Arthritis & Rheumatology

An Official Journal of the American College of Rheumatology
www.arthritisrheum.org and wileyonlinelibrary.com

Cover design: Todd Machen

♾ This journal is printed on acid-free paper.

Arthritis & Rheumatology
An Official Journal of the American College of Rheumatology
www.arthritisrheum.org and wileyonlinelibrary.com

VOLUME 69 JUNE 2017 NO. 6

Cover image: The figure on the cover (from Stock et al, page 1241) shows a Goldner's trichrome–stained section of the primary spongiosa of a *Ucma*-deficient mouse with experimental osteoarthritis. As demonstrated in this image, *Ucma*-deficient mice, in contrast to their wild-type littermates, did not exhibit elevated counts of osteoblasts aligning the bone surface (dark green staining of collagen in the extracellular matrix) adjacent to growth plate cartilage (light green). Cells are stained in red (cytoplasm) and brownish black (nuclei).

In this Issue

Highlights from this issue of *A&R* | By Lara C. Pullen, PhD

Relatives of Patients with Rheumatoid Arthritis Have Anti-CCP in Sputum

Previous research has suggested that rheumatoid arthritis (RA)–related autoimmunity is initiated at a mucosal site. However, the factors associated with the mucosal generation of autoimmunity remain unknown, and studies in individuals who are at risk of future RA are particularly lacking. In this issue, Demoruelle et al build upon their previous research on sputum RA-related antibodies in patients with RA. In this study, the investigators sought to better understand the factors associated with the earliest steps of the formation of isotype-specific antibodies to citrullinated proteins/peptides (ACPAs). They focused their efforts on RA-free, first-degree relatives (FDRs) of patients with RA, since these individuals carry a known elevated risk of developing ACPAs.

p. 1165

The researchers report that anti–cyclic citrullinated peptide (anti-CCP) is elevated in the sputum of FDRs of patients with RA. Specifically, 70% of patients with RA and 25% of FDRs had sputum that was positive for IgA and/or IgG anti-CCP. Moreover, antibodies were present in the sputum of some FDRs, even though the serum of FDRs tested negative. The investigators concluded that the lung may be a site of anti-CCP generation in a portion of FDRs. IgA anti-CCP was also associated with a history of smoking and/or elevated levels of sputum citrulline.

Further analysis revealed that elevations of sputum IgA and IgG anti-CCP in FDRs were associated with elevated sputum cell counts and neutrophil extracellular trap (NET) complex levels. This is particularly interesting because elevated NETosis has been associated with established RA. The authors explained that the association is also consistent with the hypothesis that local airway inflammation and NET formation in FDRs drives anti-CCP production in the lung. Airway inflammation might thus be said to promote the early stages of the development of RA. The researchers call for longitudinal studies to follow the evolution of these immunologic processes relative to the development of systemic autoimmunity and articular RA.

Serum Urate Levels Predict Joint Space Narrowing in Knee Osteoarthritis Patients Without Gout

Osteoarthritis (OA) has both mechanical and inflammatory pathologic features. Research aimed at understanding the pathology of OA has revealed synovial fluid uric acid (UA) to be a potential biomarker for OA. Although some researchers believe that elevated UA levels may reflect chondrocyte damage, others propose that the elevated UA levels actually contribute to and promote the cartilage damage. Still others have countered that UA levels and OA progression might reflect a common predisposing factor, rather than a causal relationship.

p. 1213

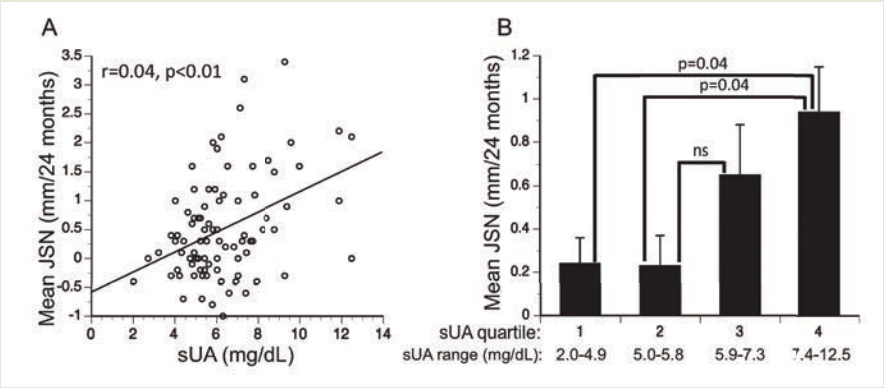

Figure 1. Association of baseline serum uric acid (sUA) levels with joint space narrowing (JSN) at 24 months, as shown by **A**, Pearson's correlation (scatterplot), and **B**, quartile groups, with designated serum UA ranges. Values are the mean ± SEM.

In this issue, Krasnokutsky et al report on their investigation of whether serum UA levels predict OA progression in a knee OA population without gout. They found that serum UA levels do predict future JSN in non-gout patients with knee OA. Specifically, they report that not only did UA levels correlate with JSN values, but there was a significant difference in mean JSN after dichotomization at a serum UA cut point of 6.8 mg/dl (the solubility point for serum urate).

In their study, the investigators found that baseline serum UA levels were able to distinguish between progressors and nonprogressors. In addition, serum UA levels correlated with synovial volume (a possible biomarker of JSN). The investigators noted, however, that the correlation did not persist once they controlled for age, sex, and body mass index. They concluded that serum UA could serve as a biomarker for OA progression.

Tocilizumab Does Not Appear to Increase Cardiovascular Risk in Rheumatoid Arthritis

A number of studies have found that tocilizumab (TCZ) increases low-density lipoprotein (LDL) cholesterol levels. It remains

p.1154

unclear whether TCZ increases cardiovascular risk in patients with rheumatoid arthritis (RA). In this issue, Kim et al report the results of their comparison of the cardiovascular risk associated with receiving TCZ versus tumor necrosis factor inhibitors (TNFi).

The investigators performed a multidatabase, population-based cohort study of 9,218 patients with RA who started treatment with TCZ. Using a variable ratio propensity score matching method, the investigators matched the TCZ initiators to 18,810 TNFi initiators from 3 different databases. All patients had previously taken a different TNFi, abatacept, or tofacitinib. The mean age of the patients was 72 years in the Medicare database, 51 years in the PharMetrics database, and 53 years in the MarketScan database. The study's primary outcome was a composite cardiovascular end point of hospitalization for myocardial infarction or stroke. The investigators found that, at baseline, cardiovascular disease was present in 14.3% of TCZ initiators and 13.5% of TNFi initiators.

During the study period, the researchers documented 125 composite cardiovascular events, which translated into an incidence rate of 0.52 per 100 person-years for TCZ initiators and 0.59 per 100 person-years for TNFi initiators. They thus found no evidence that patients with RA who switched from a different biologic drug or tofacitinib to TCZ, versus switching to TNFi had increased cardiovascular risk. The results suggest that while patients treated with TCZ have elevated lipid levels, the increases do not appear to be associated with an increased risk of cardiovascular events. These data should help physicians with their clinical decision-making in the management of RA.

Lifetime Risk of Symptomatic Hand Osteoarthritis

Symptomatic hand osteoarthritis (OA) is common, and its effect is most pronounced on hand strength and function. Not surprisingly, therefore, hand OA can cause disability in some activities of daily

p.1204

living. Although prior studies have estimated the lifetime risk of symptomatic knee OA at 45% and hip OA at 25%, up until now, there has not been an estimate of the lifetime risk of symptomatic hand OA.

In this issue, Qin et al report their estimate of the overall lifetime risk of symptomatic hand OA, as well as the stratified lifetime risk according to potential risk factors. They evaluated data from 2,218 adult subjects in the Johnston County Osteoarthritis Project, a population-based prospective cohort of residents of North Carolina. Data were collected from 1999 to 2004 and from 2005 to 2010. The researchers defined symptomatic hand OA as the presence of both self-reported symptoms and radiographic OA in the same hand.

The investigators calculated lifetime risk estimates with the hope that an individual might find such estimates to be informative and useful. They determined that 40% of adults who live to the age of 85 years will develop symptomatic hand OA. The risk was particularly high for women (47%) as opposed to men (25%). This is consistent with previous epidemiologic studies that have found that women are at higher risk of OA than men.

The burden of hand OA is especially pronounced in specific sociodemographic and clinical subgroups. In particular, the researchers estimated race-specific symptomatic hand OA risk to be 41% among whites and 29% among African Americans. The lifetime risk of symptomatic hand OA for individuals with obesity was 11 percentage points higher than that for individuals who were not obese. The authors concluded that public health and clinical interventions are necessary to address the impact of hand OA.

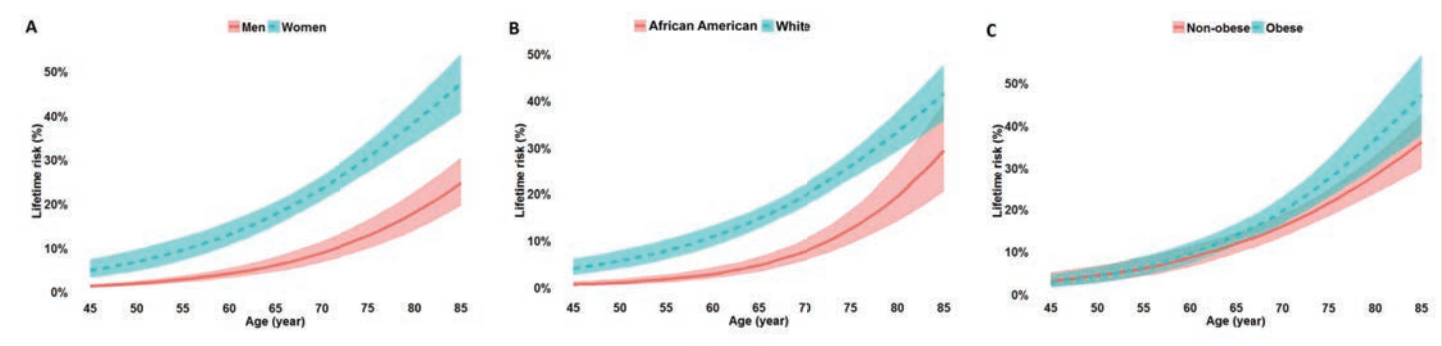

Figure 1. Cumulative risk curves by age for subgroups stratified by sex (men versus women) (**A**), race (white versus African American) (**B**), and body mass index (obese [≥30 kg/m^2] versus nonobese) (**C**). The shaded bands represent the 95% confidence intervals for the estimated cumulative risks.

Clinical Connections

Treatment of Tumor Necrosis Factor–Transgenic Mice With Anti–Tumor Necrosis Factor Restores Lymphatic Contractions, Repairs Lymphatic Vessels, and May Increase Monocyte/Macrophage Egress

Bouta et al, *Arthritis Rheumatol* 2017;69:1187-1193.

CORRESPONDENCE

Edward M. Schwarz, PhD: Edward_Schwarz@URMC.Rochester.edu.

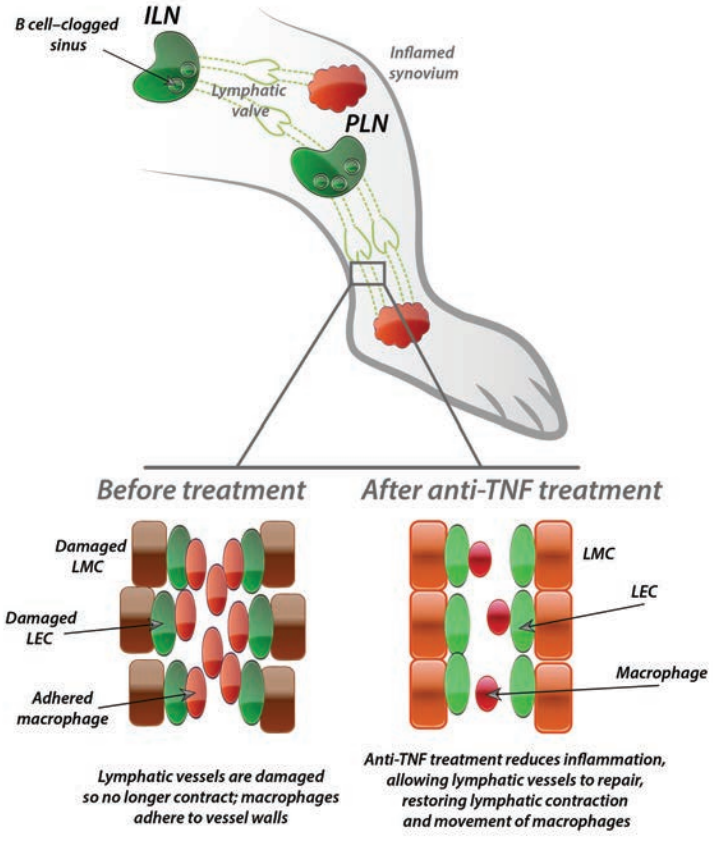

SUMMARY

Joint homeostasis is maintained by contraction of the lymphatic vessels to transport immune cells and interstitial fluid back to the circulation. In a murine model of advanced erosive inflammatory arthritis, lymphatic vessels stop contracting following damage to lymphatic endothelial cells (LECs) and lymphatic muscle cells (LMCs), which halts the migration of inflammatory cells and mediators from arthritic joints in the lower limb to the popliteal lymph nodes (PLNs) and inguinal lymph nodes (ILNs). This also contributes to B cell clogging of the lymphatic sinuses in the lymph nodes. Bouta et al found that treatment with antibodies against tumor necrosis factor (anti-TNF) promotes lymphatic vessel repair, recovery of contractions, and restoration of leukocyte transport. These findings suggest that anti-TNF therapy ameliorates erosive inflammatory arthritis, in part, via restoration of lymphatic vessel contractions that facilitate egress of inflammatory cells from inflamed synovial tissue and fluid.

KEY POINTS

- Mice with chronic erosive inflammatory arthritis have damaged lymphatic vessels that fail to contract and significantly reduced inflammatory cell egress from arthritic joints.
- Anti-TNF treatment promotes lymphatic vessel repair and restores lymphatic contractions.
- Restoration of lymphatic contractions is associated with increased inflammatory cell transport from the joint and amelioration of inflammatory arthritis.

Pathogenesis of Diffuse Alveolar Hemorrhage in Murine Lupus

Zhuang et al, *Arthritis Rheumatol* 2017;69:1280-1293.

CORRESPONDENCE
Haoyang Zhuang, PhD: haoyang.zhuang@medicine.ufl.edu
Westley H. Reeves, MD: whreeves@ufl.edu

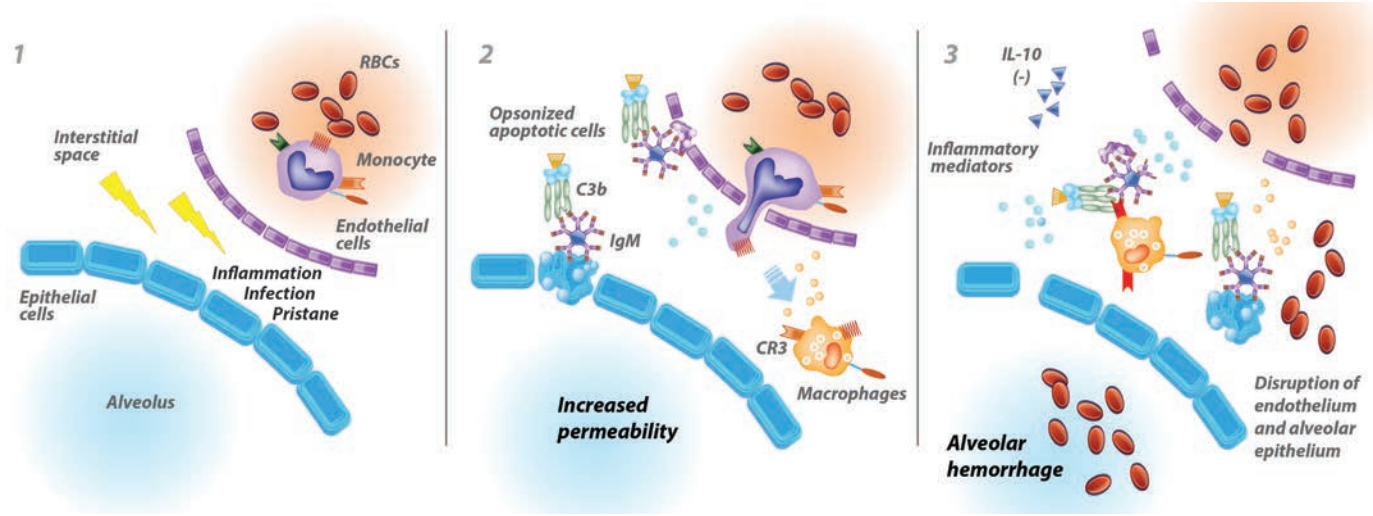

KEY POINTS

- The pathogenesis of DAH in the pristane-induced lupus model involves an inflammatory response to dead cells opsonized by "natural" IgM autoantibodies and complement component C3, followed by the engagement of CR3 on macrophages. DAH can be prevented by inhibiting complement activation or depleting immunoglobulin.
- Inflammatory macrophages (rather than neutrophils) play a central role in the pathogenesis of DAH and small vessel vasculitis (capillaritis), a feature of DAH in murine and human lupus. Both DAH and vasculitis are prevented by macrophage depletion.
- The inflammatory response is independent of Toll-like receptors, type I interferon, tumor necrosis factor, inflammasomes, and inducible nitric oxide, but is limited by IL-10.
- Inhibition of complement and/or macrophage activation or administration of IL-10 may be strategies worth testing for the treatment of DAH.

SUMMARY

Diffuse alveolar hemorrhage (DAH) is an often fatal complication of lupus. Zhuang et al report that the pathogenesis of DAH in mice with pristane-induced lupus may involve 3 steps. First, migration of pristane from the peritoneum to the lung initiates lung inflammation and death of endothelial and/or alveolar epithelial cells. In systemic lupus erythematosus patients, inflammation and cell death may be initiated by pulmonary infection. Second, chemokines and vasoactive mediators released during the initial inflammatory response increase vascular permeability and promote monocyte transmigration into the interstitial space, followed by differentiation into inflammatory macrophages and the onset of pulmonary vasculitis. The dead cells are opsonized by natural IgM and complement component C3. Third, opsonized apoptotic cells are recognized by complement receptor 3 (CR3; CD11b/CD18) on the surface of inflammatory macrophages, releasing additional inflammatory mediators. The antiinflammatory cytokine interleukin-10 (IL-10) limits this step. The inflammatory mediators disrupt endothelial and alveolar epithelial integrity, resulting in leakage of red blood cells (RBCs) into the alveolar spaces (alveolar hemorrhage).

ARTHRITIS & RHEUMATOLOGY
Vol. 69, No. 6, June 2017, pp 1127–1130
DOI 10.1002/art.40089

Arthritis & Rheumatology
An Official Journal of the American College of Rheumatology
www.arthritisrheum.org and wileyonlinelibrary.com

EDITORIAL

"Weighing in" on the Framingham Osteoarthritis Study: Measuring Biomechanical and Metabolic Contributions to Osteoarthritis

C. Thomas Appleton,[1] Gillian A. Hawker,[2] Catherine L. Hill,[3] and Janet E. Pope[1]

Thirty years ago, Altman et al told us that osteoarthritis (OA) is not a single disease (1). That 1986 description of OA as "a heterogeneous group of conditions that lead to joint symptoms and signs…" remains true today. But the simple recognition of OA as a group of related but distinct joint disorders among clinicians and researchers is hampered by the lack of a clearly accepted set of criteria to distinguish independent clinical OA phenotypes. Moreover, the description of these clinical OA phenotypes in molecular, anatomic, and physiologic domains remains a formidable, yet fundamental task before us in the field of OA research. Notwithstanding, the blanket term "OA" should no longer be used in isolation to describe the typical joint pathology and symptoms of the most common form of arthritis in humans. An effort should be made in all OA cases to apply accompanying adjectives to at least describe the context in which the joint disease arose. Candidate clinical phenotypes include OA related to joint trauma (posttraumatic OA), advanced age at disease onset (age-related/senescent OA), strong family history (inherited/genetic OA), pain sensitization, inflammatory features, and metabolic syndrome (metabolic OA) (2). Given that ~25% of the world's adult population develops metabolic syndrome (3), the association of metabolic syndrome with OA is especially alarming.

Metabolic syndrome consists of 4 core features, variably defined, including hypertension, atherogenic dyslipidemias, visceral obesity, and insulin resistance. The most recent metabolic syndrome definitions from the US National Cholesterol Education Program Adult Treatment Panel III and the International Diabetes Federation were presented in 2005. Regardless of the definition of metabolic syndrome, a clear link between metabolic syndrome and OA has been established in many different studies. Analyses of Third National Health and Nutrition Examination Survey (NHANES-III) data show that metabolic syndrome prevalence is higher among people with OA than those without OA (59% versus 23%, respectively) and that this form of OA occurs in younger age groups (ages 45–65 years) than age-related OA (4). The individual components of metabolic syndrome are also associated with excess OA risk. For example, in the Japanese Research on Osteoarthritis Against Disability (ROAD) study, the risk of OA increased with each additional component of metabolic syndrome (5), although that was a cross-sectional analysis without adjustment for body mass index (BMI).

The nature of the interaction between metabolic syndrome and OA remains unresolved. It is unclear whether the most important link is due to an influence of OA on metabolic syndrome (e.g., decreased mobility due to OA leads to obesity and therefore metabolic syndrome), vice versa (abnormal joint loading—with or without metabolic derangement—fuels OA pathophysiology), or if a common set of risk factors exist which drive both conditions in parallel. A shared etiology in the latter case would suggest that metabolic OA is an underrecognized fifth (or sixth) feature of metabolic syndrome rather than a separate condition per se, as some have suggested (6). As is often the case, the answer may lie in a combination of these possibilities. But the reliance on prevalence data and cross-sectional analyses in most OA/metabolic syndrome studies

[1]C. Thomas Appleton, MD, PhD, FRCPC, Janet E. Pope, MD, MPH, FRCPC: Western University and St. Joseph's Health Care, London, Ontario, Canada; [2]Gillian A. Hawker, MD, MSc, FRCPC: University of Toronto, Women's College Research Institute, Women's College Hospital, and Institute for Clinical Evaluative Sciences, Toronto, Ontario, Canada; [3]Catherine L. Hill, MBBS, MD, MSc, FRACP: The Queen Elizabeth Hospital, Woodville, South Australia, Australia, and the Health Observatory, University of Adelaide, Adelaide, South Australia, Australia.

Address correspondence to C. Thomas Appleton, MD, PhD, FRCPC, St. Joseph's Health Care London, 268 Grosvenor Street, London, Ontario N6A 4V2, Canada. E-mail: tom.appleton@sjhc.london.on.ca.

Submitted for publication January 14, 2017; accepted in revised form March 2, 2017.

makes it difficult to resolve such "chicken-or-the-egg" questions. Nevertheless, the balance of the literature suggests that metabolic syndrome and increased BMI or body weight are each associated with an increased risk of incident knee OA especially. Increased BMI or body weight and metabolic syndrome (given that BMI is a core component) clearly cause increased or abnormal knee joint loading (7). Therefore, the fundamental question that remains is whether metabolic syndrome increases incident OA risk purely driven by the biomechanical consequences of increased body weight, or if metabolic derangement (e.g., from increased visceral fat–driven systemic inflammation or other mechanisms yet to be confirmed) confers additive risk beyond that explained by biomechanics alone.

In this issue of *Arthritis & Rheumatology*, Niu et al (8) present longitudinal data from the Framingham OA Study, demonstrating an association of preexisting metabolic syndrome and its components with an increased risk of incident radiographic and symptomatic knee OA over 10 years of follow-up. A dose-response relationship was also seen for the association of the number of metabolic syndrome components with incident radiographic OA. The assessment of metabolic syndrome occurred a year or so before the OA examination. The prospective study design and inclusion of incident OA outcomes allowed for risk factors to be determined, in contrast to previous studies that showed only correlations or associations. The unique statistical approach for examining the various contributions to OA development due to BMI versus body weight versus waist circumference suggested a very high correlation among these measures, which is useful methodologically for future studies.

The incidence data presented by Niu et al are particularly noteworthy, since they show that preexisting metabolic syndrome and its components are risk factors for subsequent symptomatic OA and not just radiographic OA. Their study also provides circumstantial evidence supporting the hypothesis that at least one or more of the metabolic syndrome components may cause OA. Of course, the increased risk may alternately belie the existence of common risk factors for both metabolic syndrome and OA, where OA may be a later-occurring additional component of metabolic syndrome. However, we feel it is most appropriate to consider metabolic OA as a complication of metabolic syndrome, similar to cardiovascular disease.

Understanding how metabolic syndrome underlies the manifestation of metabolic OA is confounded further by the duality of pathobiology and biomechanics impelling OA pathophysiology. Obesity is the only metabolic syndrome component that is consistently associated with OA across most studies, suggesting that increased weight plays a role in OA development through increased joint loading. However, increased joint loading may not fully explain the effects of metabolic syndrome on all aspects of metabolic OA, since hand OA is also associated with obesity with or without other metabolic syndrome components (9) and is independent of abnormal joint loading. It should be noted, though, that the hypothesis that hand OA is related to obesity remains a subject of controversy, in part due to the cross-sectional design of the studies in which a significant association was found. Nevertheless, failure to adjust for any contribution of increased joint loading in knee OA due to increased body weight in metabolic syndrome will overestimate the contribution of metabolic processes to metabolic OA.

Teasing out the relative contributions of abnormal biomechanics versus metabolic derangement to the development of metabolic OA is an essential step that we must achieve to realize the best approaches to treatment. Niu et al astutely raise this issue in the Framingham OA analysis and attempt to isolate the contribution of metabolic derangement due to metabolic syndrome from abnormal joint loading by adjusting for BMI or body weight. Such adjustment nullified the association between incident radiographic OA and symptomatic OA with metabolic syndrome and each of the metabolic syndrome components, with the exception of diastolic blood pressure, which remained significantly associated with symptomatic OA. Associations between metabolic syndrome components and knee OA after adjustment for BMI were also nullified in the Korean National Health and Nutrition Examination Survey (10), among others.

Unfortunately, BMI and body weight are not ideal surrogates for joint loading, especially in metabolic syndrome, due to a close correlation with central obesity. Indeed, the correlation of BMI and body weight with central obesity is strong (Niu et al calculate a Pearson's correlation coefficient of 0.84–0.88). Measurement of body composition, which better delineates the contribution of fat and muscle to body mass, has led to interesting findings in knee OA. A recent study has suggested that the effect of BMI in asymptomatic knee OA is predominantly mediated by fat mass (and not lean mass), suggesting that differentiating between fat mass and weight may also be beneficial in predicting incident OA (11). Moreover, adjustment for body composition rather than BMI or body weight may be a better approach in future studies, which will be required to determine if a significant contribution to incident OA risk from fat mass–driven metabolic derangement truly does exist beyond biomechanics.

In addition to adding to body weight, central (visceral) obesity is strongly linked to important metabolic functions. For example, beginning with the discovery of leptin in 1994 (12), adipose tissue has been identified as

having an important endocrine function through the secretion of adipokines. In the Invecchiare in Chianti (Aging in the Chianti area; InCHIANTI) study, high leptin levels were associated with metabolic syndrome in obese and nonobese patients (13), and high levels of leptin were associated with incident radiographic knee OA in the American Study of Women's Health Across the Nation (SWAN) (14). Central obesity is also tied to the development of metabolic syndrome components, including dyslipidemia and insulin resistance. So, while central obesity contributes to abnormal joint loading via increased body weight, it may also influence joint homeostasis via systemic metabolic derangements. Since BMI/weight (which captures central obesity) encompasses both metabolic and mechanical loading variables, it follows that adjustment for BMI or body weight in studies may simultaneously adjust for both joint loading and metabolic factors associated with central obesity. Even though the intention is to adjust for abnormal joint loading in isolation, this strategy limits the ability to draw conclusions about the relative contributions of abnormal joint loading versus metabolic syndrome (or its components) with incident OA. Inventively, Niu et al try to address this issue with residuals of waist circumference after removing variation caused by BMI and body weight, but this also negated any associations with incident OA.

What is needed is an alternative factor for adjustment that more precisely estimates the magnitude of abnormal joint loading without encompassing any metabolic effects of adipose tissue. An ideal measure would be to quantify knee joint load directly, but this is quite difficult to measure externally, and force-measuring joint implants are expensive, are invasive, and would not be feasible for incident radiographic OA or symptomatic OA studies. Knee adduction moment (KAM) is a close surrogate of medial tibiofemoral compartment force, especially components of KAM such as peak KAM. Changes in peak KAM in obese patients are due to weight and not obesity distribution, making this a suitable alternative measure to use for adjustment of joint loading (7). Future studies exploring associations between metabolic syndrome and OA could include and adjust for KAM and compare with adjustment for BMI and body weight.

There are some limitations to the study by Niu et al. Despite the large sample size, incident OA was rare, so the borderline effect of blood pressure on incident OA may have been due to the study not having adequate power to detect a more robust effect. Moreover, all knee OA was combined (medial, lateral, and patellofemoral). The latter may have been a limitation since perhaps medial OA is affected more by metabolic syndrome than patellofemoral OA. The numbers of different subsets with incident OA were too small to allow for subset calculations for robust answers regarding associations with metabolic syndrome. The date of onset of OA could not be precisely determined since subjects were only examined at fixed dates. Since OA symptoms might motivate participants to make lifestyle changes (e.g., to lose weight), future studies need to carefully consider how to take such prior exposures into account for adjustment. There was a protective effect of glucose (after adjustment for BMI), which warrants further research since this could be real or spurious due to the use of numerous statistical tests.

Considering the likely confounding of body weight between mechanical and metabolic processes, the fact that any component of metabolic syndrome remained significantly associated with symptomatic OA after adjusting for BMI and body weight argues strongly for a metabolic driver of OA pathophysiology. A 2012 cross-sectional study in 352 OA patients showed that 60% of patients with prevalent OA had hypertension after correcting for age and BMI (15). In NHANES-III, 77% of subjects with OA had hypertension versus 30% of those without OA (4). Again, this does not help us to sort out whether it's the chicken (OA-related loss of mobility causing hypertension) or the egg (hypertension leading to OA). Mechanistically, subchondral ischemia is the best described hypothesis for hypertension contributing directly to OA pathogenesis. Narrowing of subchondral vessels may reduce nutrient exchange and devitalize the overlying articular cartilage (16) or stimulate apoptosis of osteocytes and subsequent osteoclast activation and subchondral bone remodeling (17). Much work is left to be done in this area to delineate the mechanisms involved, but clinical studies investigating the impact of antihypertensive therapy in patients with hypertension and comorbid metabolic OA would offer insights.

Metabolic OA should be considered and studied separately from other types of OA. The development or updating of classification criteria would aid significantly in defining metabolic OA. While such a task is best suited to a classification criteria committee, possible minimum criteria to consider might include a) the presence of metabolic syndrome according to an accepted definition, b) symptomatic OA and/or radiographic OA, and c) exclusion of alternative etiologies such as prior joint trauma, family history of genetic OA, advanced age at onset (e.g., $>$75 years), and underlying comorbid risks (e.g., inflammatory arthritis, hemochromatosis, calcium pyrophosphate deposition disease, etc.). Adjustment for confounders is a key issue in clinical studies, but biomechanics are especially important in OA and musculoskeletal diseases. Thus, working with our expert colleagues in OA biomechanics research continues to be a vital collaboration in our field. OA and metabolic syndrome are complex diseases with an unresolved

etiology, but the work presented by Niu et al further emphasizes the link between these conditions.

Whether metabolic OA should be considered a component of metabolic syndrome is still open for debate, but Niu et al have provided data on incident OA in the setting of preexisting metabolic syndrome, the Framingham OA Study, suggesting that OA may be a consequence of metabolic syndrome rather than the reverse. Carefully designed future studies are still required to determine the relative impact of increased body mass in metabolic syndrome on joint loading versus metabolic derangements (including systemic inflammation). Such future studies should be a top priority for our field. Studies employing a life course approach including past history of elevated BMI (e.g., obesity during childhood and early adulthood) are also needed. Ruling in or out a clinically important impact of altered metabolism on incident OA risk independent of biomechanics would be a significant breakthrough in our understanding of metabolic OA and other OA phenotypes. It would also provide a strong foundation for the development of rational treatment approaches for this pervasive and disabling disease.

AUTHOR CONTRIBUTIONS

Dr. Appleton drafted the article, and all authors revised it critically for important intellectual content and approved the final version to be published.

REFERENCES

1. Altman R, Asch E, Bloch D, Bole G, Borenstein D, Brandt K, et al. Development of criteria for the classification and reporting of osteoarthritis: classification of osteoarthritis of the knee. Arthritis Rheum 1986;29:1039–49.
2. Bijlsma JW, Berenbaum F, Lafeber FP. Osteoarthritis: an update with relevance for clinical practice. Lancet 2011;377:2115–26.
3. Eckel RH, Grundy SM, Zimmet PZ. The metabolic syndrome. Lancet 2005;365:1415–28.
4. Puenpatom RA, Victor TW. Increased prevalence of metabolic syndrome in individuals with osteoarthritis: an analysis of NHANES III data. Postgrad Med 2009;121:9–20.
5. Yoshimura N, Muraki S, Oka H, Kawaguchi H, Nakamura K, Akune T. Association of knee osteoarthritis with the accumulation of metabolic risk factors such as overweight, hypertension, dyslipidemia, and impaired glucose tolerance in Japanese men and women: the ROAD study. J Rheumatol 2011;38:921–30.
6. Velasquez MT, Katz JD. Osteoarthritis: another component of metabolic syndrome? Metab Syndr Relat Disord 2010;8:295–305.
7. Segal NA, Yack HJ, Khole P. Weight, rather than obesity distribution, explains peak external knee adduction moment during level gait. Am J Phys Med Rehabil 2009;88:180–8.
8. Niu J, Clancy M, Aliabadi P, Vasan R, Felson DT. Metabolic syndrome, its components, and knee osteoarthritis: the Framingham Osteoarthritis Study. Arthritis Rheumatol 2017;69:1194–1203.
9. Dahaghin S, Bierma-Zeinstra SM, Koes BW, Hazes JM, Pols HA. Do metabolic factors add to the effect of overweight on hand osteoarthritis? The Rotterdam Study. Ann Rheum Dis 2007;66:916–20.
10. Han C, Yang I, Lee W, Park Y, Park K. Correlation between metabolic syndrome and knee osteoarthritis: data from the Korean National Health and Nutrition Examination Survey (KNHANES). BMC Public Health 2013;13:603.
11. Ho-Pham LT, Lai TQ, Mai LD, Doan MC, Nguyen TV. Body composition in individuals with asymptomatic osteoarthritis of the knee. Calcif Tissue Int 2016;98:165–71.
12. Zhang Y, Proenca R, Maffei M, Barone M, Leopold L, Friedman JM. Positional cloning of the mouse obese gene and its human homologue. Nature 1994;372:425–32.
13. Stenholm S, Koster A, Alley DE, Visser M, Maggio M, Harris TB, et al. Adipocytokines and the metabolic syndrome among older persons with and without obesity: the InCHIANTI Study. Clin Endocrinol (Oxford) 2010;73:55–65.
14. Karvonen-Gutierrez CA, Harlow SD, Mancuso P, Jacobson J, de Leon CF, Nan B. Association of leptin levels with radiographic knee osteoarthritis among a cohort of midlife women. Arthritis Care Res (Hoboken) 2013;65:936–44.
15. Morović-Vergles J, Šalamon L, Marasović-Krstulović D, Kehler T, Šakić D, Badovinac O, et al. Is the prevalence of arterial hypertension in rheumatoid arthritis and osteoarthritis associated with disease? Rheumatol Int 2013;33:1185–92.
16. Imhof H, Sulzbacher I, Grampp S, Czerny C, Youssefzadeh S, Kainberger F. Subchondral bone and cartilage disease: a rediscovered functional unit. Invest Radiol 2000;35:581–8.
17. Aguirre IJ, Plotkin LI, Stewart SA, Weinstein RS, Parfitt MA, Manolagas SC, et al. Osteocyte apoptosis is induced by weightlessness in mice and precedes osteoclast recruitment and bone loss. J Bone Miner Res 2006;21:605–15.

ARTHRITIS & RHEUMATOLOGY
Vol. 69, No. 6, June 2017, pp 1131–1134
DOI 10.1002/art.40082

EDITORIAL

Choosing New Targets for Rheumatoid Arthritis Therapeutics: Too Interesting to Fail?

Iain B. McInnes, Duncan Porter, and Stefan Siebert

Progress in the treatment of rheumatoid arthritis (RA) in the last 2 decades has been remarkable, leading to substantial improvements in the quality of life for many patients. This has arisen from 2 fundamental developments. First, the advent of pathogenesis-led therapeutics has generated a growing armamentarium of effective medicines available to the practitioner (1). The introduction of tumor necrosis factor (TNF) inhibition arose from a careful in vitro cellular immunology and in vivo murine arthritis model program that generated sufficient preclinical validation to encourage successful testing in RA of TNF inhibitors in clinical studies. Subsequently, other therapies emerged that antagonize proinflammatory cytokines (for example, interleukin-6 [IL-6]), inhibit T cell costimulatory activation, or deplete CD20-positive B cells (1). More recently, a small-molecule inhibitor of intracellular signaling in the form of the JAK-1/JAK-3 inhibitor tofacitinib has heralded a new era of targeted synthetic disease-modifying antirheumatic drugs.

A second substantial development has arisen from the advent of "strategically smart" approaches, encapsulated in "treat early" and "treat to target" approaches (1). Together, these developments have significantly improved the prognosis of patients with RA, leading to reductions in joint damage, functional disability, comorbidity, and mortality. Moreover, these therapeutic developments have brought about the possibility of remission induction and maintenance of response in the treatment of RA, concepts that, even 2 decades ago, were inconceivable.

In the midst of such excitement, it is salutary to consider briefly the cost of this journey of improvement and learn lessons to inform further progress. In particular, there have been numerous clinical targets selected on the basis of robust data sets that have failed to meet success in phase II or phase III trials. This attrition rate may not be sustainable for either the pharmaceutical industry or the clinical trial community. This is pertinent since, in our view, there remains significant unmet clinical need in RA. True remission is still achieved only in a minority of patients and usually requires ongoing treatment, with its attendant risks and significant financial cost. Moreover, there is a group of patients who become refractory to all existing therapies or who never respond in the first place. Against this background of unmet clinical need in RA and rising drug development costs yet burgeoning knowledge about the disease pathobiology, it is timely to reconsider the methodology that might lead to the accurate identification of novel immune targets for use in the treatment of RA.

In this issue of *Arthritis & Rheumatology*, Blanco and colleagues present the findings from a very interesting phase III clinical trial evaluating the use of an IL-17A inhibitor, secukinumab, in patients with active RA who have previously had an inadequate response to TNF inhibitors (2). The authors and editors alike are to be congratulated for bringing these data into the public domain—publishing such data represents a significant step forward in planning for success in the future. The trial examined the therapeutic impact of 2 doses of secukinumab compared with either abatacept or placebo. While the primary outcome, the American College of Rheumatology 20% improvement response at week 24 (3), was met at the predetermined statistically significant level in patients who received the higher dose of 150 mg of secukinumab, this was achieved by only a

Iain B. McInnes, MD, PhD, Duncan Porter, MD, Stefan Siebert, MD, PhD: University of Glasgow, Glasgow, UK.

Prof. McInnes has received honoraria from Novartis, AbbVie, BMS, UCB, Janssen, Roche, and Pfizer (less than $10,000 each) and research funds from BMS, UCB, Janssen, Roche, and Pfizer. Dr. Porter has received honoraria from Janssen, BMS, Biogen, UCB, AbbVie, Roche, and Pfizer (less than $10,000 each) and research funding from Roche and Pfizer. Dr. Siebert has received honoraria from Novartis, Janssen, Pfizer, AbbVie, UCB, and Boehringer-Ingelheim (less than $10,000 each) and research funding from UCB, Celgene, and Pfizer.

Address correspondence to Iain B. McInnes, MD, PhD, College of Medical, Veterinary and Life Sciences, University of Glasgow, 120 University Place, Glasgow G12 8TA, UK. E-mail: iain.mcinnes@glasgow.ac.uk.

Submitted for publication January 26, 2017; accepted in revised form February 23, 2017.

modest proportion of patients, and significant improvement in key secondary end points was not achieved. Overall, the study demonstrates, at best, only modest superiority for secukinumab over placebo, with a response that was probably inferior to that seen with abatacept and does not support further development of secukinumab for use in patients with RA in whom TNF inhibitors have previously failed.

The study by Blanco et al should be considered in the wider context of discouraging findings from other studies of IL-17 inhibition in RA. Thus, an IL-17 receptor inhibitor, brodalumab, which blocks IL-17 receptor A and thus all IL-17 family cytokine signaling, failed to show any effect in patients with RA (4), and modest benefit, at best, was elicited upon treatment with ixekizumab, another IL-17A inhibitor (5). From this therapeutic trial set, we may conclude that IL-17A inhibition as monotherapy does not represent a satisfactory target for the treatment of RA.

It is worth considering the experimental narrative that brought us to the present phase III clinical trial. IL-17A is a member of a large cytokine family that contains both pro- and antiinflammatory members. It exhibits highly plausible biologic effector functions, working either alone or, especially, in synergy with other inflammatory cytokines such as TNF and IL-1, to promote synovial fibroblast activation, neutrophil activation and recruitment, B cell activation and antibody production, and a variety of prodestructive effects via osteoclast maturation and effector function (6). Results of in vivo experiments in relevant inflammatory arthritis models have suggested that IL-17A occupies a position of hierarchical primacy, rendering it an attractive therapeutic target. The concept that Th17 cells have dominant roles in a range of murine models of autoimmunity is now well-established and, together with the demonstration of IL-17A expression in human tissue types of clinical relevance, has led to the adoption of IL-17A as a therapeutic target in a range of cutaneous, gastrointestinal, neurologic, and articular immune-mediated diseases (6).

These observations have translated into rather mixed clinical results when appropriate human clinical trials have been performed (7). Thus, IL-17A blockade in psoriasis has yielded remarkable clinical responses, with close to 50% of participants achieving complete clearance of skin disease, as represented by Psoriasis Area and Severity Index 100% improvement (8). Successful trials of IL-17A blockade have been conducted in patients with psoriatic arthritis (9–11) and those with ankylosing spondylitis (12), but with less spectacular musculoskeletal responses when compared to those achieved in the skin (13). In contrast, no benefit accrued in patients with Crohn's disease upon receipt of secukinumab (14).

From these studies, we draw a number of conclusions. First, the emerging group of IL-17A inhibitors represents a new class of medicines with viable pharmacologic and pharmacodynamic properties. Second, secukinumab, and indeed other IL-17 inhibitors, can be highly effective when used to treat disease states in which IL-17A enjoys functional hierarchical supremacy, such as cutaneous psoriasis. Third, we have learned again from these studies that simply identifying an inflammatory cytokine as a potential target through documentation of its presence in clinical tissues of relevance and postulating plausible biologic effector functions is not sufficient to guarantee future therapeutic success. Moreover, we have learned once again that animal models of arthritis, although helpful in allowing us to dissect intact immune systems, have distinct translational limitations. Finally, the data suggest the value in building a compendium of trial outcomes across different inflammatory immune targets and immune-mediated diseases to drive us toward a molecular taxonomy for inflammation medicine that could eventually complement the clinical phenotyping upon which current clinical trials are based.

Where does this leave us in terms of current clinical target selections in RA? Happily, the field continues to progress with targets selected across a range of immune pathways. These include agents designed to inhibit innate immune activation, for example, those targeting Toll-like receptors and the intracellular molecular machinery that allows innate immune activation, such as the inflammasome. There are ongoing efforts to develop new effector cytokine inhibitors, including "look alike" agents targeting both the IL-6 receptor and IL-6 ligand and novel agents targeting granulocyte–macrophage colony-stimulating factor or its receptor α subunit. Other JAK inhibitors are emerging, including baricitinib, a JAK-1/2 inhibitor (15,16), and filgotinib, a JAK-1 inhibitor (17,18). There is also interest in developing novel small-molecule inhibitors of cellular signaling pathways, for example, inhibitors of the phosphatidylinositol 3-kinase family and Bruton's tyrosine kinase, and also some interesting studies looking at epigenetic modifiers.

The search for immunologic homeostasis continues. It is worth noting the development of cellular therapies, including the transfer of tolerogenic dendritic cells and also immune therapeutics that are designed to achieve the same effect in vivo using, for example, drug-loaded liposomes. Rather innovative approaches, such as those targeting the peptidylarginine deiminase enzyme system, those stimulating the vagal nerve, and those modulating the neuroendocrine inflammatory system using

gonadotropin-releasing hormone antagonists (for example, cetrorelix), have offered provisional evidence of benefit. This plethora of potential targets may well yield new opportunities. However, what marks all of them is the absence of definitive, consistently applied discovery pathways that can give high levels of confidence a priori that they will either target a hierarchically sufficiently prominent molecule or a particularly vulnerable point in the inflammatory cascade (19).

How then could we change our approach to the development of new therapeutic agents while celebrating the successes annotated above? It is important to recall the failure of clinical trials in RA that targeted, for example, CD4, CD5, IL-1, IL-12, IL-20, and IL-23. These clinical trial development programs all arose from rational and plausible preclinical biologic packages and, although there were subtle differences between the weight of evidence and the nature of the experimental systems employed, few could be considered to be rash development decisions based on the knowledge of that time. Perhaps it is now appropriate to consider a systems-based approach to the development and validation of targets. We currently possess unparalleled access to digital information and computational power. If this could be combined with the depth of biologic experimentation possible at the molecular and cellular level to generate a high volume and high quality of data, it would offer intriguing and powerful possibilities. Specifically, it may be possible to interrogate potential future therapeutic targets using in silico models of the rheumatic disease state, reflecting the accumulation of knowledge from preclinical biology studies, many clinical trials, and ex vivo biomarker programs, regardless of whether they are successful.

Comprehensive data sets can be generated that describe the genome, epigenome, transcriptome, proteome, and metabolome from a range of biologic samples—the so-called "polyome." Bioinformatics algorithms capable of integrating the discrete information contained across the polyome are emerging. Such data can be obtained from in vivo animal model studies in which pathways have been specifically targeted, together with in vitro leukocyte and synovial biology studies in which complex cellular contributions can be explored along with the signal pathways that subserve such biology. This should permit the creation of computational models that mimic RA pathways of inflammation and damage accrual that, in turn, can be targeted in silico to estimate the likely outcomes of novel interventions. In parallel, mode of action studies could be conducted in RA patients, in which blood and synovial responses to interventions should be mandatory parameters so as to gather new ex vivo data sets that could be fed into the models to offer refinement on an ongoing basis.

This systems approach to target discovery and validation could be usefully coupled with an increasing move toward stratification of the clinical and molecular phenotype of RA to improve success rates in the longer term. We should give greater deference to the stage of disease for which a drug is to be developed—it is probably reasonable to assume that the immune system will adapt over time as articular damage accrues in RA, and our approaches should be amended accordingly. Models of early disease will therefore be required, but models of late disease may equally be required as we consider development of agents for refractory RA. For the latter, we especially need to understand the mechanisms that underpin therapeutic failure and acquired loss of response. As we come to recognize the molecular heterogeneity of RA, so we will recognize the value of enriching the likelihood of responses to a given target by appropriate clinical selection of patients for trial entry. Similarly, adaptive trial designs may allow us to more quickly discard ineffective therapies and direct patients within the trial to those agents to which they are more likely to respond. In this respect, it is likely that important lessons can be learned, and adapted, from the rapidly expanding use of immunotherapies and innovative trial designs emerging in the treatment of cancer. Taken together, if we are more prepared to learn from unsuccessful trials and to perform detailed mechanistic analysis, not only of why studies have succeeded but also of why others have failed, we will enrich the possibilities for future generations as they meet the challenges of the "RA disease" that we will bequeath to them.

AUTHOR CONTRIBUTIONS

All authors were involved in drafting the article or revising it critically for important intellectual content, and all authors approved the final version to be published.

REFERENCES

1. Smolen JS, Aletaha D, McInnes IB. Rheumatoid arthritis. Lancet 2016;388:2023–38.
2. Blanco FJ, Möricke R, Dokoupilova E, Codding C, Neal J, Andersson M, et al. Secukinumab in active rheumatoid arthritis: a phase III randomized, double-blind, active comparator– and placebo-controlled study. Arthritis Rheumatol 2017;69:1144–53.
3. Felson DT, Anderson JJ, Boers M, Bombardier C, Furst D, Goldsmith C, et al. American College of Rheumatology preliminary definition of improvement in rheumatoid arthritis. Arthritis Rheum 1995;38:727–35.
4. Pavelka K, Chon Y, Newmark R, Lin SL, Baumgartner S, Erondu N. A study to evaluate the safety, tolerability, and efficacy of brodalumab in subjects with rheumatoid arthritis and an inadequate response to methotrexate. J Rheumatol 2015;42:912–9.

5. Genovese MC, Greenwald M, Cho CS, Berman A, Jin L, Cameron GS, et al. A phase II randomized study of subcutaneous ixekizumab, an anti–interleukin-17 monoclonal antibody, in rheumatoid arthritis patients who were naive to biologic agents or had an inadequate response to tumor necrosis factor inhibitors. Arthritis Rheumatol 2014;66:1693–704.
6. Beringer A, Noack M, Miossec P. IL-17 in chronic inflammation: from discovery to targeting. Trends Mol Med 2016;22:230–41.
7. Fragoulis GE, Siebert S, McInnes IB. Therapeutic targeting of IL-17 and IL-23 cytokines in immune-mediated diseases. Annu Rev Med 2016;67:337–53.
8. Fredriksson T, Pettersson U. Severe psoriasis—oral therapy with a new retinoid. Dermatologica 1978;157:238–44.
9. McInnes IB, Mease PJ, Kirkham B, Kavanaugh A, Ritchlin CT, Rahman P, et al. Secukinumab, a human anti-interleukin-17A monoclonal antibody, in patients with psoriatic arthritis (FUTURE 2): a randomised, double-blind, placebo-controlled, phase 3 trial. Lancet 2015;386:1137–46.
10. Mease PJ, McInnes IB, Kirkham B, Kavanaugh A, Rahman P, van der Heijde D, et al. Secukinumab inhibition of interleukin-17A in patients with psoriatic arthritis. N Engl J Med 2015;373:1329–39.
11. Mease PJ, van der Heijde D, Ritchlin CT, Okada M, Cuchacovich RS, Shuler CL, et al. Ixekizumab, an interleukin-17A specific monoclonal antibody, for the treatment of biologic-naive patients with active psoriatic arthritis: results from the 24-week randomised, double-blind, placebo-controlled and active (adalimumab)-controlled period of the phase III trial SPIRIT-P1. Ann Rheum Dis 2017;76:79–87.
12. Baeten D, Sieper J, Braun J, Baraliakos X, Dougados M, Emery P, et al. Secukinumab, an interleukin-17A inhibitor, in ankylosing spondylitis. N Engl J Med 2015;373:2534–48.
13. Farahnik B, Beroukhim K, Nakamura M, Abrouk M, Zhu TH, Singh R, et al. Anti-IL-17 agents for psoriasis: a review of phase III data. J Drugs Dermatol 2016;15:311–6.
14. Hueber W, Sands BE, Lewitzky S, Vandemeulebroecke M, Reinisch W, Higgins PD, et al. Secukinumab, a human anti-IL-17A monoclonal antibody, for moderate to severe Crohn's disease: unexpected results of a randomised, double-blind placebo-controlled trial. Gut 2012;61:1693–700.
15. Genovese MC, Kremer J, Zamani O, Ludivico C, Krogulec M, Xie L, et al. Baricitinib in patients with refractory rheumatoid arthritis. N Engl J Med 2016;374:1243–52.
16. Fleischmann R, Schiff M, van der Heijde D, Ramos-Remus C, Spindler A, Stanislav M, et al. Baricitinib, methotrexate, or combination in patients with rheumatoid arthritis and no or limited prior disease-modifying antirheumatic drug treatment. Arthritis Rheumatol 2017;69:506–17.
17. Kavanaugh A, Kremer J, Ponce L, Cseuz R, Reshetko OV, Stanislavchuk M, et al. Filgotinib (GLPG0634/GS-6034), an oral selective JAK1 inhibitor, is effective as monotherapy in patients with active rheumatoid arthritis: results from a randomised, dose-finding study (DARWIN 2). Ann Rheum Dis 2016. E-pub ahead of print.
18. Westhovens R, Taylor PC, Alten R, Pavlova D, Enríquez-Sosa F, Mazur M, et al. Filgotinib (GLPG0634/GS-6034), an oral JAK1 selective inhibitor, is effective in combination with methotrexate (MTX) in patients with active rheumatoid arthritis and insufficient response to MTX: results from a randomised, dose-finding study (DARWIN 1). Ann Rheum Dis 2016. E-pub ahead of print.
19. McInnes IB, Buckley CD, Isaacs JD. Cytokines in rheumatoid arthritis: shaping the immunological landscape. Nat Rev Rheumatol 2015;12:63–8.

ARTHRITIS & RHEUMATOLOGY
Vol. 69, No. 6, June 2017, pp 1135–1143
DOI 10.1002/art.40071

REVIEW

Cytokine Storm Syndrome

Looking Toward the Precision Medicine Era

Edward M. Behrens[1] and Gary A. Koretzky[2]

Introduction

"Cytokine storm syndrome" is a diverse set of conditions unified by a clinical phenotype of systemic inflammation, multi-organ failure, hyperferritinemia, and, if untreated, often death. This clinical constellation is caused by the elaboration of extreme amounts of inflammatory mediators resulting from unchecked feedforward immune activation and amplification. The initiating factors leading to the end state of cytokine storm are heterogeneous and derive from rheumatologic, oncologic, and infectious origins.

The first member of the cytokine storm family to be recognized by physicians was sepsis. The appreciation that the consequences of sepsis are a result not of the pathogen, but rather the immune response to the pathogen, dates back to observations made by William Osler in 1904 in his book, *The Evolution of Modern Medicine*. Accordingly, the idea that sepsis might be most effectively treated by immunomodulation is not new. With the identification of tumor necrosis factor (TNF) and interleukin-1β (IL-1β) as major inflammatory cytokines in models of sepsis in the last part of the twentieth century, trials were undertaken to block these cytokines to treat septic cytokine storm. The failure of blockade of these molecules to improve outcomes in sepsis (1–3) dampened enthusiasm for this approach for many years. In addition to the timing of therapeutic intervention (i.e., patients were typically not enrolled in the clinical trials at an early enough time point for immunomodulation therapy to potentially be successful), these trials likely failed because the situation is more complicated than Osler first recognized, with complex host–pathogen interactions playing a role beyond the simple notion that sepsis is due solely to an excessive immune response.

Further complicating matters, cytokine storm cannot be considered a disease itself, but rather the common end point of different initial insults: infectious, autoimmune/inflammatory, and iatrogenic. Even within those broad categories significant differences exist, making the landscape unlikely to be amenable to a "one-size-fits-all" therapy. Quite the opposite, we are approaching the beginning of a new era of precision medicine for cytokine storm, in which understanding of the immunologic derangement of each individual trigger, and perhaps in each individual patient, will inform the choice of intervention.

Success in personalization of therapy will require the practitioner to consider the similarities and differences in a wide array of conditions under the moniker of "cytokine storm." Common to the cytokine storm syndrome, and exemplified by all of the diseases discussed here, is a loss of negative feedback on the immune system, resulting in the overproduction of inflammatory cytokines. In turn, these inflammatory cytokines drive a positive feedback on their own production, begetting the common syndrome of exponentially growing inflammation and multi-organ failure. Commonly, but not exclusively, the main effector cytokine in these syndromes is interferon-γ (IFNγ). In contrast, distinguishing these diverse syndromes are the initial triggers that set off this chain of events, as well as the individual cytokines responsible for the loss of negative feedback and gain of positive feedback

Supported by the NIH (grant R01-AI-121250-01A1).
[1]Edward M. Behrens, MD: Children's Hospital of Philadelphia, University of Pennsylvania Perelman School of Medicine, Philadelphia; [2]Gary A. Koretzky, MD, PhD: Weill Cornell Medical College, New York, New York.

Dr. Behrens has received consulting fees from AB2Bio (less than $10,000). Dr. Koretzky has received consulting fees from Rigel Pharmaceuticals, Inc. (less than $10,000).

Address correspondence to Gary A. Koretzky, MD, PhD, Weill Cornell Medical College, 1300 York Avenue, A-125, New York, NY 10065. E-mail: gak2008@med.cornell.edu.

Submitted for publication October 20, 2016; accepted in revised form February 9, 2017.

leading to the amplified response. In this review, we will outline the advances made in basic investigation into pathogenesis of cytokine storm syndromes of genetic, autoimmune/inflammatory, and iatrogenic causes and then discuss how such advances have informed therapy, moving from empiricism to the more finely tuned "precision" approaches.

Pathogenesis of cytokine storm syndromes

Monogenic cytokine storm syndrome. The most progress in understanding of cytokine storm has been made in familial hemophagocytic lymphohistiocytosis (FHLH), a genetic syndrome caused by deficiency in cytotoxic cell function. Deficiency in perforin or in molecules essential for perforin vesicular transport and release results in infection-triggered cytokine release and the resultant multi-organ inflammation and other pathology characteristic of cytokine storm. The monogenic nature of FHLH makes it amenable for study in animal models using targeted mice with deletions in genes discovered in humans. This work has identified IFNγ as a causative cytokine in generating the multi-organ pathology leading to mortality in this disorder (4,5). In FHLH, IFNγ is produced in excessive amounts by cytotoxic CD8+ T cells that are unable to kill infected target cells due to the absence of perforin activity or delayed cytolytic granule depolarization (6). This in turn results in prolonged contact with target cells (7) and subsequent inability to eliminate them (ultimately preventing the signal for producing IFNγ from being terminated), and release of excessive amounts of cytokine. This IFNγ release is not due to the inability to clear the pathogen itself, but rather is the result of altered antigen presentation due to the inability of cytotoxic cells to prune the antigen-presenting cell populations correctly (8). Both neutralization of IFNγ and depletion of CD8+ T cells have been shown to ameliorate disease in murine models (4,5).

Given the strong evidence of a central role of IFNγ in FHLH, it has been tempting to speculate that this cytokine has a role in all cytokine storm syndromes. Both in patients and in animal models of disease, however, multiple scenarios have been observed in which features of cytokine storm syndrome develop in the absence of IFNγ or its receptor (9–11), indicating that the causes are more complex that just this single cytokine. It has also been argued that similar mechanisms of ineffective cytotoxic cell killing are responsible for cytokine storm in non-FHLH settings (12–14). However, the diverse array of rheumatologic conditions that can lead to cytokine storm, not necessarily associated with defects in perforin function, make such a simple model unlikely.

Autoimmune/inflammatory cytokine storm syndrome. Among rheumatic diseases, systemic juvenile idiopathic arthritis (JIA) and its adult analog, adult-onset Still's disease (AOSD), have the highest association with cytokine storm. In this context, cytokine storm is often called macrophage activation syndrome (MAS), a reference to activated macrophages often seen on tissue biopsy, despite lack of evidence that these cells cause the syndrome (although they do, at least under some circumstances, produce inflammatory cytokines) (15). The cause of MAS in systemic JIA and AOSD remains unclear. Some work suggests that, at least in a subset of patients, there are defects in perforin function, although not of the same magnitude as seen in FHLH (14,16). These data are confounded by inflammatory activity (17) and treatment effect, both of which alter cytotoxic cell killing, particularly when measured with standard natural killer cell cytotoxicity assays. Whole exome analysis has suggested that patients with systemic JIA, and in particular those who have had an MAS episode, are more likely to have a variant in FHLH-associated genes (12). Nonetheless, such findings represent only ~35% of patients with systemic JIA–MAS, indicating that the majority do not have alterations in genes known to be associated with FHLH. Although this percentage may in fact be shown to be higher as additional genes are identified and noncoding mutations are accounted for, recent data call into question whether there is any defect at all in natural killer cell cytotoxic function in systemic JIA (18).

While the pathogenesis of systemic JIA and associated MAS has not been elucidated, a role of cytokines in at least some patients has been established. In a report published in 2005, IL-1β was identified as being dysregulated in systemic JIA, leading to the successful use of anakinra, an IL-1 receptor antagonist, as therapy (19). Subsequent randomized controlled clinical trials have shown efficacy of IL-1 blockade in large populations of patients with systemic JIA (20). IL-6 was additionally recognized as a potential target, with large trials showing efficacy of blockade of its receptor (21). However, neither IL-1β nor IL-6 has been directly linked to the development of MAS. Rather, elevated IL-18 levels have been associated with the predisposition to MAS development in patients with systemic JIA (22,23), as well as with MAS from various secondary causes (24). IL-18 blockade improved some parameters of organ dysfunction in an FHLH mouse model, though ultimately not reducing mortality (25). Intriguingly, IL-18 receptor signaling has been shown to be defective in systemic JIA (26), although this phenomenon has not been studied in great detail in patients who have had MAS. It is therefore difficult to resolve precisely how IL-18 might contribute to MAS associated with systemic JIA, given this apparent conflict between elevated IL-18

levels in MAS and defective IL-18 receptor signaling. One possibility is that suppressed IL-18 receptor signaling in systemic JIA is a compensatory mechanism that prevents progression to MAS; when this mechanism fails, and there is a large amount of IL-18 present, MAS ensues.

Additional evidence supporting the notion that IL-18 has a role in autoinflammatory MAS comes from the recently described NLRC4-MAS syndrome (27,28). NLRC4-MAS is caused by an activating mutation in the NLRC4 inflammasome. Unlike patients with inflammasomopathies not associated with MAS, such as activating NLRP3 mutations, patients with NLRC4-MAS develop high levels of serum IL-18, suggesting a potential causal link. NLRC4-MAS is anticipated to be an excellent genetic model to provide additional insights into possible etiologies of cytokine storm, as studies of patients with this genetic defect exhibit no concomitant abnormalities in perforin function or cytotoxicity. Placing IL-18 into the pathogenic model of systemic JIA–MAS remains consistent with the established pathogenic role of IFNγ in cytokine storm, given that IL-18 is well known to result in IFNγ production by many cells. Thus, pathogenic IFNγ may arise either from a more proximal defect in perforin cytotoxicity as in the case of FHLH, from overproduction of IL-18 in autoinflammatory conditions, or from yet-to-be-defined defects in immune regulation in other settings. Recent evidence of elevated levels of IFNγ and IFNγ-responsive genes in systemic JIA with MAS is consistent with the notion of the importance of IFNγ, even in systemic JIA–MAS (29).

MAS has been associated with other rheumatic diseases, including systemic lupus erythematosus (SLE) (30), Kawasaki disease (31), spondyloarthritis (32), and juvenile dermatomyositis (DM) (33). As these are rarer disorders than systemic JIA–associated MAS, reports are scarce and systematic studies are limited. There are presumably multiple different underlying mechanisms across this diverse range of diseases, although systemic inflammation remains a common link. The development of lupus pancreatitis appears to be associated with risk of MAS (34), although a causal link has not been established. In the case of SLE-associated MAS, serum TNF levels have been reported to be elevated with normal serum levels of IL-18, suggesting a qualitatively distinct cytokine pattern from that in systemic JIA–MAS and therefore, a distinct pathogenic mechanism. On the other hand, the same activating polymorphism of IFN regulatory factor 5 that has been associated with risk of SLE conferred a 4-fold increased risk of MAS development in patients with systemic JIA (35), suggesting common pathogenic links. In the case of juvenile DM–associated MAS, serum IL-6 and IL-18 concentrations were reported to be elevated, declining as disease improved, also suggesting some common features with systemic JIA–MAS (36). To comprehensively compare and contrast these MAS phenotypes in different rheumatic diseases, prospective multicenter efforts with collection and study of larger numbers of specimens will be necessary.

Iatrogenic cytokine storm syndrome. Iatrogenic causes of cytokine storm can also be informative as these cases are, in a sense, controlled experiments from which mechanistic insights can be gained. The entire list of iatrogenic causes of cytokine storm is too extensive to enumerate, but they range from pharmacologic, as in the case of rituximab therapy (37), to procedural, such as cardiac bypass (38). The recent use of chimeric antigen receptor (CAR) T cells for the treatment of CD19+ B cell malignancy is a striking example in which patients develop a cytokine storm referred to as cytokine release syndrome (CRS) (39). A detailed dissection of the mechanisms by which CAR T cells induce CRS is beyond the scope of this review. Studies suggest a few key points related to the mechanism of CRS following immunotherapy (39–42): 1) lysis of sufficient targets is required, whether they be tumor or normal endogenous B cells; 2) diverse targets may be sufficient for CRS, as 2 distinct antigenic CAR T cell–directed therapies have been shown to cause CRS; and 3) both macrophages and IL-6 appear related to the development of CRS. The extent to which the mechanisms of CRS may relate to FHLH or MAS is unknown, and further work to test these mechanisms should be undertaken.

Treatment of cytokine storm syndromes

Put in simplest terms, treatment of cytokine storm syndromes consists of immunosuppression accompanied by attempts to control the underlying trigger or disease. In the case of genetically defined syndromes in which replacement of the hematopoietic system with genetically normal bone marrow would be "curative," allogeneic bone marrow transplant also plays an important role. In rheumatic disease–associated cytokine storm, treatment of the underlying disease is essential. Clearly, antimicrobial agents are warranted for any patient with an infectious trigger. With increased understanding of disease mechanisms and the ever-expanding armamentarium of biologic agents and other treatments that inhibit specific pathways, targeted therapy for the various cytokine storm syndromes is becoming a reality.

A discussion of the management of every cytokine storm variant is beyond the scope of this review. Rather, we will review the evidence, from both human studies and animal models, for various classes of immunomodulating therapies, underscoring the value of structured mechanistic investigations to inform a rational treatment approach. We note both the "blunt tools"

Table 1. Cytokine storm syndromes*

Syndrome	Pathologic effectors	Potential precision therapy
FHLH	CD8+ T cells, IFNγ, IL-33	T cell inhibitors, IFNγ neutralization, IL-33 receptor blockade
EBV-HLH	Viremia, IFNγ	B cell–depleting therapy
Systemic JIA–MAS	IL-1β, myeloid cell autoinflammation, IFNγ	IL-1β blockade, IFNγ neutralization
NLRC4-MAS	IL-18, IL-18–induced IFNγ	IL-18 binding protein, IFNγ neutralization
Non–systemic JIA–MAS	Unknown	Unknown
CRS	IL-6, macrophages	IL-6 receptor blockade, IL-6 neutralization
Sepsis	Heterogeneous and multifactorial	More precise geno- and phenotyping required

* FHLH = familial hemophagocytic lymphohistiocytosis; IFNγ = interferon-γ; IL-33 = interleukin-33; EBV-HLH = Epstein-Barr virus–associated HLH; systemic JIA–MAS = systemic juvenile idiopathic arthritis–associated macrophage activation syndrome; CRS = cytokine release syndrome.

originally used empirically for their general ability to suppress the immune system and the "sharper tools" of rationally selected immunomodulators that have begun to herald an era of "precision medicine" for cytokine storm. As this approach continues to advance, it is worth remembering that the terms "MAS" and "cytokine storm" refer to a common end point of multiple different underlying conditions, rather than a single disease. We therefore call attention, where it exists, to evidence for each therapy for use in specific subsets of cytokine storm (Table 1). Investigators conducting future trials should bear in mind this heterogeneity and test therapies in select subsets, rather than in MAS as a whole.

Corticosteroids. As with most inflammatory disease, cytokine storm can be treated effectively with corticosteroids. The specific choice of agent often varies between syndromes and disciplines. Methylprednisolone, used in most rheumatic diseases, has been the most widely reported in treatment of MAS, whether associated with systemic JIA or with SLE. In contrast, dexamethasone is often used in the treatment of FHLH and is the recommended agent in the widely used FHLH treatment protocol (43). It has been argued that dexamethasone has better central nervous system penetration than other corticosteroids and is therefore preferred in FHLH. However, consideration should also be given to effective corticosteroid equivalency of the various regimens, as the reported methylprednisolone-based regimens are often 20-fold more potent than the reported dexamethasone-based regimens. The side effect profile of corticosteroids is well known, and much effort has been—and continues to be—dedicated to finding other agents that can spare the need for extended periods of high-dose steroid treatment.

Cytoablation. The oldest approach to steroid sparing is cytoablative therapy, which is aimed at removing the specific cells that may be driving cytokine storm. In reports of systemic JIA– and SLE-associated MAS, cyclophosphamide was noted to have potential efficacy (30,44). Likewise, in FHLH, etoposide has been a mainstay of therapy for >20 years (43). More recently, studies of animal models of FHLH demonstrated that these drugs work by selectively destroying activated CD8+ T cells (45), consistent with the central role of these T cells as IFN producers in FHLH pathogenesis. No such data exist for other cytokine storm syndromes, and the fact that these drugs are capable of eliminating multiple immune populations likely contributes to their widespread use and efficacy in treating cytokine storm of multiple etiologies and association with a spectrum of underlying diseases.

B cell ablation with rituximab has been observed to have efficacy in Epstein-Barr virus (EBV)–associated HLH (46). The proposed mechanism is reduction in the reservoir of cells for EBV infection and replication, thereby reducing viral load. It should be noted, however, that EBV has tropism for other immune cells, including natural killer cells and T cells, particularly in EBV-HLH and chronic active EBV (47). As a case in point, one of us has had personal experience with an EBV-HLH patient who had an initial reduction in viral load with rituximab therapy, only to have a rebound in viremia shortly thereafter. Flow cytometric sorting of various immune populations revealed that the virus had indeed infected non–B cell populations, thereby escaping the rituximab therapy (Behrens EM, Teachey DT: unpublished observations).

T cell ablation with antithymocyte globulin has been reported both in the treatment phase and in the conditioning for bone marrow transplant phase of FHLH therapy, as well as in MAS (48). In the case of FHLH, depletion of the pathogenic CD8+ T cells presumably contributes to the effectiveness of T cell ablation. A formal trial of antithymocyte globulin in combination with etoposide and dexamethasone (the Hybrid Immunotherapy for

HLH [HIT-HLH]) trial has recently been completed in FHLH, and results are forthcoming.

Alemtuzumab has also been reported to be effective in both FHLH (49) and SLE-associated MAS (50). Alemtuzumab is a monoclonal antibody that depletes cells bearing the CD52 marker, which includes all lymphocytes as well as some myeloid cells, such as monocytes and dendritic cells. It is therefore potentially more potent than more lineage-specific cytoablative antibodies, but at the cost of more potent immunosuppression and infection risk.

T cell–directed immunomodulation. Given the central role of CD8+ T cells in FHLH, nonablative inhibitors of T cell function are also attractive therapeutic choices in this subset of cytokine storm. Cyclosporine and other calcineurin inhibitors work by blocking key signaling pathways downstream of the T cell antigen receptor, thereby preventing the production of IL-2, a cytokine that is essential for T cell survival and proliferation. Thus, cyclosporine blunts the magnitude of T cell responses, making it a rational choice for treatment of T cell–mediated diseases. It has been a part of FHLH therapy for >20 years (43) and has also been used in MAS associated with a number of rheumatic diseases (30,51), although no formal trials have been conducted in this population.

Abatacept, an Fc fusion protein designed to bind and inhibit CD28 signaling of T cells, is another potentially attractive approach. CD28 is critical for providing the "second signal" for robust T cell activation. A small case series of 4 patients with systemic JIA, including 2 with "mild MAS" with disease refractory to standard intervention (including IL-1β blockade), demonstrated responsiveness to the addition of abatacept to the treatment regimen (52). This finding suggests that abatacept therapy may be efficacious, perhaps in combination with IL-1β blockade; however, more formal study is needed to validate its use in this condition. Enthusiasm may be tempered by the report of a rheumatoid arthritis patient in whom EBV-HLH actually developed while the patient was receiving abatacept therapy (53). Notably, virtually every medication used to treat MAS has also been reported to cause MAS. In these MAS cases, it is difficult to determine precisely whether the drug or the underlying rheumatic disease was the true trigger; thus, caution must be applied when interpreting such reports.

IFNγ blockade. Targeted cytokine therapy has resulted in a dramatic change in the landscape of treatment of immune disorders. With the identification of IFNγ as a necessary cytokine for the development of FHLH in murine models (4,5), there has been much excitement about the use of agents to block this cytokine for the treatment of human disease. Further enthusiasm has been generated by a recent report of elevated IFNγ signals in patients with systemic JIA–MAS (29). At the time of preparation of this manuscript, a trial is underway to test IFNγ-neutralizing therapy in FHLH. Results are not currently available, but individual patient outcomes reported in abstracts suggest promise for this approach (54). Safety concerns are always important and may be informed, in part, by reports of naturally occurring IFNγ-neutralizing autoantibodies in some patients (55). Serious mycobacterial infections occur in such patients, suggesting that long-term treatment with IFNγ-neutralizing antibodies may be limited by such complications. Pending the results of the ongoing trials, IFNγ blockade may indeed become a rational therapeutic modality.

Blockade of IL-1 family member cytokines. The IL-1 family cytokines are composed of related proteins, including IL-1β, IL-18, and IL-33, all of which are of interest in cytokine storm syndromes. IL-1β has received the most attention, as approved drugs have been available to block this cytokine. There have been numerous published case reports and case series supporting the use of IL-1β blockade in MAS associated with various rheumatic diseases (56,57). At least in the case of systemic JIA, use of IL-1β blockade in MAS may reflect the principle of treating the underlying disease as a trigger. Consistent with this, multiple authors have suggested an "occult MAS" phenotype in systemic JIA (58,59); that is, patients with systemic JIA may have elements of MAS without the full severe MAS phenotype. If MAS is indeed along the spectrum of severity of systemic JIA disease activity, it should logically follow that therapies known to treat systemic JIA should also treat MAS. Contrary to this notion is the observation that ongoing treatment of systemic JIA with IL-1β blockade does not appear to prevent the onset of MAS, despite the efficacy of IL-1β blockade in reducing disease activity (60). However, because those trials were not powered to detect prevention of MAS and revealed a trend toward protection that did not reach statistical significance, this question remains open.

At a minimum, there are at least some patients in whom IL-1β blockade does not prevent MAS. Ascertaining why this subpopulation is different at the immunologic level could prove enlightening with regard to both pathogenesis and treatment approaches. In some patients, increasing the dosage of anakinra was effective in controlling previously refractory MAS (61,62), suggesting that perhaps in some cases it is actually tachyphylaxis to IL-1β blockade that results in the apparent lack of efficacy. Alternatively, it is possible that the ability of anakinra to block IL-1α is important for its efficacy at higher doses. This would have important implications with regard to the use of canakinumab to treat or prevent MAS, since this drug is selective only for IL-1β. To

date, IL-1 blockade remains untested in FHLH, but given the likely differences in pathogenesis between systemic JIA–MAS and FHLH, there is no specific reason to suspect that IL-1 blockade may have efficacy in this disorder.

As discussed above, IL-18 levels are elevated in patients with systemic JIA who are prone to MAS. IL-18 exists in equilibrium with IL-18 binding protein, in which bound IL-18 is inactive and free IL-18 is active. Measurements of free IL-18 have not been reported in patients with systemic JIA–MAS. However, a pediatric patient with NLRC4-MAS and highly elevated serum levels of free IL-18 was recently reported (63). The child had been treated unsuccessfully with numerous therapies, including IL-1β and TNF blockade. Treatment with compassionate-use recombinant IL-18 binding protein (tadekinig alfa) resulted in complete resolution of symptoms and normalization of laboratory values, even after withdrawal of other medications including steroids. Although this was only a single-patient experience, the dramatic response suggests that cytokine storm syndromes characterized by elevated levels of free IL-18 might benefit from such a therapy, and this warrants further investigation.

Although IL-33 is also an IL-1 family member, it is distinguished by not being a product of the inflammasome, but rather is an alarmin, a molecule that is constitutively expressed but released only upon necrotic cell death. Based on its role in driving "type 2 immune responses" characterized by Th2 CD4+ T cells, eosinophils, and the cytokines IL-4, IL-5, and IL-13, most clinical focus on IL-33 has been on atopic disease, with trials in asthma underway. However, a role of IL-33 in IFNγ production by CD8+ T cells was recently reported (64) and, likely related to this, blockade of IL-33 protects against mortality and morbidity in a murine model of FHLH (65). The safety risks of IL-33 blockade may not be as serious as those of IFNγ blockade, making this an attractive therapeutic strategy for human disease. Just as the murine model has provided preclinical rationale for ongoing trials of IFNγ neutralization in FHLH, IL-33 may also be an important target for FHLH. Furthermore, a report of patients developing FHLH-like syndromes despite having genetic mutations that result in the absence of the IFNγ receptor (11) suggests that it will be important to develop other therapeutic targets beyond IFNγ.

IL-6 blockade. Paralleling the logic behind the use of IL-1β blockade in systemic JIA–MAS, the efficacy of IL-6 blockade with the IL-6 receptor–blocking antibody tocilizumab in systemic JIA might also make this an attractive target for MAS. Unfortunately, as in the case of IL-1β blockade, IL-6 blockade does not seem to prevent the development of MAS in systemic JIA. Other authors have suggested that while IL-6 receptor blockade does not prevent MAS, it may mask its appearance by subduing the laboratory changes that normally occur in MAS (66), creating a greater challenge for the treating physician by confusing the clinical picture. Distinguishing "masked MAS" from "partially treated MAS" is somewhat arbitrary and difficult, though, and an alternate explanation is that IL-6 blockade has an incomplete ability to treat MAS. Further investigation will be needed to clarify this point. However, it is clear that IL-6 is not the central cytokine in systemic JIA–MAS, even if blocking it has a partial effect.

In complete contradistinction to systemic JIA–MAS, the CRS associated with CAR T cell therapy appears to be completely dependent on IL-6. Using tocilizumab to treat patients with CAR T cell therapy–induced CRS results in a dramatic reversal of the syndrome and has become part of the protocol for its management (67). This serves to further highlight that, while clinical end point presentations of cytokine storm syndromes may be similar, the driving forces in their initiation and propagation may differ dramatically.

TNF blockade. TNF initially appeared to be an attractive target for cytokine storm of sepsis, despite its failure in actual clinical trials. Undoubtedly, TNF blockade is an important therapeutic modality for treatment of inflammation associated with a number of rheumatic diseases, and so the possibility remains that, as with IL-6, selection of the correct subpopulation of cytokine storms may be critical. Case reports describing patients in whom TNF blockade successfully treated—as well as reports describing patients in whom it caused—systemic JIA–MAS can be found (68–70). There have been no systematic investigations into the use of TNF blockade in MAS or FHLH, and, given that other targets currently seem more promising, further investigation of TNF blockade in cytokine storm will likely be of lower priority.

JAK inhibition. JAK/STAT signaling is a common mechanism used by many different cytokine receptors, including IFNγ. With the recent clinical availability of inhibitors of JAK signaling for rheumatoid arthritis, consideration of repurposing these drugs for treatment of cytokine storm seems natural. Studies by 2 different groups showed efficacy of JAK inhibition in murine models of FHLH and MAS (71,72), providing important preclinical evidence supporting this approach. Whether the effects of JAK inhibition can be accounted for solely by IFNγ blockade has not been resolved. The attraction of inhibition of JAK signaling is that multiple cytokine–receptor pairs can be targeted simultaneously, obviating the need to know the specific cytokines essential in any particular scenario. Furthermore, the oral bioavailability of these small-molecule drugs makes their use in long-term therapy more tolerable

to patients than injectable medications. However, the obvious tradeoff of the first benefit is the greater possibility for on-target, but deleterious, side effects due to the blockade of multiple pathways at once, as opposed to targeting of a single cytokine or receptor. Indeed, plasmapheresis, another modality that can remove multiple cytokines concurrently, has also been reported as a successful modality in treating cytokine storm (73), providing additional support for this approach.

Conclusions

Much progress has been made in understanding the mechanisms that initiate and propagate cytokine storm. Data from animal models have informed the development and deployment of novel cytokine-blocking strategies in humans and have ushered in the possibility of repurposing existing drugs to treat cytokine storm. Continued focus on fundamental mechanisms, coupled with human observational and interventional studies, will allow us to more precisely define in which populations and in which phase of their disease these therapies will be most effective. Indeed, returning to Osler's original observation about the role of the immune system in sepsis, the results of the original "failed" trial of IL-1β blockade in sepsis were recently reanalyzed to focus only on the subgroup with elevated levels of ferritin, akin to FHLH/MAS (74). In this subgroup, IL-1β blockade had a beneficial effect that had been lost in the analysis of the entire cohort. Undoubtedly, such post hoc analyses are fraught with potential confounders (75); however, the findings in that study emphasize that the time is ripe to reconsider immune-directed therapy for even this "oldest" of cytokine storms. A precision medicine approach, achieved by understanding the immune mechanisms that lead to cytokine storm in subpopulations, and perhaps even individual patients, is likely to yield benefits in other heterogeneous groups of patients with cytokine storm, such as those with systemic JIA or SLE. Continued basic, translational, and clinical investigation will be needed to make such an approach possible. Fortunately, the pace at which new investigations are being conducted and reported suggests that if support for these efforts continues, we can succeed at achieving this.

AUTHOR CONTRIBUTIONS

Drs. Behrens and Koretzky drafted the article, revised it critically for important intellectual content, and approved the final version to be published.

REFERENCES

1. Abraham E, Wunderink R, Silverman H, Perl TM, Nasraway S, Levy H, et al. Efficacy and safety of monoclonal antibody to human tumor necrosis factor α in patients with sepsis syndrome: a randomized, controlled, double-blind, multicenter clinical trial. JAMA 1995;273:934–41.
2. Clark MA, Plank LD, Connolly AB, Streat SJ, Hill AA, Gupta R, et al. Effect of a chimeric antibody to tumor necrosis factor-α on cytokine and physiologic responses in patients with severe sepsis: a randomized, clinical trial. Crit Care Med 1998;26:1650–9.
3. Fisher CJ Jr, Dhainaut JF, Opal SM, Pribble JP, Balk RA, Slotman GJ, et al. Recombinant human interleukin 1 receptor antagonist in the treatment of patients with sepsis syndrome: results from a randomized, double-blind, placebo-controlled trial. JAMA 1994;271:1836–43.
4. Jordan MB, Hildeman D, Kappler J, Marrack P. An animal model of hemophagocytic lymphohistiocytosis (HLH): CD8+ T cells and interferon γ are essential for the disorder. Blood 2004;104:735–43.
5. Pachlopnik Schmid J, Ho CH, Chretien F, Lefebvre JM, Pivert G, Kosco-Vilbois M, et al. Neutralization of IFNγ defeats haemophagocytosis in LCMV-infected perforin- and Rab27a-deficient mice. EMBO Mol Med 2009;1:112–24.
6. Zhang M, Bracaglia C, Prencipe G, Bemrich-Stolz CJ, Beukelman T, Dimmitt RA, et al. A heterozygous RAB27A mutation associated with delayed cytolytic granule polarization and hemophagocytic lymphohistiocytosis. J Immunol 2016;196:2492–503.
7. Jenkins MR, Rudd-Schmidt JA, Lopez JA, Ramsbottom KM, Mannering SI, Andrews DM, et al. Failed CTL/NK cell killing and cytokine hypersecretion are directly linked through prolonged synapse time. J Exp Med 2015;212:307–17.
8. Lykens JE, Terrell CE, Zoller EE, Risma K, Jordan MB. Perforin is a critical physiologic regulator of T-cell activation. Blood 2011;118:618–26.
9. Canna SW, Wrobel J, Chu N, Kreiger PA, Paessler M, Behrens EM. Interferon-γ mediates anemia but is dispensable for fulminant Toll-like receptor 9–induced macrophage activation syndrome and hemophagocytosis in mice. Arthritis Rheum 2013;65:1764–75.
10. Krebs P, Crozat K, Popkin D, Oldstone MB, Beutler B. Disruption of MyD88 signaling suppresses hemophagocytic lymphohistiocytosis in mice. Blood 2011;117:6582–8.
11. Tesi B, Sieni E, Neves C, Romano F, Cetica V, Cordeiro AI, et al. Hemophagocytic lymphohistiocytosis in 2 patients with underlying IFN-γ receptor deficiency. J Allergy Clin Immunol 2015;135:1638–41.
12. Kaufman KM, Linghu B, Szustakowski JD, Husami A, Yang F, Zhang K, et al. Whole-exome sequencing reveals overlap between macrophage activation syndrome in systemic juvenile idiopathic arthritis and familial hemophagocytic lymphohistiocytosis. Arthritis Rheumatol 2014;66:3486–95.
13. Schulert GS, Zhang M, Fall N, Husami A, Kissell D, Hanosh A, et al. Whole-exome sequencing reveals mutations in genes linked to hemophagocytic lymphohistiocytosis and macrophage activation syndrome in fatal cases of H1N1 influenza. J Infect Dis 2016;213:1180–8.
14. Vastert SJ, van Wijk R, D'Urbano LE, de Vooght KM, de Jager W, Ravelli A, et al. Mutations in the perforin gene can be linked to macrophage activation syndrome in patients with systemic onset juvenile idiopathic arthritis. Rheumatology (Oxford) 2010;49:441–9.
15. Billiau AD, Roskams T, van Damme-Lombaerts R, Matthys P, Wouters C. Macrophage activation syndrome: characteristic findings on liver biopsy illustrating the key role of activated, IFN-γ-producing lymphocytes and IL-6- and TNF-α-producing macrophages. Blood 2005;105:1648–51.
16. Wulffraat NM, Rijkers GT, Elst E, Brooimans R, Kuis W. Reduced perforin expression in systemic juvenile idiopathic arthritis is restored by autologous stem-cell transplantation. Rheumatology (Oxford) 2003;42:375–9.
17. Cifaldi L, Prencipe G, Caiello I, Bracaglia C, Locatelli F, de Benedetti F, et al. Inhibition of natural killer cell cytotoxicity by

interleukin-6: implications for the pathogenesis of macrophage activation syndrome. Arthritis Rheumatol 2015;67:3037–46.
18. Put K, Vandenhaute J, Avau A, van Nieuwenhuijze A, Brisse E, Dierckx T, et al. Inflammatory gene expression profile and defective interferon-γ and granzyme K in natural killer cells from systemic juvenile idiopathic arthritis patients. Arthritis Rheumatol 2016;69:213–24.
19. Pascual V, Allantaz F, Arce E, Punaro M, Banchereau J. Role of interleukin-1 (IL-1) in the pathogenesis of systemic onset juvenile idiopathic arthritis and clinical response to IL-1 blockade. J Exp Med 2005;201:1479–86.
20. Ruperto N, Brunner HI, Quartier P, Constantin T, Wulffraat N, Horneff G, et al. Two randomized trials of canakinumab in systemic juvenile idiopathic arthritis. N Engl J Med 2012;367:2396–406.
21. Yokota S, Imagawa T, Mori M, Miyamae T, Takei S, Iwata N, et al. Longterm safety and effectiveness of the anti-interleukin 6 receptor monoclonal antibody tocilizumab in patients with systemic juvenile idiopathic arthritis in Japan. J Rheumatol 2014;41:759–67.
22. Shimizu M, Nakagishi Y, Inoue N, Mizuta M, Ko G, Saikawa Y, et al. Interleukin-18 for predicting the development of macrophage activation syndrome in systemic juvenile idiopathic arthritis. Clin Immunol 2015;160:277–81.
23. Shimizu M, Yokoyama T, Yamada K, Kaneda H, Wada H, Wada T, et al. Distinct cytokine profiles of systemic-onset juvenile idiopathic arthritis-associated macrophage activation syndrome with particular emphasis on the role of interleukin-18 in its pathogenesis. Rheumatology (Oxford) 2010;49:1645–53.
24. Mazodier K, Marin V, Novick D, Farnarier C, Robitail S, Schleinitz N, et al. Severe imbalance of IL-18/IL-18BP in patients with secondary hemophagocytic syndrome. Blood 2005;106:3483–9.
25. Chiossone L, Audonnet S, Chetaille B, Chasson L, Farnarier C, Berda-Haddad Y, et al. Protection from inflammatory organ damage in a murine model of hemophagocytic lymphohistiocytosis using treatment with IL-18 binding protein. Front Immunol 2012;3:239.
26. De Jager W, Vastert SJ, Beekman JM, Wulffraat NM, Kuis W, Coffer PJ, et al. Defective phosphorylation of interleukin-18 receptor β causes impaired natural killer cell function in systemic-onset juvenile idiopathic arthritis. Arthritis Rheum 2009;60:2782–93.
27. Canna SW, de Jesus AA, Gouni S, Brooks SR, Marrero B, Liu Y, et al. An activating NLRC4 inflammasome mutation causes autoinflammation with recurrent macrophage activation syndrome. Nat Genet 2014;46:1140–6.
28. Romberg N, Al Moussawi K, Nelson-Williams C, Stiegler AL, Loring E, Choi M, et al. Mutation of NLRC4 causes a syndrome of enterocolitis and autoinflammation. Nat Genet 2014;46: 1135–9.
29. Bracaglia C, de Graaf K, Pires Marafon D, Guilhot F, Ferlin W, Prencipe G, et al. Elevated circulating levels of interferon-γ and interferon-γ-induced chemokines characterise patients with macrophage activation syndrome complicating systemic juvenile idiopathic arthritis. Ann Rheum Dis 2017;76:166–72.
30. Bennett TD, Fluchel M, Hersh AO, Hayward KN, Hersh AL, Brogan TV, et al. Macrophage activation syndrome in children with systemic lupus erythematosus and children with juvenile idiopathic arthritis. Arthritis Rheum 2012;64:4135–42.
31. Avcin T, Tse SM, Schneider R, Ngan B, Silverman ED. Macrophage activation syndrome as the presenting manifestation of rheumatic diseases in childhood. J Pediatr 2006;148:683–6.
32. Lou YJ, Jin J, Mai WY. Ankylosing spondylitis presenting with macrophage activation syndrome. Clin Rheumatol 2007;26: 1929–30.
33. Lilleby V, Haydon J, Sanner H, Krossness BK, Ringstad G, Flato B. Severe macrophage activation syndrome and central nervous system involvement in juvenile dermatomyositis. Scand J Rheumatol 2014;43:171–3.
34. Gormezano NW, Otsuzi CI, Barros DL, da Silva MA, Pereira RM, Campos LM, et al. Macrophage activation syndrome: a severe and frequent manifestation of acute pancreatitis in 362 childhood-onset compared to 1830 adult-onset systemic lupus erythematosus patients. Semin Arthritis Rheum 2016;45:706–10.
35. Yanagimachi M, Naruto T, Miyamae T, Hara T, Kikuchi M, Hara R, et al. Association of IRF5 polymorphisms with susceptibility to macrophage activation syndrome in patients with juvenile idiopathic arthritis. J Rheumatol 2011;38:769–74.
36. Wakiguchi H, Hasegawa S, Hirano R, Kaneyasu H, Wakabayashi-Takahara M, Ohga S. Successful control of juvenile dermatomyositis-associated macrophage activation syndrome and interstitial pneumonia: distinct kinetics of interleukin-6 and -18 levels. Pediatr Rheumatol Online J 2015;13:49.
37. Winkler U, Jensen M, Manzke O, Schulz H, Diehl V, Engert A. Cytokine-release syndrome in patients with B-cell chronic lymphocytic leukemia and high lymphocyte counts after treatment with an anti-CD20 monoclonal antibody (rituximab, IDEC-C2B8). Blood 1999;94:2217–24.
38. Nebelsiek T, Beiras-Fernandez A, Kilger E, Mohnle P, Weis F. Routine use of corticosteroids to prevent inflammation response in cardiac surgery. Recent Pat Cardiovasc Drug Discov 2012;7: 170–4.
39. Grupp SA, Kalos M, Barrett D, Aplenc R, Porter DL, Rheingold SR, et al. Chimeric antigen receptor-modified T cells for acute lymphoid leukemia. N Engl J Med 2013;368:1509–18.
40. Teachey DT, Rheingold SR, Maude SL, Zugmaier G, Barrett DM, Seif AE, et al. Cytokine release syndrome after blinatumomab treatment related to abnormal macrophage activation and ameliorated with cytokine-directed therapy. Blood 2013;121:5154–7.
41. Morgan RA, Yang JC, Kitano M, Dudley ME, Laurencot CM, Rosenberg SA. Case report of a serious adverse event following the administration of T cells transduced with a chimeric antigen receptor recognizing ERBB2. Mol Ther 2010;18:843–51.
42. Van der Stegen SJ, Davies DM, Wilkie S, Foster J, Sosabowski JK, Burnet J, et al. Preclinical in vivo modeling of cytokine release syndrome induced by ErbB-retargeted human T cells: identifying a window of therapeutic opportunity? J Immunol 2013;191:4589–98.
43. Trottestam H, Horne A, Arico M, Egeler RM, Filipovich AH, Gadner H, et al. Chemoimmunotherapy for hemophagocytic lymphohistiocytosis: long-term results of the HLH-94 treatment protocol. Blood 2011;118:4577–84.
44. Sawhney S, Woo P, Murray KJ. Macrophage activation syndrome: a potentially fatal complication of rheumatic disorders. Arch Dis Child 2001;85:421–6.
45. Johnson TS, Terrell CE, Millen SH, Katz JD, Hildeman DA, Jordan MB. Etoposide selectively ablates activated T cells to control the immunoregulatory disorder hemophagocytic lymphohistiocytosis. J Immunol 2014;192:84–91.
46. Chellapandian D, Das R, Zelley K, Wiener SJ, Zhao H, Teachey DT, et al. Treatment of Epstein Barr virus-induced haemophagocytic lymphohistiocytosis with rituximab-containing chemo-immunotherapeutic regimens. Br J Haematol 2013;162: 376–82.
47. Kasahara Y, Yachie A. Cell type specific infection of Epstein-Barr virus (EBV) in EBV-associated hemophagocytic lymphohistiocytosis and chronic active EBV infection. Crit Rev Oncol Hematol 2002;44:283–94.
48. Ouachee-Chardin M, Elie C, de Saint Basile G, Le Deist F, Mahlaoui N, Picard C, et al. Hematopoietic stem cell transplantation in hemophagocytic lymphohistiocytosis: a single-center report of 48 patients. Pediatrics 2006;117:e743–50.
49. Marsh RA, Allen CE, McClain KL, Weinstein JL, Kanter J, Skiles J, et al. Salvage therapy of refractory hemophagocytic lymphohistiocytosis with alemtuzumab. Pediatr Blood Cancer 2013; 60:101–9.
50. Keith MP, Pitchford C, Bernstein WB. Treatment of hemophagocytic lymphohistiocytosis with alemtuzumab in systemic lupus erythematosus. J Clin Rheumatol 2012;18:134–7.

51. Mouy R, Stephan JL, Pillet P, Haddad E, Hubert P, Prieur AM. Efficacy of cyclosporine A in the treatment of macrophage activation syndrome in juvenile arthritis: report of five cases. J Pediatr 1996;129:750–4.
52. Record JL, Beukelman T, Cron RQ. Combination therapy of abatacept and anakinra in children with refractory systemic juvenile idiopathic arthritis: a retrospective case series. J Rheumatol 2011;38:180–1.
53. Dalal RS, LeGolvan MP, Stachurski DR, Goldberg LR. Epstein-Barr virus associated hemophagocytic lymphohistiocytosis in a rheumatic patient receiving abatacept therapy. R I Med J (2013) 2014;97:28–31.
54. Jordan M, Locatelli F, Allen C, de Benedetti F, Grom AA, Ballabio M, et al. A novel targeted approach to the treatment of hemophagocytic lymphohistiocytosis (HLH) with an anti-interferon γ (IFNγ) monoclonal antibody (mAb), NI-0501: first results from a pilot phase 2 study in children with primary HLH. Blood 2015;126:LBA–3.
55. Browne SK, Burbelo PD, Chetchotisakd P, Suputtamongkol Y, Kiertiburanakul S, Shaw PA, et al. Adult-onset immunodeficiency in Thailand and Taiwan. N Engl J Med 2012;367:725–34.
56. Behrens EM, Kreiger PA, Cherian S, Cron RQ. Interleukin 1 receptor antagonist to treat cytophagic histiocytic panniculitis with secondary hemophagocytic lymphohistiocytosis. J Rheumatol 2006;33:2081–4.
57. Miettunen PM, Narendran A, Jayanthan A, Behrens EM, Cron RQ. Successful treatment of severe paediatric rheumatic disease-associated macrophage activation syndrome with interleukin-1 inhibition following conventional immunosuppressive therapy: case series with 12 patients. Rheumatology (Oxford) 2011;50:417–9.
58. Behrens EM, Beukelman T, Paessler M, Cron RQ. Occult macrophage activation syndrome in patients with systemic juvenile idiopathic arthritis. J Rheumatol 2007;34:1133–8.
59. Bleesing J, Prada A, Siegel DM, Villanueva J, Olson J, Ilowite NT, et al. The diagnostic significance of soluble CD163 and soluble interleukin-2 receptor α-chain in macrophage activation syndrome and untreated new-onset systemic juvenile idiopathic arthritis. Arthritis Rheum 2007;56:965–71.
60. Grom AA, Ilowite NT, Pascual V, Brunner HI, Martini A, Lovell D, et al. Rate and clinical presentation of macrophage activation syndrome in patients with systemic juvenile idiopathic arthritis treated with canakinumab. Arthritis Rheumatol 2016;68:218–28.
61. Kahn PJ, Cron RQ. Higher-dose anakinra is effective in a case of medically refractory macrophage activation syndrome. J Rheumatol 2013;40:743–4.
62. Nigrovic PA, Mannion M, Prince FH, Zeft A, Rabinovich CE, van Rossum MA, et al. Anakinra as first-line disease-modifying therapy in systemic juvenile idiopathic arthritis: report of forty-six patients from an international multicenter series. Arthritis Rheum 2011;63:545–55.
63. Canna SW, Girard C, Malle L, de Jesus A, Romberg N, Kelsen J, et al. Life-threatening NLRC4-associated hyperinflammation successfully treated with IL-18 inhibition. J Allergy Clin Immunol 2016. E-pub ahead of print.
64. Bonilla WV, Frohlich A, Senn K, Kallert S, Fernandez M, Johnson S, et al. The alarmin interleukin-33 drives protective antiviral $CD8^+$ T cell responses. Science 2012;335:984–9.
65. Rood JE, Rao S, Paessler M, Kreiger PA, Chu N, Stelekati E, et al. ST2 contributes to T-cell hyperactivation and fatal hemophagocytic lymphohistiocytosis in mice. Blood 2016;127:426–35.
66. Shimizu M, Nakagishi Y, Kasai K, Yamasaki Y, Miyoshi M, Takei S, et al. Tocilizumab masks the clinical symptoms of systemic juvenile idiopathic arthritis-associated macrophage activation syndrome: the diagnostic significance of interleukin-18 and interleukin-6. Cytokine 2012;58:287–94.
67. Barrett DM, Teachey DT, Grupp SA. Toxicity management for patients receiving novel T-cell engaging therapies. Curr Opin Pediatr 2014;26:43–9.
68. Maeshima K, Ishii K, Iwakura M, Akamine M, Hamasaki H, Abe I, et al. Adult-onset Still's disease with macrophage activation syndrome successfully treated with a combination of methotrexate and etanercept. Mod Rheumatol 2012;22:137–41.
69. Makay B, Yilmaz S, Turkyilmaz Z, Unal N, Oren H, Unsal E. Etanercept for therapy-resistant macrophage activation syndrome. Pediatr Blood Cancer 2008;50:419–21.
70. Stern A, Riley R, Buckley L. Worsening of macrophage activation syndrome in a patient with adult onset Still's disease after initiation of etanercept therapy. J Clin Rheumatol 2001;7:252–6.
71. Das R, Guan P, Sprague L, Verbist K, Tedrick P, An QA, et al. Janus kinase inhibition lessens inflammation and ameliorates disease in murine models of hemophagocytic lymphohistiocytosis. Blood 2016;127:1666–75.
72. Maschalidi S, Sepulveda FE, Garrigue A, Fischer A, de Saint Basile G. Therapeutic effect of JAK1/2 blockade on the manifestations of hemophagocytic lymphohistiocytosis in mice. Blood 2016;128:60–71.
73. Demirkol D, Yildizdas D, Bayrakci B, Karapinar B, Kendirli T, Koroglu TF, et al. Hyperferritinemia in the critically ill child with secondary hemophagocytic lymphohistiocytosis/sepsis/multiple organ dysfunction syndrome/macrophage activation syndrome: what is the treatment? Crit Care 2012;16:R52.
74. Shakoory B, Carcillo JA, Chatham WW, Amdur RL, Zhao H, Dinarello CA, et al. Interleukin-1 receptor blockade is associated with reduced mortality in sepsis patients with features of macrophage activation syndrome: reanalysis of a prior phase III trial. Crit Care Med 2016;44:275–81.
75. Johnson DW, Kalil AC. Is interleukin-1 receptor blockade ready for prime time in patients with severe sepsis and macrophage activation syndrome? Crit Care Med 2016;44:443–4.

ARTHRITIS & RHEUMATOLOGY
Vol. 69, No. 6, June 2017, pp 1144–1153
DOI 10.1002/art.40070

Secukinumab in Active Rheumatoid Arthritis

A Phase III Randomized, Double-Blind, Active Comparator– and Placebo-Controlled Study

Francisco J. Blanco,[1] Rüdiger Möricke,[2] Eva Dokoupilova,[3] Christine Codding,[4] Jeffrey Neal,[5] Mats Andersson,[6] Susanne Rohrer,[6] and Hanno Richards[6]

Objective. **To evaluate the efficacy and safety of secukinumab in patients with active rheumatoid arthritis (RA) who had an inadequate response to or intolerance of tumor necrosis factor (TNF) inhibitors.**

Methods. **In this phase III study, 551 patients were randomized (1:1:1:1) to receive intravenous secukinumab at a dose of 10 mg/kg (at baseline and weeks 2 and 4) followed by subcutaneous secukinumab at a dose of either 150 mg or 75 mg every 4 weeks or, alternatively, abatacept or placebo on the same dosing schedule. The primary end point was the proportion of patients achieving 20% improvement in disease activity according to the American College of Rheumatology response criteria (ACR20) at week 24 in the secukinumab 150 mg or 75 mg treatment groups as compared with placebo. Key secondary end points included change from baseline to week 24 in the Disease Activity Score in 28 joints using C-reactive protein level (DAS28-CRP) and the Health Assessment Questionnaire disability index (HAQ DI), as well as the ACR 50% improvement (ACR50) response rate at week 24.**

Results. **The primary efficacy end point was met in patients receiving 150 mg secukinumab, in whom the ACR20 response rate at week 24 was significantly higher than that in the placebo group. The ACR20 response rates at week 24 were 30.7% in patients receiving 150 mg secukinumab ($P = 0.0305$), 28.3% in those receiving 75 mg secukinumab ($P = 0.0916$), and 42.8% in those receiving abatacept, compared with 18.1% in the placebo group. A significant reduction in the DAS28-CRP was seen in patients treated with 150 mg secukinumab ($P = 0.0495$), but not in patients treated with 75 mg secukinumab. Improvements in the HAQ DI and ACR50 response rates were not significant in the 2 secukinumab dose groups compared with the placebo group. The overall safety profile was similar across all treatment groups.**

Conclusion. **Secukinumab at a dose of 150 mg resulted in improvement in signs and symptoms and reduced disease activity in patients with active RA who had an inadequate response to TNF inhibitors. Improvements observed with abatacept were numerically higher than with secukinumab. There were no new or unexpected safety signals with secukinumab in this study.**

Rheumatoid arthritis (RA) is a chronic inflammatory autoimmune disease characterized by progressive synovial inflammation and destruction of joint cartilage and bone (1). RA affects ~0.5–1.0% of the population worldwide and is associated with decline in functional status, significant morbidity, reduced health-related quality of life, and premature mortality (2,3). Current guidelines recommend treatment with nonsteroidal antiinflammatory drugs (NSAIDs) or conventional synthetic disease-modifying antirheumatic drug (csDMARD) therapy with or without concomitant glucocorticoid therapy as the first line of treatment (4).

ClinicalTrials.gov identifier: NCT01350804.
Supported by Novartis Pharma AG, Basel, Switzerland.
[1]Francisco J. Blanco, MD, PhD: Hospital Universitario A Coruña, A Coruña, Spain; [2]Rüdiger Möricke, MD, PhD: Institut für Präventive Medizin & Klinische Forschung, Magdeburg, Germany; [3]Eva Dokoupilova, MD: Medical Plus, Uherske Hradiste, Czech Republic; [4]Christine Codding, MD: Health Research of Oklahoma, Oklahoma City; [5]Jeffrey Neal, MD: Bluegrass Community Research, Lexington, Kentucky; [6]Mats Andersson, MSc, Susanne Rohrer, PhD, Hanno Richards, MD, PhD: Novartis Pharma, Basel, Switzerland.
Dr. Möricke has received consulting fees from Novartis (less than $10,000). Drs. Rohrer and Richards own stock or stock options in Novartis.
Address correspondence to Francisco J. Blanco, MD, PhD, Hospital Universitario A Coruña, Servicio de Reumatologia, Laboratorio de Investigacion C, Xubias 84, A Coruña 15006, Spain. E-mail: fblagar@sergas.es.
Submitted for publication August 23, 2016; accepted in revised form February 9, 2017.

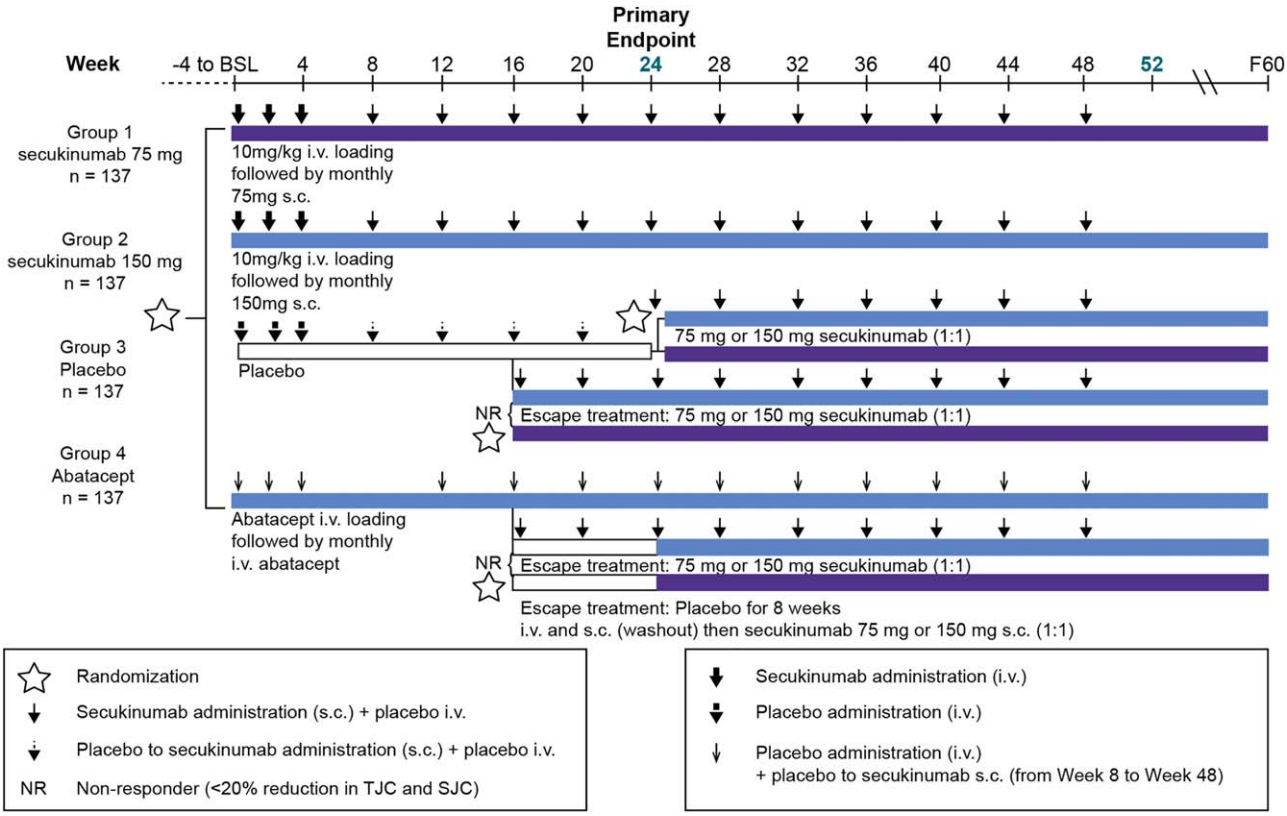

Figure 1. Study design. BSL = baseline; i.v. = intravenous; s.c. = subcutaneous; NR = nonresponder; TJC = tender joint count; SJC = swollen joint count.

Tumor necrosis factor (TNF) inhibitors are considered the initial choice for patients in whom NSAIDs and csDMARDs are ineffective and/or for whom toxicity is a concern (4). However, alternatives to anti-TNF therapies are needed, since some patients treated with anti-TNF agents may have an inadequate treatment response or the medication may have unacceptable toxicity. Abatacept is one of the biologic DMARDs with proven efficacy in patients with RA who have an inadequate response to TNF inhibitors (5). Abatacept selectively modulates a CD28-mediated costimulation required for full T cell activation (6).

Interleukin-17A (IL-17A) has been considered a potential therapeutic target for the treatment of RA (7–13). IL-17A, the principal effector cytokine of Th17 cells identified as being prominent in the pathogenesis of RA (14,15), has been implicated in the promotion of osteoclastogenesis (16), cartilage breakdown (17), and bone erosion (7). Although IL-17A is elevated in the synovium of patients with RA (18), the exact role of IL-17 in comparison with other relevant inflammation pathways (19) in RA has not yet been studied in a large phase III trial.

Secukinumab is a high-affinity, fully human IgG1 monoclonal antibody that selectively binds to and neutralizes IL-17A. Secukinumab is approved for the treatment of moderate-to-severe psoriasis, psoriatic arthritis (PsA), and ankylosing spondylitis (AS) (20). Findings from a proof-of-concept trial and 3 phase II dose-finding trials have suggested that secukinumab may provide benefit for RA patients, although efficacy was variable between the different study populations (10,21,22).

The present study evaluated the efficacy and safety of secukinumab compared with abatacept and placebo from a pivotal phase III active comparator– and placebo-controlled study in RA patients who had an inadequate response to or intolerance of TNF inhibitors. Data from a respective extension trial are also included in this report. However, due to early closure of the extension trial, only safety data are reported.

PATIENTS AND METHODS

Study design. This double-blind, double-dummy, randomized, parallel-group, active comparator– and placebo-controlled study was conducted across 121 centers in 15 countries. The study assessed efficacy at 24 weeks and up to 1 year in patients with active RA who had an inadequate response to TNF inhibitors. The study design is shown in Figure 1. Patients who received secukinumab and who completed 1 year of treatment were eligible to join an extension study with a planned follow-up

of a total of 5 years, although the mean total follow-up was 1.4 years due to early closure of the extension trial.

After a 4-week screening period, patients were randomly assigned (randomization ratio 1:1:1:1) to receive intravenous (IV) secukinumab at a dose of 10 mg/kg (at baseline and weeks 2 and 4) followed by subcutaneous (SC) secukinumab at a dose of either 150 mg or 75 mg every 4 weeks up to week 48 or, alternatively, abatacept (IV loading followed by monthly IV dosing: 500 mg for <60 kg body weight, 750 mg for 60–100 kg body weight, and 1,000 mg for >100 kg body weight) or placebo on the same IV and SC dosing schedule (Figure 1).

At week 16, patients receiving placebo who were nonresponders (response defined as ≥20% improvement from baseline in both the tender joint count and swollen joint count) were rerandomized (1:1) to receive secukinumab at 150 mg SC or 75 mg SC every 4 weeks. Patients who were placebo responders at week 16 were rerandomized (1:1) to receive secukinumab at 75 mg SC or 150 mg SC every 4 weeks starting at week 24. Patients receiving abatacept who were nonresponders at week 16 were rerandomized (1:1) to receive secukinumab at 150 mg SC or 75 mg SC every 4 weeks starting at week 24, after an 8-week washout period during which they received placebo, administered in a blinded manner, at weeks 16 and 20.

A double-dummy design was used throughout the study, as the study treatments differed in their forms and routes of administration (Figure 1). IV infusion bags with reconstituted secukinumab/placebo or abatacept/placebo solutions identical in appearance were used in the 52-week core study. At each treatment time point starting at week 8, 2 SC injections in the form of prefilled syringes (PFS) were administered, as secukinumab was available in either 0.5 ml (75 mg) PFS or 1.0 ml (150 mg) PFS. Placebo was also available in 0.5 ml and 1.0 ml PFS to match the active drug. Only patients who received secukinumab during the 52-week core study were eligible to participate in the extension study, during which they received the same dose of secukinumab as they had received in the core study.

Efficacy data are presented for the core study (placebo-controlled up to week 24). Safety information is presented from the entire core study and includes all available data from the extension study.

Patients. Patients at least 18 years of age who had been diagnosed at least 3 months before screening as having RA using the American College of Rheumatology/European League Against Rheumatism 2010 revised criteria for RA (23) were eligible for the study. Patients were also required to have active disease at baseline, defined as the presence of ≥6 tender joints (of 68 total) and ≥6 swollen joints (of 66 total), together with a positive result on either the anti–cyclic citrullinated peptide antibody test or the rheumatoid factor test, and either a high-sensitivity C-reactive protein (hsCRP) level of ≥10 mg/liter or erythrocyte sedimentation rate (ESR) of ≥28 mm/first hour at screening. Patients had to have been receiving methotrexate (dosage of 7.5–25 mg/week) or any other DMARD for at least 3 months before randomization, and the DMARD should have been administered in a stable dose for at least 4 weeks before randomization. For any patients who were taking more than 1 DMARD, study participation was allowed after an appropriate washout period. Patients also had to have received at least 1 TNF inhibitor for at least 3 months before randomization and to have experienced an inadequate response to or intolerance of at least 1 dose of the anti-TNF agent. Patients may have been receiving more than 1 TNF inhibitor. The major exclusion criteria included ongoing rheumatic or inflammatory joint diseases other than RA, evidence of malignancy or infection seen on chest radiography, active tuberculosis infection, or previous use of biologic immunomodulating agents except for those targeting TNF.

The study protocol and all amendments were reviewed by the Independent Ethics Committee or Institutional Review Board for each center. The study was conducted in accordance with the ethics principles of the Declaration of Helsinki, and patients provided written informed consent before enrollment for the core study and separately for the extension study.

Outcome measures. The primary end point was the efficacy of secukinumab (administered at a dose of 150 mg or 75 mg) compared with placebo at week 24. Efficacy was measured as the proportion of patients achieving 20% improvement in disease activity based on the American College of Rheumatology response criteria (ACR20) (24).

The key secondary efficacy outcome measures were the change from baseline in the Disease Activity Score in 28 joints (25) using C-reactive protein level (DAS28-CRP) and the Health Assessment Questionnaire disability index (HAQ DI) (26) as well as the proportion of patients achieving an ACR 50% improvement response (ACR50) at week 24. Other secondary efficacy end points included the ACR20, ACR50, and ACR70 (70% improvement) response rates and the change from baseline in the DAS28-CRP, the DAS28 using ESR (DAS28-ESR), and the HAQ DI at time points other than week 24. Subgroup analyses were conducted for a limited number of parameters, including baseline CRP level and change from baseline in the DAS28-CRP.

Safety was assessed throughout the core and extension periods by evaluation of all treatment-emergent adverse events (AEs) and serious AEs (SAEs), laboratory assessments, and assessment of immunogenicity (antisecukinumab antibodies). Safety analysis was performed separately for the initial period (up to week 16) and the entire treatment period including all available data from the extension study. Use of data up to and including week 16 provided an unbiased comparison between secukinumab, placebo, and abatacept, since, up to week 16, there was no switch in any treatment arm (see study design in Figure 1). Data collected beyond week 16 were included in analyses that summarized the entire treatment period, including the extension study.

Statistical analysis. Sample size calculations were performed using Fisher's exact test assuming an ACR20 response rate of 20% in the placebo group and 50% in the secukinumab dose groups at week 24. Including 137 patients per group with a Type I error rate of 2.5% provided 99% power to detect a difference between the secukinumab and placebo groups. The range of power for the secondary end points was between 89% and 99%.

The primary end point was analyzed via logistic regression analysis, with treatment as a factor and weight as a covariate. Odds ratios were computed for comparisons of the secukinumab regimens with the placebo regimen, utilizing a fitted logistic regression model. For patients meeting the criteria for early escape at week 16, their ACR20 response rate was set to nonresponse at week 24. This applied for all 4 treatment regimens in order to minimize bias. A hierarchical testing strategy was used to analyze the primary and secondary efficacy end points in order to maintain a family-wise error rate of 5% across the secukinumab groups and end points.

Binary variables up to week 24 were analyzed via a logistic regression model that included treatment as a factor and weight as

a covariate. Missing values, including those due to discontinuation of the study treatment, were imputed as nonresponses through week 24 (nonresponder imputation). Between-group differences in continuous variables up to week 24 were evaluated with the use of a mixed-effects model repeated-measures approach. Weight and baseline value of the outcome variable were included in the model as continuous covariates. Treatment by analysis visit and baseline score by analysis visit were included as interaction terms in the model.

The analyses of efficacy variables were performed in all patients who were randomized and to whom study treatment had been assigned (full analysis set). The safety set comprised all patients who received at least 1 dose of the study drug during the treatment period. Up to week 16, safety group assignments were those determined by the randomization schedule (secukinumab, abatacept, or placebo); beyond week 16, safety is reported on the basis of the treatment assigned.

RESULTS

Characteristics of the patients. In total, 551 patients with RA were randomized to 1 of the 4 treatment groups, of whom 390 (70.8%) completed 52 weeks of treatment. Details of the disposition of patients and the reasons for discontinuation are shown in Figure 2. The maximum exposure time for any secukinumab dose in the period including the extension study was 184 weeks, with a mean exposure of 537 days and a median exposure of 478 days.

The patients' demographic and baseline clinical characteristics were comparable across the treatment groups (Table 1). The mean age ranged from 51.6 years to 55.9 years across the treatment groups. The majority of patients were female (77.5–86.2% across the treatment groups) and at least 70% in each group were white. Furthermore, 122 patients reported a previous exposure to more than 1 TNF inhibitor, and 52.2–62.8% of patients across the groups reported concomitant use of glucocorticoids. Between 5.8% and 13.0% of patients were taking methotrexate, and between 16.7% and 23.4% of patients were taking leflunomide. Baseline values for the mean tender joint count ranged between 24.1 and 25.6, while the mean swollen joint count was between 15.8 and 17.0. Moreover, the mean DAS28-CRP was between 5.7 and 5.9, and the median hsCRP level was between 9.3 and 10.8 mg/liter.

Efficacy. *Primary efficacy outcomes.* At week 24, the ACR20 response rates were 30.7% among patients receiving 150 mg secukinumab, 28.3% among those

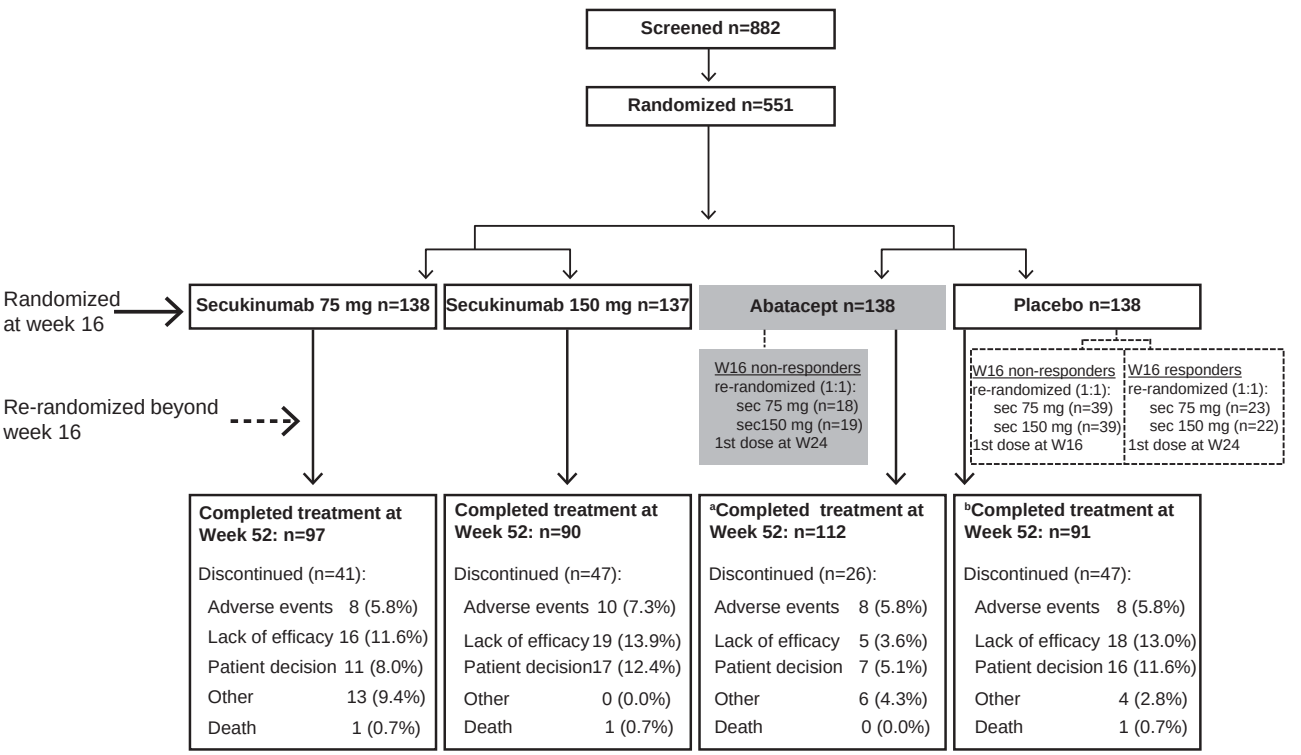

Figure 2. Disposition of patients. Patients were classified as responders or nonresponders at week 16 (W16) and were rerandomized to receive 75 mg secukinumab (sec) subcutaneously (SC) or 150 mg secukinumab SC. Only patients receving secukinumab at week 52 were eligible to enter the extension study. a = All of the patients in the abatacept group who completed treatment from week 1 to week 52 irrespective of rerandomization. b = All of the patients in the placebo group who completed treatment from week 1 to week 52. Groups in the boxes with broken outlines are rerandomized groups.

Table 1. Demographic and baseline clinical characteristics of the patients in each randomized group*

	Secukinumab 150 mg (n = 137)	Secukinumab 75 mg (n = 138)	Abatacept (n = 138)	Placebo (n = 138)
Age, mean ± SD years	55.9 ± 12.3	54.9 ± 11.3	51.6 ± 12.4	55.5 ± 12.1
Female, no. (%)	109 (79.6)	119 (86.2)	107 (77.5)	115 (83.3)
Weight, mean ± SD kg	76.0 ± 19.8	76.8 ± 19.4	77.6 ± 18.9	77.5 ± 19.7
Race, no. (%)				
White	101 (73.7)	107 (77.5)	105 (76.1)	97 (70.3)
Black	3 (2.2)	4 (2.9)	4 (2.9)	7 (5.1)
Asian	2 (1.5)	2 (1.4)	0 (0.0)	1 (0.7)
Other	31 (22.6)	25 (18.1)	29 (21.0)	33 (23.9)
68-joint TJC, mean ± SD	25.5 ± 14.2	25.6 ± 15.4	24.1 ± 14.1	24.4 ± 15.0
66-joint SJC, mean ± SD	17.0 ± 8.9	17.0 ± 9.1	15.8 ± 8.8	16.4 ± 9.1
Duration of RA, mean ± SD years	9.5 ± 8.0	10.2 ± 8.7	10.2 ± 8.1	10.3 ± 7.7
DAS28-CRP, mean ± SD	5.9 ± 0.9	5.7 ± 1.0	5.7 ± 1.0	5.8 ± 0.9
DAS28-ESR, mean ± SD	6.8 ± 0.9	6.6 ± 1.0	6.6 ± 1.0	6.6 ± 0.9
hsCRP, mg/liter				
Level >10 mg/liter, no. (%)	70 (51)	67 (49)	64 (46)	71 (51)
Median (range)	10.8 (0.1–264.1)	9.6 (0.1–300)	9.3 (0.2–142.3)	10.8 (0.3–100.8)
Positive for RF, no. (%)†	131 (94.9)	131 (95.6)	130 (94.2)	133 (96.4)
Positive for anti-CCP, no. (%)	115 (83.9)	115 (83.3)	114 (82.6)	121 (87.7)
HAQ DI, mean ± SD	1.7 ± 0.6	1.7 ± 0.6	1.7 ± 0.6	1.8 ± 0.6
TNF-naive patients, no. (%)‡	1 (0.7)	1 (0.7)	0 (0.0)	0 (0.0)
Prior use of other biologic DMARD, no. (%)§	1 (0.7)	1 (0.7)	1 (0.7)	2 (1.4)
Use of oral DMARDs at randomization, no. (%)	117 (85.4)	116 (84.1)	121 (87.7)	112 (81.2)
Methotrexate	11 (8.0)	15 (10.9)	8 (5.8)	18 (13.0)
Leflunomide	32 (23.4)	30 (21.7)	26 (18.8)	23 (16.7)
Other	1 (0.7)	1 (0.7)	1 (0.7)	2 (1.4)
Dosage of MTX at randomization, mean ± SD mg/week	15.4 ± 4.8	15.7 ± 5.2	15.2 ± 4.9	16.4 ± 9.8
Systemic glucocorticoids use, no. (%)	86 (62.8)	72 (52.2)	73 (52.9)	80 (58.0)

* TJC = tender joint count; SJC = swollen joint count; RA = rheumatoid arthritis; DAS28-CRP = Disease Activity Score in 28 joints using C-reactive protein level; DAS28-ESR = DAS28 using erythrocyte sedimentation rate; hsCRP = high-sensitivity C-reactive protein; anti-CCP = anti–cyclic citrullinated peptide; HAQ DI = Health Assessment Questionnaire disability index; MTX = methotrexate.
† Negative was defined as a rheumatoid factor (RF) titer of <14 units/ml.
‡ These patients who had not previously taken anti–tumor necrosis factor (anti-TNF) agents were protocol deviators.
§ These patients who previously took other biologic disease-modifying antirheumatic drugs (DMARDs) were protocol deviators.

receiving 75 mg secukinumab, and 42.8% among those receiving abatacept, compared with 18.1% in the placebo group (Table 2 and Figure 3A). The primary end point of the ACR20 response rate at week 24 was met in patients receiving 150 mg secukinumab, whose ACR20 response rates were statistically significantly higher than those in the placebo group, as determined using the predefined statistical testing hierarchy (adjusted $P = 0.0305$). For the secukinumab 75 mg group, the primary end point was not met (adjusted $P = 0.0916$).

Key secondary efficacy results. The first key secondary end point, change in the DAS28-CRP from baseline to week 24, was met in the secukinumab 150 mg group, whose DAS28-CRP showed a statistically significant reduction at week 24, as determined using the predefined statistical testing hierarchy (adjusted $P = 0.0495$) (Figure 3B). None of the other key secondary end points (HAQ DI and ACR50 response rates) were met in the secukinumab 150 mg group at week 24. In the secukinumab 75 mg group, none of the key secondary end points were met.

The least squares mean (LSM) change in the DAS28-CRP from baseline to week 24 was −1.47 in both secukinumab dose groups, −2.07 in the abatacept group, and −1.02 in the placebo group. The LSM change in the HAQ DI from baseline to week 24 was −0.39 in the secukinumab 150 mg group, −0.30 in the secukinumab 75 mg group, −0.61 in the abatacept group, and −0.26 in the placebo group. The ACR50 response rates at week 24 were 16.8% in those receiving 150 mg secukinumab, 11.6% in those receiving 75 mg secukinumab, 27.5% in those receiving abatacept, and 9.4% in those receiving placebo (Table 2).

Other secondary efficacy results. The trends in the ACR50 and ACR70 response rates were similar to those in the ACR20 response rate up to week 24 (Table 2). Patients who received secukinumab showed numerically

Table 2. Summary of primary and secondary end points at weeks 24 and 52

End point, week	Secukinumab 150 mg (n = 137)	Secukinumab 75 mg (n = 138)	Abatacept (n = 138)	Placebo (n = 138)
ACR20*				
Week 24	42 (30.7)†	39 (28.3)	59 (42.8)†	25 (18.1)
Week 52	55 (62.5)	52 (56.5)	59 (74.7)	NA‡
DAS28-CRP§				
Week 24	−1.5 ± 0.1†	−1.5 ± 0.1	−2.1 ± 0.1†	−1.0 ± 0.2
Week 52	−2.1 ± 1.4	−1.8 ± 1.4	−2.7 ± 1.4	NA
HAQ DI§				
Week 24	−0.4 ± 0.1	−0.3 ± 0.5	−0.6 ± 0.1†	−0.3 ± 0.1
Week 52	−0.5 ± 0.6	−0.3 ± 0.5	−0.8 ± 0.7	NA
ACR50 response rate*				
Week 24	23 (16.8)	16 (11.6)	38 (27.5)†	13 (9.4)
Week 52	40 (45.5)	24 (26.1)	41 (51.9)	NA
ACR70 response rate*				
Week 24	14 (10.2)	7 (5.1)	17 (12.3)†	7 (5.1)
Week 52	17 (19.3)	6 (6.5)	18 (22.8)	NA
DAS28-ESR§				
Week 24	−1.7 ± 0.1†	−1.7 ± 0.1†	−2.3 ± 0.1†	−1.2 ± 0.2
Week 52	−2.5 ± 1.3	−2.1 ± 1.4	−3.0 ± 1.4	NA

* Values for the American College of Rheumatology 20% (ACR20), 50% (ACR50), and 70% (ACR70) improvement response rates are the number (%) of patients, based on nonresponder imputation data at week 24 and observed data at week 52.
† $P < 0.05$ versus placebo, adjusted for multiplicity of testing.
‡ NA = not applicable.
§ Values for the Disease Activity Score in 28 joints using C-reactive protein level (DAS28-CRP), Health Assessment Questionnaire disability index (HAQ DI), and DAS28 using erythrocyte sedimentation rate (DAS28-ESR) are the mixed-effects model repeated-measures least squares mean ± SEM change from baseline at week 24 and least squares mean ± SD change from baseline at week 52.

higher response rates at week 24, both with the ACR50 (in both secukinumab dose groups) and the ACR70 (only in the secukinumab 150 mg group), as compared with patients who received placebo. The ACR50 and ACR70 responses were higher in the abatacept dose group compared with both secukinumab dose groups. ACR20, ACR50, and ACR70 responses achieved at week 24 were sustained up to week 52 in both secukinumab dose groups (Table 2).

Reductions in the mean DAS28-CRP from baseline up to week 24 were greater in patients receiving either of the secukinumab regimens compared with those receiving placebo. DAS28-CRP response rates were sustained from week 8 through week 52 in both secukinumab dose

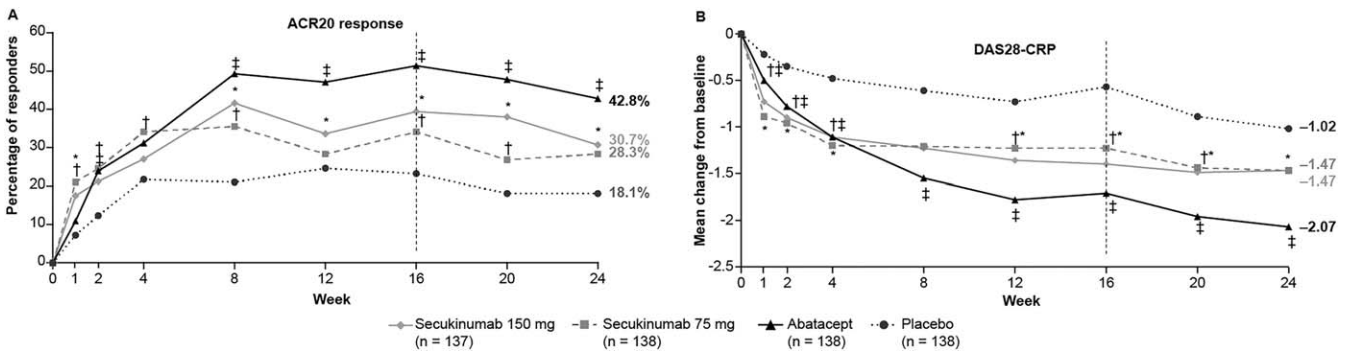

Figure 3. A, Rates of 20% improvement in disease activity according to the American College of Rheumatology response criteria (ACR20) over the first 24 weeks of treatment, using data from nonresponder imputation. **B,** Change from baseline through week 24 in the Disease Activity Score in 28 joints using C-reactive protein level (DAS28-CRP). All footnote symbols above the lines indicate significant differences versus placebo at $P \leq 0.05$. *P* values are adjusted for multiplicity of testing for secukinumab 150 mg and secukinumab 75 mg versus placebo. The broken vertical line at week 16 indicates that patients receiving placebo could escape to active treatment at week 16 if they did not respond to treatment based on 20% improvement in the tender and swollen joint counts. Values next to lines indicate the number of subjects randomized.

Table 3. Treatment-emergent AEs over 16 weeks and over the entire treatment period*

Variable	Up to week 16					During entire period†			
	Secukinumab 150 mg (n = 136)	Secukinumab 75 mg (n = 137)	Pooled secukinumab (n = 273)	Abatacept (n = 137)	Placebo (n = 139)	Secukinumab 150 mg (n = 215)	Secukinumab 75 mg (n = 218)	Pooled secukinumab (n = 433)	Abatacept (n = 137)
Any AE, no. (%)	77 (56.6)	83 (60.6)	160 (58.6)	74 (54.0)	62 (44.6)	167 (77.7)	177 (81.2)	344 (79.4)	97 (70.8)
SAEs, no. (%)	6 (4.4)	3 (2.2)	9 (3.3)	4 (2.9)	6 (4.3)	28 (13.0)	30 (13.8)	58 (13.4)	9 (6.6)
Discontinued study treatment due to any AEs, no. (%)	5 (3.7)	5 (3.6)	10 (3.7)	3 (2.2)	1 (0.7)	21 (9.8)	17 (7.8)	38 (8.8)	5 (3.6)
Death, no. (%)	1 (0.7)	0	1 (0.4)	0	0	1 (0.5)	3 (0.1)	4 (0.1)	0
Common AEs, no. (%)									
Rheumatoid arthritis	3 (2.2)	3 (2.2)	6 (2.2)	3 (2.2)	5 (3.6)	23 (10.7)	19 (8.7)	42 (9.7)	6 (4.4)
Influenza	7 (5.1)	3 (2.2)	10 (3.7)	0	1 (0.7)	13 (6.0)	7 (3.2)	20 (4.6)	1 (0.7)
Nasopharyngitis	4 (2.9)	4 (2.9)	8 (2.9)	6 (4.4)	4 (2.9)	17 (7.9)	24 (11.0)	41 (9.5)	8 (5.8)
Upper respiratory tract infection	6 (4.4)	3 (2.2)	9 (3.3)	1 (0.7)	6 (4.3)	21 (9.8)	18 (8.3)	39 (9.0)	6 (4.4)
Arthralgia	5 (3.7)	2 (1.5)	7 (2.6)	2 (1.5)	1 (0.7)	15 (7.0)	17 (7.8)	32 (7.4)	5 (3.6)
Hypertension	4 (2.9)	6 (4.4)	10 (3.7)	1 (0.7)	4 (2.9)	10 (4.7)	20 (9.2)	30 (6.9)	5 (3.6)
Headache	5 (3.7)	6 (4.4)	11 (4.0)	6 (4.4)	4 (2.9)	11 (5.1)	18 (8.3)	29 (6.7)	9 (6.6)
Diarrhea	4 (2.9)	8 (5.8)	12 (4.4)	6 (4.4)	0	12 (5.6)	16 (7.3)	28 (6.5)	9 (6.6)
Urinary tract infection	2 (1.5)	1 (0.7)	3 (1.1)	3 (2.2)	2 (1.4)	10 (4.7)	16 (7.3)	26 (6.0)	8 (5.8)
Back pain	1 (0.7)	4 (2.9)	5 (1.8)	3 (2.2)	1 (0.7)	11 (5.1)	14 (6.4)	25 (5.8)	6 (4.4)
Bronchitis	4 (2.9)	3 (2.2)	7 (2.6)	3 (2.2)	0	12 (5.6)	10 (4.6)	22 (5.1)	5 (3.6)
AEs of special interest‡									
MACE	3 (2.2)	0	3 (1.1)	0	0	3 (1.0)	2 (0.6)	5 (0.8)	0
Esophageal candidiasis	2 (1.5)	5 (3.6)	7 (2.6)	0	0	5 (1.6)	10 (3.2)	15 (2.4)	3 (2.5)
Neutropenia	2 (1.5)	3 (2.2)	5 (1.8)	3 (2.2)	1 (0.7)	5 (1.6)	8 (2.6)	13 (2.1)	3 (2.5)

* AEs = adverse events; SAEs = serious AEs; MACE = major adverse cardiovascular event (myocardial infarction, stroke, cardiovascular death).
† AEs with a frequency of ≥5% in any secukinumab group during the entire treatment period are shown.
‡ Values up to week 16 are the number (%) of patients. Values during the entire treatment period are the number of patients (exposure-adjusted incidence rate).

groups. A larger reduction in the DAS28-CRP from baseline was seen in patients with a baseline hsCRP level of >10 mg/liter compared with those with a baseline hsCRP level of ≤10 mg/liter. At week 24, in the subgroup of patients with a baseline hsCRP level of ≤10 mg/liter, the LSM changes from baseline in the DAS28-CRP were −1.32 in the secukinumab 150 mg group ($P = 0.0304$), −1.37 in the secukinumab 75 mg group ($P = 0.0171$), and −1.86 in the abatacept group ($P = 0.0001$), as compared with an LSM change of −0.70 in the placebo group. In the subgroup of patients with a baseline hsCRP level of >10 mg/liter, the LSM changes from baseline in the DAS28-CRP were −1.64 in those receiving 150 mg secukinumab ($P = 0.3878$), −1.57 in those receiving 75 mg secukinumab ($P = 0.5443$), and −2.32 in those receiving abatacept ($P = 0.0021$), as compared with −1.39 in those receiving placebo.

With regard to the DAS28-ESR, the LSM change from baseline was greater in both secukinumab dose groups compared with the placebo group at all time points up to week 24. Specifically, at week 24, the DAS28-ESR LSM changes from baseline were −1.73 in the secukinumab 150 mg group ($P = 0.0232$), −1.68 in the secukinumab 75 mg group ($P = 0.0385$), and −2.31 in the abatacept group ($P < 0.0001$), as compared with −1.23 in the placebo group. The improvement in the DAS28-ESR achieved at week 24 was sustained through week 52 (Table 2).

The improvements in the HAQ DI score achieved at week 24 were sustained up to week 52 in both secukinumab dose groups. In addition, further improvements in the HAQ DI were seen in the abatacept group during this period (Table 2).

Safety. *Initial 16-week period.* As shown in Table 3, treatment-emergent AEs were reported to occur in a higher proportion of patients in the secukinumab and abatacept groups compared with the placebo group in the initial 16-week period. The most frequently reported treatment-emergent AEs, by system organ class, were infections and infestations (Table 3). Within that class, the most commonly reported AEs were influenza, upper respiratory tract infection, and nasopharyngitis. Musculoskeletal and connective tissue disorders as well as gastrointestinal disorders occurred at comparable rates in patients in both secukinumab dose groups and the abatacept group (Table 3).

During the initial 16-week period, the most commonly reported AEs, by preferred term, in the secukinumab group were diarrhea, headache, hypertension, and influenza (Table 3). The majority of AEs reported up to week 16 were mild or moderate in severity. During the initial 16-week period, 14 patients discontinued the study treatment due to an AE: 5 in each of the secukinumab groups, 3 in the abatacept group, and 1 in the placebo group (Table 3).

The incidence of SAEs was low and comparable between the groups during the initial 16-week period (Table 3). The incidence of AEs of special interest, which included major adverse cardiac events (MACEs), *Candida* infection, and neutropenia, was low during the initial 16-week period, including 3 cases of MACEs (all in the secukinumab 150 mg group), 7 cases of esophageal candidiasis, and 9 cases of neutropenia. One death was reported during the 16-week period, in the secukinumab 150 mg group. This was attributed to fulminant pulmonary artery embolism.

Entire treatment period. Treatment-emergent AEs were reported in a higher proportion of patients in the secukinumab and abatacept groups compared with the placebo group over the entire treatment period (Table 3). The most frequently reported treatment-emergent AEs, by system organ class, were infections and infestations (Table 3). Within that class, the most commonly reported AEs were nasopharyngitis and upper respiratory tract infection.

During the entire study period, rheumatoid arthritis, nasopharyngitis, upper respiratory tract infection, arthralgia, and hypertension were the most frequently reported AEs, by preferred term, in the secukinumab groups (Table 3). Most of the AEs reported over the entire treatment period were mild or moderate in severity. During the entire study period, 43 patients discontinued the study treatment due to an AE (38 in the secukinumab groups and 5 in the abatacept group) (Table 3).

SAEs over the entire study period were reported at a rate of 9.7 per 100 patient-years (13.4%) in the secukinumab groups and 7.7 per 100 patient-years (6.6%) in the abatacept group (Table 3). Among these SAEs, the most frequently affected system organ classes were musculoskeletal and connective tissue disorders, which occurred in 11 patients (5.1%) who received 150 mg secukinumab, 9 patients (4.1%) who received 75 mg secukinumab, and 1 patient (0.7%) who received abatacept.

In terms of AEs of special interest, the overall exposure-adjusted incidence rate (EAIR) of MACEs was 0.8 per 100 patient-years in the secukinumab groups and 0 per 100 patient-years in the abatacept group (Table 3). For esophageal candidiasis and neutropenia, the EAIRs were low and similar between the active treatment groups (Table 3). No cases of tuberculosis were reported.

Three deaths occurred during the entire treatment period after week 16. All of the deaths occurred in the secukinumab 75 mg group (1 of unknown cause and 2 due to cardiac insufficiency).

Treatment-emergent antisecukinumab antibodies (developing after secukinumab treatment in patients

negative for these antibodies at baseline) were detected in 7 patients in the secukinumab groups. Antisecukinumab titers were measured and were low. Neutralizing antibodies were not detected.

DISCUSSION

Several phase II studies of secukinumab (12) and other IL-17A inhibitor molecules, such as ixekizumab, have demonstrated preliminary efficacy in the treatment of patients with RA (13,27). This is the first report to compare the efficacy of an IL-17A inhibitor with that of abatacept in a phase III randomized, double-blinded study of patients with RA in whom TNF inhibitor therapy has failed.

Secukinumab at a dose of 150 mg was statistically superior to placebo at week 24 in the treatment of patients with RA, and thus the primary end point of the study was achieved. A statistically significant change in the DAS28-CRP at week 24 was met only in the secukinumab 150 mg group, whereas none of the other key secondary end points, including the HAQ DI and the ACR50 response rate, were met. For the secukinumab 75 mg group, neither the primary end point nor any of the key secondary end points were met. Although this trial was not powered for intergroup statistical comparisons, it is noteworthy that the response to abatacept, as measured using the ACR20, ACR50, and ACR70 response rates, the DAS28-CRP, and the HAQ DI, indicated numerically larger responses in the abatacept group compared with the 2 secukinumab dose groups at most time points from week 8 through week 24 and up to week 52. Efficacy responses for abatacept were similar to those observed in other trials of this compound in patients in whom TNF inhibitor therapy has failed. The ACR50 response rate in patients receiving abatacept in this study (27.5% at week 24) was similar to the efficacy previously observed in phase III trials of abatacept in patients with an inadequate response to TNF inhibitors (20.3% at week 24) (5).

Other second-line therapies, including anti–IL-6 therapies such as tocilizumab (28) and B cell–targeting therapies such as rituximab (29), have demonstrated good efficacy in RA patients in whom treatment with TNF inhibitors has failed. Indirect comparisons of efficacy from such agents, in conjunction with the results of the direct comparison against abatacept in this trial, suggest that inhibition of IL-17A with secukinumab proffers no additional benefit to RA patients with an inadequate response to TNF inhibitors over currently approved therapies. Thus, the extension period of this trial was closed early.

Safety data from this trial confirmed the safety profile of secukinumab as previously reported in phase III trials in patients with psoriasis, PsA, or AS, and these data allow for a comparison with abatacept in terms of common events such as infectious, gastrointestinal, and musculoskeletal AEs. With respect to rare events such as MACEs and deaths, no such events occurred in the abatacept and placebo groups, and therefore direct comparisons of EAIRs for these events were not possible in this trial. However, the EAIRs for MACEs and deaths are comparable to those observed for other biologic agents in patients with RA (30,31).

In conclusion, in this study, secukinumab at a dose of 150 mg demonstrated efficacy for the treatment of patients with active RA who had an inadequate response to TNF inhibitors. However, no incremental benefit of IL-17A inhibition was seen over other agents currently approved for use in patients in whom TNF inhibitors have failed. These data, along with the findings from phase II studies (11,12) and data related to the use of other anti–IL-17A agents (13,27), suggest that IL-17A plays a lesser role in the pathogenesis of RA. Thus, blockade of IL-17A alone may not add to the armamentarium for clinicians in the treatment of patients with RA in whom anti-TNF therapy has failed. This stands in contrast to the results seen in patients with spondyloarthropathies, including PsA and AS, in whom inhibition of IL-17A with secukinumab has demonstrated robust efficacy. The safety profile of secukinumab in this study of patients with RA was comparable to the safety profile of secukinumab in PsA and AS.

AUTHOR CONTRIBUTIONS

All authors were involved in drafting the article or revising it critically for important intellectual content, and all authors approved the final version to be published. Dr. Blanco had full access to all of the data in the study and takes responsibility for the integrity of the data and the accuracy of the data analysis.

Study conception and design. Blanco, Richards.

Acquisition of data. Blanco, Möricke, Dokoupilova, Codding, Neal, Richards.

Analysis and interpretation of data. Blanco, Andersson, Rohrer, Richards.

ROLE OF THE STUDY SPONSOR

Novartis Pharma facilitated the study design, provided writing assistance for the manuscript, and reviewed and approved the manuscript prior to submission. The authors independently collected the data, interpreted the results, and had the final decision to submit the manuscript for publication. Publication of this article was not contingent upon approval by Novartis Pharma.

ADDITIONAL DISCLOSURES

Author Dokoupilova is an employee of Medical Plus.

REFERENCES

1. McInnes IB, Schett G. The pathogenesis of rheumatoid arthritis. N Engl J Med 2011;365:2205–19.
2. Gabriel SE, Michaud K. Epidemiological studies in incidence, prevalence, mortality, and comorbidity of the rheumatic diseases. Arthritis Res Ther 2009;11:229.
3. Uhlig T, Moe RH, Kvien TK. The burden of disease in rheumatoid arthritis. Pharmacoeconomics 2014;32:841–51.
4. Smolen JS, Landewe R, Breedveld FC, Buch M, Burmester G, Dougados M, et al. EULAR recommendations for the management of rheumatoid arthritis with synthetic and biological disease-modifying antirheumatic drugs: 2013 update. Ann Rheum Dis 2014;73:492–509.
5. Genovese MC, Becker JC, Schiff M, Luggen M, Sherrer Y, Kremer J, et al. Abatacept for rheumatoid arthritis refractory to tumor necrosis factor α inhibition. N Engl J Med 2005;353:1114–23.
6. Emery P. The therapeutic potential of costimulatory blockade with CTLA4Ig in rheumatoid arthritis. Expert Opin Investig Drugs 2003;12:673–81.
7. Chabaud M, Page G, Miossec P. Enhancing effect of IL-1, IL-17, and TNF-α on macrophage inflammatory protein-3α production in rheumatoid arthritis: regulation by soluble receptors and Th2 cytokines. J Immunol 2001;167:6015–20.
8. Lubberts E, Koenders MI, Oppers-Walgreen B, van den Bersselaar L, Coenen-de Roo CJ, Joosten LA, et al. Treatment with a neutralizing anti-murine interleukin-17 antibody after the onset of collagen-induced arthritis reduces joint inflammation, cartilage destruction, and bone erosion. Arthritis Rheum 2004;50:650–9.
9. Park JS, Park MK, Lee SY, Oh HJ, Lim MA, Cho WT, et al. TWEAK promotes the production of interleukin-17 in rheumatoid arthritis. Cytokine 2012;60:143–9.
10. Hueber W, Patel DD, Dryja T, Wright AM, Koroleva I, Bruin G, et al. Effects of AIN457, a fully human antibody to interleukin-17A, on psoriasis, rheumatoid arthritis, and uveitis. Sci Transl Med 2010;2:52ra72.
11. Genovese MC, Durez P, Richards HB, Supronik J, Dokoupilova E, Mazurov V, et al. Efficacy and safety of secukinumab in patients with rheumatoid arthritis: a phase II, dose-finding, double-blind, randomised, placebo controlled study. Ann Rheum Dis 2013;72:863–9.
12. Genovese MC, Durez P, Richards HB, Supronik J, Dokoupilova E, Aelion JA, et al. One-year efficacy and safety results of secukinumab in patients with rheumatoid arthritis: phase II, dose-finding, double-blind, randomized, placebo-controlled study. J Rheumatol 2014;41:414–21.
13. Genovese MC, Greenwald M, Cho CS, Berman A, Jin L, Cameron GS, et al. A phase II randomized study of subcutaneous ixekizumab, an anti–interleukin-17 monoclonal antibody, in rheumatoid arthritis patients who were naive to biologic agents or had an inadequate response to tumor necrosis factor inhibitors. Arthritis Rheumatol 2014;66:1693–704.
14. Leipe J, Grunke M, Dechant C, Reindl C, Kerzendorf U, Schulze-Koops H, et al. Role of Th17 cells in human autoimmune arthritis. Arthritis Rheum 2010;62:2876–85.
15. Miao J, Geng J, Zhang K, Li X, Li Q, Li C, et al. Frequencies of circulating IL-17-producing CD4+CD161+ T cells and CD4+CD161+ T cells correlate with disease activity in rheumatoid arthritis. Mod Rheumatol 2014;24:265–570.
16. Kotake S, Udagawa N, Takahashi N, Matsuzaki K, Itoh K, Ishiyama S, et al. IL-17 in synovial fluids from patients with rheumatoid arthritis is a potent stimulator of osteoclastogenesis. J Clin Invest 1999;103:1345–52.
17. Cai L, Yin JP, Starovasnik MA, Hogue DA, Hillan KJ, Mort JS, et al. Pathways by which interleukin 17 induces articular cartilage breakdown in vitro and in vivo. Cytokine 2001;16:10–21.
18. Van Baarsen LG, Lebre MC, van der Coelen D, Aarrass S, Tang MW, Ramwadhdoebe TH, et al. Heterogeneous expression pattern of interleukin 17A (IL-17A), IL-17F and their receptors in synovium of rheumatoid arthritis, psoriatic arthritis and osteoarthritis: possible explanation for nonresponse to anti-IL-17 therapy? Arthritis Res Ther 2014;16:426.
19. Van den Berg WB, Miossec P. IL-17 as a future therapeutic target for rheumatoid arthritis. Nat Rev Rheumatol 2009;5:549–53.
20. Cosentyx (secukinumab) highlights of prescribing information. East Hanover (NJ): Novartis Pharmaceuticals Corporation; 2015. URL: https://www.pharma.us.novartis.com/product/pi/pdf/cosentyx.pdf.
21. Tlustochowicz W, Rahman P, Seriolo B, Krammer G, Porter B, Widmer A, et al. Efficacy and safety of subcutaneous and intravenous loading dose regimens of secukinumab in patients with active rheumatoid arthritis: results from a randomized phase II study. J Rheumatol 2016;43:495–503.
22. Burmester GR, Durez P, Shestakova G, Genovese MC, Schulze-Koops H, Li Y, et al. Association of HLA-DRB1 alleles with clinical responses to the anti-interleukin-17A monoclonal antibody secukinumab in active rheumatoid arthritis. Rheumatology (Oxford) 2016;55:49–55.
23. Aletaha D, Neogi T, Silman AJ, Funovits J, Felson DT, Bingham CO III, et al. 2010 rheumatoid arthritis classification criteria: an American College of Rheumatology/European League Against Rheumatism collaborative initiative. Arthritis Rheum 2010;62:2569–81.
24. Felson DT, Anderson JJ, Boers M, Bombardier C, Furst D, Goldsmith C, et al. American College of Rheumatology preliminary definition of improvement in rheumatoid arthritis. Arthritis Rheum 1995;38:727–35.
25. Prevoo ML, van 't Hof MA, Kuper HH, van Leeuwen MA, van de Putte LB, van Riel PL. Modified disease activity scores that include twenty-eight–joint counts: development and validation in a prospective longitudinal study of patients with rheumatoid arthritis. Arthritis Rheum 1995;38:44–8.
26. Fries JF, Spitz P, Kraines RG, Holman HR. Measurement of patient outcome in arthritis. Arthritis Rheum 1980;23:137–45.
27. Genovese MC, Braun DK, Erickson JS, Berclaz PY, Banerjee S, Heffernan MP, et al. Safety and efficacy of open-label subcutaneous ixekizumab treatment for 48 weeks in a phase II study in biologic-naive and TNF-IR patients with rheumatoid arthritis. J Rheumatol 2016;43:289–97.
28. Jones G, Sebba A, Gu J, Lowenstein MB, Calvo A, Gomez-Reino JJ, et al. Comparison of tocilizumab monotherapy versus methotrexate monotherapy in patients with moderate to severe rheumatoid arthritis: the AMBITION study. Ann Rheum Dis 2010;69:88–96.
29. Cohen SB, Emery P, Greenwald MW, Dougados M, Furie RA, Genovese MC, et al. Rituximab for rheumatoid arthritis refractory to anti–tumor necrosis factor therapy: Results of a multicenter, randomized, double-blind, placebo-controlled, phase III trial evaluating primary efficacy and safety at twenty-four weeks. Arthritis Rheum 2006;54:2793–806.
30. Zhang J, Xie F, Yun H, Chen L, Muntner P, Levitan EB, et al. Comparative effects of biologics on cardiovascular risk among older patients with rheumatoid arthritis. Ann Rheum Dis 2016;75:1813–8.
31. Burmester GR, Panaccione R, Gordon KB, McIlraith MJ, Lacerda AP. Adalimumab: long-term safety in 23 458 patients from global clinical trials in rheumatoid arthritis, juvenile idiopathic arthritis, ankylosing spondylitis, psoriatic arthritis, psoriasis and Crohn's disease. Ann Rheum Dis 2013;72:517–24.

ARTHRITIS & RHEUMATOLOGY
Vol. 69, No. 6, June 2017, pp 1154–1164
DOI 10.1002/art.40084

Cardiovascular Safety of Tocilizumab Versus Tumor Necrosis Factor Inhibitors in Patients With Rheumatoid Arthritis

A Multi-Database Cohort Study

Seoyoung C. Kim,[1] Daniel H. Solomon,[1] James R. Rogers,[1] Sara Gale,[2] Micki Klearman,[2] Khaled Sarsour,[2] and Sebastian Schneeweiss[1]

Objective. **While tocilizumab (TCZ) is known to increase low-density lipoprotein (LDL) cholesterol levels, it is unclear whether TCZ increases cardiovascular risk in patients with rheumatoid arthritis (RA). This study was undertaken to compare the cardiovascular risk associated with receiving TCZ versus tumor necrosis factor inhibitors (TNFi).**

Methods. **To examine comparative cardiovascular safety, we conducted a cohort study of RA patients who newly started TCZ or TNFi using claims data from Medicare, IMS PharMetrics, and MarketScan. All patients were required to have previously used a different TNFi, abatacept, or tofacitinib. The primary outcome measure was a composite cardiovascular end point of hospitalization for myocardial infarction or stroke. TCZ initiators were propensity score matched to TNFi initiators with a variable ratio of 1:3 within each database, controlling for >65 baseline characteristics. A fixed-effects model combined database-specific hazard ratios (HRs).**

Results. **We included 9,218 TCZ initiators propensity score matched to 18,810 TNFi initiators across all 3 databases. The mean age was 72 years in Medicare, 51 in PharMetrics, and 53 in MarketScan. Cardiovascular disease was present at baseline in 14.3% of TCZ initiators and 13.5% of TNFi initiators. During the study period (mean ± SD 0.9 ± 0.7 years; maximum 4.5 years), 125 composite cardiovascular events occurred, resulting in an incidence rate of 0.52 per 100 person-years for TCZ initiators and 0.59 per 100 person-years for TNFi initiators. The risk of cardiovascular events associated with TCZ use versus TNFi use was similar across all 3 databases, with a combined HR of 0.84 (95% confidence interval 0.56–1.26).**

Conclusion. **This multi-database population-based cohort study showed no evidence of an increased cardiovascular risk among RA patients who switched from a different biologic drug or tofacitinib to TCZ versus to a TNFi.**

Epidemiologic studies of patients with rheumatoid arthritis (RA) have shown a 1.5–2.0 times increased risk of cardiovascular morbidity and mortality (1,2). This excess cardiovascular risk is thought to be the result of not only traditional cardiovascular risk factors but also RA severity or active systemic inflammation (3,4). The 2015 American College of Rheumatology guidelines for the treatment of RA recommend a treat-to-target strategy to better control disease activity in both early and established RA (5). Use

Supported by Genentech.

[1]Seoyoung C. Kim, MD, ScD, MSCE, Daniel H. Solomon, MD, MPH, James R. Rogers, BS, BA, Sebastian Schneeweiss, MD, ScD: Brigham and Women's Hospital, Boston, Massachusetts; [2]Sara Gale, PhD, MPH, Micki Klearman, MD, Khaled Sarsour, PhD, MPH: Genentech, South San Francisco, California.

Dr. Kim has received research funding from Lilly, Genentech, Pfizer, Bristol-Myers Squibb, and AstraZeneca (grants to Brigham and Women's Hospital). Dr. Solomon has received research funding from Lilly, Pfizer, AstraZeneca, Genentech, Amgen, and the Consortium of Rheumatology Researchers of North America (CORRONA) (grants to Brigham and Women's Hospital). Dr. Schneeweiss is a paid consultant to Whiscon, LLC and Aetion, Inc., a software manufacturer in which he owns equity; he is also principal investigator on research grants to Brigham and Women's Hospital from Genentech and Boehringer Ingelheim.

Address correspondence to Seoyoung C. Kim, MD, ScD, MSCE, 1620 Tremont Street, Suite 3030, Boston, MA 02120. E-mail: skim62@partners.org.

Submitted for publication September 7, 2016; accepted in revised form February 23, 2017.

of tumor necrosis factor inhibitors (TNFi) or other biologic agents is recommended for patients who have moderate-to-high disease activity while taking a traditional disease-modifying antirheumatic drug (DMARD) (5). Over the past decade, a number of studies have suggested potential cardiovascular benefits of using DMARDs in patients with RA (6). In particular, a number of cohort studies showed that treatment with TNFi may be associated with a decreased cardiovascular risk, probably related to a reduction in systemic inflammation (7–9), although some studies did not find a beneficial effect on cardiovascular risk in patients receiving TNFi compared with patients receiving DMARDs (10,11).

Tocilizumab (TCZ), an interleukin-6 receptor antagonist, is an effective biologic agent that reduces inflammatory disease activity in RA. In several clinical trials in humans, elevations in serum lipid levels were noted among subjects receiving TCZ (12–14). In a head-to-head randomized controlled trial (RCT) of TCZ monotherapy versus adalimumab monotherapy in 325 patients with RA, TCZ was superior to adalimumab for the reduction of signs and symptoms of RA, but more patients in the TCZ group had increased low-density lipoprotein (LDL) cholesterol levels than in the adalimumab group (15,16). Post hoc analyses of clinical trials and extension studies of TCZ suggest that RA disease activity, but not changes in lipid levels during treatment, may be independently associated with cardiovascular risk in RA patients treated with TCZ (17). Nonetheless, whether increases in lipid levels with TCZ treatment compared with treatment with other biologic agents leads to an excess cardiovascular risk has not been determined, although the ENTRACTE trial (ClinicalTrials.gov identifier: NCT01331837), a post-marketing open-label RCT that has just been completed, focused on evaluating the risk of cardiovascular events with TCZ versus etanercept in RA patients with elevated cardiovascular risk at baseline.

The main objective of this study was to compare the risk of cardiovascular events, including myocardial infarction (MI) and stroke, in patients who newly started TCZ versus those who newly started TNFi in a multidatabase population-based cohort of RA patients. The secondary aim was to compare the risk of other cardiovascular events, such as coronary revascularization, acute coronary syndrome (ACS), heart failure, and all-cause deaths, in TCZ initiators compared with TNFi initiators.

PATIENTS AND METHODS

Data sources. We conducted a cohort study using data from 3 large US health care claims databases: Medicare (Parts A/B/D 2010–2013), IMS PharMetrics Plus (2011–2014), and Truven MarketScan (2011–June 2015). Medicare is a federally funded program and provides health care coverage for nearly all legal residents of the US age 65 and older and some disabled patients younger than 65. Briefly, Medicare Part A is generally for inpatient care, Part B for outpatient medical services including some drugs given in a physician's office or clinic, and Part D for outpatient prescription drug coverage (18). The PharMetrics and MarketScan databases contain longitudinal medical and pharmacy claims from a number of different managed care plans and are representative of a national commercially insured population in the US (10,19,20). All 3 databases include data from all 50 US states. The Institutional Review Board of the Brigham and Women's Hospital approved the study protocol and privacy precautions. The study protocol is registered at www.encepp.eu (EUPAS11327).

Study cohort and design. Adults age 18 years or older with at least 2 outpatient visits 7–365 days apart, or 1 inpatient visit, coded with the International Classification of Diseases, Ninth Revision, Clinical Modification (ICD-9-CM) code 714.x for RA were identified. Of these RA patients, we defined 2 mutually exclusive groups of biologic DMARD initiators, TCZ initiators and TNFi initiators, based on either Healthcare Common Procedure Coding System codes or National Drug Codes. Because TCZ is largely used as a second-line biologic agent for RA, we required patients in both groups to have previously used at least 1 other biologic agent (i.e., TNFi or abatacept) or targeted synthetic DMARD (i.e., tofacitinib). The cohort entry date (i.e., index date) was defined as the date of starting TCZ or TNFi after $\geq$365 days of continuous enrollment in the health plan to ensure that we identified study patients with a complete claims history for medical services and prescription dispensing in order to identify new users and control for baseline confounding appropriately. New users of TCZ were defined as those who had not received TCZ within the last 12 months. TNFi initiators had not received a specific TNFi within the last 12 months (Figure 1). At the index date, all of the patients included in this study were required to have had at least 1 inpatient or 2 outpatient visits for RA and at least 2 prescriptions filled for a biologic DMARD or tofacitinib (one for the prior biologic DMARD or tofacitinib and the other for TCZ or TNFi). A previous study showed that RA patients can be accurately identified using a combination of diagnosis codes for RA and any DMARD prescriptions in claims data with a positive predictive value of $>$86% (21).

We excluded nursing home residents, patients with HIV/AIDS, patients with malignancy other than nonmelanoma skin cancer, and those who had end-stage renal disease or had undergone dialysis or renal transplant prior to the index date. Patients who received rituximab were excluded to minimize confounding by indication and misclassification bias since rituximab is often given to patients with malignancy. We further excluded patients with hospitalizations for MI, stroke, ACS, or heart failure in the 90 days prior to the index date.

For the primary as-treated analysis, follow-up time started the day after the index date and ended on the day of treatment discontinuation plus 30 days, outcome occurrence, disenrollment, death, or the end of study period, whichever occurred first. For the secondary intent-to-treat (ITT 365-day) analysis, follow-up time ended on the 365th day of follow-up, outcome occurrence, disenrollment, death, or the end of study period, whichever occurred first. Patients were only allowed to enter the study cohort once.

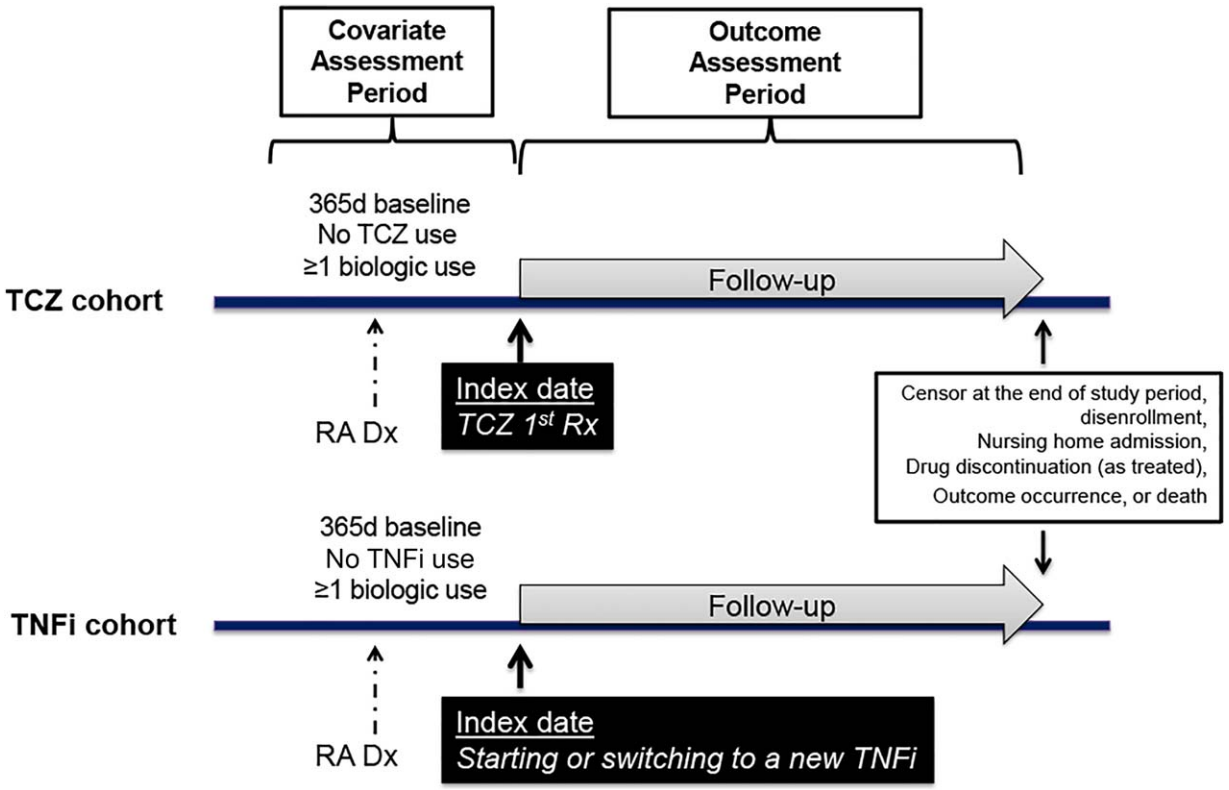

Figure 1. Study design overview. Patients with rheumatoid arthritis (RA) who had not received tocilizumab (TCZ) or tumor necrosis factor inhibitors (TNFi) in the previous 365 days were enrolled in the TCZ cohort or TNFi cohort, respectively. The index date was defined as the date of first TCZ dispensing or the date of switching to a new TNFi after being treated with at least 1 other biologic drug (i.e., abatacept, TNFi, or tofacitinib). Dx = diagnosis; Rx = prescription.

Outcome definition. The primary outcome measure was a composite cardiovascular end point of MI and stroke. MI was identified with a hospital discharge diagnosis code of acute MI (ICD-9 code 410.x excluding 410.x2) in the primary or secondary position. The length of hospitalization for MI was required to be 3–180 days, unless the patient died during the first 3 days of hospitalization (22). Stroke was defined with a hospital discharge diagnosis code of ischemic or hemorrhagic stroke (ICD-9-CM 430, 431, 433.x1, 434.x1, and 436) in the principal position. These claims-based algorithms have been validated and found to have a positive predictive value of >92% (22–24). The secondary definition of the composite cardiovascular event was based on a hospital discharge diagnosis code of MI in the primary or secondary position for any length of hospitalization or a hospital discharge diagnosis code of ischemic or hemorrhagic stroke in the primary position. This definition also had a positive predictive value of >92% (22).

Other secondary outcomes were the individual cardiovascular end points of MI and stroke, coronary revascularization, hospitalization for ACS, any cardiovascular events including MI, stroke, coronary revascularization, or ACS, and hospitalization for heart failure and all-cause mortality.

Covariate assessment. During the 12-month baseline period, we measured >90 predefined variables potentially related to RA severity or activity or development of cardiovascular events in each database. We assessed the cohort entry year, demographic characteristics, regions, comorbid conditions, use of other prescription drugs, and markers of health care utilization intensity. To assess RA-related covariates for confounding control, we determined patients' history of DMARD use during all available days before the cohort entry date, including both the 365 days prior to the index date and any other available days prior to the pre-index 365 days. While we did not have information on RA duration or disease activity, we used the previously validated claims-based index for RA severity (25). We also calculated the combined Comorbidity Score that included 47 conditions (26). Physician orders of outpatient laboratory tests (Table 1 and Supplementary Table 1, available on the *Arthritis & Rheumatology* web site at http://onlinelibrary.wiley.com/doi/10.1002/art.40084/abstract) were included because these laboratory tests may be selectively ordered depending on patients' risk factors corresponding to current practice patterns and treatment guidelines (27).

Statistical analysis. For each database, we compared the baseline characteristics of the patients in the TCZ and TNFi groups. To control for >65 potential confounders, including demographics (age, sex, region, race/ethnicity [only available in the Medicare data]), prior DMARD use, cardiovascular comorbidities, other chronic diseases, cardiovascular medications, other long-term medications, and markers of health care utilization intensity, we used propensity score matching within each database (28). The propensity score was defined as the predicted probability of a patient starting TCZ

Table 1. Selected characteristics of the RA patients in the 365 days before study entry*

	Medicare (n = 7,397)		PharMetrics (n = 8,119)		MarketScan (n = 12,512)	
	TCZ (n = 2,531)	TNFi (n = 4,866)	TCZ (n = 2,614)	TNFi (n = 5,505)	TCZ (n = 4,073)	TNFi (n = 8,439)
Demographic characteristics						
Age, mean ± SD years	72.2 ± 6.2	72.0 ± 6.1	51.3 ± 11.9	51.0 ± 11.5	53.2 ± 12.5	52.7 ± 12.4
Male	15.4	15.3	18.3	18.9	16.8	18.1
Comorbidities						
Atrial fibrillation	10.3	9.8	2.1	1.8	2.7	2.3
Myocardial infarction	1.7	1.6	0.3	0.5	0.5	0.5
Acute/subacute CAD	5.9	5.8	1.5	1.6	1.9	1.8
Chronic CAD	8.3	8.3	1.4	1.5	1.3	1.1
Atherosclerosis	24.5	24.4	6.0	5.9	6.9	6.4
Heart failure	11.2	11.2	1.8	1.9	2.6	2.0
Stroke	3.4	3.2	1.1	0.8	0.9	0.9
TIA	3.2	2.7	1.0	0.9	1.0	0.9
Peripheral vascular disease	11.2	11.8	2.1	2.1	2.5	2.4
Hypertension	83.9	83.5	50.3	49.3	47.7	46.1
Diabetes	30.2	31.0	14.2	13.9	16.0	15.0
Hyperlipidemia	67.2	65.5	36.0	34.6	34.2	32.6
Chronic kidney disease	12.9	12.6	3.8	3.8	4.2	3.9
Comorbidity Index, mean ± SD	1.3 ± 2.0	1.3 ± 2.0	0.4 ± 1.2	0.4 ± 1.2	0.4 ± 1.2	0.4 ± 1.2
CIRAS, mean ± SD	5.9 ± 1.3	5.8 ± 1.3	6.7 ± 1.7	6.6 ± 1.7	6.5 ± 1.9	6.5 ± 1.8
RA-related treatment						
No. of prior DMARDs						
1	25.8	30.9	20.1	24.3	26.6	30.8
2	35.8	36.7	27.7	31.9	31.6	35.1
≥3	38.4	32.4	52.1	43.8	41.8	34.1
Methotrexate, any use†	72.1	71.6	73.1	72.9	66.2	67.2
Steroids, any use†	74.2	72.4	71.9	71.0	67.5	67.1
Steroids, recent use‡	32.5	32.0	33.3	32.4	30.5	29.7
NSAIDs	34.3	34.9	39.9	40.7	39.7	40.9
COX-2 inhibitors	9.7	10.2	10.2	10.1	9.3	9.2
Opioids	74.8	73.4	67.6	66.6	66.3	66.9
Other medications						
Nitrates	6.5	6.4	1.8	1.6	2.1	2.1
Statins	45.1	44.3	21.0	20.0	22.4	22.6
Non-statin lipid-lowering drugs	7.7	7.8	4.0	4.3	4.6	4.8
Insulin	6.4	6.3	3.6	3.4	4.2	3.9
Beta blockers	39.2	38.4	16.5	15.9	18.2	18.0
Calcium channel blockers	28.1	28.1	10.3	10.5	12.4	12.2
Health care utilization, mean ± SD						
No. of lipid tests ordered	1.5 ± 1.3	1.4 ± 1.4	1.1 ± 1.4	0.9 ± 1.6	1.0 ± 1.7	0.8 ± 1.6
No. of PCP visits	5.0 ± 5.1	5.0 ± 5.0	2.9 ± 5.9	2.9 ± 7.6	3.1 ± 6.4	3.0 ± 5.6
No. of cardiology visits	0.8 ± 1.8	0.8 ± 1.9	0.6 ± 1.8	0.6 ± 2.0	0.7 ± 2.2	0.6 ± 2.1
No. of ED visits	0.6 ± 1.1	0.6 ± 1.2	0.6 ± 1.2	0.6 ± 1.5	0.3 ± 1.5	0.2 ± 1.6

* The tocilizumab (TCZ) and tumor necrosis factor inhibitor (TNFi) cohorts were propensity score matched with a 1:3 variable ratio. Except where indicated otherwise, values are the percent of patients. RA = rheumatoid arthritis; CAD = coronary artery disease; TIA = transient ischemic attack; CIRAS = claims-based index for RA severity; DMARDs = disease-modifying antirheumatic drugs; NSAIDs = nonsteroidal antiinflammatory drugs; COX-2 = cyclooxygenase 2; PCP = primary care physician; ED = emergency department.
† Any time before the cohort entry date.
‡ In the 30 days before the cohort entry date.

versus a TNFi given patient characteristics at baseline. For each data set, we estimated the propensity score using multivariable logistic regression that included all of the aforementioned covariates (Table 1) and the cohort entry calendar year. In order to increase study power, we implemented sequential propensity score matching with a variable ratio of up to 1:3 based on a matching caliper of 0.02 on the propensity score scale (29,30). The propensity score balance achieved within each database was inspected by tabulating all patient characteristics by treatment status and by examining the standardized differences (30,31).

After propensity score matching, we estimated incidence rates (IRs) of the primary and secondary outcomes in the TCZ group compared with the TNFi group separately in each database. Kaplan-Meier plots were used to inspect proportionality of hazards, and the follow-up time between treatment groups was

compared in each database. Cox proportional hazards models conditioning on the matching set were fitted to estimate hazard ratios (HRs) and 95% confidence intervals (95% CIs) (32,33). HRs from the 3 propensity score–matched cohorts were then combined using an inverse variance-weighted, fixed-effects model. We also conducted a further analysis to correct variance for potential overlaps in person-time between the 2 commercial cohorts by 10% or 20% (34).

Protocol-specified subgroup analyses were performed by age group (i.e., younger than 60 years or 60 years or older), the presence of preexisting cardiovascular disease or diabetes, and concomitant use of methotrexate. In addition, we conducted subgroup analysis according to baseline use of oral steroids and statins. Within each of these subgroups, TCZ and TNFi initiators were propensity score–matched with a variable ratio of 1:3. All analyses, reports, and audit trails were conducted using the Aetion platform including R version 2.1.2. The Medicare data were additionally analyzed with SAS version 9.4, yielding the same results.

RESULTS

Cohort selection. There were 88,375 RA patients who started either TCZ or a TNFi with prior use of biologic agents or targeted synthetic DMARDs in the study databases. After applying exclusion criteria, our study cohort included a total of 40,119 RA patients starting either TCZ (n = 9,917) or TNFi (n = 30,202). After performing propensity score matching with a variable ratio of 1:3, the final cohort comprised a total of 28,028 RA patients, including 9,218 TCZ and 18,810 TNFi initiators (Figure 2). On average, each TCZ initiator was matched to 2 TNFi initiators across the 3 databases.

Patient characteristics. Table 1 shows selected baseline characteristics of the propensity score–matched cohorts in each database. As expected with the difference in the demographic characteristics of enrollees in Medicare versus the commercial health plans, the mean ± SD age was 72 ± 6 years in the Medicare database versus 51 ± 11 years in the PharMetrics database and 53 ± 12 years in the MarketScan database. Similarly, cardiovascular comorbidities were more common in patients enrolled in Medicare than in those enrolled in the commercial health plans. For example, 2% of TCZ or TNFi initiators in the Medicare database had a history of MI at baseline, whereas <1% of

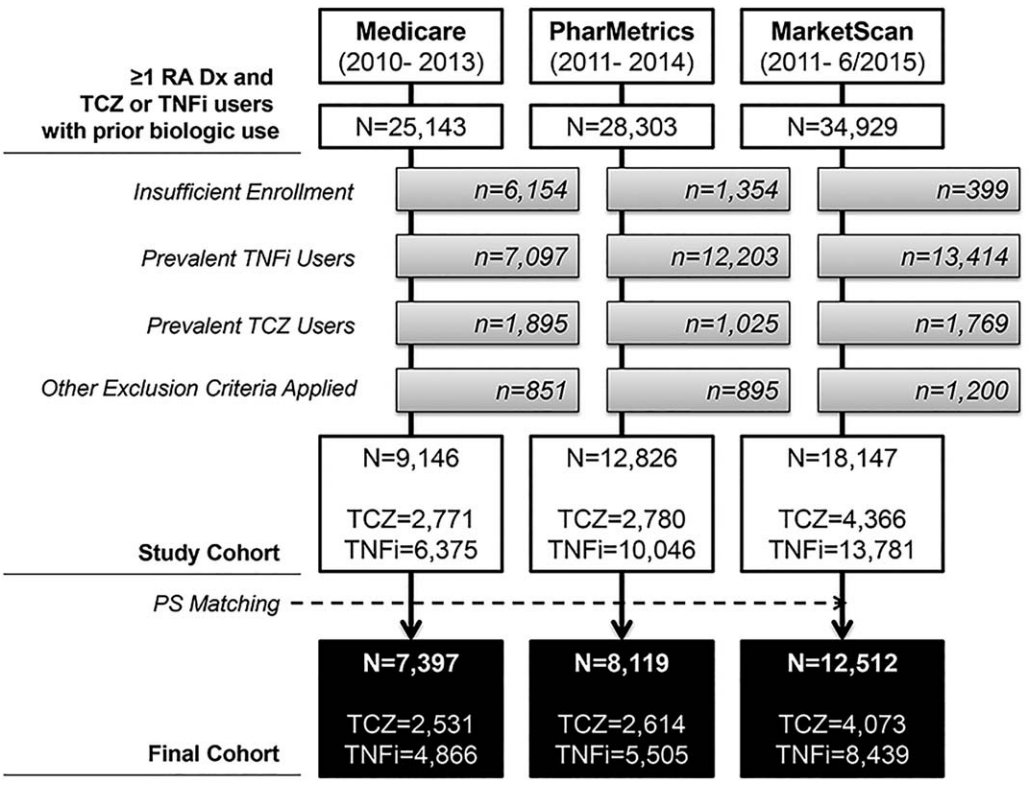

Figure 2. Selection of the study cohort. After the inclusion and exclusion criteria were applied, the study cohort included a total of 40,119 patients with rheumatoid arthritis (RA) who started treatment with tocilizumab (TCZ) or a tumor necrosis factor inhibitor (TNFi), including 9,146 from the Medicare database, 12,826 from the PharMetrics database, and 18,147 from the MarketScan database. After propensity score (PS) matching with a variable ratio of up to 1:3, the final cohort consisted of 28,028 patients, including 9,218 TCZ initiators and 18,810 TNFi initiators. Dx = diagnosis.

Table 2. IRs and HRs of cardiovascular events in RA patients treated with TCZ versus those treated with TNFi*

	TCZ					TNFi				
	No. of subjects	No. of events	Person-years	IR (95% CI)†	HR (95% CI)	No. of subjects	No. of events	Person-years	IR (95% CI)†	HR
As-treated analysis										
Composite cardiovascular events										
Medicare	2,531	17	1,841	0.92 (0.56–1.44)	0.70 (0.40–1.24)	4,866	50	3,954	1.27 (0.95–1.65)	1.0
PharMetrics	2,614	10	2,061	0.49 (0.25–0.86)	1.00 (0.45–2.22)	5,505	20	4,465	0.45 (0.28–0.68)	1.0
MarketScan	4,073	9	2,999	0.30 (0.15–0.55)	1.03 (0.46–2.34)	8,439	19	6,726	0.28 (0.18-–0.43)	1.0
Combined	9,218	36	6,901	0.52 (0.37–0.71)	0.84 (0.56–1.26)‡	18,810	89	15,145	0.59 (0.47–0.72)	1.0
MI requiring hospitalization ≥3 days§										
Medicare	2,531	NR	NR	NR	0.64 (0.25–1.65)	4,866	20	3,965	0.50 (0.32–0.77)	1.0
PharMetrics	2,614	3	2,063	0.15 (0.04–0.40)	0.74 (0.19–2.89)	5,505	9	4,472	0.20 (0.10–0.37)	1.0
MarketScan	4,073	4	3,001	0.13 (0.04–0.32)	0.77 (0.24–2.44)	8,439	12	6,729	0.18 (0.10–0.30)	1.0
Combined	9,218	NR	NR	NR	0.70 (0.37–1.34)‡	18,810	41	15,166	0.27 (0.20–0.36)	1.0
Stroke										
Medicare	2,531	11	1,843	0.60 (0.31–1.04)	0.74 (0.36–1.51)	4,866	30	3,964	0.76 (0.52–1.07)	1.0
PharMetrics	2,614	7	2,062	0.34 (0.15–0.67)	1.18 (0.43–3.22)	5,505	11	4,468	0.25 (0.13-–0.43)	1.0
MarketScan	4,073	5	3,001	0.17 (0.06–0.37)	1.33 (0.41–4.25)	8,439	8	6,730	0.12 (0.05–0.23)	1.0
Combined	9,218	23	6,906	0.33 (0.21–0.49)	0.94 (0.56–1.59)‡	18,810	49	15,162	0.32 (0.24–0.42)	1.0
Secondary definition of composite cardiovascular events¶										
Medicare	2,531	28	1,831	1.53 (1.04–2.18)	0.79 (0.51–1.24)	4,866	73	3,944	1.85 (1.46–2.31)	1.0
PharMetrics	2,614	12	2,060	0.58 (0.32–0.99)	0.79 (0.40–1.58)	5,505	32	4,460	0.72 (0.50–1.00)	1.0
MarketScan	4,073	11	2,998	0.37 (0.19–0.64)	1.13 (0.53–2.41)	8,439	21	6,726	0.31 (0.20–0.47)	1.0
Combined	9,218	51	6,889	0.74 (0.56–0.97)	0.85 (0.61–1.19)‡	18,810	126	15,130	0.83 (0.70–0.99)	1.0
Intent-to-treat analysis up to 365 days#										
Composite cardiovascular events										
Medicare	2,531	21	2,009	1.05 (0.66–1.57)	0.72 (0.43–1.21)	4,866	54	3,991	1.35 (1.03–1.75)	1.0
PharMetrics	2,614	12	2,080	0.58 (0.31–0.98)	0.85 (0.42–1.75)	5,505	23	4,338	0.53 (0.34–0.78)	1.0
MarketScan	4,037	10	3,147	0.32 (0.16–0.57)	0.79 (0.37–1.66)	8,439	26	6,447	0.40 (0.27–0.58)	1.0
Combined	9,218	43	7,236	0.59 (0.44–0.79)	0.77 (0.53–1.11)‡	18,810	103	14,776	0.70 (0.57–0.84)	1.0

* Cohorts were propensity score–matched with a 1:3 variable ratio. Propensity score models included >90 covariates, including demographics, prior disease-modifying antirheumatic drug use, cardiovascular comorbidities, medications, and health care utilization. IR = incidence rate; HR = hazard ratio; RA = rheumatoid arthritis; TCZ = tocilizumab; TNFi = tumor necrosis factor inhibitors; 95% CI = 95% confidence interval.

† Per 100 person-years.

‡ Combined using an inverse variance-weighted, fixed-effects model.

§ Not reported (NR) for the Medicare population due to the small size (<11) of the data cell and other cells that could indirectly be used to calculate the small cell count based on the data use agreement with the Centers for Medicare & Medicaid Services.

¶ Defined as a discharge diagnosis of myocardial infarction (MI) in the principal position for any length of hospitalization or a hospital discharge diagnosis of ischemic or hemorrhagic stroke in the principal position.

Exposure status at cohort entry was carried forward until day 365 of follow-up.

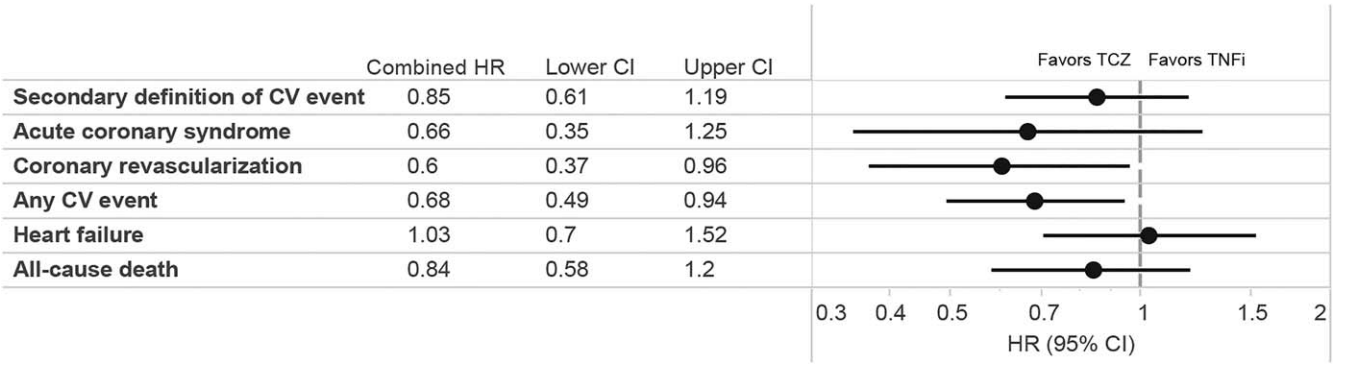

Figure 3. Secondary end points in a 1:3 variable ratio propensity score–matched as-treated analysis of rheumatoid arthritis patients starting treatment with tocilizumab (TCZ) or a tumor necrosis factor inhibitor (TNFi). Hazard ratios (HRs) were combined using an inverse variance-weighted, fixed-effects model. A "secondary definition of cardiovascular (CV) event" refers to a discharge diagnosis of myocardial infarction in the principal position for any length of hospitalization or a hospital discharge diagnosis of ischemic or hemorrhagic stroke in the principal position. "Any CV event" includes myocardial infarction, stroke, coronary revascularization, or acute coronary syndrome. 95% CI = 95% confidence interval.

TCZ or TNFi initiators in the PharMetrics or MarketScan databases did. Within each database, all of the baseline covariates were well-balanced between TCZ and TNFi initiators, with a standardized difference of <10% (30). At baseline, 14.3% of TCZ initiators and 13.5% of TNFi initiators had cardiovascular disease.

Baseline characteristics of the study cohort for each database before propensity score matching are presented in Supplementary Table 2, available on the *Arthritis & Rheumatology* web site at http://onlinelibrary.wiley.com/doi/10.1002/art.40084/abstract. In general, even before propensity score matching, the 2 groups, TCZ and TNFi initiators, were similar with regard to cardiovascular comorbidities, comorbidity index, medication use, and health care utilization patterns. TCZ initiators used a greater number of prior DMARDs and more steroids and opioids at baseline compared with TNFi initiators. Statin use at baseline was also greater in TCZ initiators versus TNFi initiators in the Medicare and PharMetrics databases.

Cardiovascular risk associated with TCZ. During a mean ± SD followup of 0.9 ± 0.7 years and a maximum observational period of 4.5 years for the primary as-treated analysis, in the 1:3 variable ratio propensity score–matched cohort, a total of 125 composite cardiovascular events of MI or stroke (36 in TCZ initiators and 89 in TNFi initiators) were recorded in the 3 databases (Table 2). The overall IR of composite cardiovascular events was 0.52 per 100 person-years in the TCZ group and 0.59 per 100 person-years in the TNFi group. The database-specific IR ranged from 0.3 per 100 person-years (MarketScan) to 0.9 per 100 person-years (Medicare) in the TCZ group and 0.3 per 100 person-years (MarketScan) to 1.3 per 100 person-years (Medicare) in the TNFi group. In general, the IR was 2–3 times higher in the older Medicare population compared with the population in the PharMetrics or MarketScan databases.

The HR for composite cardiovascular events associated with TCZ versus TNFi use was 0.70 (95% CI 0.40–1.24) in the Medicare database, 1.00 (95% CI 0.45–2.22) in the PharMetrics database, and 1.03 (95% CI 0.46–2.34) in the MarketScan database, with a combined HR of 0.84 (95% CI 0.56–1.26, *P* for heterogeneity = 0.7). After accounting for potential overlap between the PharMetrics and MarketScan populations, the 95% CI for the combined HR for composite cardiovascular events associated with TCZ use versus TNFi became slightly wider (combined HR 0.84 [95% CI 0.56–1.27 for 10% overlap and 0.55–1.28 for 20% overlap]). The Kaplan-Meier plots confirmed that there were no differences in rates of composite cardiovascular events between the TCZ and TNFi groups (Supplementary Figure 1, available on the *Arthritis & Rheumatology* web site at http://onlinelibrary.wiley.com/doi/10.1002/art.40084/abstract).

The combined HR (Table 2) for MI associated with TCZ versus TNFi was 0.70 (95% CI 0.37–1.34; *P* for heterogeneity = 1.0), and the HR for stroke was 0.94 (95% CI 0.56–1.59; *P* for heterogeneity = 0.6). Using the secondary definition of composite cardiovascular event (i.e., MI in the principal position for any length of hospitalization or a hospital discharge diagnosis code of ischemic or hemorrhagic stroke), there were a total of 177 composite cardiovascular events (51 in TCZ initiators and 126 in TNFi initiators) in the 3 databases (Table 2). The HR for composite cardiovascular events associated with TCZ versus TNFi use was 0.79 (95% CI 0.51–1.24) in Medicare, 0.79 (95% CI 0.40–1.58) in PharMetrics, and 1.13 (95% CI 0.53–2.41) in MarketScan, with a combined HR of 0.85

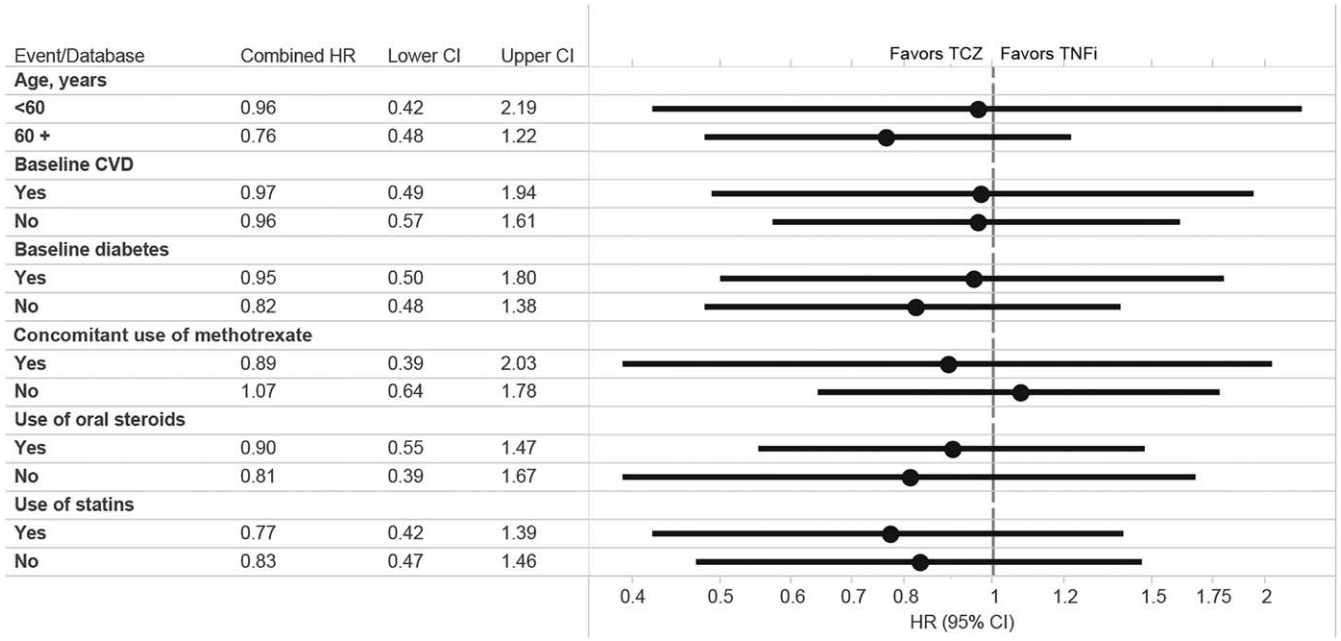

Figure 4. Subgroup analysis in a 1:3 variable ratio propensity score–matched as-treated analysis of rheumatoid arthritis patients starting treatment with tocilizumab (TCZ) or a tumor necrosis factor inhibitor (TNFi). Hazard ratios (HRs) were combined by an inverse variance-weighted, fixed-effects model. For the age <60 subgroup, only PharMetrics and MarketScan data were used since there were no cardiovascular events in the age <60 Medicare population. CVD = cardiovascular disease; 95% CI = 95% confidence interval.

(95% CI 0.61–1.19; *P* for heterogeneity = 0.71). With adjustment for potential overlap between the PharMetrics and MarketScan populations, the combined HR for the secondary definition of composite cardiovascular events was 0.84 (combined HR 0.77 [95% CI 0.53–1.12 for 10% overlap and 0.52–1.13 for 20% overlap]).

The secondary ITT 365-day analysis also showed similar results (Table 2), with a combined HR of 0.77 for composite cardiovascular events associated with TCZ versus TNFi (95% CI 0.53–1.11; *P* for heterogeneity = 0.9). After accounting for potential overlap between the PharMetrics and MarketScan populations, the 95% CI for the combined HR for composite cardiovascular events became slightly wider, but the inference remained the same (combined HR 0.77 [95% CI 0.53–1.12 for 10% overlap and 0.52–1.13 for 20% overlap]). Results from the as-treated analysis for the secondary outcomes also showed no increased risk of various individual cardiovascular end points in the TCZ group compared with the TNFi group (Figure 3). The combined HR for all-cause deaths was 0.84 in the TCZ group versus the TNFi group (95% CI 0.58–1.20; *P* for heterogeneity = 0.2).

Figure 4 summarizes the results from subgroup analyses. TCZ use versus TNFi use was not associated with a greater risk of composite cardiovascular events in a subgroup of patients age <60 years or ≥60 years, or those with baseline cardiovascular disease or diabetes, although the 95% CIs were wide. No association was found between TCZ use and cardiovascular risk in patients who were receiving methotrexate at baseline (combined HR 0.89 [95% CI 0.39–2.03]) or those who were not receiving methotrexate at baseline (combined HR 1.07 [95% CI 0.64–1.78]). The combined HR associated with TCZ versus TNFi was 0.90 (95% CI 0.55–1.47) in patients who were taking oral steroids at baseline and 0.81 (95% CI 0.39–1.67) in those who were not taking oral steroids at baseline. Among patients who were taking statins at baseline, the combined HR associated with TCZ versus TNFi was 0.77 (95% CI 0.42–1.39) for the primary cardiovascular end point, which was similar to the combined HR of 0.83 (95% CI 0.47–1.46) in patients who were not taking statins at baseline.

DISCUSSION

In a number of RCTs and observational studies, TCZ has been shown to increase LDL cholesterol levels. However, the effect of TCZ on clinical cardiovascular risk has not been fully understood. Since RA patients have a nearly 2-fold increased risk of cardiovascular disease and cardiovascular mortality compared with the general population (1,2), increases in LDL cholesterol levels with TCZ have been a concern. In this large US population-based multi-database cohort study of 28,028 patients with RA

who had previously received at least 1 biologic drug, we found no increase in the risk of a composite cardiovascular end point of MI or stroke between TCZ initiators and TNFi initiators. In fact, we found a numeric decrease in risk and ruled out a risk increase of >26% based on the upper limit of the 95% CI for the combined HR. We also did not find an increased risk of secondary end points, including the individual end points of MI, stroke, ACS, coronary revascularization, heart failure, and all-cause mortality, in TCZ initiators compared with TNFi initiators. Furthermore, in patients with a history of cardiovascular disease or diabetes or those who were receiving steroids, statins, or methotrexate at baseline, we consistently found no association of TCZ treatment with increased cardiovascular risk.

This study has important clinical implications. While elevations in lipid levels occur in patients treated with TCZ (12–14), such increases do not appear to be associated with an increased risk of clinical cardiovascular events. Rao et al reported that the risk of major cardiovascular events in patients with RA who were receiving TCZ was associated with control of RA disease activity but not changes in lipid levels based on post hoc analyses of clinical trials and extension studies of TCZ (17). Several studies demonstrated a similar complex relationship between cholesterol levels, disease activity/systemic inflammation, and cardiovascular risk in patients with RA and showed no clear association between LDL cholesterol levels and cardiovascular risk (35–38). In patients with active systemic inflammation such as sepsis or RA, LDL levels tend to be low (37). In other words, generally, systemic inflammation has lipid-lowering effects. Therefore, it may not be surprising to observe elevated levels of total cholesterol or LDL cholesterol with treatment with powerful antiinflammatory biologic drugs such as TCZ. There are also some reports of a significant increase in total cholesterol levels after TNFi treatment, correlating with lower RA disease activity (37,39). Our finding that there was no increased cardiovascular risk with TCZ versus TNFi use is reassuring, particularly given the potential beneficial cardiovascular effects of TNFi seen in several cohort studies (7–9).

This population-based comparative safety study provides much needed data for clinical decision making in the management of RA. Furthermore, a prior cohort study that showed comparative cardiovascular safety of different biologic agents, including TCZ versus abatacept, in patients with RA did not show an elevated risk of incident MI or composite coronary heart disease (40). With the completion of the ENTRACTE study, a postmarketing open-label RCT that examines the risk of cardiovascular events in RA patients treated with TCZ compared with those treated with etanercept, more head-to-head safety data will be available soon.

The main strength of this study is its large size and generalizability, since the study cohort is based on 3 large population-representative insurance databases in the US. Since TCZ is a relatively new therapy, using multiple databases was necessary to achieve an adequate study size. Combining the results from 3 databases, we were able to include a total of 9,218 TCZ initiators after propensity score matching. This study was planned to have at least 80% power to refute a 30% increase in the risk of the primary end point in TCZ initiators versus TNFi initiators. The upper limit of the 95% confidence interval of HR for the primary end point was 1.26. Unlike enrollees in clinical trials, our study cohort is representative of older adults (Medicare) and the working population and their dependents (PharMetrics and MarketScan) in the US. Detailed longitudinal information on patients' drug use in pharmacy claims data linked to comprehensive medical claims is another advantage of the study data sources.

To yield findings with high validity, this study used rigorous pharmacoepidemiologic approaches, such as the inclusion of study drug initiators (i.e., new user design), specific outcome definition, use of an active comparator, and propensity score matching with a variable ratio to perform appropriate statistical control for a large number of confounders and to minimize confounding by indication and immortal time bias (41,42). We required a relatively long baseline period to define "new users" of either TCZ or TNFi and assess patients' baseline characteristics for confounding control. Because TCZ is mostly used as a second-line treatment for RA in routine practice, the requirement of prior biologic or targeted synthetic use in both TCZ and TNFi initiators likely further reduced the degree of confounding by RA duration or severity between the 2 groups. Given known differences in patient demographics and other characteristics across the 3 databases, we used a prespecified analysis plan in each data set separately and combined the results using a meta-analysis technique. Finally, the null association between TCZ use and cardiovascular risk, compared with TNFi use, was consistently observed in all of the prespecified secondary and subgroup analyses.

This study has several limitations. First, since we relied on claims data, we had no data on RA disease duration or activity, seropositivity, systemic inflammation, lipid levels, blood pressure, family history of cardiovascular disease, use of over-the-counter drugs such as aspirin or some nonsteroidal antiinflammatory drugs, smoking, or body mass index, although we captured many proxies of these clinical covariates. Second, while we adjusted for >65 baseline variables potentially related to cardiovascular risk

using propensity score matching, residual confounding cannot be ruled out. Third, there is a potential for outcome misclassification since outcomes were identified with claims-based definitions, although we used validated algorithms with high specificity. Fourth, there is a potential for duplicate person-years between the PharMetrics and MarketScan databases. While the exact degree of overlap between the 2 data sets is unknown, it does not appear to have a substantial impact on our estimates based on a sensitivity analysis accounting for 10–20% overlap. Finally, since the mean follow-up was <1 year for the majority of the study population, the long-term cardiovascular effect of TCZ or TNFi may need to be further examined. However, 7,142 patients (25% of the study cohort) were followed up for >1 year, and 2,271 (8%) were followed up for >2 years in the study. The maximum observational period was 4.5 years in both exposure groups.

In conclusion, this multi-database population-representative cohort study showed no evidence of an increased risk of cardiovascular events in patients with RA who switched from a biologic or targeted synthetic DMARD to TCZ compared with those who switched to a different TNFi. Our results were consistent in secondary and clinically important subgroup analyses.

AUTHOR CONTRIBUTIONS

All authors were involved in drafting the article or revising it critically for important intellectual content, and all authors approved the final version to be published. Dr. Kim had full access to all of the data in the study and takes responsibility for the integrity of the data and the accuracy of the data analysis.

Study conception and design. Kim, Solomon, Gale, Klearman, Sarsour, Schneeweiss.

Acquisition of data. Kim, Rogers, Schneeweiss.

Analysis and interpretation of data. Kim, Solomon, Rogers, Gale, Klearman, Sarsour, Schneeweiss.

ROLE OF THE STUDY SPONSOR

This study was funded by Genentech but solely conducted at the Brigham and Women's Hospital. Genentech provided the funding to conduct the study and obtain the study databases but had no role in the analysis. The sponsor was given the opportunity to make nonbinding comments on interpretation of the data and a draft of the manuscript, but the authors retained the right of publication and to determine the final wording.

REFERENCES

1. Solomon DH, Karlson EW, Rimm EB, Cannuscio CC, Mandl LA, Manson JE, et al. Cardiovascular morbidity and mortality in women diagnosed with rheumatoid arthritis. Circulation 2003; 107:1303–7.
2. Avina-Zubieta JA, Choi HK, Sadatsafavi M, Etminan M, Esdaile JM, Lacaille D. Risk of cardiovascular mortality in patients with rheumatoid arthritis: a meta-analysis of observational studies. Arthritis Rheum 2008;59:1690–7.
3. Meissner Y, Zink A, Kekow J, Rockwitz K, Liebhaber A, Zinke S, et al. Impact of disease activity and treatment of comorbidities on the risk of myocardial infarction in rheumatoid arthritis. Arthritis Res Ther 2016;18:183.
4. Solomon DH, Kremer J, Curtis JR, Hochberg MC, Reed G, Tsao P, et al. Explaining the cardiovascular risk associated with rheumatoid arthritis: traditional risk factors versus markers of rheumatoid arthritis severity. Ann Rheum Dis 2010;69:1920–5.
5. Singh JA, Saag KG, Bridges SL Jr, Akl EA, Bannuru RR, Sullivan MC, et al. 2015 American College of Rheumatology guideline for the treatment of rheumatoid arthritis. Arthritis Rheumatol 2016;68:1–26.
6. Roubille C, Richer V, Starnino T, McCourt C, McFarlane A, Fleming P, et al. The effects of tumour necrosis factor inhibitors, methotrexate, non-steroidal anti-inflammatory drugs and corticosteroids on cardiovascular events in rheumatoid arthritis, psoriasis and psoriatic arthritis: a systematic review and meta-analysis. Ann Rheum Dis 2015;74:480–9.
7. Barnabe C, Martin BJ, Ghali WA. Systematic review and meta-analysis: anti–tumor necrosis factor α therapy and cardiovascular events in rheumatoid arthritis. Arthritis Care Res (Hoboken) 2011;63:522–9.
8. Greenberg JD, Kremer JM, Curtis JR, Hochberg MC, Reed G, Tsao P, et al. Tumour necrosis factor antagonist use and associated risk reduction of cardiovascular events among patients with rheumatoid arthritis. Ann Rheum Dis 2011;70:576–82.
9. Solomon DH, Curtis JR, Saag KG, Lii J, Chen L, Harrold LR, et al. Cardiovascular risk in rheumatoid arthritis: comparing TNF-α blockade with nonbiologic DMARDs. Am J Med 2013; 126:730.e9–17.
10. Desai RJ, Rao JK, Hansen RA, Fang G, Maciejewski M, Farley J. Tumor necrosis factor-α inhibitor treatment and the risk of incident cardiovascular events in patients with early rheumatoid arthritis: a nested case-control study. J Rheumatol 2014;41: 2129–36.
11. Dixon WG, Watson KD, Lunt M, Hyrich KL, British Society for Rheumatology Biologics Register Control Centre Consortium, Silman AJ, et al, on behalf of the British Society for Rheumatology Biologics Register. Reduction in the incidence of myocardial infarction in patients with rheumatoid arthritis who respond to anti–tumor necrosis factor α therapy: results from the British Society for Rheumatology Biologics Register. Arthritis Rheum 2007;56:2905–12.
12. Jones G, Sebba A, Gu J, Lowenstein MB, Calvo A, Gomez-Reino JJ, et al. Comparison of tocilizumab monotherapy versus methotrexate monotherapy in patients with moderate to severe rheumatoid arthritis: the AMBITION study. Ann Rheum Dis 2010;69:88–96.
13. Nishimoto N, Yoshizaki K, Miyasaka N, Yamamoto K, Kawai S, Takeuchi T, et al. Treatment of rheumatoid arthritis with humanized anti–interleukin-6 receptor antibody: a multicenter, double-blind, placebo-controlled trial. Arthritis Rheum 2004;50: 1761–9.
14. Smolen JS, Beaulieu A, Rubbert-Roth A, Ramos-Remus C, Rovensky J, Alecock E, et al. Effect of interleukin-6 receptor inhibition with tocilizumab in patients with rheumatoid arthritis (OPTION study): a double-blind, placebo-controlled, randomised trial. Lancet 2008;371:987–97.
15. Gabay C, McInnes IB, Kavanaugh A, Tuckwell K, Klearman M, Pulley J, et al. Comparison of lipid and lipid-associated cardiovascular risk marker changes after treatment with tocilizumab or adalimumab in patients with rheumatoid arthritis. Ann Rheum Dis 2016;75:1806–12.
16. Gabay C, Emery P, van Vollenhoven R, Dikranian A, Alten R, Pavelka K, et al. Tocilizumab monotherapy versus adalimumab monotherapy for treatment of rheumatoid arthritis (ADACTA): a randomised, double-blind, controlled phase 4 trial. Lancet 2013;381:1541–50.
17. Rao VU, Pavlov A, Klearman M, Musselman D, Giles JT, Bathon JM, et al. An evaluation of risk factors for major

adverse cardiovascular events during tocilizumab therapy. Arthritis Rheumatol 2015;67:372–80.
18. Hennessy S, Freeman C, Cunningham F. US government claims databases. In: Strom B, Kimmel S, Hennessy S, editors. Pharmacoepidemiology. 5th ed. Philadelphia: Wiley-Blackwell; 2012. p. 209–23.
19. Kappelman MD, Rifas-Shiman SL, Kleinman K, Ollendorf D, Bousvaros A, Grand RJ, et al. The prevalence and geographic distribution of Crohn's disease and ulcerative colitis in the United States. Clin Gastroenterol Hepatol 2007;5:1424–9.
20. Quek RG, Fox KM, Wang L, Li L, Gandra SR, Wong ND. A US claims-based analysis of real-world lipid-lowering treatment patterns in patients with high cardiovascular disease risk or a previous coronary event. Am J Cardiol 2016;117:495–500.
21. Kim SY, Servi A, Polinski JM, Mogun H, Weinblatt ME, Katz JN, et al. Validation of rheumatoid arthritis diagnoses in health care utilization data. Arthritis Res Ther 2011;13:R32.
22. Kiyota Y, Schneeweiss S, Glynn RJ, Cannuscio CC, Avorn J, Solomon DH. Accuracy of Medicare claims-based diagnosis of acute myocardial infarction: estimating positive predictive value on the basis of review of hospital records. Am Heart J 2004;148:99–104.
23. Andrade SE, Harrold LR, Tjia J, Cutrona SL, Saczynski JS, Dodd KS, et al. A systematic review of validated methods for identifying cerebrovascular accident or transient ischemic attack using administrative data. Pharmacoepidemiol Drug Saf 2012;21 Suppl 1:100–28.
24. Kumamaru H, Judd SE, Curtis JR, Ramachandran R, Hardy NC, Rhodes JD, et al. Validity of claims-based stroke algorithms in contemporary Medicare data: reasons for geographic and racial differences in stroke (REGARDS) study linked with Medicare claims. Circ Cardiovasc Qual Outcomes 2014;7:611–9.
25. Ting G, Schneeweiss S, Scranton R, Katz JN, Weinblatt ME, Young M, et al. Development of a health care utilisation data-based index for rheumatoid arthritis severity: a preliminary study. Arthritis Res Ther 2008;10:R95.
26. Gagne JJ, Glynn RJ, Avorn J, Levin R, Schneeweiss S. A combined comorbidity score predicted mortality in elderly patients better than existing scores. J Clin Epidemiol 2011;64:749–59.
27. Schneeweiss S, Rassen JA, Glynn RJ, Myers J, Daniel GW, Singer J, et al. Supplementing claims data with outpatient laboratory test results to improve confounding adjustment in effectiveness studies of lipid-lowering treatments. BMC Med Res Methodol 2012;12:180.
28. Rubin DB. Estimating causal effects from large data sets using propensity scores. Ann Intern Med 1997;127:757–63.
29. Rassen JA, Shelat AA, Myers J, Glynn RJ, Rothman KJ, Schneeweiss S. One-to-many propensity score matching in cohort studies. Pharmacoepidemiol Drug Saf 2012;21 Suppl 2:69–80.
30. Austin PC. Optimal caliper widths for propensity-score matching when estimating differences in means and differences in proportions in observational studies. Pharm Stat 2011;10:150–61.
31. Franklin JM, Rassen JA, Ackermann D, Bartels DB, Schneeweiss S. Metrics for covariate balance in cohort studies of causal effects. Stat Med 2014;33:1685–99.
32. Cummings P, McKnight B, Weiss NS. Matched-pair cohort methods in traffic crash research. Accid Anal Prev 2003;35:131–41.
33. Walker AM, Jick H, Hunter JR, Danford A, Watkins RN, Alhadeff L, et al. Vasectomy and non-fatal myocardial infarction. Lancet 1981;1:13–5.
34. Munder T, Brutsch O, Leonhart R, Gerger H, Barth J. Researcher allegiance in psychotherapy outcome research: an overview of reviews. Clin Psychol Rev 2013;33:501–11.
35. Liao KP, Liu J, Lu B, Solomon DH, Kim SC. Association between lipid levels and major adverse cardiovascular events in rheumatoid arthritis compared to non–rheumatoid arthritis patients. Arthritis Rheumatol 2015;67:2004–10.
36. Myasoedova E, Crowson CS, Kremers HM, Roger VL, Fitz-Gibbon PD, Therneau TM, et al. Lipid paradox in rheumatoid arthritis: the impact of serum lipid measures and systemic inflammation on the risk of cardiovascular disease. Ann Rheum Dis 2011;70:482–7.
37. Robertson J, Peters MJ, McInnes IB, Sattar N. Changes in lipid levels with inflammation and therapy in RA: a maturing paradigm. Nat Rev Rheumatol 2013;9:513–23.
38. Navarro-Millán I, Yang S, DuVall SL, Chen L, Baddley J, Cannon GW, et al. Association of hyperlipidaemia, inflammation and serological status and coronary heart disease among patients with rheumatoid arthritis: data from the National Veterans Health Administration. Ann Rheum Dis 2016;75:341–7.
39. Seriolo B, Paolino S, Sulli A, Fasciolo D, Cutolo M. Effects of anti-TNF-α treatment on lipid profile in patients with active rheumatoid arthritis. Ann N Y Acad Sci 2006;1069:414–9.
40. Zhang J, Xie F, Yun H, Chen L, Muntner P, Levitan EB, et al. Comparative effects of biologics on cardiovascular risk among older patients with rheumatoid arthritis. Ann Rheum Dis 2016; 75:1813–8.
41. Ray WA. Evaluating medication effects outside of clinical trials: new-user designs. Am J Epidemiol 2003;158:915–20.
42. Yoshida K, Solomon DH, Kim SC. Active-comparator design and new-user design in observational studies. Nat Rev Rheumatol 2015;11:437–41.

ARTHRITIS & RHEUMATOLOGY
Vol. 69, No. 6, June 2017, pp 1165–1175
DOI 10.1002/art.40066

Anti–Citrullinated Protein Antibodies Are Associated With Neutrophil Extracellular Traps in the Sputum in Relatives of Rheumatoid Arthritis Patients

M. Kristen Demoruelle,[1] Kylie K. Harrall,[1] Linh Ho,[1] Monica M. Purmalek,[2] Nickie L. Seto,[2] Heather M. Rothfuss,[3] Michael H. Weisman,[4] Joshua J. Solomon,[5] Aryeh Fischer,[1] Yuko Okamoto,[1] Lindsay B. Kelmenson,[1] Mark C. Parish,[1] Marie Feser,[1] Chelsie Fleischer,[1] Courtney Anderson,[1] Michael Mahler,[6] Jill M. Norris,[1] Mariana J. Kaplan,[2] Brian D. Cherrington,[3] V. Michael Holers,[1] and Kevin D. Deane[1]

Objective. **Studies suggest that rheumatoid arthritis (RA)–related autoimmunity is initiated at a mucosal site. However, the factors associated with the mucosal generation of this autoimmunity are unknown, especially in individuals who are at risk of future RA. Therefore, we tested anti–cyclic citrullinated peptide (anti-CCP) antibodies in the sputum of RA-free first-degree relatives (FDRs) of RA patients and patients with classifiable RA.**

Methods. **We evaluated induced sputum and serum samples from 67 FDRs and 20 RA patients for IgA anti-CCP and IgG anti-CCP, with cutoff levels for positivity determined in a control population. Sputum was also evaluated for cell counts, neutrophil extracellular traps (NETs) using sandwich enzyme-linked immunosorbent assays for protein/nucleic acid complexes, and total citrulline.**

Results. **Sputum was positive for IgA and/or IgG anti-CCP in 14 of 20 RA patients (70%) and 17 of 67 FDRs (25%), including a portion of FDRs who were serum anti-CCP negative. In the FDRs, elevations of sputum IgA and IgG anti-CCP were associated with elevated sputum cell counts and NET levels. IgA anti-CCP was associated with ever smoking and with elevated sputum citrulline levels.**

Conclusion. **Anti-CCP is elevated in the sputum of FDRs, including seronegative FDRs, suggesting that the lung may be a site of anti-CCP generation in this population. The association of anti-CCP with elevated cell counts and NET levels in FDRs supports a hypothesis that local airway inflammation and NET formation may drive anti-CCP production in the lung and may promote the early stages of RA development. Longitudinal studies are needed to follow the evolution of these processes relative to the development of systemic autoimmunity and articular RA.**

Seropositive rheumatoid arthritis (RA) is characterized by disease-associated autoantibodies, including

The contents of this article are solely the responsibility of the authors and do not necessarily represent the official views of the National Institutes of Health.

Supported by the NIH (National Institute of Arthritis and Musculoskeletal and Skin Diseases [NIAMS] grant AR-066712, National Institute of Allergy and Infectious Diseases grants AI-101990 and AI-103023, Office of Research on Women's Health grant HD-057022, National Center for Advancing Translational Sciences grant TR-001082, and NIAMS Intramural Research Program project ZIAAR-041199), the Rheumatology Research Foundation (Scientist Development Awards to Drs. Demoruelle and Kelmenson and a Disease-Targeted Research Initiative award to Dr. Holers), and the Walter S. and Lucienne Driskill Foundation.

[1]M. Kristen Demoruelle, MD, Kylie K. Harrall, MS, Linh Ho, BS, Aryeh Fischer, MD, Yuko Okamoto, MD, Lindsay B. Kelmenson, MD, Mark C. Parish, BS, Marie Feser, MPH, Chelsie Fleischer, MA, Courtney Anderson, BS, Jill M. Norris, PhD, V. Michael Holers, MD, Kevin D. Deane, MD, PhD: University of Colorado Denver at Aurora; [2]Monica M. Purmalek, BA, Nickie L. Seto, BS, Mariana J. Kaplan, MD: NIH, Bethesda, Maryland; [3]Heather M. Rothfuss, PhD, Brian D. Cherrington, PhD: University of Wyoming, Laramie; [4]Michael H. Weisman, MD: Cedars-Sinai Medical Center, Los Angeles, California; [5]Joshua J. Solomon, MD: National Jewish Health, Denver, Colorado; [6]Michael Mahler, PhD: Inova Diagnostics, San Diego, California.

Drs. Holers and Deane are co-holders of a patent owned by Stanford University related to the use of biomarkers to predict rheumatoid arthritis development.

Address correspondence to M. Kristen Demoruelle, MD, University of Colorado School of Medicine, Division of Rheumatology, 1775 Aurora Court, Mail Stop B-115, Aurora, CO 80045. E-mail: Kristen.Demoruelle@UCDenver.edu.

Submitted for publication September 27, 2016; accepted in revised form February 2, 2017.

antibodies to citrullinated proteins/peptides (ACPAs) that are commonly measured using anti–cyclic citrullinated peptide (anti-CCP) assays. In established RA, ACPA isotypes, including IgA and IgG, are prevalent, specific, and associated with higher levels of disease activity, suggesting that they play an important role in the pathogenesis of RA (1–4). Understanding the development of ACPA isotypes could therefore provide further insight into the cause of RA.

It is well established that ACPAs can be present for years prior to the onset of inflammatory arthritis, during a period of systemic autoimmunity associated with RA that can be called preclinical RA and can be defined as the presence of circulating RA-related autoantibodies prior to the onset of clinically apparent synovitis (2–10). Importantly, individuals without classifiable RA who have circulating ACPAs do not exhibit synovitis, as assessed by physical examination (5,11), imaging with ultrasound or magnetic resonance (5,11–13), or synovial biopsy (12,13). These findings strongly suggest that in order to understand the initial steps in the generation of ACPAs, studies must examine individuals who have not yet developed clinically apparent synovitis and classifiable RA. These data also indicate that ACPAs originate at a site outside the joint.

As to where that site is, emerging data support the hypothesis that ACPAs may be initially generated at a mucosal surface (2–5,14–20). For example, serum levels of IgA ACPAs are elevated in populations who are at risk of developing RA, including first-degree relatives (FDRs) of RA patients (2–4). The strong association between smoking, lung disease, and ACPA-positive RA further support the idea that the lung mucosa may be a particularly relevant site of ACPA generation (17–19). In addition, our group previously demonstrated that circulating RA-related autoantibodies were associated with airway abnormalities in the absence of inflammatory arthritis (5), and ACPAs were detectable in the lung of a portion of inflammatory arthritis–free FDRs, as determined by testing of induced sputum samples (14).

While these data are intriguing, the mechanisms that trigger local ACPA production in the lung are unknown. However, understanding the factors that may drive the initial development of ACPAs and IgA ACPAs in particular, given the role of IgA in mucosal immunity, may ultimately lead to novel approaches to the prediction, treatment, and prevention of RA.

Several candidates may be potential factors associated with ACPA formation at the mucosal surface, including exposure to environmental agents such as smoking and local inflammation, which can lead to citrullination. In addition, multiple studies have suggested a role of neutrophil extracellular trap (NET) formation (or, NETosis) in RA. NETosis is a peptidylarginine deiminase type 4 (PAD4)–mediated process by which neutrophils decondense and externalize their DNA in complex with neutrophil cytoplasmic granule proteins, such as myeloperoxidase (MPO) and neutrophil elastase (NE) (21–23). Enhanced NETosis has been associated with ACPAs peripherally and in the joints of patients with established RA (24–26). While NET formation in sputum has been associated with lung disease (27–29), it is unknown whether NETs are associated with ACPAs in the lung of subjects at risk of developing RA.

In order to explore factors associated with the generation of APCAs in the lung, we evaluated inflammatory arthritis–free FDRs of RA patients, who are at higher risk of developing RA. We investigated levels of isotype-specific anti-CCP as well as a variety of factors, including demographic features, environmental exposures, genetic factors, and sputum biomarkers including cell counts, total citrullination, and markers of NETosis, in induced sputum samples from FDRs.

PATIENTS AND METHODS

Study subjects. Subjects were recruited from the Studies of the Etiology of RA (SERA) cohort, which is described in detail elsewhere (30,31). Briefly, SERA evaluates in a prospective manner the FDRs of RA patients, with these FDRs being at elevated risk of RA based on their family history of disease (32,33), making them a reasonable group in which to evaluate the earliest stages of RA. For this study, SERA subjects were recruited from the Denver, CO, study site between January 2011 and October 2015.

FDRs. We recruited SERA FDRs who had no evidence of inflammatory arthritis. FDRs were not selected based on serum anti-CCP status, but as our group and others have reported, inflammatory arthritis–free FDRs have a higher prevalence of serum anti-CCP positivity compared to the general population, including 9.5% positivity for the commercially available anti–CCP-3.1 antibody (IgG/IgA; Inova Diagnostics) (3,6).

Patients with early RA. We recruited patients who had classifiable RA that had been diagnosed within the past 1 year and were seropositive for anti–CCP-3.1. RA patients were recruited sequentially from rheumatology clinics or from SERA research study visits if a subject developed incident inflammatory arthritis that met classification criteria during prospective follow-up. RA was confirmed by medical chart review, and all patients met the American College of Rheumatology/European League Against Rheumatism 2010 classification criteria (34).

Healthy control subjects. In order to determine cutoff levels for anti-CCP isotype positivity, we recruited healthy control subjects from the community through local advertisements, seeking those who were serum anti–CCP-3.1 negative, did not have RA or inflammatory arthritis, and did not have an FDR with RA.

All study procedures were approved by the Colorado Multiple Institutional Review Board. Informed consent was obtained from all study subjects.

Study visit. All study subjects underwent collection of paired samples of blood and sputum on the same day, except for 3 subjects, who had sputum collected within 2 weeks of blood samples. Subjects without RA underwent a joint-focused interview and examination of 66 joints by a trained rheumatologist (MKD, LBK, or KDD) to assure that there was no clinically evident inflammatory arthritis. Standardized questionnaires were used to obtain demographic information and self-reported histories of smoking and chronic lung disease.

Genetic testing. Blood was tested for the presence of alleles containing the shared epitope (SE) using previously described methods (30). The following alleles were considered to contain the SE: DRB1*04:01, 04:04, 04:05, 04:08, 04:09, 04:10, and DR1 01:01 and 01:02.

Sputum collection. Induced sputum was collected and processed using established protocols, which are described in detail elsewhere (14). Briefly, sputum samples were collected over 15 minutes using hypertonic nebulized saline. The entire sputum sample was diluted with phosphate buffered saline (PBS), followed by syringe-based mechanical homogenization. Samples collected after September 2013 underwent manual cell counts, with differential cell counts performed using a hemocytometer and cytocentrifugation. Cell counts were reported as the number $\times 10^4$/ml. To minimize salivary contamination of sputum samples, subjects underwent oral wash prior to sputum collection. In addition, per established methods, subjects were asked to spit any saliva during the sputum collection into a separate plastic container, and they were instructed to only use the sputum collection cup when producing a sputum sample from coughing (35). Only samples that were consistent with lower airways origin, as demonstrated by <10 squamous epithelial cells/high-power field on light microscopy or $<80\%$ squamous epithelial cells on cell differential (35,36), were used for the analyses.

After homogenization, samples were centrifuged and proteinase inhibitors (phenylmethylsulfonyl fluoride) and EDTA were added to the supernatant. A mucolytic agent, such as dithiothreitol, was not used so as to avoid the destruction of disulfide bonds that could affect antibody structure and conformation. All sputum biomarker testing was performed on the cell-free supernatants, except for the cell count and differential cell count, which were performed prior to centrifugation. Because sputum testing was performed on diluted samples, all sputum results reported herein have been multiplied by the sample's dilution factor, which was calculated based on the amount of PBS added and the original weight of the sample.

Serum and sputum testing for IgA and IgG anti-CCP. Serum and sputum samples underwent enzyme-linked immunosorbent assay (ELISA) for IgA anti-CCP and IgG anti-CCP at the University of Colorado Division of Rheumatology Clinical Research Laboratory, using a CCP-3 plate and the respective conjugate (for research only; Inova Diagnostics). A positive control sample was provided by the manufacturer for each isotype. The levels in sputum and serum are reported as relative units based on the optical density (OD) of the test sample divided by the OD of the positive control. This approach allowed us to account for any plate-to-plate variation. Cutoff levels for positivity of the anti-CCP isotypes were set at a level that was present in $<5\%$ of our healthy control subjects, thereby corresponding to a level at or above the 95th percentile in controls. Of note, anti-CCP isotype cutoff levels for both serum and sputum were set using the same control group.

In this study, serum and sputum anti-CCP levels were measured in duplicate wells. For sputum, the mean coefficient of variation between wells was 4.8% for IgA anti-CCP and 5.3% for IgG anti-CCP. To further validate the anti-CCP isotype assays, we tested serum from 6 subjects without RA, 3 of whom were previously found to have high anti-CCP isotype levels and 3 had low levels. We determined intraassay variability for each isotype by testing serum from each subject in 10 wells each. The mean coefficient of variation was 8.4% for IgA anti-CCP and 8.0% for IgG anti-CCP.

Total Ig testing. In subjects with adequate sputum volume available after anti-CCP testing, the levels of total IgA and IgG (in mg/dl) were also tested in the sputum (Siemens BN II nephelometry cerebrospinal fluid assessment system) and serum (Beckman-Coulter Synchron nephelometry system).

NET levels. In samples collected prior to January 2015 that had adequate sputum volume following anti-CCP and Ig testing, the level of NETosis was measured as NET remnants in cell-free supernatant of sputum. Specifically, NET-associated protein–nucleic acid complexes were quantified using a sandwich ELISA that detects complexes of DNA–MPO and DNA–NE, as previously described (37), and as follows: for DNA–MPO complexes, high-binding 96-well ELISA microplates were incubated overnight at 4°C with mouse anti-human MPO (clone 4A4; AbD Serotec) in coating buffer from a Cell Death Detection ELISA kit (Roche). After blocking with 1% bovine serum albumin, plates were incubated overnight at 4°C with 10% sputum in blocking buffer, washed and peroxidase-conjugated anti-DNA (Roche) was added for 1.5 hours at room temperature. Tetramethylbenzidine substrate (Sigma) was then added, and absorbance was measured at 450 nm after addition of stop reagent (Sigma).

The methods for the DNA–NE complexes were similar as those for the DNA–MPO complexes. The antibody used to coat plates was rabbit anti-human NE (Calbiochem). After overnight incubation with sputum, plates were incubated for 1 hour at room temperature with mouse anti–double-stranded DNA monoclonal antibody (Millipore), followed by horseradish peroxidase–conjugated anti-mouse IgG (Bio-Rad). The procedure was then completed as for the DNA–MPO complexes.

Total citrulline content. In sputum samples that were tested for NETs, the total citrulline level was quantified (in nmoles/ml) using the detection step of the Color Development Reagent assay and quantified as previously described (38–40). To avoid detection of urea and methylurea with this assay, a 20-fold excess of urease was added to each sputum sample for 15 minutes at 25°C prior to testing.

Statistical analysis. Prevalence of positivity was compared between groups using chi-square/Fisher's exact test and within groups using McNemar's test. Because of a non-normal distribution of anti-CCP isotype levels, nonparametric testing was used to compare anti-CCP levels across groups (Mann-Whitney U test) and to perform correlation analyses between anti-CCP levels and other factors (Spearman's correlation coefficient). In addition, linear regression was used to evaluate the relationship between sputum anti-CCP levels and sputum cell counts as well as between NET and citrulline levels,

Table 1. Characteristics of the study subjects

	FDRs of RA patients (n = 67)*	RA patients (n = 20)†	Healthy controls (n = 70)
Age, median (range) years	52 (23–77)	54 (33–66)	36 (20–71)‡
Female, no. (%)	47 (70)	13 (65)	56 (80)
Non-Hispanic white, no. (%)	48 (72)	9 (45)§	49 (70)
Ever smoker, no. (%)	24 (36)	9 (45)	19 (27)
Current smoker, no. (%)	5 (8)	7 (35)¶	0 (0)‡
Shared epitope (≥1 allele), no. (%)#	42 (63)	10 (59)	24 (35)‡
History of chronic lung disease, no. (%)**	14 (21)	3 (15)	8 (11)

* Sera from 7 of the 67 rheumatoid arthritis (RA)–free first-degree relatives (FDRs) (10%) were positive for anti–cyclic citrullinated peptide 3.1 (anti–CCP-3.1). There was no significant difference in age, sex, race, history of smoking, shared epitope positivity, or chronic lung disease between the CCP-3.1–seropositive and the CCP-3.1–seronegative groups.
† Thirteen of the 20 RA patients (65%) were taking nonbiologic disease-modifying antirheumatic drugs.
‡ $P < 0.01$ versus the FDR and RA groups, as determined by Kruskal-Wallis test for age and by chi-square or Fisher's exact test for the other features.
§ $P = 0.03$ versus the FDR group, as determined by chi-square test.
¶ $P < 0.01$ versus the FDR group, as determined by Fisher's exact test.
# Blood for shared epitope testing was available from only 17 of the 20 RA patients and 69 of the 70 controls.
** The presence of chronic lung disease was determined by self-report using a questionnaire that asked whether subjects had a health care provider–diagnosed history of asthma, emphysema, chronic bronchitis, bronchiectasis, interstitial lung disease, lung cancer, pulmonary artery hypertension, obstructive sleep apnea, or other chronic lung disease.

accounting for adjustment variables when necessary. We report the T statistic and *P* value for each relationship. In these linear models, sputum anti-CCP levels and cell counts were log-transformed to meet the assumption of normality for linear regression. The potential confounders of age, sex, ever smoking, SE positivity, and citrulline level were included in the models and were removed at a level of $\alpha > 0.10$.

Analyses were performed using SPSS (version 23) and SAS (version 9.4). Figures were generated in GraphPad Prism (version 7).

RESULTS

Characteristics of the study subjects. We evaluated 67 FDRs, 20 RA patients, and 70 healthy control subjects. The characteristics of these subjects are shown in Table 1. There was no statistically significant difference in age, sex, presence of ≥1 SE allele, history of ever smoking, or chronic lung disease between the FDRs and the RA patients. RA patients were more likely to be current smokers and less likely to be non-Hispanic white. Compared to the FDRs and RA patients, the controls were younger, less likely to be smokers, and less likely to be SE positive.

Sputum IgA and IgG anti-CCP positivity in FDRs and RA patients. Seventeen of the 67 FDRs (25.4%) had IgA anti-CCP and/or IgG anti-CCP in their sputum (Table 2). Among the FDR group, there was a nonsignificant trend toward greater prevalence of sputum IgA anti-CCP positivity than IgG anti-CCP positivity (16 of 67 [23.9%] versus 11 of 67 [16.4%]; $P = 0.13$). Data on the controls are included in Figure 1, and because this group was used to establish cutoff values, these subjects were not studied relative to the FDR or RA populations.

Table 2. Sputum and serum anti-CCP positivity in RA patients and FDRs

	FDRs of RA patients (n = 67)	RA patients (n = 20)
Sputum anti-CCP isotype, no. (%)		
IgA+ and/or IgG+*	17 (25)	14 (70)†
IgA+/IgG+	10 (15)	8 (40)‡
IgA+/IgG–	6 (9)	0 (0)
IgA–/IgG+	1 (1)	6 (30)†
IgA–/IgG–	50 (75)	6 (30)†
Serum anti-CCP isotype, no. (%)		
IgA+ and/or IgG+§	12 (18)	20 (100)†
IgA+/IgG+	2 (3)	12 (60)†
IgA+/IgG–	8 (12)	1 (5)
IgA–/IgG+	2 (3)	7 (35)†
IgA–/IgG–	55 (82)	0 (0)†

* For sputum, the rheumatoid arthritis (RA)–free first-degree relatives (FDRs) more often had IgA than IgG anti–cyclic citrullinated peptide (anti-CCP) ($P = 0.13$ by McNemar's test), whereas the RA patients more often had IgG than IgA anti-CCP ($P = 0.03$ by McNemar's test).
† $P < 0.01$ for the prevalence of positivity versus the FDR group, as determined by chi-square test.
‡ $P = 0.03$ for the prevalence of positivity versus the FDR group, as determined by chi-square test.
§ For serum, the FDRs more often had IgA than IgG anti-CCP ($P = 0.11$ by McNemar's test), whereas the RA patients more often had IgG than IgA anti-CCP ($P = 0.07$ by McNemar's test).

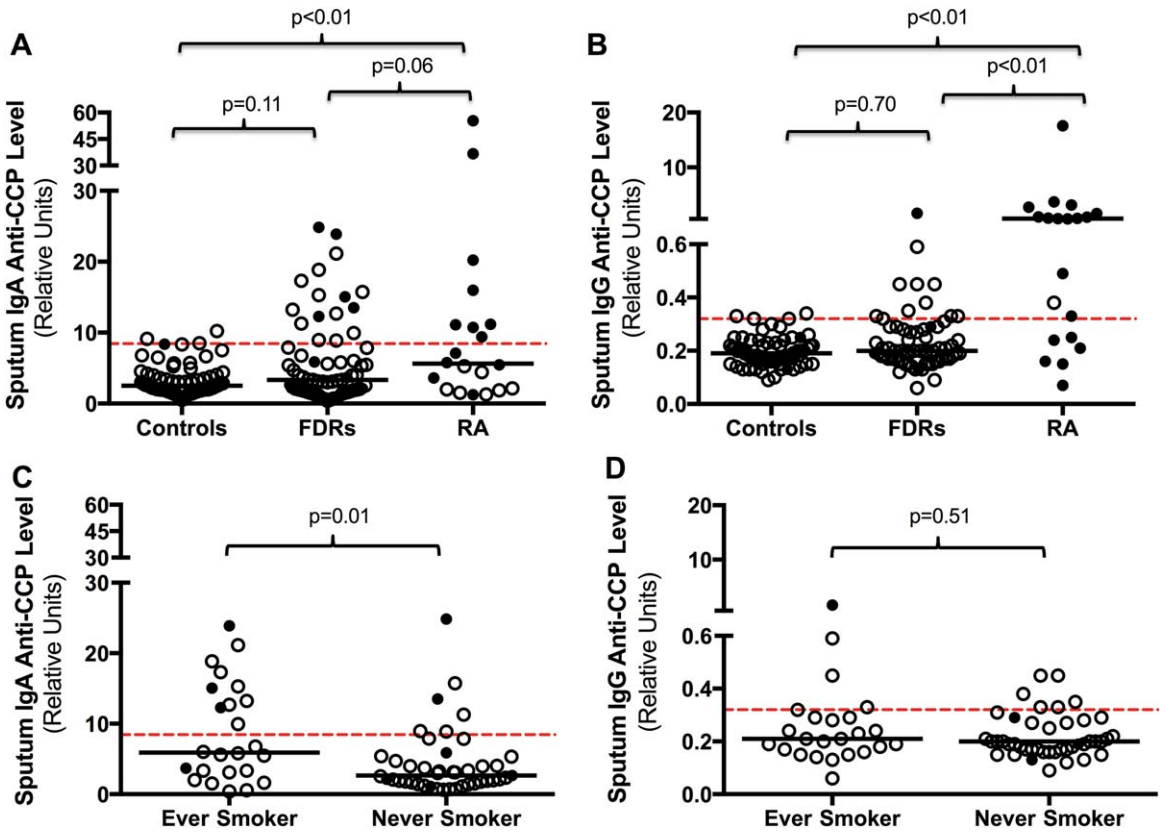

Figure 1. Distribution of sputum IgA and IgG anti–cyclic citrullinated peptide (anti-CCP) levels in all study subjects and in rheumatoid arthritis (RA)–free first-degree relatives (FDRs) stratified by smoking status. **A** and **B,** Distribution of sputum IgA anti-CCP (**A**) and IgG anti-CCP (**B**) in healthy control subjects, FDRs, and RA patients. **C** and **D,** Distribution of sputum IgA anti-CCP (**C**) and IgG anti-CCP (**D**) in FDRs stratified by history of smoking (ever smoked versus never smoked). *P* values were determined by nonparametric testing. Open symbols represent serum anti-CCP–negative subjects and solid symbols represent serum anti-CCP–positive subjects; horizontal lines show the median. Broken line indicates the cutoff level for anti-CCP positivity.

Fourteen of 20 RA patients (70.0%) were positive for IgA anti-CCP and/or IgG anti-CCP in sputum, which was significantly higher than in the FDRs (70.0% versus 25.4%; $P < 0.01$). RA patients also demonstrated higher rates of positivity for sputum IgG anti-CCP compared to the FDRs (14 of 20 [70.0%] versus 11 of 67 [16.4%]; $P < 0.01$), whereas sputum IgA anti-CCP positivity was not significantly higher in RA patients as compared to FDRs (8 of 20 [40.0%] versus 16 of 67 [23.9%]; $P = 0.26$). In addition, sputum IgA and IgG anti-CCP levels were highest in the RA patients (Figures 1A and B).

When comparing rates of autoantibody positivity within groups, the rates of sputum IgG anti-CCP positivity were higher than IgA anti-CCP in the RA patients (14 of 20 [70.0%] versus 8 of 20 [40.0%]; $P = 0.03$). In the FDRs, IgG anti-CCP was not significantly more positive than IgA anti-CCP (11 of 67 [16.4%] versus 16 of 67 [23.9%]; $P = 0.13$).

Comparison of sputum and serum anti-CCP. To evaluate the relationship between sputum and serum anti-CCP positivity, we stratified the FDRs based on their serum anti-CCP isotype status. Overall, 12 of the 67 FDRs (17.9%) and 20 of the 20 RA patients (100%) were positive for serum IgA and/or IgG anti-CCP.

Among the FDRs, 10 were serum IgA anti-CCP positive, of whom 5 (50%) were also sputum IgA anti-CCP positive. There were 57 serum IgA anti-CCP negative FDRs, of whom 11 (19%) were sputum IgA anti-CCP positive (Supplementary Figure 1A, available on the *Arthritis & Rheumatology* web site at http://onlinelibrary.wiley.com/doi/10.1002/art.40066/abstract). Furthermore, there were 4 serum IgG anti-CCP–positive FDRs, of whom 1 (25%) was also sputum IgG anti-CCP positive, and there were 63 serum IgG anti-CCP–negative FDRs, of whom 10 (16%) were sputum IgG anti-CCP positive (Supplementary Figure 1B). Among

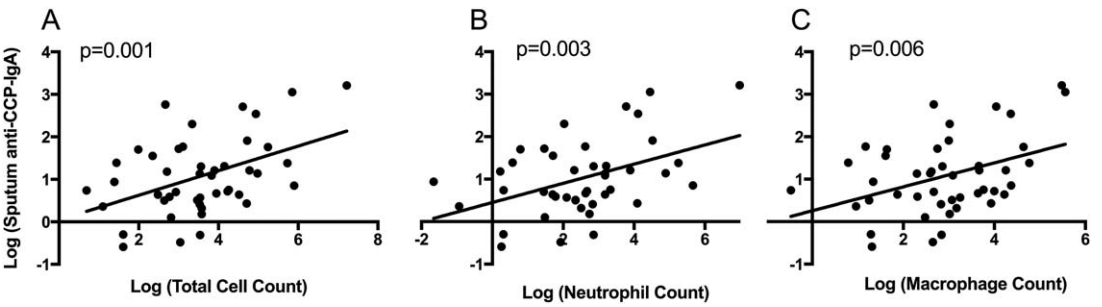

Figure 2. Relationship between sputum IgA anti–cyclic citrullinated peptide (anti-CCP) levels and sputum cell counts in rheumatoid arthritis–free first-degree relatives. Log-transformed levels of the sputum total cell count (**A**), total neutrophil count (**B**), and total macrophage count (**C**) are plotted against the log-transformed levels of sputum IgA anti-CCP. *P* values were calculated using linear regression.

the RA patients, 13 were serum IgA anti-CCP positive, of whom 8 (62%) were also sputum IgA anti-CCP positive, and 7 were serum IgA anti-CCP negative, of whom none were sputum IgA anti-CCP positive (Supplementary Figure 1C). In addition, there were 19 serum IgG anti-CCP–positive RA patients, of whom 13 (68%) were also sputum IgG anti-CCP positive, and there was 1 serum IgG anti-CCP–negative RA patient who was sputum IgG anti-CCP positive (Supplementary Figure 1D).

To evaluate the potential for translocation of anti-CCP from serum to sputum, we compared the ratios of anti-CCP to total Ig levels for each isotype in sputum and serum, with the rationale that a higher ratio at one site supports the idea that the antibody is generated at that site (41,42). In the sputum anti-CCP–positive FDRs, 11 of 14 (79%) had a higher ratio of IgA anti-CCP to total IgA in the sputum compared to the serum, and 9 of 10 (90%) had a higher ratio of IgG anti-CCP to total IgG in the sputum, which supports the notion that the anti-CCP was generated in the lung in the majority of these subjects. In the sputum anti-CCP–positive RA patients, 3 of 8 (38%) had a higher ratio of IgA anti-CCP to total IgA in the sputum, and 11 of 13 (85%) had a higher ratio of IgG anti-CCP to total IgG in the sputum. In addition, the median total IgA and IgG levels in sputum did not differ between the FDRs and the RA patients, but the total sputum IgA levels in both groups was higher than that in the controls (Supplementary Figure 2, available at http://onlinelibrary.wiley.com/doi/10.1002/art.40066/abstract).

Comparison of subject characteristics and sputum anti-CCP isotypes. Because smoking has been associated with an increased risk of serum anti-CCP–positive RA and is relevant in sputum studies (17), we analyzed subjects stratified by smoking history. In the FDRs, sputum IgA, but not IgG, anti-CCP positivity was significantly higher in ever smokers compared to never smokers (Figures 1C and D). A similar, but not significant, association was seen in the RA patients (Supplementary Figure 3, available at http://onlinelibrary.wiley.com/doi/10.1002/art.40066/abstract).

In the FDRs, there were no associations between sputum IgA or IgG anti-CCP positivity and sex, race, ≥1 SE allele, or history of lung disease (data not shown). Correlation analysis did not identify a significant correlation between age and sputum anti-CCP isotype levels.

Similarly, in RA patients and control subjects, there were no significant correlations or associations between sputum anti-CCP isotypes and age, sex, race, SE positivity, or history of lung disease (data not shown).

Sputum cell counts and sputum anti-CCP isotypes. The known predominant cell types in sputum are neutrophils and macrophages (35,36), and we focused our analyses on these cell types. In the FDRs, there was a median of 12.3×10^4/ml neutrophils (interquartile range [IQR] 4.3–26.3×10^4/ml) and 17.5×10^4/ml macrophages (IQR 8.2–47.1×10^4/ml). In the RA patients, there was a median of 24.7×10^4/ml neutrophils (IQR 6.5–44.0×10^4/ml) and 12.7×10^4/ml macrophages (IQR 4.6–27.2×10^4/ml).

Using regression analyses, we evaluated the association of anti-CCP levels with signs of airway inflammation as measured by sputum total cell counts (excluding squamous epithelial cells), and neutrophil and macrophage counts. In the FDRs, sputum IgA anti-CCP was significantly associated with total ($t = 3.5$, $P = 0.001$), neutrophil ($t = 3.2$, $P = 0.003$), and macrophage ($t = 2.9$, $P = 0.006$) counts (Figure 2). Similar associations were demonstrated for sputum IgG anti-CCP and total ($t = 1.8$, $P = 0.080$), neutrophil ($t = 2.5$, $P = 0.018$), and macrophage ($t = 2.0$, $P = 0.048$) counts in this group of subjects (Figure 3). In RA patients, sputum IgA anti-CCP was significantly associated with the total cell count ($t = 2.3$, $P = 0.039$), but no other significant associations were seen between sputum IgA or IgG anti-CCP levels and cell counts in these patients (data not shown).

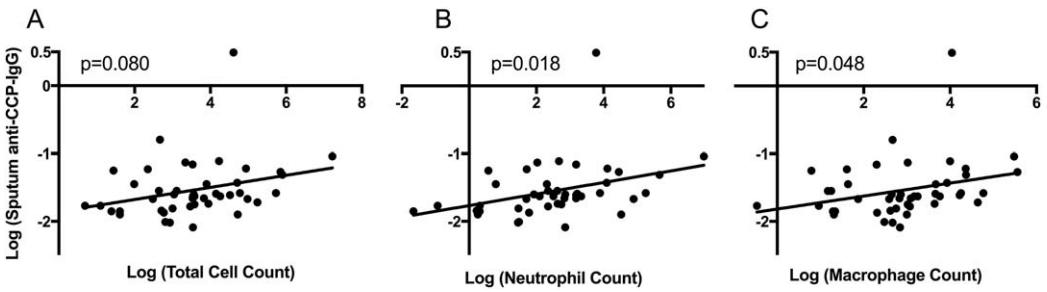

Figure 3. Relationship between sputum IgG anti–cyclic citrullinated peptide (anti-CCP) levels and sputum cell counts in rheumatoid arthritis–free first-degree relatives. Log-transformed levels of the sputum total cell count (**A**), total neutrophil count (**B**), and total macrophage count (**C**) are plotted against the log-transformed levels of sputum IgG anti-CCP. *P* values were calculated using linear regression.

Sputum neutrophil and macrophage counts were higher in sputum anti-CCP isotype–positive FDRs compared to sputum anti-CCP isotype–negative healthy controls, with a median neutrophil count of 43.8×10^4/ml (IQR 7.6–85.5×10^4/ml) versus 9.2×10^4/ml (IQR 3.9–31.8×10^4/ml) ($P = 0.14$) and a median macrophage count of 56.9×10^4/ml (IQR 20.5–240.5×10^4/ml) versus 17.2×10^4/ml (IQR 6.7–41.5×10^4/ml) ($P < 0.01$). However, sputum levels of neutrophils and macrophages were similar in sputum anti-CCP isotype–negative FDRs and controls ($P = 0.69$ and $P = 0.58$, respectively).

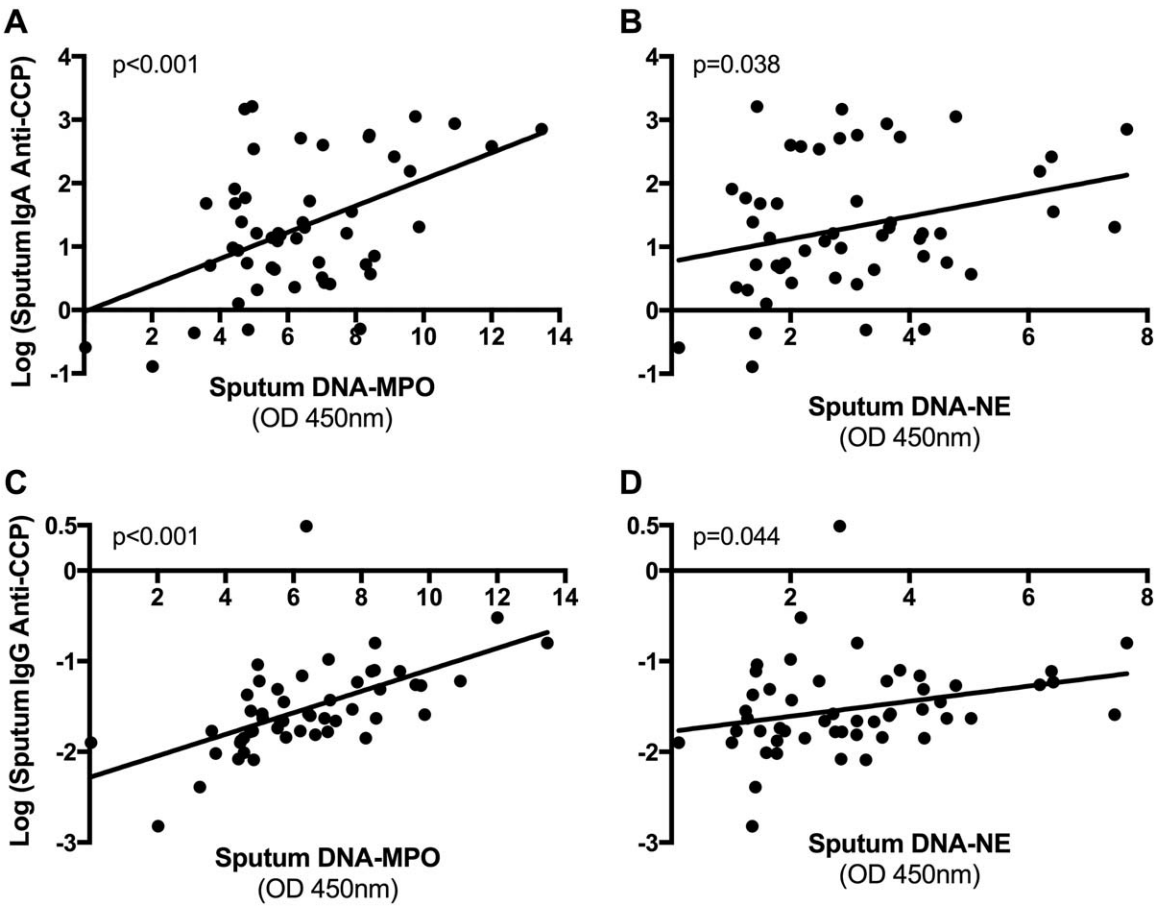

Figure 4. Associations of sputum anti–cyclic citrullinated peptide (anti-CCP) isotypes and sputum neutrophil extracellular trap (NET) levels in rheumatoid arthritis–free first-degree relatives. Log-transformed sputum NET levels, as measured by DNA–myeloperoxidase (MPO) complexes (**A** and **C**) and DNA–neutrophil elastase (NE) complexes (**B** and **D**), are plotted against the log-transformed levels of sputum IgA (**A** and **B**) and IgG (**C** and **D**) anti-CCP. *P* values were calculated using linear regression.

Sputum NET levels and sputum anti-CCP isotypes. We next studied the association between sputum levels of anti-CCP and NETs. Using log-transformed anti-CCP levels, sputum levels of IgA and IgG anti-CCP in the FDRs were significantly associated with sputum levels of NETs, as determined by measuring DNA–MPO and DNA–NE complexes (Figure 4). In analyses adjusting for ever smoking and citrulline levels, the association between sputum IgA anti-CCP and NET levels in the FDRs remained significant (by DNA–MPO complexes, $t = 3.75$, $P < 0.01$; by DNA–NE complexes, $t = 2.10$, $P = 0.04$). In particular, for every 1-unit increase in NET level as measured by DNA–MPO complexes, there was an increase of 1.20 (95% confidence interval [95% CI] 1.09–1.33) in sputum IgA anti-CCP levels and 1.13 (95% CI 1.07–1.18) in sputum IgG anti-CCP. Similarly, for every 1-unit increase in NET level as measured by DNA–NE complexes, there was an increase of 1.17 (95% CI 1.01–1.37) in sputum IgA anti-CCP and 1.09 (95% CI 1.00–1.18) in sputum IgG anti-CCP. No significant associations between sputum IgA or IgG anti-CCP levels and NET levels were found in RA patients (data not shown).

Sputum citrulline levels and sputum anti-CCP isotypes. In the FDRs, there was a significant association between sputum citrulline and sputum IgA anti-CCP levels ($t = 3.2$, $P < 0.01$), but not between sputum citrulline and sputum IgG anti-CCP ($t = 0.7$, $P = 0.50$). Sputum citrulline levels were higher in ever smokers compared to never smokers, but in analyses adjusted for ever smoking, sputum IgA anti-CCP remained significantly associated with the total citrulline level ($t = 2.7$, $P < 0.01$). In the RA patients, there were no significant associations between sputum IgA or IgG anti-CCP levels and total citrulline levels (data not shown).

Of note, as presented in Supplementary Figure 4 (available at http://onlinelibrary.wiley.com/doi/10.1002/art.40066/abstract), due to sample volume restrictions, a subset of 51 FDRs and 9 RA patients had sufficient sputum volume available for testing of NET and citrulline levels. To ensure that there was no selection bias in the subjects who had larger volumes of sputum, we compared FDRs and RA patients who did and did not undergo NET and citrulline testing. In these analyses, we found no significant difference in age, sex, race, SE positivity, history of ever smoking, serum anti-CCP positivity, or sputum anti-CCP positivity.

DISCUSSION

Similar to our previous work (14) but studying an expanded cohort and newly discriminating isotype-specific ACPA reactivity, we found that elevations of ACPA levels in the lung/sputum, as characterized by anti-CCP isotypes, is prevalent in a portion of FDRs (25%) and RA patients (70%). Of particular interest, this study is the first to demonstrate IgA anti-CCP in sputum, and we determined that IgA and IgG anti-CCP are associated with increased sputum cell counts and NET remnants in FDRs. Importantly, these findings provide support for the conclusion that sputum ACPA elevations are associated with local airway inflammation. This study also provides the first evidence that NET formation is associated with ACPAs in the lung, suggesting that NETosis may drive ACPA production locally in FDRs who are at an elevated risk of developing RA.

The relationship between ACPA elevations and NET formation in FDRs is of particular interest for several reasons. Elevated NETosis has been associated with established RA, can expose citrullinated proteins to the immune system, including RA-associated proteins such as citrullinated histone H3, and can release PAD4, which could citrullinate other local proteins (24–26,43). Although it is possible that NET formation could have been induced in our study during sputum collection or processing, this is less likely given that all samples underwent the same protocols, while elevated NET remnants were identified only in a subset. In addition, previous studies have applied immunostaining techniques that visually demonstrate the formation of NETs from sputum neutrophils (28,29). It will be important to understand the mechanisms contributing to higher sputum NETosis levels in these FDRs. Specific questions to be addressed are whether neutrophils from FDRs are more likely than those from non-FDRs to undergo NETosis and whether increased NETosis in the sputum can be generated by another source (e.g., microbiota, inflammatory cytokines, or ACPAs triggered by another mechanism). A recent study showed that microbial factors may affect neutrophil-related citrullination through pore-forming mechanisms (44); therefore, other mechanisms aside from NETosis by which neutrophils or other factors may contribute to mucosal citrullination need to be explored.

Because we wanted to study factors associated with the earliest steps of ACPA formation and in order to enhance our ability to find RA-related autoimmunity, we focused on FDRs as a population that is known to be at elevated risk of developing ACPAs (2,3,6). It is worth noting, however, that we did not find associations between sputum ACPA isotypes and cell counts or NET levels in the RA patients. This lack of association could be due to the small number of RA patients studied or their use of immunosuppressive medications. However,

it could also be that the mechanisms that drive ACPAs change during the evolution of disease or after the onset of synovitis in RA. For example, only after arthritis is present in RA have ACPAs been identified in synovial tissues (42,45). This will need to be explored in prospective evaluations of the evolution of sputum and serum ACPAs and other biomarkers in individuals who develop classifiable RA.

Citrullination in the lung has been associated with smoking and inflammation (16,20). In the present study, we demonstrated that sputum IgA, but not IgG, ACPAs were associated with smoking and increased citrulline levels. Although the Color Development Reagent assay quantifies ureido groups that can include citrullinated as well as homocitrullinated peptides, this finding suggests that perhaps IgA ACPA is more likely than IgG ACPA to be formed in response to nonspecific inflammation in the lung and that other factors may be required to drive IgG ACPA formation. This finding also highlights the fact that different ACPA isotypes may play different roles in the pathogenesis of RA. Previous studies demonstrated that serum IgG ACPA positivity is higher in patients with established RA as compared to unaffected FDRs, who were more often serum IgA ACPA positive (2,3). In our study, we found similar associations in serum as well as sputum. Although prospective studies are needed, this finding raises the question as to whether the development of IgG ACPA is an important step in the transition from preclinical RA to clinically apparent arthritis.

We also found that a subset of FDRs demonstrated sputum ACPA isotype positivity in the absence of serum ACPA positivity. This finding further validates our previous work showing that the lung may be a site where ACPAs originate, and indeed, we have demonstrated in subset analyses that sputum IgA anti-CCP does not appear to be from a salivary source (see Supplementary Materials, available at http://onlinelibrary.wiley.com/doi/10.1002/art.40066/abstract). However, we also found some FDRs who were serum ACPA positive in the absence of sputum ACPA positivity, which suggests that in some FDRs, ACPAs may have originated at a site outside the lung. This underscores the importance of comprehensively examining additional mucosal surfaces as potential sites of initiation of RA-related autoimmunity.

While FDRs are at increased risk of developing RA-related autoimmunity, it is clear that the number of FDRs demonstrating sputum ACPA positivity exceeds the number that statistically will develop classifiable RA. This suggests that local ACPA formation may be necessary but not sufficient to progress to systemic RA-related autoimmunity and eventually arthritis. In addition, sputum ACPAs could have been translocated from the serum in the FDRs. We believe this is unlikely because many FDRs were ACPA positive only in sputum, and the ratios of Ig to anti-CCP were higher in sputum as compared to serum for the majority of FDRs. Furthermore, the primary goal in the selection of our control population was to set cutoff levels for sputum ACPA positivity. Our control subjects were younger than the FDRs or RA patients. Because there was not an association between age and ACPA level, this difference was unlikely to influence the establishment of a positive cutoff level.

Additional longitudinal studies of the prevalence and evolution of sputum ACPAs in individuals who develop classifiable RA and in carefully matched controls will be needed to better understand these issues. Specifically, studies should be conducted to validate the diagnostic accuracy of sputum ACPA isotypes for ultimate progression to classifiable RA, as well as to explore the mechanisms by which ACPA generation at a mucosal surface may occur in broader populations, perhaps as a natural response to mucosal inflammation. These latter studies are especially important if the detection of sputum autoantibodies becomes a method by which to identify subjects who may be at risk of developing RA.

Emerging data suggest that antibody reactivity to native or noncitrullinated/arginine peptides may play a role in the early development of autoimmunity in RA (19,46,47). Older studies have demonstrated that in non-RA populations, serum ACPA reactivity can be nonspecific or cross-reactive with arginine peptides (48). While our study only tested antibody reactivity to the citrullinated CCP-3 plate substrate, based on these other studies, it would be expected that a portion of our subjects could have antibodies to native proteins. Further studies are needed to address whether antibodies to native proteins precede the development of ACPAs in FDRs, whether FDRs demonstrate simultaneous generation of antibodies to citrullinated and noncitrullinated targets, and whether sputum ACPAs in FDRs are less specific and cross-react with noncitrullinated antigens.

In conclusion, ACPA isotypes as measured by anti-CCP are present in the sputum of a portion of FDRs and subjects with early classifiable disease. In FDRs, sputum ACPA is associated with elevated cell counts and NET remnants, which supports the idea that the lung plays an important role in the early phases of RA-related autoimmunity. Longitudinal and additional mechanism-based studies in broader populations are needed to further investigate this relationship.

AUTHOR CONTRIBUTIONS

All authors were involved in drafting the article or revising it critically for important intellectual content, and all authors approved the final version to be published. Dr. Demoruelle had full access to all of the data in the study and takes responsibility for the integrity of the data and the accuracy of the data analysis.

Study conception and design. Demoruelle, Rothfuss, Kaplan, Cherrington, Holers, Deane.

Acquisition of data. Demoruelle, Purmalek, Rothfuss, Weisman, Solomon, Fischer, Kelmenson, Parish, Feser, Fleischer, Anderson, Norris, Kaplan, Cherrington, Holers, Deane.

Analysis and interpretation of data. Demoruelle, Harrall, Ho, Purmalek, Seto, Rothfuss, Okamoto, Kelmenson, Mahler, Kaplan, Cherrington, Holers, Deane.

ADDITIONAL DISCLOSURES

Author Mahler is an employee of Inova Diagnostics.

REFERENCES

1. Svard A, Kastbom A, Reckner-Olsson A, Skogh T. Presence and utility of IgA-class antibodies to cyclic citrullinated peptides in early rheumatoid arthritis: the Swedish TIRA project. Arthritis Res Ther 2008;10:R75.
2. Barra L, Scinocca M, Saunders S, Bhayana R, Rohekar S, Racape M, et al. Anti–citrullinated protein antibodies in unaffected first-degree relatives of rheumatoid arthritis patients. Arthritis Rheum 2013;65:1439–47.
3. Arlestig L, Mullazehi M, Kokkonen H, Rocklov J, Rönnelid J, Dahlqvist SR. Antibodies against cyclic citrullinated peptides of IgG, IgA and IgM isotype and rheumatoid factor of IgM and IgA isotype are increased in unaffected members of multicase rheumatoid arthritis families from northern Sweden. Ann Rheum Dis 2012;71:825–9.
4. Kokkonen H, Mullazehi M, Berglin E, Hallmans G, Wadell G, Rönnelid J, et al. Antibodies of IgG, IgA and IgM isotypes against cyclic citrullinated peptide precede the development of rheumatoid arthritis. Arthritis Res Ther 2011;13:R13.
5. Demoruelle MK, Weisman MH, Simonian PL, Lynch DA, Sachs PB, Pedraza IF, et al. Airways abnormalities and rheumatoid arthritis–related autoantibodies in subjects without arthritis: early injury or initiating site of autoimmunity? Arthritis Rheum 2012;64:1756–61.
6. Demoruelle MK, Parish MC, Derber LA, Kolfenbach JR, Hughes-Austin JM, Weisman MH, et al. Performance of anti–cyclic citrullinated peptide assays differs in subjects at increased risk of rheumatoid arthritis and subjects with established disease. Arthritis Rheum 2013;65:2243–52.
7. Deane KD, O'Donnell CI, Hueber W, Majka DS, Lazar AA, Derber LA, et al. The number of elevated cytokines and chemokines in preclinical seropositive rheumatoid arthritis predicts time to diagnosis in an age-dependent manner. Arthritis Rheum 2010;62:3161–72.
8. Rantapää-Dahlqvist S, de Jong BA, Berglin E, Hallmans G, Wadell G, Stenlund H, et al. Antibodies against cyclic citrullinated peptide and IgA rheumatoid factor predict the development of rheumatoid arthritis. Arthritis Rheum 2003;48:2741–9.
9. Sokolove J, Bromberg R, Deane KD, Lahey LJ, Derber LA, Chandra PE, et al. Autoantibody epitope spreading in the preclinical phase predicts progression to rheumatoid arthritis. PLoS One 2012;7:e35296.
10. Van de Stadt LA, Witte BI, Bos WH, van Schaardenburg D. A prediction rule for the development of arthritis in seropositive arthralgia patients. Ann Rheum Dis 2013;72:1920–6.
11. Van de Stadt LA, Bos WH, Meursinge Reynders M, Wieringa H, Turkstra F, van der Laken CJ, et al. The value of ultrasonography in predicting arthritis in auto-antibody positive arthralgia patients: a prospective cohort study. Arthritis Res Ther 2010; 12:R98.
12. De Hair MJ, van de Sande MG, Ramwadhdoebe TH, Hansson M, Landewé R, van der Leij C, et al. Features of the synovium of individuals at risk of developing rheumatoid arthritis: implications for understanding preclinical rheumatoid arthritis. Arthritis Rheumatol 2014;66:513–22.
13. Van de Sande MG, de Hair MJ, van der Leij C, Klarenbeek PL, Bos WH, Smith MD, et al. Different stages of rheumatoid arthritis: features of the synovium in the preclinical phase. Ann Rheum Dis 2011;70:772–7.
14. Willis VC, Demoruelle MK, Derber LA, Chartier-Logan CJ, Parish MC, Pedraza IF, et al. Sputum autoantibodies in patients with established rheumatoid arthritis and subjects at risk of future clinically apparent disease. Arthritis Rheum 2013;65:2545–54.
15. Reynisdottir G, Karimi R, Joshua V, Olsen H, Hensvold AH, Harju A, et al. Structural changes and antibody enrichment in the lungs are early features of anti–citrullinated protein antibody–positive rheumatoid arthritis. Arthritis Rheumatol 2014;66:31–9.
16. Lugli EB, Correia RE, Fischer R, Lundberg K, Bracke KR, Montgomery AB, et al. Expression of citrulline and homocitrulline residues in the lungs of non-smokers and smokers: implications for autoimmunity in rheumatoid arthritis. Arthritis Res Ther 2015;17:9.
17. Klareskog L, Stolt P, Lundberg K, Kallberg H, Bengtsson C, Grunewald J, et al. A new model for an etiology of rheumatoid arthritis: smoking may trigger HLA–DR (shared epitope)–restricted immune reactions to autoantigens modified by citrullination. Arthritis Rheum 2006;54:38–46.
18. Fischer A, Solomon JJ, du Bois RM, Deane KD, Olson AL, Fernandez-Perez ER, et al. Lung disease with anti-CCP antibodies but not rheumatoid arthritis or connective tissue disease. Respir Med 2012;106:1040–7.
19. Janssen KM, de Smit MJ, Brouwer E, de Kok FA, Kraan J, Altenburg J, et al. Rheumatoid arthritis-associated autoantibodies in non-rheumatoid arthritis patients with mucosal inflammation: a case-control study. Arthritis Res Ther 2015;17:174.
20. Makrygiannakis D, Hermansson M, Ulfgren AK, Nicholas AP, Zendman AJ, Eklund A, et al. Smoking increases peptidylarginine deiminase 2 enzyme expression in human lungs and increases citrullination in BAL cells. Ann Rheum Dis 2008;67:1488–92.
21. Brinkmann V, Reichard U, Goosmann C, Fauler B, Uhlemann Y, Weiss DS, et al. Neutrophil extracellular traps kill bacteria. Science 2004;303:1532–5.
22. Papayannopoulos V, Metzler KD, Hakkim A, Zychlinsky A. Neutrophil elastase and myeloperoxidase regulate the formation of neutrophil extracellular traps. J Cell Biol 2010;191:677–91.
23. Wang Y, Li M, Stadler S, Correll S, Li P, Wang D, et al. Histone hypercitrullination mediates chromatin decondensation and neutrophil extracellular trap formation. J Cell Biol 2009;184:205–13.
24. Khandpur R, Carmona-Rivera C, Vivekanandan-Giri A, Gizinski A, Yalavarthi S, Knight JS, et al. NETs are a source of citrullinated autoantigens and stimulate inflammatory responses in rheumatoid arthritis. Sci Transl Med 2013;5:178ra40.
25. Spengler J, Lugonja B, Ytterberg AJ, Zubarev RA, Creese AJ, Pearson MJ, et al. Release of active peptidyl arginine deiminases by neutrophils can explain production of extracellular citrullinated autoantigens in rheumatoid arthritis synovial fluid. Arthritis Rheumatol 2015;67:3135–45.
26. Sur Chowdhury C, Giaglis S, Walker UA, Buser A, Hahn S, Hasler P. Enhanced neutrophil extracellular trap generation in rheumatoid arthritis: analysis of underlying signal transduction pathways and potential diagnostic utility. Arthritis Res Ther 2014;16:R122.
27. Pedersen F, Marwitz S, Holz O, Kirsten A, Bahmer T, Waschki B, et al. Neutrophil extracellular trap formation and extracellular DNA in sputum of stable COPD patients. Respir Med 2015;109: 1360–2.

28. Wright TK, Gibson PG, Simpson JL, McDonald VM, Wood LG, Baines KJ. Neutrophil extracellular traps are associated with inflammation in chronic airway disease. Respirology 2016;21:467–75.
29. Obermayer A, Stoiber W, Krautgartner WD, Klappacher M, Kofler B, Steinbacher P, et al. New aspects on the structure of neutrophil extracellular traps from chronic obstructive pulmonary disease and in vitro generation. PLoS One 2014;9:e97784.
30. Kolfenbach JR, Deane KD, Derber LA, O'Donnell C, Weisman MH, Buckner JH, et al. A prospective approach to investigating the natural history of preclinical rheumatoid arthritis (RA) using first-degree relatives of probands with RA. Arthritis Rheum 2009;61:1735–42.
31. Deane KD, Striebich CC, Goldstein BL, Derber LA, Parish MC, Feser ML, et al. Identification of undiagnosed inflammatory arthritis in a community health fair screen. Arthritis Rheum 2009;61:1642–9.
32. Frisell T, Holmqvist M, Kallberg H, Klareskog L, Alfredsson L, Askling J. Familial risks and heritability of rheumatoid arthritis: role of rheumatoid factor/anti–citrullinated protein antibody status, number and type of affected relatives, sex, and age. Arthritis Rheum 2013;65:2773–82.
33. Sparks JA, Chen CY, Hiraki LT, Malspeis S, Costenbader KH, Karlson EW. Contributions of familial rheumatoid arthritis or lupus and environmental factors to risk of rheumatoid arthritis in women: a prospective cohort study. Arthritis Care Res (Hoboken) 2014;66:1438–46.
34. Aletaha D, Neogi T, Silman AJ, Funovits J, Felson DT, Bingham CO III, et al. 2010 rheumatoid arthritis classification criteria: an American College of Rheumatology/European League Against Rheumatism collaborative initiative. Arthritis Rheum 2010;62:2569–81.
35. Gershman NH, Wong HH, Liu JT, Mahlmeister MJ, Fahy JV. Comparison of two methods of collecting induced sputum in asthmatic subjects. Eur Respir J 1996;9:2448–53.
36. In 't Veen JC, de Gouw HW, Smits HH, Sont JK, Hiemstra PS, Sterk PJ, et al. Repeatability of cellular and soluble markers of inflammation in induced sputum from patients with asthma. Eur Respir J 1996;9:2441–7.
37. Lood C, Blanco LP, Purmalek MM, Carmona-Rivera C, de Ravin SS, Smith CK, et al. Neutrophil extracellular traps enriched in oxidized mitochondrial DNA are interferogenic and contribute to lupus-like disease. Nat Med 2016;22:146–53.
38. Kearney PL, Bhatia M, Jones NG, Yuan L, Glascock MC, Catchings KL, et al. Kinetic characterization of protein arginine deiminase 4: a transcriptional corepressor implicated in the onset and progression of rheumatoid arthritis. Biochemistry 2005;44:10570–82.
39. Knuckley B, Causey CP, Jones JE, Bhatia M, Dreyton CJ, Osborne TC, et al. Substrate specificity and kinetic studies of PADs 1, 3, and 4 identify potent and selective inhibitors of protein arginine deiminase 3. Biochemistry 2010;49:4852–63.
40. Knipp M, Vasak M. A colorimetric 96-well microtiter plate assay for the determination of enzymatically formed citrulline. Anal Biochem 2000;286:257–64.
41. Masson-Bessiere C, Sebbag M, Durieux JJ, Nogueira L, Vincent C, Girbal-Neuhauser E, et al. In the rheumatoid pannus, anti-filaggrin autoantibodies are produced by local plasma cells and constitute a higher proportion of IgG than in synovial fluid and serum. Clin Exp Immunol 2000;119:544–52.
42. Snir O, Widhe M, Hermansson M, von Spee C, Lindberg J, Hensen S, et al. Antibodies to several citrullinated antigens are enriched in the joints of rheumatoid arthritis patients. Arthritis Rheum 2010;62:44–52.
43. Sohn DH, Rhodes C, Onuma K, Zhao X, Sharpe O, Gazitt T, et al. Local joint inflammation and histone citrullination in a murine model of the transition from preclinical autoimmunity to inflammatory arthritis. Arthritis Rheumatol 2015;67:2877–87.
44. Konig MF, Abusleme L, Reinholdt J, Palmer RJ, Teles RP, Sampson K, et al. Aggregatibacter actinomycetemcomitans-induced hypercitrullination links periodontal infection to autoimmunity in rheumatoid arthritis. Sci Transl Med 2016;8:369ra176.
45. Humby F, Bombardieri M, Manzo A, Kelly S, Blades MC, Kirkham B, et al. Ectopic lymphoid structures support ongoing production of class-switched autoantibodies in rheumatoid synovium. PLoS Med 2009;6:e1.
46. Brink M, Hansson M, Rönnelid J, Klareskog L, Rantapää Dahlqvist S. The autoantibody repertoire in periodontitis: a role in the induction of autoimmunity to citrullinated proteins in rheumatoid arthritis? Antibodies against uncitrullinated peptides seem to occur prior to the antibodies to the corresponding citrullinated peptides. Ann Rheum Dis 2014;73:e46.
47. Konig MF, Giles JT, Nigrovic PA, Andrade F. Antibodies to native and citrullinated RA33 (hnRNP A2/B1) challenge citrullination as the inciting principle underlying loss of tolerance in rheumatoid arthritis. Ann Rheum Dis 2016;75:2022–8.
48. Kakumanu P, Yamagata H, Sobel ES, Reeves WH, Chan EK, Satoh M. Patients with pulmonary tuberculosis are frequently positive for anti–cyclic citrullinated peptide antibodies, but their sera also react with unmodified arginine-containing peptide. Arthritis Rheum 2008;58:1576–81.
49. Svard A, Kastbom A, Sommarin Y, Skogh T. Salivary IgA antibodies to cyclic citrullinated peptides (CCP) in rheumatoid arthritis. Immunobiology 2013;218:232–7.

ARTHRITIS & RHEUMATOLOGY
Vol. 69, No. 6, June 2017, pp 1176–1186
DOI 10.1002/art.40053

Persistence of Disease-Associated Anti–Citrullinated Protein Antibody–Expressing Memory B Cells in Rheumatoid Arthritis in Clinical Remission

Adam J. Pelzek,[1] Caroline Grönwall,[1] Pamela Rosenthal,[1] Jeffrey D. Greenberg,[1] Mandy McGeachy,[2] Larry Moreland,[2] William F. C. Rigby,[3] and Gregg J. Silverman[1]

Objective. **In rheumatoid arthritis (RA), autoreactive B cells are pathogenic drivers and sources of anti–citrullinated protein antibodies (ACPAs) that are a diagnostic biomarker and predictor of worse long-term prognosis. Yet, the immunobiologic significance of persistent ACPA production at the cellular level is poorly understood. This study was undertaken to investigate the representation of ACPA-expressing switched-memory B cells in RA.**

Methods. **In a cross-sectional study of RA patients, we investigated the presence of continued defects in immune homeostasis as a function of disease activity. Using an enzyme-linked immunosorbent assay (ELISA) and a sensitive multiplex bead-based immunoassay, we characterized fine binding antibody specificities in sera, synovial fluid (SF), and B cell culture supernatants. In this manner, we determined the frequency and epitope reactivity patterns of ACPAs produced by SF B cells and switched-memory blood B cells and compared the latter to serum ACPA levels and disease activity scores.**

Results. **Cultured B cells from SF were shown to spontaneously secrete ACPAs, while constitutive IgG autoantibody production by peripheral blood mononuclear cells (PBMCs) was substantially less frequent. After in vitro stimulation, PBMCs secreted IgG ACPA that was overwhelmingly from switched-memory B cells, across all patient groups treated with methotrexate and/or a tumor necrosis factor inhibitor. Intriguingly, the frequencies of ACPA-expressing switched-memory B cells significantly correlated with serum IgG anti–cyclic citrullinated peptide 3 ($r = 0.57$, $P = 0.003$). Moreover, treatment-induced clinical remission had little or no effect on the circulating burden of switched-memory ACPA-expressing B cells, in part explaining the continued dysregulation of humoral immunity.**

Conclusion. **Our findings rationalize why therapeutic cessation most often results in disease reactivation and clinical flare. Hence, a clinical disease activity score is not a reliable indicator of the resolution of pathologic recirculating B cell autoimmunity.**

Rheumatoid arthritis (RA) is a chronic inflammatory disease affecting ~1–2% of Western populations that can lead to joint destruction, disability, and early mortality (1,2). Disease is postulated to be initiated by an inflammatory response in periodontal tissue, pulmonary airways, and/or the intestine (3–6). Progression to tissue injury is linked to a specific breach in immunologic tolerance to autoantigens generated by a posttranslational enzymatic process, citrullination, that modifies the side chains of arginine residues. In fact, circulating anti–citrullinated protein antibodies (ACPAs), which recognize a progressively expanding number of citrullinated protein epitopes, may arise years before symptomatic joint

Supported by the NIH (National Institute of Allergy and Infectious Diseases [NIAID] grants R01-AI-090118, R01-AI-068063, and N01-AR-4-2271 [to Dr. Silverman], National Institute of Arthritis and Musculoskeletal and Skin Diseases grant R01-AR42455 [to Dr. Silverman], and NIAID training grant T32-AI-100853 [to NYU School of Medicine, Immunology & Inflammation]), the American Recovery and Reinvestment Act (supplement to Dr. Silverman), the Rheumatology Research Foundation of the American College of Rheumatology (Disease-Targeted Innovative Research grant to Dr. Silverman), the P. Robert Majumder Charitable Trust (grant to Dr. Silverman), and the Stewart and Judith Colton Autoimmunity Center (grant to Dr. Silverman).

[1]Adam J. Pelzek, MS, Caroline Grönwall, PhD (current address: Karolinska Institutet, Stockholm, Sweden), Pamela Rosenthal, MD, Jeffrey D. Greenberg, MD, Gregg J. Silverman, MD: New York University School of Medicine, New York, New York; [2]Mandy McGeachy, PhD, Larry Moreland, MD: University of Pittsburgh, Pittsburgh, Pennsylvania; [3]William F. C. Rigby, MD: Dartmouth Medical School, Lebanon, New Hampshire.

Address correspondence to Gregg J. Silverman, MD, New York University School of Medicine, 450 East 29th Street, Alexandria East Room 804, New York, NY 10016. E-mail: Gregg.silverman@nyumc.org.

Submitted for publication August 19, 2016; accepted in revised form January 17, 2017.

involvement (7,8). ACPAs themselves and ACPA-containing immune complexes have been postulated to be directly pathogenic (9). Moreover, B lymphocytes, which infiltrate the inflamed synovial membranes of affected joints and locally produce ACPAs and rheumatoid factor (RF), also contribute to pathogenesis through antigen presentation, costimulation of CD4+ T cells, and secretion of chemokines and cytokines such as interleukin-6 (IL-6), tumor necrosis factor (TNF), and RANKL (10–13).

The presence of serum ACPAs, as detected by a cyclic citrullinated peptide (CCP) assay, both serves as a diagnostic biomarker and predicts a worse prognosis for progressive joint damage (14). At clinical onset, RA patients also have expansions of memory B cell subset(s) that correlate with worse long-term clinical outcomes (15). Importantly, even though treat-to-target strategies can more dependably induce low disease activity and clinical remission, serum ACPAs nonetheless generally persist. The immunobiologic basis for this persistence remains obscure, since ACPA production in ectopic synovial lymphoid tissue is presumably diminished with disease remission. It can be postulated that ACPAs continue to be spontaneously produced by long-lived plasma cells in the bone marrow or other sites, which have become disconnected from a previous pathogenic synovial process. We decided to test this model by determining whether disease-associated autoreactive peripheral B cells disappeared or persisted in patients in treatment-induced clinical remission.

Herein, we have compared the binding specificities of serum antibodies and peripheral blood B cells, with special focus on the representation of ACPA-expressing switched-memory B cells, which require additional stimuli to secrete antibodies. We have also characterized the fine binding specificities of these memory B cells, and enumerated their frequencies in the peripheral blood. Importantly, to better understand the effect of treatment on the underlying autoimmune process, we assessed relationships with clinical disease activity (16). Our findings show that recirculating ACPA-expressing memory B cells generally persist despite treatment with conventional disease-modifying antirheumatic drugs or TNF inhibition. Thus, the dysregulation of systemic autoimmunity in RA persists, even with remission of clinically relevant disease, which likely accounts for the failure of most treatment regimens to induce drug-free remission.

PATIENTS AND METHODS

Study design, human subjects, and sample procurement. All patients fulfilled the 2010 American College of Rheumatology/European League Against Rheumatism criteria for RA (17) (see Supplementary Table 1, available on the *Arthritis & Rheumatology* web site at http://onlinelibrary.wiley.com/doi/10.1002/art.40053/abstract). For initial classification, patients were defined as "seropositive" or "seronegative" based on the CCP2 clinical test (Axis-Shield) (18). Patients were recruited at New York University and as part of the Rheumatoid Arthritis Comparative Effectiveness Research (RACER) trial at the University of Pittsburgh. All patients and healthy donors provided written informed consent in accordance with protocols approved by the Human Subjects Institutional Review Board of the New York University School of Medicine and the University of Pittsburgh.

Enzyme-linked immunosorbent assay (ELISA) and multiplex bead-based assays. In a central laboratory, serum samples from all donors were tested for IgM-RF and IgG CCP3 (Inova Diagnostics) (19) (Supplementary Table 1). Samples with high activity were further evaluated at multiple dilutions for accurate activity assignment. Reactivity patterns for autocyclizing biotinylated peptides (20–28) (see Supplementary Table 2, available on the *Arthritis & Rheumatology* http://onlinelibrary.wiley.com/doi/10.1002/art.40053/abstract, for citrullinated and native peptides) were then defined (see Supplementary Figure 1, available on the *Arthritis & Rheumatology* web site at http://onlinelibrary.wiley.com/doi/10.1002/art.40053/abstract). Using a panel of avidin-coated microspheres and the same peptides/proteins, we also refined a multiplex bead-based array (Luminex), which has enhancements compared to methods described in a recent report (29). Signal strength was quantified according to the median fluorescence intensity from >35 beads for each analyte per well. During assay development, an additive (SurModics) was included to limit the potential influence of RF in a sample. A recombinant human IgG1 antibody to citrullinated fibrinogen (clone 1F11; ModiQuest) was used as a positive control.

Synovial fluid mononuclear cell (SFMC) culture. Briefly, after joint aspiration, an aliquot of SF was cleared by centrifugation and then treated with hyaluronidase (20 units/ml). Cells were recovered by Ficoll separation, washed, assessed for viability, and cultured in RPMI 1640 with 10% fetal bovine serum (FBS), 10 m*M* HEPES, 0.1% 2-mercaptoethanol, penicillin/streptomycin/glutamine with or without CpG 2006, IL-21, and the CD40L-expressing feeder line, MS40L (30).

Detection of antigen-specific or IgG-secreting cells (ISCs). To determine the frequencies of total IgG and antigen-specific IgG-secreting B cells, we adapted methodology for enzyme-linked immunospot (ELISpot) detection (31,32). Peripheral blood mononuclear cells (PBMCs), cultured with or without stimulants, were added at 2×10^5/well to 96-well PVDF membrane plates (Millipore) coated with anti-human IgG Fc-specific $F(ab')_2$ (Jackson ImmunoResearch) to capture ISC products. To detect specificity, we added biotinylated CCP3, biotinylated cyclic glutamine–containing peptide 3 (CQP3), biotinylated tetanus toxoid (TT), or anti-human IgG antibody. To develop, we used streptavidin-HRP80 (RDI; Fitzgerald) and aminoethylcarbazole substrate. The enumeration of antigen-specific ISCs was normalized per 10^6 PBMCs.

PBMC cultures. To assess the capacity for in vitro antibody secretion, PBMCs were isolated and cryopreserved, and later cultured at 10^6 cells per well for 6 days in 1 ml of RPMI complete media with 10% FBS, with or without CpG 2006 (6 μg/ml), IL-21 (50 ng/ml), and soluble CD40L (500 ng/ml), adapting previously reported conditions (31). We used fluorescence-activated cell sorting to isolate four B cell subpopulations: CD27+IgD–,

CD27+IgD+, CD27–IgD–, and CD27–IgD+ (see Supplementary Figure 2, available on the *Arthritis & Rheumatology* web site at http://onlinelibrary.wiley.com/doi/10.1002/art.40053/abstract).

Statistical analysis. We assessed nonparametric paired-sample comparisons by Spearman's correlation using Prism software version 6.0e (GraphPad). *P* values less than 0.05 were considered significant.

RESULTS

Patient cohorts and the development of citrulline-specific immunoassays. Given our goal of investigating the contributions of circulating ACPA-specific B lymphocytes to RA pathogenesis, we first assembled cohorts of well-characterized patients. A cross-sectional cohort was established at New York University that included patients with new-onset RA and patients with established RA (Supplementary Table 1). Assays for IgG CCP3 demonstrated nearly complete concordance with the IgG CCP2 results obtained at enrollment (data not shown).

Development of a bead-based multiplex ACPA assay. To evaluate patterns of antibody reactivity with citrulline-containing proteins and autocyclizing synthetic peptides, we first independently evaluated reactivity by ELISA (Supplementary Figure 1). These same peptides and proteins were then adapted to a multiplex bead-based array using a panel of avidin-coated microspheres, and we found significant correlations between results obtained with ELISA and our custom bead-based multiplex assays (see Supplementary Figure 3, available on the *Arthritis & Rheumatology* web site at http://onlinelibrary.wiley.com/doi/10.1002/art.40053/abstract).

To better assess the limits of detection, we evaluated the binding reactivity pattern of a recombinant human antibody to citrullinated fibrinogen, 1F11. This IgG1 antibody demonstrated a dose-dependent hierarchy of reactivity with a range of citrulline-containing antigenic ligands; with the most active antigenic ligands, reactivity was detectable at 0.1 ng/ml (data not shown).

With this multiplex assay, we characterized the circulating autoantibody fine specificity of sera from seropositive and seronegative RA patients (Figure 1a). The strongest IgG binding reactivity was generally with the CCP3 peptide, while only infrequent and, at best, weak reactivity was observed for the CQP3 peptide (which contains the neutral side chain of glutamine residues instead of charged arginine residues). Otherwise, RA patient sera displayed great heterogeneity in the fine specificities of the ACPAs when tested with a range of citrulline-containing antigens (Figures 1a and b).

We also evaluated ACPA responses in the sera of RA patients who had received different treatment regimens (i.e., patient groups receiving oral MTX and/or a TNF inhibitor [TNFi]). We observed no major differences between these groups with respect to ACPA fine binding

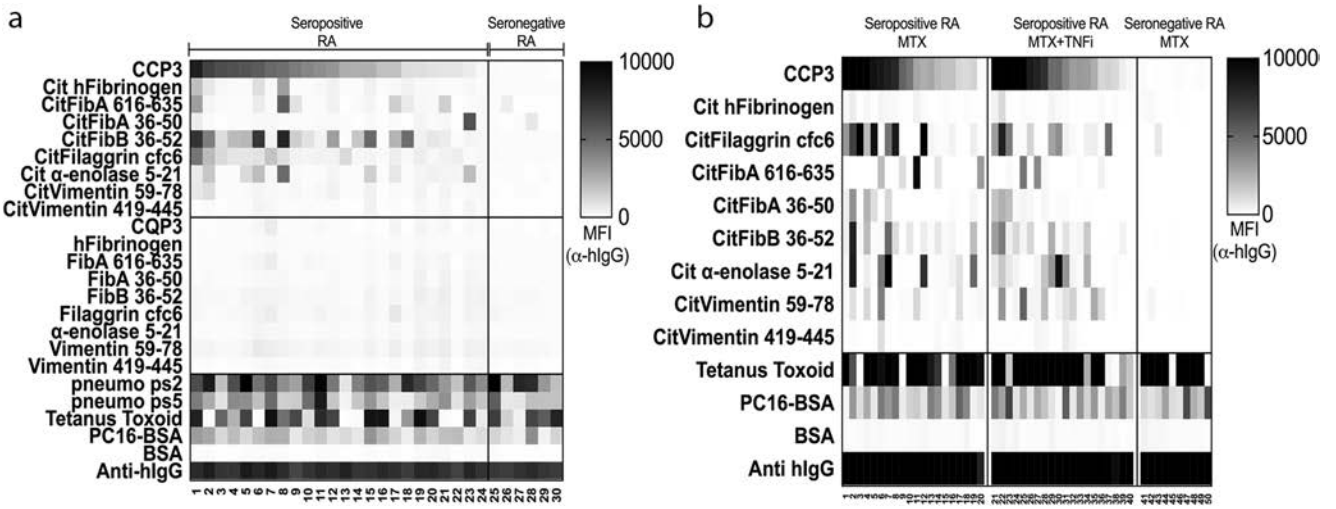

Figure 1. Serum IgG from cyclic citrullinated peptide 3 (CCP3)–positive (seropositive) rheumatoid arthritis (RA) patients reacts with citrullinated, but not native, cyclized peptide epitopes in a multiplex bead-based array. **a,** Serum samples from seropositive RA patients (n = 24) and seronegative RA patients (n = 6) were diluted 1:1,000 and assessed for IgG anti–citrullinated protein antibody (ACPA) reactivity by multiplex bead-based array. **b,** A custom multiplex bead-based antigen array was used to assess ACPAs in serum from RA patients receiving different treatments. Samples from seropositive RA patients treated with methotrexate (MTX; n = 20), seropositive RA patients treated with MTX and tumor necrosis factor inhibitor (TNFi; n = 20), and seronegative RA patients treated with MTX (n = 10) were analyzed for IgG ACPA fine specificities. Similar epitope specificity patterns were detected in the different treatment groups. Data are presented as the median fluorescence intensity (MFI). Cit hFibrinogen = citrullinated human fibrinogen; CitFibA = Cit-fibrinogen A; CQP3 = cyclic glutamine-containing peptide 3; pneumo ps2 = pneumococcal capsular polysaccharide 2; BSA = bovine serum albumin; anti-hIgG = anti-human IgG.

specificity, qualitatively or quantitatively, although we again found that seropositive RA patients were highly heterogeneous with respect to their IgG ACPA epitope specificity profiles (Figure 1b). Samples from seronegative RA patients, as defined by CCP2 and CCP3 assays, were generally nonreactive with other citrulline-containing antigens, since our multiplex assay detected infrequent (0–4%) recognition, as assessed by IgG binding of Cit-peptides/proteins, and then with only weak reactivity (Figure 1), which is consistent with prior findings (33,34).

To further evaluate the clinical specificity of our assay, we tested sera from healthy subjects and patients with other rheumatic diseases, including osteoarthritis, systemic lupus erythematosus, psoriatic arthritis, and Sjögren's syndrome (see Supplementary Table 3, available on the *Arthritis & Rheumatology* web site at http://onlinelibrary.wiley.com/doi/10.1002/art.40053/abstract). Our findings confirmed that the detection of IgG anti-citrulline antigen reactivity with our assay was highly specific for patients with RA, since among these 87 disease-specific controls, we found that IgG reactivity with the CCP3 peptide or other citrullinated antigens was distinctly uncommon.

Specificity and frequency of disease-associated autoreactive B cells at the site of disease. To evaluate ACPAs produced at the site of disease, we assessed the capacity of our multiplex assay to detect ACPAs in SF samples from 2 seropositive RA patients. Substantial levels of CCP3+ IgG were present, while no reactivity with the CQP3 control ligand was seen (Figure 2). Despite similar levels of CCP3 reactivity in these 2 SF samples, there were notable differences in the detection of IgG ACPA fine binding specificities with the other citrulline-containing peptides in the assay.

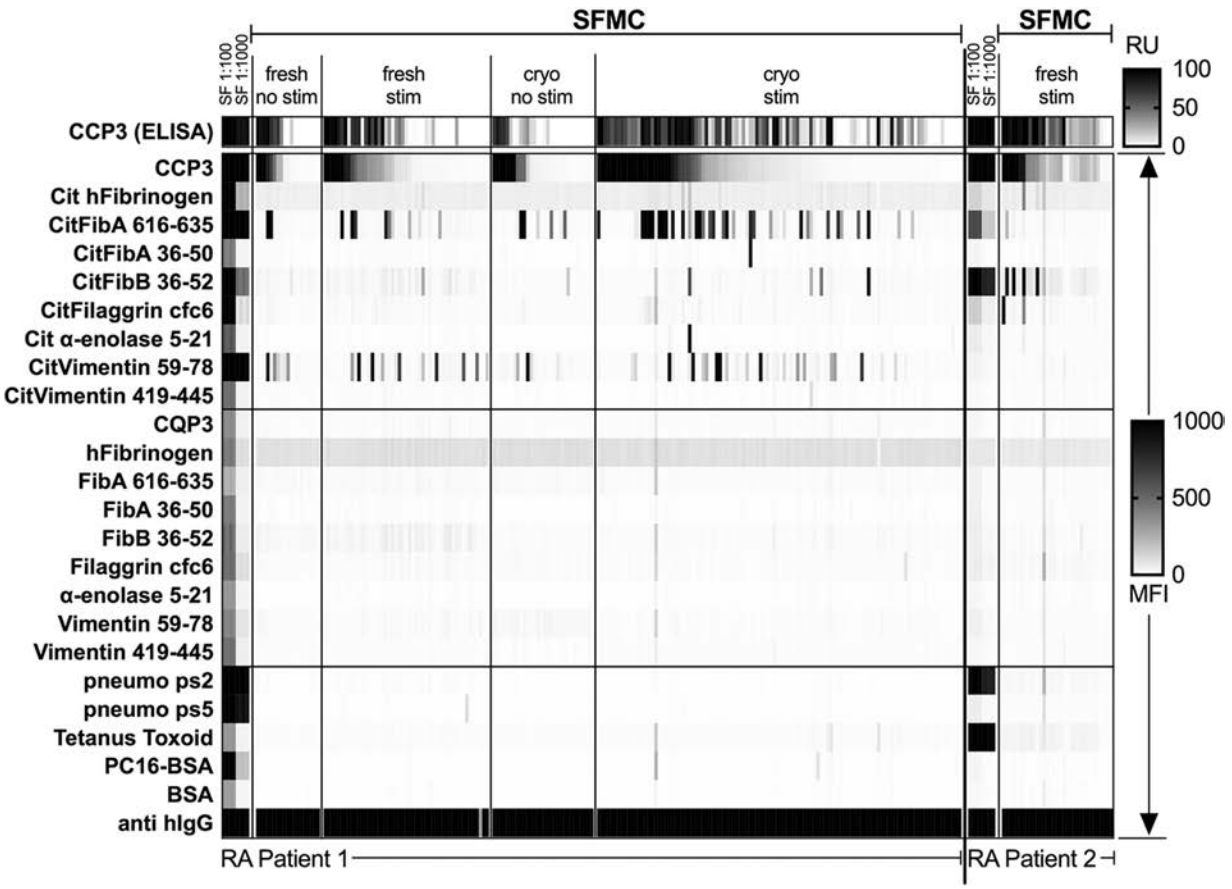

Figure 2. ACPA-reactive B cells are common in RA synovial fluid (SF), and SF mononuclear cell (SFMC) culture supernatant epitope reactivity patterns mirror those in autologous SF. SF was obtained from 2 RA patients, and SFMCs were isolated. SFMCs (1,000 or 10,000 per well) were cultured for 12 days with or without 3,000 MS40L cells/well and CpG 2006 and interleukin-21 (stim). Culture supernatants were analyzed using an enzyme-linked immunosorbent assay (ELISA) to detect IgG anti-CCP3, followed by a multiplex assay for epitope specificity of all positive and some negative wells. SF was tested at 1:100 and 1:1,000 dilutions by ELISA and multiplex assay. "Fresh" indicates directly ex vivo–cultured cells, and "cryo" indicates previously cryopreserved, thawed cells. RU = relative units (see Figure 1 for other definitions).

These SF mononuclear cell (SFMC) samples contained a substantial representation of lymphocytes with the surface phenotype of switched-memory B cells (data not shown). SFMCs were cultured in media supplemented with IL-21/CpG 2006, in the presence of the MS40L feeder cell line that enables in vitro clonal expansion of preactivated B cells (30), which also induced 20-fold higher total IgG levels compared to unstimulated cultures (data not shown). IgG ACPAs were commonly detected in wells with 10,000 SFMCs, but were infrequent at 1,000 SFMCs/well, and never detected at 100 SFMCs/well. In each well, IgG ACPA fine specificity was heterogeneous, with the most common secreted ACPA epitope reactivities reiterating the same immunodominant ACPA specificities found in SF (Figure 2). While these studies document the high frequency of ACPA-expressing B cells at the site of disease, blood samples from these particular donors were, unfortunately, not available for comparison.

Detection of circulating antigen-specific peripheral B cells by ELISpot assay. To investigate the representation of circulating autoreactive B cells, we adapted ELISpot methods to evaluate the representation of ACPA-expressing B cells capable of constitutive ex vivo secretion (i.e., plasma cells/blasts) and B cells that required in vitro stimulation for IgG ACPA production (i.e., memory B cells) (31,32). Without in vitro stimulation, we detected only a very low frequency of spontaneous total ISCs (range 200–321/10^6 PBMCs), and by this method, we detected neither ACPA reactivity nor other TT-specific antibodies (data not shown). In stimulated PBMCs from seropositive RA patients, we found CCP3-reactive IgG spots in a mean ± SEM of 41.3 ± 0.5 ISCs/10^6 PBMCs (range 0–205), representing 0.13% of all ISCs (Figure 3a). Only background levels were detected with the control peptide CQP3 (mean ± SEM 1.9 ± 0.6 ISCs/10^6 PBMCs). In contrast, for seronegative RA patients and healthy adults, CCP3 and CQP3 ISCs were below the limit of detection. These results confirmed that only RA patients have disease-specific circulating B cells capable of secreting IgG ACPAs.

As an internal control, we found that almost all RA patients and healthy subjects had detectable circulating IgG-expressing memory B cells reactive with the control bacterial antigen TT from the preventative vaccine that has been given to almost every adult. RA patients had a mean ± SEM of 71.1 ± 2.6 IgG anti-TT ISCs (range 0–205) and healthy adults had 65.4 ± 1.2 anti-TT ISCs/10^6 PBMCs (range 0–220) (Figure 3a), with no significant difference between the 2 groups. Notably, these experiments showed that the frequencies of recirculating anti-TT memory B cells overlap with the frequencies of ACPA-specific B cells in seropositive RA patients. Although these ELISpot assays were informative, we sought to develop a more efficient means of illuminating the broader range of fine binding autospecificities expressed by peripheral B cells in a donor.

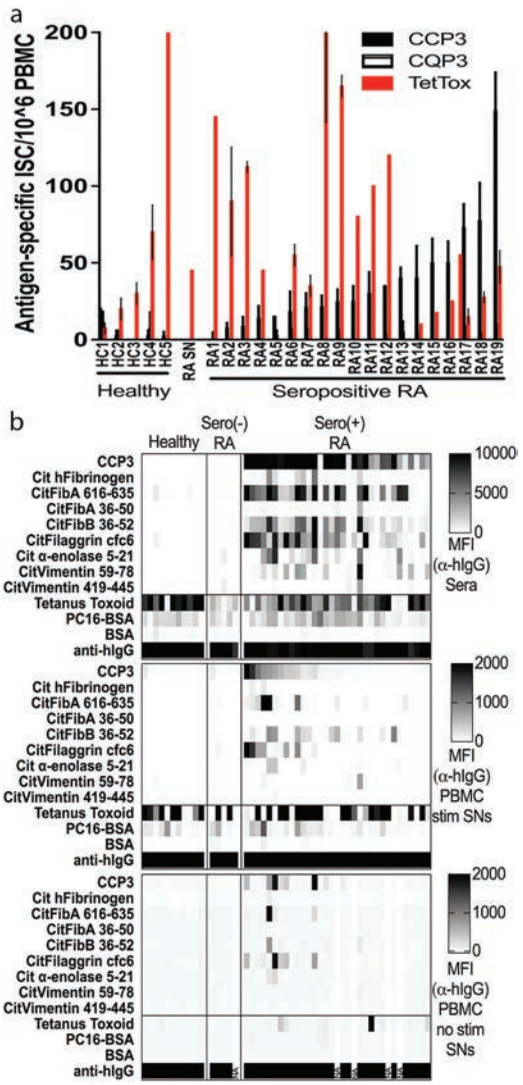

Figure 3. ACPA-expressing B cells are present in the circulation of seropositive RA patients, and peripheral blood mononuclear cell (PBMC) cultures from seropositive RA patients secrete IgG ACPAs with epitope reactivity patterns that recapitulate ACPA patterns in serum. **a,** Day 6 PBMC cultures (with or without CpG 2006, interleukin-21, and CD40L) from seropositive RA patients (n = 19), a seronegative (SN) RA patient, and healthy controls (HC; n = 5) were assessed by enzyme-linked immunospot assay for antigen-specific B cells using 200,000 cells per well after overnight culture. ISCs = Ig-secreting cells; TetTox = tetanus toxoid. **b,** PBMCs from healthy controls (n = 11), seronegative RA patients (n = 5), and seropositive RA patients (n = 33) were isolated and cultured with or without stimulation (stim), adapting previously described conditions (31). Culture supernatants were assayed for antibody content by multiplex antigen bead assay using anti-human IgG (Fc-specific) R-phycoerythrin (eBioscience). Data are presented as the MFI. See Figure 1 for other definitions.

Table 1. RA patient data for memory B cell studies*

	All RA patients (n = 24)	Patients receiving MTX (n = 12)	Patients receiving TNFi with or without MTX (n = 12)†	Healthy controls (n = 5)
Sex, no. (%) female/male	20 (83.3)/4 (16.7)	10 (83.3)/2 (16.7)	10 (83.3)/2 (16.7)	2 (40)/3 (60)
Age, years	53.5 ± 11.5 (27–82)	51.1 ± 13.5 (27–82)	56.0 ± 9.1 (42–72)	36.6 ± 12.6 (25–58)
DAS28	3.0 ± 1.8 (1.1–7.2)	3.1 ± 2.0 (1.3–7.2)	3.0 ± 1.7 (1.1–6.8)	
Anti-CCP3 IgG, RU‡	1,675.3 ± 1,906.7 (49.2–7,725.9)	1,192.9 ± 1,105.4 (104.8–3,424.3)	2,157.6 ± 2,423.2 (49.2–7,725.9)	2.9 ± 1.1 (2.1–4.8)
ACPA-expressing switched-memory B cells, % wells	1.4 ± 2.3 (0–7.7)	0.86 ± 2.2 (0–7.7)	1.9 ± 2.4 (0–7.7)	0
ACPA-expressing switched-memory B cells/1 × 10^4 switched-memory B cells	2.8 ± 4.6 (0–15.4)	1.7 ± 4.4 (0–15.4)	3.8 ± 4.8 (0–15.4)	0
Disease duration, days	4,200.5 ± 4,243.9 (226–16,342)	2,379.2 ± 1,830.5 (239–6,022)	6,187.5 ± 5,254.9 (315–16,342)	–
Duration of MTX treatment, days	1,711.3 ± 2,854.1 (119–11,204)	1,061.9 ± 1,490.5 (119–3,878)	2,360.7 ± 3,760.2 (148–11,204)	–
Duration of TNFi treatment, days	–	–	866.1 ± 1,301.2 (148–3,584)	–

* Except where indicated otherwise, values are the mean ± SD (range). RA = rheumatoid arthritis; DAS28 = Disease Activity Score in 28 joints; RU = relative units; ACPA = anti–citrullinated protein antibody.
† Eleven patients received methotrexate (MTX) and tumor necrosis factor inhibitor (TNFi), and 1 patient received TNFi only.
‡ The anti–cyclic citrullinated peptide 3 (anti-CCP3) test (Inova) was performed using sera diluted 1:1,616.

ACPA production by PBMCs from RA patients. To investigate the fine binding specificity of circulating citrulline antigen–reactive B cells, the PBMC culture conditions described above were used to induce B cell differentiation and antibody production, which we evaluated by multiplex bead array. Indeed, without stimulation, we detected only low levels of IgG (mean 0.16 μg/ml [range 0.01–0.56 μg/ml]), while with 6 days of stimulation, IgG levels were greatly increased (mean 7.65 μg/ml [range 1.85–20.95 μg/ml]). Based on IgG CCP3 reactivity, ACPAs were found in 15 of 33 supernatants (45.5%) from stimulated seropositive RA PBMCs (Figure 3b). In general, wells that contained IgG anti-CCP3 antibodies also displayed a range of reactivities for other citrulline-containing epitopes (but not arginine-containing analogs) that greatly varied between different RA donors. Taken together with the ELISpot results described above, these findings confirmed that seropositive RA patients commonly have circulating citrulline epitope–specific B cells.

Overall, IgG ACPAs were only detected in cultures of PBMCs from seropositive RA patients, and in most cases, only after 4–6 days of in vitro stimulation. ACPAs were infrequently detected in wells with unstimulated cells (i.e., 7 of 29 [24.1%] of seropositive RA patients) (Figure 3b). Furthermore, the autoreactive blood B cell clones in different donors appeared to vary broadly by fine specificity for citrulline-containing self-antigen variants. These findings support the notion that RA patients have quiescent switched-memory B cells that can express ACPAs in their blood, while circulating constitutively IgG-secreting cells (i.e., plasma cells/plasmablasts) are much less commonly detected.

The relationship between the fine specificity of serum ACPAs and of the stimulated circulating ACPA-expressing memory B cells within the PBMCs was evaluated. Intriguingly, we found significant correlations between the serum IgG reactivities and in vitro secreted autoantibodies to CCP3 ($P < 0.0001$), Cit-filaggrin cfc6 ($P = 0.0001$), and 7 other citrullinated antigens that were tested (see Supplementary Figure 4, available on the Arthritis & Rheumatology web site at http://onlinelibrary.wiley.com/doi/10.1002/art.40053/abstract). Correlations for serum and in vitro–produced anti-TT antibody responses were also observed ($P = 0.03$). These results strongly support the notion that there is a connection between epitope-specific ACPAs in serum and the fine specificities of circulating autoreactive B cells. However, clinical disease activity, based on the Disease Activity Score in 28 joints (DAS28) (35), correlated with neither the level nor the ACPA specificity in serum or supernatant (data not shown).

Evaluation of sorted peripheral blood B cells by multiplex assay. To directly determine which B cell subsets in the peripheral blood are the source of RA disease-associated ACPAs, we used flow cytometry to isolate CD3–CD14–CD19+ B cells from PBMCs into 4 subpopulations: CD27+IgD– cells, CD27+IgD+ cells, CD27–IgD– cells, and CD27–IgD+ cells. The MS40L

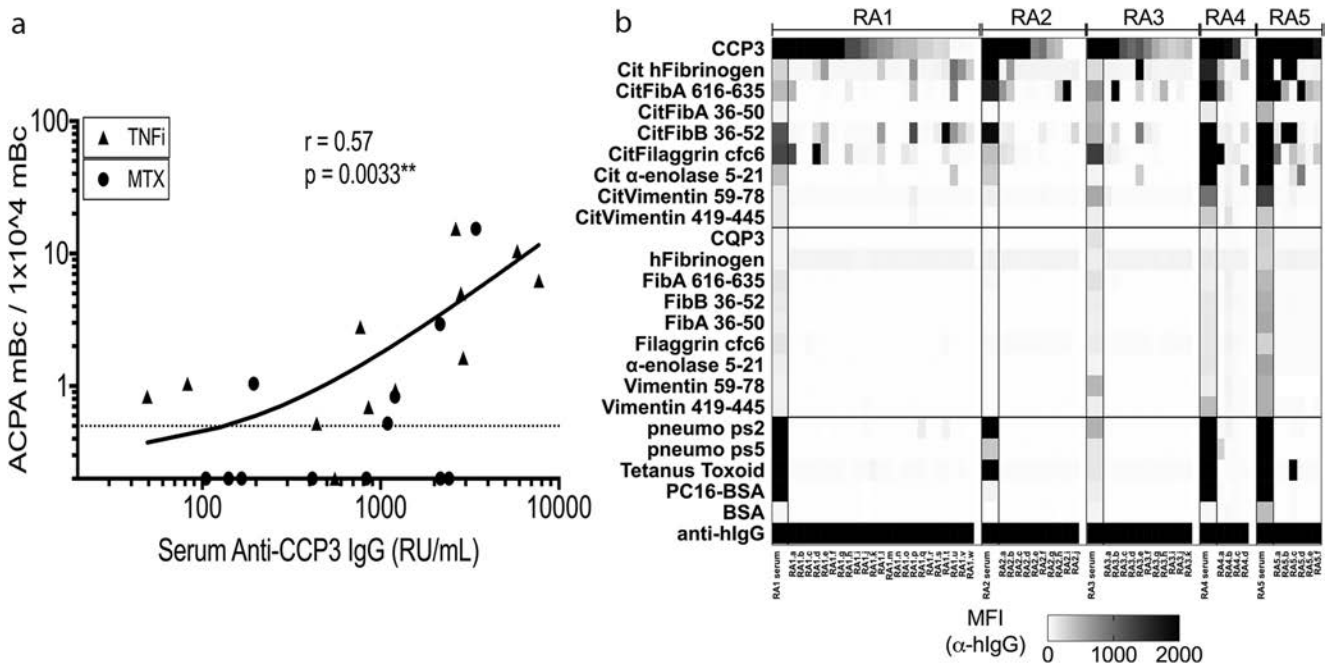

Figure 4. A high burden of ACPA-expressing switched-memory B cells (mBc) correlates with a high serum ACPA level, and epitope specificities largely recapitulate those in circulating serum ACPAs in the same subject. Peripheral blood mononuclear cells (PBMCs) from seropositive RA patients were stained, and switched-memory (CD19+IgD–CD27+) B cells were separated by fluorescence-activated cell sorting and cultured for 12 days at 50 cells/well with MS40L cells plus CpG 2006 and interleukin-21. Wells that were determined to be positive for CCP3 by enzyme-linked immunosorbent assay prescreening were subjected to multiplex analysis for citrullinated epitope reactivity. Multiplex wells were counted as positive if reactivity of a citrullinated peptide (based on MFI) was >50 MFI and ≥2-fold that of the native peptide. **a,** For samples from patients with seropositive RA who were receiving a TNFi (n = 12) or MTX (n = 12), ACPA-positive wells were counted, since these were assumed to contain 1 or more ACPA-expressing memory B cells per well. Data were converted to switched-memory B cells per 10,000 memory B cells cultured, and then plotted against serum IgG anti-CCP3 (with relative units [RU]/ml determined by IgG CCP3 clinical test and with additional serum dilutions performed when required). **b,** Representative multiplex data for samples from 5 seropositive RA patients, depicting serum (diluted 1:1,000) and supernatant (diluted 1:2) IgG ACPA reactivity, are shown. ** = *P* for Spearman's correlation ≤ 0.01. See Figure 1 for other definitions.

cell line was then used for in vitro expansion of each sorted B cell subset of defined surface phenotype (30). Sorted B cell subsets from 10 RA patients and 5 healthy individuals (see Supplementary Figure 2 for strategy) were separately cultured at 50 viable B cells per well. In a multiplex assay and confirmed by ELISA, only low or undetectable IgG levels were present after 0–2 days of in vitro culture, and ACPA reactivity was not detectable. Following culture of switched-memory B cells with stimulants for 12 days, we detected 10-fold greater levels of total IgG (mean ± SD 3.2 ± 2.4 μg/ml) than was associated with any other defined B cell subset.

Cultured switched-memory B cells (CD27+IgD–) most consistently produced high levels of IgG ACPAs. Otherwise, ACPAs were only infrequently detected in wells from "double-negative" B cells (CD27–IgD–). Other sorted subsets had no detectable ACPA activity (data not shown), since IgG ACPAs were never detected among preswitched-memory B cells (CD27+IgD+) or naive/transitional B cells (CD27–IgD+).

Overall, these data document that IgG ACPAs primarily derive from switched-memory B cells (i.e., ACPA-expressing memory B cells) in the circulation of RA patients (Table 1). Moreover, ACPA-expressing memory B cells were detected in the circulation of seropositive RA patients in both treatment groups tested (MTX or TNFi), with detection most frequently based on reactivity with the CCP3 ligand, while there was much greater heterogeneity with other individual citrulline-containing peptides, but neither had detectable reactivity with B cells from seronegative RA patients or unaffected control subjects. We also surveyed for IgM autoantibodies, but every case of IgM reactivity with citrulline-containing ligands was associated with high polyreactivity with other antigens as well (data not shown), and therefore, no truly monospecific IgM ACPAs were detected.

Correlation of the burden of circulating ACPA-expressing B cells with serum levels of ACPAs. Based on evidence that seropositive RA patients commonly have circulating B cells that are capable of secreting IgG

ACPAs, we wondered whether there was a relationship between the levels of these autoantibody-expressing memory B cells and their serum IgG ACPA levels. We therefore performed surveys on samples from a cross-sectional study of RA patients.

Overall, we found ACPA secretion in a mean of 1.4% of wells containing 50 viable switched-memory B cells (CD19+CD27+IgD–) (range 0–7.7%), while IgG ACPA-expressing B cells were never detected in healthy donors (Table 1). Considering the number of B cells that were tested, we estimated that ACPA reactivity was expressed by a mean ± SD of 0.03 ± 0.04% of switched-memory B cells in a seropositive RA patient (range 0–0.15%). Notably, we found a significant direct correlation between the proportion of wells with detectable IgG ACPAs and serum levels of IgG anti-CCP3 (Spearman's correlation $r = 0.57$, $P = 0.003$) (Figure 4a). In general, ACPA-expressing B cells in individual wells exhibited great heterogeneity in their recognition of multiple autoantigenic determinants (Figure 4b). Taken together, the data indicate that there is a biologic link between the frequencies of recirculating anti-citrulline memory B cells and serum ACPA levels.

Lack of correlation of levels of circulating ACPA-expressing B cells with disease activity. Over the past 2 decades, there have been remarkable advances in the efficacy of treatment regimens, and in our capacity to accurately gauge overall disease activity in individual RA patients. Neither total blood levels of memory B cells nor IgG CCP3 antibody levels correlated with disease activity (data not shown). We therefore next sought to determine whether we could find relationships between RA clinical disease activity and levels of recirculating citrulline antigen–reactive memory B cells. Our cross-sectional studies were performed on patients who displayed a wide range of serum IgG anti-CCP3 levels, and based on the DAS28 (36), disease activity ranged from high (DAS28 >5.1) in some patients to clinical remission (DAS28 <2.6) in others. ACPA switched-memory B cells were found in the majority of seropositive RA patients (16 of 24 [66.7%]) (Figures 4 and 5). Yet, from quantitation of the frequency of wells with detectable ACPAs, we found only a nonsignificant trend toward a higher frequency of ACPA-expressing blood memory B cells in patients with higher DAS28 scores (Figure 5). Further analyses in subsets of patients who received treatment with either methotrexate (MTX) or a biologic agent (TNFi) also failed to show a significant correlation. Most importantly, ACPA-expressing memory B cells were detected in most seropositive RA patients in clinical remission (8 of 14), based on DAS28 scores of <2.6 (Figure 5).

In summary, treatment with standard of care regimens, while sufficient to reduce disease activity and, in some patients, to attain clinical remission, was not sufficient to eliminate ACPA-expressing memory B cells from the peripheral circulation, regardless of the DAS28 score (Figure 5). A subset of RA patients had very high frequencies of circulating ACPA-expressing memory B cells, with a variety of ACPA epitope reactivity patterns in individual patients (Figure 4b). Serum IgG CCP3 was also detected in the patient subsets with high, moderate, and low disease activity, as well as those in remission according to the DAS28, although this association was not significant (data not shown). Taken together, our results suggest that the presence of a high burden of circulating ACPA-expressing memory B cells may persist despite seemingly effective therapeutic interventions and is not reflected by standard measures of disease activity.

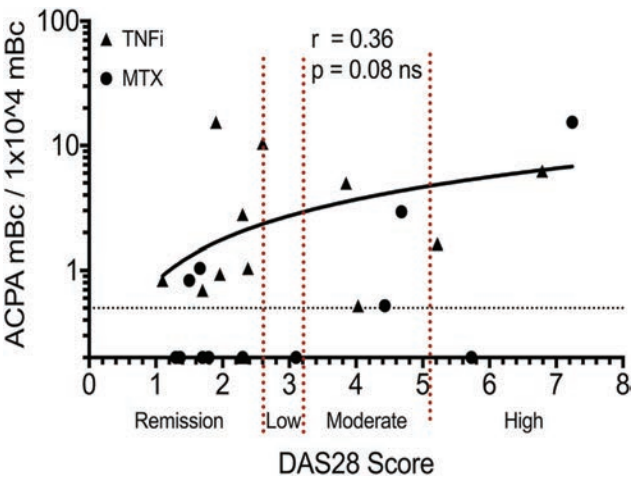

Figure 5. High burdens of circulating anti–citrullinated protein antibody (ACPA) switched-memory B cells (mBc) can be detected in the circulation of treated rheumatoid arthritis (RA) patients, including those whose disease is in clinical remission. For samples from patients with seropositive RA who were receiving tumor necrosis factor inhibitor (TNFi) therapy (n = 12) or methotrexate (MTX; n = 12), ACPA-positive switched-memory B cells (per 10,000 switched-memory B cells cultured) were quantified as described in Figure 4, plotted against the Disease Activity Score in 28 joints (DAS28), and analyzed by Spearman's correlation. The DAS28 using the C-reactive protein level (DAS28-CRP) was used in 21 patients, and the DAS28 using the erythrocyte sedimentation rate (DAS28-ESR) was used in 3 patients for whom CRP data were not available. Levels of ACPA-expressing switched-memory B cells did not correlate significantly with DAS28 scores. Results of correlation analyses with DAS28-CRP and DAS28-ESR were equivalent. NS = not significant.

DISCUSSION

We found that seropositive RA patients, but not seronegative RA patients or healthy adults, have substantial levels of circulating anticitrullinated epitope-specific B

cells, at frequencies akin to those for an antigen-specific protective B cell response. Circulating RA-associated ACPA-expressing B cells were predominantly switched-memory (i.e., CD27+IgD–) B cells (37–39) that do not spontaneously secrete ACPAs without in vitro activation. These B cells displayed a range of binding autospecificities for different citrullinated epitopes and were also cross-reactive with the synthetic CCP3 peptide widely used to confirm the clinical diagnosis of RA, while they did not recognize native arginine-containing self–protein/peptide analogs.

Our surveys of a cross-sectional cohort of adult RA patients also revealed that the frequency of activatable citrullinated antigen–reactive B cells in a subject was directly proportional to serum IgG ACPA levels. While the range of IgG ACPA specificities expressed varied greatly between individual patients, for an individual RA patient the serum ACPA binding reactivity pattern was very similar to that induced by in vitro stimulation of disease-associated memory B cells. Whereas it has been argued that serum autoantibodies may be primarily produced by antibody-secreting B lineage cells that infiltrate affected synovial linings (20,40) and/or the bone marrow (41), our findings suggest that the same clonal sets may be represented among the memory B cells in the bloodstream.

Progressive advances in our understanding of RA pathogenesis have led to the introduction of therapeutic agents that often provide high-hurdle clinical benefits, and biopsy/rebiopsy studies have shown this is generally paralleled by resolution of the pathogenic lymphocytic and myeloid synovial infiltrates in affected joints (42–44). Yet despite these therapeutic advancements, such treatments are generally associated with only modest decreases in circulating IgM-RF or IgG ACPA/CCP, and very rarely do these serologic disease markers become undetectable.

In this study, we demonstrated that therapeutic interventions (MTX and/or TNFi) did not dependably abolish the recirculating autoantigen-targeted memory B cells that reflect the disease-associated defect in B cell immunologic tolerance, even in patients who attained clinical remission. Our findings therefore confirm that, despite the capacity of TNF inhibition to apparently disengage autoreactive B cells from the inflammatory destructive effector pathways in the rheumatoid synovial apparently disease process, these treatments do not appear to substantially impact the underlying pathogenic autoimmunity (as recently discussed [15]).

Our integrated technical approach provided insights that complement other cutting-edge methods for the isolation and characterization of individual B cells in the RA autoimmune response. Recombinant monoclonal antibodies have been recovered and expressed from single synovium-infiltrating B cells, and RA B cell receptor repertoire studies have also provided the molecular characterization of ACPA binding specificity, B cell clonal relatedness, and immunogenetic origins (39,45). Tetramer technology for flow cytometric sorting has also been adapted for the study of autoantigen-specific B cells from RA patients (39). While these approaches provide important perspectives, single B cell analyses enable detailed examinations of individual antigen-reactive lymphocytes (akin to the in-depth study of "individual trees"), while the latter approaches provide broad surveys of disease-associated B cell lineage "forests." Our approach provided an informative middle ground since it was designed to quantitate memory B cells and also elucidate autoantibody fine specificity and cross-reactivity in groups of patients. Our approach may require larger blood samples to derive more-accurate frequencies when in vivo levels of ACPA-expressing B cells among peripheral B cells are low. In the future, we would like to apply our now validated methods to longitudinal studies of individuals before and after starting a new agent.

Our investigations have provided direct evidence that memory B cells are not eradicated in peripheral blood following therapeutic attainment of clinical remission. Therefore, the regimens that we examined are insufficient for induction of long-term immune remission. In fact, patients with high serum IgG anti-CCP3 levels were significantly more likely to have high frequencies of ACPA-expressing switched-memory B cells, suggesting there are likely ongoing roles for these cells in the production of serum ACPAs. Our findings also suggest that serum ACPA levels are closely intertwined with the persistence of circulating ACPA-expressing memory B cells. We therefore wonder about the relationship between memory B cells and long-lived plasma cells, as our findings are consistent with a model in which memory B cells are required to replenish ACPA-secreting plasma cells in the bone marrow and potentially at other sites.

The contributions of B cells to RA pathogenesis have been best documented by the clinical efficacy of rituximab, the prototypical anti-CD20 antibody, which induces efficient eradication of B cells from the blood. However, the impact at other sites may not be accurately reflected in the bloodstream levels. In treated RA patients with clinical benefits, when in vivo therapeutic anti-CD20 levels later wane, the return of detectable levels of blood B cells is often associated with an overall reduction in the levels of different CD27+ B cell subsets that can persist for years (46). Yet, to the best of our knowledge, the proportions of these posttreatment recovery memory B cells linked to host immune defenses versus disease-associated autoimmunity have not been investigated.

In conclusion, our results highlight the fact that commonly used treatment regimens are deficient in affecting the underlying pathologic autoimmune disease process. These findings therefore help to rationalize the outcome of 2 large trials in which cessation of therapy in RA patients in clinical remission led to relapse in the great majority of RA patients within the first year (47–49). Indeed, these regimens fail to provide an effective cure for RA because they do not have the capacity to target the reservoirs of pathogenic autoreactive B cells (as well as T cells).

We therefore propose that the next phase in the development of RA therapy should have a goal of deleting pathologic memory cells and reversing the defect in immune tolerance. Progress toward this goal will require the adoption of a new standard for differentiating clinical remission from true immune remission, which includes an assessment of cellular autoimmune players that will otherwise be responsible for disease reactivation and clinical relapse. Our technical approach for assessing the autoimmune B cell burden in RA patients may therefore provide this essential tool for assessing the capacity of treatment regimens to target and eliminate disease-specific autoimmunity, as well as for making better and more informed treatment decisions in daily clinical practice.

ACKNOWLEDGMENTS

We are grateful to Rufus Burlingame and Inova Diagnostics for providing the CCP3 and CQP3 peptides. We acknowledge the assistance of the NYU Immune Monitoring Core and the NYU Flow Cytometry Core Facility (supported by NYU-HHC CTSI grant UL1-TR-000038) and the NYU Laura and Isaac Perlmutter Cancer Center support (grant P30-CA-016087 from the National Center for Advancing Translational Sciences [NCATS]).

AUTHOR CONTRIBUTIONS

All authors were involved in drafting the article or revising it critically for important intellectual content, and all authors approved the final version to be published. Dr. Silverman had full access to all of the data in the study and takes responsibility for the integrity of the data and the accuracy of the data analysis.

Study conception and design. Pelzek, Silverman.

Acquisition of data. Pelzek, Greenberg, McGeachy, Moreland, Rigby, Silverman.

Analysis and interpretation of data. Pelzek, Grönwall, Rosenthal, Silverman.

REFERENCES

1. Sokka T, Abelson B, Pincus T. Mortality in rheumatoid arthritis: 2008 update. Clin Exp Rheumatol 2008;26 Suppl 51:S35–61.
2. Dadoun S, Zeboulon-Ktorza N, Combescure C, Elhai M, Rozenberg S, Gossec L, et al. Mortality in rheumatoid arthritis over the last fifty years: systematic review and meta-analysis. Joint Bone Spine 2013;80:29–33.
3. Catrina AI, Joshua V, Klareskog L, Malmström V. Mechanisms involved in triggering rheumatoid arthritis. Immunol Rev 2016; 269:162–74.
4. De Smit MJ, Brouwer E, Vissink A, van Winkelhoff AJ. Rheumatoid arthritis and periodontitis: a possible link via citrullination. Anaerobe 2011;17:196–200.
5. Demoruelle MK, Weisman MH, Simonian PL, Lynch DA, Sachs PB, Pedraza IF, et al. Airways abnormalities and rheumatoid arthritis–related autoantibodies in subjects without arthritis: early injury or initiating site of autoimmunity? Arthritis Rheum 2012;64:1756–61.
6. Scher JU, Sczesnak A, Longman RS, Segata N, Ubeda C, Bielski C, et al. Expansion of intestinal Prevotella copri correlates with enhanced susceptibility to arthritis. Elife 2013;2: e01202.
7. Nielen MM, van Schaardenburg D, Reesink HW, van de Stadt RJ, van der Horst-Bruinsma IE, de Koning MH, et al. Specific autoantibodies precede the symptoms of rheumatoid arthritis: a study of serial measurements in blood donors. Arthritis Rheum 2004;50:380–6.
8. Van der Woude D, Rantapää-Dahlqvist S, Ioan-Facsinay A, Onnekink C, Schwarte CM, Verpoort KN, et al. Epitope spreading of the anti-citrullinated protein antibody response occurs before disease onset and is associated with the disease course of early arthritis. Ann Rheum Dis 2010;69:1554–61.
9. Holers VM. Antibodies to citrullinated proteins: pathogenic and diagnostic significance. Curr Rheumatol Rep 2007;9:396–400.
10. Silverman GJ, Carson DA. Roles of B cells in rheumatoid arthritis. Arthritis Res Ther 2003;5 Suppl 4:S1–6.
11. Dorner T. Crossroads of B cell activation in autoimmunity: rationale of targeting B cells. J Rheumatol Suppl 2006;77:3–11.
12. Marston B, Palanichamy A, Anolik JH. B cells in the pathogenesis and treatment of rheumatoid arthritis. Curr Opin Rheumatol 2010;22:307–15.
13. Meednu N, Zhang H, Owen T, Sun W, Wang V, Cistrone C, et al. Production of RANKL by memory B cells: a link between B cells and bone erosion in rheumatoid arthritis. Arthritis Rheumatol 2016;68:805–16.
14. Singh JA, Furst DE, Bharat A, Curtis JR, Kavanaugh AF, Kremer JM, et al. 2012 update of the 2008 American College of Rheumatology recommendations for the use of disease-modifying antirheumatic drugs and biologic agents in the treatment of rheumatoid arthritis. Arthritis Care Res (Hoboken) 2012;64:625–39.
15. Silverman GJ, Pelzek A. Rheumatoid arthritis clinical benefits from abatacept, cytokine blockers, and rituximab are all linked to modulation of memory B cell responses. J Rheumatol 2014; 41:825–8.
16. Fransen J, van Riel PL. The Disease Activity Score and the EULAR response criteria. Rheum Dis Clin North Am 2009;35: 745–57, vii–viii.
17. Aletaha D, Neogi T, Silman AJ, Funovits J, Felson DT, Bingham CO III, et al. 2010 rheumatoid arthritis classification criteria: an American College of Rheumatology/European League Against Rheumatism collaborative initiative. Arthritis Rheum 2010;62: 2569–81.
18. Van Venrooij WJ, Zendman AJ. Anti-CCP2 antibodies: an overview and perspective of the diagnostic abilities of this serological marker for early rheumatoid arthritis. Clin Rev Allergy Immunol 2008;34:36–9.
19. Debaugnies F, Servais G, Badot V, Noubouossie D, Willems D, Corazza F. Anti-cyclic citrullinated peptide antibodies: a comparison of different assays for the diagnosis of rheumatoid arthritis. Scand J Rheumatol 2013;42:108–14.
20. Snir O, Widhe M, Hermansson M, von Spee C, Lindberg J, Hensen S, et al. Antibodies to several citrullinated antigens are

enriched in the joints of rheumatoid arthritis patients. Arthritis Rheum 2010;62:44–52.
21. Hill JA, Bell DA, Brintnell W, Yue D, Wehrli B, Jevnikar AM, et al. Arthritis induced by posttranslationally modified (citrullinated) fibrinogen in DR4-IE transgenic mice. J Exp Med 2008; 205:967–79.
22. Chandra PE, Sokolove J, Hipp BG, Lindstrom TM, Elder JT, Reveille JD, et al. Novel multiplex technology for diagnostic characterization of rheumatoid arthritis. Arthritis Res Ther 2011; 13:R102.
23. Sebbag M, Moinard N, Auger I, Clavel C, Arnaud J, Nogueira L, et al. Epitopes of human fibrin recognized by the rheumatoid arthritis-specific autoantibodies to citrullinated proteins. Eur J Immunol 2006;36:2250–63.
24. Verpoort KN, Cheung K, Ioan-Facsinay A, van der Helm-van Mil AH, de Vries-Bouwstra JK, Allaart CF, et al. Fine specificity of the anti–citrullinated protein antibody response is influenced by the shared epitope alleles. Arthritis Rheum 2007;56:3949–52.
25. Schellekens GA, de Jong BA, van den Hoogen FH, van de Putte LB, van Venrooij WJ. Citrulline is an essential constituent of antigenic determinants recognized by rheumatoid arthritis-specific autoantibodies. J Clin Invest 1998;101:273–81.
26. Schellekens GA, Visser H, de Jong BA, van den Hoogen FH, Hazes JM, Breedveld FC, et al. The diagnostic properties of rheumatoid arthritis antibodies recognizing a cyclic citrullinated peptide. Arthritis Rheum 2000;43:155–63.
27. Dubucquoi S, Solau-Gervais E, Lefranc D, Marguerie L, Sibilia J, Goetz J, et al. Evaluation of anti-citrullinated filaggrin antibodies as hallmarks for the diagnosis of rheumatic diseases. Ann Rheum Dis 2004;63:415–9.
28. Lundberg K, Kinloch A, Fisher BA, Wegner N, Wait R, Charles P, et al. Antibodies to citrullinated α-enolase peptide 1 are specific for rheumatoid arthritis and cross-react with bacterial enolase. Arthritis Rheum 2008;58:3009–19.
29. Wagner CA, Sokolove J, Lahey LJ, Bengtsson C, Saevarsdottir S, Alfredsson L, et al. Identification of anticitrullinated protein antibody reactivities in a subset of anti-CCP-negative rheumatoid arthritis: association with cigarette smoking and HLA-DRB1 'shared epitope' alleles. Ann Rheum Dis 2015;74:579–86.
30. Luo XM, Maarschalk E, O'Connell RM, Wang P, Yang L, Baltimore D. Engineering human hematopoietic stem/progenitor cells to produce a broadly neutralizing anti-HIV antibody after in vitro maturation to human B lymphocytes. Blood 2009;113: 1422–31.
31. Cao Y, Gordic M, Kobold S, Lajmi N, Meyer S, Bartels K, et al. An optimized assay for the enumeration of antigen-specific memory B cells in different compartments of the human body. J Immunol Methods 2010;358:56–65.
32. Bonsignori M, Moody MA, Parks RJ, Holl TM, Kelsoe G, Hicks CB, et al. HIV-1 envelope induces memory B cell responses that correlate with plasma antibody levels after envelope gp120 protein vaccination or HIV-1 infection. J Immunol 2009;183: 2708–17.
33. Van Venrooij WJ, van Beers JJ, Pruijn GJ. Anti-CCP antibodies: the past, the present and the future. Nat Rev Rheumatol 2011;7:391–8.
34. Sakkas LI, Bogdanos DP, Katsiari C, Platsoucas CD. Anti-citrullinated peptides as autoantigens in rheumatoid arthritis-relevance to treatment. Autoimmun Rev 2014;13:1114–20.
35. Prevoo ML, van 't Hof MA, Kuper HH, van Leeuwen MA, van de Putte LB, van Riel PL. Modified disease activity scores that include twenty-eight–joint counts: development and validation in a prospective longitudinal study of patients with rheumatoid arthritis. Arthritis Rheum 1995;38:44–8.
36. Anderson J, Caplan L, Yazdany J, Robbins ML, Neogi T, Michaud K, et al. Rheumatoid arthritis disease activity measures: American College of Rheumatology recommendations for use in clinical practice. Arthritis Care Res (Hoboken) 2012;64:640–7.
37. Bellatin MF, Han M, Fallena M, Fan L, Xia D, Olsen N, et al. Production of autoantibodies against citrullinated antigens/peptides by human B cells. J Immunol 2012;188:3542–50.
38. Szarka E, Babos F, Magyar A, Huber K, Szittner Z, Papp K, et al. Recognition of new citrulline-containing peptide epitopes by autoantibodies produced in vivo and in vitro by B cells of rheumatoid arthritis patients. Immunology 2014;141:181–91.
39. Kerkman PF, Fabre E, van der Voort EI, Zaldumbide A, Rombouts Y, Rispens T, et al. Identification and characterisation of citrullinated antigen-specific B cells in peripheral blood of patients with rheumatoid arthritis. Ann Rheum Dis 2016;75: 1170–6.
40. Amara K, Steen J, Murray F, Morbach H, Fernandez-Rodriguez BM, Joshua V, et al. Monoclonal IgG antibodies generated from joint-derived B cells of RA patients have a strong bias toward citrullinated autoantigen recognition. J Exp Med 2013;210:445–55.
41. Hiepe F, Dörner T, Hauser AE, Hoyer BF, Mei H, Radbruch A. Long-lived autoreactive plasma cells drive persistent autoimmune inflammation. Nat Rev Rheumatol 2011;7:170–8.
42. Kavanaugh A, Rosengren S, Lee SJ, Hammaker D, Firestein GS, Kalunian K, et al. Assessment of rituximab's immunomodulatory synovial effects (ARISE trial). Part 1: clinical and synovial biomarker results. Ann Rheum Dis 2008;67:402–8.
43. Buch MH, Boyle DL, Rosengren S, Saleem B, Reece RJ, Rhodes LA, et al. Mode of action of abatacept in rheumatoid arthritis patients having failed tumour necrosis factor blockade: a histological, gene expression and dynamic magnetic resonance imaging pilot study. Ann Rheum Dis 2009;68:1220–7.
44. Klaasen R, Thurlings RM, Wijbrandts CA, van Kuijk AW, Baeten D, Gerlag DM, et al. The relationship between synovial lymphocyte aggregates and the clinical response to infliximab in rheumatoid arthritis: a prospective study. Arthritis Rheum 2009; 60:3217–24.
45. Tan YC, Kongpachith S, Blum LK, Ju CH, Lahey LJ, Lu DR, et al. Barcode-enabled sequencing of plasmablast antibody repertoires in rheumatoid arthritis. Arthritis Rheumatol 2014;66: 2706–15.
46. Roll P, Mahmood Z, Muhammad K, Feuchtenberger M, Dörner T, Tony HP. Long-term repopulation of peripheral B-cell subsets after single and repeated rituximab infusions in patients with rheumatoid arthritis. Clin Exp Rheumatol 2015; 33:347–53.
47. Smolen JS, Nash P, Durez P, Hall S, Ilivanova E, Irazoque-Palazuelos F, et al. Maintenance, reduction, or withdrawal of etanercept after treatment with etanercept and methotrexate in patients with moderate rheumatoid arthritis (PRESERVE): a randomised controlled trial. Lancet 2013;381:918–29.
48. Nagy G, van Vollenhoven RF. Sustained biologic-free and drug-free remission in rheumatoid arthritis, where are we now? Arthritis Res Ther 2015;17:181.
49. Ghiti Moghadam M, Vonkeman HE, Ten Klooster PM, Tekstra J, van Schaardenburg D, Starmans-Kool M, et al. Stopping tumor necrosis factor inhibitor treatment in patients with established rheumatoid arthritis in remission or with stable low disease activity: a pragmatic multicenter, open-label randomized controlled trial. Arthritis Rheumatol 2016;68:1810–7.

ARTHRITIS & RHEUMATOLOGY
Vol. 69, No. 6, June 2017, pp 1187–1193
DOI 10.1002/art.40047

BRIEF REPORT

Treatment of Tumor Necrosis Factor–Transgenic Mice With Anti–Tumor Necrosis Factor Restores Lymphatic Contractions, Repairs Lymphatic Vessels, and May Increase Monocyte/Macrophage Egress

Echoe M. Bouta,[1] Igor Kuzin,[2] Karen de Mesy Bentley,[1] Ronald W. Wood,[1] Homaira Rahimi,[1] Rui-Cheng Ji,[3] Christopher T. Ritchlin,[1] Andrea Bottaro,[2] Lianping Xing,[1] and Edward M. Schwarz[1]

Objective. **Recent studies have demonstrated that there is an inverse relationship between lymphatic egress and inflammatory arthritis in affected joints. As a model, tumor necrosis factor (TNF)–transgenic mice develop advanced arthritis following draining lymph node (LN) collapse, and loss of lymphatic contractions downstream of inflamed joints. It is unknown if these lymphatic deficits are reversible. This study was undertaken to test the hypothesis that anti-TNF therapy reduces advanced erosive inflammatory arthritis, associated with restoration of lymphatic contractions, repair of damaged lymphatic vessels, and evidence of increased monocyte egress.**

Methods. **TNF-transgenic mice with advanced arthritis and collapsed popliteal LNs were treated with anti-TNF monoclonal antibody (10 mg/kg weekly) or placebo for 6 weeks, and effects on knee synovitis, lymphatic vessel ultrastructure and function, and popliteal LN cellularity were assessed by ultrasound, histology, transmission electron microscopy (TEM), near-infrared indocyanine green imaging, and flow cytometry.**

Results. **Anti-TNF therapy significantly decreased synovitis (~5-fold; $P < 0.05$ versus placebo), restored lymphatic contractions, and significantly increased the number of popliteal LN monocyte/macrophages (~2-fold; $P < 0.05$ versus placebo). TEM demonstrated large activated macrophages attached to damaged lymphatic endothelium in mice with early arthritis, extensively damaged lymphatic vessels in placebo-treated mice with advanced arthritis, and rolling leukocytes in repaired lymphatic vessels in mice responsive to anti-TNF therapy.**

Conclusion. **These findings support the concept that anti-TNF therapy ameliorates erosive inflammatory arthritis, in part via restoration of lymphatic vessel contractions and potential enhancement of inflammatory cell egress.**

Despite the establishment of tumor necrosis factor (TNF) inhibitors as standard of care for rheumatoid arthritis (RA), the mechanisms by which they ameliorate synovitis in inflamed joints remain incompletely understood. Specifically, how an anti-TNF agent reduces synovial macrophage numbers independent of apoptosis (1,2), and alters monocyte influx into the synovium (3), remains an open question. One possible explanation is that TNF inhibition increases the efflux of monocyte/macrophages from the synovium, which is supported by studies demonstrating that anti-TNF increases lymphangiogenesis in murine inflammatory arthritis and in RA patients (4,5). However, anti-TNF–induced cellular egress from joints during flare has yet to be formally demonstrated.

Previously, we demonstrated that progression of arthritis in the knee joints of TNF-transgenic mice is paralleled by dramatic changes in the draining lymph nodes (LNs) (6–8). Those longitudinal imaging studies combining contrast-enhanced magnetic resonance imaging (CE-MRI) of the synovium and popliteal LNs (6) with quantitation of lymphatic drainage via near-infrared (NIR) imaging of an injected dye (indocyanine green [ICG]) (9) demonstrated that prior to detectable synovial hyperplasia in the knee, the adjacent popliteal LN expands due to increased lymphangiogenesis, lymphatic fluid accumulation, CD11b+ macrophage infiltration, and the expansion of a unique subset of CD23+/CD21^{high} B cells in inflamed

Supported by the NIH (PHS awards T32-AR-053459, K08-AR-067885, R01-AR-069000, R01-AR-048697, R01-AR-056702, P01-AI-078907, and P30-AR-069655).

[1]Echoe M. Bouta, PhD, Karen de Mesy Bentley, MS, Ronald W. Wood, PhD, Homaira Rahimi, MD, Christopher T. Ritchlin, MD, MPH, Lianping Xing, BM, PhD, Edward M. Schwarz, PhD: University of Rochester School of Medicine and Dentistry, Rochester, New York; [2]Igor Kuzin, PhD, Andrea Bottaro, PhD: Cooper Medical School of Rowan University, Camden, New Jersey; [3]Rui-Cheng Ji, MD, PhD: Oita University, Oita, Japan.

Address correspondence to Edward M. Schwarz, PhD, The Center for Musculoskeletal Research, University of Rochester Medical Center, 601 Elmwood Avenue, Box 665, Rochester, NY 14642. E-mail: Edward_Schwarz@URMC.Rochester.edu.

Submitted for publication October 4, 2016; accepted in revised form January 12, 2017.

nodes (5,9–14). This asymptomatic "expansion" phase is followed by a sudden "collapse" of the popliteal LN, which is identified by CE-MRI or power Doppler imaging of the popliteal LN (6,15). This collapse, which occurs at variable time intervals in ~80% of TNF-transgenic mice, is associated with the translocation of CD23+/CD21^{high} B cells in inflamed nodes from the follicles to lymphatic vessel endothelial hyaluronan receptor 1–positive lymphatic vessels of the paracortical sinuses, and a reduction in LN volume and increase in popliteal LN fluid pressure (6,8,16). Thereafter, lymphatic drainage declines significantly due to loss of intrisic lymphatic contractions and passive flow (7,8,10,13).

It has also been demonstrated that B cell depletion therapy with anti-CD20 antibodies ameliorated knee flare afferent to collapsed popliteal LNs by clearing the LN sinuses and restoring passive lymphatic flow in the absence of lymphatic contractions (8). However, whether agents that target the underlying etiology of inflammatory arthritis can restore lymphatic vessel contractions during the collapsed phase of the disease remains unknown. To this end, we evaluated the effects of anti-TNF treatment on advanced knee arthritis in TNF-transgenic mice to determine if lymphatic contraction can be restored.

MATERIALS AND METHODS

Animals and treatment. All animal research was conducted using protocols approved by the University of Rochester Institutional Animal Care and Use Committee. TNF-transgenic mice (3647 line) (17) were originally acquired from Dr. G. Kollias (Alexander Fleming Institute, Athens, Greece), and were maintained as heterozygotes on a C57BL/6 background. For all imaging, mice were anesthetized with 1.5–2% isoflurane. Male TNF-transgenic mice (8–10 months old) with collapsed popliteal LNs were treated with anti-TNF (provided by Janssen Pharmaceuticals) or nonspecific IgG1 isotype placebo control monoclonal antibodies (CNTO12 and CNTO151; Janssen) 10 mg/kg per week intraperitoneally, as previously described (6).

CE-MRI acquisition and analysis. MRI and analysis were performed as previously described (6,10,11). Briefly, TNF-transgenic mice were anesthetized and the knee and ankle were inserted into a customized coil and imaged in a Siemens Trio 3T scanner. After a precontrast scan, 0.5 ml/kg of gadolinium diethylenetriaminepentaacetic acid (Gd-DTPA) contrast agent (Omniscan; Amersham Health) was injected into the orbital venous plexus. The postcontrast scan was started 5 minutes after injection to allow for circulation of Gd-DTPA.

Histologic analysis. For histologic analysis, mouse knees were harvested and fixed in 10% neutral buffered formalin. The joints were then decalcified in 14% EDTA at room temperature for 21 days. Joints were then embedded in paraffin and cut into 5-μm sections. Sections were deparaffinized and stained with Alcian blue–hematoxylin/orange G, tartrate-resistant acid phosphatase, or F4/80 (AbD Serotec) as previously described (6,10,11).

Power Doppler ultrasound (PDUS). The popliteal LNs of TNF-transgenic mice were phenotyped and classified as collapsed using PDUS as previously described (15). PDUS was also performed on the mouse knee joints as previously described (18). Each joint was imaged with a high-resolution small-animal ultrasound system (VisualSonics 770) using a 704b scanhead.

NIR ICG imaging. Mice were placed on a heated surface (Indus Instruments), hair was removed with a depilatory cream, and the footpad was injected with 10 μl of 0.1% ICG (Akorn) as previously described (8). The imaging system was composed of a lens (Zoom 7000; Navitar), ICG filter set (Semrock), and camera (Prosilica GT1380; Allied Vision Technologies). ICG was excited with a tungsten halogen bulb (IT 9596ER; Illumination Technologies) through a ring illuminator (Schott). Imaging settings and recordings were obtained using a custom-built LabVIEW program (National Instruments). Real-time NIR imaging was performed for 60 minutes after ICG injection into the footpad to quantify the lymphatic contraction frequency, and mice were imaged 24 hours later to quantify percent ICG clearance as previously described (8).

Flow cytometric analysis. Single-cell suspensions were prepared from LNs by mechanical disruption and stained with a mixture of fluorochrome-conjugated monoclonal antibodies: CD3 (clone 17A2), CD11b (clone M1/70), major histocompatibility complex class II (clone M5/114.15.2), and Gr1 (clone RB6-8C5) (all from BioLegend), CD19 (clone 1D3) and CD11c (clone HL3) (both from BD PharMingen), and F4/80 (BM8; eBioscience), as previously described (13). All of the samples were stained for dead cell exclusion using a Live/Dead Fixable Violet Dead Cell Stain kit (Invitrogen) and fixed in 1% formaldehyde before running on the instrument. Samples were run on a 12-color LSRII flow cytometer (BD PharMingen) and analyzed using FlowJo software (Tree Star).

Transmission electron microscopy (TEM). The lymphatic vessel afferent to the popliteal LN was identified by injecting Evans blue into the mouse footpad and was then excised and immersion-fixed at 4°C using a combination fixative of 2.5% glutaraldehyde and 4.0% paraformaldehyde in 0.1*M* sodium cacodylate buffer for 24 hours. The specimens were rinsed in 0.1*M* sodium cacodylate buffer and postfixed with buffered 1% osmium tetroxide. The tissue was dehydrated in a graded series of ethanol to 100%, transitioned into propylene oxide, and infiltrated with Epon–Araldite epoxy resin, followed by embedding in fresh resin and polymerization for 2 days at 60°C. To identify the lymphatic vessel in the specimen, the epoxy-embedded block was cut serially into 1μ slices and stained with toluidine blue. The lymphatic vessel was then trimmed of excess surrounding tissue and thin sectioned at 70 nm using a diamond knife and ultramicrotome. The thin sections were placed onto Formvar/carbon slot nickel grids and stained with uranyl acetate and lead citrate. A Hitachi 7650 transmission electron microscope with an 11-megapixel Erlangshen digital camera (Gatan) was used to image the grids.

Statistical analysis. Significance was determined by Mann-Whitney test for non-normally distributed data or *t*-test for normally distributed data. Normality was tested using a Shapiro-Wilk normality test. Longitudinal data were analyzed using two-way analysis of variance with multiple comparisons corrected for by controlling the false discovery rate or Bonferroni post hoc test. *P* values less than 0.05 were considered significant.

RESULTS

Consistent with our prior studies (10), anti-TNF therapy significantly decreased mouse knee synovial volume

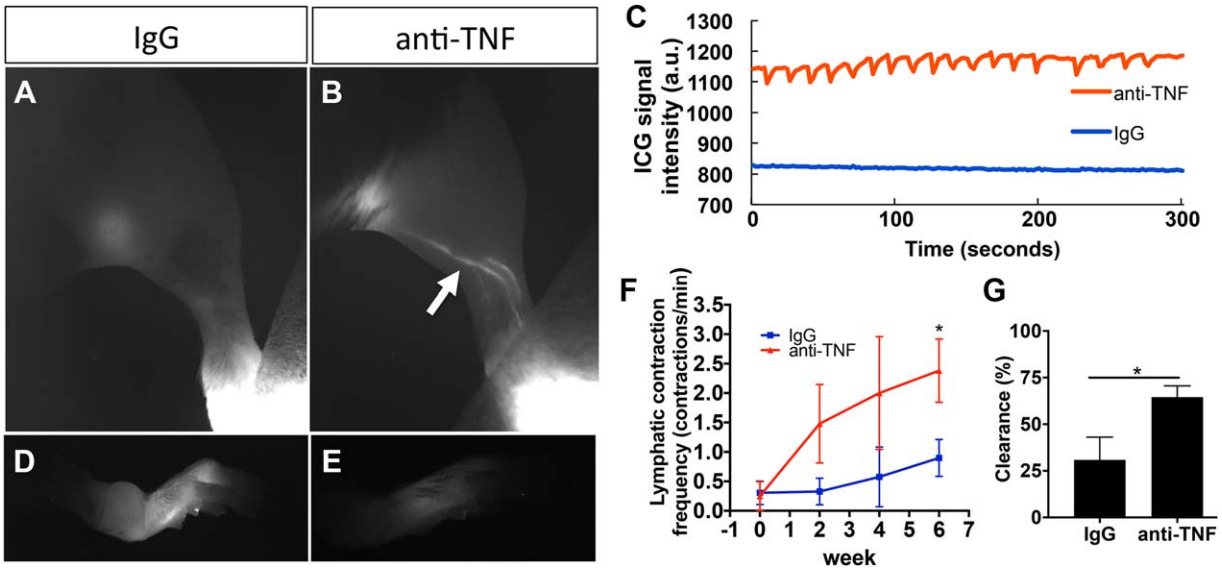

Figure 1. Restoration of lymphatic contractions in anti–tumor necrosis factor (anti-TNF)–treated TNF-transgenic mice with advanced arthritis. Male TNF-transgenic mice (n = 6) were randomized to receive IgG placebo or anti-TNF treatment following power Doppler ultrasound to confirm popliteal lymph node collapse and baseline near-infrared (NIR) indocyanine green (ICG) imaging to confirm loss of lymphatic contractions. After beginning therapy, the mice underwent NIR ICG imaging every 2 weeks for 6 weeks to assess recovery of lymphatic contractions. **A** and **B,** Representative NIR images of the lower limb obtained 1 hour after ICG injection in mice treated for 6 weeks with placebo or anti-TNF. Note that ICG-filled lymphatic vessels are most apparent in the anti-TNF–treated mouse (**arrow** in **B**). **C,** Representative examples of the raw signal intensity data used to quantify lymphatic contractions. Recovery was observed at 6 weeks in the anti-TNF–treated mice, while no contractions were observed in the placebo-treated mice. **D** and **E,** Representative NIR images of the injected foot obtained 24 hours after ICG injection in mice treated for 6 weeks with placebo or anti-TNF. Note that residual ICG is greater in the foot of the placebo-treated mouse. **F,** Quantification of the frequency of lymphatic contractions in placebo-treated and anti-TNF–treated mice. Values are the mean ± SEM. * = $P = 0.01$ by two-way analysis of variance with multiple comparisons corrected for by controlling the false discovery rate. **G,** Percent ICG clearance in placebo-treated and anti-TNF–treated mice after 6 weeks of treatment. Values are the mean ± SEM. * = $P < 0.05$ by Mann-Whitney test. Color figure can be viewed in the online issue, which is available at http://onlinelibrary.wiley.com/doi/10.1002/art.40047/abstract.

versus placebo as assessed by CE-MRI (Supplementary Figure 1, available on the *Arthritis & Rheumatology* web site at http://onlinelibrary.wiley.com/doi/10.1002/art.40047/abstract). Anti-TNF therapy reduced joint inflammation, bone erosion, and osteoclast numbers as assessed by histology (Supplementary Figures 2A–D, available on the *Arthritis & Rheumatology* web site at http://onlinelibrary.wiley.com/doi/10.1002/art.40047/abstract). Furthermore, immunohistochemistry demonstrated that numbers of F4/80+ macrophages in knee synovium were markedly reduced in anti-TNF–treated mice versus placebo-treated mice (Supplementary Figures 2E and F). We also performed PD volume measurements in the mouse knee joint space as an additional assessment of synovial vascularity and

Table 1. Increased monocyte and granulocyte numbers in anti-TNF–treated arthritic TNF-transgenic mice*

	IgG-treated mice	Anti-TNF–treated mice	*P*†
B cells (CD19+)	1.4 ± 0.3	2.4 ± 0.8	NS
T cells (CD3+)	0.5 ± 0.09	2.0 ± 0.7	NS
Non–B/non–T cells (CD19−, CD3−)	1.8 ± 0.3	5.2 ± 1.0	0.009
Monocyte/macrophages (CD3–, CD19–, CD11b+, CD11c−, F4/80+)	0.8 ± 0.1	1.7 ± 0.4	0.047
Granulocytes (CD3–, CD19–, CD11b+, CD11c−, F4/80−, Gr1+)	0.7 ± 0.09	2.0 ± 0.05	0.024

* Popliteal lymph nodes (LNs) from the tumor necrosis factor (TNF)–transgenic mice described in Figure 1 were harvested after 6 weeks of treatment and analyzed by flow cytometry to quantify cells per popliteal LN. Values are the mean ± SEM $\times 10^6$ cells per popliteal LN. NS = not significant.
† By unpaired *t*-test.

inflammation. After 6 weeks of treatment, a higher PD signal was obvious in the placebo group, compared to the anti-TNF treatment group (Supplementary Figures 2G and H). Longitudinally, US showed a dramatic and continual increase in PD volume in the placebo group, while anti-TNF prevented an increase in joint inflammation (Supplementary Figure 2I).

Longitudinal NIR ICG imaging demonstrated a remarkable increase in lymphatic transport in anti-TNF–treated mice compared to placebo-treated mice, in which ICG uptake was low or absent at 6 weeks (Figure 1). Quantification of the frequency of lymphatic contractions confirmed that the anti-TNF effects were due in part to active transport (Figures 1C and F), which resulted in increased lymphatic clearance (Figure 1G). Notably, anti-TNF–treated mice showed consistent, regular lymphatic contractions that were significantly increased versus placebo-treated mice, and equivalent to findings in wild-type mice (~2 contractions/minute), similar to previous studies (8). Moreover, this is the first demonstration that lymphatic contractions can be recovered after popliteal LN collapse in this model.

To further dissect the mechanisms of action of anti-TNF therapy, we assessed drug effects on the cellular composition of the popliteal LNs by flow cytometry. The results showed that the increased cellular egress from inflamed joints following anti-TNF treatment was accompanied by higher total cell numbers in the collapsed

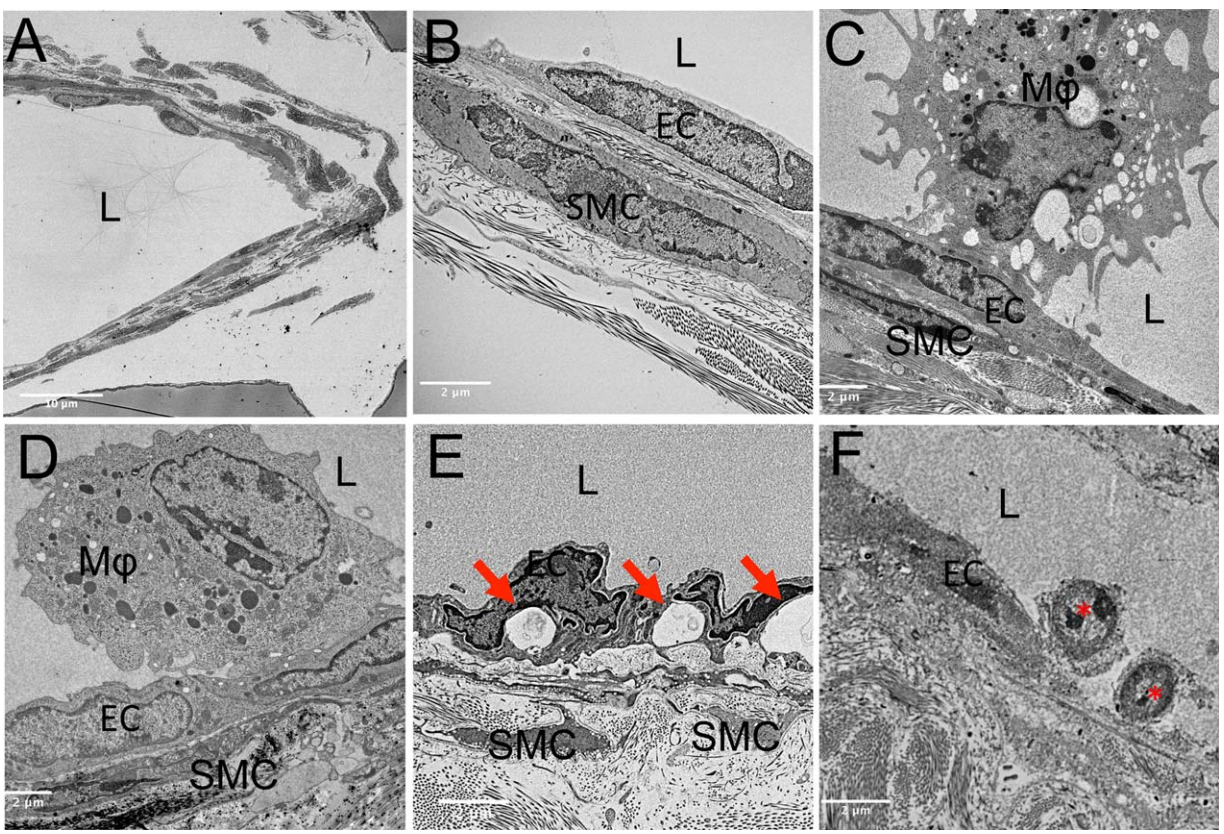

Figure 2. Ultrastructural evidence of lymphatic vessel repair and rolling leukocytes in anti–tumor necrosis factor (anti-TNF)–treated TNF-transgenic mice that recovered lymphatic vessel contractions. Wild-type and TNF-transgenic mice (n = 3 per group) underwent transmission electron microscopy imaging as described in Materials and Methods. Low-magnification imaging was used to identify lymphatic vessels. After the lymphatic vessel was identified, vessel walls were imaged at 10,000× magnification. **A,** Representative low-magnification image of lymphatic vessels in a wild-type mouse. Original magnification × 2,500. **B,** Representative image of the vessel wall in a wild-type mouse. Note the absence of cells in the lumen (**L**). **C,** Representative image of the vessel wall in an untreated TNF-transgenic mouse with expanding popliteal lymph nodes (LNs). Note the activated macrophage (**M*ϕ***) with initial pseudopod attachment to endothelial cells (**EC**) afferent to the expanded popliteal LNs. **D,** Representative image of the vessel wall in an untreated TNF-transgenic mouse with collapsed popliteal LNs. Note the complete macrophage attachment to ECs afferent to collapsed popliteal LNs. **E,** Representative image of the vessel wall in a placebo (IgG)–treated TNF-transgenic mouse with collapsed popliteal LNs. Note the exacerbated destruction of the lymphatic vessel as evidenced by vacuole formation in ECs (**arrows**). **F,** Representative image of the vessel wall in an anti-TNF–treated TNF-transgenic mouse with collapsed popliteal LNs. Note the mononucleated leukocytes that appear to be rolling along the endothelium (**asterisks**), indicative of restored cellular egress. **SMC** = smooth muscle cell. Original magnification × 10,000 in **B–F**.

popliteal LNs of TNF-transgenic mice (Table 1). Although our cellular subset analysis displayed trends suggesting increased numbers of B cells and T cells in anti-TNF–treated mice, the only significant changes observed in the popliteal LN populations in mice treated with anti-TNF therapy were a 2.1-fold increase in monocyte/macrophages (CD3−CD19−CD11b+) and a 2.9-fold increase in granulocytes (CD3−CD19−CD11b+CD11c−F4/80−Gr1+). Taken together, these findings support a model in which anti-TNF therapy ameliorates synovitis potentially by enhancing cellular egress from the joint via active lymphatic transport through the draining LNs.

To corroborate our finding of anti-TNF–induced monocyte/macrophage egress, we performed TEM on the lymphatic vessels afferent to popliteal LNs. Wild-type mouse lymphatic vessels showed intact lymphatic endothelial and muscle cells (Figures 2A and B) with lumens devoid of cells. Vessels afferent to expanding popliteal LNs showed initial, and what appeared as weak, luminal attachment of large (>5 μm) macrophages to the endothelial cells (Figure 2C), while vessels afferent to collapsed popliteal LNs showed these activated macrophages firmly attached to the endothelial cells, indicated by the increased surface area of macrophage attachment (Figure 2D). TEM images of lymphatic vessels from placebo-treated mice displayed extensive tissue destruction as evidenced by large vacuoles in endothelial cells and degenerated muscle cells (Figure 2E). Notably, mice with collapsed popliteal LNs treated with anti-TNF showed evidence of restored cellular egress; TEM revealed small (<2 μm) leukocytes with a rolling cell morphology on the luminal endothelium (Figure 2F). In particular, we did not observe cytoplasmic vacuoles in endothelial cells, a finding associated with damaged lymphatic vessels, providing additional support to explain the recovery of lymphatic contraction (15).

DISCUSSION

Advances in drug development over the last 2 decades have provided an array of treatment options in RA (19,20). Despite this progress, major unmet clinical needs remain for a significant proportion of RA patients (~40%) who are partial responders, or whose disease is refractory to all currently available therapies including anti-TNF. There is also a larger group of RA patients who experience periodic arthritis flares. Thus, new therapeutic strategies are needed, which requires formal elucidation of the mechanisms of action of drugs currently in use. To this end, we have focused on lymphatic changes during arthritis progression and flare (6,8,10,13,21) and the effects of interventions that specifically target lymphatic contractions, whose physiologic importance in supporting lymphatic drainage and subsequent onset of lymphedema have been established in preclinical and clinical studies (22,23).

It is well known that monocyte/macrophages (type A synoviocytes) are the most abundant cell type in RA inflamed synovium, and that these cells are a major source of inflammatory mediators and catabolic factors in pannus tissue (24). Moreover, results from RA trials with various drug therapies have shown that clinical efficacy directly correlates with an observed decrease in CD68+ synovial sublining macrophages (25,26). Many studies have addressed the mechanisms responsible for the reduction in RA monocyte/macrophages in response to anti-TNF treatment, but the findings have been inconclusive and contradictory. For example, while anti-TNF–induced apoptosis of synoviocytes in RA has been reported (27), other studies failed to show these effects (1,2). Other investigations demonstrated that anti-TNF therapy reduced the generation of osteoclasts and bone erosion (28). In contrast, we found that anti-TNF decreases macrophage/monocyte numbers in the joint by increasing lymphatic transport and potentially cell egress from inflamed joints. These findings are further supported by previous studies demonstrating that anti-TNF therapy increased lymphangiogenesis both in a murine model and in RA patients (4).

Our data demonstrate that reduction in joint inflammation (Supplementary Figures 1 and 2, available on the *Arthritis & Rheumatology* web site at http://onlinelibrary.wiley.com/doi/10.1002/art.40047/abstract) is accompanied by an increase in lymphatic contraction frequency and lymphatic clearance (Figure 1), and a significant increase in the number of CD11b+ cells in the draining LNs (Table 1). Previously, we have shown that CD11b+ cells migrate in lymphatic vessels afferent to expanding popliteal LNs, and are immobile within these lymphatic vessels during the popliteal LN collapsed phase (8). Therefore, the best explanation for the concomitant decrease in myeloid synoviocytes and increased CD11b+ cells in the popliteal LNs after 6 weeks of anti-TNF therapy is increased cell egress through the lymphatic system, as evidenced by the rolling leukocytes in lymphatic vessels (Figure 2F). However, important points that were not addressed in the present study include the possibility that CD11b+ cells enter the popliteal LNs through high endothelial venules and a potential increase in T cells and B cells. Therefore, formal histology studies to determine the temporal and spatial increases in distinct myeloid and lymphocytic populations in the popliteal LNs following anti-TNF therapy are planned. It may also be possible to assess increased lymphatic clearance following anti-TNF treatment of RA patients using new NIR ICG imaging methods (21).

In addition to our studies of anti-TNF treatment of TNF-transgenic mice described here and elsewhere (6,10,11), we have assessed the effects of anti-CD20 in this RA model (8,13). Although head-to-head efficacy studies have yet to be performed, there were several general findings that highlight distinct drug mechanisms of action on joint inflammation and lymphatic clearance. The first is that anti-TNF therapy ameliorates arthritis in both ankle and knee joints, while anti-CD20 and genetic B cell depletion affect only knee arthritis (8). This may be due to anti-TNF effects on both tenosynovitis, which drives ankle arthritis in this model (29), and knee flare triggered by the loss of lymphatic drainage (Supplementary Figure 1), while anti-CD20 affects only the latter (8,13). Second, anti-CD20 efficacy appears to be due to "unclogging" of lymphatic vessels to restore passive lymphatic flow, as evidenced by a dramatic increase in popliteal LN contrast enhancement on CE-MRI and loss of CD23+/CD21^{high} B cells in inflamed nodes without lymphatic contractions (8), while anti-TNF targets the underling etiology in this model to decrease inflammation and restore lymphatic contractions (Figure 1) without decreasing popliteal LN B cell numbers (Table 1).

In summary, these data show that in a murine model of arthritis, TNF inhibition is followed by increased lymphatic drainage from the joint, providing a possible clearance mechanism for inflammatory cells. More importantly, we demonstrate for the first time that a therapeutic agent can restore steady normal lymphatic contractions subsequent to arthritic flare associated with collapsed draining LNs and the loss of lymphatic contractions. Thus, drugs specifically designed to facilitate lymphatic vessel repair and return of lymphatic contractions remain intriguing and novel treatments for additional exploration.

ACKNOWLEDGMENTS

We thank Pat Weber for technical assistance with CE-MRI, Gayle Schneider for assistance with thin sectioning for TEM, and Sarah Mack and Kathy Maltby for technical assistance with histology.

AUTHOR CONTRIBUTIONS

All authors were involved in drafting the article or revising it critically for important intellectual content, and all authors approved the final version to be published. Dr. Schwarz had full access to all of the data in the study and takes responsibility for the integrity of the data and the accuracy of the data analysis.

Study conception and design. Bouta, Kuzin, Ritchlin, Bottaro, Xing, Schwarz.

Acquisition of data. Bouta, Kuzin, Ji.

Analysis and interpretation of data. Bouta, Kuzin, de Mesy-Bentley, Wood, Rahimi, Ji, Ritchlin, Bottaro, Xing, Schwarz.

REFERENCES

1. Smeets TJ, Kraan MC, van Loon ME, Tak PP. Tumor necrosis factor α blockade reduces the synovial cell infiltrate early after initiation of treatment, but apparently not by induction of apoptosis in synovial tissue. Arthritis Rheum 2003;48:2155–62.
2. Wijbrandts CA, Remans PH, Klarenbeek PL, Wouters D, van den Bergh Weerman MA, et al. Analysis of apoptosis in peripheral blood and synovial tissue very early after initiation of infliximab treatment in rheumatoid arthritis patients. Arthritis Rheum 2008;58:3330–9.
3. Herenius MM, Thurlings RM, Wijbrandts CA, Bennink RJ, Dohmen SE, Voermans C, et al. Monocyte migration to the synovium in rheumatoid arthritis patients treated with adalimumab. Ann Rheum Dis 2011;70:1160–2.
4. Polzer K, Baeten D, Soleiman A, Distler J, Gerlag DM, Tak PP, et al. Tumour necrosis factor blockade increases lymphangiogenesis in murine and human arthritic joints. Ann Rheum Dis 2008;67:1610–6.
5. Zhang Q, Lu Y, Proulx S, Guo R, Yao Z, Schwarz EM, et al. Increased lymphangiogenesis in joints of mice with inflammatory arthritis. Arthritis Res Ther 2007;9:R118.
6. Proulx ST, Kwok E, You Z, Papuga MO, Beck CA, Shealy DJ, et al. Longitudinal assessment of synovial, lymph node, and bone volumes in inflammatory arthritis in mice by in vivo magnetic resonance imaging and microfocal computed tomography. Arthritis Rheum 2007;56:4024–37.
7. Li J, Zhou Q, Wood R, Kuzin I, Bottaro A, Ritchlin CT, et al. CD23^{+}/CD21^{hi} B-cell translocation and ipsilateral lymph node collapse is associated with asymmetric arthritic flare in TNF-Tg mice. Arthritis Res Ther 2011;13:R138.
8. Li J, Ju Y, Bouta EM, Xing L, Wood RW, Kuzin I, et al. Efficacy of B cell depletion therapy for murine joint arthritis flare is associated with increased lymphatic flow. Arthritis Rheum 2013;65:130–8.
9. Zhou Q, Wood R, Schwarz EM, Wang YJ, Xing L. Near-infrared lymphatic imaging demonstrates the dynamics of lymph flow and lymphangiogenesis during the acute versus chronic phases of arthritis in mice. Arthritis Rheum 2010;62:1881–9.
10. Proulx ST, Kwok E, You Z, Beck CA, Shealy DJ, Ritchlin CT, et al. MRI and quantification of draining lymph node function in inflammatory arthritis. Ann N Y Acad Sci 2007;1117:106–23.
11. Proulx ST, Kwok E, You Z, Papuga MO, Beck CA, Shealy DJ, et al. Elucidating bone marrow edema and myelopoiesis in murine arthritis using contrast-enhanced magnetic resonance imaging. Arthritis Rheum 2008;58:2019–29.
12. Guo R, Zhou Q, Proulx ST, Wood R, Ji RC, Ritchlin CT, et al. Inhibition of lymphangiogenesis and lymphatic drainage via vascular endothelial growth factor receptor 3 blockade increases the severity of inflammation in a mouse model of chronic inflammatory arthritis. Arthritis Rheum 2009;60:2666–76.
13. Li J, Kuzin I, Moshkani S, Proulx ST, Xing L, Skrombolas D, et al. Expanded CD23+/CD21^{hi} B cells in inflamed lymph nodes are associated with the onset of inflammatory-erosive arthritis in TNF-transgenic mice and are targets of anti-CD20 therapy. J Immunol 2010;184:6142–50.
14. Kuzin II, Kates SL, Ju Y, Zhang L, Rahimi H, Wojciechowski W, et al. Increased numbers of CD23^{+}CD21^{hi} Bin-like B cells in human reactive and rheumatoid arthritis lymph nodes. Eur J Immunol 2016;46:1752–7.
15. Bouta EM, Ju Y, Rahimi H, de Mesy-Bentley KL, Wood RW, Xing L, et al. Power Doppler ultrasound phenotyping of expanding versus collapsed popliteal lymph nodes in murine inflammatory arthritis. PLoS One 2013;8:e73766.
16. Bouta EM, Wood RW, Brown EB, Rahimi H, Ritchlin CT, Schwarz EM. In vivo quantification of lymph viscosity and pressure in lymphatic vessels and draining lymph nodes of arthritic joints in mice. J Physiol 2014;592:1213–23.
17. Keffer J, Probert L, Cazlaris H, Georgopoulos S, Kaslaris E, Kioussis D, et al. Transgenic mice expressing human tumour

necrosis factor: a predictive genetic model of arthritis. EMBO J 1991;10:4025–31.
18. Bouta EM, Banik PD, Wood RW, Rahimi H, Ritchlin CT, Thiele RG, et al. Validation of power Doppler versus contrast enhanced magnetic resonance imaging quantification of joint inflammation in murine inflammatory arthritis. J Bone Miner Res 2015;30:690–4.
19. Smolen JS, Landewe R, Breedveld FC, Dougados M, Emery P, Gaujoux-Viala C, et al. EULAR recommendations for the management of rheumatoid arthritis with synthetic and biological disease-modifying antirheumatic drugs. Ann Rheum Dis 2010;69:964–75.
20. Keystone EC, Smolen J, van Riel P. Developing an effective treatment algorithm for rheumatoid arthritis. Rheumatology (Oxford) 2012;51 Suppl 5:v48–54.
21. Rahimi H, Bell R, Bouta EM, Wood RW, Xing L, Ritchlin CT, et al. Lymphatic imaging to assess rheumatoid flare: mechanistic insights and biomarker potential. Arthritis Res Ther 2016;18:194.
22. Zawieja DC. Contractile physiology of lymphatics. Lymphat Res Biol 2009;7:87–96.
23. Mallick A, Bodenham AR. Disorders of the lymph circulation: their relevance to anaesthesia and intensive care. Br J Anaesth 2003;91:265–72.
24. Firestein GS. Evolving concepts of rheumatoid arthritis. Nature 2003;423:356–61.
25. Zwerina J, Hayer S, Tohidast-Akrad M, Bergmeister H, Redlich K, Feige U, et al. Single and combined inhibition of tumor necrosis factor, interleukin-1, and RANKL pathways in tumor necrosis factor–induced arthritis: effects on synovial inflammation, bone erosion, and cartilage destruction. Arthritis Rheum 2004;50:277–90.
26. Mould AW, Tonks ID, Cahill MM, Pettit AR, Thomas R, Hayward NK, et al. Vegfb gene knockout mice display reduced pathology and synovial angiogenesis in both antigen-induced and collagen-induced models of arthritis. Arthritis Rheum 2003;48:2660–9.
27. Catrina AI, Trollmo C, af Klint E, Engstrom M, Lampa J, Hermansson Y, et al. Evidence that anti–tumor necrosis factor therapy with both etanercept and infliximab induces apoptosis in macrophages, but not lymphocytes, in rheumatoid arthritis joints: extended report. Arthritis Rheum 2005;52:61–72.
28. Binder NB, Puchner A, Niederreiter B, Hayer S, Leiss H, Bluml S, et al. Tumor necrosis factor–inhibiting therapy preferentially targets bone destruction but not synovial inflammation in a tumor necrosis factor–driven model of rheumatoid arthritis. Arthritis Rheum 2013;65:608–17.
29. Hayer S, Redlich K, Korb A, Hermann S, Smolen J, Schett G. Tenosynovitis and osteoclast formation as the initial preclinical changes in a murine model of inflammatory arthritis. Arthritis Rheum 2007;56:79–88.

DOI: 10.1002/art.40088

Clinical Images: Arytenoid chondritis

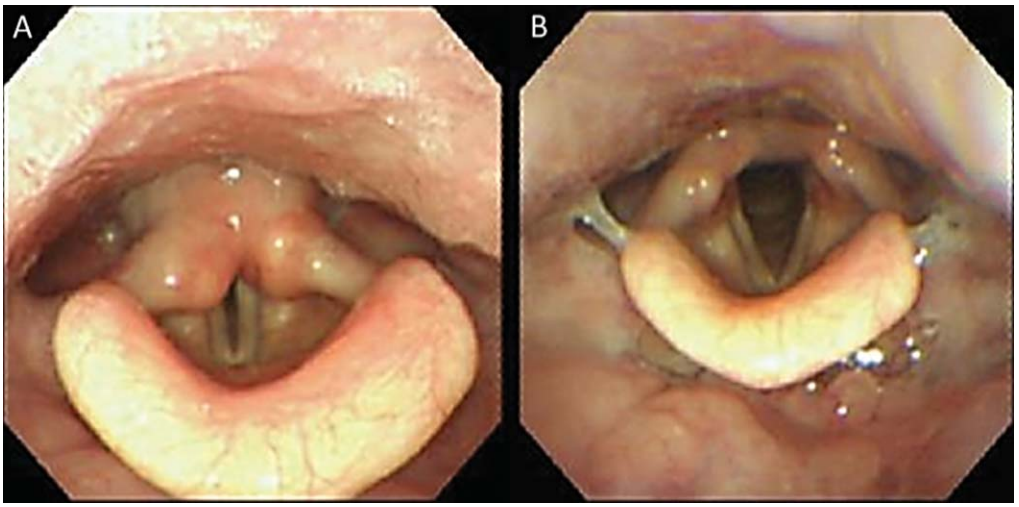

The patient, a 50-year-old woman, was admitted with a 2-week history of fever (39°C) and antinuclear antibody positivity. Physical examination revealed oral ulcers, malar rash, and poly-lymphadenopathy. Inflammation of the cartilage of the nose and auricles was also detected. Based on these findings, along with laboratory results of lymphopenia and anti-Sm antibody positivity, relapsing polychondritis (RP) related to systemic lupus erythematosus (SLE) was diagnosed. On the second day of admission, she reported hoarseness. Although contrast computed tomography did not reveal cricoiditis or bronchial stents, otorhinolaryngologic examination demonstrated arytenoid chondritis (**A**). She was treated with prednisone (25 mg every other day) and her symptoms were alleviated. Follow-up otorhinolaryngologic examination showed resolution of the arytenoid chondritis (**B**). RP is an autoimmune disorder with chondritis as a prominent clinical feature. It has been found to coexist in some patients with SLE (1). Airway involvement is one of the critical symptoms and a risk factor for intensive care unit admission (2). It is therefore necessary to detect and treat arytenoid chondritis early.

1. Zeuner M, Straub RH, Rauh G, Albert ED, Schölmerich J, Lang B. Relapsing polychondritis: clinical and immunogenetic analysis of 62 patients. J Rheumatol 1997;24:96–101.
2. Dion J, Costedoat-Chalumeau N, Sène D, Cohen-Bittan J, Leroux G, Dion C, et al. Relapsing polychondritis can be characterized by three different clinical phenotypes: analysis of a recent series of 142 patients. Arthritis Rheumatol 2016;68:2992–3001.

Yasuhiro Suyama, MD
Shin-ichi Ishimoto, MD
Kiyofumi Hagiwara, MD
JR Tokyo General Hospital
Tokyo, Japan

necrosis factor: a predictive genetic model of arthritis. EMBO J 1991;10:4025–31.
18. Bouta EM, Banik PD, Wood RW, Rahimi H, Ritchlin CT, Thiele RG, et al. Validation of power Doppler versus contrast enhanced magnetic resonance imaging quantification of joint inflammation in murine inflammatory arthritis. J Bone Miner Res 2015;30:690–4.
19. Smolen JS, Landewe R, Breedveld FC, Dougados M, Emery P, Gaujoux-Viala C, et al. EULAR recommendations for the management of rheumatoid arthritis with synthetic and biological disease-modifying antirheumatic drugs. Ann Rheum Dis 2010;69:964–75.
20. Keystone EC, Smolen J, van Riel P. Developing an effective treatment algorithm for rheumatoid arthritis. Rheumatology (Oxford) 2012;51 Suppl 5:v48–54.
21. Rahimi H, Bell R, Bouta EM, Wood RW, Xing L, Ritchlin CT, et al. Lymphatic imaging to assess rheumatoid flare: mechanistic insights and biomarker potential. Arthritis Res Ther 2016;18:194.
22. Zawieja DC. Contractile physiology of lymphatics. Lymphat Res Biol 2009;7:87–96.
23. Mallick A, Bodenham AR. Disorders of the lymph circulation: their relevance to anaesthesia and intensive care. Br J Anaesth 2003;91:265–72.
24. Firestein GS. Evolving concepts of rheumatoid arthritis. Nature 2003;423:356–61.
25. Zwerina J, Hayer S, Tohidast-Akrad M, Bergmeister H, Redlich K, Feige U, et al. Single and combined inhibition of tumor necrosis factor, interleukin-1, and RANKL pathways in tumor necrosis factor–induced arthritis: effects on synovial inflammation, bone erosion, and cartilage destruction. Arthritis Rheum 2004;50:277–90.
26. Mould AW, Tonks ID, Cahill MM, Pettit AR, Thomas R, Hayward NK, et al. Vegfb gene knockout mice display reduced pathology and synovial angiogenesis in both antigen-induced and collagen-induced models of arthritis. Arthritis Rheum 2003;48:2660–9.
27. Catrina AI, Trollmo C, af Klint E, Engstrom M, Lampa J, Hermansson Y, et al. Evidence that anti–tumor necrosis factor therapy with both etanercept and infliximab induces apoptosis in macrophages, but not lymphocytes, in rheumatoid arthritis joints: extended report. Arthritis Rheum 2005;52:61–72.
28. Binder NB, Puchner A, Niederreiter B, Hayer S, Leiss H, Bluml S, et al. Tumor necrosis factor–inhibiting therapy preferentially targets bone destruction but not synovial inflammation in a tumor necrosis factor–driven model of rheumatoid arthritis. Arthritis Rheum 2013;65:608–17.
29. Hayer S, Redlich K, Korb A, Hermann S, Smolen J, Schett G. Tenosynovitis and osteoclast formation as the initial preclinical changes in a murine model of inflammatory arthritis. Arthritis Rheum 2007;56:79–88.

DOI: 10.1002/art.40088

Clinical Images: Arytenoid chondritis

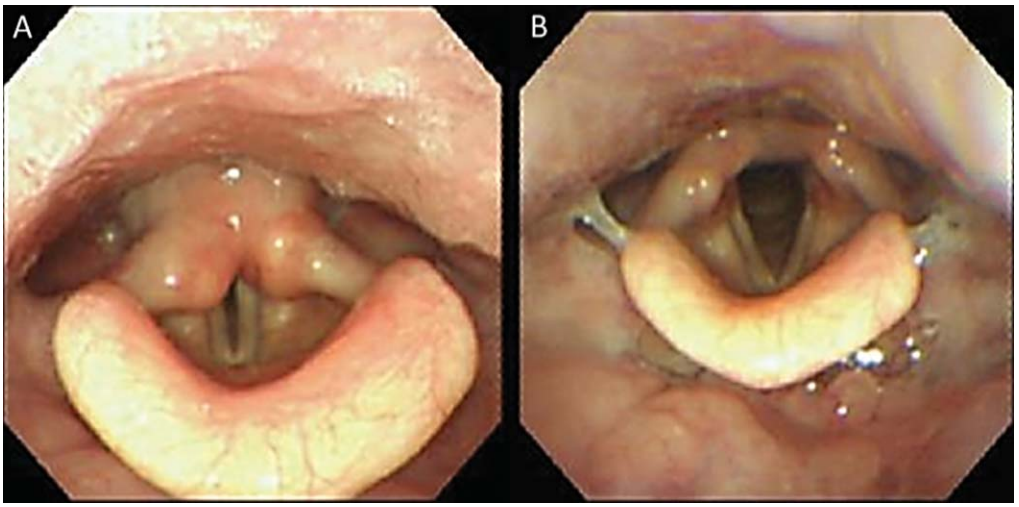

The patient, a 50-year-old woman, was admitted with a 2-week history of fever (39°C) and antinuclear antibody positivity. Physical examination revealed oral ulcers, malar rash, and poly-lymphadenopathy. Inflammation of the cartilage of the nose and auricles was also detected. Based on these findings, along with laboratory results of lymphopenia and anti-Sm antibody positivity, relapsing polychondritis (RP) related to systemic lupus erythematosus (SLE) was diagnosed. On the second day of admission, she reported hoarseness. Although contrast computed tomography did not reveal cricoiditis or bronchial stents, otorhinolaryngologic examination demonstrated arytenoid chondritis (**A**). She was treated with prednisone (25 mg every other day) and her symptoms were alleviated. Follow-up otorhinolaryngologic examination showed resolution of the arytenoid chondritis (**B**). RP is an autoimmune disorder with chondritis as a prominent clinical feature. It has been found to coexist in some patients with SLE (1). Airway involvement is one of the critical symptoms and a risk factor for intensive care unit admission (2). It is therefore necessary to detect and treat arytenoid chondritis early.

1. Zeuner M, Straub RH, Rauh G, Albert ED, Schölmerich J, Lang B. Relapsing polychondritis: clinical and immunogenetic analysis of 62 patients. J Rheumatol 1997;24:96–101.
2. Dion J, Costedoat-Chalumeau N, Sène D, Cohen-Bittan J, Leroux G, Dion C, et al. Relapsing polychondritis can be characterized by three different clinical phenotypes: analysis of a recent series of 142 patients. Arthritis Rheumatol 2016;68:2992–3001.

Yasuhiro Suyama, MD
Shin-ichi Ishimoto, MD
Kiyofumi Hagiwara, MD
JR Tokyo General Hospital
Tokyo, Japan

ARTHRITIS & RHEUMATOLOGY
Vol. 69, No. 6, June 2017, pp 1194–1203
DOI 10.1002/art.40087

Metabolic Syndrome, Its Components, and Knee Osteoarthritis

The Framingham Osteoarthritis Study

Jingbo Niu,[1] Margaret Clancy,[1] Piran Aliabadi,[2] Ramachandran Vasan,[1] and David T. Felson[3]

Objective. **Previous studies have suggested that metabolic syndrome is associated with osteoarthritis (OA). However, analyses have often not included adjustment for body mass index (BMI) and have not addressed whether levels of individual metabolic syndrome components are related to OA. This study was undertaken to examine the relationship of metabolic syndrome and its components with radiographic and symptomatic knee OA.**

Methods. **Framingham Study subjects were assessed for OA in 1992–1995 and again in 2002–2005. Near the baseline visit, subjects had components of metabolic syndrome assessed. We defined incident radiographic OA as present when a knee without radiographic OA at baseline had a Kellgren/Lawrence grade of ≥2 at follow-up, and defined incident symptomatic OA as present when a knee developed the new combination of radiographic OA and knee pain. After excluding knees with prevalent OA at baseline, we tested the relationship of metabolic syndrome according to the National Cholesterol Education Program Adult Treatment Panel III criteria and its components with the risk of incident radiographic OA and symptomatic OA before and after adjusting for BMI using the risk ratio from a binary regression with generalized estimating equations.**

Results. **A total of 991 subjects (55.1% women) with a mean age of 54.2 years were studied, and 26.7% of men and 22.9% of women had metabolic syndrome. Metabolic syndrome and many of its components were associated with both incident radiographic OA and symptomatic OA, but after adjustment for BMI, almost all of these associations became weak and nonsignificant. An association of high blood pressure, especially diastolic pressure, with OA outcomes persisted in both men and women.**

Conclusion. **After adjustment for BMI, neither metabolic syndrome nor its components were associated with incident OA. There may be an association between OA and high blood pressure that needs further study.**

Metabolic syndrome (1,2), whose elements include central obesity, dyslipidemia, impaired fasting glucose, and hypertension, increases the risk of cardiovascular disease (3) and mortality (4). Recent work has focused on identifying the relationship of particular components of metabolic syndrome with diseases to better understand its influence on disease pathogenesis (3).

In the musculoskeletal field, there has been considerable interest in the association of metabolic syndrome with osteoarthritis (OA). Central obesity, a component of metabolic syndrome, is related to body mass index (BMI), a well-known risk factor for knee OA (5). Other components of metabolic syndrome may affect the occurrence of OA through low-grade inflammation, by altering the microvasculature of subchondral bone, or by causing neuromuscular impairment (6,7).

Previous studies have suggested a strong and consistent relationship of metabolic syndrome with an increase in knee OA before adjustment for BMI (8–13). After adjusting for BMI or body weight, especially as a continuous variable, most of the positive findings on metabolic syndrome and OA have weakened (8,11,12), while some, especially findings regarding the number of metabolic syndrome components and OA, have persisted (9,14). In studies of individual components of

Supported by the NIH (National Institute of Arthritis and Musculoskeletal and Skin Diseases grant AR-47785).

[1]Jingbo Niu, DSc, Margaret Clancy, MPH, Ramachandran Vasan, MD, DM: Boston University School of Medicine, Boston, Massachusetts; [2]Piran Aliabadi, MD: Brigham and Women's Hospital, Boston, Massachusetts; [3]David T. Felson, MD, MPH: Boston University School of Medicine, Boston, Massachusetts, and National Institute for Health Research Manchester Biomedical Research Unit, Manchester, UK.

Address correspondence to David T. Felson, MD, MPH, Clinical Epidemiology Research and Training Unit, Boston University School of Medicine, 650 Albany Street, X-200, Boston, MA 02118. E-mail: dfelson@bu.edu.

Submitted for publication June 6, 2016; accepted in revised form February 28, 2017.

metabolic syndrome, central obesity has been the component most frequently associated with knee OA (8,10–12,14,15), and in some studies, this relationship has persisted even after adjusting for BMI (11,13). Hypertension, especially high diastolic blood pressure, was related to knee OA in some studies (9,10,13,16) but not others (8,11).

BMI (and body weight) confer a loading effect both directly on the joint and by causing an increase in muscle force across the joint to accommodate this increased load (5). In animal models, increased weight and other causes of increased focal load across the joint (malalignment; meniscal tear) all strongly increase OA risk (17). Thus, some measure of obesity-related load must be adjusted for when evaluating the effect of metabolic syndrome and its components. Further, there is a strong relationship between central obesity and overall BMI, such that conventional regression adjustment for BMI may be insufficient to evaluate the independent effect of central obesity.

Prior studies have almost all been cross-sectional, with the exception of Japanese and Swedish studies with radiographic knee OA as the outcome and a study following up persons with OA for hip or knee replacement (9,11,13). Few prior studies focused on the occurrence of symptomatic knee OA.

Metabolic syndrome and its relation to heart disease has been a major focus of the Framingham Heart Study, and components of metabolic syndrome have been carefully assessed. Metabolic syndrome is defined by dichotomizing these components, but dichotomizing disease risk factors may compromise power and limit the ability to detect the threshold effect of risk factors (18). Using data from the Framingham OA Study, a substudy of the Heart Study, we examined the longitudinal relationship of metabolic syndrome and its components with radiographic and symptomatic knee OA.

PATIENTS AND METHODS

Study design and subjects. Subjects were recruited from the Framingham Offspring Cohort, which consists of the descendants of the original Framingham Heart Study cohort and their spouses. The OA study focused on surviving members of the Offspring Cohort whose parents, members of the original Framingham cohort, had participated in an OA study and their spouses. These subjects were invited to participate in the OA study in 1992–1995 (baseline visit), and came back for a follow-up visit in 2002–2005 (19). We included subjects who were 40 years and older at baseline because the incidence of knee OA increases dramatically after age 50 (20). The study was approved by the Boston University Medical Center Institutional Review Board. All participants provided written informed consent.

Metabolic syndrome. Since specific family members of the original cohort were asked to come in for an examination for the OA Study after exam 5 of the Offspring Cohort (which took place in 1990–1993), the assessment of metabolic syndrome occurred a year or so before the OA examination. Participants in the Offspring Cohort fasted overnight and had plasma samples taken for the measurement of glucose and lipids, answered questionnaires about sociodemographic and lifestyle characteristics, and underwent a physical examination. Plasma glucose was measured in fresh specimens with a hexokinase reagent kit (A-gent glucose test; Abbott). Glucose assays were run in duplicate; the intraassay coefficient of variation was 3%. The fasting plasma total cholesterol and plasma triglyceride levels were measured enzymatically, and the high-density lipoprotein (HDL) cholesterol fraction was measured after precipitation of low-density lipoprotein (LDL) cholesterol and very low-density lipoprotein cholesterol with Dextran sulfate–magnesium (21). LDL cholesterol was estimated indirectly when triglyceride levels were <4.52 mmoles/liter (22). The Framingham laboratory participates in the lipoprotein cholesterol laboratory standardization program administered by the Centers for Disease Control and Prevention in Atlanta, Georgia (23). Waist circumference was measured as part of the physical examination. Blood pressure was measured twice after subjects had been seated for at least 5 minutes, and the average of the 2 measurements was calculated.

We classified subjects as having metabolic syndrome according to the National Cholesterol Education Program Adult Treatment Panel III (ATP III) criteria (24). Subjects were considered to have metabolic syndrome if they met at least 3 of the following 5 criteria: 1) abdominal obesity (waist circumference $\geq$102 cm [$\geq$40 inches] in men and $\geq$88 cm [$\geq$35 inches] in women), 2) high triglyceride levels ($\geq$150 mg/dl), 3) low HDL cholesterol ($<$40 mg/dl in men and $<$50 mg/dl in women), 4) high blood pressure (systolic blood pressure $\geq$130 mm Hg or diastolic blood pressure $\geq$85 mm Hg or treatment for high blood pressure), and 5) high fasting glucose ($\geq$110 mg/dl or diagnosis of diabetes). We also defined metabolic syndrome using modified ATP III criteria, in which high fasting glucose is based on the cut point of $\geq$100 mg/dl suggested by the American Diabetes Association (25).

Knee radiographic and pain assessment. At baseline and follow-up, bilateral weight-bearing anteroposterior (AP) knee radiographs were obtained using a fixed-flexion approach, and lateral view radiographs were obtained using a validated protocol (26). Longitudinal knee radiographs were read by a musculoskeletal radiologist (PA) and a rheumatologist. If there was a disagreement as to whether the knee had radiographic OA, the reading was adjudicated by a panel of 3 readers, including the 2 who read all films and a third reader (DTF). A consensus reading was reached when at least 2 of 3 readers agreed.

The Kellgren/Lawrence grade was determined using AP view radiographs, and joint space narrowing and osteophytes were scored on lateral view radiographs. A knee was defined as having radiographic OA in the tibiofemoral joint if it had a Kellgren/Lawrence grade of $\geq$2 on the AP view, and as having radiographic OA in the patellofemoral joint if it had any osteophyte grade of $\geq$2, or any osteophyte grade of $\geq$1 plus a joint space narrowing grade of $\geq$2 in the patellofemoral joint on the lateral view (27).

Subjects were asked "on most days do you have pain, aching or stiffness in your knee" for each knee at both baseline

Table 1. Baseline characteristics of the subjects, by sex and presence of metabolic syndrome based on ATP III criteria*

	Men		Women	
	No metabolic syndrome (n = 326)	Metabolic syndrome (n = 119)	No metabolic syndrome (n = 421)	Metabolic syndrome (n = 125)
Age, mean ± SD years	54 ± 8.0	55.6 ± 7.6	53.2 ± 7.9	57.2 ± 8.2
BMI, mean ± SD kg/m^2	27.1 ± 3.2	30.9 ± 3.8	24.9 ± 3.9	30.7 ± 5.6
Body weight, mean ± SD pounds	183.7 ± 24.5	209.1 ± 29.3	143.2 ± 24.5	175.9 ± 33.6
Physical activity index, mean ± SD	37.4 ± 37.4	36.5 ± 36.5	36.9 ± 36.9	36.7 ± 36.7
Smoking, no. (%)	39 (12.0)	22 (18.5)	68 (16.2)	16 (12.8)
Alcohol consumption, no. (%)	252 (77.3)	82 (68.9)	305 (72.4)	72 (57.6)
College education, no. (%)	232 (71.2)	76 (63.9)	274 (65.1)	65 (52.0)
Abdominal obesity, no. (%)	64 (19.6)	79 (66.4)	77 (18.3)	105 (84)
High triglycerides, no. (%)	77 (23.6)	96 (80.7)	51 (12.1)	103 (82.4)
Low HDL, no. (%)	91 (27.9)	97 (81.5)	90 (21.4)	99 (79.2)
High BP, no. (%)	102 (31.3)	101 (84.9)	102 (24.2)	104 (83.2)
High fasting glucose (≥100 mg/dl), no. (%)	110 (33.7)	72 (60.5)	47 (11.2)	69 (55.2)
High fasting glucose (≥110 mg/dl), no. (%)	22 (6.7)	36 (30.3)	8 (1.9)	40 (32)
Waist circumference, mean ± SD cm	96 ± 9.0	105.5 ± 9.1	80 ± 10.8	98 ± 11.3
Triglycerides, mean ± SD mg/dl	130.1 ± 78.1	240.8 ± 139.7	105.3 ± 45.1	228.4 ± 142.0
HDL, mean ± SD mg/dl	45.6 ± 10.4	34.8 ± 8.7	60.4 ± 13.9	43.4 ± 9.9
Systolic blood pressure, mean ± SD mm Hg	121.8 ± 14.3	133.8 ± 15.3	115.3 ± 16.5	136.7 ± 19.4
Diastolic blood pressure, mean ± SD mm Hg	74.2 ± 8.5	80 ± 10.8	69 ± 9.6	76.5 ± 9.7
Fasting blood glucose, mean ± SD mg/dl	98.7 ± 21.1	111.8 ± 32	90.7 ± 8.1	113.5 ± 42.8

* ATP III = Adult Treatment Panel III; BMI = body mass index; HDL = high-density lipoprotein; BP = blood pressure.

and follow-up visits. Subjects were considered to have symptomatic knee OA if they had both knee pain and radiographic OA in either tibiofemoral or patellofemoral joint on radiographs.

Covariates. We used data from the Offspring examination on covariates including age, sex, educational attainment, current smoking, physical activity (28), and alcohol consumption (≥1 drink/week). Height and weight were measured, and BMI was calculated as weight in kilograms divided by the square of height in meters (kg/m^2).

Statistical analysis. Since differential association by sex was observed between some components of metabolic syndrome and prevalent radiographic knee OA in a previous study (15), we performed sex-specific analyses. Baseline characteristics were explored among subjects with and those without metabolic syndrome prior to all analyses. We also examined the correlation of continuous measurements used to define metabolic syndrome with BMI and body weight.

Metabolic syndrome and incident radiographic OA. Among knees without radiographic OA in both tibiofemoral and patellofemoral joints at baseline, incident radiographic OA was defined as the development of radiographic OA in either tibiofemoral or patellofemoral joint or knee replacement at the follow-up visit. For each exposure at baseline, i.e., metabolic syndrome (yes versus no) and each of its 5 components (yes versus no), we used the risk ratio from a binary regression model to estimate its association with incident radiographic OA. Generalized estimating equations were used to control for the correlation between 2 knees in a subject. We adjusted for age, education level, current smoking, alcohol consumption, and physical activity level in the analysis. To show whether obesity was the main confounding factor to the association of interest, we further adjusted for BMI in another model, and adjusted for body weight instead of BMI in a third model.

To explore whether there was a dose-response relationship between the severity of metabolic syndrome and incident radiographic OA, we used the number of components (1, 2, 3, and 4–5 versus 0) and sex-specific quartiles of each continuous measurement in the definition of metabolic syndrome (2nd–4th quartiles versus the lowest quartile) as exposures. We used the binary regression models described above to assess the association between each severity exposure and incident radiographic OA. If the results suggested a dose-response relationship, we used the median of continuous measurement in each quartile as continuous exposure to test for a linear trend.

Since waist circumference is highly correlated with BMI and body weight, we used the residual of waist circumference as one way to control for weight-related confounding. The residual of waist circumference was the difference between the observed and expected value from a linear regression model with waist circumference as the dependent variable and BMI as the independent variable in each sex. We classified the BMI-adjusted residual into sex-specific quartiles. Then we replaced BMI with body weight to get the weight-adjusted residual of waist circumference and repeated the analysis.

Metabolic syndrome and incident symptomatic OA. Among knees without symptomatic OA at baseline, incident symptomatic OA was defined as the development of symptomatic OA or knee replacement by the time of the follow-up visit. We used the same method as described above to assess the association between each baseline exposure and incident symptomatic OA.

RESULTS

Subject characteristics. Among 1,083 subjects with longitudinal radiograph reading in the Framingham OA Study, 4 subjects with metabolic syndrome not assessed, 55 subjects age <40 years, and 33 subjects with bilateral radiographic OA at baseline were excluded. The mean ± SD age of the 991 remaining subjects was 54.2 ± 8.1 years at baseline, 55.1% were women, 26.7% of the men and 22.9% of the women had metabolic syndrome according to the ATP III criteria, and 34.2% of the men and 25.1% of the women had metabolic syndrome according to the modified ATP III criteria. Subjects with metabolic syndrome were older, less likely to drink alcohol or have a college education, and had a higher BMI compared with those without metabolic syndrome, especially among women (Table 1). BMI and body weight were strongly correlated with waist circumference (Pearson's correlation coefficient = 0.87–0.88 in

Table 2. Metabolic syndrome, its components, and incident radiographic knee OA*

	Men					Women				
Metabolic syndrome and its components	No. of knees	Incident radiographic OA, no. (%)	RR (95% CI)†	RR (95% CI)‡	RR (95% CI)§	No. of knees	Incident radiographic OA, no. (%)	RR (95% CI)†	RR (95% CI)‡	RR (95% CI)§
Metabolic syndrome, ATP III criteria										
No	587	43 (7.3)	1.0	1.0	1.0	790	74 (9.4)	1.0	1.0	1.0
Yes	213	35 (16.4)	2.0 (1.2–3.4)	1.5 (0.9–2.6)	1.4 (0.8–2.5)	213	31 (14.6)	1.4 (0.9–2.3)	0.8 (0.5–1.4)	0.8 (0.5–1.4)
Metabolic syndrome, modified ATP III criteria										
No	537	41 (7.6)	1.0	1.0	1.0	767	71 (9.3)	1.0	1.0	1.0
Yes	263	37 (14.1)	1.7 (1.0–2.8)	1.2 (0.7–2.0)	1.2 (0.7–2.0)	236	34 (14.4)	1.4 (0.9–2.3)	0.8 (0.5–1.4)	0.8 (0.5–1.3)
Abdominal obesity										
No	558	39 (7.0)	1.0	1.0	1.0	691	53 (7.7)	1.0	1.0	1.0
Yes	242	39 (16.1)	2.4 (1.5–3.9)	1.7 (0.9–3.1)	1.3 (0.6–2.8)	312	52 (16.7)	2.1 (1.3–3.2)	1.0 (0.6–1.9)	0.9 (0.5–1.7)
High triglycerides										
No	490	42 (8.6)	1.0	1.0	1.0	732	74 (10.1)	1.0	1.0	1.0
Yes	310	36 (11.6)	1.3 (0.8–2.2)	1.2 (0.7–1.9)	1.2 (0.8–2.0)	271	31 (11.4)	1.0 (0.6–1.6)	0.7 (0.5–1.2)	0.8 (0.5–1.2)
Low HDL										
No	463	36 (7.8)	1.0	1.0	1.0	664	71 (10.7)	1.0	1.0	1.0
Yes	337	42 (12.5)	1.8 (1.1–2.9)	1.5 (0.9–2.5)	1.5 (0.9–2.4)	339	34 (10.0)	0.9 (0.6–1.5)	0.7 (0.4–1.2)	0.7 (0.4–1.1)
High BP										
No	447	32 (7.2)	1.0	1.0	1.0	643	51 (7.9)	1.0	1.0	1.0
Yes	353	46 (13.0)	1.6 (1.0–2.6)	1.3 (0.8–2.1)	1.2 (0.7–2.0)	360	54 (15.0)	1.7 (1.0–2.7)	1.3 (0.8–2.0)	1.2 (0.8–1.9)
Fasting glucose ≥110 mg/dl										
No	695	63 (9.1)	1.0	1.0	1.0	920	92 (10.0)	1.0	1.0	1.0
Yes	105	15 (14.3)	1.3 (0.7–2.5)	1.1 (0.6–2.2)	1.1 (0.6–2.1)	83	13 (15.7)	1.4 (0.8–2.7)	0.9 (0.4–1.7)	0.9 (0.5–1.7)
Fasting glucose ≥100 mg/dl										
No	474	48 (10.1)	1.0	1.0	1.0	794	76 (9.6)	1.0	1.0	1.0
Yes	326	30 (9.2)	0.8 (0.5–1.4)	0.7 (0.4–1.2)	0.7 (0.4–1.2)	209	29 (13.9)	1.3 (0.8–2.2)	0.9 (0.5–1.5)	0.9 (0.5–0.4)

* OA = osteoarthritis; RR = relative risk; 95% CI = 95% confidence interval; ATP III = Adult Treatment Panel III; HDL = high-density lipoprotein; BP = blood pressure.
† Adjusted for age, education, smoking status, alcohol consumption, and physical activity level.
‡ Adjusted for age, education, smoking status, alcohol consumption, physical activity level, and body mass index.
§ Adjusted for age, education, smoking status, alcohol consumption, physical activity level, and body weight.

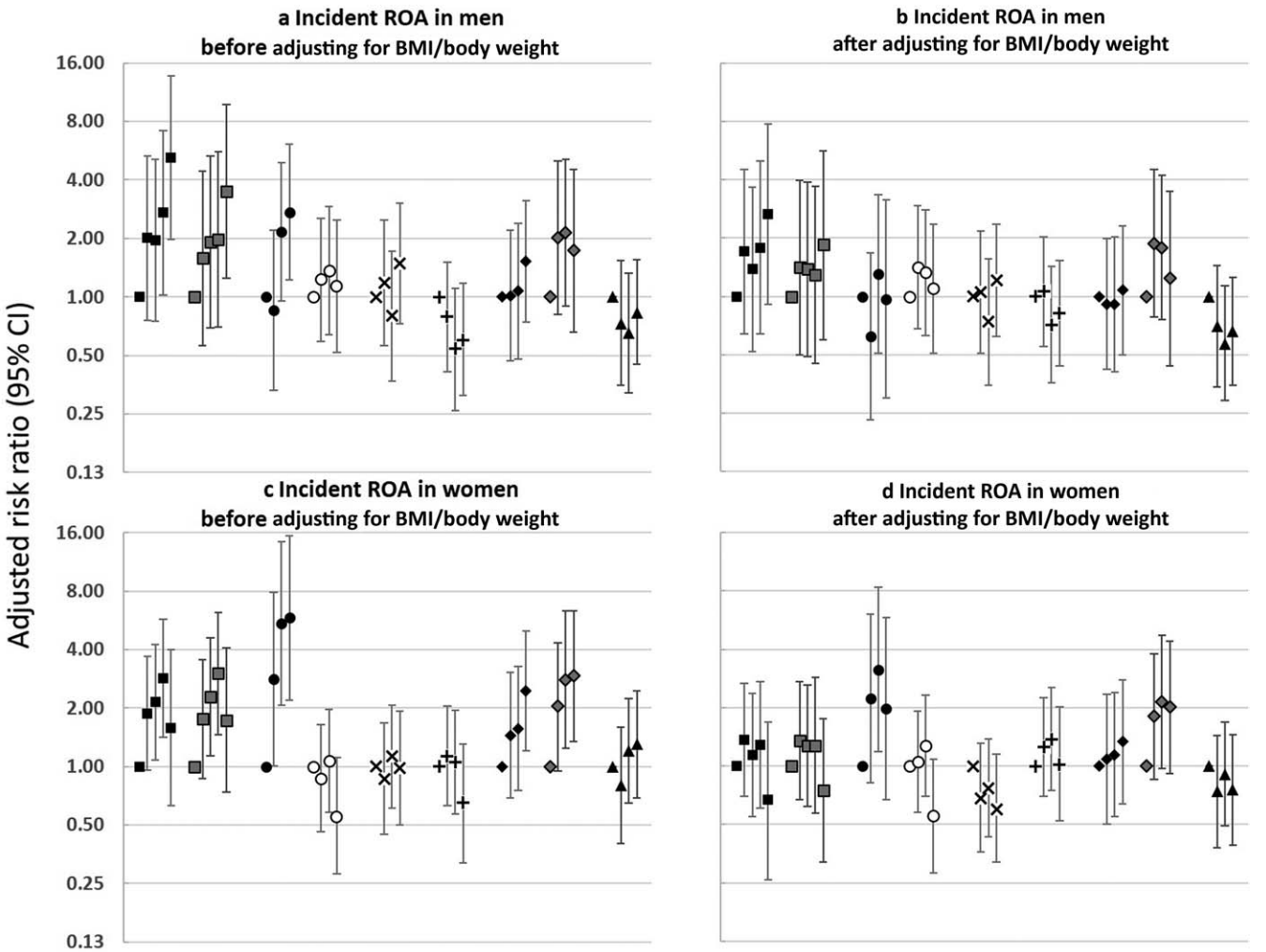

Figure 1. Severity of metabolic syndrome components and incident radiographic knee osteoarthritis (ROA) by sex. Adjusted relative risks (RRs) of incident radiographic knee OA for the number of metabolic syndrome components (0, 1, 2, 3, 4, or 5) based on Adult Treatment Panel III (ATP III) criteria (■), number of metabolic syndrome components based on modified ATP III criteria (■), and sex-specific quartiles (lowest, second, third, and highest) of waist circumference (●), residual of waist circumference from regression on body weight (○), triglycerides (×), high-density lipoprotein (+), systolic blood pressure (◆), diastolic blood pressure (◆), and fasting blood glucose (▲) are shown. **a** and **c** show RRs from models adjusted for age, education, smoking status, alcohol consumption, and physical activity level. **b** and **d** show RRs from models adjusted for age, education, smoking status, alcohol consumption, physical activity level, and body mass index (BMI) or body weight.

men and 0.84–0.85 in women), but only weakly correlated with other continuous measurements used to define metabolic syndrome (Pearson's correlation coefficients <0.4).

Metabolic syndrome and incident radiographic OA. Among the knees without radiographic OA at baseline, the incidence of radiographic OA was 9.8% (78 of 800 knees) in men and 10.5% (105 of 1,003 knees) in women. After adjusting for age, education, smoking status, alcohol consumption, and physical activity level, metabolic syndrome, abdominal obesity, and low HDL were associated with an increased incidence of radiographic OA among men (Table 2). Among women, abdominal obesity and high blood pressure were associated with incident radiographic OA, but metabolic syndrome was not. After adjusting for BMI or body weight, none of these associations remained significant.

As with metabolic syndrome, the number of metabolic syndrome components was associated with the incidence of radiographic OA before adjustment for BMI or body weight, especially in men, but the association was markedly attenuated and no longer significant

Table 3. Metabolic syndrome, its components, and incident symptomatic knee OA*

	Men					Women				
Metabolic syndrome and its components	No. of knees	Incident symptomatic OA, no. (%)	RR (95% CI)†	RR (95% CI)‡	RR (95% CI)§	No. of knees	Incident symptomatic OA, no. (%)	RR (95% CI)†	RR (95%CI)‡	RR (95% CI)§
Metabolic syndrome, ATP III criteria										
No	617	35 (5.7)	1.0	1.0	1.0	803	43 (5.4)	1.0	1.0	1.0
Yes	220	18 (8.2)	1.2 (0.6–2.2)	0.8 (0.4–1.6)	0.8 (0.4–1.6)	234	32 (13.7)	2.3 (1.4–4.0)	1.2 (0.7–2.1)	1.2 (0.7–2.1)
Metabolic syndrome, modified ATP III criteria										
No	554	26 (4.7)	1.0	1.0	1.0	780	42 (5.4)	1.0	1.0	1.0
Yes	283	27 (9.5)	1.7 (0.9–3.0)	1.3 (0.6–2.5)	1.3 (0.7–2.5)	257	33 (12.8)	2.2 (1.3–3.8)	1.1 (0.6–2.0)	1.1 (0.6–1.9)
Abdominal obesity										
No	574	23 (4.0)	1.0	1.0	1.0	694	29 (4.2)	1.0	1.0	1.0
Yes	263	30 (11.4)	2.7 (1.5–4.9)	2.2 (1.0–4.9)	2.2 (0.9–5.4)	343	46 (13.4)	3.1 (1.8–5.3)	1.5 (0.8–2.9)	1.4 (0.8–2.7)
High triglycerides										
No	515	34 (6.6)	1.0	1.0	1.0	746	43 (5.8)	1.0	1.0	1.0
Yes	322	19 (5.9)	0.8 (0.4–1.5)	0.7 (0.4–1.3)	0.7 (0.4–1.4)	291	32 (11.0)	1.7 (0.9–2.9)	1.1 (0.6–1.9)	1.1 (0.6–1.9)
Low HDL										
No	494	31 (6.3)	1.0	1.0	1.0	680	45 (6.6)	1.0	1.0	1.0
Yes	343	22 (6.4)	1.0 (0.5–1.8)	0.8 (0.4–1.5)	0.8 (0.5–1.6)	357	30 (8.4)	1.2 (0.7–2.0)	0.8 (0.5–1.4)	0.8 (0.4–1.4)
High BP										
No	458	17 (3.7)	1.0	1.0	1.0	643	29 (4.5)	1.0	1.0	1.0
Yes	379	36 (9.5)	2.2 (1.2–3.9)	1.8 (1.0–3.4)	1.8 (1.0–3.5)	394	46 (11.7)	2.5 (1.4–4.4)	1.7 (1.0–3.0)	1.6 (0.9–2.8)
Fasting glucose ≥100 mg/dl										
No	724	44 (6.1)	1.0	1.0	1.0	947	65 (6.9)	1.0	1.0	1.0
Yes	113	9 (8.0)	0.9 (0.4–2.0)	0.8 (0.3–1.7)	0.8 (0.4–1.7)	90	10 (11.1)	1.7 (0.9–3.4)	0.9 (0.4–1.9)	0.9 (0.4–1.9)
Fasting glucose ≥110 mg/dl										
No	494	30 (6.1)	1.0	1.0	1.0	815	56 (6.9)	1.0	1.0	1.0
Yes	343	23 (6.7)	0.9 (0.5–1.6)	0.8 (0.4–1.5)	0.8 (0.4–1.5)	222	19 (8.6)	1.2 (0.7–2.2)	0.7 (0.4–1.3)	0.7 (0.4–1.3)

* OA = osteoarthritis; RR = relative risk; 95% CI = 95% confidence interval; ATP III = Adult Treatment Panel III; HDL = high-density lipoprotein; BP = blood pressure.
† Adjusted for age, education, smoking status, alcohol consumption, and physical activity level.
‡ Adjusted for age, education, smoking status, alcohol consumption, physical activity level, and body mass index.
§ Adjusted for age, education, smoking status, alcohol consumption, physical activity level, and body weight.

when we adjusted for BMI or weight. Increasing waist circumference was associated with an increased incidence of radiographic OA in both sexes, but the trend did not remain after adjusting for either BMI or body weight, and this null association was confirmed by using the residual of waist circumference as exposure (Figure 1). The associations of both high systolic blood pressure and high diastolic blood pressure with radiographic OA diminished greatly and became nonsignificant after adjustment for weight or BMI (Table 2 and Figure 1). Even so, women with diastolic blood pressure in the highest quartile tended to have a higher incidence of radiographic OA than women with diastolic blood pressure in the lowest quartile (Figure 1).

Metabolic syndrome and incident symptomatic OA. Among knees without symptomatic OA at baseline, the incidence of symptomatic OA was 6.3% in men (53 of 837) and 7.2% in women (75 of 1,037). Metabolic syndrome was not associated with incident symptomatic OA in men either before or after adjusting for BMI or weight. The association between metabolic syndrome and incident symptomatic OA was observed in women before adjustment but disappeared after controlling for weight-related confounding (Table 3). The association

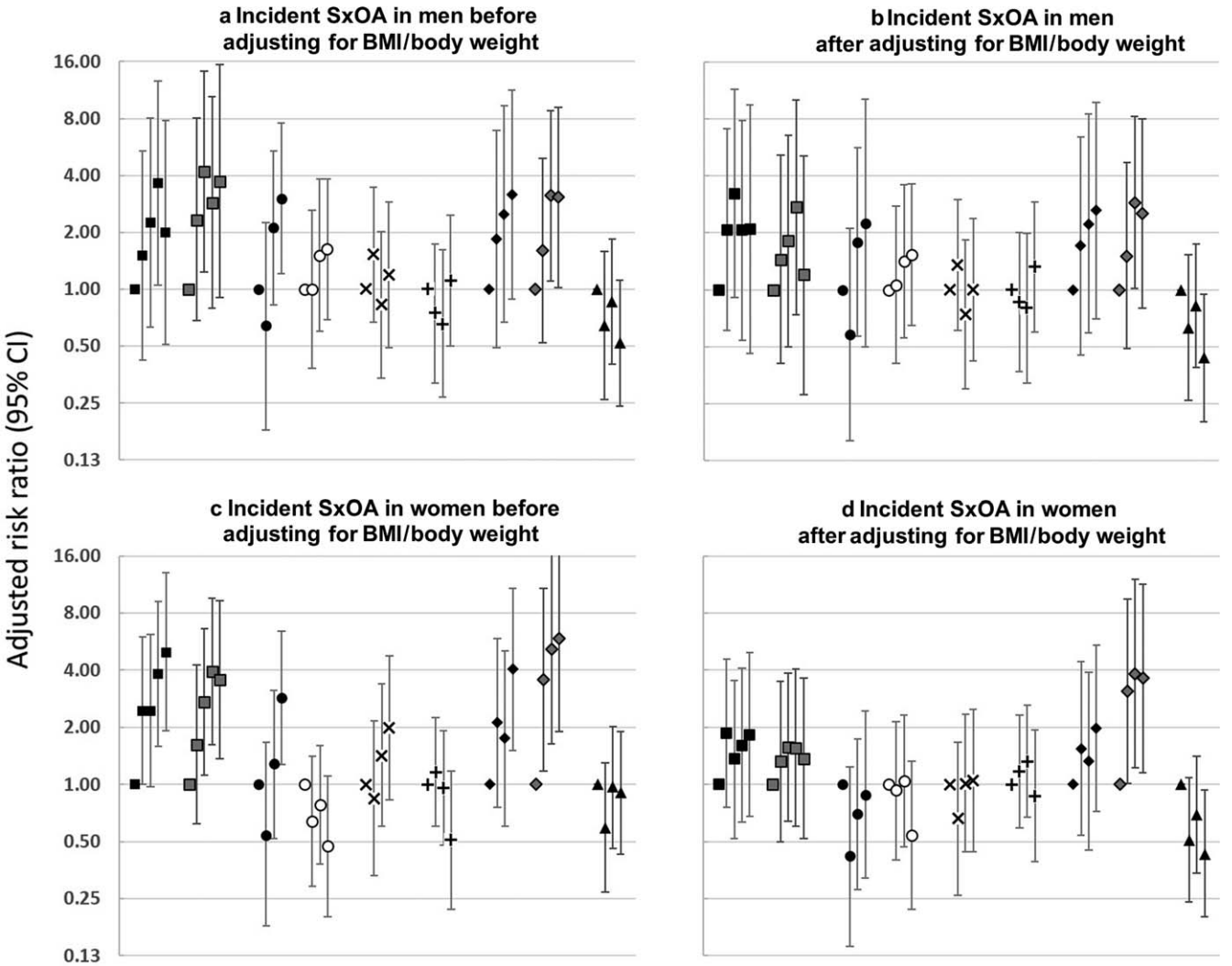

Figure 2. Severity of metabolic syndrome components and incident symptomatic knee osteoarthritis (SxOA) by sex. Adjusted relative risks (RRs) of incident symptomatic knee OA for the number of metabolic syndrome components (0, 1, 2, 3, or 4) based on Adult Treatment Panel III (ATP III) criteria (■), number of metabolic syndrome components based on modified ATP III criteria (■) and sex-specific quartiles (lowest, second, third, and highest) of waist circumference (●), residual of waist circumference from regression on body weight (○), triglycerides (×), high-density lipoprotein (+), systolic blood pressure (◆), diastolic blood pressure (◆), and fasting blood glucose (▲) are shown. **a** and **c** show RRs from models adjusted for age, education, smoking status, alcohol consumption, and physical activity level. **b** and **d** show RRs from models adjusted for age, education, smoking status, alcohol consumption, physical activity level, and body mass index (BMI) or body weight.

of abdominal obesity and high blood pressure with incident symptomatic OA among men and women became weaker and not statistically significant after adjusting for BMI or body weight (Table 3 and Figure 2).

Before adjusting for BMI or weight, a trend toward an increase in incident symptomatic OA with the number of metabolic syndrome components was observed among men and remained after adjusting for BMI or body weight for up to 3 components (weight-adjusted relative risk = 1.0, 2.1, 3.2, 2.1, and 2.1 for having 0 to 4 components, respectively, according to ATP III criteria). The trend for number of components and incident symptomatic OA observed in women disappeared after adjusting for BMI or body weight.

Before adjustment for BMI or weight, a higher incidence of symptomatic OA was observed among both men and women with higher waist circumference, systolic blood pressure and diastolic blood pressure quartile, and among women with higher triglyceride levels (Figure 2). The trend for waist circumference diminished greatly and became nonsignificant after adjusting for BMI or body weight (Table 3 and Figure 2). The trend was attenuated

and became nonsignificant for systolic blood pressure quartiles (weight-adjusted P for trend = 0.082 in men and 0.162 in women), but remained for diastolic blood pressure quartiles (weight-adjusted P for trend = 0.053 in men and 0.026 in women) after adjusting for BMI or weight. On the other hand, subjects in higher fasting blood glucose quartiles tended to have a lower incidence of symptomatic OA after adjusting for weight-related confounders (P for linear trend = 0.044 in men and 0.080 in women) (Figure 2).

DISCUSSION

Before adjustment for BMI and body weight, metabolic syndrome was associated with an increased incidence of radiographic OA in men and increased incidence of symptomatic OA in women, while the association between the number of components of metabolic syndrome and incident OA was consistent in both sexes and for both radiographic OA and symptomatic OA. After controlling for BMI or weight, the associations of these measures with OA were all markedly attenuated and almost all were no longer significant. Only high diastolic blood pressure remained associated with an increased incidence of symptomatic OA in both men and women after adjusting for body weight.

The strong correlation between the degree of abdominal obesity and BMI or body weight could make it hard to separate the effects of these risk factors in multivariate models. We computed residuals of waist circumference by removing the variation caused by BMI or body weight and assessed the relationship between waist circumference residual and OA. This tended to nullify any association observed (Figures 1 and 2). This method showed that abdominal obesity, BMI, and body weight are likely to be measures of the same potential factor.

High blood pressure is another metabolic syndrome component that has been associated with OA in previous studies before adjusting for BMI (9,10,13,16), and some studies also reported this association after adjusting for BMI (9,13,16). While we found that diastolic blood pressure was related to incident symptomatic OA even after adjustment for BMI, the relationship between systolic blood pressure and incident symptomatic OA was nearly significant also, suggesting that both might be related to symptomatic OA. Any cross-sectional analysis of this relationship would be challenging to interpret since treatment for symptomatic OA includes nonsteroidal antiinflammatory drugs, which can raise blood pressure.

Although symptomatic knee OA is the form of OA that affects quality of life, it has not been as well studied as radiographic OA in terms of its relationship to metabolic syndrome. There is evidence of a role of inflammatory mediators in nociception and pain in arthritis (29). People with metabolic syndrome, which is accompanied by systemic inflammation, may have higher levels of pain for the same severity of structural OA (13,29). The definitions of symptomatic OA in previous studies were inconsistent, including self-reported OA (15), clinical OA (12), and severe symptomatic OA as assessed by knee replacement as the outcome (11). The findings from these studies were also inconsistent. Our study was the first to define symptomatic OA based on both radiographs and knee symptoms and using incident symptomatic OA as the outcome.

After adjustment for BMI, we also found, surprisingly, an inverse association between fasting blood sugar and OA, especially symptomatic OA. In several previous studies, diabetes and elevated blood glucose levels were reported to be positively associated with OA and joint replacement (7). However, in the Multicenter OA Study, investigators reported no association of diabetes with incident OA in men, whereas in women, the presence of diabetes and an increase in insulin resistance protected against OA onset after adjusting for BMI (30). Given the inconsistent findings, the relationship between blood sugar and knee OA needs further study.

Our study has strengths and limitations. Strengths include the use of a longitudinal sample with components of metabolic syndrome characterized by state-of-the-art methods. We were able to test different levels of the components of metabolic syndrome rather than just dichotomizing them. We carried out the first attempt to examine the independent effect of central obesity on OA by using the residual approach for adjustment for collinear measures.

Among the limitations of the present study, we have no data to account for change in metabolic syndrome and its components during the 10-year follow-up period, so the exposures were susceptible to misclassification. Metabolic syndrome is a risk factor for several disabling or fatal diseases, so subjects with metabolic syndrome were more likely to be lost to follow-up and this could introduce bias. Further, since we did not know the date of onset of symptomatic OA, we could not adjust for competing risks of death. While metabolic syndrome increases the risk of death, this would bias our results only if the combination of incident OA and metabolic syndrome increased mortality risk more than metabolic syndrome alone, and in the Framingham Study, we have found no association of OA with overall

mortality risk in hand OA (31). Even if symptomatic knee OA were associated with enhanced mortality, this is not likely to be true for new-onset disease, and increases in OA mortality risk seen in other studies are small and would be unlikely to confound our findings (32). Also, larger numbers of incident OA cases may have led us to identify blood pressure as a significant risk factor for OA, given that our weight-adjusted analysis suggested a persistent association of OA risk with blood pressure. Most of our incident cases were knees with tibiofemoral OA, which limited our ability to examine whether risk for patellofemoral and tibiofemoral OA differed.

In conclusion, this study revealed that metabolic syndrome, the number of its components, and individual components, such as central obesity, are associated with incident knee OA but not independent of BMI and body weight. Incident symptomatic knee OA occurred more frequently with an increase in blood pressure, an association that needs further exploration.

AUTHOR CONTRIBUTIONS

All authors were involved in drafting the article or revising it critically for important intellectual content, and all authors approved the final version to be published. Dr. Felson had full access to all of the data in the study and takes responsibility for the integrity of the data and the accuracy of the data analysis.

Study conception and design. Niu, Vasan, Felson.
Acquisition of data. Clancy, Aliabadi, Felson.
Analysis and interpretation of data. Niu.

REFERENCES

1. Isomaa B, Almgren P, Tuomi T, Forsen B, Lahti K, Nissen M, et al. Cardiovascular morbidity and mortality associated with the metabolic syndrome. Diabetes Care 2001;24:683–9.
2. Reaven GM. Banting lecture 1988: role of insulin resistance in human disease. Diabetes 1988;37:1595–607.
3. Kaur J. A comprehensive review on metabolic syndrome. Cardiol Res Pract 2014;2014:21.
4. Trevisan M, Liu J, Bahsas FB, Menotti A. Syndrome X and mortality: a population-based study. Am J Epidemiol 1998;148: 958–66.
5. Sowers MR, Karvonen-Gutierrez CA. The evolving role of obesity in knee osteoarthritis. Curr Opin Rheumatol 2010;22: 533–7.
6. Findlay DM. Vascular pathology and osteoarthritis. Rheumatology (Oxford) 2007;46:1763–8.
7. Berenbaum F. Diabetes-induced osteoarthritis: from a new paradigm to a new phenotype. Ann Rheum Dis 2011;70: 1354–6.
8. Shin D. Association between metabolic syndrome, radiographic knee osteoarthritis, and intensity of knee pain: results of a national survey. J Clin Endocrinol Metab 2014;99:3177–83.
9. Yoshimura N, Muraki S, Oka H, Tanaka S, Kawaguchi H, Nakamura K, et al. Accumulation of metabolic risk factors such as overweight, hypertension, dyslipidaemia, and impaired glucose tolerance raises the risk of occurrence and progression of knee osteoarthritis: a 3-year follow-up of the ROAD study. Osteoarthritis Cartilage 2012;20:1217–26.
10. Yoshimura N, Muraki S, Oka H, Kawaguchi H, Nakamura K, Akune T. Association of knee osteoarthritis with the accumulation of metabolic risk factors such as overweight, hypertension, dyslipidemia, and impaired glucose tolerance in Japanese men and women: the ROAD study. J Rheumatol 2011;38: 921–30.
11. Engstrom G, Gerhardsson de Verdier M, Rollof J, Nilsson PM, Lohmander LS. C-reactive protein, metabolic syndrome and incidence of severe hip and knee osteoarthritis: a population-based cohort study. Osteoarthritis Cartilage 2009; 17:168–73.
12. Visser AW, de Mutsert R, le Cessie S, den Heijer M, Rosendaal FR, Kloppenburg M. The relative contribution of mechanical stress and systemic processes in different types of osteoarthritis: the NEO study. Ann Rheum Dis 2015;74:1842–7.
13. Hussain SM, Wang Y, Cicuttini FM, Simpson JA, Giles GG, Graves S, et al. Incidence of total knee and hip replacement for osteoarthritis in relation to the metabolic syndrome and its components: a prospective cohort study. Semin Arthritis Rheum 2014;43:429–36.
14. Hussain SM, Cicuttini FM, Bell RJ, Robinson PJ, Davis SR, Giles GG, et al. Incidence of total knee and hip replacement for osteoarthritis in relation to circulating sex steroid hormone concentrations in women. Arthritis Rheumatol 2014;66:2144–51.
15. Han CD, Yang IH, Lee WS, Park YJ, Park KK. Correlation between metabolic syndrome and knee osteoarthritis: data from the Korean National Health and Nutrition Examination Survey (KNHANES). BMC Public Health 2013;13:603.
16. Hart DJ, Doyle DV, Spector TD. Association between metabolic factors and knee osteoarthritis in women: the Chingford study. J Rheumatol 1995;22:1118–23.
17. Kuyinu EL, Narayanan G, Nair LS, Laurencin CT. Animal models of osteoarthritis: classification, update, and measurement of outcomes. J Orthop Surg Res 2016;11:19.
18. Felson DT, Lavalley MP. The ACR20 and defining a threshold for response in rheumatic diseases: too much of a good thing. Arthritis Res Ther 2014;16:101.
19. Felson DT, Niu J, McClennan C, Sack B, Aliabadi P, Hunter DJ, et al. Knee buckling: prevalence, risk factors, and associated limitations in function. Ann Intern Med 2007;147:534–40.
20. Oliveria SA, Felson DT, Reed JI, Cirillo PA, Walker AM. Incidence of symptomatic hand, hip, and knee osteoarthritis among patients in a health maintenance organization. Arthritis Rheum 1995;38:1134–41.
21. McNamara JR, Schaefer EJ. Automated enzymatic standardized lipid analyses for plasma and lipoprotein fractions. Clin Chim Acta 1987;166:1–8.
22. Friedewald WT, Levy RI, Fredrickson DS. Estimation of the concentration of low-density lipoprotein cholesterol in plasma, without use of the preparative ultracentrifuge. Clin Chem 1972; 18:499–502.
23. Meigs JB, Wilson PW, Nathan DM, D'Agostino RB Sr, Williams K, Haffner SM. Prevalence and characteristics of the metabolic syndrome in the San Antonio Heart and Framingham Offspring studies. Diabetes 2003;52:2160–7.
24. Expert Panel on Detection, Evaluation, and Treatment of High Blood Cholesterol in Adults. Executive summary of the third report of the National Cholesterol Education Program (NCEP) expert panel on detection, evaluation, and treatment of high blood cholesterol in adults (adult treatment panel III). JAMA 2001;285:2486–97.
25. Genuth S, Alberti KG, Bennett P, Buse J, Defronzo R, Kahn R, et al. Follow-up report on the diagnosis of diabetes mellitus. Diabetes Care 2003;26:3160–7.
26. Lavalley MP, McLaughlin S, Goggins J, Gale D, Nevitt MC, Felson DT. The lateral view radiograph for assessment of the tibiofemoral joint space in knee osteoarthritis: its reliability, sensitivity to change, and longitudinal validity. Arthritis Rheum 2005;52:3542–7.

27. Felson DT, McAlindon TE, Anderson JJ, Naimark A, Weissman BW, Aliabadi P, et al. Defining radiographic osteoarthritis for the whole knee. Osteoarthritis Cartilage 1997;5: 241–50.
28. Kannel WB, Sorlie P. Some health benefits of physical activity: the Framingham Study. Arch Intern Med 1979;139: 857–61.
29. Kidd BL, Photiou A, Inglis JJ. The role of inflammatory mediators on nociception and pain in arthritis. Novartis Found Symp 2004;260:122–33; discussion 133–8, 277–9.
30. Walimbe M, Schwartz AV, Tolstykh I, McCulloch CE, Felson DT, Lewis CE, et al. Hyperglycemia and risk of osteoarthritis [abstract]. Arthritis Rheumatol 2014;66 Suppl:S559.
31. Haugen IK, Ramachandran VS, Misra D, Neogi T, Niu J, Yang T, et al. Hand osteoarthritis in relation to mortality and incidence of cardiovascular disease: data from the Framingham Heart study. Ann Rheum Dis 2015;74:74–81.
32. Walker AM. Observation and inference: an introduction to the methods of epidemiology. Chestnut Hill (MA): Epidemiology Resources, Inc.; 1991.

ARTHRITIS & RHEUMATOLOGY
Vol. 69, No. 6, June 2017, pp 1204–1212
DOI 10.1002/art.40097

Lifetime Risk of Symptomatic Hand Osteoarthritis

The Johnston County Osteoarthritis Project

Jin Qin,[1] Kamil E. Barbour,[1] Louise B. Murphy,[1] Amanda E. Nelson,[2] Todd A. Schwartz,[2] Charles G. Helmick,[1] Kelli D. Allen,[2] Jordan B. Renner,[2] Nancy A. Baker,[3] and Joanne M. Jordan[2]

Objective. **Symptomatic hand osteoarthritis (OA) is a common condition that affects hand strength and function, and causes disability in activities of daily living. Prior studies have estimated that the lifetime risk of symptomatic knee OA is 45% and that of hip OA is 25%. The objective of the present study was to estimate the overall lifetime risk of symptomatic hand OA, and the stratified lifetime risk according to potential risk factors.**

Methods. **Data were obtained from 2,218 adult subjects (age ≥45 years) in the Johnston County Osteoarthritis Project, a population-based prospective cohort study among residents of Johnston County, North Carolina. Data for the present study were collected from 2 of the follow-up cycles (1999–2004 and 2005–2010). Symptomatic hand OA was defined as the presence of both self-reported symptoms and radiographic OA in the same hand. Lifetime risk, defined as the proportion of the population who will develop symptomatic hand OA in at least 1 hand by age 85 years, was estimated from models using generalized estimating equations.**

Results. **Overall, the lifetime risk of symptomatic hand OA was 39.8% (95% confidence interval [95% CI] 34.4–45.3%). In this population, nearly 1 in 2 women (47.2%, 95% CI 40.6–53.9%) had an estimated lifetime risk of developing symptomatic hand OA by age 85 years, compared with 1 in 4 men (24.6%, 95% CI 19.5–30.5%). Race-specific symptomatic hand OA risk estimates were 41.4% (95% CI 35.5–47.6%) among whites and 29.2% (95% CI 20.5–39.7%) among African Americans. The lifetime risk of symptomatic hand OA among individuals with obesity (47.1%, 95% CI 37.8–56.7%) was 11 percentage points higher than that in individuals without obesity (36.1%, 95% CI 29.7–42.9%).**

Conclusion. **These findings demonstrate the substantial burden of symptomatic hand OA overall and in sociodemographic and clinical subgroups. Increased use of public health and clinical interventions is needed to address its impact.**

The hand is one of the sites most frequently affected by osteoarthritis (OA), characterized by bony enlargements of the finger joints and deformities of the hand (1). Many people with hand OA experience symptoms of pain or aching, stiffness, loss of mobility, and decreased grip strength, leading to impaired hand function and disability in activities of daily living (2,3). Contrary to the common belief that it is a disease of older people, hand OA can occur relatively early in life (i.e., middle age), impairing an individual's capacity to work (4).

Studies of hand OA, particularly epidemiologic assessments of its prevalence and incidence, are sparse. Hand OA with active symptoms is associated with functional limitations, greater disability, and increased health care utilization (3,5); therefore, symptomatic hand OA has both clinical and public health implications. The prevalence estimates for symptomatic hand OA in the general population of adults among various countries range

The findings and conclusions herein are those of the authors and do not necessarily represent the official position of the Centers for Disease Control and Prevention.

Supported by the Centers for Disease Control and Prevention (cooperative agreements S043 and S3486) and the NIH (National Institute of Arthritis and Musculoskeletal and Skin Diseases grants 5-P60-AR-30701 and 5-P60-AR-49465).

[1]Jin Qin, ScD, Kamil E. Barbour, PhD, Louise B. Murphy, PhD, Charles G. Helmick, MD: Centers for Disease Control and Prevention, Atlanta, Georgia; [2]Amanda E. Nelson, MD, Todd A. Schwartz, DrPH, Kelli D. Allen, PhD, Jordan B. Renner, MD, Joanne M. Jordan, MD, MPH: University of North Carolina at Chapel Hill; [3]Nancy A. Baker, ScD: University of Pittsburgh, Pittsburgh, Pennsylvania.

Address correspondence to Jin Qin, ScD, 4770 Buford Highway, F76, Atlanta, GA 30341. E-mail: jqin@cdc.gov.

Submitted for publication September 27, 2016; accepted in revised form March 9, 2017.

between 3% and 8% (6–11). Higher prevalence values have been reported among older adults, with prevalence estimates of 13% in men and 26% in women age >70 years in the Framingham Osteoarthritis Study (3), a prevalence of 15% among individuals age ≥65 years in an Italian community (10), and the lowest estimate, 5%, among a Chinese population of adults age ≥60 years (11). In the Framingham Osteoarthritis Study, the 9-year cumulative incidence (proportion of new cases) of symptomatic hand OA in adults was 7% (12). The 10-year cumulative incidence of doctor-diagnosed hand OA in a Norwegian adult cohort was 6% (13). The incidence rate of symptomatic hand OA observed for up to 4 years among members of the Fallon Community Plan (Massachusetts) was 100 per 100,000 person-years (5).

Lifetime risk is the probability of developing a condition over the course of a lifetime. The lifetime risk has been previously estimated for other chronic conditions, including cancer, heart diseases, and diabetes mellitus (14–16). Using data from the Johnston County (JoCo) OA Project, the lifetime risk was estimated to be 45% for development of symptomatic knee OA (17) and 25% for symptomatic hip OA (18). To our knowledge, the lifetime risk of symptomatic hand OA has not been reported. Estimating the lifetime risk of symptomatic hand OA provides a risk estimate that is useful both for an individual's prognosis and for those seeking a better understanding of its public health burden. Using longitudinal data from the JoCo OA Project, we estimated the overall lifetime risk of symptomatic hand OA in the study population, and also stratified the risk by potential influential factors. It was not our objective to examine the association between risk factors and symptomatic hand OA, but rather to provide an estimated probability of having symptomatic hand OA by a certain age, and to determine whether this probability might differ by sex, race, education level, obesity status, hand injury history, and occupational factors that have been reported to be potential risk factors of OA or that may affect other risk factors (19–21).

SUBJECTS AND METHODS

Study design and data source. The JoCo OA Project is an ongoing population-based prospective cohort study monitoring the occurrence and natural history of OA in residents of Johnston County, North Carolina. Data collection and evaluation were conducted at baseline during 1991–1997 (n = 3,068) and at 3 follow-up cycles (time 1 during 1999–2004, time 2 during 2005–2010, and time 3 during 2011–2015). The study protocol used probability sampling to select a representative sample of noninstitutionalized civilians, comprising African American and white men and women age ≥45 years who were residents of 1 of 6 selected townships of Johnston County and who were physically and mentally capable of completing the study protocol. The protocol included both home interviews and clinic visits. Project methods are described in detail elsewhere (22). The study protocol was approved by the Institutional Review Boards of the Centers for Disease Control and Prevention and the University of North Carolina.

Radiographs were obtained during the clinic visits by a standard protocol involving bilateral posteroanterior views of the hands. A single experienced musculoskeletal radiologist (JBR) read the images using standard atlases (23,24) for features of radiographic OA at each of the 30 joints of both hands, using the radiographic films obtained in each data-collection cycle. We performed a reliability assessment of the radiographic readings by comparing a sample of those films read singly and those films read in series (paired readings) (see Supplementary Appendix and Supplementary Tables 1 and 2, available on the *Arthritis & Rheumatology* web site at http://onlinelibrary.wiley.com/doi/10.1002/art.40097/abstract), which showed good-to-excellent reliability (kappa coefficients 0.72 for time 1 and 0.86 for time 2), thus allowing us to use the original (read singly) radiographic readings.

In this study, we analyzed data from the time 1 and time 2 follow-up cycles, because hand OA symptoms and radiographic measurements were collected in these cycles (hand symptoms and radiographic features were not measured at baseline in the JoCo OA Project). Symptomatic hand OA was defined as the presence of both self-reported symptoms and radiographic OA in the same hand. Participants were considered to have symptomatic hand OA if they had symptomatic hand OA in at least 1 hand. Presence of hand symptoms was ascertained by a response of "yes" to the question, "On most days, do you have pain, aching, or stiffness in your left/right hand?" Radiographic hand OA was defined according to the following 2 criteria (25): 1) a Kellgren/Lawrence (K/L) radiographic severity grade of ≥2 (i.e., mild-to-severe radiographic OA) (24) in at least 3 total joints in each hand, excluding the metacarpophalangeal (MCP) joints; and 2) at least 1 of the affected joints being the distal interphalangeal (DIP) joint. The thumb interphalangeal joint was considered to be a proximal interphalangeal (PIP) joint, and the carpometacarpal (CMC) joint was included in the count of the total number of joints affected (as described in criterion 1).

Various definitions of radiographic hand OA have been used in different studies (26). Our definition was based on the descriptions of generalized OA phenotypes in prior studies (25,27,28), as well as on the intent to represent subjects commonly seen in clinical settings and the presence of hand OA sufficiently severe to likely affect quality of life. We believe our definition has both clinical and public health implications, and therefore the definition that we applied is appropriate for lifetime estimation of the symptomatic hand OA risk from a population perspective.

We conducted a sensitivity analysis for an alternative definition of radiographic hand OA that includes the MCP joint. The results of the sensitivity analysis showed little difference from the analyses excluding the MCP joint, and therefore those results are not reported herein. Additional sensitivity analyses using radiographic hand OA as the outcome measure were also performed separately for men and for women, and for individuals with and those without obesity.

Lifetime risk estimation. Lifetime risk is the cumulative probability (i.e., cumulative incidence) of a condition in a cohort—the number of people who develop the disease by a specified age (age 85 years in this analysis) as a proportion of the total

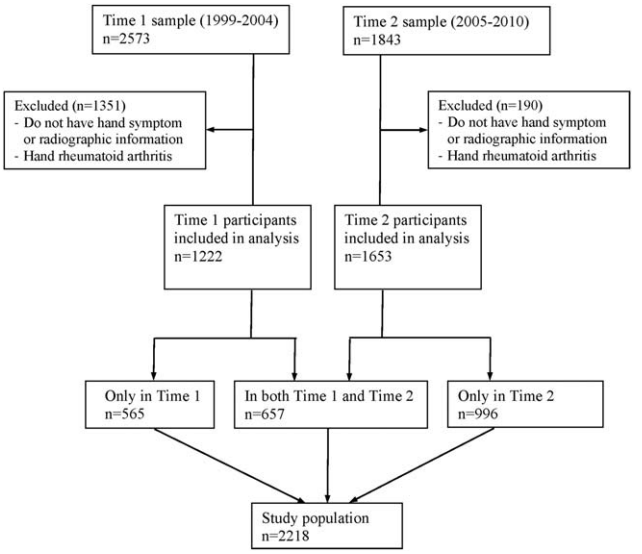

Figure 1. Distribution of subjects in the symptomatic hand osteoarthritis study sample from the Johnston County Osteoarthritis Project. In the time 2 sample, subjects (n = 730) were deemed ineligible for the following reasons: physically/mentally unable to participate (n = 165), moved away (n = 160), deceased (n = 358), or unknown (n = 47).

population at risk during the same time period. Lifetime risk estimation of other diseases has typically used life table analysis or modified time-to-event analysis, which require complete registry of the disease (in the case of life table analysis) or frequent follow-up (in the case of time-to-event analysis). To our knowledge, there are no population-based OA data sources with these characteristics. In addition, there are 3 methodologic challenges to the use of these conventional methods. First, the time to onset of symptomatic hand OA cannot be precisely determined, because OA develops slowly over time. Second, 137 participants in our sample had preexisting symptomatic hand OA at their first measurement (prevalent cases) that might thereby be excluded from a time-to-event analysis, meaning that we would lose more than one-third of the symptomatic hand OA cases in the cohort. Third, 70% of the study participants had only 1 observation at either time 1 or time 2, and therefore, in a typical time-to-event analysis, they would be managed through censoring or might be excluded from the study, thus further reducing the sample size. Because of the considerable attrition between baseline and follow-up commonly seen in cohort studies, life table analysis may result in an overestimation of risk because of the extensive censoring among participants who would be absent at follow-up.

We estimated the lifetime risk as a model-predicted prevalence of symptomatic hand OA at age 85 years for those who survived to this age, which is equal to the cumulative incidence by age 85 years, because 1) the joint structural changes defined in radiographic OA are irreversible, and 2) symptomatic hand OA has not been shown to be associated with total mortality (29). We analyzed all individuals with either single or multiple observations using a generalized estimating equations (GEE) approach, to account for within-person correlation (i.e., multiple observations per person) and to estimate the population-averaged prediction at a given age. All cohort members, regardless of symptomatic hand OA status at time 1, were included in this analysis. The inclusion of both prevalent and incident cases ensures a greater likelihood that individuals who have ever had symptomatic hand OA are included in the estimate.

Study population. Our study population comprised 2,218 participants for whom both information on hand symptoms and hand radiographs were available during at least 1 data-collection cycle (Figure 1). Among these participants, 657 individuals (29.6%) had complete information on hand symptoms and radiographic measurements at both time 1 and time 2, with a median follow-up time of 6.0 years (range 4.0–8.4 years); the rest of the study population had only 1 observation of hand symptoms and radiographic measurements, at either time 1 (n = 565) or time 2 (n = 996). Participants with radiographic evidence of rheumatoid arthritis (n = 11) were excluded from this analysis. All 2,218 eligible participants were included in the data analysis for lifetime risk estimation of symptomatic hand OA.

Statistical analysis. We estimated the lifetime risk of symptomatic hand OA using the GEE method. Age served as the

Table 1. Sociodemographic and clinical characteristics of the study population at time 1*

	Unweighted, no. of subjects	Weighted, % of subjects
Age range		
45–54 years	414	29.2
55–64 years	386	31.2
65–74 years	253	22.7
≥75 years	169	16.9
Sex		
Women	812	60.6
Men	410	39.4
Race		
White	769	71.3
African American	453	28.7
Education		
Less than high school	289	23.8
High school completed	617	48.0
Vocational school/college or higher	309	27.7
Missing	7	0.5
Obesity (BMI ≥30 kg/m^2)		
Yes	603	45.5
No	619	54.5
History of hand injury		
Yes	137	11.2
No	1,083	88.7
Missing	2	0.1
Occupational hand-held tool use in the longest job†		
Less frequent	317	25.4
More frequent	862	71.2
Missing	43	3.4

* The Johnston County Osteoarthritis Project population from time 1 (1999–2004) contained 1,222 subjects. For the weighted percentage, sampling weights were applied to be representative of the target population. BMI = body mass index.

† Categories were assessed in response to the question, "For the job that you held longest in your life, how often did you have to use hand-held tools or equipment (pen, keyboard, computer mouse, drill, hairdryer, sander, etc.)?" The participants in whom use was categorized as less frequent were those who answered "never," "seldom," or "sometimes" to this question. Those in whom use was categorized as more frequent were those who answered "often" or "always."

independent variable, binary status of symptomatic hand OA (yes versus no) was the outcome variable, and lifetime risk was estimated as the model-predicted probability of developing symptomatic hand OA at age 85 years, using conditional marginal probability. We chose the age of 85 years because it is a reasonable life expectancy for individuals in the US (30). For stratified analysis, we estimated the lifetime risk from models that contained the stratification variable (e.g., sex) one at a time and the interaction term of the variable with age. To test the linearity of the age effect, a preliminary analysis was conducted to include the quadratic term age^2. We also estimated the model-predicted probability of having symptomatic hand OA for ages 45 years through 85 years, and plotted cumulative risk curves by age and stratification variables.

To ensure that our estimates were representative of the target population (i.e., the 6 selected townships of Johnston County), we incorporated sampling weights to account for oversampling of African Americans and differential rates of nonresponse at different data-collection cycles. The weights were also calibrated to the population counts from the 2000 US Census for those 6 townships in Johnston County. In addition, the statistical analyses were adjusted for within-cluster correlation from potential correlation of repeated measures for participants (for those with data from both cycles), using an exchangeable working correlation structure, and the within-cluster correlation from the stratified random sampling design at 3 levels (stratum [townships], the primary sampling unit [streets], and the secondary sampling unit [households]). A Taylor series linearization method was used to estimate the standard error of the probabilities with 95% confidence interval (95% CI). Adjusted F-statistics from Wald's test were used to test the risk difference between levels of the stratification variables. Statistical testing used an alpha level of 0.05. All analyses were performed using SAS callable SUDAAN software (version 11; RTI International).

Stratification variables. The estimated lifetime risk of symptomatic hand OA was stratified for the following 6 known or potential risk factors for symptomatic hand OA: sex, race, education level, obesity, prior hand injury, and occupational hand activities (19–21). Age and stratification variables were self-reported in an interviewer-administered questionnaire during home interviews. Obesity was defined as a body mass index (BMI) of $\geq$30 kg/m^2, with the participants' weight and height measured during clinic visits. Prior hand injury for the right and left hands was determined based on the participant's response to the question, "Has a doctor ever told you that you had broken or fractured any fingers of your hands?" Participants answering "yes" for at least 1 hand were considered to have prior hand injury. Occupational hand activities were assessed by the question, "For the job that you held longest in your life, how often did you have to use hand-held tools or equipment (pen, keyboard, computer mouse, drill, hairdryer, sander, etc.)?" For participants who answered "never," "seldom," or "sometimes" use was categorized as "less frequent," and for those who answered "often" or "always" use was categorized as "more frequent."

RESULTS

Overall, 352 participants in the study population had symptomatic hand OA in at least 1 hand. The unweighted prevalence of symptomatic hand OA was 10.8% at time 1 and 15.5% at time 2, and the unweighted prevalence of pain, aching, or stiffness in at least 1 hand was 46.2% at time 1 and 36.3% at time 2.

The mean $\pm$ SD age of the 1,222 study participants at time 1 was 61.0 $\pm$ 10.7 years (range 45–94 years). The weighted proportion of women was higher than that of men (60.6% versus 39.4%), and there were more whites than African Americans (71.3% versus 28.7%) (Table 1). About three-fourths of the cohort had completed at least high school (75.7%), and nearly one-half of the cohort (45.5%) were obese. These characteristics were similar at time 2, except that the subjects at time 2 were older. The quadratic term age^2 was not statistically significant (at a level of $\alpha = 0.05$). First-order continuous age was used in the remaining analyses, because its association with lifetime risk provides a simpler (linear) interpretation.

Table 2. Lifetime risk of symptomatic hand osteoarthritis (OA) overall and by OA risk factor stratification variable*

	Lifetime risk, % of subjects (95% CI)	*P*†
Symptomatic hand OA overall (in at least 1 hand)	39.8 (34.4–45.3)	NA
Symptomatic OA in 1 hand	13.5 (11.4–16.1)	NA
Symptomatic OA in both hands	27.3 (22.1–33.2)	NA
Stratification variable‡		
Sex		<0.0001
Women	47.2 (40.6–53.9)	
Men	24.6 (19.5–30.5)	
Race		0.031
White	41.4 (35.5–47.6)	
African American	29.2 (20.5–39.7)	
Education level		≥0.255§
Less than high school	43.7 (37.0–50.6)	
High school completed	39.6 (30.5–49.4)	
Higher than high school	38.3 (32.3–44.7)	
Obesity (BMI ≥30 kg/m^2)		0.063
Yes	47.1 (37.8–56.7)	
No	36.1 (29.7–42.9)	
Hand injury history		0.427
Yes	53.7 (22.0–82.6)	
No	39.3 (33.9–45.0)	
Occupational hand-held tool use in the longest job¶		0.392
Less frequent	37.2 (31.6–43.2)	
More frequent	41.5 (34.1–49.2)	

* The Johnston County Osteoarthritis Project study population comprised 2,218 subjects. 95% CI = 95% confidence interval; NA = not applicable; BMI = body mass index.
† Calculated using adjusted F-statistics (*P* values) from Wald's test (testing the risk difference between levels of the stratification variables).
‡ Estimated from models that contained the stratification variable (e.g., sex) and the interaction term of the variable with age.
§ The smallest of the 3 pairwise comparisons.
¶ Categories were assessed in response to the question, "For the job that you held longest in your life, how often did you have to use hand-held tools or equipment (pen, keyboard, computer mouse, drill, hairdryer, sander, etc.)?" The participants in whom use was categorized as less frequent were those who answered "never," "seldom," or "sometimes" to this question. Those in whom use was categorized as more frequent were those who answered "often" or "always."

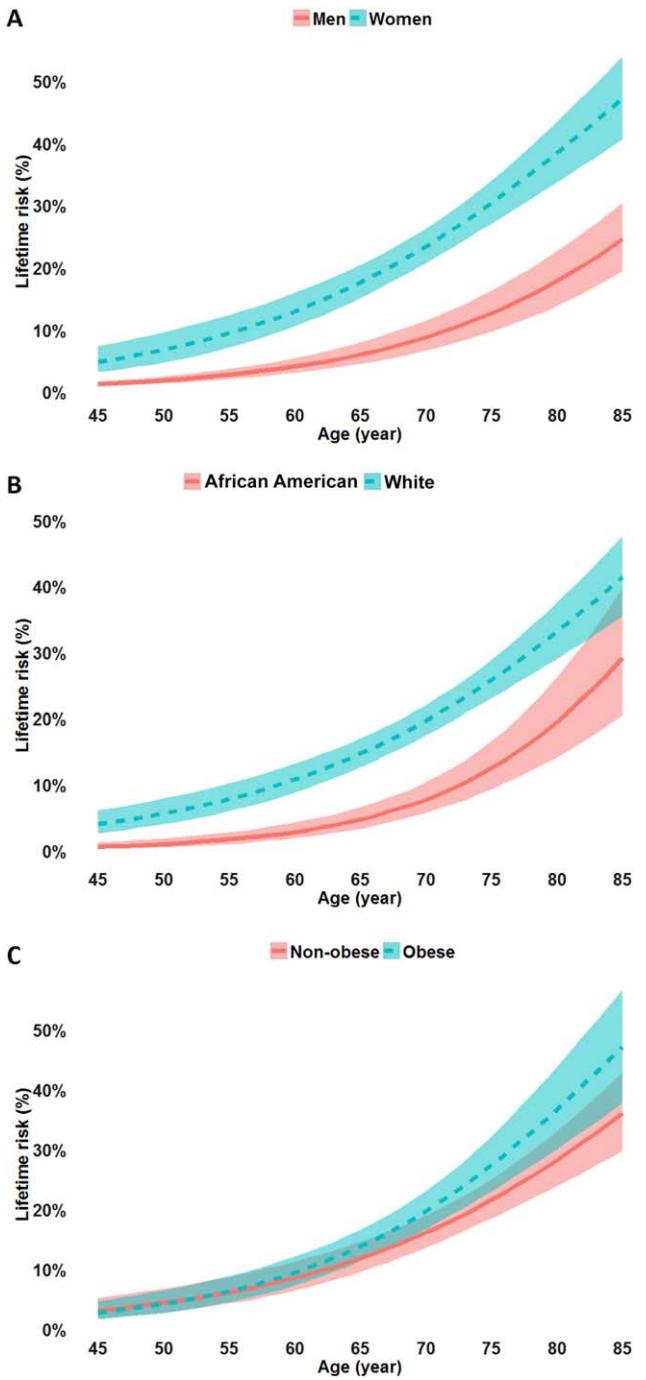

Figure 2. Cumulative risk curves by age for subgroups stratified by sex (men versus women) **(A)**, race (white versus African American) **(B)**, and body mass index (obese [≥30 kg/m^2] versus nonobese) **(C)**. The shaded bands represent the 95% confidence intervals for the estimated cumulative risks.

The overall lifetime risk of symptomatic hand OA (i.e., the proportion of those who will develop the condition by age 85 years) was 39.8% (95% CI 34.4–45.3%) (Table 2). The lifetime risk was nearly 1 in 2 for women (47.2%, 95% CI 40.6–53.9%) compared with 1 in 4 for men (24.6%, 95% CI 19.5–30.5%). The curve of cumulative incidence of symptomatic hand OA showed a consistently significantly higher risk in women than in men at all ages analyzed, and this difference became greater with increasing age (Figure 2A).

The lifetime risk of symptomatic hand OA was 12.2 percentage points higher in whites than in African Americans ($P = 0.031$) (Table 2). The curve of cumulative incidence of symptomatic hand OA indicated a significantly higher risk in whites than in African Americans throughout the middle to older ages (Figure 2B).

Among individuals with obesity, the lifetime risk of symptomatic hand OA was 47.1% (95% CI 37.8–56.7%), compared with 36.1% (95% CI 29.7–42.9%) among those without obesity ($P = 0.063$) (Table 2). In individuals classified as obese compared with those who were not obese, there was little difference in the cumulative risk of symptomatic hand OA up to the mid-60s in age, but thereafter the difference in cumulative risk in obese individuals compared with nonobese individuals increased with older age (Figure 2C).

Moreover, the lifetime risk of symptomatic hand OA was 53.7% (95% CI 22.0–82.6%) in individuals with prior hand injury compared with 39.3% (95% CI 33.9–45.0%) among those without prior hand injury ($P = 0.427$) (Table 2; see also Supplementary Figure 1A, available on the *Arthritis & Rheumatology* web site at http://onlinelibrary.wiley.com/doi/10.1002/art.40097/abstract). There was no statistically significant difference in lifetime risk by education level or occupational hand-held tool use (Table 2; see also Supplementary Figures 1B and C, available on the *Arthritis & Rheumatology* web site at http://onlinelibrary.wiley.com/doi/10.1002/art.40097/abstract).

DISCUSSION

Our estimates of lifetime risk from this population-based study of adults suggest that 40% will develop symptomatic hand OA by age 85 years. The lifetime risk of symptomatic hand OA was slightly lower than that of symptomatic knee OA (45%), but higher than that of symptomatic hip OA (25%) in the same population (17,18). Similarly, estimates of OA prevalence in the general population are usually the highest for the knee, followed by the hand (using a definition similar to ours), and lower for the hip (10,25).

Lifetime risk estimates provide an informative and helpful prediction from an individual perspective if one anticipates living to an older age. In addition, estimation of lifetime risk presents the scope of the problem from a

population perspective. Given the aging population and increasing life expectancy in the US (31), it is reasonable to expect that more Americans will be affected by this painful and debilitating condition in the years to come.

The lifetime risk was particularly high among women; we estimated that nearly 1 in 2 women will develop symptomatic hand OA by age 85 years compared with 1 in 4 men. Women are consistently at higher risk of OA than men in epidemiologic studies (19–21), particularly in the hand. In a large prospective cohort study, the adjusted female-to-male OA rate ratios were 2.5 for hand OA, 1.5 for knee OA, and 1.2 for hip OA; the risk of hand OA among women peaked at ages 60–64 years (32). Several hypotheses have been proposed to explain the higher risk of OA in women. One probable explanation is a hormonal effect: the higher incidence of OA in women just after menopause suggests that estrogen deficiency may play a role in causing the disease (21). Other hypotheses include differences in pain perception and sensitivity (33) and anatomic differences between men and women (34), as well as differences in reporting of pain (3). It has been previously shown in the Framingham Osteoarthritis Study that the prevalence of radiographic hand OA was similar between women and men (94.4% versus 88.6%), whereas symptomatic hand OA was twice as common in women as in men (26.2% versus 13.4%) (3). We performed a sensitivity analysis that analyzed radiographic hand OA as the outcome measure, and the lifetime risk of radiographic hand OA at age 85 years was 79% (95% CI 74–83%) in women and 63% (95% CI 57–68%) in men. The difference was statistically significant ($P < 0.01$). One possible explanation for the difference between the findings in our study and those in the Framingham Osteoarthritis Study is that the definition of radiographic hand OA used in the Framingham Study was presence of OA in ≥1 finger joint.

Consistent with our findings, prior studies using data from the JoCo OA Project demonstrated that whites were more likely to have symptomatic hand OA and to have hand radiographic OA phenotypes as compared with African Americans, after adjusting for sex, age, and BMI (25,35). In another population of middle-aged women, the unadjusted prevalence of radiographic OA was found to be similar between African American women and white women in the DIP, PIP, and CMC joints, but was markedly higher in the MCP joints among African American women (36). The biologic mechanism for these observed differences is unknown and warrants further investigation.

Obesity is an important, and modifiable, risk factor for both the incidence and the progression of OA. The evidence of association between obesity and OA in the load-bearing knee joint is strong, whereas evidence of association between obesity and hand OA is moderate in different studies (13,37–42). These studies used multivariate analyses to examine the association between obesity and OA, adjusting for other potential confounders (e.g., sex). The goal of our analyses was not to investigate the risk factors for symptomatic hand OA, but rather to estimate the scale of the burden and to assess the risk via simple stratification analyses based on known OA risk factors, analyzed one at a time. Nevertheless, our results still showed a difference of 11 percentage points in the lifetime risk of symptomatic hand OA by obesity status. Sensitivity analyses using radiographic hand OA as the outcome measure estimated the lifetime risk at age 85 years to be 78% (95% CI 72–84%) for individuals with obesity and 70% (95% CI 63–77%) for those without obesity (test-of-difference $P = 0.076$), suggesting that the difference in estimates of lifetime risk of symptomatic hand OA by obesity status may not be fully explained by differences in the reporting of pain.

Recent studies have suggested that the pathogenesis of hand OA is likely different than the pathogenesis of OA in the load-bearing joints (i.e., knee and hip). Unlike knee and hip OA, in which abnormal biomechanics due to excessive weight are known to play an essential role, systemic processes, such as aberrant metabolic regulation and inflammation associated with obesity, may be more important than mechanical factors in the pathogenesis and progression of hand OA (43–45).

Joint injury and occupational activities are known modifiable risk factors for OA (19–21). Severe injury to the structure of the knee is strongly linked to the subsequent onset of OA and musculoskeletal symptoms (46,47). However, similar evidence with regard to the effects of injury in the hand is lacking, because almost all such injury studies have focused on the knee. The lifetime risk of symptomatic hand OA was 54% among those with hand injury compared with 39% among those without hand injury, but the small number of participants with hand injury precluded statistically significant findings. Occupational activities that involve repetitive motion, high biomechanical loading, or vibration could initiate or accelerate structural changes in the cartilage, bones, and other joint tissues, and cause injuries (48). Extensive precision pinch or grip, as seen in occupations such as dentists and textile workers, is associated with increased risk of OA in the DIP joint, whereas forceful and prolonged gripping, common in heavy manual work, is associated with increased risk in the MCP joint (48). Our single question on hand-held tool use tried to assess occupational activities that would be relevant to the hand, but did not directly address gripping or pinching.

Our analysis is subject to the following limitations. First, Johnston County, North Carolina is a lower-income, semirural area in the southern US, and our findings may not be generalizable to other regions of the US or other

populations. However, we expect that the lifetime risk of symptomatic hand OA is likely high in the US, given the aging population and the high prevalence of obesity (49), both of which are important risk factors for OA. A comparison of the US and Johnston County populations in 2010 (50) showed that 50.8% were women in both populations, approximately one-third were obese (35.7% versus 34.4%), and race distributions were similar (whites, 72.4% versus 74.2%; African Americans, 12.6% versus 15.1%). Compared with the US population, the Johnston County population was slightly younger (age ≥45 years, 39.5% versus 35.6%, respectively; age ≥65 years, 13.0% versus 10.2%, respectively). Moreover, the Johnston County population was less educated (18.8% had not completed high school versus 14.9% in the US population) and had lower income (median annual household income $49,745 versus $51,914 in the US population). However, Johnston County had substantially more people living in rural areas (52% versus 19.3% of the US population).

Second, the hand symptom question was not joint-specific, which may affect specificity of symptomatic hand OA ascertainment, as the joints having radiographic OA and those showing symptoms may not be the same ones. Questions about hand symptoms with more details (e.g., which joints are affected and level of severity) may help to improve the specificity of the symptomatic hand OA definition.

Third, the hand injury question asks participants if they ever had broken or fractured fingers. This question is likely to result in an underestimation of less severe hand injuries.

Fourth, the assessment of occupational hand-held tool use was limited in 2 ways. 1) Participants self-reported the frequency of hand-held tool use in the longest job held in their lives, which may be subject to misclassification of exposure due to recall bias. 2) The occupational hand-held tool question listed examples ranging from pens, keyboards, and a computer mouse to hairdryers, drills, and sanders; the latter typically involves vibration and greater force relative to the other tools. Mixing them together would likely cause nondifferential misclassification of occupational exposure, and would increase the similarity between the high-exposure and low-exposure groups, thus resulting in an underestimate (dilution) of the true difference between stratified lifetime risks.

Fifth, although the onset of hand OA occurs most commonly after the age of 40 years (21), selecting a study sample with ages ≥45 years may miss cases of symptomatic hand OA in the younger population. This may contribute to a slight underestimation of the lifetime risk.

Sixth, the method used in this study did not adjust for potential changes in BMI over time.

Seventh, models of stratified lifetime risk estimates only included a single factor at a time, in addition to age. Therefore, residual confounding may exist.

Finally, the limited sample size decreased the precision of the point estimates. This would likely prevent detection of statistically significant differences between subgroups.

This study had several strengths. First, our approach provided lifetime risk estimation of symptomatic hand OA that included all participants with either 1 measurement or multiple measurements in the analysis, which is otherwise unfeasible using conventional methods, given the difficulties described earlier.

Second, as far as we know, the JoCo OA Project is the only longitudinal OA cohort study in the US that includes oversampling of African Americans (33% in the JoCo OA Project baseline cohort) for analysis of racial differences.

Third, the probability sampling design of the JoCo OA Project allowed us to make population-based inferences.

Lifetime risk, or the probability of developing a condition over a lifetime, is conceptually accessible to the public; it may be easier for the general population to understand absolute risk estimates such as the lifetime risk, as opposed to relative risk estimates. Moreover, greater understanding of lifetime risks may motivate health care providers and researchers to develop preventive strategies and provide earlier interventions for hand OA.

Symptomatic hand OA has substantial public health implications, considering its high lifetime risk, its effect on functional impairment and disability of the hand, and its association with decreased quality of life. These findings underscore the need for increased use of public health and clinical prevention and intervention measures to address and mitigate the impact of symptomatic hand OA on individuals and society. There are effective and inexpensive public health interventions (51) as well as other nonpharmacologic strategies and pharmacologic therapies (52) that may help manage OA symptoms, maintain better function, and improve quality of life. Our lifetime risk estimates of symptomatic hand OA, together with those previously ascertained for knee OA and hip OA (17,18), further illustrate the significant burden of symptomatic OA.

ACKNOWLEDGMENTS

We would like to thank the dedicated staff of the Johnston County Osteoarthritis Project, William Kalsbeek, PhD for his consultation in sampling design and statistical analysis, and Amy Shi, PhD for her assistance in reliability assessments of the hand radiographs.

AUTHOR CONTRIBUTIONS

All authors were involved in drafting the article or revising it critically for important intellectual content, and all authors approved the final version to be published. Dr. Qin had full access to all of the data in the study and takes responsibility for the integrity of the data and the accuracy of the data analysis.

Study conception and design. Nelson, Schwartz, Helmick, Allen, Renner, Jordan.

Acquisition of data. Jordan.

Analysis and interpretation of data. Qin, Barbour, Murphy, Schwartz, Renner, Baker.

REFERENCES

1. Zhang W, Doherty M, Leeb BF, Alekseeva L, Arden NK, Bijlsma JW, et al. EULAR evidence-based recommendations for the diagnosis of hand osteoarthritis: report of a task force of ESCISIT. Ann Rheum Dis 2009;68:8–17.
2. Michon M, Maheu E, Berenbaum F. Assessing health-related quality of life in hand osteoarthritis: a literature review. Ann Rheum Dis 2011;70:921–8.
3. Zhang Y, Niu J, Kelly-Hayes M, Chaisson CE, Aliabadi P, Felson DT. Prevalence of symptomatic hand osteoarthritis and its impact on functional status among the elderly: the Framingham Study. Am J Epidemiol 2002;156:1021–7.
4. Kloppenburg M, Stamm T, Watt I, Kainberger F, Cawston TE, Birrell FN, et al. Research in hand osteoarthritis: time for reappraisal and demand for new strategies: an opinion paper. Ann Rheum Dis 2007;66:1157–61.
5. Oliveria SA, Felson DT, Reed JI, Cirillo PA, Walker AM. Incidence of symptomatic hand, hip, and knee osteoarthritis among patients in a health maintenance organization. Arthritis Rheum 1995;38:1134–41.
6. Andrianakos AA, Kontelis LK, Karamitsos DG, Aslanidis SI, Georgountzos AI, Kaziolas GO, et al. Prevalence of symptomatic knee, hand, and hip osteoarthritis in Greece: the ESORDIG study. J Rheumatol 2006;33:2507–13.
7. Carmona L, Ballina J, Gabriel R, Laffon A, on behalf of the EPISER Study Group. The burden of musculoskeletal diseases in the general population of Spain: results from a national survey. Ann Rheum Dis 2001;60:1040–5.
8. Dillon CF, Hirsch R, Rasch EK, Gu Q. Symptomatic hand osteoarthritis in the United States: prevalence and functional impairment estimates from the third U.S. National Health and Nutrition Examination Survey, 1991–1994. Am J Phys Med Rehabil 2007;86:12–21.
9. Grotle M, Hagen KB, Natvig B, Dahl FA, Kvien TK. Prevalence and burden of osteoarthritis: results from a population survey in Norway. J Rheumatol 2008;35:677–84.
10. Mannoni A, Briganti MP, Di Bari M, Ferrucci L, Costanzo S, Serni U, et al. Epidemiological profile of symptomatic osteoarthritis in older adults: a population based study in Dicomano, Italy. Ann Rheum Dis 2003;62:576–8.
11. Zhang Y, Xu L, Nevitt MC, Niu J, Goggins JP, Aliabadi P, et al. Lower prevalence of hand osteoarthritis among Chinese subjects in Beijing compared with white subjects in the United States: the Beijing Osteoarthritis Study. Arthritis Rheum 2003;48:1034–40.
12. Haugen IK, Englund M, Aliabadi P, Niu J, Clancy M, Kvien TK, et al. Prevalence, incidence and progression of hand osteoarthritis in the general population: the Framingham Osteoarthritis Study. Ann Rheum Dis 2011;70:1581–6.
13. Grotle M, Hagen KB, Natvig B, Dahl FA, Kvien TK. Obesity and osteoarthritis in knee, hip and/or hand: an epidemiological study in the general population with 10 years follow-up. BMC Musculoskelet Disord 2008;9:132.
14. Feuer EJ, Wun LM, Boring CC, Flanders WD, Timmel MJ, Tong T. The lifetime risk of developing breast cancer. J Natl Cancer Inst 1993;85:892–7.
15. Lloyd-Jones DM, Larson MG, Beiser A, Levy D. Lifetime risk of developing coronary heart disease. Lancet 1999;353:89–92.
16. Narayan KM, Boyle JP, Thompson TJ, Sorensen SW, Williamson DF. Lifetime risk for diabetes mellitus in the United States. JAMA 2003;290:1884–90.
17. Murphy L, Schwartz TA, Helmick CG, Renner JB, Tudor G, Koch G, et al. Lifetime risk of symptomatic knee osteoarthritis. Arthritis Rheum 2008;59:1207–13.
18. Murphy LB, Helmick CG, Schwartz TA, Renner JB, Tudor G, Koch GG, et al. One in four people may develop symptomatic hip osteoarthritis in his or her lifetime. Osteoarthritis Cartilage 2010;18:1372–9.
19. Neogi T, Zhang Y. Epidemiology of osteoarthritis. Rheum Dis Clin North Am 2013;39:1–19.
20. Suri P, Morgenroth DC, Hunter DJ. Epidemiology of osteoarthritis and associated comorbidities. PM R 2012;4 Suppl:S10–9.
21. Zhang Y, Jordan JM. Epidemiology of osteoarthritis. Clin Geriatr Med 2010;26:355–69.
22. Jordan JM, Helmick CG, Renner JB, Luta G, Dragomir AD, Woodard J, et al. Prevalence of knee symptoms and radiographic and symptomatic knee osteoarthritis in African Americans and Caucasians: the Johnston County Osteoarthritis Project. J Rheumatol 2007;34:172–80.
23. Burnett S, Hart DJ, Cooper C, Spector TD. A radiographic atlas of osteoarthritis. London: Springer-Verlag; 1994.
24. Kellgren JH, Lawrence JS. Radiological assessment of osteo-arthrosis. Ann Rheum Dis 1957;16:494–502.
25. Nelson AE, Golightly YM, Renner JB, Schwartz TA, Kraus VB, Helmick CG, et al. Differences in multijoint symptomatic osteoarthritis phenotypes by race and sex: the Johnston County Osteoarthritis Project. Arthritis Rheum 2013;65:373–7.
26. Marshall M, Dziedzic KS, van der Windt DA, Hay EM. A systematic search and narrative review of radiographic definitions of hand osteoarthritis in population-based studies. Osteoarthritis Cartilage 2008;16:219–26.
27. Kraus VB, Jordan JM, Doherty M, Wilson AG, Moskowitz R, Hochberg M, et al. The Genetics of Generalized Osteoarthritis (GOGO) study: study design and evaluation of osteoarthritis phenotypes. Osteoarthritis Cartilage 2007;15:120–7.
28. Nelson AE, Smith MW, Golightly YM, Jordan JM. "Generalized osteoarthritis": a systematic review. Semin Arthritis Rheum 2014;43:713–20.
29. Haugen IK, Ramachandran VS, Misra D, Neogi T, Niu J, Yang T, et al. Hand osteoarthritis in relation to mortality and incidence of cardiovascular disease: data from the Framingham Heart Study. Ann Rheum Dis 2015;74:74–81.
30. Arias E. United States life tables, 2011. Natl Vital Stat Rep 2015;64:1–63.
31. Vincent GK, Velkoff VA. The next four decades: the older population in the United States: 2010 to 2050. Washington (DC): US Department of Commerce, Economics and Statistics Administration, US Census Bureau; 2010.
32. Prieto-Alhambra D, Judge A, Javaid MK, Cooper C, Diez-Perez A, Arden NK. Incidence and risk factors for clinically diagnosed knee, hip and hand osteoarthritis: influences of age, gender and osteoarthritis affecting other joints. Ann Rheum Dis 2014;73:1659–64.
33. Racine M, Tousignant-Laflamme Y, Kloda LA, Dion D, Dupuis G, Choiniere M. A systematic literature review of 10 years of research on sex/gender and experimental pain perception. Part 1. Are there really differences between women and men? Pain 2012;153:602–18.
34. Maleki-Fischbach M, Jordan JM. New developments in osteoarthritis: sex differences in magnetic resonance imaging-based biomarkers and in those of joint metabolism. Arthritis Res Ther 2010;12:212.
35. Nelson AE, Renner JB, Schwartz TA, Kraus VB, Helmick CG, Jordan JM. Differences in multijoint radiographic osteoarthritis phenotypes among African Americans and Caucasians: the

Johnston County Osteoarthritis project. Arthritis Rheum 2011; 63:3843–52.
36. Sowers M, Lachance L, Hochberg M, Jamadar D. Radiographically defined osteoarthritis of the hand and knee in young and middle-aged African American and Caucasian women. Osteoarthritis Cartilage 2000;8:69–77.
37. Carman WJ, Sowers M, Hawthorne VM, Weissfeld LA. Obesity as a risk factor for osteoarthritis of the hand and wrist: a prospective study. Am J Epidemiol 1994;139:119–29.
38. Oliveria SA, Felson DT, Cirillo PA, Reed JI, Walker AM. Body weight, body mass index, and incident symptomatic osteoarthritis of the hand, hip, and knee. Epidemiology 1999;10:161–6.
39. Reyes C, Leyland KM, Peat G, Cooper C, Arden NK, Prieto-Alhambra D. Association between overweight and obesity and risk of clinically diagnosed knee, hip, and hand osteoarthritis: a population-based cohort study. Arthritis Rheumatol 2016;68:1869–75.
40. Szoeke C, Dennerstein L, Guthrie J, Clark M, Cicuttini F. The relationship between prospectively assessed body weight and physical activity and prevalence of radiological knee osteoarthritis in postmenopausal women. J Rheumatol 2006;33:1835–40.
41. Visser AW, Ioan-Facsinay A, de Mutsert R, Widya RL, Loef M, de Roos A, et al. Adiposity and hand osteoarthritis: the Netherlands Epidemiology of Obesity study. Arthritis Res Ther 2014;16:R19.
42. Yusuf E, Nelissen RG, Ioan-Facsinay A, Stojanovic-Susulic V, DeGroot J, van Osch G, et al. Association between weight or body mass index and hand osteoarthritis: a systematic review. Ann Rheum Dis 2010;69:761–5.
43. Kluzek S, Newton JL, Arden NK. Is osteoarthritis a metabolic disorder? Br Med Bull 2015;115:111–21.
44. Mathiessen A, Slatkowsky-Christensen B, Kvien TK, Hammer HB, Haugen IK. Ultrasound-detected inflammation predicts radiographic progression in hand osteoarthritis after 5 years. Ann Rheum Dis 2016;75:825–30.
45. Visser AW, de Mutsert R, le Cessie S, den Heijer M, Rosendaal FR, Kloppenburg M, et al. The relative contribution of mechanical stress and systemic processes in different types of osteoarthritis: the NEO study. Ann Rheum Dis 2015;74: 1842–7.
46. Blagojevic M, Jinks C, Jeffery A, Jordan KP. Risk factors for onset of osteoarthritis of the knee in older adults: a systematic review and meta-analysis. Osteoarthritis Cartilage 2010;18:24–33.
47. Muthuri SG, McWilliams DF, Doherty M, Zhang W. History of knee injuries and knee osteoarthritis: a meta-analysis of observational studies. Osteoarthritis Cartilage 2011;19:1286–93.
48. Felson DT. Do occupation-related physical factors contribute to arthritis? Baillieres Clin Rheumatol 1994;8:63–77.
49. Ogden CL, Carroll MD, Kit BK, Flegal KM. Prevalence of childhood and adult obesity in the United States, 2011–2012. JAMA 2014;311:806–14.
50. US Census Bureau. DP-1. Profile of general population and housing characteristics. 2010: Johnston County, North Carolina & United States. URL: https://factfinder.census.gov/faces/nav/jsf/pages/community_facts.xhtml.
51. Brady TJ, Jernick SL, Hootman JM, Sniezek JE. Public health interventions for arthritis: expanding the toolbox of evidence-based interventions. J Womens Health (Larchmt) 2009;18: 1905–17.
52. Hochberg MC, Altman RD, April KT, Benkhalti M, Guyatt G, McGowan J, et al. American College of Rheumatology 2012 recommendations for the use of nonpharmacologic and pharmacologic therapies in osteoarthritis of the hand, hip, and knee. Arthritis Care Res (Hoboken) 2012;64:465–74.

ARTHRITIS & RHEUMATOLOGY
Vol. 69, No. 6, June 2017, pp 1213–1220
DOI 10.1002/art.40069

Serum Urate Levels Predict Joint Space Narrowing in Non-Gout Patients With Medial Knee Osteoarthritis

Svetlana Krasnokutsky, Charles Oshinsky, Mukundan Attur, Sisi Ma, Hua Zhou, Fangfei Zheng, Meng Chen, Jyoti Patel, Jonathan Samuels, Virginia C. Pike, Ravinder Regatte, Jenny Bencardino, Leon Rybak, Steven Abramson, and Michael H. Pillinger

Objective. **The pathogenesis of osteoarthritis (OA) includes both mechanical and inflammatory features. Studies have implicated synovial fluid uric acid (UA) as a potential OA biomarker, possibly reflecting chondrocyte damage. Whether serum UA levels reflect/contribute to OA is unknown. We investigated whether serum UA levels predict OA progression in a non-gout knee OA population.**

Methods. **Eighty-eight patients with medial knee OA (body mass index [BMI] <33 kg/m^2) but without gout were studied. Baseline serum UA levels were measured in previously banked serum samples. At 0 and 24 months, patients underwent standardized weight-bearing fixed-flexion posteroanterior knee radiography to determine joint space width (JSW) and Kellgren/Lawrence grades. Joint space narrowing (JSN) was calculated as the change in JSW from 0 to 24 months. Twenty-seven patients underwent baseline contrast-enhanced 3T knee magnetic resonance imaging for assessment of synovial volume.**

Results. **Serum UA levels correlated with JSN values in both univariate (r = 0.40, $P < 0.01$) and multivariate (r = 0.28, $P = 0.01$) analyses. There was a significant difference in mean JSN after dichotomization at a serum UA cut point of 6.8 mg/dl, the solubility point for serum urate, even after adjustment (JSN of 0.90 mm for a serum UA ≥6.8 mg/dl and 0.31 mm for a serum UA <6.8 mg/dl; $P < 0.01$). Baseline serum UA levels distinguished progressors (JSN >0.2 mm) and fast progressors (JSN >0.5 mm) from nonprogressors (JSN ≤0.0 mm) in multivariate analyses (area under the receiver operating characteristic curve 0.63 [$P = 0.03$] and 0.62 [$P = 0.05$], respectively). Serum UA levels correlated with the synovial volume (r = 0.44, $P < 0.01$), a possible marker of JSN, although this correlation did not persist after controlling for age, sex, and BMI (r = 0.13, $P = 0.56$).**

Conclusion. **In non-gout patients with knee OA, the serum UA level predicted future JSN and may serve as a biomarker for OA progression.**

Osteoarthritis (OA), the most prevalent form of arthritis, remains poorly understood. Though historically regarded as a disease of mechanical degeneration, it is now appreciated that inflammation, on both the tissue and biochemical levels, plays an important role in OA pathogenesis (1–4). Various inflammatory molecules have been studied for their ability to reflect the presence of OA or predict its progression. For example, levels of 15-hydroxyeicosatetraenoic acid and prostaglandin E_2 are elevated in patients with symptomatic knee OA, and interleukin-1β (IL-1β) and IL-1 receptor antagonist have been reported to be associated with joint space narrowing (JSN) (5–7). The potential for these molecules to serve as OA biomarkers is a matter of ongoing investigation. In addition to prognostic utility, biomarkers that predict JSN would be of considerable value when defining enrollment criteria for prospective OA clinical trials, in which limiting heterogeneity and enriching for more rapid disease progression would have significant practical benefit (8).

Supported by the NIH (National Institute of Arthritis and Musculoskeletal and Skin Diseases grant R01-AR-052873 to Dr. Abramson) and the Rheumatology Research Foundation (Investigator Award to Dr. Krasnokutsky). Dr. Pillinger's work was supported in part by the NIH (NYU Clinical and Translational Science Award 1UL1-TR-001445 from the National Center for Advancing Translational Sciences).

Svetlana Krasnokutsky, MD, MS, Charles Oshinsky, BA, Mukundan Attur, PhD, Sisi Ma, PhD, Hua Zhou, PhD, Fangfei Zheng, MD, Meng Chen, MD, Jyoti Patel, BS, Jonathan Samuels, MD, Virginia C. Pike, BA, Ravinder Regatte, PhD, Jenny Bencardino, MD, Leon Rybak, MD, Steven Abramson, MD, Michael H. Pillinger, MD: New York University School of Medicine, New York, New York.

Dr. Krasnokutsky and Mr. Oshinsky are co–first authors and contributed equally to this work.

Address correspondence to Charles Oshinsky, BA, NYU Hospital for Joint Diseases, 301 East 17th Street, Suite 1410, Division of Rheumatology, New York, NY 10003. E-mail: charlie4910@gmail.com.

Submitted for publication June 8, 2016; accepted in revised form February 7, 2017.

Uric acid (UA) is the end product of human purine catabolism, and in the form of soluble serum urate, it has been recognized as a biomarker in diseases such as heart failure, hypertension, and renal disease (9,10). UA is metabolically active and has been reported to act both intracellularly and extracellularly and to denote and/or promote inflammatory states (11). In addition, UA precipitates monosodium urate monohydrate (MSU) crystals (in macroscopic or microscopic forms) and drives inflammation by engaging and activating leukocytes and other cells (12). MSU crystals are responsible for not only the acute, painful attacks of gout, but also the lower-level, chronic inflammatory states (13).

A small but accumulating body of evidence suggests that UA may participate in the pathogenesis of OA (14). Previous reports noted an association between UA and OA (15). Gout and OA often colocalize within the same joint (16), and studies have shown that, even in the absence of gout, synovial fluid UA levels correlate with OA severity (17,18). We have reported that patients with gout are more likely than control subjects with a serum UA of <6.8 mg/dl and no gout to have OA, with hyperuricemic non-gout patients having an intermediate level of knee OA prevalence and severity. When present, OA is also likely to be more severe in patients with gout as compared to those without it (19).

Whether serum UA may serve as a biomarker to convey or predict OA risk is not known. To assess this possibility, we investigated whether serum UA levels are associated with the radiographic severity of knee OA and with synovial volume, as determined by contrast-enhanced magnetic resonance imaging (MRI), and whether serum UA levels predict OA JSN, in a non-gout population with knee OA.

PATIENTS AND METHODS

Patient population. We assessed a subset of patients enrolled in a previously described, 24-month prospective, natural history study of knee OA with a focus on inflammatory biomarker discovery. At initial enrollment, patients met the American College of Rheumatology (ACR) clinical criteria for knee OA (20) and had symptomatic OA of at least 1 knee (index knee), with a Kellgren/Lawrence (K/L) score of ≥1 in that knee (21). Exclusion criteria included any other form of arthritis (e.g., rheumatoid arthritis, spondyloarthritis, gout, pyrophosphate disease, or other crystal arthropathy), a body mass index (BMI) ≥33 kg/m^2 (chosen to minimize the impact of obesity on OA/inflammatory biomarkers without adversely impairing recruitment potential), and other characteristics as previously described (7). For the current study, we included only patients whose baseline knee OA was predominantly medial (i.e., medial joint space width [JSW] less than lateral JSW on radiographic assessment), consistent with the Osteoarthritis Research Society International recommendations (22). Study patients additionally had both baseline and 24-month radiographic measurements, as well as stored serum samples available for baseline serum UA measurement. The study was approved by the Institutional review Board of New York University Medical Center, and informed consent had previously been obtained from all patients.

Clinical and laboratory assessments. All patients completed pain assessments by visual analog scale (VAS) and Western Ontario and McMaster Universities Osteoarthritis Index (WOMAC) (23) at baseline and every 6 months thereafter for the duration of the study. Pain questions were specific to the more painful knee (index knee). Blood samples from patients had been collected in serum collection tubes, and serum had been isolated within 60 minutes of collection. Serum samples were placed in aliquots and stored at −70°C until thawing for assessment of serum UA levels. Serum UA measurements were performed by the New York University Hospitals Clinical Laboratory and were determined by automated colorimetric assay using a Vitros analyzer (Ortho Clinical Diagnostics).

Radiographic and MRI measurements. All patients underwent weight-bearing, fixed-flexion posteroanterior knee radiography, which was performed in a standardized manner using a SynaFlexer radiographic positioning frame (Synarc), at baseline and at 24 months, as previously described (24). Beam position was optimized for the medial joint space compartment. The patient's index knee was evaluated radiographically with respect to both K/L grade and medial JSW, the latter measured at the mid-portion of the joint space using electronic calipers. Lateral joint space width was also assessed. JSN was calculated as the change in JSW (in millimeters) from baseline to the month 24 follow-up. All baseline radiographs were read and measured by 2 experienced musculoskeletal radiologists (LR and JB) who were blinded with regard to the patient's identity and clinical information. There was a high correlation between readers (kappa values for interrater agreement were 0.85 and 0.77 for the K/L scores in the right and left knees, respectively, and kappa scores for JSW were ≥0.93 for the medial compartments of both the right and left knees). Based on the high interreader correlations, a single reader (LR) was used for assessing the 24-month follow-up results.

A subset of patients enrolled in the parent study (n = 58) had undergone a dynamic gadolinium-enhanced 3.0T MRI of the index knee at baseline that was read for quantitative synovial volume. Of these patients, 27 met our additional requirements for the current study and were analyzed. The complete technical details of the MRI evaluation and the criteria for initial inclusion into the MRI assessment have been previously described (24). Briefly, the precontrast portion of the imaging protocol included a sagittal 3-dimensional (3-D) high-resolution T1-weighted fast low-angle shoot (FLASH) sequence with selective water excitation, as well as a sagittal T2-weighted fat-saturated spin-echo sequence. The postcontrast portion of the examination consisted of a dynamic gadolinium-enhanced 3-D T1-weighted FLASH sequence obtained in the sagittal plane. Assessment of the synovial volume was performed with MatLab custom tools for manual segmentation of the entire knee joint, using contrast-enhanced dynamic images of the knees in relation to the precontrast images obtained at baseline. Patterns of signal enhancement were evaluated in the infrapatellar and suprapatellar fat pads, in the intercondylar notch, and along the periphery of joint effusion. All MRIs were evaluated in a blinded manner by a single expert reader (RR).

Outcomes and analysis. Our primary objective was to determine whether baseline serum UA levels are associated with medial JSN over 2 years. Secondary outcomes included the

association of baseline serum UA levels with the baseline K/L grade, JSW, synovial volume on dynamic enhanced contrast MRI, and pain scores by VAS and WOMAC.

Statistical analysis. The relationships between baseline serum UA levels and clinical and demographic variables, including WOMAC pain, VAS pain, JSW, MRI-determined baseline synovial volume, age, and BMI, were determined by Pearson's correlation. Associations between serum UA and MRI-determined synovial volume were assessed by partial correlations, controlling for age, sex, and BMI. Given the limited number of patients in our analyses of MRI-determined synovial volume, this patient sample was assessed for normality in multiple ways. We confirmed a normal distribution on quantile–quantile plot, Lilliefors test ($P = 0.14$), and square root transforms of the data, applying Lilliefors ($P = 0.50$) and Shapiro-Wilk's ($P = 0.29$) tests. However, Shapiro-Wilk's test on untransformed data did not support normality ($P = 0.01$). Given that most, but not all, test results supported normality, MRI-determined synovial volume was interpreted as generally, but not strongly, normal in distribution.

The relationship between serum UA levels and binary baseline clinical and demographic variables, including diuretic intake and sex, were determined by Student's *t*-test. To analyze the relationship between serum UA and JSN, correlations were computed with and without controlling for age, sex, and BMI. Additionally, thresholds were chosen to examine the potential difference in JSN at different serum UA cut points (serum UA population median for the sample 5.85 mg/dl), ACR treatment target (6.0 mg/dl), and the solubility threshold for urate (6.8 mg/dl), as assessed by Student's *t*-test. One-way analysis of variance (ANOVA) was used to examine the potential differences in serum UA levels among patients defined as having no (JSN $\leq$0 mm), slow (0 $<$ JSN $<$ 0.5 mm), and fast (JSN $\geq$0.5 mm) progression of JSN. Post hoc Tukey-Kramer tests were used to assess pairwise comparisons when the omnibus test was significant. To determine the predictive value of serum UA for progression, receiver operating characteristic curves were constructed and areas under the curve (AUCs) computed (range 0–1, where 1 indicates perfect predictivity and 0.5 indicates random guessing). For these analyses, we defined nonprogression versus progression in the following 3 ways: 1) JSN $\leq$0 mm versus JSN $>$0 mm; 2) JSN $\leq$0 mm versus JSN $>$0.2 mm; and 3) JSN $\leq$0 mm versus JSN $>$0.5 mm. AUC values were compared against random models for significance using Delong's test. In addition, the relationship between the change in pain scores on the WOMAC and VAS measured at 24 months were correlated with serum UA levels to examine the potential relationship between serum UA levels and progression of pain.

RESULTS

Demographic characteristics. From among 146 completers of the original OA natural history study, 111 participants had medial disease at baseline. Of those, 88 had frozen serum of sufficient quantity to be enrolled in the current study. The demographic features of the enrolled patients are summarized in Table 1. Twenty-seven of the 88 patients had also undergone baseline dynamic contrast-enhanced MRI of the knee, with synovial volume measurements available for analysis. The demographic features and baseline synovial volumes in patients who enrolled in the original OA natural history study, but were lost to follow-up after the baseline assessment, were similar to those in our current study cohort (data not shown).

Table 1. Baseline demographic and clinical features of the 88 osteoarthritis patients*

Age, mean ± SEM years	61.26 ± 1.01
Sex, %	
Male	32.95
Female	67.05
BMI, mean ± SEM kg/m^2	26.86 ± 0.38
Serum UA, mean ± SEM mg/dl	6.30 ± 0.22
Synovial volume, mean ± SEM mm^3	15.49 ± 1.49
Joint space width, mean ± SEM mm	3.51 ± 0.15
K/L grade, % affected	
1	22.72
2	20.45
3	47.73
4	9.09

* Data on synovial volume were available for 27 patients. BMI = body mass index; UA = uric acid; K/L = Kellgren/Lawrence.

Relationship of serum UA levels to baseline OA severity and other characteristics. In an initial cross-sectional analysis, serum UA levels did not correlate with baseline WOMAC pain scores (r = 0.12, $P = 0.28$) or VAS pain scores (r = 0.08, $P = 0.48$). Consistent with a previous study (17), the serum UA levels also did not correlate with baseline OA severity measured as JSW (r = −0.15, $P = 0.15$) and K/L grade (F[3,84] = 1.82, $P = 0.15$). The ages of the patients, which ranged from 43 to 85 years, did not correlate with serum UA levels (r = 0.14, $P = 0.19$) in our cohort, despite reported associations in the literature. Consistent with previously published studies, serum UA levels significantly correlated with the BMI at study entry (r = 0.23, $P = 0.03$) and the mean serum UA levels in men were significantly higher than those in women (7.56 mg/dl versus 5.67 mg/dl; $P < 0.01$). There was no significant difference between baseline serum UA levels in the 8 patients taking a diuretic (all taking hydrochlorothiazide) and the patients not taking diuretics (6.10 mg/dl versus 6.32 mg/dl; $P = 0.63$). Serum UA levels correlated significantly (r = 0.44, $P < 0.01$) with MRI-determined baseline synovial volume on univariate analysis (Figure 1). However, the synovial volume did not correlate with the serum UA level after multivariate adjustment for age, sex, and BMI, with the loss of association driven by sex (r = 0.13, $P = 0.56$). Because synovial volume has been suggested as a potential marker of OA progression (25), we next examined the relationship between serum UA levels and medial JSN.

Serum UA levels and 24-month radiographic disease progression. Serum UA levels were significantly correlated with the progression of OA measured as the medial JSN at 24 months (r = 0.40, $P < 0.01$) (Figure 2A).

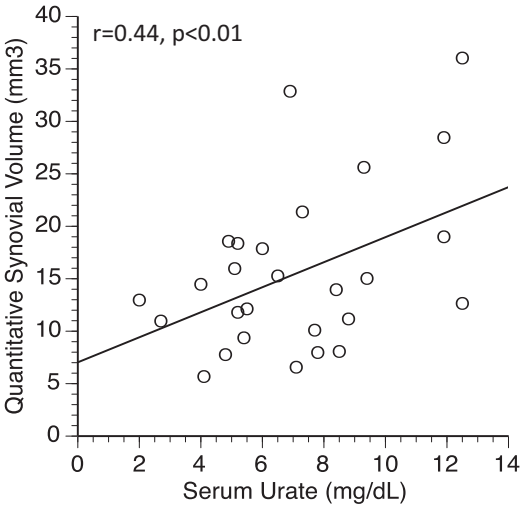

Figure 1. Pearson's correlation of baseline serum uric acid levels and quantitative synovial volume determined by contrast-enhanced magnetic resonance imaging.

This correlation was retained (r = 0.28, $P = 0.01$) after controlling for age, sex, and BMI. Analysis of the data according to quartiles revealed an apparent step-off in 24-month JSN between the second and third quartiles (Figure 2B). One-way ANOVA revealed an overall difference in mean JSN between the 4 quartiles (F[3,84] = 3.54, $P = 0.02$), with significant differences in mean JSN between quartiles 1 and 4 (0.24 mm versus 0.94 mm; $P = 0.04$) and between quartiles 2 and 4 (0.23 mm versus 0.94 mm; $P = 0.04$). We therefore assessed the difference in JSN by dichotomizing the data across 3 possibly relevant cut points: the median serum UA level in the study population (5.85 mg/dl), the ACR serum UA treatment target for urate-lowering therapy among gout patients (6.0 mg/dl), and the solubility threshold for urate (6.8 mg/dl). We observed significant differences in mean JSN across all 3 cut points. After adjustment for age, sex, and BMI, significance was retained only around the cut point of 6.8 mg/dl (Table 2).

We next stratified patients by radiographic progression and analyzed for differences in serum UA levels between groups. We defined nonprogressors as individuals who had JSN of ≤0 mm over 24 months, slow progressors as those with 0 mm < JSN of <0.5 mm over 24 months, and fast progressors as those with JSN of ≥0.5 mm over 24 months. We observed a significant difference in serum UA levels among the 3 progression groups (F[2,87] = 5.51, $P < 0.01$). Post hoc testing confirmed a significant difference between the mean serum UA levels in nonprogressors versus fast progressors (5.8 mg/dl versus 7.1 mg/dl; $P = 0.02$) and slow versus fast progressors (5.6 mg/dl versus 7.1 mg/dl; $P < 0.01$). In contrast, the difference between mean serum UA levels in nonprogressors versus slow progressors was not significant ($P = 0.69$). After controlling for age, sex, and BMI, one-way ANOVA continued to confirm an overall significant difference in serum UA among the 3 progression groups (F[2,87] = 3.64, $P = 0.03$), with borderline significance for the difference between the mean serum UA level in nonprogressors versus fast progressors and in slow progressors versus fast progressors ($P = 0.07$ and $P = 0.07$, respectively). The discrepancy between the omnibus and post hoc test results was likely due to the greater statistical power of the omnibus test. As was the case for pain at baseline, the serum UA level did not correlate with the change in scores for the WOMAC pain (r = 0.05, $P = 0.68$) or VAS pain (r = −0.04, $P = 0.72$) over 24 months.

Additionally, we defined a range of JSN thresholds (according to the degree of 24-month JSN) as outcomes and used these to generate AUC curves and to determine

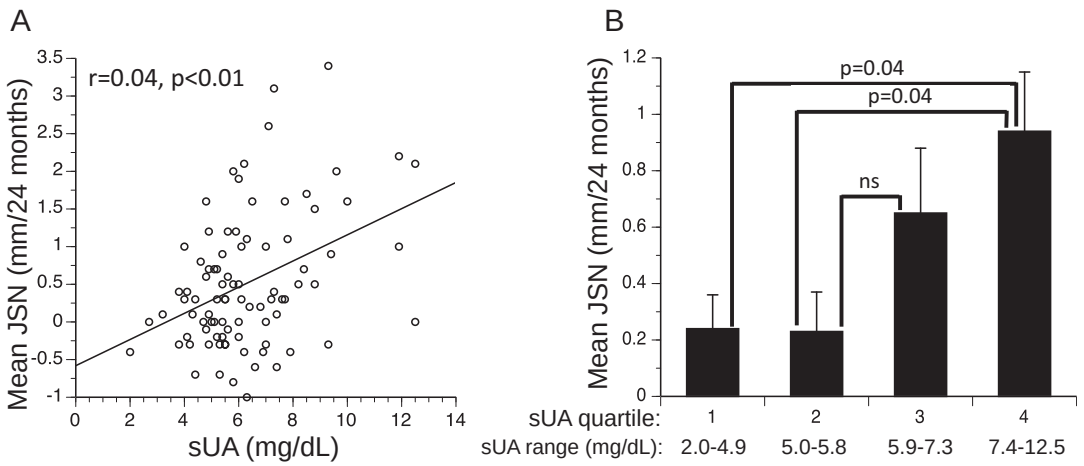

Figure 2. Association of baseline serum uric acid (sUA) levels with joint space narrowing (JSN) at 24 months, as shown by **A,** Pearson's correlation (scatterplot), and **B,** quartile groups, with designated serum UA ranges. Values are the mean ± SEM.

Table 2. Mean differences in JSN over 24 months, categorized by serum uric acid cut point*

	Mean JSW at study entry, mm			Mean JSN over 24 months, mm			
Serum uric acid cut point	Below cut point	Above cut point	*P*	Below cut point	Above cut point	*P*	P_{adj}†
5.85 mg/dl	3.67	3.41	0.39	0.24	0.79	<0.01	0.06
6.0 mg/dl	3.74	3.33	0.16	0.26	0.78	<0.01	0.09
6.8 mg/dl	3.74	3.15	0.04	0.31	0.90	<0.01	<0.01

* JSN = joint space narrowing; JSW = joint space width.
† Adjusted *P* (P_{adj}) for age, sex, and body mass index.

the capacity of the serum UA level to predict 24-month radiographic knee OA progression. For this analysis, nonprogressors were defined as JSN ≤0.0 mm; progressor thresholds were JSN of >0.0 mm, >0.2 mm, and >0.5 mm after 24 months. Baseline serum UA distinguished nonprogressors in all 3 categories of progression (AUC 0.62, $P = 0.03$; AUC 0.64, $P = 0.01$; and AUC 0.68, $P < 0.01$ for JSN >0.0 mm, >0.2 mm, and >0.5 mm, respectively). After inclusion of age, sex, and BMI in the model, serum UA levels continued to significantly distinguish nonprogressors from progressors, with JSN >0.2 mm (AUC 0.63, $P = 0.03$) and >0.5 mm (AUC 0.62, $P = 0.05$) over 24 months (Table 3).

Exclusion of joint-widening artifacts. A minority of our patients experienced apparent widening of the medial compartment during the 2-year observation period. Although many investigators have ascribed such phenomena to a normal distribution within the measuring process (26,27), there are several reasons such widening might occur. Positioning errors or changes in weight bearing during imaging could hinder accurate joint space measurement. In our study, these sources of errors were mitigated through the use of standardized, fixed-flexion, weight-bearing imaging using a SynaFlexer device, which has been used in numerous other studies, including those of the Osteoarthritis Initiative (5,7,24,28). Additionally, in some cases, medial compartment widening can reflect mechanical shifts resulting from lateral compartment narrowing. This phenomenon, referred to as pseudowidening, could therefore reflect OA progression in the lateral compartment (29,30) rather than any actual medial change. To assess for possible pseudowidening, we first determined the degree of lateral compartment change in patients with medial compartment widening versus those with medial compartment narrowing. We observed no significant difference in the lateral compartment change between these 2 groups (lateral JSN for those with medial compartment narrowing versus those with medial compartment widening 0.16 mm versus 0.16 mm, $P = 1.00$).

To further examine the possibility that lateral compartment narrowing could have affected our medial compartment observations, we reanalyzed our data after first excluding all patients with both medial joint space widening (any degree) and substantial lateral compartment narrowing (≥0.5 mm over 2 years). In this analysis, 9 patients were excluded, leaving 79 patients for medial compartment assessments (Supplementary Table 1, available on the *Arthritis & Rheumatology* web site at http://onlinelibrary.wiley.com/doi/10.1002/art.40069/abstract). We continued to observe a direct correlation between serum urate and

Table 3. Determination of the capacity of serum UA to predict 24-month radiographic knee OA progression, by JSN progression group*

Comparison group, model	No. of progressors	AUC (95% CI)	*P*
Any progressor (JSN >0.0 mm)			
Serum UA	56	0.62 (0.50–0.75)	0.03
Serum UA + age, sex, and BMI	56	0.56 (0.43–0.69)	0.17
Moderate-to-fast progressors (JSN >0.2 mm)			
Serum UA	50	0.64 (0.52–0.77)	0.01
Serum UA + age, sex, and BMI	50	0.63 (0.50–0.75)	0.03
Fast progressors (JSN >0.5 mm)			
Serum UA	33	0.68 (0.54–0.81)	0.01
Serum UA + age, sex, and BMI	33	0.62 (0.48–0.76)	0.05

* To determine the value of serum uric acid (UA) for predicting the progression of knee osteoarthritis (OA), receiver operating characteristic curves were constructed and areas under the curve (AUCs) with 95% confidence intervals (95% CIs) were computed. All comparisons are versus nonprogressors (joint space narrowing [JSN] of ≤0 mm). BMI = body mass index.

medial JSN ($r = 0.43$, $P = 0.01$), as well as an apparent serum UA step-off for medial JSN progression in the range of 6.0–6.8 mg/dl (Supplementary Figures 1A and B, available at http://onlinelibrary.wiley.com/doi/10.1002/art.40069/abstract). Specified serum UA cut points (Supplementary Table 2, available at http://onlinelibrary.wiley.com/doi/10.1002/art.40069/abstract) and AUC analyses also remained significant (Supplemental Table 3, available at http://onlinelibrary.wiley.com/doi/10.1002/art.40069/abstract), even after adjustment for other potential confounders. Moreover, exclusion of the above-specified patients from the MRI synovial volume assessments resulted in improved correlation of serum UA levels with synovial volume (Supplementary Figure 2, available at http://onlinelibrary.wiley.com/doi/10.1002/art.40069/abstract) ($r = 0.54$, $P < 0.01$).

DISCUSSION

To our knowledge, these results are the first to suggest that current baseline serum UA levels predict future progression of knee OA. Increased serum UA levels were associated with increased JSN, a widely used, Food and Drug Administration–endorsed marker of OA progression (31,32), in both univariate and multivariate analyses. Subjects with serum UA levels ≥6.8 mg/dl had significantly higher JSN at 24 months than did patients with serum UA levels of <6.8 mg/dl (33). Synovial tissue proliferation, as measured using gadolinium-enhanced MRI, also correlated with serum UA levels, although this correlation did not persist after multivariate analysis. This latter observation is consistent with reports that synovial volume correlates with radiographic OA (24) and that MRI-detected synovitis may be a risk factor for OA incidence and progression (34–36). In contrast to several previous studies (37,38), the synovial volume did not correlate with OA pain in our study (data not shown), possibly because our MRI protocol involved global synovial examination, whereas pain has been most closely correlated with peripatellar synovitis (39,40). Finally, baseline serum UA levels distinguished both the mild progressors with JSN of >0.2 mm over 24 months and the fast progressors with JSN of >0.5 mm over 24 months from the nonprogressors through AUC analyses.

The observed association between serum UA levels and JSN could reflect a causal relationship, with secondarily elevated synovial fluid urate levels promoting cartilage damage, as synovial fluid is largely an ultrafiltrate of serum (17). Chondrocytes express plasma membrane urate transporters, indicating that they can take up soluble urate with a potential for an intracellular pro-oxidant effect (41). Alternatively, synovial fluid urate could act in its crystallized rather than soluble form. Indeed, our observation that an increased risk of JSN was best dichotomized around a serum UA level of 6.8 mg/dl (the saturation point for urate crystallization) supports a model in which MSU crystals promote synovitis (19,42,43) and cartilage disruption. Consistent with this possibility, UA has been shown to deposit on cartilage in patients with hyperuricemia who do not have gout (44), and Martinon and others (41,45) have demonstrated the ability of MSU crystals to activate the NLRP3 inflammasome and drive the generation of IL-1β, a major candidate cytokine in OA progression. Alternatively, OA progression could be accelerated intrinsically by chondrocyte death in a forward-feedback, UA-dependent cycle (17,46–48). As reported by Shi et al (47), dying cells locally generate UA that, at concentrations sufficient to permit MSU crystallization, act as a danger signal to activate neighbor cell inflammatory responses. Although it is unlikely that chondrocyte death locally in an OA joint could be sufficient to increase systemic serum UA levels, it is possible that elevated serum and resultant synovial fluid UA concentrations create an environment in which chondrocyte death raises pericellular local UA concentrations sufficient to support MSU precipitation.

Finally, it is possible that the relationship between serum UA levels and OA progression is not causal, but instead, is due to a common predisposing factor(s). Given concerns for confounding, we controlled for age, sex, and BMI, and the correlation between JSN and serum UA levels persisted, revealing no significant effect of these factors. However, serum UA levels could predict progression of OA in a noncausative manner, reflecting processes that are not at present fully appreciated and therefore were not adjusted for in our model. It is worth noting that while our AUC analyses support an association between the serum UA level and OA progression, thus making it a candidate biomarker for progression, exploration of the efficacy of the serum UA level as a biomarker in the clinical setting would additionally require evaluation of its sensitivity and specificity tradeoff. Nevertheless, the AUC values we observed are consistent with those of other recently reported serum biomarkers of knee OA progression (5,49).

Strengths of our study include the use of a clinical laboratory for measuring serum UA levels in a standardized manner, the standardized acquisition of radiographs using the SynaFlexer positioning frame, the blinding of radiologists reading the radiographs for JSW and the MRI-based synovial volume, and a follow-up time of 2 years. Our cohort was also mostly community-based and likely representative of patients with knee OA in the general population.

Limitations of our study are that our population was restricted to patients with knee OA, a BMI of <33 kg/m^2, and no gout, and the results may therefore not be generalizable to patients with knee OA without these features.

In contrast to JSN over 24 months, we observed no correlation between serum UA levels and JSW at study entry; however, our study did not set strict entry criteria on the duration of disease prior to the study, and the limitations of our data do not permit us to extrapolate in order to ascertain the rate of OA progression before study entry. We note, moreover, that analyses around the serum UA cut point of 6.8 mg/dl indicated that patients with supersaturated serum UA levels may have had significantly reduced JSW at entry (Table 2).

We did not measure all factors associated with OA progression, such as meniscal pathology or malalignment. We clinically determined the absence of gout and did not perform knee aspirations to confirm the absence of crystals. We included patients with symptoms and baseline K/L scores of ≥1, instead of the more conventionally defined K/L score ≥2 for defining OA, because a K/L score of 1 has recently been described as representing early OA (50). Finally, our study, especially the subset of patients undergoing MRI, would have benefited from a larger sample size. Indeed, our data set for MRI analysis was normally distributed according to most, but not all, of the tests we applied. Prospective studies and greater sample sizes will be needed to assess the possibility of causality.

In conclusion, this is the first longitudinal study to report that serum UA levels may serve as a biomarker of OA progression. As serum UA measurements are inexpensive and readily obtainable, such results have the potential to affect the study of OA treatment by permitting the identification of patients who are more likely to experience progression for inclusion in investigational studies. Measurement of serum UA levels could also potentially provide a mechanism for determining the risk of progression and could facilitate monitoring the treatment of patients living with OA. Whether UA-lowering therapy could potentially help limit OA progression also deserves investigation.

ACKNOWLEDGMENTS

The authors thank Chio Yokose, Aaron Garza, and Rochelle Yates.

AUTHOR CONTRIBUTIONS

All authors were involved in drafting the article or revising it critically for important intellectual content, and all authors approved the final version to be published. Dr. Krasnokutsky had full access to all of the data in the study and takes responsibility for the integrity of the data and the accuracy of the data analysis.

Study conception and design. Krasnokutsky, Attur, Abramson, Pillinger.

Acquisition of data. Krasnokutsky, Oshinsky, Attur, Patel, Samuels, Regatte, Bencardino, Rybak, Abramson, Pillinger.

Analysis and interpretation of data. Krasnokutsky, Oshinsky, Attur, Ma, Zhou, Zheng, Chen, Patel, Samuels, Pike, Regatte, Bencardino, Rybak, Abramson, Pillinger.

REFERENCES

1. Liu-Bryan R, Terkeltaub R. Emerging regulators of the inflammatory process in osteoarthritis. Nat Rev Rheumatol 2015;11:35–44.
2. Sellam J, Berenbaum F. The role of synovitis in pathophysiology and clinical symptoms of osteoarthritis. Nat Rev Rheumatol 2010;6:625–35.
3. Benito MJ, Veale DJ, FitzGerald O, van den Berg WB, Bresnihan B. Synovial tissue inflammation in early and late osteoarthritis. Ann Rheum Dis 2005;64:1263–7.
4. D'Agostino MA, Conaghan P, Le Bars M, Baron G, Grassi W, Martin-Mola E, et al. EULAR report on the use of ultrasonography in painful knee osteoarthritis. Part 1. Prevalence of inflammation in osteoarthritis. Ann Rheum Dis 2005;64:1703–9.
5. Attur M, Krasnokutsky S, Statnikov A, Samuels J, Li Z, Friese O, et al. Low-grade inflammation in symptomatic knee osteoarthritis: prognostic value of inflammatory plasma lipids and peripheral blood leukocyte biomarkers. Arthritis Rheumatol 2015;67:2905–15.
6. Attur M, Krasnokutsky-Samuels S, Samuels J, Abramson SB. Prognostic biomarkers in osteoarthritis. Curr Opin Rheumatol 2013;25:136–44.
7. Attur M, Belitskaya-Levy I, Oh C, Krasnokutsky S, Greenberg J, Samuels J, et al. Increased interleukin-1β gene expression in peripheral blood leukocytes is associated with increased pain and predicts risk for progression of symptomatic knee osteoarthritis. Arthritis Rheum 2011;63:1908–17.
8. Attur M, Statnikov A, Samuels J, Li Z, Alekseyenko AV, Greenberg JD, et al. Plasma levels of interleukin-1 receptor antagonist (IL1Ra) predict radiographic progression of symptomatic knee osteoarthritis. Osteoarthritis Cartilage 2015;23:1915–24.
9. Johnson RJ, Kang DH, Feig D, Kivlighn S, Kanellis J, Watanabe S, et al. Is there a pathogenetic role for uric acid in hypertension and cardiovascular and renal disease? Hypertension 2003;41:1183–90.
10. Leyva F, Anker SD, Godsland IF, Teixeira M, Hellewell PG, Kox WJ, et al. Uric acid in chronic heart failure: a marker of chronic inflammation. Eur Heart J 1998;19:1814–22.
11. Shi Y, Evans JE, Rock K/L. Molecular identification of a danger signal that alerts the immune system to dying cells. Nature 2003;425:516–21.
12. Dalbeth N, Haskard DO. Mechanisms of inflammation in gout. Rheumatology (Oxford) 2005;44:1090–6.
13. Choi HK, Mount DB, Reginato AM. Pathogenesis of gout. Ann Intern Med 2005;143:499–516.
14. Yokose C, Chen M, Berhanu A, Pillinger MH, Krasnokutsky S. Gout and osteoarthritis: associations, pathophysiology, and therapeutic implications. Curr Rheumatol Rep 2016;18:65.
15. Acheson RM, Collart AB. New Haven survey of joint diseases. XVII. Relationship between some systemic characteristics and osteoarthrosis in a general population. Ann Rheum Dis 1975;34:379–87.
16. Roddy E, Zhang W, Doherty M. Are joints affected by gout also affected by osteoarthritis? Ann Rheum Dis 2007;66:1374–7.
17. Denoble AE, Huffman KM, Stabler TV, Kelly SJ, Hershfield MS, McDaniel GE, et al. Uric acid is a danger signal of increasing risk

for osteoarthritis through inflammasome activation. Proc Natl Acad Sci U S A 2011;108:2088–93.
18. Stabler TV, Heinrichs A, McDaniel G, et al. Synovial fluid uric acid as a marker of joint tissue degradation in osteoarthritis [abstract]. Osteoarthritis Cartilage 2009;17:S69–70.
19. Howard RG, Samuels J, Gyftopoulos S, Krasnokutsky S, Leung J, Swearingen CJ, et al. Presence of gout is associated with increased prevalence and severity of knee osteoarthritis among older men: results of a pilot study. J Clin Rheumatol 2015;21: 63–71.
20. Altman R, Asch E, Bloch D, Bole G, Borenstein D, Brandt K, et al. Development of criteria for the classification and reporting of osteoarthritis: classification of osteoarthritis of the knee. Arthritis Rheum 1986;29:1039–49.
21. Kellgren JH, Lawrence JS. Radiological assessment of osteo-arthrosis. Ann Rheum Dis 1957;16:494–502.
22. Hunter DJ, Altman RD, Cicuttini F, Crema MD, Duryea J, Eckstein F, et al. OARSI clinical trials recommendations: knee imaging in clinical trials in osteoarthritis. Osteoarthritis Cartilage 2015;23:698–715.
23. Bellamy N, Buchanan WW, Goldsmith CH, Campbell J, Stitt LW. Validation study of WOMAC: a health status instrument for measuring clinically important patient relevant outcomes to antirheumatic drug therapy in patients with osteoarthritis of the hip or knee. J Rheumatol 1988;15:1833–40.
24. Krasnokutsky S, Belitskaya-Levy I, Bencardino J, Samuels J, Attur M, Regatte R, et al. Quantitative magnetic resonance imaging evidence of synovial proliferation is associated with radiographic severity of knee osteoarthritis. Arthritis Rheum 2011;63:2983–91.
25. Atukorala I, Kwoh CK, Guermazi A, Roemer FW, Boudreau RM, Hannon MJ, et al. Synovitis in knee osteoarthritis: a precursor of disease? Ann Rheum Dis 2016;75:390–5.
26. Bingham CO III, Buckland-Wright JC, Garnero P, Cohen SB, Dougados M, Adami S, et al. Risedronate decreases biochemical markers of cartilage degradation but does not decrease symptoms or slow radiographic progression in patients with medial compartment osteoarthritis of the knee: results of the two-year multinational knee osteoarthritis structural arthritis study. Arthritis Rheum 2006;54:3494–507.
27. Bartlett SJ, Ling SM, Mayo NE, Scott SC, Bingham CO III. Identifying common trajectories of joint space narrowing over two years in knee osteoarthritis. Arthritis Care Res (Hoboken) 2011;63:1722–8.
28. Nevitt MC, Felson DT, Lester G. The Osteoarthritis Initiative: protocol for the cohort study. University of California, San Francisco (data coordinating center); 2006. URL: http://oai.epi-ucsf.org/datarelease/docs/StudyDesignProtocol.pdf.
29. Guermazi A, Roemer FW, Hayashi D. Imaging of osteoarthritis: update from a radiological perspective. Curr Opin Rheumatol 2011;23:484–91.
30. Wirth W, Duryea J, Hellio Le Graverand MP, John MR, Nevitt M, Buck RJ, et al. Direct comparison of fixed flexion, radiography and MRI in knee osteoarthritis: responsiveness data from the Osteoarthritis Initiative. Osteoarthritis Cartilage 2013;21: 117–25.
31. Emrani PS, Katz JN, Kessler CL, Reichmann WM, Wright EA, McAlindon TE, et al. Joint space narrowing and Kellgren-Lawrence progression in knee osteoarthritis: an analytic literature synthesis. Osteoarthritis Cartilage 2008;16:873–82.
32. Ravaud P, Giraudeau B, Auleley GR, Chastang C, Poiraudeau S, Ayral X, et al. Radiographic assessment of knee osteoarthritis: reproducibility and sensitivity to change. J Rheumatol 1996;23: 1756–64.
33. Khanna D, Fitzgerald JD, Khanna PP, Bae S, Singh MK, Neogi T, et al. 2012 American College of Rheumatology guidelines for management of gout. Part 1. Systematic nonpharmacologic and pharmacologic therapeutic approaches to hyperuricemia. Arthritis Care Res (Hoboken) 2012;64:1431–46.
34. Felson DT, Niu J, Neogi T, Goggins J, Nevitt MC, Roemer F, et al. Synovitis and the risk of knee osteoarthritis: the MOST Study. Osteoarthritis Cartilage 2016;24:458–64.
35. Roemer FW, Kwoh CK, Hannon MJ, Hunter DJ, Eckstein F, Fujii T, et al. What comes first? Multitissue involvement leading to radiographic osteoarthritis: magnetic resonance imaging–based trajectory analysis over four years in the osteoarthritis initiative. Arthritis Rheumatol 2015;67:2085–96.
36. Attur M, Samuels J, Krasnokutsky S, Abramson SB. Targeting the synovial tissue for treating osteoarthritis (OA): where is the evidence? Best Pract Res Clin Rheumatol 2010;24:71–9.
37. Kaukinen P, Podlipska J, Guermazi A, Niinimaki J, Lehenkari P, Roemer FW, et al. Associations between MRI-defined structural pathology and generalized and localized knee pain: the Oulu Knee Osteoarthritis study. Osteoarthritis Cartilage 2016;24: 1565–76.
38. Neogi T, Guermazi A, Roemer F, Nevitt MC, Scholz J, Arendt-Nielsen L, et al. Association of joint inflammation with pain sensitization in knee osteoarthritis: the multicenter osteoarthritis study. Arthritis Rheumatol 2016;68:654–61.
39. De Lange-Brokaar BJ, Ioan-Facsinay A, Yusuf E, Visser AW, Kroon HM, van Osch GJ, et al. Association of pain in knee osteoarthritis with distinct patterns of synovitis. Arthritis Rheumatol 2015;67:733–40.
40. Riis RG, Gudbergsen H, Henriksen M, Ballegaard C, Bandak E, Rottger D, et al. Synovitis assessed on static and dynamic contrast-enhanced magnetic resonance imaging and its association with pain in knee osteoarthritis: a cross-sectional study. Eur J Radiol 2016;85:1099–108.
41. Mobasheri A, Neama G, Bell S, Richardson S, Carter SD. Human articular chondrocytes express three facilitative glucose transporter isoforms: GLUT1, GLUT3 and GLUT9. Cell Biol Int 2002;26:297–300.
42. Agudelo CA, Schumacher HR. The synovitis of acute gouty arthritis: a light and electron microscopic study. Hum Pathol 1973;4:265–79.
43. Nowatzky J, Howard R, Pillinger MH, Krasnokutsky S. The role of uric acid and other crystals in osteoarthritis. Curr Rheumatol Rep 2010;12:142–8.
44. Howard RG, Pillinger MH, Gyftopoulos S, Thiele RG, Swearingen CJ, Samuels J. Reproducibility of musculoskeletal ultrasound for determining monosodium urate deposition: concordance between readers. Arthritis Care Res (Hoboken) 2011;63:1456–62.
45. Martinon F, Petrilli V, Mayor A, Tardivel A, Tschopp J. Gout-associated uric acid crystals activate the NALP3 inflammasome. Nature 2006;440:237–41.
46. Kono H, Chen CJ, Ontiveros F, Rock K/L. Uric acid promotes an acute inflammatory response to sterile cell death in mice. J Clin Invest 2010;120:1939–49.
47. Shi Y. Caught red-handed: uric acid is an agent of inflammation. J Clin Invest 2010;120:1809–11.
48. McQueen FM, Chhana A, Dalbeth N. Mechanisms of joint damage in gout: evidence from cellular and imaging studies. Nat Rev Rheumatol 2012;8:173–81.
49. Kraus VB, Collins JE, Hargrove D, Losina E, Nevitt M, Katz JN, et al. Predictive validity of biochemical biomarkers in knee osteoarthritis: data from the FNIH OA Biomarkers Consortium. Ann Rheum Dis 2017;76:186–95.
50. De Klerk BM, Willemsen S, Schiphof D, van Meurs JB, Koes BW, Hofman A, et al. Development of radiological knee osteoarthritis in patients with knee complaints. Ann Rheum Dis 2012; 71:905–10.

ARTHRITIS & RHEUMATOLOGY
Vol. 69, No. 6, June 2017, pp 1221–1232
DOI 10.1002/art.40056

Profibrotic Infrapatellar Fat Pad Remodeling Without M1 Macrophage Polarization Precedes Knee Osteoarthritis in Mice With Diet-Induced Obesity

Erika Barboza,[1] Joanna Hudson,[1] Wan-Pin Chang,[1] Susan Kovats,[1] Rheal A. Towner,[1] Robert Silasi-Mansat,[1] Florea Lupu,[1] Collin Kent,[1] and Timothy M. Griffin[2]

Objective. **To test the hypothesis that high-fat (HF) diet–induced obesity increases proinflammatory cytokine expression, macrophage infiltration, and M1 polarization in the infrapatellar fat pad (IFP) prior to knee cartilage degeneration.**

Methods. **We characterized the effect of HF feeding on knee OA pathology, body adiposity, and glucose intolerance in male C57BL/6J mice and identified a diet duration that induces metabolic dysfunction prior to cartilage degeneration. Magnetic resonance imaging and histomorphology were used to quantify changes in the epididymal, subcutaneous, and infrapatellar fat pads and in adipocyte sizes. Finally, we used targeted gene expression and protein arrays, immunohistochemistry, and flow cytometry to quantify differences in fat pad markers of inflammation and immune cell populations.**

Results. **Twenty weeks of feeding with an HF diet induced marked obesity, glucose intolerance, and early osteoarthritis (OA), including osteophytes and cartilage tidemark duplication. This duration of HF feeding increased the IFP volume. However, it did not increase IFP inflammation, macrophage infiltration, or M1 macrophage polarization as observed in epididymal fat. Furthermore, leptin protein levels were reduced. This protection from obesity-induced inflammation corresponded to increased IFP fibrosis and the absence of adipocyte hypertrophy.**

Conclusion. **The IFP does not recapitulate classic abdominal adipose tissue inflammation during the early stages of knee OA in an HF diet–induced model of obesity. Consequently, these findings do not support the hypothesis that IFP inflammation is an initiating factor of obesity-induced knee OA. Furthermore, the profibrotic and antihypertrophic responses of IFP adipocytes to HF feeding suggest that intraarticular adipocytes are subject to distinct spatiotemporal structural and metabolic regulation among fat pads.**

Obesity significantly increases the risk of osteoarthritis (OA) (1,2), and clinical and preclinical studies support a role of both biomechanical and inflammatory factors in the pathogenesis of OA (3). OA involves a mosaic pattern of altered systemic and local inflammation (4,5). For example, circulating markers of inflammation can indicate the presence of symptomatic knee OA that is at risk of progression (6). Locally, cytokines and chemokines are elevated in the synovium, cartilage, meniscus, and synovial fluid (7–10). Innate mediators of inflammation drive many facets of obesity-induced metabolic dysfunction, providing a potential link to OA pathogenesis (11–13). Recent studies have shown that activated synovial macrophages are present in at least some OA joints (14–16), and there is mounting evidence that innate inflammatory networks, such as those involving

The contents of this article are solely the responsibility of the authors and do not necessarily represent the official views of the National Institutes of Health or the Arthritis Foundation.

Supported by the NIH (National Center for Research Resources grant P20-RR-018758 and National Institute of General Medical Sciences grant P20-GM-103441 to Drs. Griffin, Towner, and Lupu, and National Institute of Arthritis and Musculoskeletal and Skin Diseases grant R03-AR-066828 to Dr. Griffin) and the Arthritis Foundation (Arthritis Investigator Award to Dr. Griffin).

[1]Erika Barboza, PhD, Joanna Hudson, BS, Wan-Pin Chang, PhD, Susan Kovats, PhD, Rheal A. Towner, PhD, Robert Silasi-Mansat, PhD, Florea Lupu, PhD, Collin Kent, BS: Oklahoma Medical Research Foundation, Oklahoma City; [2]Timothy M. Griffin, PhD: Oklahoma Medical Research Foundation, Reynolds Oklahoma Center on Aging, and University of Oklahoma Health Sciences Center, Oklahoma City.

Address correspondence to Timothy M. Griffin, PhD, Aging and Metabolism Research Program, Oklahoma Medical Research Foundation, MS 21, 825 NE 13th Street, Oklahoma City, OK 73104. E-mail: Tim-Griffin@omrf.org.

Submitted for publication October 19, 2016; accepted in revised form January 24, 2017.

complement and alarmins, are critical mediators of OA progression and pain (17).

Understanding how metabolic inflammation contributes to OA risk is challenging because obesity triggers systemic and tissue-specific cellular immune responses, particularly within adipose tissue. We previously reported that knee OA develops in proportion to total body fat and the adipokine leptin, but not other cytokines, in mice with high-fat (HF) diet–induced obesity (18). In humans, leptin is elevated in synovial fluid relative to serum, indicating the potential for local metabolic inflammation (19). In a comparison of patient-matched infrapatellar and subcutaneous fat, the infrapatellar fat pad (IFP) was shown to secrete higher levels of adiponectin, adipsin, interleukin-6 (IL-6), tumor necrosis factor (TNF), and visfatin per tissue weight (20,21). Clinical imaging studies also support a role of the IFP in OA, linking changes in IFP size or magnetic resonance signal intensity to changes in OA symptoms and to structural pathology (22,23). However, most evidence of IFP inflammation is based on samples collected from patients undergoing total joint arthroplasty (24). Therefore, we wanted to understand the effect of obesity on IFP inflammation during the initiation of knee OA.

Macrophages are central mediators of adipose tissue inflammation (25). Resident adipose tissue macrophages suppress inflammation similar to alternatively activated M2 macrophages. Obesity stimulates chemokine-mediated macrophage infiltration and proinflammatory (M1) polarization, particularly in abdominal fat. Given the proinflammatory phenotype of the IFP in OA joints, we hypothesized that obesity increases knee OA by inducing IFP macrophage infiltration, M1 polarization, and proinflammatory cytokine production prior to the development of cartilage degeneration. Previous findings in humans with OA characterized IFP macrophages as primarily M2 regardless of obesity status (26). However, M2-like macrophages are prevalent during wound healing; consequently, the inflammatory characteristics at the end stage of OA may greatly differ from those at the onset of disease. Therefore, we evaluated IFP inflammation and macrophage polarization markers prior to the onset of cartilage damage.

We tested our hypothesis using a widely studied HF diet–induced mouse model of obesity in mice obtained from The Jackson Laboratory. We first characterized the temporal effects of HF feeding on knee OA pathology, body adiposity, and glucose tolerance to identify a diet duration that induces metabolic dysfunction prior to cartilage degeneration. We then used magnetic resonance imaging (MRI) and histomorphology to quantify changes in the size of the epididymal fat pad (EFP), the subcutaneous fat pad (SFP), and the IFP and corresponding changes in adipocyte size. Finally, we conducted quantitative gene expression profiling, immunohistochemistry, and flow cytometry to characterize differences in markers of inflammation and cell types among the different fat pads and in response to an HF diet.

MATERIALS AND METHODS

Animals. Experiments were conducted in accordance with protocols approved by the AAALAC International–accredited Institutional Animal Care and Use Committee at the Oklahoma Medical Research Foundation (OMRF). Male C57BL/6J mice were purchased from the JAX Diet-Induced Obesity (DIO) service (The Jackson Laboratory), which randomizes mice to receive diets containing either 10% kcal of fat (control; D12450Bi) or 60% kcal of fat (HF; D12492i) beginning at 6 weeks of age (Research Diets). DIO animals were purchased at 24 weeks of age and maintained on the same diets in the OMRF vivarium (specific pathogen–free facility) until experimental end points at 26 and 52 weeks of age. Mice were group-housed ($\leq$5 animals/cage) in ventilated cages in a temperature-controlled room with 12-hour light/dark cycles and with ad libitum access to food and water and routine veterinary assessment. Multiple cohorts of animals were purchased from the JAX DIO service to complete all experiments (Supplementary Table 1, available on the *Arthritis & Rheumatology* web site at http://onlinelibrary.wiley.com/doi/10.1002/art.40056/abstract). Sample sizes for specific experiments are given below.

Body composition, fat pad volume, and glucose analyses. Body fat content (excluding the head) was measured under isoflurane anesthesia using a dual-energy x-ray absorptiometry system (Piximus II; GE Lunar) at 24 and 50 weeks of age (27). Infrapatellar, subcutaneous, and peritoneal fat pad volumes were measured in 24-week-old animals receiving control and HF diets using water-suppressed MRI, as previously described (28). Intraperitoneal glucose tolerance tests were performed in mice subjected to overnight fasting ~1 week prior to euthanasia, as previously described (29).

Histologic and immunohistochemical analyses. Animals were euthanized by CO_2 asphyxiation, alternating between groups. Intact knees were isolated, processed, and stained with hematoxylin, fast green, and Safranin O for histologic grading, as described previously (18,30). Modified Mankin OA scoring was conducted by 2 experienced graders under blinded conditions, assessing 4 locations: lateral femur, lateral tibia, medial femur, and medial tibia. Osteophyte severity along the anterior and posterior margins of the medial and lateral tibial plateaus was quantified using a 0–3 grading system for each region, as previously described (31).

EFPs, SFPs (femoroinguinal), and IFPs were harvested following death and stabilized in Zamboni's fixative prior to paraffin processing. Sections (6 μm) were collected at 48-μm intervals for the EFPs and SFPs and continuously for the IFPs. For adipocyte analyses, 2 slides per sample were stained with hematoxylin and eosin. Two images per slide were captured using a Nikon E200 microscope equipped with a DS-Fi1 digital camera. Adipocytes intersecting a digital grid overlay were

manually traced to calculate the average adipocyte area per sample using NIS Elements software (Nikon). For macrophage quantification, 3 slides per fat pad per animal were prepared for F4/80 staining. Slides underwent antigen retrieval (0.05% proteinase K), nonspecific blocking (5% normal donkey serum in phosphate buffered saline [PBS] at 0.1% Triton X), and incubation with rat anti-mouse F4/80 monoclonal antibody (1:100 dilution; Invitrogen catalog no. MF48000) for 1 hour at room temperature. Slides were washed and stained with Cy3 secondary antibody (Jackson ImmunoResearch) and Hoechst for visualization and quantitation by fluorescence microscopy using a Nikon Eclipse 80i microscope, an X-cite 120Q light source, and a DS-Qi1Mc camera. Primary antibody was omitted for negative controls.

Fat pad fibrosis was evaluated by sirius red staining. Slides were stained in saturated picric acid with 0.1% sirius red F3B (VWR), washed in 0.5% acetic acid, and counterstained with 0.5% Harris' hematoxylin (VWR). Slides were examined under epipolarized ultraviolet light with a Nikon E800 microscope equipped with an Omax 14 MP digital camera and Omax ToupView acquisition software. Three 10× images per sample were selected for quantification with ImageJ software (version 1.49o; National Institutes of Health) using the color deconvolution 2 plugin to generate a threshold-based binary image of the epifluorescent signal. Fibrosis was quantified as the area of epifluorescent signal within a central 1,400-pixel–diameter region of interest free of tissue artifact or vasculature.

RNA and protein extraction. Extracted fat pad samples were immediately placed in TRIzol reagent (Ambion) on ice and stored at −80°C until homogenization. Although it was not possible to isolate the IFP from the immediate underlying synovium, IFP samples were carefully dissected under a stereomicroscope using McPherson-Vannas scissors and fine forceps to minimize the inclusion of adjacent synovium and other connective joint tissues. To obtain sufficient messenger RNA (mRNA), IFPs from both knees were pooled for 2 animals per analysis sample. EFP and SFP mRNA samples were pooled for the same animal pairs to facilitate comparisons among fat pads. The mRNA and protein were isolated according to the manufacturer's protocol, and mRNA was purified using RNeasy Mini (IFP) and RNeasy Micro (SFP and EFP) kits (Qiagen).

Quantitative reverse transcription–polymerase chain reaction (RT-PCR) and protein array analyses. Gene expression was measured using RT^2 Profiler PCR inflammatory cytokine and receptors (PAMM-011D) and extracellular matrix and adhesion molecules (PAMM-013D) mouse arrays (Qiagen) according to the manufacturer's protocols. A total of 200 ng of mRNA per array was synthesized into complementary DNA using an RT^2 First-Strand kit (Qiagen and SABiosciences) following the manufacturers' instructions. Samples were analyzed on a CFX96 thermocycler (Bio-Rad), and gene expression was quantified relative to the geometric mean of 5 stable reference genes: *Gusb*, *Hprt1*, *Hsp90ab1*, *Gapdh*, and *Actb*. Protein samples were diluted in PBS with 1% Triton X-100 and analyzed using a Proteome Profiler Mouse Adipokine Array kit (catalog no. ARY013; R&D Systems) following the manufacturer's instructions. Membranes were incubated with 250 μg of protein, and bound antigen was detected by autoradiography using streptavidin–horseradish peroxidase secondary antibody and ChemiReagent Substrate mixture. Densitometry was conducted using a G:BOX imaging system and Gene Tools software (Syngene).

Flow cytometry. The EFP and IFP tissues were placed in PBS with 5% fetal bovine serum (FBS) prior to cell isolation. Stromal vascular fraction cells were obtained by digesting fat at 37°C for 1 hour on an orbital shaker in a buffer containing Dulbecco's modified Eagle's medium (DMEM)/F-12 complete medium, 1 mg/ml of type IA collagenase (Sigma-Aldrich), 0.1 mg/ml of DNase I, 0.8 m*M* zinc chloride, 1.5% bovine serum albumin, and 25 m*M* HEPES (Life Technologies). Collagenase activity was neutralized with Hanks' balanced salt solution (catalog no. 21-022-CV; Cellgro Mediatech) and 10% FBS. The mixture was filtered (70 μm) and then centrifuged at 400*g* for 10 minutes at 4°C.

The cell filtrate was incubated in 1× red blood cell lysis solution for 1 minute at room temperature followed by a DMEM wash and centrifugation. Freshly isolated cells were resuspended in fluorescence-activated cell sorting buffer (1× PBS with 5% FBS), counted, and labeled for 30 minutes on ice with fluorochrome-conjugated monoclonal antibodies (BioLegend) against mouse CD45.2 (clone 104), CD3 (145-2C11), CD19 (6D5), F4/80 (BM8), CD11c (N418), and CD206 (C068C2). Propidium iodide was used to determine cell viability (BioLegend). Compensation was done using a CompBead anti-rat and anti-hamster Igκ/negative control compensation particles set from BD Biosciences. Experiments were analyzed with a BD LSR II flow cytometer and FlowJo software (Tree Star).

Statistical analysis. Imaging analyses were evaluated in a blinded manner. Scoring and quantitative analyses were averaged for all images, sections, and/or anatomical sites to generate an average value per animal for the statistical analyses. Differences in semiquantitative scores were determined using Mann-Whitney U tests (Prism 6.0f software). Gene expression array analyses included a 10% false discovery rate adjustment following the Benjamini-Hochberg procedure, as indicated. All other data were analyzed by Student's *t*-test, one-way analysis of variance (ANOVA), or two-way ANOVA followed by Dunnett's or Holm-Sidak's multiple comparisons test, respectively (Prism 6.0f). Data are expressed as the mean ± SEM except where indicated otherwise. *P* values less than 0.05 were considered significant.

RESULTS

Time course of HF diet–induced knee OA pathogenesis. We examined knee OA pathology in mice after 20 and 46 weeks of feeding them a control or HF diet. There were no differences in knee OA at 20 weeks based on modified Mankin scores, whereas 46 weeks of an HF diet increased OA severity (Figure 1A). Between 26 and 52 weeks of age, the OA scores increased 21.2% in the group receiving a control diet and 44.6% in the group receiving an HF diet ($P = 0.0098$). Scores on the modified Mankin subcomponents showed a significant increase in tidemark duplication in the HF diet group after 20 weeks (Figures 1B and D). HF feeding also accelerated osteophyte formation after 20 weeks of

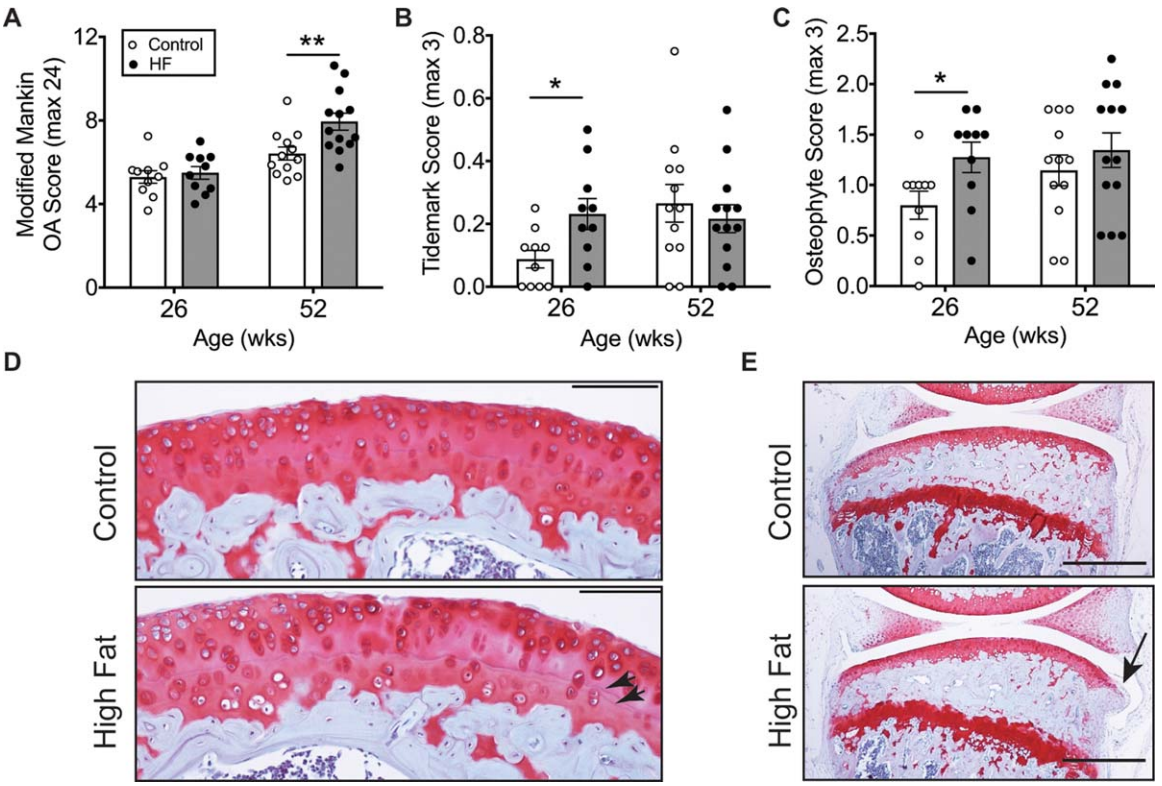

Figure 1. Age-dependent pathologic changes of knee osteoarthritis (OA) in mice with high-fat (HF) diet–induced obesity. Animals were fed a diet consisting of either 10% kcal of fat (control diet) or 60% kcal of fat (HF diet) beginning at 6 weeks of age. **A,** Increased severity of cartilage OA after 46 weeks of an HF diet, but not 20 weeks. OA in knee cartilage was determined by the modified Mankin score, which was averaged for multiple sections and sites throughout the joint, including the medial and lateral tibia and femur. **B,** Increased duplication of the tidemark separating the uncalcified and calcified cartilage after 20 weeks of an HF diet. After 46 weeks, however, both diet groups were similar. **C,** Accelerated development of tibial osteophytes after 20 weeks of an HF diet. However, after 46 weeks, control and HF diet groups were no longer different. Each symbol represents an individual mouse. Values are the mean ± SEM of 10 mice per group at 26 weeks and 12 mice per control group and 13 mice per HF group at 52 weeks. $* = P < 0.05$; $** = P < 0.01$. **D** and **E,** Sagittal sections of the medial tibia (**D**) and the medial compartment of the knee (**E**) after 20 weeks in mice fed a control diet or an HF diet. **Arrowheads** indicate tidemarks; **arrow** indicates an osteophyte. Bars = 100 μm in **D**; 500 μm in **E**.

eating an HF diet (Figures 1C and E), indicating the presence of early-stage OA. Therefore, we selected a 20-week period of HF diet to test the hypothesis that obesity induces IFP inflammation prior to the development of pathologic changes of overt OA in knee cartilage.

Distinct infrapatellar adipocyte response to HF diet–induced obesity and fat pad hypertrophy. Twenty weeks of eating an HF diet increased body mass by 41% ($P < 0.0001$) and increased total body fat from 14.8% to 36.7% of body mass ($P < 0.0001$) (Figure 2A). The fasting blood glucose level was not elevated at this time point, but blood glucose levels remained elevated in mice in the HF group 30–90 minutes following a glucose challenge (Figure 2B). We next compared the effect of HF feeding on the sizes of the EFP, SFP, and IFP depots and their respective adipocytes. In animals eating the control diet, IFP adipocytes were significantly smaller than SFP and EFP adipocytes (Figure 2C). Following 20 weeks of HF feeding, the infrapatellar, subcutaneous, and peritoneal (i.e., epididymal plus mesenteric) adipose tissue volumes increased by 1.54-fold ($P = 0.005$), 5.63-fold ($P = 0.0004$), and 3.98-fold ($P = 0.0003$), respectively (Figure 2D). When adipocyte cross-sectional areas were examined, IFP adipocytes did not become hypertrophic like the SFP and EFP adipocytes had (Figures 2C and E). Thus, although the IFP volume increased in response to HF feeding, adipocyte hypertrophy did not contribute to the increase in IFP size.

Comparison of HF diet–induced changes in IFP versus EFP immune cell populations. We next evaluated the effect of an HF diet on the immune cell populations in the stromal vascular fraction of the IFP and EFP (Figure 3 and Supplementary Figure 1, available at

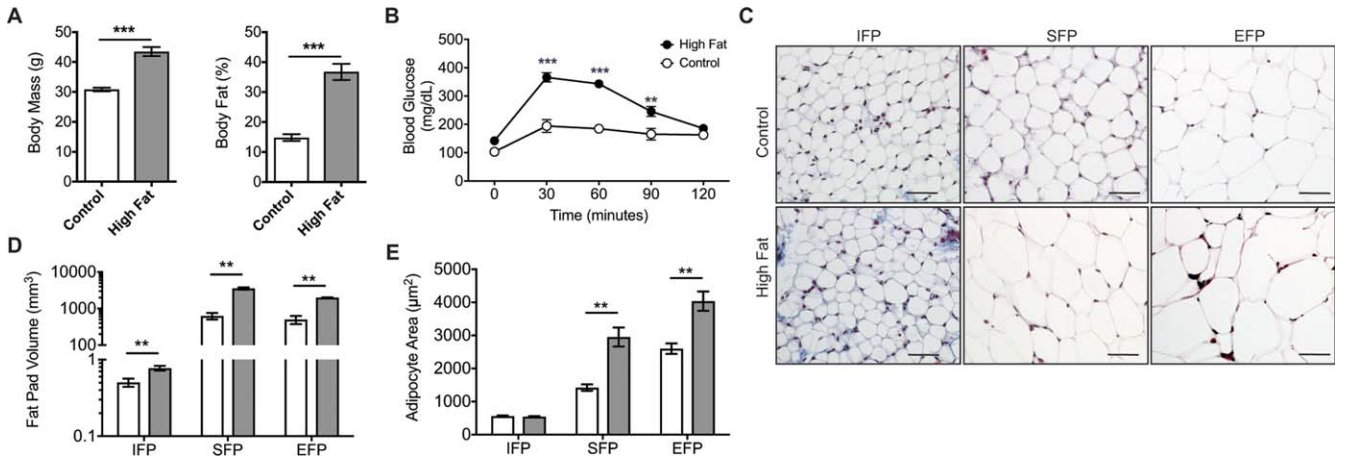

Figure 2. High-fat (HF) diet–induced changes in systemic metabolism and location-specific changes in fat pad and adipocyte size. Mice were fed a control diet or an HF diet for 20 weeks beginning at 6 weeks of age. **A,** Substantial increase in body mass (left) and body fat (right) in mice fed an HF diet. **B,** Significantly elevated fasting blood glucose levels at 30, 60, and 90 minutes after glucose challenge in mice fed an HF diet, indicating impaired glucose tolerance. **C,** Trichrome-stained sections of the infrapatellar fat pad (IFP), subcutaneous fat pad (SFP), and epididymal fat pad (EFP) of mice fed a control or HF diet. IFP adipocytes were substantially smaller than SFP or EFP adipocytes for either diet. Bars = 50 μm. **D,** Fat pad volumes in mice fed a control (open bars) or HF (solid bars) diet, as determined on water-suppressed magnetic resonance imaging (MRI) sequences. Image data were acquired with a 7T, 30-cm horizontal bore USR Bruker MRI system. A validated automated segmenting procedure (28) and manual segmenting were used. **E,** Increased adipocyte area in SFPs and EFPs, but not IFPs, in the HF diet group (solid bars), indicating that adipocyte hypertrophy did not contribute to the increase in IFP size. Values are the mean ± SEM of 8 mice per control group and 10 mice per HF group in **A**, 4 mice per control group and 5 mice per HF group in **B**, 9 mice per group for the IFP and 3 mice per group for the SFP and EFP in **D**, and 5 mice per group in **E**. ** = $P < 0.01$; *** = $P < 0.001$.

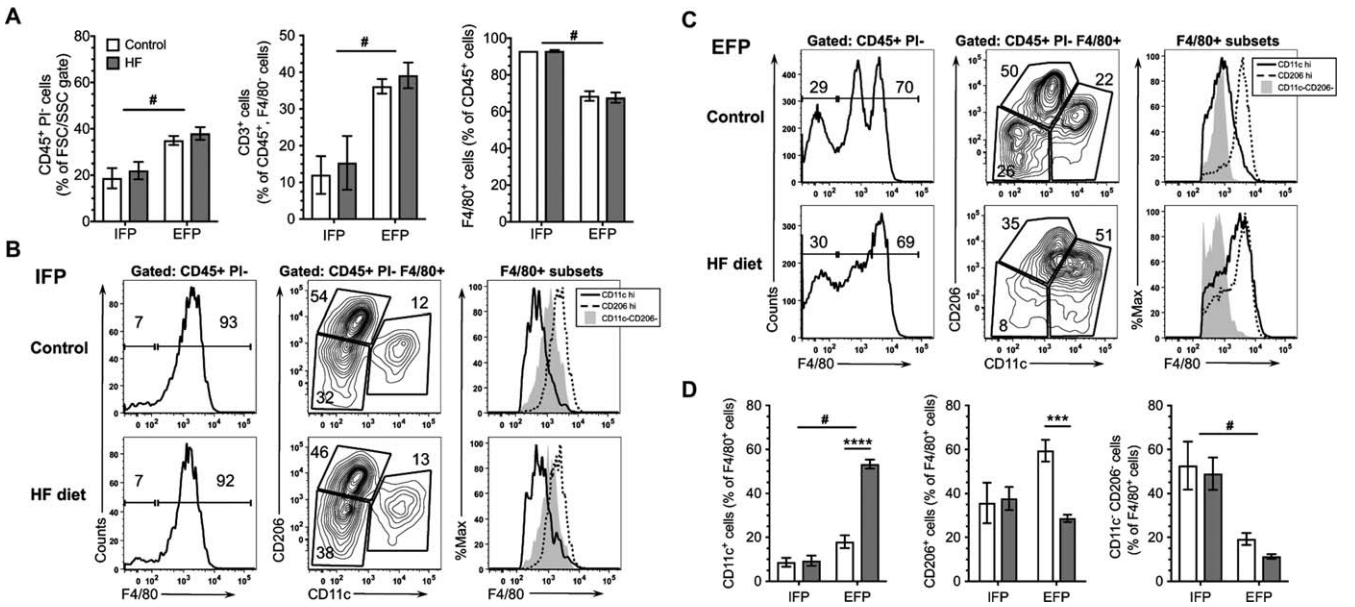

Figure 3. Effect of a high-fat (HF) diet on immune cell populations in the infrapatellar fat pad (IFP) and epididymal fat pad (EFP). Stromal vascular fraction cells were isolated from IFPs and EFPs after 20 weeks of an HF diet. IFP samples were pooled from 6 animals per experiment, and EFP samples were collected from 2 of the same 6 animals. Experiments were performed 3 times (n = 3 independent experiments for IFP and 6 for EFP). **A,** Effect of an HF diet on adipose tissue leukocytes (propidium iodide [PI]–negative, CD45+) (left), T cells (CD45+, CD3+, F4/80–) (middle), and macrophages (CD45+, F4/80+) (right). **B,** Effect of an HF diet on the distribution of F4/80+ adipose tissue leukocytes (PI–, CD45+) in the IFP. Macrophages were further identified within the population of F4/80+ cells based on CD11c and CD206 expression and F4/80 staining intensity among CD11c^{high}, CD206^{high}, and CD11c–CD206– populations. **C,** Effect of an HF diet on the distribution of F4/80+ adipose tissue leukocytes (PI–, CD45+) in the EFP. Unlike the IFP, HF feeding increased the number of CD11c+ cells and shifted the expression of CD11c+ cells from F4/80^{intermediate} to F4/80^{high}, indicating M1 polarization. **D,** Effect of an HF diet on the percentage of PI–CD45+F4/80+ cells expressing the M1 macrophage marker CD11c (left), the M2 macrophage marker CD206 (middle), or neither marker (right) in the IFP and the EFP. Values in **A** and **D** are the mean ± SEM. # = $P < 0.05$ between fat pads; *** = $P < 0.001$ between diets; **** = $P < 0.0001$ between diets.

http://onlinelibrary.wiley.com/doi/10.1002/art.40056/abstract). The EFP contained a greater percentage of CD45+ cells compared to the IFP, and this was independent of diet ($P < 0.0001$) (Figure 3A). There were also significant differences in T cell (CD3+) and macrophage (F4/80+) populations between the EFP and IFP depots (Figure 3A). Notably, the IFP contained a lower percentage of T cells ($P < 0.0001$) and a higher percentage of macrophages ($P < 0.0001$) compared to the EFP, and these differences were independent of an HF diet (Figure 3A). B cell populations from the IFP were negligible for either diet.

We then evaluated the effect of an HF diet on CD206+ and CD11c+ adipose tissue macrophages, as determined with F4/80 staining (25). In the IFP, the intensity of F4/80 staining and the relative proportion of CD206+ and CD11c+ cells did not change with an HF diet (Figures 3B and D). The $CD206^{high}$ cells were also $F4/80^{high}$, as expected for macrophages, whereas the $CD11c^{high}$ cells had lower F4/80 expression, consistent with their potential identity as dendritic cells rather than M1 macrophages (32). The $F4/80^{intermediate}$CD11c–CD206– cells in the IFP showed an SSC/FSC pattern similar to that of the CD206+ and CD11c+ populations in both the IFP and EFP (data not shown), suggesting that these cells are undifferentiated monocytes rather than neutrophils or eosinophils, as recently reported for the EFP (32). In contrast to the IFP, an HF diet significantly altered the intensity of F4/80 staining and the relative proportion of CD206+ and CD11c+ cells in the EFP (Figures 3C and D). The proportion of CD11c+ cells and intensity of F4/80 staining in $CD11c^{high}$ cell population increased with an HF diet, consistent with an increase in M1-like macrophages. Furthermore, macrophage crown-like structures, another characteristic of adipose tissue inflammation, were increased with an HF diet in the EFP ($P = 0.019$) but were not significantly altered in the SFP, and none were observed in the IFP (data not shown).

No effect of HF diet–induced obesity on IFP inflammation. To further characterize fat pad– and HF diet–specific effects on adipose tissue inflammation, we compared the expression of proinflammatory and antiinflammatory genes and chemokine ligand and receptor genes using a targeted gene expression array. In mice consuming the control diet, *Tnf* and *Il1b* were more highly expressed in the IFP compared to the SFP (Figure 4A). The proinflammatory mediator *Casp1* was also more highly expressed in the IFP compared to the EFP. An HF diet increased the expression of *Tnf* and *Il1b* in the SFP and *Casp1* in the EFP, but none were altered in the IFP (Figure 4A). Among key antiinflammatory genes, *Il4* and *Il13* were more highly expressed in the IFP compared to the EFP, and only *Il13* expression in the EFP was increased following an HF diet (Figure 4B). There were no differences in the expression of the macrophage chemokine ligands *Ccl2*, *Ccl3*, and *Ccl7* in animals consuming a control diet (Figure 4C). However, following an HF diet, the expression of *Ccl2*, *Ccl3*, and *Ccl7* increased in the EFP, and the expression of *Ccl2* and *Ccl7* increased in the SFP, but no significantly increased expression occurred in the IFP (Figure 4C). Expression of the chemokine receptors *Ccr1*, *Ccr3*, and *Ccr5*, however, were nearly all elevated in the IFP relative to the other fat pads, independently of diet (Figure 4D). Thus, under basal nonobese conditions, the expression of proinflammatory genes and chemokine receptor genes was elevated in the IFP compared to the SFP and EFP, but the IFP was insensitive to HF diet–induced changes.

We then performed an unsupervised cluster analysis of both fat pad type and macrophage polarization effector status on the HF diet–induced fold change in gene expression (Figure 4E). Although M1 and M2 subtypes can be ambiguous and overlapping, we selected a panel of genes previously found to be associated with these designations (33) to assess general patterns of inflammatory gene expression among the fat pads. Depot-specific fat pad samples clustered together based on their HF diet–induced changes in inflammatory gene expression. Notably, the expression patterns in the SFP more closely followed those in the EFP than in the IFP (Figure 4E). The genes clustered together into 2 major groups and were significantly associated with the M1 versus M2 gene designations (left and right clusters, respectively; $P = 0.036$) (Figure 4A). Consistent with the findings of flow cytometry, the EFP samples, and to a lesser extent SFP samples, were characterized by an up-regulation of M1 effector genes and down-regulation of M2 effector genes. The IFP samples, however, did not show a discernible pattern of M1 versus M2 HF diet–induced gene expression. An analysis of adipokine and cytokine protein levels in the IFP also showed minimal effects of an HF diet, with a minor increase in IL-10 (mean ± SEM HF-induced fold change 1.19 ± 0.05; $P = 0.03$) and a reduction in leptin (mean ± SEM HF-induced fold change 0.61 ± 0.10; $P = 0.03$) (Supplementary Figure 2, available at http://onlinelibrary.wiley.com/doi/10.1002/art.40056/abstract).

Robust increase in IFP fibrosis caused by HF diet–induced obesity. To better understand the factors that differentiate the remodeling response of infrapatellar and subcutaneous fat pads to HF diet–induced obesity, we examined changes in adipose tissue fibrosis and the expression of genetic regulators of extracellular matrix homeostasis. Quantification of sirius red staining

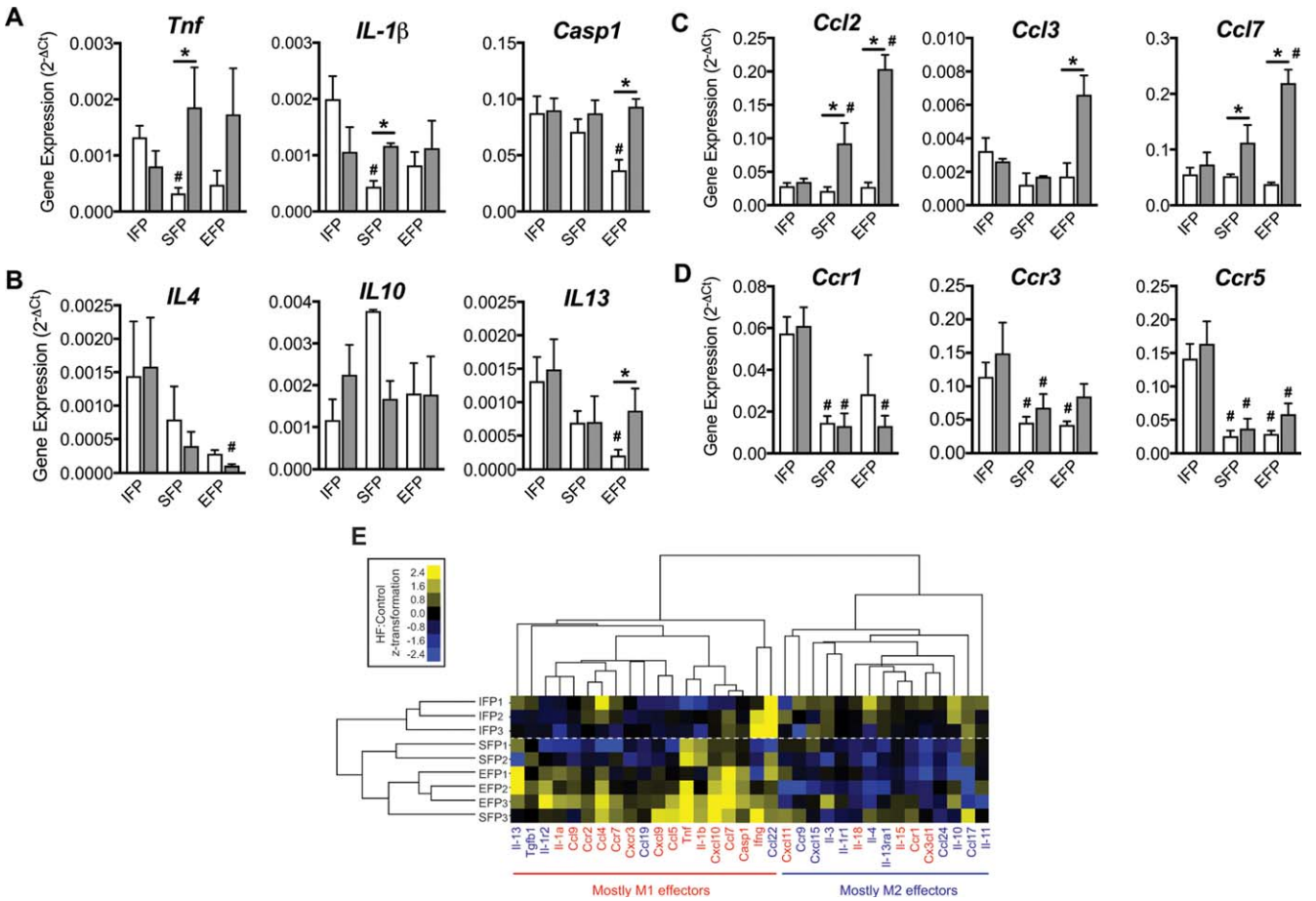

Figure 4. Effect of a high-fat (HF) diet on fat pad–specific proinflammatory and antiinflammatory gene expression. Gene expression ($2^{-\Delta C_t}$) was measured using RT^2 Profiler PCR inflammatory cytokine and receptors targeted arrays following 20 weeks of a control (open bars) or HF (solid bars) diet. The infrapatellar fat pads (IFPs) from both knees were pooled from 2 animals per gene array. Subcutaneous fat pad (SFP) and epididymal fat pad (EFP) samples were pooled in parallel from the same animals. Experiments were performed 3 times, and the values were log-transformed for statistical analyses. **A–D,** Expression of the indicated proinflammatory (**A**), antiinflammatory (**B**), chemokine ligand (**C**), and chemokine receptor (**D**) genes in the IFPs, SFPs, and EFPs. Values are the mean ± SEM. # = $P < 0.05$ versus IFP control; * = $P < 0.05$ HF versus control for the same fat pad type. **E,** Heatmap showing unsupervised cluster analysis of both fat pad type and macrophage polarization effector status using the HF diet–induced fold change in gene expression, as calculated by the $\Delta\Delta C_t$ method. Fat pad samples clustered by anatomic location, and macrophage polarization effector genes clustered primarily by M1 versus M2 effector bias. M1 effector genes tended to be up-regulated and M2 effector genes down-regulated in EFP and SFP samples.

showed that the collagen content of adipose tissue was greater in the IFP compared to the SFP in mice fed a control diet ($P = 0.003$) (Figures 5A and B). This difference was magnified following an HF diet, whereby the adipose tissue collagen content increased 2.0-fold (from 1.84% to 3.74% in the IFP; $P = 0.001$), but did not change in the SFP (0.24% versus 0.25%) (Figure 5B). This same pattern remained even when collagen content was normalized to adipocyte size to account for baseline differences in adipocyte size and HF diet–induced SFP adipocyte hypertrophy (Figure 5C).

This profibrotic response in the IFP was accompanied by a greater number of differentially expressed genes involved in extracellular matrix remodeling (Figure 5D and Supplementary Table 2, available at http://onlinelibrary.wiley.com/doi/10.1002/art.40056/abstract). Of 84 genes evaluated, 34 were differentially expressed in the IFP in response to an HF diet, with 19 being up-regulated and 15 being down-regulated. The up-regulated genes included several that encode extracellular matrix proteins, such as types III, IV, and VI collagen as well as fibronectin and fibronectin receptors

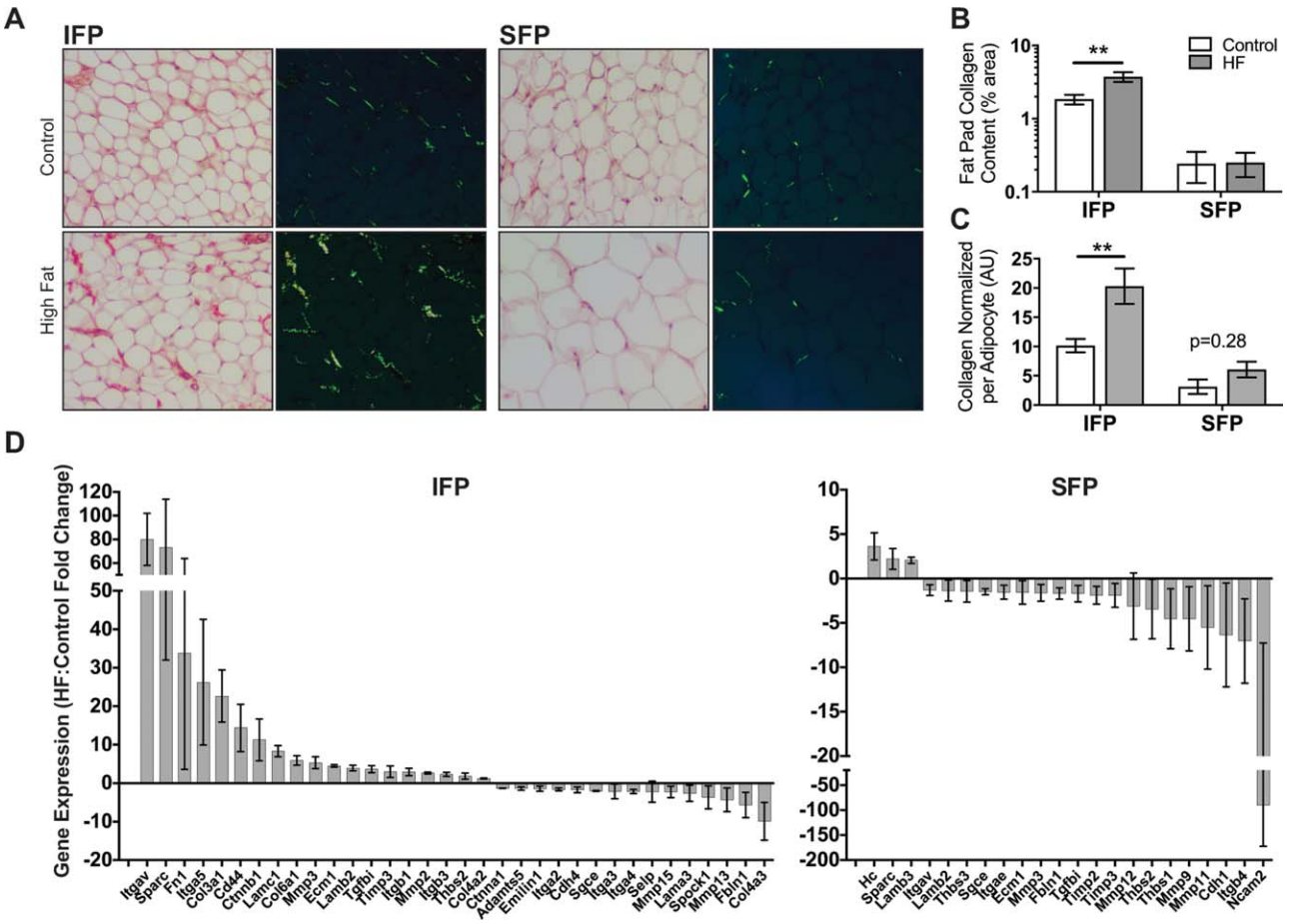

Figure 5. High-fat (HF) diet–induced infrapatellar and subcutaneous adipose tissue fibrosis and extracellular matrix gene expression. **A,** Brightfield (left) and epipolarized ultraviolet light (right) images of sirius red–stained paraffin sections of the infrapatellar fat pad (IFP) and subcutaneous fat pad (SFP) of mice fed a control or HF diet for 20 weeks. Yellow-green pixels from epipolarized images were quantified to determine the collagen content of adipose tissue. Original magnification × 10. **B,** Significant increase in IFP collagen content, but no alteration of SFP collagen content, after an HF diet. **C,** Elevated IFP, but not SFP, collagen content after an HF diet, even with normalization. Fat pad collagen content was normalized to the average adipocyte area per fat pad to adjust for anatomic and HF diet–associated differences in adipocyte size. Values in **B** and **C** are the mean ± SEM of 5 mice per group. **D,** Gene expression in the IFP and SFP following 20 weeks of an HF diet, as measured by RT^2 Profiler PCR extracellular matrix and adhesion molecules targeted arrays. Significantly differentially expressed genes due to the HF diet as compared with the control diet are plotted from the highest to the lowest for the IFP and SFP ($P < 0.05$ based on the 95% confidence interval [95% CI] of the fold-change value). Values are the mean and 95% CI. Sample sizes are same as in Figure 4. ** = $P < 0.01$. (Values shown graphically in **D** are reported as actual values in Supplementary Table 2, available at http://onlinelibrary.wiley.com/doi/10.1002/art.40056/abstract).

Itga5 and *Itgb1*. In contrast, 22 genes were differentially expressed in the SFP, with the majority being down-regulated (3 up-regulated versus 19 down-regulated). Only 1 gene, *Sparc*, was up-regulated in both fat pads in response to an HF diet; *Sparc* is a profibrotic glycoprotein that inhibits adipogenesis (34). Three genes were down-regulated in the IFP and SFP: *Fbln1*, *Itga4*, and *Sgce*. Several genes were up-regulated in the IFP in response to an HF diet that were down-regulated in the SFP, including cell adhesion and extracellular matrix binding proteins (*Ecm1*, *Itgav*, *Lamb2*, *Tgfbi*, and *Thbs2*) and regulators of matrix proteostasis (*Mmp3* and *Timp3*).

Given these differences in extracellular matrix regulation, we compared differences in gene expression in the IFP relative to the SFP of mice fed a control diet in order to gain insight into basal differences in transcription. We included both inflammatory and extracellular matrix arrays because inflammation can contribute to adipose tissue fibrosis. Of 168 genes, 10 were up-regulated and 16 were down-regulated in the IFP (Table 1). A smaller subset retained significance after corrections for multiple comparisons (4 up-regulated and 8 down-regulated). Of these, most were cytokine receptors and chemokines associated with

Table 1. Genes differentially expressed in the IFP versus SFP of mice fed a control diet*

Gene	Fold regulation (IFP:SFP), mean (95% CI)	*P*
Up-regulated in the IFP		
Ccl17	17.4 (9.54, 25.3)	0.0122
Ccl19	10.9 (9.64, 12.1)	0.0008†
Ccr5	6.79 (2.15, 11.4)	0.0330
Tnf	4.54 (1.46, 7.62)	0.0385
Ccr1	4.17 (1.68, 6.67)	0.0319
Il13ra1	3.45 (2.82, 4.08)	0.0035†
Itgam	3.36 (3.31, 3.42)	<0.0001†
Thbs3	2.06 (1.28, 2.83)	0.0279
Il1r1	1.48 (1.33, 1.62)	0.0049†
Scye1	1.19 (1.04, 1.34)	0.0328
Down-regulated in the IFP		
Adamts2	−1.26 (–1.30, −1.23)	<0.0001†
Cxcl10	−1.26 (–1.87, −0.656)	0.0039†
Ccl25	−1.48 (–2.72, 0.241)	0.0132
Cxcl9	−1.66 (–1.98, −1.33)	0.0008†
Mif	−1.66 (–3.00, −0.335)	0.0132
Cxcr3	−1.72 (–2.07, −1.38)	0.0009†
Cdh1	−1.80 (–2.95, −0.658)	0.0089
Ccl6	−1.89 (–3.84, 0.0579)	0.0237
Ccl5	−1.91 (–2.57, −1.25)	0.0028†
Col4a2	−1.94 (–2.97, −0.914)	0.0065†
Ccl11	−2.19 (–3.05, −1.32)	0.0040†
Ccr10	−2.25 (–3.93, −0.570)	0.0141
Thbs1	−2.41 (–5.61, 0.787)	0.0443
Col4a1	−2.77 (–6.28, 0.734)	0.0436
Il2rg	−2.85 (–1.36, −0.811)	0.0009†
Mmp9	−10.4 (–19.1, −1.74)	0.0298

* Values for the infrapatellar fat pad (IFP) are expressed relative to the subcutaneous fat pad (SFP). Results are for mice consuming the control diet.
† Significance was retained after controlling for a 10% false discovery rate (exploratory analysis) following the Benjamini-Hochberg procedure.

reduced T cell chemotaxis and increased innate immune responses. These findings suggest that basal differences in adipose tissue mediators of inflammation, rather than the extracellular matrix per se, contribute to the robust profibrotic response in the IFP of obese mice.

DISCUSSION

The IFP is considered a paracrine mediator of cartilage catabolism due to the niche it provides for immune cells and its proinflammatory phenotype in OA joints (19–21,24). We hypothesized that obesity stimulates IFP inflammation by increasing macrophage infiltration and M1 polarization prior to the development of cartilage degeneration. Although we observed elevated basal IFP inflammation compared to other fat depots, diet-induced obesity did not further increase the number of immune cells in the IFP or induce a proinflammatory shift in cytokine expression or macrophage polarization after 20 weeks of consuming an HF diet. Given that this duration of feeding induced early-stage OA changes, such as osteophyte formation and cartilage tidemark duplication, the findings do not support a role of IFP inflammation as a central initiating factor of obesity-induced knee OA. We did not, however, evaluate IFP inflammation after 46 weeks of HF feeding, when cartilage degeneration was significantly elevated, which raises the possibility that IFP inflammation contributes to OA progression.

Unlike subcutaneous or epididymal adipocytes, IFP adipocytes did not become hypertrophic in response to HF feeding despite an overall increase in fat pad size. This unique response to HF feeding suggests that IFP size increases by hyperplasia (i.e., adipogenesis), which has previously been reported to occur transiently in the epididymal fat of male C57BL/6 mice following high-fat feeding (35). In addition, high-fat feeding also increased IFP fibrosis. Adipose tissue fibrosis is usually associated with adipocyte hypertrophy and obesity-induced metabolic dysfunction (25,36). In this context, M1 adipose tissue macrophages appear to generate proinflammatory signals that shift preadipocytes away from an adipogenic lineage and toward a myofibroblast phenotype. The localization of M1 macrophages and dense extracellular matrix deposits in crown-like structures that surround necrotic adipocytes reinforces the pathologic attributes of adipose tissue fibrosis. Therefore, the association of adipose tissue fibrosis with negligible M1 polarization and adipocyte hypertrophy in the IFP in obese mice raises questions about how it occurs and how it affects joint health. One possibility is that the temporal dynamics of inflammatory activation and resolution are accelerated in the IFP, which would require testing at earlier time points of feeding an HF diet. Alternatively, IFP fibrosis may occur via physiologic signaling mediators, such as mechanical stress, rather than pathologic proinflammatory M1 polarization.

Mechanical signals regulate stem cell fate, adipogenesis, and adipocyte hypertrophy, and the extracellular matrix mediates how cells sense these changes in the environment (37–39). In pre-adipocyte culture models, static tensile strain stimulates adipocyte differentiation, whereas compressive strain or cyclic tensile strain suppresses adipogenesis (for review, see ref. 40). Although few studies have examined IFP biomechanical stresses (41), the load-bearing aspects of this intraarticular fat pad likely underlie the basal differences in adipocyte size and response to diet-induced obesity. In a previous study, we showed that mice with diet-induced obesity maintain similar levels of spontaneous locomotor activity despite increased weight gain, which is consistent with increased joint stresses (18).

Adipocyte size is a key factor in the regulation of adipokine secretion, and our results suggest that obesity-induced IFP fibrosis may limit metabolic inflammation by inhibiting adipocyte hypertrophy. Previous work has shown that subcutaneous adipocytes in the largest size quartile produce more leptin, IL-6, IL-8, CCL2, and granulocyte colony-stimulating factor compared to the smallest quartile, even when normalized to adipocyte surface area (42). We observed few changes in adipokine protein levels in the IFPs of HF versus control mice. One notable exception was leptin, which surprisingly was reduced in mice fed an HF diet. We previously found that IL-1β decreases leptin production in the IFP of rats (43), although in the current study, IL-1β gene expression was not increased with an HF diet. Rather, the increased extracellular matrix content may limit leptin production and adipocyte hypertrophy (25,39).

Many suppressors of adipocyte hypertrophy, including types III, IV, and VI collagen and fibronectin, were transcriptionally up-regulated in the IFP following HF feeding. In particular, the matricellular protein SPARC (also known as osteonectin) negatively regulates adipose tissue expansion by both stimulating fibronectin and suppressing adipogenic transcription factors and genes, including leptin (34). HF feeding induced SPARC expression significantly more in the IFP (73-fold increase) versus the SFP (2.2-fold increase), suggesting that SPARC up-regulation is an important mediator of IFP fibrosis with obesity. Consistent with this, we observed that an HF diet increased IFP expression of α5 and β1 integrins, which form a receptor for fibronectin as well as SPARC-mimicking peptides (34). In addition, HF feeding likely stimulated IFP remodeling, as shown by the differential expression of several matrix metalloproteinases (*Mmp2*, *Mmp3*, *Mmp13*, and *Mmp15*) and tissue inhibitor of matrix metalloproteinase 3 (*Timp3*). Furthermore, macrophages are known to regulate extracellular matrix remodeling in adipose tissue (25). We found that the IFP was enriched for M2 macrophages and IL-13 expression, which are associated with fibrosis in other tissues (36).

The clinical significance of the IFP in OA development and progression is an active area of investigation (44,45). Some MRI-based cross-sectional studies have shown positive associations between IFP volume, joint inflammation, and joint pain (46,47), whereas cross-sectional and longitudinal analyses of other cohorts indicate a protective effect of IFP size on cartilage damage and pain, particularly in women (23,48,49). Age and OA progression also mediate size changes in the IFP (22,43). Our findings show that obesity can increase IFP size in a genetically and environmentally controlled animal model, but increased IFP size is not necessarily associated with increased inflammation. A more detailed understanding of the inflammatory and secretory status of the adipocytes themselves is likely needed to predict the clinical impact of the IFP on OA pathophysiology. Our results parallel recent studies reporting a profibrotic effect of the IFP on synovial fibroblasts (50,51), suggesting that adipocytes may play a central role in modulating joint tissue fibrosis.

Our findings contrast with a previous study reporting IFP adipocyte hypertrophy and inflammation in male C57BL/6J mice following HF feeding (52). However, that study used an HF diet composed of safflower oil and beef tallow versus soybean oil and lard used in the present study. That study also examined earlier time points (4, 8, and 12 weeks) compared to the present study (20 weeks). The previous study also focused its histologic analysis on a single region in the medial compartment, excluding the larger IFP area throughout the intercondylar notch, which we included in our study. Thus, the prior findings may indicate regional variation in adipocyte responses to obesity. It is also possible that including adjacent synovial tissue could produce an inflammatory phenotype, as a recent study reported HF diet–induced increases in synovial macrophages and TNF production (16). Although our study included synovium immediately deep to the IFP, it did not include adjacent peripheral synovium, and we did not observe an increase in TNF expression following HF feeding. This suggests that the synovium, rather than the IFP, is the major source of TNF in the mouse knee. This differs from studies in humans, which showed a positive correlation between IFP-derived TNF and the body mass index (20). An additional potential limitation of our study is that we only focused on male mice, as there is increasing evidence that the specific metabolic links between obesity and OA are sex dependent (53).

In conclusion, the IFP does not recapitulate the classic M1 macrophage–mediated inflammation that occurs in abdominal adipose tissue with obesity. This apparent protection from obesity-induced inflammation corresponds to the absence of adipocyte hypertrophy and an increase in adipose tissue fibrosis. These findings suggest that intraarticular adipocytes are subject to distinct spatiotemporal metabolic regulation among the fat pads, possibly due to the structural constraints and cyclic biomechanical stresses associated with the joints. Additional studies focused on earlier and later time points and the effects of altered joint loading conditions may help clarify how the IFP contributes to joint health and OA pathogenesis.

ACKNOWLEDGMENTS

We thank Melinda West, Erin Hutchison, Debra Saunders, and Drs. Yao Fu, Philippe Garteiser, Sabrina Doblas, and Bart Frank for technical assistance and Drs. Mary Beth Humphrey, Yao Fu, and Elise Donovan for advice and intellectual input.

AUTHOR CONTRIBUTIONS

All authors were involved in drafting the article or revising it critically for important intellectual content, and all authors approved the final version to be published. Dr. Griffin had full access to all of the data in the study and takes responsibility for the integrity of the data and the accuracy of the data analysis.

Study conception and design. Griffin.

Acquisition of data. Barboza, Hudson, Chang, Kovats, Silasi-Mansat, Kent, Griffin.

Analysis and interpretation of data. Barboza, Chang, Kovats, Towner, Lupu, Kent, Griffin.

REFERENCES

1. Felson DT, Anderson JJ, Naimark A, Walker AM, Meenan RF. Obesity and knee osteoarthritis: the Framingham study. Ann Intern Med 1988;109:18–24.
2. Yusuf E, Nelissen RG, Ioan-Facsinay A, Stojanovic-Susulic V, DeGroot J, van Osch G, et al. Association between weight or body mass index and hand osteoarthritis: a systematic review. Ann Rheum Dis 2010;69:761–5.
3. Issa RI, Griffin TM. Pathobiology of obesity and osteoarthritis: integrating biomechanics and inflammation. Pathobiol Aging Age Relat Dis 2012;2:17470.
4. Houard X, Goldring MB, Berenbaum F. Homeostatic mechanisms in articular cartilage and role of inflammation in osteoarthritis. Curr Rheumatol Rep 2013;15:375.
5. Berenbaum F. Osteoarthritis as an inflammatory disease (osteoarthritis is not osteoarthrosis!). Osteoarthritis Cartilage 2013;21: 16–21.
6. Attur M, Krasnokutsky S, Statnikov A, Samuels J, Li Z, Friese O, et al. Low-grade inflammation in symptomatic knee osteoarthritis: prognostic value of inflammatory plasma lipids and peripheral blood leukocyte biomarkers. Arthritis Rheumatol 2015;67:2905–15.
7. Wang Q, Rozelle AL, Lepus CM, Scanzello CR, Song JJ, Larsen DM, et al. Identification of a central role for complement in osteoarthritis. Nat Med 2011;17:1674–9.
8. Rai MF, Patra D, Sandell LJ, Brophy RH. Transcriptome analysis of injured human meniscus reveals a distinct phenotype of meniscus degeneration with aging. Arthritis Rheum 2013;65: 2090–101.
9. Ritter SY, Subbaiah R, Bebek G, Crish J, Scanzello CR, Krastins B, et al. Proteomic analysis of synovial fluid from the osteoarthritic knee: comparison with transcriptome analyses of joint tissues. Arthritis Rheum 2013;65:981–92.
10. Nair A, Gan J, Bush-Joseph C, Verma N, Tetreault MW, Saha K, et al. Synovial chemokine expression and relationship with knee symptoms in patients with meniscal tears. Osteoarthritis Cartilage 2015;23:1158–64.
11. Courties A, Gualillo O, Berenbaum F, Sellam J. Metabolic stress-induced joint inflammation and osteoarthritis. Osteoarthritis Cartilage 2015;23:1955–65.
12. Thijssen E, van Caam A, van der Kraan PM. Obesity and osteoarthritis, more than just wear and tear: pivotal roles for inflamed adipose tissue and dyslipidaemia in obesity-induced osteoarthritis. Rheumatology (Oxford) 2015;54:588–600.
13. Rai MF, Sandell LJ. Inflammatory mediators: tracing links between obesity and osteoarthritis. Crit Rev Eukaryot Gene Expr 2011;21:131–42.
14. Daghestani HN, Pieper CF, Kraus VB. Soluble macrophage biomarkers indicate inflammatory phenotypes in patients with knee osteoarthritis. Arthritis Rheumatol 2015;67:956–65.
15. Kraus VB, McDaniel G, Huebner JL, Stabler TV, Pieper CF, Shipes SW, et al. Direct in vivo evidence of activated macrophages in human osteoarthritis. Osteoarthritis Cartilage 2016;24:1613–21.
16. Hamada D, Maynard R, Schott E, Drinkwater CJ, Ketz JP, Kates SL, et al. Suppressive effects of insulin on tumor necrosis factor–dependent early osteoarthritic changes associated with obesity and type 2 diabetes mellitus. Arthritis Rheumatol 2016; 68:1392–402.
17. Liu-Bryan R, Terkeltaub R. Emerging regulators of the inflammatory process in osteoarthritis. Nat Rev Rheumatol 2015;11: 35–44.
18. Griffin TM, Fermor B, Huebner JL, Kraus VB, Rodriguiz RM, Wetsel WC, et al. Diet-induced obesity differentially regulates behavioral, biomechanical, and molecular risk factors for osteoarthritis in mice. Arthritis Res Ther 2010;12:R130.
19. Presle N, Pottie P, Dumond H, Guillaume C, Lapicque F, Pallu S, et al. Differential distribution of adipokines between serum and synovial fluid in patients with osteoarthritis. Contribution of joint tissues to their articular production. Osteoarthritis Cartilage 2006;14:690–5.
20. Klein-Wieringa IR, Kloppenburg M, Bastiaansen-Jenniskens YM, Yusuf E, Kwekkeboom JC, El-Bannoudi H, et al. The infrapatellar fat pad of patients with osteoarthritis has an inflammatory phenotype. Ann Rheum Dis 2011;70:851–7.
21. Distel E, Cadoudal T, Durant S, Poignard A, Chevalier X, Benelli C. The infrapatellar fat pad in knee osteoarthritis: an important source of interleukin-6 and its soluble receptor. Arthritis Rheum 2009;60:3374–7.
22. Chuckpaiwong B, Charles HC, Kraus VB, Guilak F, Nunley JA. Age-associated increases in the size of the infrapatellar fat pad in knee osteoarthritis as measured by 3T MRI. J Orthop Res 2010;28:1149–54.
23. Pan F, Han W, Wang X, Liu Z, Jin X, Antony B, et al. A longitudinal study of the association between infrapatellar fat pad maximal area and changes in knee symptoms and structure in older adults. Ann Rheum Dis 2015;74:1818–24.
24. Ioan-Facsinay A, Kloppenburg M. An emerging player in knee osteoarthritis: the infrapatellar fat pad. Arthritis Res Ther 2013; 15:225.
25. Martinez-Santibanez G, Nien-Kai Lumeng C. Macrophages and the regulation of adipose tissue remodeling. Annu Rev Nutr 2014;34:57–76.
26. Bastiaansen-Jenniskens YM, Clockaerts S, Feijt C, Zuurmond AM, Stojanovic-Susulic V, Bridts C, et al. Infrapatellar fat pad of patients with end-stage osteoarthritis inhibits catabolic mediators in cartilage. Ann Rheum Dis 2012;71:288–94.
27. Johnston SL, Peacock WL, Bell LM, Lonchampt M, Speakman JR. PIXImus DXA with different software needs individual calibration to accurately predict fat mass. Obes Res 2005;13:1558–65.
28. Garteiser P, Doblas S, Towner RA, Griffin TM. Calibration of a semi-automated segmenting method for quantification of adipose tissue compartments from magnetic resonance images of mice. Metabolism 2013;62:1686–95.
29. Koves TR, Li P, An J, Akimoto T, Slentz D, Ilkayeva O, et al. Peroxisome proliferator-activated receptor-γ co-activator 1α-mediated metabolic remodeling of skeletal myocytes mimics exercise training and reverses lipid-induced mitochondrial inefficiency. J Biol Chem 2005;280:33588–98.
30. Cai A, Hutchison E, Hudson J, Kawashima Y, Komori N, Singh A, et al. Metabolic enrichment of omega-3 polyunsaturated fatty acids does not reduce the onset of idiopathic knee osteoarthritis in mice. Osteoarthritis Cartilage 2014;22:1301–9.

31. Kraus VB, Huebner JL, DeGroot J, Bendele A. The OARSI histopathology initiative: recommendations for histological assessments of osteoarthritis in the guinea pig. Osteoarthritis Cartilage 2010;18:S35–52.
32. Cho KW, Zamarron BF, Muir LA, Singer K, Porsche CE, DelProposto JB, et al. Adipose tissue dendritic cells are independent contributors to obesity-induced inflammation and insulin resistance. J Immunol 2016;197:3650–61.
33. Murray PJ, Allen JE, Biswas SK, Fisher EA, Gilroy DW, Goerdt S, et al. Macrophage activation and polarization: nomenclature and experimental guidelines. Immunity 2014;41:14–20.
34. Nie J, Sage EH. SPARC inhibits adipogenesis by its enhancement of β-catenin signaling. J Biol Chem 2009;284:1279–90.
35. Jeffery E, Church CD, Holtrup B, Colman L, Rodeheffer MS. Rapid depot-specific activation of adipocyte precursor cells at the onset of obesity. Nat Cell Biol 2015;17:376–85.
36. Pessin JE, Kwon H. How does high-fat diet induce adipose tissue fibrosis? J Investig Med 2012;60:1147–50.
37. Guilak F, Cohen DM, Estes BT, Gimble JM, Liedtke W, Chen CS. Control of stem cell fate by physical interactions with the extracellular matrix. Cell Stem Cell 2009;5:17–26.
38. Chun TH. Peri-adipocyte ECM remodeling in obesity and adipose tissue fibrosis. Adipocyte 2012;1:89–95.
39. Pope BD, Warren CR, Parker KK, Cowan CA. Microenvironmental control of adipocyte fate and function. Trends Cell Biol 2016;26:745–55.
40. Shoham N, Gefen A. Mechanotransduction in adipocytes. J Biomech 2012;45:1–8.
41. Bohnsack M, Hurschler C, Demirtas T, Rühmann O, Stukenborg-Colsman C, Wirth CJ. Infrapatellar fat pad pressure and volume changes of the anterior compartment during knee motion: possible clinical consequences to the anterior knee pain syndrome. Knee Surg Sports Traumatol Arthrosc 2005;13:135–41.
42. Skurk T, Alberti-Huber C, Herder C, Hauner H. Relationship between adipocyte size and adipokine expression and secretion. J Clin Endocrinol Metab 2007;92:1023–33.
43. Fu Y, Huebner JL, Kraus VB, Griffin TM. Effect of aging on adipose tissue inflammation in the knee joints of F344BN rats. J Gerontol A Biol Sci Med Sci 2016;71:1131–40.
44. Eymard F, Chevalier X. Inflammation of the infrapatellar fat pad. Joint Bone Spine 2016;83:389–93.
45. Roemer FW, Jarraya M, Felson DT, Hayashi D, Crema MD, Loeuille D, et al. Magnetic resonance imaging of Hoffa's fat pad and relevance for osteoarthritis research: a narrative review. Osteoarthritis Cartilage 2016;24:383–97.
46. Ballegaard C, Riis RG, Bliddal H, Christensen R, Henriksen M, Bartels EM, et al. Knee pain and inflammation in the infrapatellar fat pad estimated by conventional and dynamic contrast-enhanced magnetic resonance imaging in obese patients with osteoarthritis: a cross-sectional study. Osteoarthritis Cartilage 2014;22:933–40.
47. Cowan SM, Hart HF, Warden SJ, Crossley KM. Infrapatellar fat pad volume is greater in individuals with patellofemoral joint osteoarthritis and associated with pain. Rheumatol Int 2015;35:1439–42.
48. Han W, Cai S, Liu Z, Jin X, Wang X, Antony B, et al. Infrapatellar fat pad in the knee: Is local fat good or bad for knee osteoarthritis? Arthritis Res Ther 2014;16:R145.
49. Cai J, Xu J, Wang K, Zheng S, He F, Huan S, et al. Association between infrapatellar fat pad volume and knee structural changes in patients with knee osteoarthritis. J Rheumatol 2015; 42:1878–84.
50. Eymard F, Pigenet A, Citadelle D, Flouzat-Lachaniette CH, Poignard A, Benelli C, et al. Induction of an inflammatory and prodegradative phenotype in autologous fibroblast-like synoviocytes by the infrapatellar fat pad from patients with knee osteoarthritis. Arthritis Rheumatol 2014;66:2165–74.
51. Bastiaansen-Jenniskens YM, Wei W, Feijt C, Waarsing JH, Verhaar JA, Zuurmond AM, et al. Stimulation of fibrotic processes by the infrapatellar fat pad in cultured synoviocytes from patients with osteoarthritis: a possible role for prostaglandin $F_{2\alpha}$. Arthritis Rheum 2013;65:2070–80.
52. Iwata M, Ochi H, Hara Y, Tagawa M, Koga D, Okawa A, et al. Initial responses of articular tissues in a murine high-fat diet-induced osteoarthritis model: pivotal role of the IPFP as a cytokine fountain. PLoS ONE 2013;8:e60706.
53. June RK, Liu-Bryan R, Long F, Griffin TM. Emerging role of metabolic signaling in synovial joint remodeling and osteoarthritis. J Orthop Res 2016;34:2048–58.

ARTHRITIS & RHEUMATOLOGY
Vol. 69, No. 6, June 2017, pp 1233–1245
DOI 10.1002/art.40042

A Dual Role of Upper Zone of Growth Plate and Cartilage Matrix–Associated Protein in Human and Mouse Osteoarthritic Cartilage

Inhibition of Aggrecanases and Promotion of Bone Turnover

Michael Stock,[1] Stefanie Menges,[1] Nicole Eitzinger,[1] Maria Geßlein,[1] Renate Botschner,[1] Laura Wormser,[1] Alfiya Distler,[1] Ursula Schlötzer-Schrehardt,[1] Katharina Dietel,[1] Jörg Distler,[1] Christian Beyer,[1] Kolja Gelse,[1] Klaus Engelke,[2] Marije I. Koenders,[3] Wim van den Berg,[3] Klaus von der Mark,[2] and Georg Schett[1]

Objective. **Cartilage damage and subchondral bone changes are closely connected in osteoarthritis. Nevertheless, how these processes are interlinked is, to date, incompletely understood. This study was undertaken to investigate the mechanistic role of a cartilage-derived protein, upper zone of growth plate and cartilage matrix–associated protein (UCMA), in osteoarthritis-related cartilage and bone changes.**

Methods. **UCMA expression was assessed in healthy and osteoarthritic human and mouse cartilage. For analysis of cartilage and bone changes, osteoarthritis was induced by destabilization of the medial meniscus (DMM) in wild-type (WT) and *Ucma*-deficient mice. UCMA–collagen interactions, the effect of UCMA on aggrecanase activity, and the impact of recombinant UCMA on osteoclast differentiation were studied in vitro.**

Results. **UCMA was found to be overexpressed in human and mouse osteoarthritic cartilage. DMM-triggered cartilage changes, including increased structural damage, proteoglycan loss, and chondrocyte cell death, were aggravated in *Ucma*-deficient mice compared to WT littermates, thereby demonstrating the potential chondroprotective effects of UCMA. Moreover, UCMA inhibited ADAMTS-dependent aggrecanase activity and directly interacted with cartilage-specific collagen types. In contrast, osteoarthritis-related bone changes were significantly reduced in *Ucma*-deficient mice, showing less pronounced osteophyte formation and subchondral bone sclerosis. Mechanistically, UCMA directly promoted osteoclast differentiation in vitro.**

Conclusion. **UCMA appears to link cartilage with bone changes in osteoarthritis by supporting cartilage integrity as an endogenous inhibitor of aggrecanases while also promoting osteoclastogenesis and subchondral bone turnover. Thus, UCMA represents an important link between cartilage and bone in osteoarthritis.**

Articular cartilage degeneration is a hallmark of osteoarthritis. In contrast to other mesenchymal tissues, damaged cartilage does not regenerate sufficiently, even if the trigger for cartilage loss can be controlled by clinical intervention. To date, a number of factors involved in osteoarthritis-related cartilage degradation have been identified, including the activation of aggrecanases (ADAMTS-

Supported by the Deutsche Forschungsgemeinschaft (grant STO 824/3-1), the Bundesministerium für Bildung und Forschung (project METARTHROS), the Marie Curie project OSTEOIMMUNE, the TEAM project of the European Union, and the Innovative Medicines Initiative–funded project BTCure.

[1]Michael Stock, PhD, Stefanie Menges, PhD, Nicole Eitzinger, PhD, Maria Geßlein, Renate Botschner, BSc, Laura Wormser, BSc, Alfiya Distler, PhD, Ursula Schlötzer-Schrehardt, PhD, Katharina Dietel, MSc, Jörg Distler, MD, Christian Beyer, MD, Kolja Gelse, MD, Georg Schett, MD: Friedrich Alexander University of Erlangen–Nürnberg and Universitätsklinikum Erlangen, Erlangen, Germany; [2]Klaus Engelke, PhD, Klaus von der Mark, PhD: Friedrich Alexander University of Erlangen–Nürnberg, Erlangen, Germany; [3]Marije I. Koenders, PhD, Wim van den Berg, PhD: Radboud University, Nijmegen, The Netherlands.

Address correspondence to Michael Stock, PhD, Friedrich Alexander University of Erlangen–Nürnberg, Department of Internal Medicine 3, Rheumatology and Immunology, Universitätsklinikum Erlangen, Ulmenweg 18, 91054 Erlangen, Germany. E-mail: mstock@molmed.uni-erlangen.de.

Submitted for publication September 8, 2015; accepted in revised form January 10, 2017.

4 and ADAMTS-5) and matrix metalloproteinases (MMPs) (1,2). Moreover, chondrocytes in articular cartilage hardly proliferate, and there is no efficient external cell supply for cartilage renewal (3). Therefore, increased chondrocyte apoptosis, often observed in osteoarthritis, may promote cartilage degeneration (4–7). Together, these events lead to an imbalance in matrix turnover and, eventually, to cartilage matrix degradation. Subchondral bone sclerosis and osteophyte formation are additional prominent features of osteoarthritis (8,9). Since progression of cartilage damage and subchondral bone alterations coincide during osteoarthritis, it has been difficult to elucidate how these processes in cartilage and bone are interlinked. Nevertheless, some studies suggest that targeting bone sclerosis in osteoarthritis may be beneficial for cartilage integrity (10,11).

Despite recent advances in understanding the pathophysiology of osteoarthritis, there are currently no curative approaches available for the treatment of osteoarthritis. Therefore, unraveling the molecular mechanisms of cartilage degradation and subchondral bone alterations may provide important advances in the development of novel therapies, which would prevent further cartilage loss and—ideally—induce tissue repair. Recently, we introduced a novel chondrocyte-specific protein, upper zone of growth plate and cartilage matrix–associated protein (UCMA), that is secreted into the cartilage matrix (12–14). Whereas knockdown of *Ucma* in zebrafish embryos leads to craniofacial malformations, suggesting a role of UCMA in skeletal development, *Ucma*-deficient mice develop normally (12,15). Thus, the physiologic function of UCMA in mammals has largely remained unknown.

Since the function of extracellular matrix proteins often has been revealed only under challenging conditions, we considered that UCMA might play a relevant role in joint integrity under pathologic conditions. Therefore, we studied the impact of UCMA on osteoarthritis. In the present study, we demonstrated that UCMA protein expression is up-regulated in osteoarthritic cartilage. In a mouse model of osteoarthritis induced by surgical destabilization of the medial meniscus (DMM), *Ucma*-deficient mice exhibited exacerbated cartilage degradation compared to wild-type (WT) littermates, thereby indicating the potential chondroprotective properties of UCMA. Supporting this notion, we demonstrated that UCMA is an efficient inhibitor of aggrecanases. In contrast to this chondroprotective effect, osteoarthritis-triggered bone alterations were substantially reduced in *Ucma*-deficient mice, being attributable to reduced differentiation of osteoblasts and osteoclasts. Taken together, these findings suggest a dual role of UCMA in osteoarthritis, influencing both cartilage proteoglycan degradation and subchondral bone changes.

MATERIALS AND METHODS

Mice. All experiments were performed with the approval of the local ethics authorities (University of Erlangen–Nuremberg and the Government of Mittelfranken, Ansbach, Germany) and according to the regulations of the animal facilities in Germany.

Induction of experimental osteoarthritis in mice. Sham surgery and DMM through surgical transection of the medial meniscotibial ligament were performed in mice at ages 8 weeks or 12 weeks, as previously described (16). DMM and sham operations were carried out in separate groups, with both legs undergoing surgery. At 4 weeks postsurgery (n = 3 or n = 4 mice per group) or 8 weeks postsurgery (n = 5 or n = 6 mice per group), mice were killed and frontal paraffin sections (4 μm) of the knees were prepared. The second knee was used for RNA preparation or micro–computed tomography (micro-CT) analyses.

Human cartilage samples. Samples of human cartilage were obtained from the knee joints of healthy human subjects during autopsy (n = 3). Osteoarthritic cartilage specimens were obtained from osteoarthritis patients (n = 3) who had undergone total knee joint arthroplasty at the University Hospital Erlangen. Each patient gave informed consent prior to surgery, and the institutional ethics committee approved the study protocol.

Histology. Scoring of the histologic severity of osteoarthritis was performed according to Osteoarthritis Research Society International (OARSI) recommendations, in which all 4 quadrants of the stifle joint (medial and lateral femoral condyles, and medial and lateral tibial plateaus; 8 of the most affected sections per joint) were scored in multiple-step sections through the complete joint (17). Maximal scores from all 4 quadrants were cumulated, as reported previously (16). Proteoglycan loss was quantified by determining the proportion of articular cartilage that was negative for Safranin O staining (17). Osteophytes, subchondral bone plate thickness, and bone volume of the primary spongiosa were assessed on Safranin O–stained or hematoxylin and eosin–stained sections of the articular cartilage. Osteoclast and osteoblast numbers were determined on tartrate-resistant acid phosphatase (TRAP)–stained and Goldner's trichrome–stained tissue sections. Quantification was carried out using ImageJ software or an OsteoMeasure system (OsteoMetrics) (16,18). Micro-CT analysis of the tibiae was performed in a manner as recently described (18). Bone volume was measured in the trabecular bone of the metaphysis (the first 4 mm below the primary spongiosa). All analyses were performed in a blinded manner (n = 3–4 mice per group at 4 weeks postsurgery, n = 5–6 mice per group at 8 weeks postsurgery).

Immunohistochemistry. Immunohistochemical detection of UCMA in the cartilage samples was performed as previously reported (12). After antigen retrieval with hyaluronidase and blocking, detection of UCMA was performed using a UCMA-specific antibody (ab-2, 1:500) and a SignalStain Boost immunohistochemistry detection reagent (HRP, rabbit; Cell Signaling Technologies) with diaminobenzidine. NITEGE and VDIPEN neoepitopes were detected similarly, using a rabbit anti-NITEGE antibody (Ab1320, 1:1,000; IBEX Pharmaceuticals) or affinity-purified anti-VDIPEN antibody (19), followed by staining with a biotinylated goat anti-rabbit IgG antibody or avidin–peroxidase (Vector Laboratories), respectively. Cell death analysis in sections of articular cartilage was performed by TUNEL staining using an In Situ Cell Death Detection Kit (Roche) (n = 3–4 mice per group at 4 weeks postsurgery, n = 5–6 mice per group at 8 weeks postsurgery).

Gene expression analyses. Total RNA was extracted from murine epiphyseal cartilage (n = 3 mice per group), total knee joints (n = 5 mice per group), or articular cartilage (n = 6 mice per group) using an RNeasy Fibrous Tissue Mini Kit (Qiagen). Complementary DNA was synthesized using SuperScript II reverse transcriptase (Invitrogen), and messenger RNA (mRNA) expression of each gene, relative to the values for *cyclophilin A*, was quantified by real-time reverse transcription–polymerase chain reaction, as previously described (13) (for a list of the primer sequences, see Supplementary Table 1, available on the *Arthritis & Rheumatology* web site at http://onlinelibrary.wiley.com/doi/10.1002/art.ART40042/abstract).

Protein interaction studies. Recombinant His-FLAG–tagged UCMA was episomally expressed in HEK 293–Epstein-Barr nuclear antigen cells and purified from conditioned medium by affinity chromatography on nickel–nitrilotriacetic acid–Sepharose (Qiagen), as reported previously (13). Different collagen types (all derived from chicken sources by pepsin extraction) were immobilized on PVDF membranes by vacuum blotting. After blocking with bovine serum albumin (BSA), the membranes were incubated in recombinant UCMA (100 ng/ml); after washing, bound UCMA was detected using rabbit anti-UCMA (UCMA-1, 1:1,000) or mouse anti-FLAG (1:1,000) antibodies (both from Sigma-Aldrich) or an anti-rabbit or anti-mouse horseradish peroxidase (HRP)–conjugated IgG antibody, followed by detection with an enhanced chemiluminescence (ECL)–based technique (13). Replacement of UCMA solution or the anti-UCMA antibody with BSA solution did not reveal significant signals.

Pulldown assays were performed as previously reported (20), in which 1 mg/ml type II collagen or BSA was coupled to CNBr-activated Sepharose beads. Thereafter, 20 μl BSA–Sepharose or type II collagen–Sepharose beads was incubated with 2 μg UCMA in 1 ml pulldown buffer (20 m*M* Tris, pH 8.0, 25 m*M* NaCl, 1.5 m*M* $MgCl_2$, 1 m*M* EGTA, 1% Triton X-100, 1 m*M* dithiothreitol) overnight at 4°C. After washing, coprecipitated UCMA was detected by Western blotting using a mouse anti-FLAG antibody. For solid-phase binding assays, enzyme-linked immunosorbent assay (ELISA) plates were coated with BSA (blanks; 10 μg/well) or collagens (1–10,000 ng/well). After blocking with BSA, the plates were incubated with UCMA (100 ng/ml). Bound UCMA was detected using a mouse anti-FLAG antibody (1:1,000) or an HRP-conjugated anti-mouse IgG antibody, followed by detection with an ABTS-based colorimetric technique at 405 nm.

Cartilage explant cultures. Mouse articular cartilage explants were obtained from the femoral heads of 3-week-old *Ucma*-deficient mice and WT littermates, as reported previously (21). Each cartilage specimen was cultured in 100 μl Dulbecco's modified Eagle's medium–Ham's F-12 for 1–3 days, with or without stimulants. To study the degradation of collagen and aggrecan, cartilage explants were treated with 10 ng/ml interleukin-1β (IL-1β) for 3 days (n = 5 samples) or with 50 n*M* recombinant MMP-1 (n = 2–3 samples) or 20 n*M* recombinant ADAMTS-5 (n = 5 samples or n = 3 samples) (all from PeproTech) for 24 hours (21,22). Afterward, conditioned medium was collected and cartilage specimens were extracted with 125 μg/ml papain at 60°C overnight to release residual collagens and proteoglycans. Quantification of collagens was performed through the detection of hydroxyproline, using a QuickZyme Biosciences Total Collagen Assay. The amount of released collagen was normalized against the total collagen content in the conditioned medium and papain extracts.

Proteoglycans were quantified by applying a dimethylmethylene blue–based dye binding assay (21), in which 250 μl dye solution (16 mg/ml dimethylmethylene blue in 0.5% ethanol, 2 gm/liter sodium formate, 0.2% formic acid) was added to 40 μl of sample, and absorption was measured at 595 nm, with a reference wavelength of 655 nm. The amount of released proteoglycan was normalized against the total proteoglycan content in the conditioned medium and papain extracts.

Aggrecanase activity assay. UCMA-dependent inhibition of aggrecanase activity was performed using an Aggrecanase Activity ELISA system (MD Biosciences) according to the manufacturer's instructions. A synthetic aggrecan interglobular domain was subjected to proteolytic cleavage with 0.75 n*M* recombinant ADAMTS-4 (MD Biosciences) or 1 n*M* ADAMTS-5 (PeproTech) in the presence of varying amounts of recombinant UCMA for 15 minutes at 37°C. Finally, aggrecan cleavage products were quantified using an ELISA that detects the aggrecan neoepitope ARGSVIL.

Osteoclast differentiation assays. Osteoclast progenitors were isolated from the bone marrow of 6-week-old C57BL/6 mice. For differentiation of osteoclasts, 5×10^5 cells/cm^2 were cultured in α-minimum essential medium containing 10% fetal calf serum, 1% penicillin–streptomycin, 30 ng/ml macrophage colony-stimulating factor (M-CSF) (PeproTech), 10 ng/ml RANKL (PeproTech), and varying doses of recombinant UCMA (13). After 5 days of differentiation, TRAP staining was performed using a leukocyte acid phosphatase kit (Sigma-Aldrich).

For analysis of osteoclastogenesis-related signaling pathways, the cells were differentiated for only 3 days. Thereafter, the cells were starved overnight in serum-free medium before stimulation with recombinant UCMA. For coculture experiments, WT mouse bone marrow cells were differentiated with M-CSF and only 5 ng/ml RANKL in the presence of femoral articular cartilage explants from 3-week-old *Ucma*-deficient and WT mice (n = 3 mice per group).

Western blotting. Analyses by Western blotting were performed as reported previously (23). Cell lysates were resolved by sodium dodecyl sulfate–polyacrylamide gel electrophoresis. After blotting, levels of phosphorylated and total IKKα/β, p38 MAPK, and ERK-1/2 were detected using their respective primary rabbit antibodies (each 1:1,000; Cell Signaling Technologies), an HRP-conjugated anti-rabbit IgG antibody, and an ECL-based detection technique.

Statistical analysis. Data are presented as the mean ± SEM. Statistically significant differences between 2 groups were evaluated by Mann-Whitney test. When more than 2 groups were compared, one-way analysis of variance and Tukey's test for multiple comparisons were used, after confirming normal distribution of the data using the Kolmogorov-Smirnov test. Results were analyzed using GraphPad Prism software.

RESULTS

Overexpression of UCMA in osteoarthritic cartilage. We have previously demonstrated the cartilage-specific expression of UCMA during mouse development (12,13). In the current study, we confirmed this finding using reporter mice that harbor a *lacZ* cassette replacing

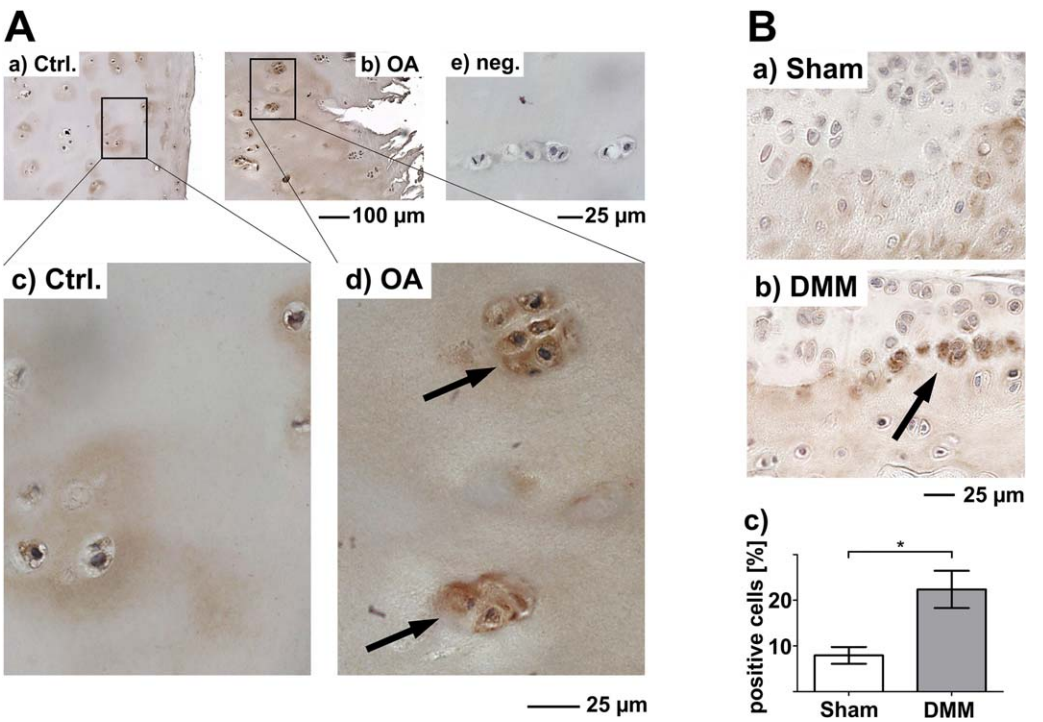

Figure 1. Overexpression of upper zone of growth plate and cartilage matrix–associated protein (UCMA) in osteoarthritic (OA) cartilage. **A,** Human cartilage samples from a healthy control (Ctrl.) (parts a and c) and a patient with knee OA (parts b and d) were analyzed by immunohistochemistry for the expression of UCMA. To confirm the specificity of the immunohistochemical signals, a negative (neg.) control without primary antibody is shown (part e). **Arrows** in part d indicate chondrones (chondrocyte clusters) with high UCMA expression. Parts c and d are higher-magnification views of the boxed areas in parts a and b. **B,** UCMA expression was analyzed by immunohistochemistry at 8 weeks postsurgery on tibial articular cartilage samples from a sham-operated mouse (part a) and a mouse with OA induced by destabilization of the medial meniscus (DMM) (part b). In part b, the **arrow** indicates high UCMA–expressing chondrocytes. UCMA-positive cells were quantified in the murine tibial articular cartilage 8 weeks after sham or DMM surgery (part c). Results are the mean ± SEM of ≥5 mice per group (~300–500 cells per joint). * = $P < 0.05$ by Mann-Whitney test. Color figure can be viewed in the online issue, which is available at http://onlinelibrary.wiley.com/doi/10.1002/art.40042/abstract.

exon 1 of the *Ucma* gene (12). Only chondrocytes, but not osteoblasts or osteoclasts, were found to express β-galactosidase, an indicator of *Ucma* expression (see Supplementary Figures 1A–C, available on the *Arthritis & Rheumatology* web site at http://onlinelibrary.wiley.com/doi/10.1002/art.ART40042/abstract). Moreover, expression of *Ucma* mRNA was negligible in mouse calvarial cells, tibial cortical bone, or osteoclasts. Barely detectable *Col2a1* expression and substantial levels of *Col1a1* and *Trap* confirmed the purity (i.e., lack of chondrocyte contamination) of the osteoblast, bone, and osteoclast samples (see Supplementary Figures 1D–I, http://onlinelibrary.wiley.com/doi/10.1002/art.ART40042/abstract).

UCMA protein was found in both the articular cartilage and growth plate cartilage, but not in the bone, of adult mice. While *Ucma*-expressing chondrocytes appeared to be located primarily within the resting and proliferative zones or above the tidemark, UCMA protein was also detected in calcified cartilage in the vicinity of the bone (see Supplementary Figure 1J, http://onlinelibrary.wiley.com/doi/10.1002/art.ART40042/abstract).

To investigate a potential role of UCMA in osteoarthritis, we studied UCMA expression in healthy and osteoarthritic human articular cartilage. While *Ucma* mRNA levels did not significantly differ between healthy and osteoarthritic human cartilage samples (data not shown), UCMA protein was substantially overexpressed in human osteoarthritic cartilage, particularly at chondrones (chondrocyte clusters) in severely affected cartilage areas (Figure 1A, part d). In the mouse model, induction of osteoarthritis by DMM in mice at ages 8 weeks (Figure 1B) or 12 weeks (Supplementary Figures 2A–D, available on the *Arthritis & Rheumatology* web site at http://onlinelibrary.wiley.com/doi/10.1002/art.ART40042/abstract) also resulted in overexpression of UCMA protein at 4 weeks after surgery (Supplementary Figures 2A and B), and this was even more pronounced at 8 weeks after surgery (Figure 1B and Supplementary Figures 2C and D). Control immunohistochemical analyses of tissue

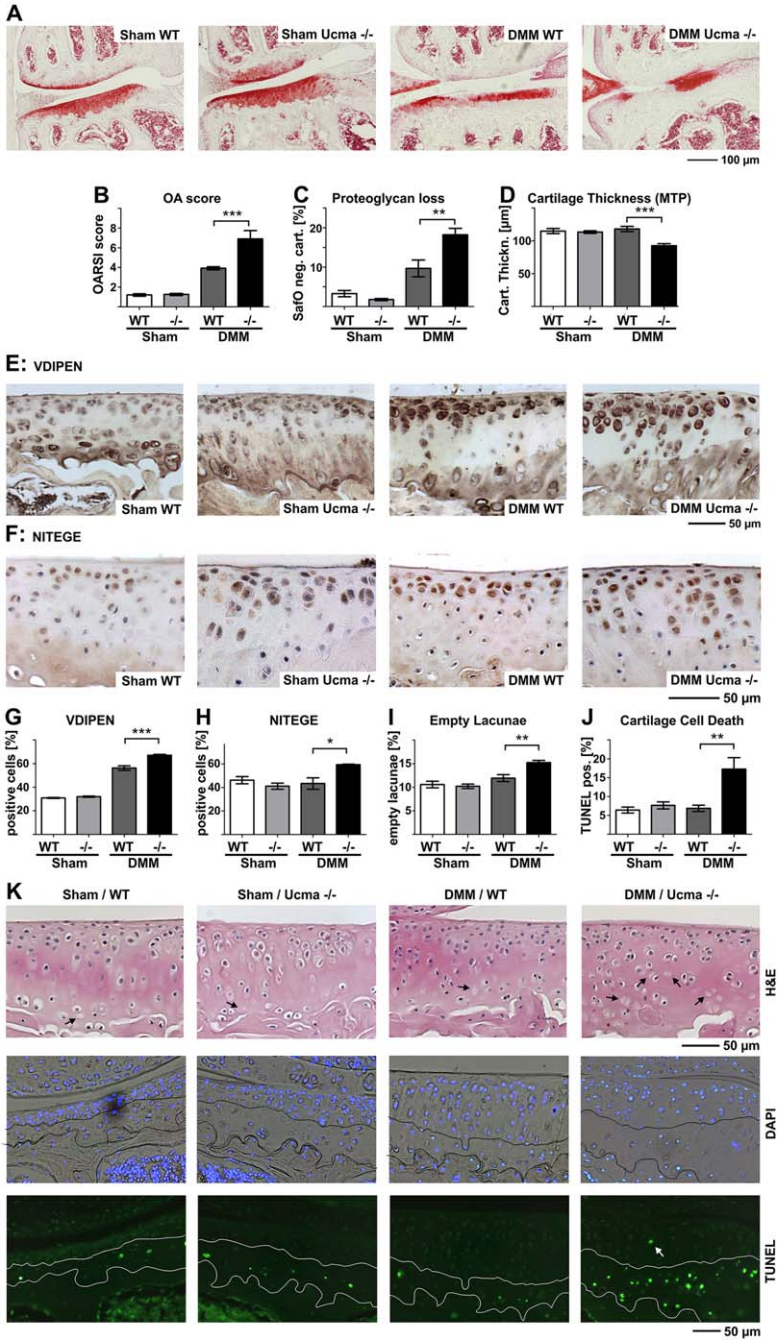

Figure 2. Increased cartilage damage during experimental OA in *Ucma*-deficient mice. OA was induced by DMM surgery in 8-week-old mice. **A** and **B,** Safranin O–stained frontal sections of the knees of sham-operated or DMM-operated wild-type (WT) and *Ucma*-deficient mice were assessed for histologic severity of OA **(A)**, with severity scores assigned based on Osteoarthritis Research Society International (OARSI) recommendations **(B)**. **C** and **D,** OA-related proteoglycan loss **(C)** and changes in articular cartilage thickness at the medial tibial plateau (MTP) **(D)** were assessed after sham or DMM surgery in WT and *Ucma*-deficient mice. **E–H,** Levels of the matrix metalloproteinase–generated VDIPEN and ADAMTS-generated NITEGE aggrecan neoepitopes were assessed by immunohistochemistry **(E** and **F)** and quantified as the percentage of positive cells **(G** and **H)**. **I–K,** The extent of cell death was assessed in mouse tibial articular cartilage samples by determining the number of empty lacunae in hematoxylin and eosin (H&E)–stained sections **(I** and **K)** and by TUNEL staining for apoptotic cells **(J** and **K)**. In **K,** the lower line delineates the cement line, while the upper line indicates the tidemark. **Black arrows** indicate empty lacunae, and the **white arrow** indicates a TUNEL+ chondrocyte above the tidemark. Counterstaining was done with DAPI. Results are the mean ± SEM of ≥5 mice per group (~300–500 chondrocytes per joint). $* = P < 0.05$; $** = P < 0.01$; $*** = P < 0.001$. See Figure 1 for other definitions.

sections from *Ucma*-deficient mice confirmed the signal specificity (Supplementary Figure 1J, http://onlinelibrary.wiley.com/doi/10.1002/art.ART40042/abstract).

Aggravation of osteoarthritis-triggered cartilage damage in *Ucma*-deficient mice. We next studied the functional role of UCMA in osteoarthritic mice. Osteoarthritis was induced by DMM in 8-week-old *Ucma*-deficient and WT mice. Eight weeks after surgery, *Ucma*-deficient mice exhibited significantly higher OARSI scores for osteoarthritis severity compared to WT littermates (Figures 2A and B), along with increased proteoglycan loss (Figure 2C) and reduced articular cartilage thickness (Figure 2D). DMM surgery in 12-week-old mice resulted in similar findings at 4 and 8 weeks after surgery (see Supplementary Figure 3, available on the *Arthritis & Rheumatology* web site at http://onlinelibrary.wiley.com/doi/10.1002/art.ART40042/abstract). These findings demonstrate that *Ucma*-deficient mice are more prone to osteoarthritis-triggered cartilage damage than that seen in WT mice, indicating that UCMA has potential chondroprotective effects.

Ucma-deficient mice with osteoarthritis exhibited significantly decreased levels of mRNA for the tissue inhibitor of metalloproteinases 2 (TIMP-2) gene, but the expression of other anabolic and catabolic chondrocyte genes, such as *Aggrecan*, *Col2a1*, *Col10a1*, *ADAMTS4*, *ADAMTS5, MMP3*, *MMP9*, *MMP13*, *Timp1*, and *Timp3*, were not altered in the epiphyseal cartilage from newborn mice or in the complete knee joints or articular knee cartilage from mice at 8 weeks after surgery (results in Supplementary Figures 4A–L, Supplementary Figures 5A–J, and Supplementary Figures 6A–K, available on the *Arthritis & Rheumatology* web site at http://onlinelibrary.wiley.com/doi/10.1002/art.ART40042/abstract). Nevertheless, increased levels of the collagenase- and aggrecanase-specific aggrecan cleavage products VDIPEN (Figures 2E and G) and NITEGE (Figures 2F and H) in articular cartilage confirmed that DMM-induced aggrecan degradation was enhanced in *Ucma*-deficient mice, which is consistent with our observations of increased proteoglycan loss in these mice. Thus, UCMA may inhibit proteoglycan-degrading enzymes such as aggrecanases.

Protection of cartilage from ADAMTS-dependent aggrecan cleavage and inhibition of ADAMTS-dependent aggrecanase activity by UCMA. To investigate whether UCMA may affect the stability of cartilage by interfering with proteolytic activity, we explanted femoral articular cartilage from 3-week-old WT and *Ucma*-deficient mice and analyzed the susceptibility of the cartilage to IL-1β–induced degradation after 3 days of in vitro culture. IL-1β–induced proteoglycan release was significantly higher in cartilage explants from *Ucma*-deficient mice than in explants from WT littermates (Figure 3A, part a).

We next tested the direct susceptibility of the articular cartilage to proteolytic cleavage, in analyses of cartilage explants from *Ucma*-deficient mice and WT littermates. Cartilage explants were subjected to collagen or aggrecan cleavage by recombinant MMP-1 or ADAMTS-5. WT and *Ucma*-deficient mouse cartilage did not differ in its susceptibility to MMP-1–mediated collagen cleavage (Figure 3B, part e), but *Ucma*-deficient mouse cartilage explants exhibited a significantly higher level of ADAMTS-5–triggered proteoglycan cleavage (Figure 3A, part b).

In order to investigate whether UCMA directly affects the proteolytic activity of ADAMTS aggrecanases, a synthetic peptide containing an ADAMTS cleavage site was subjected to ADAMTS-4 or ADAMTS-5 digestion in the absence or presence of recombinant UCMA. Aggrecanase activity was determined by the generation of an ADAMTS-specific aggrecan cleavage product, ARGSVIL. In fact, UCMA blocked the proteolytic activity of both ADAMTS-4 (Figure 3A, part c) and ADAMTS-5 (Figure 3A, part d) in a dose-dependent manner, reaching up to ~90% inhibition, suggesting that UCMA serves as a physiologic inhibitor of aggrecanases.

Direct interaction of UCMA with collagens in the cartilage matrix. Although our data show that UCMA does not inhibit collagen degradation by MMP-1, the possibility exists that UCMA may protect cartilage collagen fibrils indirectly by masking proteolytic cleavage sites. We had previously shown, by electron microscopy, that UCMA is associated with collagen fibrils in the cartilage matrix (13). We confirmed this finding in the present study, using another antibody (UCMA ab2) for immunogold labeling and subsequent detection by electron microscopy (see results in Supplementary Figure 7, available on the *Arthritis & Rheumatology* web site at http://onlinelibrary.wiley.com/doi/10.1002/art.ART40042/abstract).

To investigate whether UCMA directly binds to collagens, we immobilized different collagen types on PVDF membranes and incubated these blots with recombinant FLAG-tagged UCMA. Detection of bound UCMA using an anti-FLAG or anti-UCMA antibody revealed that UCMA directly interacts with cartilage-specific collagens, including type II and type XI collagens. In contrast, UCMA did not bind to type I collagen, which is the typical process seen in bone, tendon, and skin (Figure 3B, parts a and b).

UCMA binding to type II collagen was also confirmed in a pulldown assay using type II collagen–coupled Sepharose beads (Figure 3B, part c). Solid-phase assays using collagen-coated ELISA plates and UCMA in the liquid phase further confirmed these findings (Figure 3B, part d), suggesting that UCMA may be integrated in the cartilage matrix.

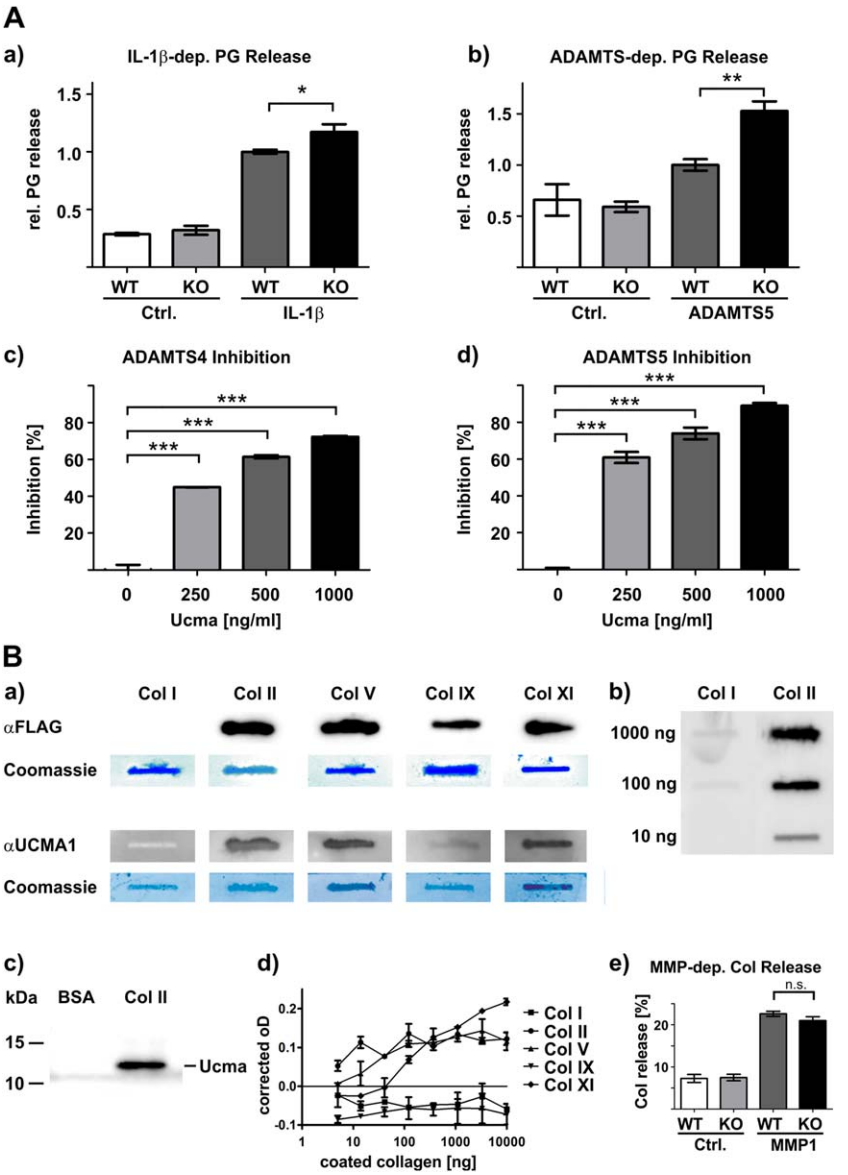

Figure 3. Blockade of ADAMTS-triggered aggrecanolysis by UCMA, and interaction of UCMA with type II collagen (Col II). **A,** Effects of UCMA on ADAMTS-dependent aggrecanase activity were assessed in articular cartilage explants from wild-type (WT) mice (n = 5) and *Ucma*-deficient (knockout [KO]) mice (n = 5 or n = 3) after culture with 10 ng/ml interleukin-1β (IL-1β) for 3 days (part a) or with 20 n*M* ADAMTS-5 for 24 hours (part b). IL-1β–dependent (dep.) or ADAMTS-dependent proteoglycan (PG) release into the medium was determined relative (rel.) to total proteoglycan content. The activity of ADAMTS-4 (part c) and ADAMTS-5 (part d) in the presence of 0–1,000 ng/ml UCMA was determined using an enzyme-linked immunosorbent assay (ELISA)–based system. Results are the mean ± SEM. **B,** Collagen types were blotted onto a PVDF membrane and incubated with a recombinant His-FLAG–tagged UCMA. Binding of UCMA to the various collagens was detected with an anti-FLAG antibody (part a) or an anti-UCMA antibody (parts a and b). Staining with Coomassie blue demonstrates equal loading. Coprecipitation of FLAG-tagged UCMA with bovine serum albumin (BSA)– or type II collagen–coupled Sepharose beads was detected by Western blotting using an anti-FLAG antibody (part c). The various collagens were coated to ELISA plates at the indicated doses and incubated with UCMA, and bound UCMA was detected with an anti-FLAG antibody and a colorimetric detection system (part d). Results are the mean ± SEM of 3 independent experiments. Articular cartilage explants from WT mice (n = 3) and *Ucma*-deficient mice (n = 2) were incubated with 50 n*M* matrix metalloproteinase 1 (MMP-1) for 24 hours, and the percentage of released hydroxyproline (measured as collagen was determined in relation to total hydroxyproline content (part e). Results are the mean ± SEM. * = $P < 0.05$; ** = $P < 0.01$; *** = $P < 0.001$. NS = not significant (see Figure 1 for other definitions). Color figure can be viewed in the online issue, which is available at http://onlinelibrary.wiley.com/doi/10.1002/art.40042/abstract.

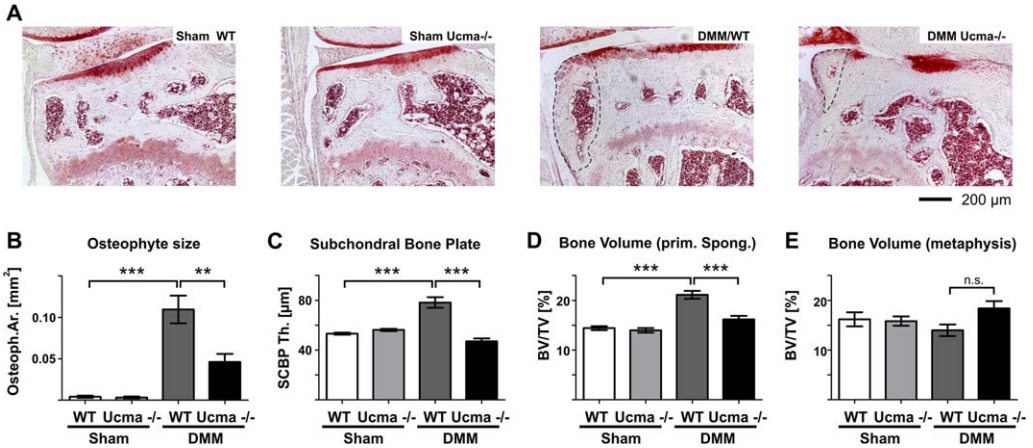

Figure 4. Development of substantially reduced levels of bone sclerosis in *Ucma*-deficient mice with experimental OA. **A,** The subchondral bones of sham-operated or DMM-operated wild-type (WT) and *Ucma*-deficient mice were analyzed for histomorphometric features. **B,** Osteophyte size at the medial tibia was determined in each group of mice. **C–E,** Subchondral bone plate thickness (SCBP Th.) (**C**), bone volume (measured as bone volume/total volume [BV/TV]) of the primary spongiosa (prim. Spong.) (**D**), and trabecular bone volume (BV/TV) of the metaphysis (the first 4 mm below the primary spongiosa) (**E**) were determined by micro–computed tomography in each group of mice. Results are the mean ± SEM of ≥5 mice per group. ** = $P < 0.01$; *** = $P < 0.001$. NS = not significant (see Figure 1 for other definitions). Color figure can be viewed in the online issue, which is available at http://onlinelibrary.wiley.com/doi/10.1002/art.40042/abstract.

Increased chondrocyte cell death in *Ucma*-deficient mice with osteoarthritis. Enhanced chondrocyte apoptosis can also contribute to osteoarthritis-related cartilage damage. To estimate the number of dying and dead chondrocytes in the articular cartilage of *Ucma*-deficient and WT mice after sham surgery or DMM surgery, we quantified the numbers of empty lacunae and TUNEL-positive cells. Intriguingly, DMM-operated *Ucma*-deficient mice exhibited a significant increase in the number of empty lacunae (Figures 2I and K) and also a significant increase in the number of TUNEL-positive cells (Figures 2J and K). While most of the TUNEL-positive cells were located in the calcified zone, we also observed more TUNEL-positive cells in the noncalcified cartilage from *Ucma*-deficient mice after DMM surgery.

Alleviation of osteophyte formation and subchondral bone sclerosis by *Ucma* deficiency during experimental osteoarthritis. Osteophyte formation and bone sclerosis are hallmarks of osteoarthritis. Overexpression of UCMA in osteoarthritic articular cartilage and its accumulation at the bone–cartilage interface suggest that UCMA may also influence subchondral bone during osteoarthritis. Therefore, we investigated the subchondral bone of WT and *Ucma*-deficient mice after sham or DMM surgery. Profound osteophyte formation was observed at 8 weeks after DMM surgery in 8-week-old WT mice. In *Ucma*-deficient mice, however, osteophyte formation was substantially reduced after DMM surgery (Figures 4A and B). Moreover, we observed significant thickening of the subchondral bone plate and increased bone volume in the tibial primary spongiosa in 8-week-old WT animals after DMM surgery, whereas these parameters remained unchanged in DMM-operated *Ucma*-deficient mice (Figures 4C and D). Similar findings were seen in 12-week-old mice at 8 weeks postsurgery, whereas at 4 weeks postsurgery, differences in bone in 12-week-old mice were not yet detectable (see results in Supplementary Figures 8A–H, available on the *Arthritis & Rheumatology* web site at http://onlinelibrary.wiley.com/doi/10.1002/art.ART40042/abstract).

Bone volume in the metaphyseal region of the tibia, excluding the primary spongiosa, was not significantly altered by DMM surgery in either the WT or *Ucma*-deficient mice (Figure 4E). These results demonstrate that *Ucma* deficiency alleviates subchondral bone sclerosis in DMM-induced osteoarthritis.

The numbers of osteoblasts and osteoclasts, as well as the osteoblast and osteoclast surface, were significantly increased in WT mice during experimental osteoarthritis, indicating that bone remodeling activity is enhanced in DMM-operated joints. In contrast, *Ucma*-deficient mice did not exhibit elevated osteoblast or osteoclast counts after DMM surgery (Figures 5A–C and E–G). The increase in osteoblast counts during osteoarthritis in WT mice, but not in *Ucma*-deficient animals, was also reflected by the elevated *osteocalcin* mRNA levels in the knee joint tissue from WT mice compared to *Ucma*-deficient mice after DMM surgery (Figure 5D). Interestingly, however, there were no significant changes in the levels of mRNA for RANKL and osteoprotegerin (OPG) in associaton with the changes in osteoclast numbers (Figures 5H and I). Thus, the RANKL:OPG ratio may not be the decisive factor responsible for changes in

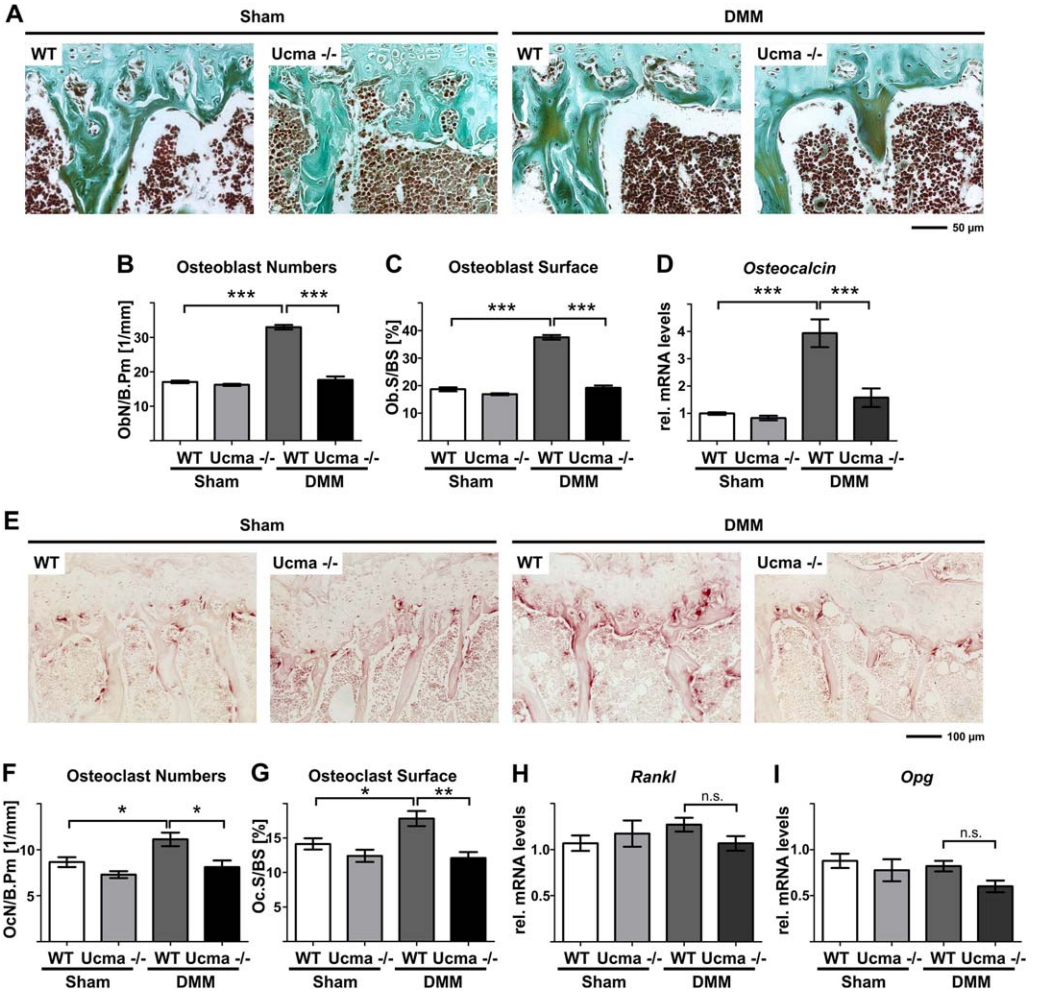

Figure 5. Reduced numbers of osteoblasts and osteoclasts during experimental OA in *Ucma*-deficient mice. Osteoblast and osteoclast counts were determined by histomorphometry in the primary spongiosa and proximal metaphysis of wild-type (WT) and *Ucma*-deficient mice after sham surgery or DMM surgery. **A** and **E,** Tibial sections were stained for osteoblasts and osteoclasts with Goldner's trichrome **(A)** or tartrate-resistant acid phosphatase **(E)**. **B–D,** Osteoblast numbers (measured as osteoblasts per bone perimeter [ObN/BPm]) (**B**), osteoblast surface per bone surface (ObS/BS) (**C**), and expression of the *osteocalcin* gene **(D)** were determined in each group of mice postsurgery. **F–I,** Osteoclast numbers (measured as osteoclasts per bone perimeter [OcN/BPm]) (**F**), osteoclast surface per bone surface (OcS/BS) (**G**), and expression of *Rankl* **(H)** and *Opg* **(I)** were determined in each group of mice postsurgery. Relative (rel.) gene expression was determined by reverse transcription–polymerase chain reaction. Results are the mean ± SEM of ≥5 mice per group. $* = P < 0.05$; $** = P < 0.01$; $*** = P < 0.001$. NS = not significant (see Figure 1 for other definitions).

osteoclast numbers after DMM in mice. These data suggest an UCMA-dependent, but RANKL/OPG-independent, mechanism that promotes osteoclastogenesis during experimental osteoarthritis.

Promotion of osteoclast differentiation by UCMA in vitro. To investigate whether UCMA directly affects osteoclastogenesis, we studied the impact of UCMA on osteoclast differentiation in vitro. When WT mouse bone marrow cells were cocultured with WT mouse articular cartilage explants, differentiation of osteoclasts was substantially promoted in close proximity to the explants. This effect decreased with increasing distance from the explants, suggesting a gradient of effect. In cocultures with cartilage explants from *Ucma*-deficient mice, however, cartilage-dependent promotion of osteoclastogenesis was substantially reduced (Figures 6A–C). These data indicate that UCMA gets released from cartilage at biologically active levels, which, although too low to detect biochemically (see Supplementary Figure 9, available on the *Arthritis & Rheumatology* web site at http://onlinelibrary.wiley.com/doi/10.1002/art.ART40042/abstract), can support the differentiation of osteoclasts outside the cartilage compartment. Accordingly, recombinant

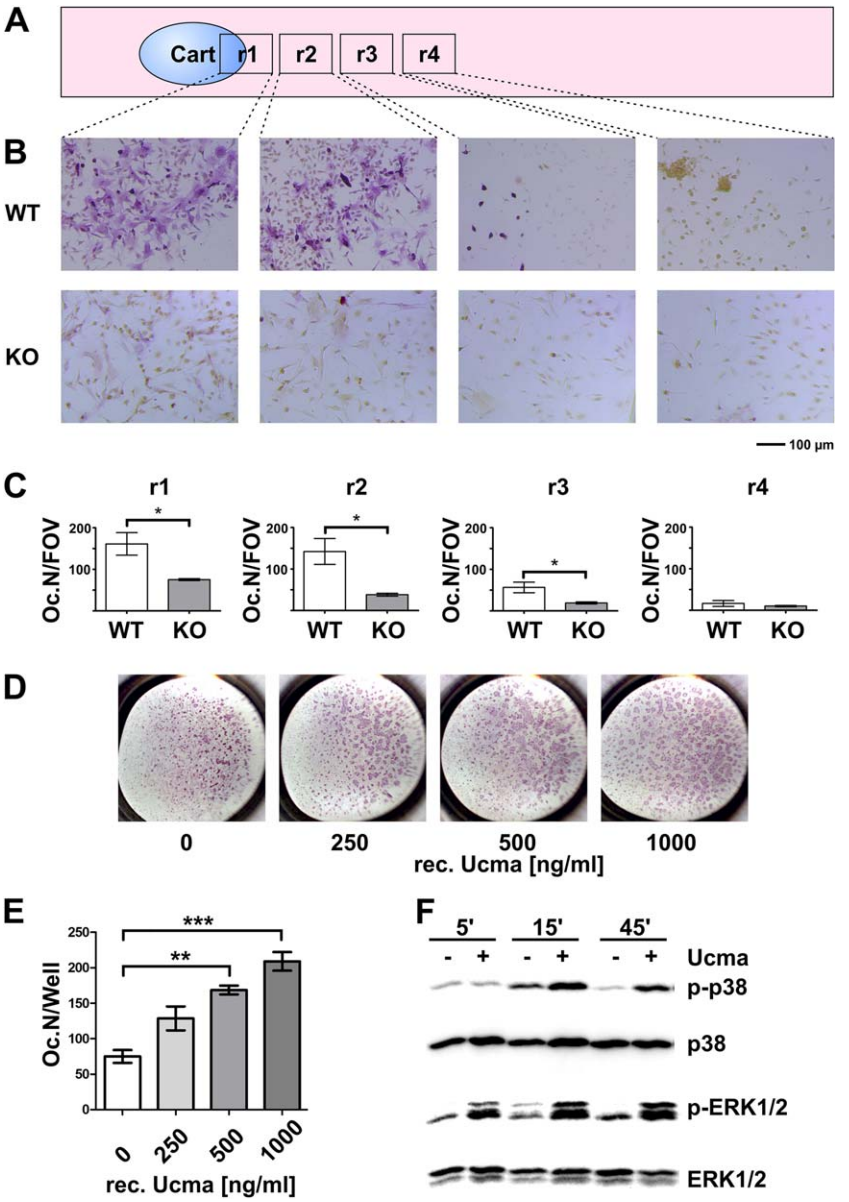

Figure 6. Promotion of osteoclast differentiation in vitro by upper zone of growth plate and cartilage matrix–associated protein (UCMA). **A–C,** Wild-type (WT) mouse bone marrow–derived osteoclast precursors were cocultured with cartilage explants from WT or *Ucma*-deficient (knockout [KO]) mice (n = 3 mice per group). Osteoclast numbers were evaluated by tartrate-resistant acid phosphatase (TRAP) staining at various distances from the cartilage explants (Cart radius 1–4 [r1–4]) **(A)**. Osteoclast–cartilage explant cocultures were assessed by TRAP staining at r1–4 **(B)**, and osteoclasts were quantified as the osteoclast number per field of vision (OcN/FOV) at r1–4 **(C)**. **D** and **E,** Induction of osteoclastogenesis by recombinant UCMA was evaluated using TRAP staining of osteoclasts **(D)** and quantification of TRAP-positive multinucleated cells **(E)** in cell cultures with various doses of recombinant (rec.) UCMA. **F,** Western blotting was used to assess the levels of total and phosphorylated p38 MAP kinase and ERK-1/2 in osteoclast precursors incubated with recombinant UCMA (500 ng/ml) for the indicated periods of time (in minutes). All experiments were repeated at least twice. Results are the mean ± SEM. $* = P < 0.05$; $** = P < 0.01$; $*** = P < 0.001$. Color figure can be viewed in the online issue, which is available at http://onlinelibrary.wiley.com/doi/10.1002/art.40042/abstract.

UCMA also promoted osteoclastogenesis in vitro (Figures 6D and E). We did not detect interactions between UCMA and RANKL/OPG (results in Supplementary Figure 10, available on the *Arthritis & Rheumatology* web site at http://onlinelibrary.wiley.com/doi/10.1002/art.ART40042/abstract), which might have explained this finding.

Moreover, UCMA induced the phosphorylation of ERK-1/2 and p38 MAPK, but not that of IKKα/β, in

osteoclast precursors in a RANKL-independent manner (Figure 6F). This finding indicates that UCMA may have direct activating effects on osteoclasts via the stimulation of signaling pathways, which thereby promotes osteoclastogenesis. These findings support the notion that UCMA induces subchondral bone turnover during osteoarthritis.

DISCUSSION

UCMA (also termed Gla-rich protein) has been reported to accumulate in calcified cartilage during osteoarthritis (24). Herein, we extended this concept, showing that UCMA is particularly overexpressed in newly forming chondrocyte clusters in the osteoarthritic cartilage. So far, the physiologic role of UCMA is largely unknown. During zebrafish development, knockdown of *Ucma* disturbs skeletal development and leads to craniofacial malformations (15). In contrast, ablation of *Ucma* in the mouse does not affect skeletal development (12).

In this study, we challenged articular cartilage integrity through surgical induction of osteoarthritis. Observations of exacerbated cartilage damage in *Ucma*-deficient mice suggest that UCMA has a chondroprotective effect. This finding also demonstrates that mechanisms compensating for the loss of UCMA during normal cartilage development cannot countervail the loss of UCMA during osteoarthritis. Interestingly, aggravated cartilage damage in *Ucma*-deficient mice was not associated with significant changes in the expression of anabolic or catabolic cartilage genes, except for a decrease in *Timp2* mRNA expression. Reduced *Timp2* expression may contribute to the cartilage phenotype seen in *Ucma*-deficient mice, since TIMP-2 can inhibit MMPs, and *Timp2*-deficient mice develop aggravated DMM-induced cartilage damage (20,21). However, in *Timp2*-deficient mice, augmented cartilage degradation was found to be associated with increased angiogenesis and osteophyte formation, both of which are events that are unlikely to result from enhanced cartilage proteolysis in the absence of TIMP-2 (21). In contrast, in *Ucma*-deficient mice, osteophyte formation was substantially reduced. Moreover, ADAMTS-related aggrecan cleavage was increased. Studies have shown that TIMP-2 does not block ADAMTS activity (20,25), and therefore, decreased *Timp2* mRNA levels cannot fully explain the observed phenotype in *Ucma*-deficient osteoarthritic mice.

We hypothesized that UCMA may exert its chondroprotective effect, at least partially, by increasing the resistance of the cartilage matrix against proteolytic degradation. In fact, we had previously shown that chondrocytes secrete UCMA into the cartilage matrix, where it colocalizes with collagen fibrils (13). Herein we demonstrated that UCMA directly interacts with different cartilage-specific collagen types, including type II collagen. Several studies have indicated that the ablation of collagen-binding cartilage matrix proteins increases the vulnerability of articular cartilage. For example, deletion of matrilin 3 or type IX collagen in mice and mutations in cartilage oligomeric matrix protein in humans will result in early onset of osteoarthritis (26–29). Accordingly, *Ucma*-deficient mouse cartilage was more susceptible to IL-1β–induced proteoglycan degradation, thus supporting our finding of increased proteoglycan loss in the articular cartilage of *Ucma*-deficient mice during experimental osteoarthritis.

Moreover, while *Ucma* deficiency did not directly affect MMP-triggered collagen degradation, *Ucma*-deficient mouse cartilage was significantly more sensitive to ADAMTS-5–dependent aggrecan cleavage. This effect could be explained either by the increased accessibility of proteoglycans or by the elevated aggrecanase activity in *Ucma*-deficient mouse cartilage. Our analysis of the effect of UCMA on aggrecanase activity clearly showed that UCMA blocked the aggrecanase activity of both ADAMTS-4 and ADAMTS-5. Therefore, along with TIMP-3, UCMA can be considered to be one of the few endogenous inhibitors of ADAMTS aggrecanases. In consequence, the observed overexpression of UCMA during osteoarthritis represents a type of rescue mechanism to reduce aggrecanase activity in diseased cartilage (25).

Apart from enhanced cartilage matrix degradation, chondrocyte apoptosis has also been suggested to be a factor promoting cartilage damage in osteoarthritis (6,7). In fact, we observed significantly increased chondrocyte death in the articular cartilage from *Ucma*-deficient mice compared to WT controls after DMM surgery. The increase in cell death was observed throughout the articular cartilage, in which UCMA protein is normally detected, although the majority of cell death was confined to the calcified cartilage. Apoptosis in articular cartilage has been associated with matrix degradation during osteoarthritis. Chondrocyte-specific deletion of MMP-13 leads to decreased matrix degradation and apoptosis during osteoarthritis (30,31). Similarly, *Ucma*-deficient mice showed an increase in MMP-generated matrix degradation and chondrocyte cell death, although a causal relationship between both events was not shown.

Bone changes are another hallmark of osteoarthritis and have been associated with high local bone turnover (32). Cartilage and bone changes are tightly coupled in osteoarthritic joints, but the molecular mechanisms of cartilage–bone interactions are not completely understood. Osteoblasts have been shown to induce phenotypic changes in human osteoarthritic chondrocytes. Osteoclasts have been associated with osteoarthritis-related cartilage

destruction (11,33,34). Likewise, several bone-derived factors that potentially influence cartilage in osteoarthritis have been identified, such as transforming growth factor β, IL-6, RANTES, and monocyte chemotactic protein 1 (10,11,33,35–37). Nonetheless, concepts that might explain how cartilage affects bone are scarcely understood to date.

Herein we show not only that cartilage is the major source of UCMA but also that UCMA is secreted into the cartilage matrix, in which it may migrate to the cartilage–bone interface (12–14). UCMA–collagen interactions may regulate this diffusion through the matrix, which is similar, for example, to the control of Indian hedgehog migration in the cartilage matrix through binding to proteoglycans (38). Accumulation of UCMA in the calcified matrix may be mediated by the binding of calcium via Gla residues on UCMA (24). At the cartilage–bone interface, UCMA may directly act on osteoclasts and influence bone homeostasis. Intriguingly, we observed that osteoarthritis-related changes in the subchondral bone, such as osteophyte formation and bone sclerosis, were alleviated in *Ucma*-deficient mice. UCMA-dependent effects on bone were, however, only detectable in close proximity to cartilage, but not at higher distances from the cartilage.

It was previously demonstrated that UCMA affects osteogenic differentiation in vitro, although osteoblast counts and differentiation of osteoblasts in *Ucma*-deficient mice are not altered during normal development (12,13,39). Elevated osteoblast counts in the subchondral bone compartment could only be detected in WT mice, but not in *Ucma*-deficient mice, indicating that UCMA may promote osteoblast differentiation during osteoarthritis. This supports the findings in a study by Lee and colleagues, who found that overexpression of UCMA in osteoblast precursors stimulates osteogenic differentiation (39). Although we had previously observed an inhibitory effect of recombinant UCMA on osteogenic differentiation in vitro, this difference may be explained by alterations in posttranslational modifications of recombinant UCMA, such as proteolytic processing, tyrosine sulfation, and Gla residues, or could be explained by the stage of differentiation (13,14,39,40).

Osteoclast numbers were increased in WT mice but not in *Ucma*-knockout mice. Analysis of cartilage organ cultures revealed that UCMA was secreted from the cartilage into the conditioned medium. WT mouse cartilage explants, but not cartilage explants from *Ucma*-deficient mice, promoted in vitro osteoclast differentiation, indicating that UCMA is released from cartilage at levels sufficient to promote osteoclastogenesis. We did not detect interaction of UCMA with either RANKL or OPG; however, UCMA rapidly induced the p38 MAPK and ERK signaling pathways, both of which are essential for osteoclast differentiation (41,42). This finding suggests that UCMA directly activates osteoclast differentiation by an as yet–unknown receptor, which in turn activates proosteoclastic signaling pathways.

In conclusion, we herein describe a dual role of UCMA in osteoarthritis. Our findings show that UCMA supports, on the one hand, the integrity of the articular cartilage by controlling aggrecanase activity, while on the other hand, it promotes osteoarthritis-related bone responses.

ACKNOWLEDGMENT

The authors gratefully acknowledge Herbert Rohrmüller for providing excellent technical assistance.

AUTHOR CONTRIBUTIONS

All authors were involved in drafting the article or revising it critically for important intellectual content, and all authors approved the final version to be published. Dr. Stock had full access to all of the data in the study and takes responsibility for the integrity of the data and the accuracy of the data analysis.

Study conception and design. Stock, Eitzinger, Beyer, Gelse, van den Berg, von der Mark, Schett.

Acquisition of data. Stock, Menges, Eitzinger, Geßlein, Botschner, Wormser, A. Distler, Schlötzer-Schrehardt, Dietel, Engelke, Koenders.

Analysis and interpretation of data. Stock, Eitzinger, J. Distler, Engelke, von der Mark.

REFERENCES

1. Van den Berg WB. Osteoarthritis year 2010 in review: pathomechanisms. Osteoarthritis Cartilage 2011;19:338–41.
2. Yang S, Kim J, Ryu JH, Oh H, Chun CH, Kim BJ, et al. Hypoxia-inducible factor-2α is a catabolic regulator of osteoarthritic cartilage destruction. Nat Med 2010;16:687–93.
3. Aigner T, Rose J, Martin J, Buckwalter J. Aging theories of primary osteoarthritis: from epidemiology to molecular biology. Rejuvenation Res 2004;7:134–45.
4. Mitrovic D, Quintero M, Stankovic A, Ryckewaert A. Cell density of adult human femoral condylar articular cartilage: joints with normal and fibrillated surfaces. Lab Invest 1983;49:309–16.
5. Hashimoto S, Ochs RL, Komiya S, Lotz M. Linkage of chondrocyte apoptosis and cartilage degradation in human osteoarthritis. Arthritis Rheum 1998;41:1632–8.
6. Blanco FJ, Guitian R, Vazquez-Martul E, de Toro FJ, Galdo F. Osteoarthritis chondrocytes die by apoptosis: a possible pathway for osteoarthritis pathology. Arthritis Rheum 1998;41:284–9.
7. Zamli Z, Sharif M. Chondrocyte apoptosis: a cause or consequence of osteoarthritis? Int J Rheum Dis 2011;14:159–66.
8. Glyn-Jones S, Palmer AJ, Agricola R, Price AJ, Vincent TL, Weinans H, et al. Osteoarthritis. Lancet 2015;386:376–87.
9. Van der Kraan PM, van den Berg WB. Osteophytes: relevance and biology. Osteoarthritis Cartilage 2007;15:237–44.
10. Mansell JP, Collins C, Bailey AJ. Bone, not cartilage, should be the major focus in osteoarthritis. Nat Clin Pract Rheumatol 2007;3:306–7.
11. Hayami T, Pickarski M, Wesolowski GA, McLane J, Bone A, Destefano J, et al. The role of subchondral bone remodeling in osteoarthritis: reduction of cartilage degeneration and prevention of osteophyte formation by alendronate in the rat anterior cruciate ligament transection model. Arthritis Rheum 2004;50:1193–206.
12. Eitzinger N, Surmann-Schmitt C, Bosl M, Schett G, Engelke K, Hess A, et al. Ucma is not necessary for normal development of the mouse skeleton. Bone 2012;50:670–80.

13. Surmann-Schmitt C, Dietz U, Kireva T, Adam N, Park J, Tagariello A, et al. Ucma, a novel secreted cartilage-specific protein with implications in osteogenesis. J Biol Chem 2008;283: 7082–93.
14. Tagariello A, Luther J, Streiter M, Didt-Koziel L, Wuelling M, Surmann-Schmitt C, et al. Ucma: a novel secreted factor represents a highly specific marker for distal chondrocytes. Matrix Biol 2008;27:3–11.
15. Neacsu CD, Grosch M, Tejada M, Winterpacht A, Paulsson M, Wagener R, et al. Ucmaa (Grp-2) is required for zebrafish skeletal development: evidence for a functional role of its glutamate γ-carboxylation. Matrix Biol 2011;30:369–78.
16. Stock M, Distler A, Distler J, Beyer C, Ruiz-Heiland G, Ipseiz N, et al. Fc-γ receptors are not involved in cartilage damage during experimental osteoarthritis. Osteoarthritis Cartilage 2015; 23:1221–5.
17. Glasson SS, Chambers MG, van den Berg WB, Little CB. The OARSI histopathology initiative: recommendations for histological assessments of osteoarthritis in the mouse. Osteoarthritis Cartilage 2010;18 Suppl 3:S17–23.
18. Stock M, Bohm C, Scholtysek C, Englbrecht M, Furnrohr BG, Klinger P, et al. Wnt inhibitory factor 1 deficiency uncouples cartilage and bone destruction in tumor necrosis factor α–mediated experimental arthritis. Arthritis Rheum 2013;65:2310–22.
19. Koenders MI, Lubberts E, Oppers-Walgreen B, van den Bersselaar L, Helsen MM, Kolls JK, et al. Induction of cartilage damage by overexpression of T cell interleukin-17A in experimental arthritis in mice deficient in interleukin-1. Arthritis Rheum 2005;52:975–83.
20. Surmann-Schmitt C, Widmann N, Dietz U, Saeger B, Eitzinger N, Nakamura Y, et al. Wif-1 is expressed at cartilage-mesenchyme interfaces and impedes Wnt3a-mediated inhibition of chondrogenesis. J Cell Sci 2009;122:3627–37.
21. Stanton H, Golub SB, Rogerson FM, Last K, Little CB, Fosang AJ. Investigating ADAMTS-mediated aggrecanolysis in mouse cartilage. Nat Protoc 2011;6:388–404.
22. Yamamoto K, Troeberg L, Scilabra SD, Pelosi M, Murphy CL, Strickland DK, et al. LRP-1-mediated endocytosis regulates extracellular activity of ADAMTS-5 in articular cartilage. FASEB J 2013;27:511–21.
23. Surmann-Schmitt C, Widmann N, Mallein-Gerin F, von der Mark K, Stock M. Stable subclones of the chondrogenic murine cell line MC615 mimic distinct stages of chondrocyte differentiation. J Cell Biochem 2009;108:589–99.
24. Rafael MS, Cavaco S, Viegas CS, Santos S, Ramos A, Willems BA, et al. Insights into the association of Gla-rich protein and osteoarthritis, novel splice variants and γ-carboxylation status. Mol Nutr Food Res 2014;58:1636–46.
25. Arpino V, Brock M, Gill SE. The role of TIMPs in regulation of extracellular matrix proteolysis. Matrix Biol 2015;44–46:247–54.
26. Briggs MD, Hoffman SM, King LM, Olsen AS, Mohrenweiser H, Leroy JG, et al. Pseudoachondroplasia and multiple epiphyseal dysplasia due to mutations in the cartilage oligomeric matrix protein gene. Nat Genet 1995;10:330–6.
27. Fassler R, Schnegelsberg PN, Dausman J, Shinya T, Muragaki Y, McCarthy MT, et al. Mice lacking α1(IX) collagen develop noninflammatory degenerative joint disease. Proc Natl Acad Sci U S A 1994;91:5070–4.
28. Nicolae C, Ko YP, Miosge N, Niehoff A, Studer D, Enggist L, et al. Abnormal collagen fibrils in cartilage of matrilin-1/matrilin-3-deficient mice. J Biol Chem 2007;282:22163–75.
29. Van der Weyden L, Wei L, Luo J, Yang X, Birk DE, Adams DJ, et al. Functional knockout of the matrilin-3 gene causes premature chondrocyte maturation to hypertrophy and increases bone mineral density and osteoarthritis. Am J Pathol 2006;169:515–27.
30. Thomas CM, Fuller CJ, Whittles CE, Sharif M. Chondrocyte death by apoptosis is associated with cartilage matrix degradation. Osteoarthritis Cartilage 2007;15:27–34.
31. Wang M, Sampson ER, Jin H, Li J, Ke QH, Im HJ, et al. MMP13 is a critical target gene during the progression of osteoarthritis. Arthritis Res Ther 2013;15:R5.
32. Burr DB, Gallant MA. Bone remodelling in osteoarthritis. Nat Rev Rheumatol 2012;8:665–73.
33. Sanchez C, Deberg MA, Piccardi N, Msika P, Reginster JY, Henrotin YE. Osteoblasts from the sclerotic subchondral bone downregulate aggrecan but upregulate metalloproteinases expression by chondrocytes. This effect is mimicked by interleukin-6, -1β and oncostatin M pre-treated non-sclerotic osteoblasts. Osteoarthritis Cartilage 2005;13:979–87.
34. Sanchez C, Deberg MA, Piccardi N, Msika P, Reginster JY, Henrotin YE. Subchondral bone osteoblasts induce phenotypic changes in human osteoarthritic chondrocytes. Osteoarthritis Cartilage 2005;13:988–97.
35. Lisignoli G, Toneguzzi S, Grassi F, Piacentini A, Tschon M, Cristino S, et al. Different chemokines are expressed in human arthritic bone biopsies: IFN-γ and IL-6 differently modulate IL-8, MCP-1 and rantes production by arthritic osteoblasts. Cytokine 2002;20:231–8.
36. Mansell JP, Bailey AJ. Abnormal cancellous bone collagen metabolism in osteoarthritis. J Clin Invest 1998;101:1596–603.
37. De Hooge AS, van de Loo FA, Bennink MB, Arntz OJ, de Hooge P, van den Berg WB. Male IL-6 gene knock out mice developed more advanced osteoarthritis upon aging. Osteoarthritis Cartilage 2005;13:66–73.
38. The I, Bellaiche Y, Perrimon N. Hedgehog movement is regulated through tout velu-dependent synthesis of a heparan sulfate proteoglycan. Mol Cell 1999;4:633–9.
39. Lee YJ, Park SY, Lee SJ, Boo YC, Choi JY, Kim JE. Ucma, a direct transcriptional target of Runx2 and Osterix, promotes osteoblast differentiation and nodule formation. Osteoarthritis Cartilage 2015;23:1421–31.
40. Viegas CS, Simes DC, Laize V, Williamson MK, Price PA, Cancela ML. Gla-rich protein (GRP), a new vitamin K-dependent protein identified from sturgeon cartilage and highly conserved in vertebrates. J Biol Chem 2008;283:36655–64.
41. Li X, Udagawa N, Itoh K, Suda K, Murase Y, Nishihara T, et al. p38 MAPK-mediated signals are required for inducing osteoclast differentiation but not for osteoclast function. Endocrinology 2002;143:3105–13.
42. Lee SE, Woo KM, Kim SY, Kim HM, Kwack K, Lee ZH, et al. The phosphatidylinositol 3-kinase, p38, and extracellular signal-regulated kinase pathways are involved in osteoclast differentiation. Bone 2002;30:71–7.

ARTHRITIS & RHEUMATOLOGY
Vol. 69, No. 6, June 2017, pp 1246–1256
DOI 10.1002/art.40080

Inhibition of Shedding of Low-Density Lipoprotein Receptor–Related Protein 1 Reverses Cartilage Matrix Degradation in Osteoarthritis

Kazuhiro Yamamoto,[1] Salvatore Santamaria,[1] Kenneth A. Botkjaer,[2] Jayesh Dudhia,[3] Linda Troeberg,[1] Yoshifumi Itoh,[1] Gillian Murphy,[2] and Hideaki Nagase[1]

Objective. **The aggrecanase ADAMTS-5 and the collagenase matrix metalloproteinase 13 (MMP-13) are constitutively secreted by chondrocytes in normal cartilage, but rapidly endocytosed via the cell surface endocytic receptor low-density lipoprotein receptor–related protein 1 (LRP-1) and subsequently degraded. This endocytic system is impaired in osteoarthritic (OA) cartilage due to increased ectodomain shedding of LRP-1. The aim of this study was to identify the LRP-1 sheddase(s) in human cartilage and to test whether inhibition of LRP-1 shedding prevents cartilage degradation in OA.**

Methods. **Cell-associated LRP-1 and soluble LRP-1 (sLRP-1) released from human cartilage explants and chondrocytes were measured by Western blot analysis. LRP-1 sheddases were identified by proteinase inhibitor profiling and gene silencing with small interfering RNAs. Specific monoclonal antibodies were used to selectively inhibit the sheddases. Degradation of aggrecan and collagen in human OA cartilage was measured by Western blot analysis using an antibody against an aggrecan neoepitope and a hydroxyproline assay, respectively.**

Results. **Shedding of LRP-1 was increased in OA cartilage compared with normal tissue. Shed sLRP-1 bound to ADAMTS-5 and MMP-13 and prevented their endocytosis without interfering with their proteolytic activities. Two membrane-bound metalloproteinases, ADAM-17 and MMP-14, were identified as the LRP-1 sheddases in cartilage. Inhibition of their activities restored the endocytic capacity of chondrocytes and reduced degradation of aggrecan and collagen in OA cartilage.**

Conclusion. **Shedding of LRP-1 is a key link to OA progression. Local inhibition of LRP-1 sheddase activities of ADAM-17 and MMP-14 is a unique way to reverse matrix degradation in OA cartilage and could be effective as a therapeutic approach.**

Osteoarthritis (OA) is the most prevalent age-related joint disorder, but there is no disease-modifying treatment available except for joint replacement surgery (1). The main cause of the disease is degradation of articular cartilage due to elevated activities of matrix metalloproteinases (MMPs) and ADAMTS. While both ADAMTS-4 and ADAMTS-5 have been considered to participate in aggrecan degradation in human OA (2,3), recent studies by Larkin et al with neutralizing monoclonal antibodies have shown that ADAMTS-5 is more effective than ADAMTS-4 in aggrecan degradation in human OA cartilage and nonhuman primates in vivo (4). Collagen fibrils are mainly degraded by collagenolytic MMPs, and MMP-13 is considered to be the major collagenase in OA cartilage (5–7).

We have recently found that both ADAMTS-5 and MMP-13 are constitutively produced in healthy human cartilage, but they are rapidly taken up by the chondrocytes via the endocytic receptor low-density lipoprotein receptor–related protein 1 (LRP-1) and degraded intracellularly (8–10). These findings suggest that they probably function for a very short period of time to maintain normal

Supported by Arthritis Research UK (grant 20563 to Dr. Yamamoto and grant 19466 to Dr. Troeberg), Arthritis Research UK Centre for Osteoarthritis Pathogenesis (grant 20205), the Kennedy Trust for Rheumatology Research, Orthopaedic Research UK (grant 483 to Dr. Dudhia), Cancer Research UK (grant C100/A8243 to Dr. Murphy), and the NIH (National Institute of Arthritis and Musculoskeletal and Skin Diseases grant AR-40994 to Dr. Nagase).

[1]Kazuhiro Yamamoto, PhD, Salvatore Santamaria, PhD, Linda Troeberg, PhD, Yoshifumi Itoh, PhD, Hideaki Nagase, PhD: University of Oxford, Oxford, UK; [2]Kenneth A. Botkjaer, PhD, Gillian Murphy, PhD: University of Cambridge, Cambridge, UK; [3]Jayesh Dudhia, PhD: Royal Veterinary College, Hertfordshire, UK.

Address correspondence to Kazuhiro Yamamoto, PhD, University of Oxford, Kennedy Institute of Rheumatology, Roosevelt Drive, Oxford OX3 7FY, UK. E-mail: kazuhiro.yamamoto@kennedy.ox.ac.uk.

Submitted for publication December 2, 2016; accepted in revised form February 21, 2017.

homeostatic turnover of extracellular matrix (ECM) components of the tissue. Other proteins that are endocytosed by LRP-1 include ADAMTS-4 (11) and tissue inhibitor of metalloproteinases 3 (TIMP-3) (12,13), indicating that LRP-1 is a key modulator of cartilage matrix degradation systems. This endocytic pathway is impaired in OA cartilage because of the reduction of protein levels of LRP-1 in chondrocytes without any significant changes in the level of messenger RNA (mRNA) for LRP-1, resulting in increased extracellular activity of ADAMTS-5 (8). We thus proposed that the loss of LRP-1 in OA cartilage is due to proteolytic shedding of the receptor, and that this process shifts normal homeostatic conditions of cartilage to a more catabolic environment, leading to the development of OA.

The aim of this study was to identify the "sheddase" activities that cleave LRP-1 and release the soluble form of LRP-1 (sLRP-1) in human cartilage. We also aimed to test whether inhibition of the sheddase(s) prevents the degradation of cartilage in OA.

MATERIALS AND METHODS

Reagents and antibodies. The sources of materials used were as follows: mouse monoclonal anti–LRP-1 α-chain antibody (8G1), mouse anti–LRP-1 β-chain monoclonal antibody (5A6) that recognizes the ectodomain, BC-3 mouse monoclonal antibody that recognizes the N-terminal ^{374}ARGSV aggrecan core protein fragments generated by aggrecanase, rabbit anti–ADAM-10 polyclonal antibody (ab1997), rabbit anti–ADAM-17 polyclonal antibody (ab2051), and rabbit anti–MMP-14 monoclonal antibody (ab51074) were from Abcam; mouse anti–FLAG M2 monoclonal antibody, chondroitinase ABC, endo-β-galactosidase, bovine nasal septum type II collagen, E-64, and 4-(2-aminoethyl)benzenesulfonyl fluoride (AEBSF) were from Sigma; human recombinant interleukin-1α (IL-1α) and tumor necrosis factor (TNF) were from PeproTech; rabbit antitubulin polyclonal antibody (no. 2148) was from Cell Signaling Technology; goat antiactin polyclonal antibody (I-19) was from Santa Cruz Biotechnology; human plasma IgG (1-001-A) was from R&D Systems; solubilized and purified full-length human LRP-1 was from BioMac; and a hydroxamate-based MMP inhibitor, CT1746, was from UCB Celltech.

Anti-human ADAMTS-5 catalytic domain rabbit polyclonal antibody was raised in rabbits and characterized (14). Inhibitory monoclonal antibodies against human ADAM-17 (D1A12) (15), MMP-14 (E2C6), desmin (negative control antibody) (16), and ADAMTS-5 (2D3) (9); bovine nasal aggrecan (17), receptor-associated protein (RAP) (8), recombinant human ADAMTS-5 lacking the C-terminus thrombospondin domain with a FLAG tag at the C-terminus (14), MMP-13 with a FLAG tag between the signal and propeptide (18), TIMP-1 (19), TIMP-2 (20), TIMP-3 (21), and N-terminal domain of human TIMP-3 (22) were prepared as described previously. All other reagents used were of the highest available analytic grade.

Human cartilage tissue preparation and isolation of chondrocytes. Cartilage from femoral condyles of human knee joints was used. Healthy normal articular cartilage was obtained from patients following knee amputation due to soft tissue sarcoma or osteosarcoma with no involvement of the cartilage. Tissue specimens were obtained from 9 patients (6 males, ages 9–57 years, mean age 35.5 years; 3 females, ages 13–19 years, mean age 15.7 years). Human OA articular cartilage was obtained from patients following total knee replacement surgery. Tissues were obtained from 16 patients (8 males, ages 51–86 years, mean age 75.1 years; 8 females, ages 50–82 years, mean age 68.1 years). Dissected cartilage ($\sim$18 mm^3, $\sim$20 mg wet weight/piece) was placed in one well of a round-bottomed 96-well plate and allowed to rest for 24 hours in 200 μl of Dulbecco's modified Eagle's medium (DMEM) containing 10% fetal calf serum (FCS) before use. The medium was replaced, and the cartilage was rested for a further 24–96 hours in 200 μl of DMEM at 37°C before the assays were performed. Chondrocytes were isolated as described previously (12). Primary chondrocytes were used in the experiments to compare normal and OA chondrocytes, and passaged cells were used in the experiments to identify the LRP-1 sheddase.

Western blot analysis of LRP-1 in cartilage. To analyze LRP-1 in the cartilage, medium was removed after incubation for various periods of time, and then total protein was extracted by adding 50 μl of 4× sodium dodecyl sulfate (SDS) sampling buffer (200 m*M* Tris HCl [pH 6.8]/8% SDS and 20% glycerol) to each explant in a 96-well plate. After 1 hour of incubation, the sample buffers were pooled from each condition (3 explants per condition), and 10 μl of samples was analyzed by SDS–polyacrylamide gel electrophoresis (PAGE) under nonreducing conditions and Western blotting using anti–LRP-1 α-chain, anti–LRP-1 β-chain, and antitubulin antibodies. Immune signals of LRP-1 and tubulin were quantified using ImageJ software (National Institutes of Health), and the relative amounts of LRP-1 α- and β-chains in the cartilage extracts were estimated using tubulin as an internal control.

Immunofluorescence staining of LRP-1. OA and normal cartilage samples (n = 3 each) were rested in culture with DMEM for 2 days. Explants were then snap-frozen and sectioned (5-μm sections) using a CM1900 cryostat (Leica Microsystems). Each sample was fixed with methanol and incubated with anti–LRP-1 β-chain antibody for 3 hours at room temperature. Incubation with Alexa Fluor 568–conjugated anti-mouse IgG (Molecular Probes) for 1 hour at room temperature was used to visualize the antigen signals. Nuclei were stained with DAPI. Samples were viewed using an Eclipse TE2000-U confocal laser scanning microscope (Nikon). Data were collated using Volocity software (Improvision).

Quantitative reverse transcriptase–polymerase chain reaction (qRT-PCR). Quantitative RT-PCR was carried out as described previously (8). Briefly, RNA was extracted and isolated from 50 mg of ground cartilage tissue using an RNeasy kit (Qiagen), and complementary DNA was then generated using a reverse transcription kit following the guidelines of the manufacturer (Applied Biosystems). Complementary DNA was then used for real-time PCR assays using TaqMan technology. The $\Delta\Delta C_t$ method of relative quantitation was used to calculate relative mRNA levels for each transcript examined. The 60S acidic ribosomal protein P0 (RPLP0) gene was used to normalize the data. Predeveloped primer/probe sets for LRP-1, ADAM-12, and RPLP0 were purchased from Applied Biosystems.

Western blot analysis of cellular LRP-1 and sLRP-1. Chondrocytes (5×10^4) were cultured in 12-well plates in 2 ml of DMEM containing 10% FCS for 2 days. Cells were rested in 1 ml of DMEM for 24 hours, and the medium was replaced

with 1 ml of DMEM and used in the experiments. After incubation for various periods of time, the medium was collected and concentrated 20-fold using spin filters (Microcon YM-30; Merck Millipore), and 20 μl of 4× SDS sampling buffer was added to 50 μl of each concentrated medium. The cells were lysed with 200 μl of 2× SDS sampling buffer, and 10 μl of samples were analyzed by SDS-PAGE under nonreducing conditions and Western blotting using anti–LRP-1 α-chain, anti–LRP-1 β-chain, and antitubulin antibodies. Immune signals of LRP-1 and tubulin were quantified using ImageJ software, and the relative amounts of LRP-1 α-chain in the medium and LRP-1 α- and β-chains in the cell lysate were estimated within the linear range of measurements (see Supplementary Figures 1A and B, available on the *Arthritis & Rheumatology* web site at http://onlinelibrary.wiley.com/doi/10.1002/art.40080/abstract) and normalized using tubulin, and those in the standard cell lysates of chondrocytes were used as internal controls. An absolute number of LRP-1 molecules released into medium was estimated by comparing various concentrations of purified LRP-1 within a reasonable linear range.

Flow cytometric analysis of LRP-1. Cells were plated in 6-well plates in DMEM containing 10% FCS and incubated until 80% confluent. Cells were rested in 2 ml of DMEM for 1 day, detached using a cell scraper, and fixed for 5 minutes at 4°C with ice-cold methanol followed by 2 washes with fluorescence-activated cell sorting (FACS) buffer (phosphate buffered saline containing 5% goat serum and 3% bovine serum albumin [BSA]). Cells were stained for 30 minutes at 25°C with anti–LRP-1 β-chain antibody, washed with FACS buffer, and then further incubated with allophycocyanin-conjugated goat anti-mouse IgG (BD PharMingen) and isotype control in FACS buffer for 20 minutes at 25°C. Cells were then washed with FACS buffer and analyzed using an LSRII flow cytometer (BD Biosciences), and postacquisition data analysis was performed using FlowJo software version 7.6.1 (Tree Star).

Analysis of endocytosis of ADAMTS-5 and MMP-13. Cells (5×10^4) cultured in 24-well plates were rested in 500 μl of DMEM for 1 day. The medium was replaced with 500 μl of fresh DMEM with 10 n*M* of ADAMTS-5 or MMP-13 in the absence or presence of 2 n*M* or 10 n*M* sLRP-1 or 500 n*M* RAP at 37°C. After incubation for 0–4 hours, media were collected and the protein was precipitated with 5% trichloroacetic acid and dissolved in 50 μl of 1× SDS sampling buffer containing 5% 2-mercaptoethanol. All samples were analyzed by SDS-PAGE under reducing conditions and Western blotting using anti–FLAG M2 antibody or anti–ADAMTS-5 antibody, respectively. Immune signals for exogenously added ADAMTS-5 and MMP-13 detected in the medium were quantified using ImageJ software within the linear range of the measurements (see Supplementary Figures 1C and D, http://onlinelibrary.wiley.com/doi/10.1002/art.40080/abstract), and the amount of each recombinant protein remaining in the medium at each time point was calculated as a percentage of the amount of each recombinant protein at 0 hours.

Analysis of aggrecanolytic activity of ADAMTS-5. Purified ADAMTS-5 (5 n*M*) was preincubated with 0–25 n*M* purified sLRP-1 in TNCB buffer (50 m*M* Tris HCl [pH 7.5]/150 m*M* NaCl/10 m*M* $CaCl_2$/0.01% BSA) containing 0.01% Brij-35 for 10 minutes at 25°C. The mixture was diluted 100-fold and incubated with 0.5 mg/ml purified bovine aggrecan for 0–4 hours at 37°C. The samples were deglycosylated as described previously (23). Briefly, aggrecan was deglycosylated in sodium acetate buffer with chondroitinase ABC and endo-β-galactosidase (each 0.01 unit/100 μg of aggrecan) for 24 hours at 37°C. Aggrecan was then precipitated using ice-cold acetone and analyzed by Western blotting using the antibody BC-3, which recognizes the N-terminal ^{374}ARGSV aggrecan core protein fragments generated by aggrecanase.

Small interfering RNA (siRNA)–mediated knockdown of membrane-bound metalloproteinases. Small interfering RNA oligonucleotides for ADAMs and MMP-14 (On-TargetPlus SMARTpool siRNA) and nontargeting oligonucleotide were purchased from Thermo Scientific Dharmacon. Cells were plated at a density of 4×10^4 cells/well (12-well plate) in DMEM containing 10% FCS and incubated until 50% confluent. INTERFERin (PeqLab) was used to transfect cells with siRNA at a final concentration of 20 n*M* in Opti-MEM I (Gibco). After 48 hours of incubation, the medium was replaced with fresh DMEM with or without 10 ng/ml IL-1 or 200 ng/ml TNF and incubated further for 24 hours. Cells were lysed with 200 μl of 2× SDS sampling buffer containing 5% 2-mercaptoethanol, and then the samples were analyzed by SDS-PAGE under reducing conditions and Western blotting using anti–ADAM-10, anti–ADAM-17, anti–MMP-14, and antiactin antibodies. Immune signals of each enzyme and actin were quantified using ImageJ software, and the relative amount of each enzyme was estimated using actin as an internal control.

Analysis of the effect of inhibitory antibodies against ADAM-17 and MMP-14 on LRP-1 protein levels. Normal chondrocytes (5×10^4) cultured in 24-well plates were rested in 500 μl of DMEM for 1 day. The medium was replaced with 500 μl of fresh DMEM with or without 10 ng/ml IL-1 in the absence or presence of various concentrations of combinations of the control antibodies (human IgG for the anti–ADAM-17 antibody [D1A12] and antidesmin intracellular domain antibody for the anti–MMP-14 antibody [E2C6]) or the anti–ADAM-17 and the anti–MMP-14 antibodies. After 24 hours of incubation, the cells were lysed with 100 μl of 2× SDS sampling buffer, and then LRP-1 α- and β-chains were detected as described above. To test the effect of inhibitory antibodies against ADAM-17 and MMP-14 on LRP-1 levels in OA chondrocytes and cartilage in culture, cells and cartilage explants were cultured for 24 hours with DMEM in the absence or presence of combinations of 250 n*M* each of the control antibodies, the anti–ADAM-17 antibody and the antidesmin antibody, the anti–MMP-14 antibody and IgG, or the anti–ADAM-17 and the anti–MMP-14 antibodies. LRP-1 α- and β-chains were then detected as described above.

Analysis of aggrecan degradation in OA cartilage. OA cartilage was cultured in a round-bottomed 96-well plate (1 explant per well) and rested in DMEM for 1 day. The cartilage was further cultured in DMEM in the absence or presence of a combination of 2 antibodies (250 n*M* each) (i.e., combination of the anti–ADAM-17 antibody and the antidesmin antibody [control], combination of the anti–MMP-14 antibody and IgG [control], combination of the anti–ADAM-17 and the anti–MMP-14 antibodies, or combination of the antidesmin antibody and IgG), or 250 n*M* of anti–ADAMTS-5 or N-terminal domain of human TIMP-3. After 12 hours of incubation, the medium was replaced with fresh DMEM containing the antibodies or TIMP and incubated further for 0–48 hours. For Western blotting, the conditioned media were pooled from each condition (3 explants per condition) and deglycosylated as described above, and immunoreactivity was measured within the linear range of the assay based on standard samples (see Supplementary Figure 1E, http://onlinelibrary.wiley.com/doi/10.1002/art.40080/abstract).

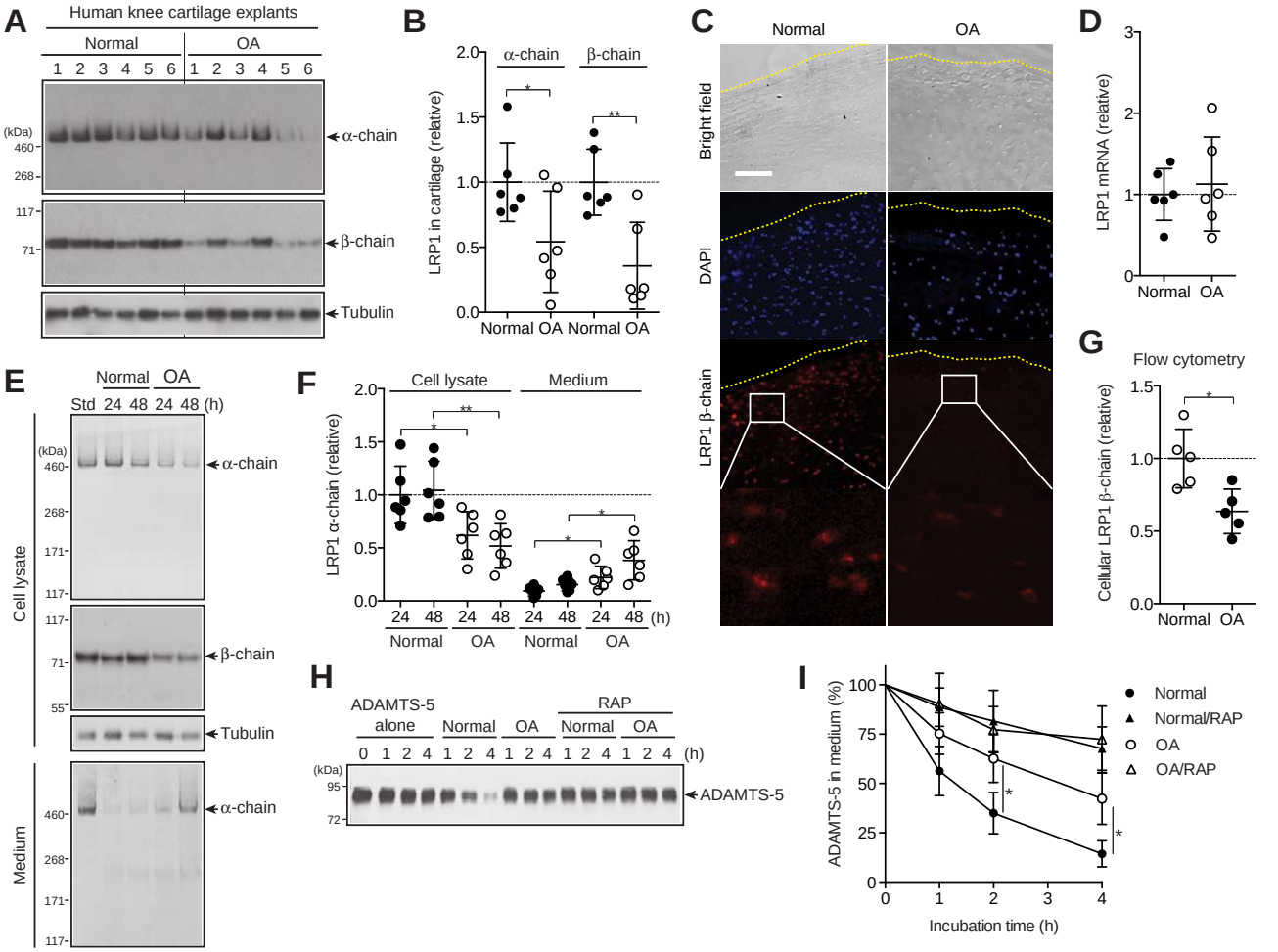

Figure 1. Increased ectodomain shedding of low-density lipoprotein receptor–related protein 1 (LRP-1) and reduced endocytic capacity of chondrocytes in human osteoarthritic (OA) cartilage. **A,** Western blotting of total proteins extracted from cartilage explants of human knee joints of OA patients and patients without arthritis (n = 6 each) with antibodies against α- and β-chains of LRP-1. **B,** Densitometric analysis of LRP-1 in **A**. Data were normalized against tubulin. **C,** Immunofluorescence staining of LRP-1 in frozen section of human knee cartilage. Dotted lines indicate the articular cartilage surface. Bar = 100 μm. **D,** Relative levels of mRNA for LRP-1 in cartilage, measured by TaqMan quantitative reverse transcriptase–polymerase chain reaction. **E,** Representative Western blotting of LRP-1 protein in cell lysates and medium of human normal and OA chondrocytes (n = 6 donors each). Std = standard cell lysates. **F,** Quantification of LRP-1 α-chain detected in **E**. **G,** Flow cytometric analysis of LRP-1 β-chain. **H,** Representative Western blotting for endocytosis of ADAMTS-5 (10 n*M*) by human normal and OA chondrocytes (n = 3 donors each) with or without the LRP-1 ligand antagonist receptor-associated protein (RAP) (500 n*M*). ADAMTS-5 in the medium was detected by Western blotting using anti–ADAMTS-5 antibody. **I,** Quantification of findings in **H**. In **B**, **D**, **F**, and **G**, symbols represent individual cartilage donors; bars show the mean ± SD. The mean values in normal cartilage and chondrocytes were set at 1 (dashed lines). In **I**, values are the mean ± SD. $* = P < 0.05$; $** = P < 0.01$, by Student's 2-tailed *t*-test.

Analysis of collagen degradation in OA cartilage. OA cartilage was cultured with various antibodies or with 250 n*M* of TIMP-1 as described above for aggrecan degradation studies, and media were harvested after 96 hours. The extent of type II collagen degradation in OA cartilage was assessed by measuring the amount of hydroxyproline released into the media using a modification of the assay described by Bergman and Loxley (24). The hydroxyproline contents in cartilage explant remnants after culture were also determined by digesting them in 500 μl of papain digest solution (0.05*M* phosphate buffer [pH 6.5]/2 m*M* *N*-acetylcysteine/2 m*M* EDTA/10 μg/ml papain) at 65°C for 24 hours. The relative amount of collagen degradation was estimated by dividing the amount of hydroxyproline released into the medium by the summed amount of hydroxyproline in the medium and in the papain digests.

Study approval. Normal human articular cartilage tissue specimens were obtained from the Stanmore BioBank, Institute of Orthopaedics, Royal National Orthopaedic Hospital, Stanmore, following informed consent from patients and approval by the Royal Veterinary College Ethics and Welfare Committee (Institutional approval Unique Reference Number 2012 0048H). Human OA cartilage tissue specimens were obtained from the Oxford Musculoskeletal Biobank and were collected with informed donor consent in full compliance with national and institutional ethical requirements, the United Kingdom Human Tissue Act, and the Declaration of Helsinki

(Human Tissue Authority Licence 12217 and Oxford Research Ethics Committee C 09/H0606/11).

Statistical analysis. All quantified data are represented as the mean ± SD where applicable. Significant differences between data sets were determined using Student's 2-tailed *t*-test or one-way analysis of variance followed by Dunnett's multiple comparison test, where indicated.

RESULTS

Increased ectodomain shedding of LRP-1 and reduced endocytic capacity in human OA cartilage. We first verified the loss of LRP-1 protein in human OA cartilage. LRP-1 consists of an extracellular 515-kd α-chain and an 85-kd β-chain that are processed from the precursor by furin. The α-chain contains the ligand-binding domains, and the β-chain has an extracellular domain, a transmembrane domain, and a cytoplasmic domain. Western blotting analyses of α- and β-chains of cartilage extracts with antibodies that recognize the N-terminus of the α-chain and the extracellular domain of the β-chain showed that both chains were reduced in OA cartilage by ~48% and ~65%, respectively, compared with normal cartilage (Figures 1A and B). The reduction of LRP-1 was further confirmed by immunofluorescence staining of β-chain in the cartilage (Figure 1C). No significant change in the level of mRNA for LRP-1 between normal and OA cartilage (Figure 1D) suggested that the loss of LRP-1 in OA cartilage was due to proteolytic shedding of the receptor.

To further investigate the increased shedding of LRP-1 in OA cartilage, chondrocytes were cultured and LRP-1 proteins were analyzed. Both α- and β-chains were reduced in OA cell lysates compared with normal chondrocytes, which was accompanied by an increased release of full-length α-chain into the medium (Figures 1E and F). Flow cytometric analysis of the β-chain with antiectodomain antibody further confirmed the reduction of cell surface LRP-1 including the β-chain in OA chondrocytes (Figure 1G), suggesting that the primary shedding site is located in the ectodomain of the β-chain. We estimated that a single normal chondrocyte released $\sim 3.9 \pm 2.7 \times 10^3$ LRP-1 molecules per hour (mean ± SD), while a single OA chondrocyte released $9.6 \pm 5.4 \times 10^3$ LRP-1 molecules per hour. As anticipated, the endocytic capacity of human OA chondrocytes was significantly reduced; the half-life of ADAMTS-5 was ~2.8-fold longer in OA chondrocytes (~210 minutes) than in normal chondrocytes (~75 minutes) (Figures 1H and I).

Soluble LRP-1 ectodomain prevents endocytosis of ADAMTS-5 and MMP-13 without interfering with their activities. We then evaluated whether sLRP-1 alters half-lives of cartilage-degrading metalloproteinases. As shown in Figures 2A and B, endocytosis of ADAMTS-5 and MMP-13 was reduced partially with 2 n*M* sLRP-1 and almost completely inhibited with 10 n*M* sLRP-1 to the level that was attained with the LRP ligand antagonist RAP. We also found that sLRP-1–bound ADAMTS-5 and MMP-13 retained activity against their natural substrates, aggrecan and collagen, respectively (Figures 2C and D). It is notable that ADAMTS-5 bound to sLRP-1 was ~3-fold more active on aggrecan cleavage compared with free ADAMTS-5 (Figure 2C). Thus, shedding of the LRP-1 ectodomain impairs the endocytic capacity of the cell not only by reducing the level of cell surface LRP-1 but also by converting membrane-anchored LRP-1 into soluble decoy receptors, leaving excess matrix-degrading proteinases extracellularly.

ADAM-17 and MMP-14 are responsible for shedding LRP-1 in human chondrocytes. To identify the LRP-1 sheddase in human chondrocytes, we first examined whether proinflammatory cytokines such as IL-1 and TNF that stimulate cartilage matrix degradation increase LRP-1 shedding, as this might facilitate characterization of the sheddase in the cartilage. As shown in Figures 3A–C, these cytokines increased LRP-1 shedding ~4.0-fold in normal human chondrocytes. The cytokine-stimulated LRP-1 shedding was inhibited by the hydroxamate metalloproteinases inhibitor CT1746, but not by a serine proteinase inhibitor (AEBSF) or a cysteine proteinase inhibitor (E-64) (Figure 3D). Among the 3 TIMPs tested, TIMP-1 was not effective but TIMP-2 and TIMP-3 were, and TIMP-3 showed the strongest inhibition (Figure 3E). Thus, we postulated that the responsible enzyme was likely to be a membrane-anchored ADAM or MMP.

ADAM-10, ADAM-12, ADAM-17, and MMP-14 have previously been reported to be LRP-1 sheddases in other cell types (25). We therefore ablated each enzyme individually using a specific siRNA. The ADAM-10 protein level was reduced by ~90%, and the ADAM-12 mRNA level was reduced by ~88% (see Supplementary Figures 2A–C, http://onlinelibrary.wiley.com/doi/10.1002/art.40080/abstract), but their knockdown did not affect LRP-1 shedding (see Supplementary Figure 2D). Small interfering RNAs targeting ADAM-17 and MMP-14 reduced their protein levels by 76% and 84%, respectively (see Supplementary Figures 2E and F), and knockdown of each partially inhibited LRP-1 shedding (Figure 3F). However, knockdown of both MMP-14 and ADAM-17 exhibited a stronger, additive effect, to the level achieved by TIMP-3 (Figure 3F), which suggests that these 2 proteinases function as LRP-1 sheddases. A low level of LRP-1 shedding occurred in unstimulated chondrocytes, and was mainly due to MMP-14.

Combination of inhibitory antibodies against ADAM-17 and MMP-14 blocks LRP-1 shedding in OA cartilage. To verify the role of ADAM-17 and MMP-14 in LRP-1 shedding, we used the recently developed

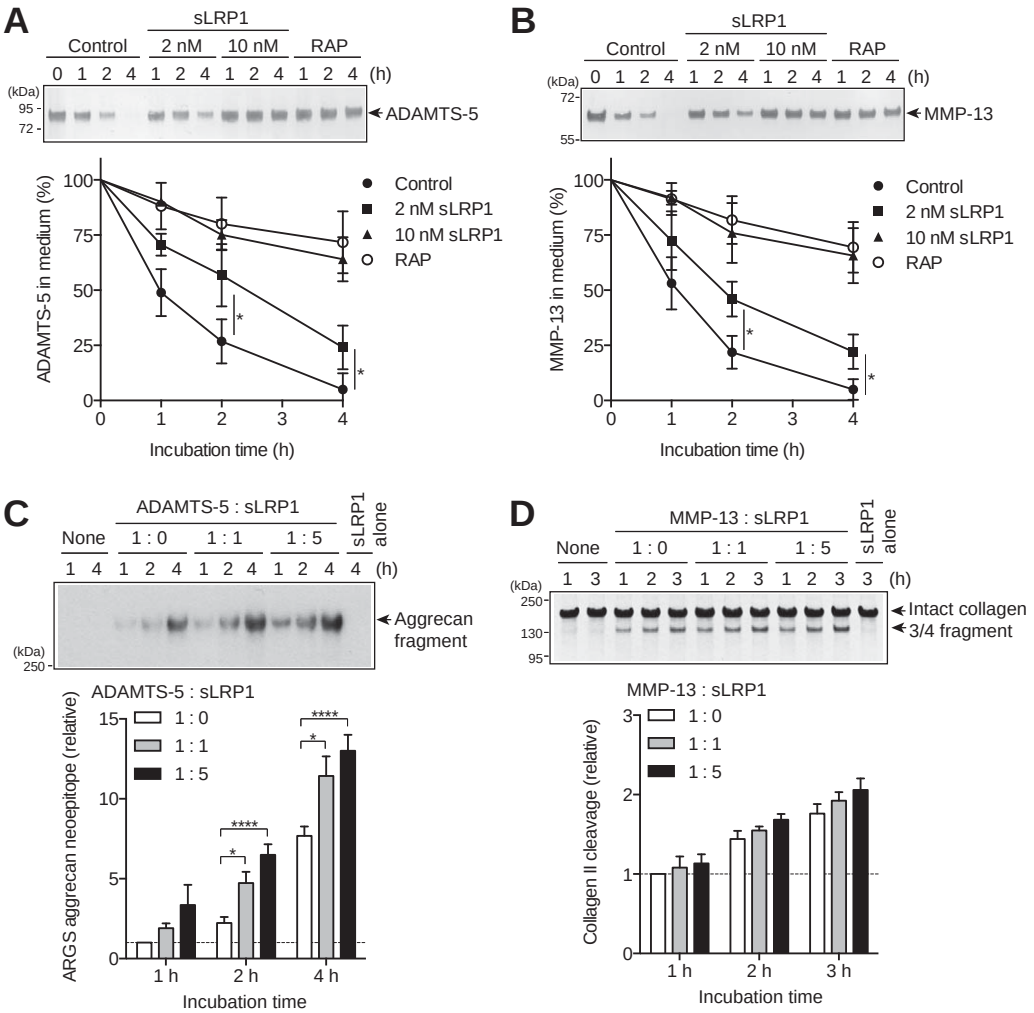

Figure 2. Ectodomain of soluble low-density lipoprotein receptor–related protein 1 (sLRP-1) prevents endocytosis of ADAMTS-5 and matrix metalloproteinase 13 (MMP-13) without interfering with their activities. **A** and **B,** Normal human chondrocytes (n = 3 donors) were cultured with Dulbecco's modified Eagle's medium containing 10 n*M* ADAMTS-5 (**A**) or 10 n*M* MMP-13 (**B**) with no additional treatment (Control) or in the presence of 2 n*M* sLRP-1, 10 n*M* sLRP-1, or 500 n*M* receptor-associated protein (RAP) for 0–4 hours. ADAMTS-5 and MMP-13 in the medium were detected by Western blotting using anti–FLAG M2 antibody. Top, Representative Western blotting. Bottom, Quantification of findings in Western blotting. **C,** Bovine aggrecan (0.5 mg/ml) was incubated with 0.05 n*M* ADAMTS-5 alone (1:0) or in the presence of 0.05 n*M* sLRP-1 (1:1) or 0.25 n*M* sLRP-1 (1:5) for 1–4 hours at 37°C. The reactions were stopped with 10 m*M* EDTA, and the reaction products were deglycosylated and subjected to Western blotting using antibody against the aggrecan neoepitope ^{374}ARGSV (ARGS). Top, Representative Western blotting. Bottom, Quantification of findings in Western blotting. **D,** Type II collagen (1 mg/ml) was incubated with 5 n*M* MMP-13 alone (1:0) or in the presence of 5 n*M* sLRP-1 (1:1) or 25 n*M* sLRP-1 (1:5) for 1–3 hours at 25°C. The reactions were stopped with 10 m*M* EDTA, and the reaction products were analyzed by sodium dodecyl sulfate–polyacrylamide gel electrophoresis (SDS-PAGE) with Coomassie brilliant blue staining. Top, Representative SDS-PAGE. Bottom, Quantification of findings in SDS-PAGE. In **C** and **D**, the mean values after 1 hour of incubation without sLRP-1 were set at 1 (dashed lines). Values are the mean ± SD. $* = P < 0.05$; $**** = P < 0.0001$, by Student's 2-tailed *t*-test (**A** and **B**) or one-way analysis of variance followed by Dunnett's multiple comparison test (**C**).

specific antibodies against ADAM-17 (D1A12) (15) and against MMP-14 (E2C6) (16), which inhibit the target enzymes with inhibition constants of 0.46 n*M* and 0.11 n*M*, respectively. The IL-1–induced loss of LRP-1 was partially inhibited by a single antibody, but a combination of the 2 antibodies blocked LRP-1 shedding to the level of IL-1–untreated cells (Figure 4A). They were similarly effective at blocking LRP-1 shedding in OA chondrocytes (Figure 4B). The anti–MMP-14 antibody increased cellular levels of the LRP-1 α- and β-chains 1.6-fold and 2.1-fold, respectively, while the anti–ADAM-17 antibody increased them 1.4-fold and 1.8-fold, respectively. A combination of the 2 antibodies increased both α- and β-chains 2.3-fold and 2.6-fold, respectively (Figure 4B). The

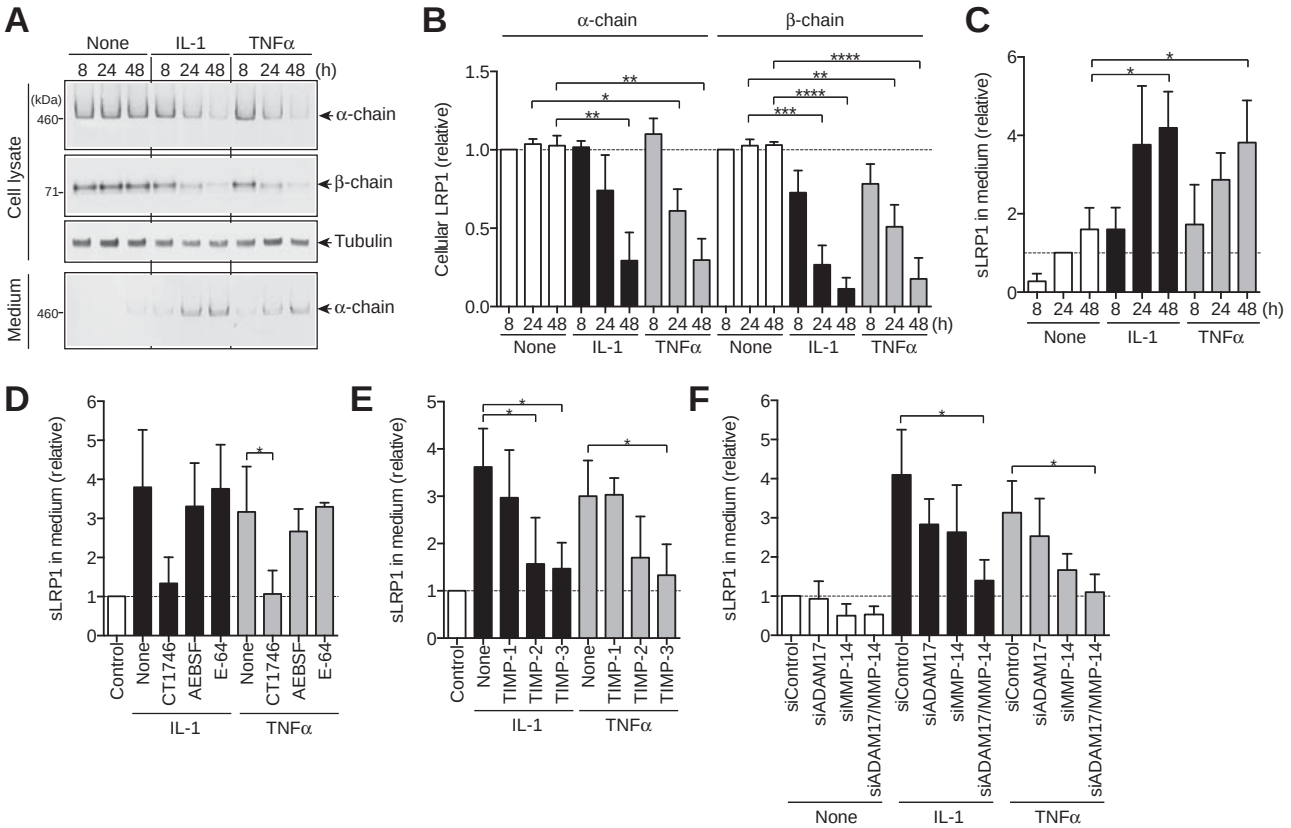

Figure 3. ADAM-17 and matrix metalloproteinase 14 (MMP-14) are the responsible sheddases of low-density lipoprotein receptor–related protein 1 (LRP-1) in human chondrocytes. **A,** Results of culturing human normal chondrocytes (n = 3 donors) with Dulbecco's modified Eagle's medium in the presence or absence of 10 ng/ml interleukin-1 (IL-1) or 200 ng/ml tumor necrosis factor (TNF) for 8–48 hours. LRP-1 proteins in the cell lysate and the medium were analyzed by Western blotting with antibodies against α- and β-chains of LRP-1. **B** and **C,** Quantification of LRP-1 protein in the cell lysate (**B**) and soluble LRP-1 (sLRP-1) released into the medium (**C**) with or without IL-1 or TNF treatment. **D,** Effect of the metalloproteinase inhibitor CT1746 (20 μM), the serine proteinase inhibitor 4-(2-aminoethyl)benzenesulfonyl fluoride (AEBSF) (50 μM), or the cysteine proteinase inhibitor E-64 (10 μM) on cytokine-induced LRP-1 shedding with or without IL-1 or TNF treatment. **E,** Effect of tissue inhibitor of metalloproteinases 1 (TIMP-1) (500 nM), TIMP-2 (500 nM), or TIMP-3 (300 nM) on cytokine-induced LRP-1 shedding with or without IL-1 or TNF treatment. **F,** Effect of small interfering RNA (siRNA)–mediated knockdown of ADAM-17 and/or MMP-14 on cytokine-induced LRP-1 shedding with or without IL-1 or TNF treatment. Values in **B–F** are the mean ± SD. In **B–D**, the mean values in the cells incubated without cytokine for 8 hours (**B**) or 24 hours (**C** and **D**) were set at 1 (dashed lines). In **E** and **F**, the mean values in the cells transfected with nontargeting siRNA were set at 1 (dashed lines). $* = P < 0.05$; $** = P < 0.002$; $*** = P < 0.0002$; $**** = P < 0.0001$, by one-way analysis of variance followed by Dunnett's multiple comparison test.

restoration of LRP-1 in OA chondrocytes by combining the 2 antibodies was time dependent, and it reached a plateau at 24 hours (Figure 4C). Addition of the 2 antibodies to OA cartilage blocked LRP-1 shedding and increased α- and β-chains 2.6-fold and 2.3-fold, respectively (Figure 4D). This indicates that the antibodies can penetrate the tissue and inhibit the LRP-1 sheddases in OA cartilage.

Blocking of LRP-1 sheddases restores endocytic capacity and reduces the degradation of aggrecan and collagen in OA cartilage. We then tested the effect of combining the 2 antibodies on the endocytic capacity of OA chondrocytes. The antibody-treated OA chondrocytes cleared exogenously added ADAMTS-5 from the medium ~2.4-fold faster (half-life ~95 minutes) than the untreated OA chondrocytes (half-life ~210 minutes) (Figure 5A), indicating that blocking LRP-1 sheddases restored the endocytic capacity of OA chondrocytes close to that of normal chondrocytes.

Remarkably, combined antibody treatment reduced the degradation of aggrecan and collagen in OA cartilage. Analysis of the same conditioned media for the aggrecanase-specific cleavage motif using the antibody against the ^{374}ARGSV neoepitope indicated that aggrecanase activity was markedly inhibited by blocking LRP-1 sheddases (Figure 5B) (see Supplementary Figure 3, http://onlinelibrary.wiley.com/doi/10.1002/art.40080/abstract). Potent inhibition with the anti–ADAMTS-5 antibody and TIMP-3 indicated that the primary

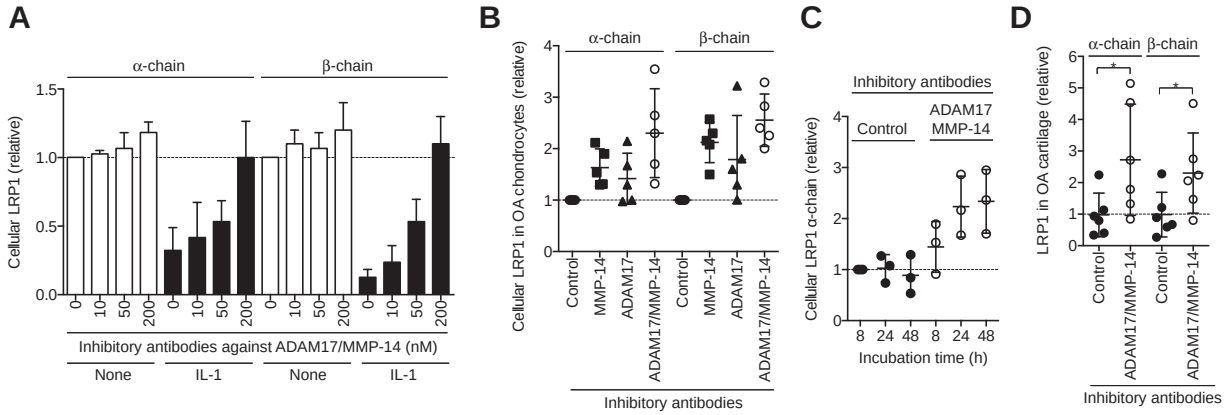

Figure 4. Combination of antibodies inhibiting ADAM-17 and matrix metalloproteinase 14 (MMP-14) blocks shedding of low-density lipoprotein receptor–related protein 1 (LRP-1) in osteoarthritic (OA) cartilage. **A,** Results of culturing human normal chondrocytes (n = 3 donors) with Dulbecco's modified Eagle's medium without (None) or with 10 ng/ml interleukin-1 (IL-1) in the absence or presence of combined anti–ADAM-17 and anti–MMP-14 (10–200 n*M* each) for 48 hours. LRP-1 proteins in the cell lysate were analyzed by Western blotting with antibodies against α- and β-chains of LRP-1. **B,** Effect of combining anti–MMP-14 and anti–ADAM-17 antibodies (200 n*M* each) on LRP-1 shedding in human OA chondrocytes (n = 5 donors). **C,** Time course analysis of the effect of combined anti–MMP-14 and anti–ADAM-17 antibodies on the recovery of cellular LRP-1. **D,** Effect of combined anti–MMP-14 and anti–ADAM-17 antibodies on LRP-1 shedding in human knee OA cartilage explants (n = 6 donors each). In **A**, values are the mean ± SD, and the mean value in the cells incubated without IL-1 or the antibodies was set at 1 (dashed line). In **B–D**, symbols represent individual cartilage donors; bars show the mean ± SD. In **B–D**, the mean values in the cells or cartilage incubated with the control antibodies for 8 hours (**C**) or 24 hours (**B** and **D**) were set at 1 (dashed lines). * = $P < 0.05$, by Student's 2-tailed *t*-test.

aggrecanase in OA cartilage was ADAMTS-5. Effective inhibition of aggrecan degradation by the combination of anti–ADAM-17 and anti–MMP-14 antibodies was further confirmed by Safranin O staining of the cartilage (see Supplementary Figure 4, http://onlinelibrary.wiley.com/doi/10.1002/art.40080/abstract).

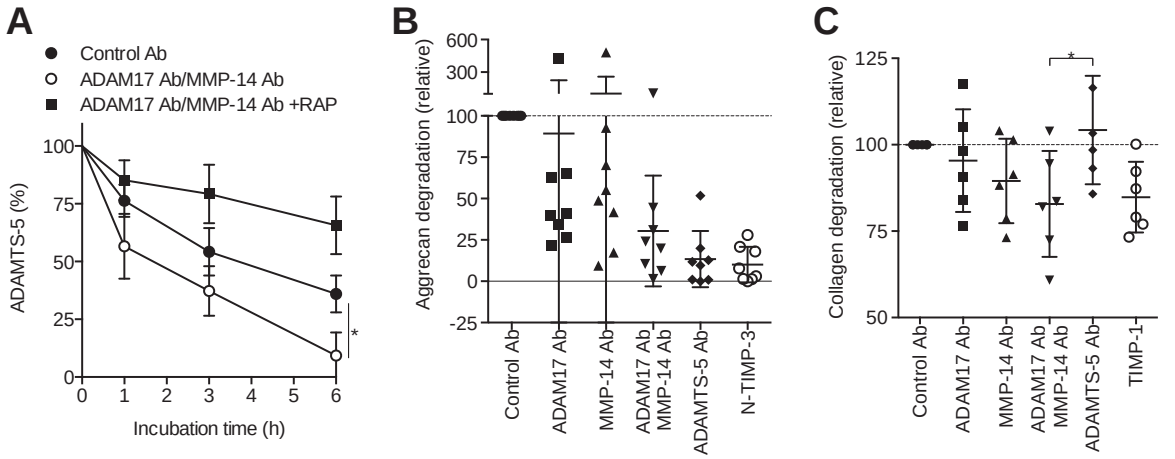

Figure 5. Blocking of low-density lipoprotein receptor–related protein 1 (LRP-1) sheddases restores endocytic capacity and reduces aggrecan and collagen degradation in osteoarthritic (OA) cartilage. **A,** Recovery of endocytic capacity in OA chondrocytes upon treatment with anti–ADAM-17 and anti–matrix metalloproteinase 14 (anti–MMP-14) antibodies (Ab). Endocytosis of ADAMTS-5 (10 n*M*) was measured as described in Figures 1H and I (n = 3 donors). **B** and **C,** Inhibition of aggrecan and collagen degradation in human OA cartilage upon treatment with combined anti–ADAM-17 and anti–MMP-14 antibodies. OA knee cartilage explants were incubated with antibodies or tissue inhibitor of metalloproteinases (TIMP) at 250 n*M*. **B,** Aggrecan degradation detected after 48 hours with an antibody against the aggrecan neoepitope ^{374}ARGSV. The mean value in medium of the cartilage incubated with the control antibodies was set at 100 (dashed line) (n = 8 donors). **C,** Collagen degradation of cultured OA cartilage after 96 hours of incubation, measured by hydroxyproline assay. The amount of hydroxyproline released with control antibodies was set at 100 (dashed line). In **A**, values are the mean ± SD. In **B** and **C**, symbols represent individual cartilage donors; bars show the mean ± SD. The mean values in media of the cartilage incubated with the control antibodies for 48 hours (**B**) or 96 hours (**C**) were set at 100 (dashed lines). * = $P < 0.05$, by Student's 2-tailed *t*-test (**A**) or one-way analysis of variance followed by Dunnett's multiple comparison test (**C**). RAP = receptor-associated protein; N-TIMP-3 = N-terminal domain of human TIMP-3.

Collagen degradation was also inhibited in the presence of anti–ADAM-17 and anti–MMP-14 antibodies by 5% and 10%, respectively, and more effective inhibition (17%) was observed upon combining the 2 antibodies (Figure 5C). In general, anti–MMP-14 showed a stronger effect than anti–ADAM-17, but there was considerable patient-to-patient variation in the effect of each antibody, which may reflect the multifactorial nature of OA. Inhibition was also detected with TIMP-1 treatment, but not with the anti–ADAMTS-5 antibody, indicating that collagen degradation is specific to collagenase. Cell viability analysis indicated that none of these treatments was toxic to chondrocytes (data not shown).

DISCUSSION

In this study, we have shown that the ectodomain shedding of LRP-1 may be an important regulator of the development of human OA. The specific inhibitory antibodies that we recently developed for human MMP-14 and ADAM-17 have allowed us to evaluate the role of LRP-1 shedding in degradation of cartilage matrix in human subjects and thus provided clinically relevant information.

Numerous membrane-anchored proteins are released from the cell surface by the process of regulated proteolysis called ectodomain shedding, and the enzymes responsible for shedding are primarily membrane-anchored proteinases. This process regulates a wide variety of cellular and physiologic functions, and dysregulated shedding is linked to numerous diseases, such as Alzheimer's disease, inflammation, rheumatoid arthritis (RA), cancer, chronic kidney disease, cardiac hypertrophy, and heart failure (26,27). LRP-1 shedding is increased under inflammatory conditions such as in RA and systemic lupus erythematosus (28), and in cancer (29,30), but the exact pathologic role of LRP-1 shedding in these diseases has not been clearly understood. We propose that LRP-1 shedding in local tissues under inflammatory or chronic pathologic conditions dysregulates normal turnover of ECM and cellular homeostasis, leading to slowly progressing chronic diseases such as in OA.

LRP-1 is widely expressed in different cell types and controls extracellular levels of numerous biologically active molecules to maintain tissue homeostasis (31). Currently, more than 50 ligands have been characterized, including lipoproteins, ECM proteins, growth factors, cell surface receptors, proteinases, proteinase inhibitors, and secreted intracellular proteins (31). In cartilage, LRP-1 controls not only ECM-degrading proteinases but also the Wnt/β-catenin signaling pathway by interacting with Frizzled-1 (32) and connective tissue growth factor (CCN2), and both regulate endochondral ossification and articular cartilage regeneration (33), emphasizing the

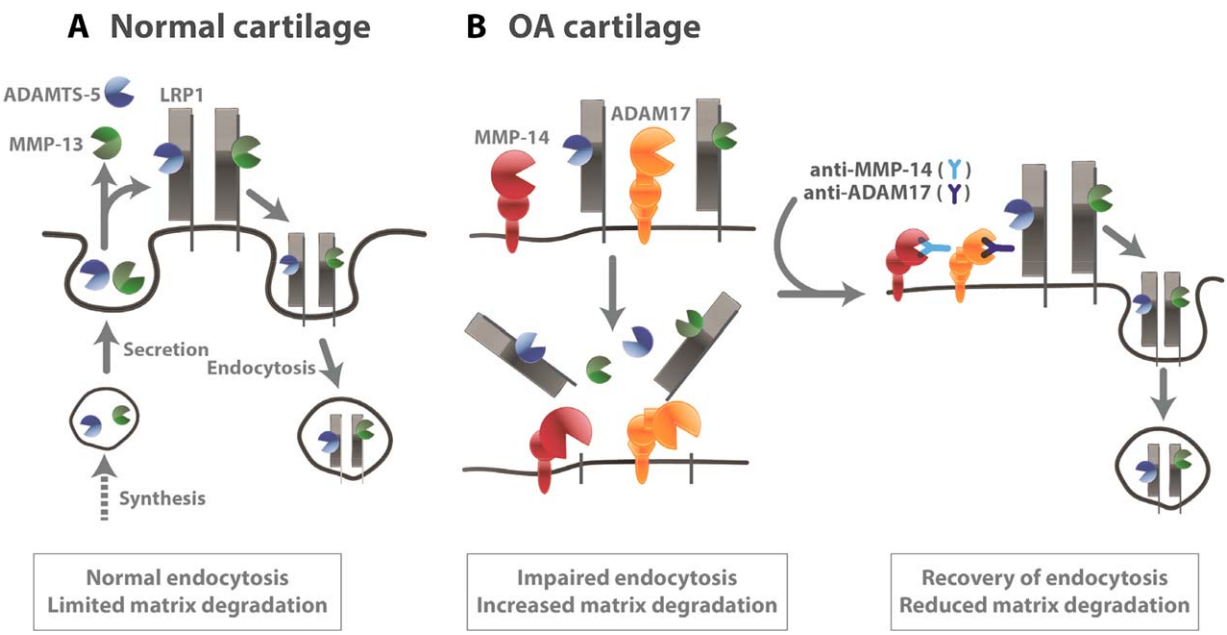

Figure 6. Low-density lipoprotein receptor–related protein 1 (LRP-1)–mediated endocytic pathways in normal and osteoarthritic (OA) cartilage. **A,** Secreted ADAMTS-5 and matrix metalloproteinase 13 (MMP-13) are largely endocytosed by LRP-1 in normal cartilage. Thus, their activities in the extracellular milieu are limited. **B,** In OA cartilage, the ectodomain of LRP-1 is shed by ADAM-17 and MMP-14, resulting in impairment of endocytic capacity of chondrocytes. Blocking of ADAM-17 and MMP-14 activities recovers the lost endocytic function of OA chondrocytes, reduces cartilage matrix degradation, and restores cartilage homeostasis.

importance of LRP-1 in skeletal development and in the maintenance of cartilage homeostasis.

Thus, the impairment of LRP-1 function due to increased shedding of the receptor is detrimental to healthy cartilage, as demonstrated in the present study. This is triggered by increased activity of ADAM-17 and MMP-14, but their protein levels were not significantly changed between healthy and OA cartilage (data not shown), which suggests that the activation of these enzymes is regulated posttranslationally. The additive but not synergistic effect of anti–ADAM-17 and anti–MMP-14 antibodies further suggests that these proteinases may be activated by different mechanisms and act independently as LRP-1 sheddases. In addition, MMP-14 and ADAM-17 cleave a number of cell membrane proteins, including growth factors, cytokines, cell adhesion molecules, and mechanosensors (26,34). Therefore, their activation may also affect the integrity of other cell surface molecules in cartilage as well as cellular behavior. We are currently investigating how ADAM-17 and MMP-14 are activated as well as their substrate selectivity in cartilage, as these may indicate additional molecular mechanisms for the development of OA, particularly in the early stages.

Another notable finding of this study is that anti–ADAM-17 and anti–MMP-14 antibodies reduced both aggrecanolytic and collagenolytic activities of human OA cartilage in culture, and this effect was due to restoration of the lost LRP-1 function by blocking the LRP-1 sheddase activities of ADAM-17 and MMP-14 (Figure 6). These results suggest that inhibition of elevated LRP-1 sheddase activities in OA cartilage may be an effective way to prevent cartilage matrix degradation. Although the systematic inhibition of ADAM-17 and MMP-14 as OA therapy may be problematic, as these enzymes are biologically important in the release of growth factors and cell surface receptors in many cell types (27,34), local administration of anti–ADAM-17 and anti–MMP-14 antibodies or small molecule inhibitors of ADAM-17 and MMP-14 may be worth investigating as disease-modifying OA drugs. This approach is an attractive option for OA therapy, as the recovery of the lost endocytic function of chondrocytes would help to maintain cartilage homeostasis. We are currently testing whether this approach is beneficial in early and advanced OA, using preclinical animal models.

ACKNOWLEDGMENTS

The authors thank Yasuyuki Shitomi for valuable discussion on the siRNA studies, Bryony Stott, Marcia Curtinha, and Ida Parisi for the histology of knee sections, and Katherine Groves and the Oxford Musculoskeletal Biobank for supplying human OA tissue.

AUTHOR CONTRIBUTIONS

All authors were involved in drafting the article or revising it critically for important intellectual content, and all authors approved the final version to be published. Dr. Yamamoto had full access to all of the data in the study and takes responsibility for the integrity of the data and the accuracy of the data analysis.

Study conception and design. Yamamoto, Murphy, Nagase.
Acquisition of data. Yamamoto, Santamaria, Botkjaer, Dudhia.
Analysis and interpretation of data. Yamamoto, Troeberg, Itoh, Murphy, Nagase.

REFERENCES

1. Goldring MB, Berenbaum F. Emerging targets in osteoarthritis therapy. Curr Opin Pharmacol 2015;22:51–63.
2. Naito S, Shiomi T, Okada A, Kimura T, Chijiiwa M, Fujita Y, et al. Expression of ADAMTS4 (aggrecanase-1) in human osteoarthritic cartilage. Pathol Int 2007;57:703–11.
3. Song RH, Tortorella MD, Malfait AM, Alston JT, Yang Z, Arner EC, et al. Aggrecan degradation in human articular cartilage explants is mediated by both ADAMTS-4 and ADAMTS-5. Arthritis Rheum 2007;56:575–85.
4. Larkin J, Lohr TA, Elefante L, Shearin J, Matico R, Su JL, et al. Translational development of an ADAMTS-5 antibody for osteoarthritis disease modification. Osteoarthritis Cartilage 2015; 23:1254–66.
5. Mitchell PG, Magna HA, Reeves LM, Lopresti-Morrow LL, Yocum SA, Rosner PJ, et al. Cloning, expression, and type II collagenolytic activity of matrix metalloproteinase-13 from human osteoarthritic cartilage. J Clin Invest 1996;97:761–8.
6. Kiani C, Chen L, Wu YJ, Yee AJ, Yang BB. Structure and function of aggrecan. Cell Res 2002;12:19–32.
7. Little CB, Barai A, Burkhardt D, Smith SM, Fosang AJ, Werb Z, et al. Matrix metalloproteinase 13–deficient mice are resistant to osteoarthritic cartilage erosion but not chondrocyte hypertrophy or osteophyte development. Arthritis Rheum 2009;60:3723–33.
8. Yamamoto K, Troeberg L, Scilabra SD, Pelosi M, Murphy CL, Strickland DK, et al. LRP-1-mediated endocytosis regulates extracellular activity of ADAMTS-5 in articular cartilage. FASEB J 2013;27:511–21.
9. Santamaria S, Yamamoto K, Botkjaer K, Tape C, Dyson MR, McCafferty J, et al. Antibody-based exosite inhibitors of ADAMTS-5 (aggrecanase-2). Biochem J 2015;471:391–401.
10. Yamamoto K, Okano H, Miyagawa W, Visse R, Shitomi Y, Santamaria S, et al. MMP-13 is constitutively produced in human chondrocytes and co-endocytosed with ADAMTS-5 and TIMP-3 by the endocytic receptor LRP1. Matrix Biol 2016;56:57–73.
11. Yamamoto K, Owen K, Parker AE, Scilabra SD, Dudhia J, Strickland DK, et al. Low density lipoprotein receptor-related protein 1 (LRP1)-mediated endocytic clearance of a disintegrin and metalloproteinase with thrombospondin motifs-4 (ADAMTS-4): functional differences of non-catalytic domains of ADAMTS-4 and ADAMTS-5 in LRP1 binding. J Biol Chem 2014;289:6462–74.
12. Troeberg L, Fushimi K, Khokha R, Emonard H, Ghosh P, Nagase H. Calcium pentosan polysulfate is a multifaceted exosite inhibitor of aggrecanases. FASEB J 2008;22:3515–24.
13. Scilabra SD, Troeberg L, Yamamoto K, Emonard H, Thogersen I, Enghild JJ, et al. Differential regulation of extracellular tissue inhibitor of metalloproteinases-3 levels by cell membrane-bound and shed low density lipoprotein receptor-related protein 1. J Biol Chem 2013;288:332–42.
14. Gendron C, Kashiwagi M, Lim NH, Enghild JJ, Thogersen IB, Hughes C, et al. Proteolytic activities of human ADAMTS-5: comparative studies with ADAMTS-4. J Biol Chem 2007;282: 18294–306.
15. Tape CJ, Willems SH, Dombernowsky SL, Stanley PL, Fogarasi M, Ouwehand W, et al. Cross-domain inhibition of TACE ectodomain. Proc Natl Acad Sci U S A 2011;108:5578–83.

16. Botkjaer KA, Kwok HF, Terp MG, Karatt-Vellatt A, Santamaria S, McCafferty J, et al. Development of a specific affinity-matured exosite inhibitor to MT1-MMP that efficiently inhibits tumor cell invasion in vitro and metastasis in vivo. Oncotarget 2016;7:16773–92.
17. Hascall VC, Sajdera SW. Proteinpolysaccharide complex from bovine nasal cartilage. The function of glycoprotein in the formation of aggregates. J Biol Chem 1969;244:2384–96.
18. Yu Z, Visse R, Inouye M, Nagase H, Brodsky B. Defining the requirements for collagenase cleavage in collagen type III using a bacterial collagen system. J Biol Chem 2012;287:22988–97.
19. Huang W, Suzuki K, Nagase H, Arumugam S, van Doren SR, Brew K. Folding and characterization of the amino-terminal domain of human tissue inhibitor of metalloproteinases-1 (TIMP-1) expressed at high yield in E. coli. FEBS Lett 1996;384:155–61.
20. Troeberg L, Tanaka M, Wait R, Shi YE, Brew K, Nagase H. E. coli expression of TIMP-4 and comparative kinetic studies with TIMP-1 and TIMP-2: insights into the interactions of TIMPs and matrix metalloproteinase 2 (gelatinase A). Biochemistry 2002;41:15025–35.
21. Troeberg L, Fushimi K, Scilabra SD, Nakamura H, Dive V, Thogersen IB, et al. The C-terminal domains of ADAMTS-4 and ADAMTS-5 promote association with N-TIMP-3. Matrix Biol 2009;28:463–9.
22. Kashiwagi M, Tortorella M, Nagase H, Brew K. TIMP-3 is a potent inhibitor of aggrecanase 1 (ADAM-TS4) and aggrecanase 2 (ADAM-TS5). J Biol Chem 2001;276:12501–4.
23. Kashiwagi M, Enghild JJ, Gendron C, Hughes C, Caterson B, Itoh Y, et al. Altered proteolytic activities of ADAMTS-4 expressed by C-terminal processing. J Biol Chem 2004;279:10109–19.
24. Bergman I, Loxley R. Lung tissue hydrolysates: studies of the optimum conditions for the spectrophotometric determination of hydroxyproline. Analyst 1969;94:575–84.
25. Etique N, Verzeaux L, Dedieu S, Emonard H. LRP-1: a checkpoint for the extracellular matrix proteolysis. Biomed Res Int 2013:152163–70.
26. Hartmann M, Herrlich A, Herrlich P. Who decides when to cleave an ectodomain? Trends Biochem Sci 2013;38:111–20.
27. Peschon JJ, Slack JL, Reddy P, Stocking KL, Sunnarborg SW, Lee DC, et al. An essential role for ectodomain shedding in mammalian development. Science 1998;282:1281–4.
28. Gorovoy M, Gaultier A, Campana WM, Firestein GS, Gonias SL. Inflammatory mediators promote production of shed LRP1/CD91, which regulates cell signaling and cytokine expression by macrophages. J Leukoc Biol 2010;88:769–78.
29. Rozanov DV, Hahn-Dantona E, Strickland DK, Strongin AY. The low density lipoprotein receptor-related protein LRP is regulated by membrane type-1 matrix metalloproteinase (MT1-MMP) proteolysis in malignant cells. J Biol Chem 2004;279:4260–8.
30. Selvais C, D'Auria L, Tyteca D, Perrot G, Lemoine P, Troeberg L, et al. Cell cholesterol modulates metalloproteinase-dependent shedding of low-density lipoprotein receptor-related protein-1 (LRP-1) and clearance function. FASEB J 2011;25:2770–81.
31. Lillis AP, van Duyn LB, Murphy-Ullrich JE, Strickland DK. LDL receptor-related protein 1: unique tissue-specific functions revealed by selective gene knockout studies. Physiol Rev 2008;88:887–918.
32. Zilberberg A, Yaniv A, Gazit A. The low density lipoprotein receptor-1, LRP1, interacts with the human frizzled-1 (HFz1) and down-regulates the canonical Wnt signaling pathway. J Biol Chem 2004;279:17535–42.
33. Kawata K, Kubota S, Eguchi T, Aoyama E, Moritani NH, Kondo S, et al. Role of LRP1 in transport of CCN2 protein in chondrocytes. J Cell Sci 2012;125:2965–72.
34. Itoh Y. Membrane-type matrix metalloproteinases: their functions and regulations. Matrix Biol 2015;44–6:207–23.

ARTHRITIS & RHEUMATOLOGY
Vol. 69, No. 6, June 2017, pp 1257–1266
DOI 10.1002/art.40086

The Biomarkers of Lupus Disease Study

A Bold Approach May Mitigate Interference of Background Immunosuppressants in Clinical Trials

Joan T. Merrill,[1] Fred Immermann,[2] Maryann Whitley,[2] Tianhui Zhou,[2] Andrew Hill,[2] Margot O'Toole,[2] Padmalatha Reddy,[2] Marek Honczarenko,[2] Aikaterini Thanou,[1] Joe Rawdon,[1] Joel M. Guthridge,[1] Judith A. James,[1] and Sudhakar Sridharan[2]

Objective. **Molecular medicine raised expectations for strategically targeted biologic agents in systemic lupus erythematosus (SLE), but clinical trial results have been disappointing and difficult to interpret. Most studies add investigational agents to various, often effective, standard therapy immunosuppressants used at baseline, with unknown treatment interactions. Eliminating polypharmacy in trials of active lupus remains controversial. We undertook the Biomarkers of Lupus Disease study to test withdrawal of immunosuppressants as a novel approach to rendering SLE trials interpretable.**

Methods. **In 41 patients with active, non–organ-threatening SLE flare (group A), temporary steroids were given while background immunosuppressants were withdrawn. Time to loss of disease suppression (time to disease flare) and safety were evaluated; standard therapy was immediately resumed when symptoms recurred. Immunologic impacts of standard therapy were studied at baseline by multiplex assay, enzyme-linked immunosorbent assay, and messenger RNA array in group A patients plus 62 additional patients donating a single sample (group B).**

Results. **Patients with lower or higher baseline disease activity had median times to flare of 71 or 45 days, respectively; 40 of 41 patients (98%) had disease flares by 6 months. All flares were treated and resolved within 6 weeks. No serious adverse events occurred from flare or infection. Type I interferon (IFN), Th17, and B lymphocyte stimulator pathways tracked together. Baseline immunosuppressants had distinct impacts on Th17 and B lymphocyte stimulator, depending on IFN signature.**

Conclusion. **Trials in active, non–organ-threatening SLE can safely withdraw background treatments if patients who have disease flares are designated nonresponders and returned to standard therapy. Immunologic effects of standard therapy vary between IFN-defined subsets. These findings provide a strategy for minimizing or optimizing treatment combinations in lupus trials and clinical care.**

Systemic lupus erythematosus (SLE) is a complex autoimmune disorder characterized by unpredictable flares of organ-threatening inflammation (1). Outlines of

ClinicalTrials.gov identifier: NCT00987831.

The contents of this article are solely the responsibility of the authors and do not necessarily represent the official views of the National Institutes of Health.

Supported by Pfizer (grant to the Oklahoma Medical Research Foundation). Biomarker evaluation was also supported by the NIH (National Institute of Allergy and Infectious Diseases, Division of Intramural Research grants U19-AI-082714 and U01-AI-101934, National Institute of Arthritis and Musculoskeletal and Skin Diseases grant P30-AR-053483, and Institutional Development awards U54-GM-104938 and P30-GM-103510 from the National Institute of General Medical Sciences).

[1]Joan T. Merrill, MD, Aikaterini Thanou, MD, Joe Rawdon, DNP, Joel M. Guthridge, PhD, Judith A. James, MD, PhD: Oklahoma Medical Research Foundation and University of Oklahoma Health Sciences Center, Oklahoma City; [2]Fred Immermann, MStat, Maryann Whitley, PhD, Tianhui Zhou, PhD (current address: GlaxoSmithKline, Boston, Massachusetts), Andrew Hill, PhD, Margot O'Toole, PhD (current address: Independent Consultant, Boston, Massachusetts), Padmalatha Reddy, PhD, Marek Honczarenko, MD, PhD (current address: Bristol-Myers Squibb, Inc., Princeton, New Jersey), Sudhakar Sridharan, MD (current address: Pharmaceutical Product Development, Inc., Rockville, Maryland): Pfizer, Inc., Cambridge, Massachusetts.

Drs. James and Sridharan contributed equally to this work.

Mr. Immermann and Drs. Whitley, Hill, and Reddy own stock or stock options in Pfizer.

Address correspondence to Joan T. Merrill, MD, Oklahoma Medical Research Foundation, 825 NE 13th Street, Oklahoma City, OK 73104. E-mail: joan-merrill@omrf.org.

Submitted for publication July 18, 2016; accepted in revised form February 28, 2017.

a common pathology have emerged (2,3), involving innate and adaptive immunity, defective immune clearance (4–9), and various combinations of multifactorial genetic risk variants (10,11). However, since patients may develop similar features via different routes in a circuitous and redundant immune system, it seems unlikely that any one treatment will work for all patients, and certainly not at a single dose.

The SLE field has seen only one approved treatment in 60 years and 25 years of disappointing clinical trial programs (12–19). Therefore, the predominant therapy for SLE remains empirical use of unapproved combinations of immunosuppressive agents that often fail to control disease adequately for long periods of time. Attempts to restore immunologic homeostasis with targeted biologic agents might be served by considering the complexity and heterogeneity of the patients. Current treatment development programs universally ignore this issue. With few exceptions (18), most trials have failed to focus on subsets of patients with immunopathology even relevant to the mechanism being addressed. Still, exploratory analyses of ambiguous study results have repeatedly uncovered, after the fact, subgroups of patients for whom each treatment might have succeeded better (14–19).

Standard therapy varies greatly between patients. Most clinical trials in SLE are add-on studies, continuing whatever variegated background immunosuppressants and steroids are being taken at entry. This background polypharmacy obscures the interpretation of pharmacodynamic data and likely contributes to apparently high "placebo" response rates, which actually reflect standard therapy temporarily optimized by rescue regimens. Some recent trials have been marginally more successful by limiting the aggressiveness of rescue interventions while allowing patients to continue a variety of immunosuppressants (14–16). However, suggestions to completely eliminate confounding background medications in SLE trials have been extremely controversial, even though patients have appreciable rates of serious infection when entering add-on trials with aggressive background medications.

In addition to obscuring pharmacodynamics and true response rates, background polypharmacy inevitably superimposes unknown immunomodulatory variables (14–19) that could have synergistic, additive, or inhibitory impact on a treatment under study. However, the impact of standard therapy on the mechanistic pathways of targeted, investigational biologic agents has never been studied in SLE. It follows that the true degree of heterogeneity innate to SLE cannot be known until the impact of therapeutic cross-talk on immunologic variables is better defined.

To provide an avenue for addressing these knowledge gaps, the Biomarkers of Lupus Disease (BOLD) study was designed to test several hypotheses. First, if patients with active but not organ-threatening SLE are given temporary relief by steroid injections, withdrawal of background immunosuppressants can be accomplished safely. Second, improvement from intramuscular steroids will gradually wane, ensuring low response rates after a few months in the absence of additional effective treatment. Third, upon flare, patients can be designated nonresponders and treated immediately with reasonable safety. The BOLD study also sought to generate hypotheses based on gene expression and protein data that background treatments may have disparate effects on different patient immunophenotypes. If the above hypotheses are correct, then withdrawing standard therapy immunosuppressants in trials could also help eliminate potential interactions between investigational and background treatments that may confound characterization of patient pathology and impact the interpretability of trial results.

PATIENTS AND METHODS

Patient enrollment. This study was performed in accordance with the Declaration of Helsinki and approved by the Institutional Review Board of the Oklahoma Medical Research Foundation. Patients provided written informed consent prior to beginning study-specific procedures.

Patients in group A (n = 41) completed both cross-sectional and prospective substudies. Patients in group B (n = 62) participated in the cross-sectional study only. Inclusion criteria for patients in groups A and B were as follows: fulfilling the American College of Rheumatology 1982 revised criteria for SLE (20) as updated in 1997 (21); receiving treatment with ≤20 mg prednisone (or equivalent) daily; having active, symptomatic disease despite standard therapy, defined as at least 2 British Isles Lupus Assessment Group (BILAG) B (moderate activity) scores (22), or at least 1 BILAG A (severe activity) score or an SLE Disease Activity Index (SLEDAI) score of at least 6 (23); and having a clinical state warranting intervention equivalent to the steroids offered to patients in group A. Additional inclusion criteria for patients in group A were ability and willingness to stop any immunosuppressants (e.g., azathioprine, methotrexate, or mycophenolate mofetil). Exclusion criteria included active infection at screening, known previous HIV or hepatitis B or C infection, pregnancy or inadequate birth control in women of childbearing potential, cancer (except basal cell or cervical carcinoma) within 5 years, and any medical condition that would interfere with the protocol or compromise patient safety, including but not limited to the investigator's opinion of risk for organ-threatening disease.

Cross-sectional substudy. One hundred three patients with active SLE (groups A and B) underwent clinical assessments and provided blood specimens (at baseline). To

Table 1. Demographic characteristics of the participants*

	Group A (n = 41)†	Group B (n = 62)‡	Groups A and B (n = 103)	Group C, controls (n = 55)
Women	39 (95.1)	56 (88.7)	94 (91.3)	53 (96.4)
Age, mean ± SD years	42.3 ± 11.9	40.87 ± 11.3	41.3 ± 11.5	40.8 ± 12.1
Race				
Caucasian	25 (61.0)	37 (59.7)	62 (60.2)	43 (78.2)
African American	11 (26.8)	12 (19.4)	23 (22.3)	10 (18.2)
American Indian	4 (9.8)	10 (16.1)	14 (13.6)	1 (1.8)
Asian	1 (2.4)	3 (4.8)	4 (3.9)	1 (1.8)

* Except where indicated otherwise, values are the number (%).
† Patients with systemic lupus erythematosus (SLE) participating in cross-sectional and prospective substudies.
‡ SLE patients participating in cross-sectional substudy only.

improve interpretability of gene expression studies (see below), 55 healthy control subjects (group C) were matched to participants in either group A or group B by race, sex, and age (within 5 years) (Table 1). Group C was used as a representative control population for scaling the principal component values and establishing normal gene expression ranges. Control subjects provided 2 samples at 2 different visits. High-quality samples from 99 of those visits were available for gene expression studies (see "Gene expression analysis" below).

Prospective substudy. After blood was obtained at baseline, group A patients discontinued immunosuppressants and received steroid injections (up to 640 mg methylprednisolone [MP] acetate within 2 weeks; maximum of 4 injections allowed). To continue in the study, patients had to demonstrate clinical improvement. Six patients required 640 mg, 19 required 480 mg, and 16 required ≤320 mg. Withdrawal of hydroxychloroquine at baseline was optional and could be overridden by patient or clinician. Patients taking low-dose oral steroids at entry continued at the same dose. Scheduled monthly disease activity assessments and adverse event collection were performed, and blood samples were obtained at each visit for safety monitoring, biomarker assessments, and coded storage in a repository. Upon clinical improvement (improving visit), patients were followed up monthly until disease activity increased (flare visit). As a safety strategy that is necessary for a trial of this design, patients were instructed to call or return to the clinic (without requiring an appointment) at any time they developed worsening symptoms. At the flare visit, standard therapy was reinitiated. Six patients with no improvement within 2 weeks of baseline were dropped from group A and immediately treated with standard therapy. Baseline samples from these patients, with their consent, were used in group B (final total of 41 patients in group A and 62 patients in group B).

Clinical assessments. We evaluated several measures at every visit. These included the hybrid SLEDAI, which is identical to the Safety of Estrogens in Lupus Erythematosus National Assessment (SELENA) version of the SLEDAI (SELENA–SLEDAI) (24,25) except for the proteinuria definition from the SLEDAI 2000 (26,27); the SELENA–SLEDAI flare index with physician's global assessment of disease activity (24,25); the BILAG 2004 index (28); the Cutaneous Lupus Erythematosus Disease Area and Severity Index (CLASI) (29,30); and tender and swollen joint counts. The SLEDAI and BILAG are commonly evaluated over the previous month (12–16), but when patients improved within 2 weeks of the entry visit, a 2-week evaluation using SLEDAI and BILAG clinical templates was performed. In these cases, the BILAG definition requiring 2 weeks of improvement was modified to 1 week.

Clinical outcome measures. The primary end point was time to flare from baseline in group A patients (n = 41), comparing patients with moderate disease at baseline (BILAG B score in ≤3 organs, no BILAG A score, and SLEDAI score ≤10) to those with significant disease (>3 BILAG B scores, at least 1 BILAG A score, SLEDAI score >10, or severe flare by clinical SELENA–SLEDAI flare index descriptors). Kaplan-Meier analysis and the log rank test were used to compare time to flare in the primary end point in subpopulations based on disease severity, steroid dose, and race.

Clinical improvement (improving visit) required clinician's opinion of significant improvement with no intention of increasing treatment, along with at least 1 grade of improvement by BILAG score in at least 1 organ or SLEDAI score decrease of at least 4 points. The flare visit was defined as clinician opinion of significant worsening and intention to treat, with at least 1 grade of worsening by BILAG score or a 4-point increase in SLEDAI score. The key secondary end point was a descriptive evaluation of adverse events.

Cytokine, chemokine, and soluble receptor measurement. Blood samples collected at baseline and at selected subsequent visits were assayed for levels of cytokines, chemokines, and soluble receptors. The Serum Analyte and Biomarker Core at the Oklahoma Medical Research Foundation uses a standardized xMAP 50-plex assay (Affymetrix/eBioscience) on the BioPlex200 platform (Bio-Rad). This 2-laser immunobead multiplex technology quantifies 50 cytokines in 250 μl of plasma (31). Serum B lymphocyte stimulator (R&D Systems) and APRIL (eBioscience) could not be multiplexed and were analyzed by enzyme-linked immunosorbent assay.

Gene expression analysis. Messenger RNA expression levels in whole blood samples were measured using TaqMan Low Density Arrays (Applied Biosystems) that included probe sets for 347 transcripts, and were then normalized to the median of endogenous control levels. Log_2-scale gene expression (ΔC_t) values for 11 interferon (IFN)–related genes (*GBP5*, *HERC5*, *IFI27*, *IRF7*, *ISG15*, *LY6E*, *MX1*, *OAS2*, *OAS3*, *RSAD2*, and *USP18*) were mean-centered and then subjected to principal components analysis using R

version 2.15.2 (www.r-project.org) (32). The first principal component (PC1) for each patient visit captured the majority of variance, providing a summarized expression measure for the 11 IFN-related genes. To make the arbitrary-scale PC1 values more interpretable, the ΔC_t values from 99 healthy volunteer visits from which high-quality samples were available were projected onto the PC1, and PC1 values for both patients and healthy volunteers were scaled linearly, where PC1 values for healthy volunteer visits had a mean of zero and unit variance, determining an "IFN index." The mclust R package was used to fit a 2-Gaussian equal-variance mixture model to the IFN index to define a single dividing value to separate "IFN low" from "IFN high." Samples from each patient visit were classified as "IFN high" or "IFN low," and patients were classified as "IFN high" or "IFN low" based on the predominant visit-level assignment. Gene expression data will be available at the NCBI GEO database (accession no. GSE92776) as of December 22, 2017.

Statistical analysis. Relationships between gene expression, IFN group (high versus low expression of IFN-inducible genes), and baseline immunosuppressants were examined using analysis of covariance with the covariates of RNA integrity number, assay batch, and percent neutrophils, based on our analysis of variable impacts. Relationships between protein concentrations (pg/ml), IFN group, and baseline immunosuppressants were evaluated using analysis of variance (ANOVA). For comparisons between subpopulations, gene expression and disease activity scores were analyzed by *t*-test, frequencies of autoantibody positivity by Fisher's exact test, and protein concentrations by ANOVA. Exploratory biomarker assessments were hypothesis-driven based on known pathology of SLE but were not adjusted for multiple comparisons.

RESULTS

Population. Participants were 91.3% women with a mean age of 41.3 years and were of Caucasian, African American, American Indian, and Asian race (Table 1). Demographics were similar between groups, but group A had fewer American Indians (Table 1). The mean ± SD cumulative BILAG score was 15.2 ± 5.73, and the mean ± SD SLEDAI score was 8.8 ± 3.73. Baseline lupus treatments included steroids, hydroxychloroquine, and immunosuppressants (32.1% azathioprine, 17.5% mycophenolate mofetil, 25.2% methotrexate) (Table 2). Overall, medications were comparable in groups A and B, with methotrexate slightly more common in group A and mycophenolate mofetil slightly more common in group B (Table 2). More group B patients used steroids and had low levels of complement (Table 2), suggesting that group B patients were sicker. However, disease activity scores did not differ between groups.

Changes in disease activity (group A). Supporting the clinician-weighted definitions of improvement and flare, scores on the BILAG 2004 index, SLEDAI, CLASI, and physician's global assessment of disease activity as well as joint counts decreased significantly at the improving visit and increased significantly at the flare visit for group A ($P < 0.0001$ in all cases except $P < 0.0012$ for the CLASI at the improving visit versus

Table 2. Baseline characteristics of the patient population*

	Group A (n = 41)†	Group B (n = 62)‡	Groups A and B (n = 103)
Baseline disease activity			
BILAG 2004 index, mean ± SD	15.0 ± 4.32	15.3 ± 6.52	15.2 ± 5.73
SLEDAI score, mean ± SD	8.1 ± 2.73	9.3 ± 4.21	8.8 ± 3.73
PGA (0–100-mm VAS), mean ± SD	1.9 ± 0.33	1.9 ± 0.33	1.89 ± 0.33
CLASI activity score, mean ± SD	5.6 ± 7.50	4.6 ± 5.18	5.0 ± 6.20
Tender joints, mean ± SD	14.3 ± 8.06	11.7 ± 8.25	12.7 ± 8.22
Swollen joints, mean ± SD	10.7 ± 7.05	9.9 ± 7.28	10.2 ± 7.15
Low C3, no. (%)	3 (7.3)	14 (22.6)	17 (16.5)
Low C4, no. (%)	8 (19.5)	21 (33.9)	29 (28.2)
Baseline treatment			
Azathioprine, no. (%)	12 (29.3)	21 (33.9)	33 (32.1)
Mycophenolate mofetil, no. (%)	6 (14.6)	12 (19.3)	18 (17.5)
Methotrexate, no. (%)	12 (29.3)	14 (22.6)	26 (25.2)
Any immunosuppressant, no. (%)§	30 (73.2)	47 (75.8)	77 (74.8)
Antimalarial, no. (%)	30 (73.2)	45 (72.6)	75 (72.8)
Prednisone (or equivalent), no. (%)	8 (20.0)	22 (35.5)	30 (29.1)
Steroid dose, mean ± SD mg/day¶	8.6 ± 5.46	13.9 ± 10.03	12.5 ± 9.26

* BILAG = British Isles Lupus Assessment Group; SLEDAI = Systemic Lupus Erythematosus Disease Activity Index; PGA = physician's global assessment of disease activity; VAS = visual analog scale; CLASI = Cutaneous Lupus Erythematosus Disease Area and Severity Index.
† SLE patients participating in cross-sectional and prospective substudies.
‡ SLE patients participating in cross-sectional substudy only.
§ Azathioprine, mycophenolate mofetil, or methotrexate.
¶ In prednisone equivalents, 1 patient entered receiving 20 mg/day; all others received ≤10 mg/day.

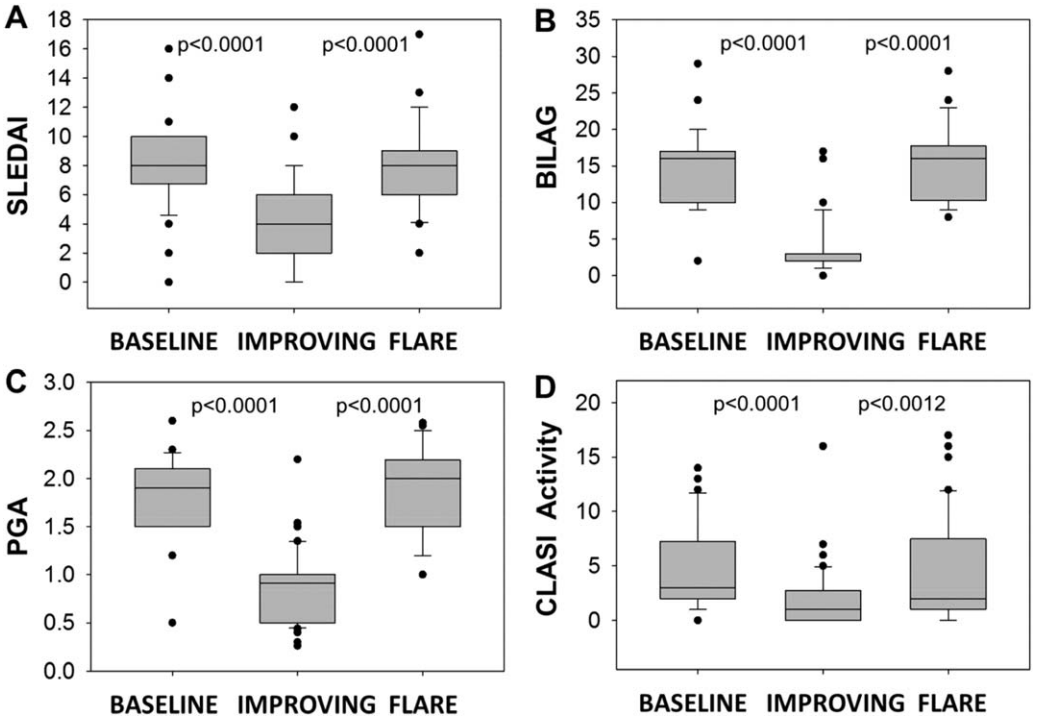

Figure 1. Standardized disease activity measures at the baseline, improving, and flare visits. Improving and flare visits in group A were designated based on clinician's opinion, with minimal input from the Systemic Lupus Erythematosus Disease Activity Index (SLEDAI) (**A**) or British Isles Lupus Assessment Group (BILAG) (**B**) tools, and no input from the physician's global assessment of disease activity (PGA) (**C**), Cutaneous Lupus Erythematosus Disease Area and Severity Index (CLASI) (**D**), or joint counts (see Supplementary Figure 1, available on the *Arthritis & Rheumatology* web site at http://onlinelibrary.wiley.com/doi/10.1002/art.40086/abstract). All disease activity measures decreased significantly from the baseline visit to the improving visit and increased significantly from the improving visit to the flare visit. Disease activity measures are defined in detail in Patients and Methods. Changes from the baseline to improving visit and from the improving to flare visit were evaluated using the nonparametric Wilcoxon rank sum test. Data are presented as box plots, where the boxes represent the 25th to 75th percentiles, the lines within the boxes represent the median, and the lines outside the boxes represent the 10th and 90th percentiles. Circles indicate values less than the 10th percentile or greater than the 90th percentile.

the flare visit) (Figure 1) (also see Supplementary Figure 1, available on the *Arthritis & Rheumatology* web site at http://onlinelibrary.wiley.com/doi/10.1002/art.40086/abstract). The prespecified primary end point was time to flare from baseline. All steroid injections were administered within the first 2 weeks of baseline. Within 6 months of baseline, 40 of the 41 group A patients exhibited flare, suggesting that analogous trials would have an extremely low placebo response rate at a 6-month milestone.

Time to flare did not differ between patients grouped by a priori definitions of moderate (n = 25; median 71 days) versus high (n = 16; median 45 days) disease activity ($P = 0.44$). However, in exploratory evaluations seeking prognostic indicators, time to flare was significantly shorter in patients with baseline cumulative BILAG scores of ≥17 compared to patients with scores of <17 ($P = 0.029$). African American patients exhibited flare sooner than other patients ($P = 0.013$) (Figure 2). Furthermore, flare occurred sooner in patients with BILAG scores of ≥17 who received ≤240 mg total MP acetate compared to those with BILAG scores of <17 who received ≥320 mg total MP acetate ($P = 0.043$). Thus, sicker patients requiring less MP acetate for an initial satisfactory response are likely to exhibit flares earlier than other patients, providing potentially useful parameters for clinical trial design (Figure 2). Use of low-dose steroids or antimalarials during the trial or withdrawal of different baseline immunosuppressants had no discernable impact on time to flare; however, this study was not powered to draw firm conclusions about these variables.

Safety. Adverse events were a prespecified, descriptive secondary end point. There were no adverse events in group B (single blood donation). Thirty-one adverse events were reported in group A; all resolved after evaluation and/or treatment. Nineteen adverse events were grade 1 or grade 2 infections. The two grade 3 adverse events (see Supplementary Table 1, http://onlinelibrary.wiley.com/doi/10.1002/art.40086/abstract) included one serious event (bleeding ulcer) and one

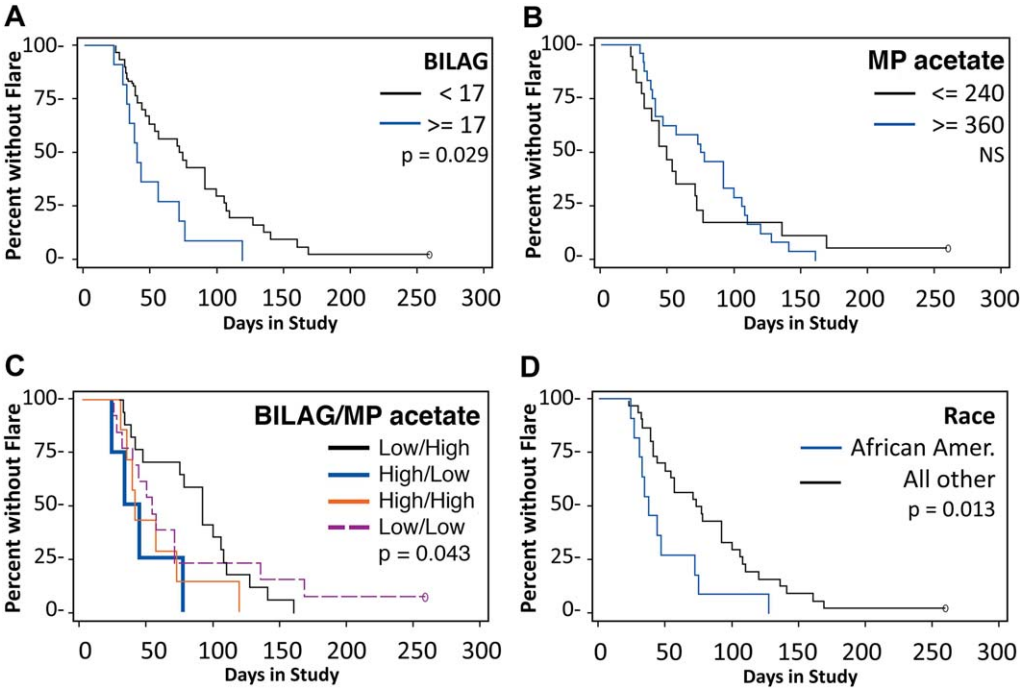

Figure 2. Time from baseline to flare visit. Flare occurred in 40 of 41 group A patients (97.6%) within 6 months of baseline. **A,** Time to flare was reduced in patients with high British Isles Lupus Assessment Group (BILAG) scores (≥17; n = 16) compared to those with low BILAG scores (<17; n = 25). **B,** Time to flare was not distinctly different in patients who received high cumulative doses of methylprednisolone (MP) acetate (≥360 mg) versus those who received low cumulative doses of MP acetate (≤240 mg). **C,** Flare was delayed significantly in patients with low BILAG scores who received high cumulative doses of MP acetate compared to patients with high BILAG scores who received low cumulative doses of MP acetate ($P = 0.043$). **D,** Time to flare was reduced in African American patients compared to all others. Comparisons were made by Kaplan-Meier analysis and log rank test. NS = not significant.

nonserious event (anal abscess that responded to oral antibiotics). Both patients recovered and remained in the study. There were no serious adverse events from lupus flare or infection.

As another safety measure, disease severity was compared between the baseline and flare visits in group A (see Supplementary Table 1, http://onlinelibrary.wiley.com/doi/10.1002/art.40086/abstract). The percentage of patients with BILAG A scores (severe activity) did not differ between the baseline visit (29%) and the flare visit (29%). Five patients (12.2%) who entered with BILAG B scores (moderate activity) exited with BILAG A scores, and 5 patients (12.2%) who entered with BILAG A scores exited with BILAG B scores. No severe flares were organ-threatening; no flares involved nephritis, the central nervous system, serious hematologic features, or solid organs. One patient was followed up for 1 year and had no flare. All end-of-study flares were treated with standard therapy and resolved within 6 weeks.

SLE immunopathology. A large percentage of patients with SLE are characterized by an elevated type I IFN–inducible gene signature (8), but it remains unclear whether IFN signals reliably discriminate optimal treatment groups. At baseline, patients in groups A and B with high type I IFN signals (IFN high) were compared to those without the signature (IFN low) (Table 3). IFN-high patients displayed markedly higher gene expression of B lymphocyte stimulator (*TNFSF13B*; $P = 0.005$) and interleukin-17 (IL-17) receptor A (*IL17RA*; $P = 0.009$), confirming previous observations that activated B lymphocyte stimulator and IL-17 pathways are associated with type I IFN activity in SLE (7–9). *IL23A* gene expression was not increased in IFN-high patients. Protein levels of B lymphocyte stimulator ($P = 0.0001$) and IL-23 (IL-23p19) ($P = 0.01$) were also higher in IFN-high patients. More IFN-high patients had antibodies to double-stranded DNA ($P = 0.0001$), SSA/Ro ($P = 0.0007$), RNP ($P = 0.0001$), and Sm ($P = 0.01$) (Table 3).

Impact of standard therapy on Th17 and B lymphocyte stimulator pathways in IFN-high and IFN-low patients. It has not been previously studied whether categorization of patients by IFN signatures could clarify understanding of standard therapy effects. Baseline *IL17RA* gene expression was modestly decreased in all

Table 3. Gene and protein expression relevant to IL-17 and B lymphocyte stimulator pathways and other clinical variables in subsets of SLE patients with or without a type I IFN signature*

	IFN-high patients (n = 49)	IFN-low patients (n = 46)	P†
Gene expression, mean ΔC_t vs. healthy controls‡			
TNFSF13B (B lymphocyte stimulator)	1.41	2.55	0.005
IL17RA	1.37	1.59	0.009
IL23A	2.23	2.27	0.77
Mediators of inflammation, mean pg/ml			
B lymphocyte stimulator	1,539.4	908.2	0.0001
IL-23p19	0.229	0.019	0.01
Autoantibodies, % positive			
Anti-dsDNA	30	2	0.0001
Anti-Ro	30	4	0.0007
Anti-Sm	13	0	0.01
Anti-RNP	37	0	0.0001
Disease activity score, mean			
SLEDAI	9.73	7.70	0.009
BILAG	16.5	14.0	0.04

* IL-17 = interleukin-17; SLE = systemic lupus erythematosus; anti-dsDNA = anti–double-stranded DNA; SLEDAI = SLE Disease Activity Index; BILAG = British Isles Lupus Assessment Group.
† Gene expression in 95 patients with evaluable RNA samples was compared by analysis of covariance with RNA integrity number, assay batch, and percent neutrophils as covariates, using a *t*-test to compare interferon (IFN)–high patients with IFN-low patients. Other values were compared by analysis of variance (protein concentrations), Fisher's exact test (frequencies of autoantibody positivity), or *t*-test (disease activity scores).
‡ Lower numbers indicate higher gene expression.

patients receiving immunosuppressants compared to those who were not (20% lower with methotrexate [$P = 0.059$]; 41% lower with mycophenolate mofetil [$P = 0.0039$]; 9% lower with azathioprine [$P = 0.33$]) (Table 4) (see Supplementary Figure 2, http://onlinelibrary.wiley.com/doi/10.1002/art.40086/abstract). However, the impact of these medications was more evident when IFN-high and IFN-low patients were examined

Table 4. Impact of standard SLE medications on gene expression in subsets of patients with or without a type I IFN signature*

	All patients (n = 95)†		IFN-high patients (n = 49)‡		IFN-low patients (n = 46)	
Gene (RNA), treatment	Difference from no treatment, %	P	Difference from no treatment, %	P	Difference from no treatment, %	P
IL17RA						
MTX	19.6	0.059	9.3	0.35	30.8	0.069
MMF	40.9	0.0039	1.2	0.15	96.2	0.0015
AZA	8.8	0.33	14.7	0.15	3.2	0.93
TNFSF13B (B lymphocyte stimulator)						
HCQ	48.9	0.22	204.1	0.0068	−27.1	0.52

* SLE = systemic lupus erythematosus; MTX = methotrexate; MMF = mycophenolate mofetil; AZA = azathioprine; HCQ = hydroxychloroquine.
† Gene expression in 95 patients with evaluable RNA samples was compared by analysis of covariance with RNA integrity number, assay batch, and percent neutrophils as covariates, using a *t*-test to compare the percent difference between those taking and those not taking a designated treatment. The overall population, interferon (IFN)–high patient subset, and IFN-low patient subset were analyzed separately. Note that despite lower numbers of patients in each defined subset, the differences, where apparent, have greater statistical significance, emphasizing the increased clarity that might be derived from analysis of meaningful patient types.
‡ The type I IFN signature was defined by *GBP5*, *HERC5*, *IFI27*, *IRF7*, *ISG15*, *LY6E*, *MX1*, *OAS2*, *OAS3*, *RSAD2*, and *USP18* (see Patients and Methods).

separately. Mycophenolate mofetil and methotrexate reduced *IL17RA* expression in the IFN-low group only (Table 4). Hydroxychloroquine treatment was associated with substantially lower *TNFSF13B* (B lymphocyte stimulator) gene expression in IFN-high patients, but not in IFN-low patients (Table 4).

Individual immunosuppressants had no consistent effects on protein or gene expression when comparing baseline visits (active disease, receiving treatment) and flare visits (not receiving treatment) in group A patients, but the numbers were small in each treatment group (data not shown). However, B lymphocyte stimulator RNA (but not protein) expression increased 2.4-fold from the baseline to the flare visit in all IFN-low patients, regardless of baseline treatments ($P = 0.0003$), reaching levels equivalent to those seen in IFN-high patients (data not shown).

DISCUSSION

Data from the BOLD study suggest that future SLE clinical trials could achieve very low placebo response rates without unacceptably compromising patient safety by enrolling SLE patients with active, non–organ-threatening disease, providing temporary steroids, and withdrawing standard therapy immunosuppressants. Risk of serious infections might even be reduced by eliminating excess immunosuppressants at baseline, but this study was not designed to test that hypothesis.

Most SLE clinical trials continue various, often effective standard therapy background medications being taken by patients at entry (12–19), based on assumptions that this minimizes risk of serious flares and that immunologic interference is minimal. However, these two assumptions are not evidence-based. Moreover, they are inconsistent with each other, since flares are only prevented by modulating immunologic pathways. In fact, data from trials indicate that patients receiving standard therapy alone have almost as many infections as those receiving standard therapy plus biologic agents (12–16); it therefore seems likely that standard therapy is at least as risky as some biologic agents. Other analyses suggest that in trials with a polypharmacy design, efficacy can only be distinguished in subsets of patients with higher grade disease activity (15,16). Since these patients are at highest risk of serious flares, it may be fortunate that interpretable studies can be performed for them without requiring treatment withdrawal.

Does this mean that clinical trials in SLE (and subsequent regulatory approvals) should be restricted to polypharmacy protocols in patients with the most severe disease? A recent shift in phase III plans for at least one agent (15) suggests that this notion is gaining traction, risking disenfranchisement of patients with chronic, moderate SLE from access to targeted biologic agents. There is a significant unmet need in this population, as even with good disease control, chronic, smoldering SLE leads to progressive organ damage, long-term morbidity, and mortality (33,34). Our data suggest that immunosuppressants can be safely withdrawn in these patients to support a safe and interpretable trial design. This approach might provide early proof of efficacy in less vulnerable patients while helping to define pharmacodynamic variables without confounding immunomodulatory signals. In turn, later trials with more vulnerable patients would be armed with better information to minimize risk of choosing untoward treatment combinations.

The need to account for confounding medications is highlighted by our exploratory observation that certain standard therapies might have unique effects on IFN-high patients versus IFN-low patients. Although they are used interchangeably in the clinic and in clinical trials, immunosuppressants may have disparate and even opposing effects in SLE subgroups; our preliminary observations support this hypothesis. If not addressed, this could confound clinical trials and selection of optimal treatment combinations in the clinic. Therefore, larger, prospective studies with prespecified biomarker end points and adjustments for multiple comparisons are needed to rigorously test the immunologic effects of antimalarials and immunosuppressants in different patient subsets. Our incidental finding that IFN-low patients exhibit uncharacteristically high B lymphocyte stimulator RNA expression at the time of acute flare also warrants further exploration. We previously described B lymphocyte stimulator as a robust marker for SLE disease activation (7), and various alternative immunologic routes can induce B lymphocyte stimulator (35). Thus, B lymphocyte stimulator could represent a common pathway for discrete SLE subpopulations at the time of flare.

Given the heterogeneity of lupus, it is likely that exceptions to the broad themes inspected in this small study will arise, drawing attention to antagonistic or synergistic pathways in smaller patient subsets. However, better knowledge of the immunologic effects of standard therapy lupus medications on major identifiable subgroups of lupus will aid more rational testing and more successful use of targeted biologic agents.

ACKNOWLEDGMENTS

We thank the many colleagues at Pfizer who contributed their research time, reagents, and laboratory infrastructure. We

also thank Dr. Jill P. Buyon (New York University, New York, NY) for serving as the safety monitor and contributing helpful discussions to the design of the study, Dr. Rebecka Bourn (Oklahoma Medical Research Foundation, Oklahoma City) for editorial assistance, and Dr. Angela Andersen (Life Science Editors, Salt Lake City, UT) for comments on the manuscript.

AUTHOR CONTRIBUTIONS

All authors were involved in drafting the article or revising it critically for important intellectual content, and all authors approved the final version to be published. Dr. Merrill had full access to all of the data in the study and takes responsibility for the integrity of the data and the accuracy of the data analysis.

Study conception and design. Merrill, James, Sridharan.

Acquisition of data. Merrill, O'Toole, Reddy, Honczarenko, Thanou, Rawdon, Guthridge, James, Sridharan.

Analysis and interpretation of data. Merrill, Immermann, Whitley, Zhou, Hill, Guthridge, James, Sridharan.

ROLE OF THE STUDY SPONSOR

Pfizer funded the study but had no role in its design or clinical conduct. Coauthors of the study, in their capacity as employees of Pfizer, participated in biomarker data collection, sample assays, data analysis, and the writing of the manuscript. This project did not include the study of any Pfizer products. Pfizer had no role in the decision to submit the manuscript for publication. Publication of this article was not contingent upon approval by Pfizer.

REFERENCES

1. Rahman A, Isenberg DA. Systemic lupus erythematosus. N Engl J Med 2008;358:929–39.
2. Cervera R, Khamashta MA, Font J, Sebastiani GD, Gil A, Lavilla P, et al. Systemic lupus erythematosus: clinical and immunologic patterns of disease expression in a cohort of 1,000 patients: the European Working Party on Systemic Lupus Erythematosus. Medicine (Baltimore) 1993;72:113–24.
3. Font J, Cervera R, Ramos-Casals M, Garcia-Carrasco M, Sents J, Herrero C, et al. Clusters of clinical and immunologic features in systemic lupus erythematosus: analysis of 600 patients from a single center. Semin Arthritis Rheum 2004;33:217–30.
4. Yao Y, Richman L, Higgs BW, Morehouse CA, de los Reyes M, Brohawn P, et al. Neutralization of interferon-α/β–inducible genes and downstream effect in a phase I trial of an anti–interferon-α monoclonal antibody in systemic lupus erythematosus. Arthritis Rheum 2009;60:1785–96.
5. Mohan C, Datta SK. Lupus: key pathogenic mechanisms and contributing factors. Clin Immunol Immunopathol 1995;77:209–20.
6. Kotzin BL. Systemic lupus erythematosus. Cell 1996;85:303–6.
7. Ritterhouse LL, Crowe SR, Niewold TB, Merrill JT, Roberts VC, Dedeke AB, et al. B lymphocyte stimulator levels in systemic lupus erythematosus: higher circulating levels in African American patients and increased production after influenza vaccination in patients with low baseline levels. Arthritis Rheum 2011;63:3931–41.
8. Brkic Z, Corneth OB, van Helden-Meeuwsen CG, Dolhain RJ, Maria NI, Paulissen SM, et al. T-helper 17 cell cytokines and interferon type I: partners in crime in systemic lupus erythematosus? Arthritis Res Ther 2014;16:R62.
9. Dolff S, Quandt D, Wilde B, Feldkamp T, Hua F, Cai X, et al. Increased expression of costimulatory markers CD134 and CD80 on interleukin-17 producing T cells in patients with systemic lupus erythematosus. Arthritis Res Ther 2010;12:R150.
10. Sestak AL, Furnrohr BG, Harley JB, Merrill JT, Namjou B. The genetics of systemic lupus erythematosus and implications for targeted therapy. Ann Rheum Dis 2011;70 Suppl 1:i37–43.
11. Bentham J, Morris DL, Cunninghame Graham DS, Pinder CL, Tombleson P, Behrens TW, et al. Genetic association analyses implicate aberrant regulation of innate and adaptive immunity genes in the pathogenesis of systemic lupus erythematosus. Nat Genet 2015;47:1457–64.
12. Navarra SV, Guzman RM, Gallacher AE, Hall S, Levy RA, Jimenez RE, et al. Efficacy and safety of belimumab in patients with active systemic lupus erythematosus: a randomised, placebo-controlled, phase 3 trial. Lancet 2011;377:721–31.
13. Furie R, Petri M, Zamani O, Cervera R, Wallace DJ, Tegzova D, et al. A phase III, randomized, placebo-controlled study of belimumab, a monoclonal antibody that inhibits B lymphocyte stimulator, in patients with systemic lupus erythematosus. Arthritis Rheum 2011;63:3918–30.
14. Wallace DJ, Kalunian K, Petri MA, Strand V, Houssiau FA, Pike M, et al. Efficacy and safety of epratuzumab in patients with moderate/severe active systemic lupus erythematosus: results from EMBLEM, a phase IIb, randomised, double-blind, placebo-controlled, multicentre study. Ann Rheum Dis 2014;73:183–90.
15. Furie RA, Leon G, Thomas M, Petri MA, Chu AD, Hislop C, et al. A phase 2, randomised, placebo-controlled clinical trial of blisibimod, an inhibitor of B cell activating factor, in patients with moderate-to-severe systemic lupus erythematosus, the PEARL-SC study. Ann Rheum Dis 2015;74:1667–75.
16. Van Vollenhoven RF, Petri MA, Cervera R, Roth DA, Ji BN, Kleoudis CS, et al. Belimumab in the treatment of systemic lupus erythematosus: high disease activity predictors of response. Ann Rheum Dis 2012;71:1343–9.
17. Merrill JT, Erkan D, Buyon JP. Challenges in bringing the bench to bedside in drug development for SLE. Nat Rev Drug Discov 2004;3:1036–46.
18. Merrill JT, Buyon JP. Connective tissue diseases: what does the death of Riquent hold for the future of SLE? Nat Rev Rheumatol 2009;5:306–7.
19. Merrill JT. Emergence of targeted immune therapies for systemic lupus. Expert Opin Emerg Drugs 2005;10:53–65.
20. Tan EM, Cohen AS, Fries JF, Masi AT, McShane DJ, Rothfield NF, et al. The 1982 revised criteria for the classification of systemic lupus erythematosus. Arthritis Rheum 1982;25:1271–7.
21. Hochberg MC. Updating the American College of Rheumatology revised criteria for the classification of systemic lupus erythematosus [letter]. Arthritis Rheum 1997;40:1725.
22. Symmons DP, Coppock JS, Bacon PA, Bresnihan B, Isenberg DA, Maddison P, et al, and Members of the British Isles Lupus Assessment Group (BILAG). Development and assessment of a computerized index of clinical disease activity in systemic lupus erythematosus. Q J Med 1988;69:927–37.
23. Bombardier C, Gladman DD, Urowitz MB, Caron D, Chang DH, and the Committee on Prognosis Studies in SLE. Derivation of the SLEDAI: a disease activity index for lupus patients. Arthritis Rheum 1992;35:630–40.
24. Buyon JP, Petri MA, Kim MY, Kalunian KC, Grossman J, Hahn BH, et al. The effect of combined estrogen and progesterone hormone replacement therapy on disease activity in systemic lupus erythematosus: a randomized trial. Ann Intern Med 2005;142:953–62.
25. Petri M, Kim MY, Kalunian KC, Grossman J, Hahn BH, Sammaritano LR, et al, for the OC-SELENA Trial. Combined oral contraceptives in women with systemic lupus erythematosus. N Engl J Med 2005;353:2550–8.
26. Gladman DD, Ibanez D, Urowitz MB: Systemic Lupus Erythematosus Disease Activity Index 2000. J Rheumatol 2002;29:288–91.
27. Touma Z, Urowitz MB, Gladman DD. SLEDAI-2K for a 30-day window. Lupus 2010;19:49–51.
28. Yee CS, Farewell V, Isenberg DA, Griffiths B, Teh LS, Bruce IN, et al. The BILAG-2004 index is sensitive to change for

assessment of SLE disease activity. Rheumatology (Oxford) 2009; 48:691–5.
29. Albrecht J, Taylor L, Berlin JA, Dulay S, Ang G, Fakharzadeh S, et al. The CLASI (Cutaneous Lupus Erythematosus Disease Area and Severity Index): an outcome instrument for cutaneous lupus erythematosus. J Invest Dermatol 2005;125:889–94.
30. Klein R, Moghadam-Kia S, LoMonico J, Okawa J, Coley C, Taylor L, et al. Development of the CLASI as a tool to measure disease severity and responsiveness to therapy in cutaneous lupus erythematosus. Arch Dermatol 2011;147:203–8.
31. Munroe ME, Vista ES, Guthridge JM, Thompson LF, Merrill JT, James JA. Proinflammatory adaptive cytokine and shed tumor necrosis factor receptor levels are elevated preceding systemic lupus erythematosus disease flare. Arthritis Rheumatol 2014;66:1888–99.
32. Hill AA, Immermann FW, Zhang Y, Reddy PS, Zhou T, O'Toole M, et al. FRI0003 determination of interferon (IFN) signatures for SLE patients may be critical for optimal treatment selection but depends on the genes chosen: report from the BOLD (Biomarkers of Lupus Disease) study. Ann Rheum Dis 2013;72 Suppl 3:A369–70.
33. Urowitz MB, Gladman DD, Tom BD, Ibanez D, Farewell VT. Changing patterns in mortality and disease outcomes for patients with systemic lupus erythematosus. J Rheumatol 2008;35:2152–8.
34. Urowitz MB, Gladman DD, Ibanez D, Fortin PR, Bae SC, Gordon C, et al. Evolution of disease burden over five years in a multicenter inception systemic lupus erythematosus cohort. Arthritis Care Res (Hoboken) 2012;64:132–7.
35. Schneider P. The role of APRIL and BAFF in lymphocyte activation. Curr Opin Immunol 2005;17:282–9.

ARTHRITIS & RHEUMATOLOGY
Vol. 69, No. 6, June 2017, pp 1267–1271
DOI 10.1002/art.40079

BRIEF REPORT

The Euro-Lupus Low-Dose Intravenous Cyclophosphamide Regimen Does Not Impact the Ovarian Reserve, as Measured by Serum Levels of Anti–Müllerian Hormone

Farah Tamirou, Séverine Nieuwland Husson, Damien Gruson, Frédéric Debière, Bernard R. Lauwerys, and Frédéric A. Houssiau

Objective. **The Euro-Lupus regimen of low-dose intravenous cyclophosphamide (IV CYC) (cumulative dose of 3 gm) was developed to reduce gonadal toxicity. To address the possibility of a marginal effect on the ovarian reserve, we measured serum titers of anti–Müllerian hormone (AMH) in patients with systemic lupus erythematosus (SLE) treated with the Euro-Lupus regimen and compared them with those measured in patients who were treated with higher doses of IV CYC or were never treated with IV CYC.**

Methods. **Serum AMH levels were measured by enzyme-linked immunosorbent assay in a cohort of 155 premenopausal SLE patients; 30 of these patients had been treated with the Euro-Lupus regimen, and 24 had received higher doses of IV CYC. None had received oral CYC. AMH levels were age-adjusted using a slope computed from levels measured across the group of SLE patients who had not been treated with IV CYC. Demographic and clinical data were collected.**

Results. **Serum titers of AMH measured in SLE patients treated with the Euro-Lupus IV CYC regimen (median dose 1.46 ng/ml) did not differ from those measured in patients never treated with the cytotoxic drug (median 1.85 ng/ml). As expected, patients given >6 gm of IV CYC had significantly lower serum titers of AMH (median 0.83 ng/ml) compared with those never treated with IV CYC ($P = 0.047$). Median serum AMH titers did not change before (1.24 ng/ml) and after (2.50 ng/ml) treatment with the Euro-Lupus IV CYC regimen in the subset of patients for whom paired samples could be tested ($P = 0.43$).**

Conclusion. **The Euro-Lupus regimen of low-dose IV CYC does not impact the ovarian reserve of SLE patients and can therefore be proposed as treatment in patients seeking to become pregnant.**

Intravenous cyclophosphamide (IV CYC) is used to treat severe disease manifestations of systemic lupus erythematosus (SLE), such as neuropsychiatric SLE or lupus nephritis (LN). It is well known that the high-dose IV CYC regimen proposed by the National Institutes of Health (NIH) (1) is gonadotoxic and may lead to early menopause in SLE patients, the risk of which is commensurate with the cumulative dose and age (2).

We proposed the use of low-dose IV CYC treatment, the so-called Euro-Lupus regimen, as induction therapy for LN to minimize gonadal side effects (3). To our knowledge, no case of early menopause after treatment with the Euro-Lupus regimen has been reported. Nonetheless, this end point is not appropriate for unmasking subtle gonadal damage in young women who still have a wide ovarian reserve and in whom cytotoxic damage may therefore remain subclinical. This issue can now be addressed by measuring serum levels of anti–Müllerian hormone (AMH), which is produced by the granulosa cells of growing follicles that shelter oocytes to maturity, thereby reflecting ovarian reserve (4). Although CYC treatment has been associated with lower serum titers of AMH in SLE patients (5,6), this was never tested in patients who received treatment with the low-dose Euro-Lupus regimen.

The aim of this study was to determine whether the Euro-Lupus regimen of low-dose IV CYC impacts the ovarian reserve, as assessed by serum levels of AMH.

Supported by the Fonds pour la Recherche Scientifique en Rhumatologie/Fonds voor Wetenschappelijke Reuma Onderzoek of the Société Royale Belge de Rhumatologie/Koninklijke Belgische Vereniging voor Reumatologie.

Farah Tamirou, MD, Séverine Nieuwland Husson, CNP, Damien Gruson, MD, PhD, Frédéric Debière, MD, PhD, Bernard R. Lauwerys, MD, PhD, Frédéric A. Houssiau, MD, PhD: Cliniques Universitaires Saint-Luc, Université catholique de Louvain, Brussels, Belgium.

Address correspondence to Farah Tamirou, MD, Rheumatology Department, Cliniques Universitaires Saint-Luc, Avenue Hippocrate 10, B-1200 Brussels, Belgium. E-mail: farah.tamirou@uclouvain.be.

Submitted for publication December 19, 2016; accepted in revised form February 16, 2017.

PATIENTS AND METHODS

Patients. Within the framework of the Louvain Lupus Cohort, clinical data and serum samples are collected on a regular basis, after informed consent is obtained. For this study, patients younger than age 50 years were included, and within this group, those who were pregnant or had undergone menopause were excluded. Pregnancy and menopause are indeed conditions associated with decreased and undetectable levels of AMH, respectively. Importantly, none of the patients who received the Euro-Lupus regimen were excluded because of early menopause, while 2 patients who received a cumulative IV CYC dose of 13 gm and experienced gonadal failure at age 34 years and age 42 years, respectively, were excluded. Table 1 shows the demographic data for the patients as well as past and current treatments, disease activity, and damage. Of note, most patients were white, half of them were receiving steroids at the time of serum sampling, and one-third had received IV CYC. None had received oral CYC.

Serum AMH measurements. Serum titers of AMH were measured using the ultrasensitive quantitative 3-step enzyme-linked immunosorbent assay method developed by Ansh Laboratories. This assay measures levels of AMH and proAMH. All samples were tested in the same assay. Because AMH titers decrease with age, we adjusted AMH levels for a standard age of 30 years, using a slope computed from AMH levels measured across the group of SLE patients not treated with IV CYC (n = 101) who were ages 18–48 years.

Table 1. Characteristics of the patients at the time of serum AMH measurement*

Demographic data	
Age, mean ± SD years	35 ± 7
Ethnicity	
White European	72
African	7
Other	21
Disease duration, mean ± SD years	10 ± 7
Treatment	
Prednisolone	
Ever	94
Current	54
Dose, mean ± SD mg†	10 ± 8
Hydroxychloroquine	
Ever	99
Current	88
IV CYC ever	35
Mycophenolate mofetil	
Ever	30
Current	23
Azathioprine	
Ever	48
Current	21
Methotrexate	
Ever	15
Current	7
Current SLEDAI-2K, median (range)	2 (0–16)
Current SDI, median (range)	0 (0–7)

* Except where indicated otherwise, values are the percent. AMH = anti–Müllerian hormone; IV CYC = intravenous cyclophosphamide; SLEDAI-2K = Systemic Lupus Erythematosus Disease Activity Index 2000; SDI = Systemic Lupus International Collaborating Clinics/American College of Rheumatology Damage Index.
† Calculated for patients currently receiving prednisolone.

In the cross-sectional analysis, the mean ± SD time interval between the last IV CYC treatment and measurement of serum levels of AMH was 7 ± 5 years. When available, longitudinal data (before and after IV CYC treatment) were collected. The mean ± SD time interval between collection of the 2 samples was 19 ± 13 months.

Statistical analysis. The unpaired *t*-test, Mann-Whitney test, Wilcoxon's signed rank test, and Fisher's exact test were used, as appropriate.

RESULTS

Cross-sectional analysis of serum titers of AMH. As shown in Table 2, the mean body mass index (BMI) did not differ between groups, thereby excluding a confounding bias related to the known inverse relationship between BMI and AMH levels (7). The mean age of the patients at the time of the AMH assay was significantly higher in the high-dose IV CYC group (>6 gm) compared with patients not treated with IV CYC, but this difference was taken into account by adjusting for age when serum levels of AMH were measured. As expected, treatment with high-dose IV CYC (>6 gm) was associated with a longer disease duration and a higher Systemic Lupus International Collaborating Clinics/American College of Rheumatology Damage Index (8). Not surprisingly, renal involvement was statistically more common in all IV CYC–treated groups compared with patients who were not treated with IV CYC.

As shown in Figure 1, age-adjusted serum levels of AMH in patients who received the Euro-Lupus IV CYC regimen (cumulative dose of 3 gm) did not differ from those measured in patients who were never treated with IV CYC (median 1.46 ng/ml versus 1.85 ng/ml). Patients who received more than 3 gm and up to 6 gm of IV CYC (mean ± SD 5.54 ± 0.85 gm) had a median serum level of AMH of 2.75 ng/ml, which also was not statistically different from that in the group not treated with IV CYC. Conversely, and as expected, patients who received more than 6 gm of IV CYC (mean ± SD dose 9.49 ± 4.02 gm) had significantly lower serum titers of AMH compared with patients who did not receive IV CYC (median 0.83 ng/ml; $P = 0.047$ by Mann-Whitney test).

Longitudinal analysis of serum titers of AMH. In 10 patients treated with the Euro-Lupus IV CYC regimen, we had the opportunity to measure serum levels of AMH before and after treatment. The median age-adjusted serum titers of AMH did not differ (1.24 ng/ml before and 2.50 ng/ml after; $P = 0.43$ by Wilcoxon's test).

DISCUSSION

The Euro-Lupus regimen of low-dose IV CYC, which consists of 6 IV CYC pulses of 500 mg every

Table 2. Clinical features of the SLE patients at the time of serum AMH measurement, according to the cumulative dose of IV CYC*

Clinical features	No IV CYC (n = 101)	IV CYC, 3 gm (n = 30)	IV CYC, >3 but ≤ 6 gm (n = 11)	IV CYC, >6 gm (n = 13)
Age, mean ± SD years	35 ± 8	34 ± 6	32 ± 8	39 ± 6†
Disease duration, mean ± SD years	8.72 ± 6.78	9.14 ± 5.19	11.14 ± 5.28	15.52 ± 8.78‡
BMI, mean ± SD kg/m^2	24.66 ± 4.70	24.76 ± 4.78	26.38 ± 7.14	26.77 ± 5.42
Hormonal contraception use	47 (52)	17 (57)	4 (50)	7 (70)
ACR criteria				
Malar rash	32 (32)§	17 (57)	7 (64)	7 (54)
Discoid rash	11 (11)	4 (13)	0 (0)	0 (0)
Photosensitivity	41 (41)	8 (27)	1 (9)	4 (31)
Oral ulcers	32 (32)	5 (17)	2 (18)	3 (23)
Nonerosive arthritis	71 (70)	18 (60)	4 (36)	9 (69)
Pleuritis or pericarditis	27 (27)	5 (17)	1 (9)	4 (31)
Renal disorder	24 (24)¶	30 (100)	9 (82)	11 (85)
Neurologic disorder	4 (4)#	1 (3)	3 (27)	0 (0)
Hematologic disorder	83 (82)	26 (87)	10 (91)	13 (100)
Immunologic disorder	83 (82)	29 (97)	11 (100)	12 (92)
ANA positive	101 (100)	30 (100)	11 (100)	13 (100)
Time between last IV CYC dose and AMH measurement, mean ± SD years	NA	6.35 ± 4.69	4.10 ± 3.09	9.68 ± 6.70#
SDI, median (range)	0 (0–3)	0 (0–7)	0 (0–1)	1 (0–5)**
Age-adjusted serum titer of AMH, median ng/ml	1.85	1.46	2.75	0.83

* Except where indicated otherwise, values are the percent. *P* values were calculated by unpaired *t*-test, Mann-Whitney test, or Fisher's exact test, as appropriate. SLE = systemic lupus erythematosus; AMH = anti–Müllerian hormone; BMI = body mass index; ANA = antinuclear antibody; SDI = Systemic Lupus International Collaborating Clinics/American College of Rheumatology (ACR) Damage Index.
† $P < 0.05$ versus no intravenous cyclophosphamide (IV CYC), 3 gm IV CYC, and >3 but ≤ 6 gm IV CYC.
‡ $P < 0.005$ versus no IV CYC and 3 gm IV CYC.
§ $P < 0.05$ versus 3 gm IV CYC and >3 but ≤ 6 gm IV CYC.
¶ $P < 0.0005$ versus 3 gm IV CYC, >3 but ≤ 6 gm IV CYC, and >6 gm IV CYC.
# $P < 0.05$ versus >3 but ≤ 6 gm IV CYC.
** $P < 0.001$ versus no IV CYC.

2 weeks (cumulative dose 3 gm), is prescribed as a remission-inducing immunosuppressive treatment for LN (3). This low-dose IV CYC regimen was developed to reduce gonadal toxicity associated with higher doses, such as those used in the regimen proposed by the NIH (1,2). Although no case of early menopause after treatment with the Euro-Lupus IV CYC regimen has been reported, uncertainty persists regarding a marginal effect on the ovarian reserve that could result, for example, in earlier menopause.

For a long time, this specific issue has been difficult to address for 2 reasons. First, a very long-term follow-up period is needed to ascertain whether gonadal failure has occurred. Second, other factors may interfere, such as maternal age at the time of menopause, consistent with the wide variability of age at the time of menopause in the general population. In this respect, AMH testing has opened a new avenue for understanding, because serum titers of this hormone, produced by the granulosa of the small growing antral ovarian follicles, correlate with follicle counts as determined by ultrasonography, which is still the gold standard for assessing the ovarian reserve (4). AMH is therefore considered a good marker of CYC-induced ovarian damage in women with rheumatic diseases (9).

In the current study, using an AMH assay, we demonstrate for the first time that the Euro-Lupus IV CYC regimen does not impact the ovarian reserve (a very welcome and reassuring piece of information), which was anticipated but not proven so far. The cross-sectional data were confirmed in a small longitudinal cohort of SLE patients who were tested before and after receiving treatment with the Euro-Lupus IV CYC regimen. According to the results of the current study, the minimum gonadotoxic IV CYC cumulative dose was likely to be >6 gm. This suggests that even 2 courses of treatment with the Euro-Lupus regimen of low-dose IV CYC could be safely administered over time without affecting the ovarian reserve. In patients with LN, induction of a second course immunosuppressive treatment is indeed often required, given the high relapse rate (10). This 6-gm threshold is consistent with that observed in a

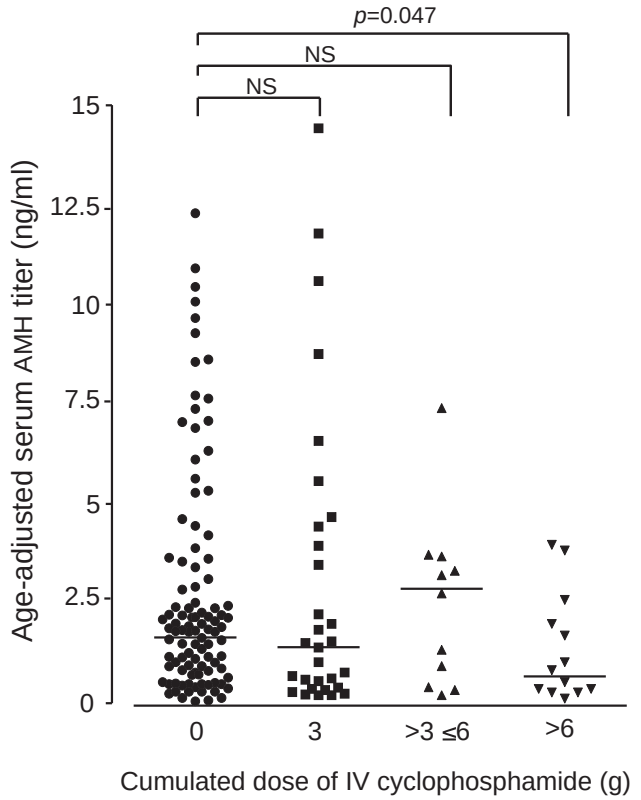

Figure 1. Age-adjusted serum levels of anti–Müllerian hormone (AMH) in patients with systemic lupus erythematosus, according to cumulative dose of intravenous (IV) cyclophosphamide. Symbols represent individual patients; bars show the median. *P* values were calculated by Mann-Whitney test. NS = not significant.

study by Mok et al, which showed that in patients ages 30 years and younger, a cumulative CYC dose cutoff of 5.9 gm yielded a sensitivity of 0.75 and a specificity of 0.80 for the prediction of undetectable AMH on receiver operating curve analysis; the area under the curve was 0.88 (5). Of note, 29 of the 48 CYC-treated patients tested in that study had received oral CYC, whereas our patients were treated exclusively with IV CYC (or were not treated with IV CYC).

We examined the possibility that factors other than the cumulative IV CYC dose might have influenced serum titers of AMH in our cohort. First, the well-known effect of aging on lowering AMH levels was taken into account by age adjustment of the measured serum values. Second, pregnant patients were excluded, because AMH titers decrease during pregnancy (11). Third, it has been suggested that SLE per se is associated with lower AMH titers, regardless of CYC exposure, disease duration, and disease activity (12). Because all of the patients in the current study had SLE, a potential "disease effect" cannot explain the differences between the IV CYC groups. Of note, within the group of patients who were not treated with IV CYC, in whom a relatively large range of serum AMH values was observed, we could not identify any correlation with clinical or biologic data (not shown). Fourth, no difference in the mean BMI was observed between IV CYC groups, thereby making it unlikely that differences in serum AMH titers were related to BMI.

Although the serum level of AMH is a good quantitative biomarker of the ovarian reserve, it does not allow for the prediction of fertility in either the general population or in SLE patients. As shown by Morel et al, CYC-treated SLE patients had significantly lower mean serum titers of AMH, but no correlation with the probability of subsequent pregnancy was observed (6). In our study, the percentage of patients who had at least one successful pregnancy after receiving IV CYC treatment (30%, 9%, and 38% in the 3 gm, >3 but ≤6 gm, and >6 gm groups, respectively) did not statistically differ from that observed in patients who were not exposed to IV CYC (46%). Of note, these values were obtained in the entire cohort, irrespective of a woman's desire to become pregnant or potential contraindications to pregnancy such as a renal flare. In this respect, it should be stressed that serum titers of AMH not be used for family planning counseling, because many other factors contribute to fertility.

Actually, the purpose of this study was not to evaluate the impact of the Euro-Lupus regimen of low-dose IV CYC on fertility, a much more complex issue, but rather the impact on the ovarian reserve. On the whole, the data presented here demonstrate that the Euro-Lupus low-dose IV CYC regimen can be proposed as treatment for SLE patients trying to become pregnant.

AUTHOR CONTRIBUTIONS

All authors were involved in drafting the article or revising it critically for important intellectual content, and all authors approved the final version to be published. Dr. Houssiau had full access to all of the data in the study and takes responsibility for the integrity of the data and the accuracy of the data analysis.

Study conception and design. Tamirou, Nieuwland Husson, Houssiau.
Acquisition of data. Tamirou, Nieuwland Husson, Gruson, Houssiau.
Analysis and interpretation of data. Tamirou, Gruson, Debiève, Lauwerys, Houssiau.

REFERENCES

1. Austin HA III, Klippel JH, Balow JE, le Riche NG, Steinberg AD, Plotz PH, et al. Therapy of lupus nephritis: controlled trial of prednisone and cytotoxic drugs. N Engl J Med 1986;314:614–9.
2. Boumpas DT, Austin HA III, Vaughan EM, Yarboro CH, Klippel JH, Balow JE. Risk for sustained amenorrhea in patients with systemic lupus erythematosus receiving intermittent pulse cyclophosphamide therapy. Ann Intern Med 1993;119:366–9.

3. Houssiau FA, Vasconcelos C, D'Cruz D, Sebastiani GD, de Ramon Garrido E, Danieli MG, et al. Immunosuppressive therapy in lupus nephritis: the Euro-Lupus Nephritis Trial, a randomized trial of low-dose versus high-dose intravenous cyclophosphamide. Arthritis Rheum 2002;46:2121–31.
4. Visser JA, de Jong FH, Laven JS, Themmen AP. Anti-Müllerian hormone: a new marker for ovarian function. Reproduction 2006;131:1–9.
5. Mok CC, Chan PT, To CH. Anti–Müllerian hormone and ovarian reserve in systemic lupus erythematosus. Arthritis Rheum 2013;65:206–10.
6. Morel N, Bachelot A, Chakhtoura Z, Ghillani-Dalbin P, Amoura Z, Galicier L, et al. Study of anti-Müllerian hormone and its relation to the subsequent probability of pregnancy in 112 patients with systemic lupus erythematosus, exposed or not to cyclophosphamide. J Clin Endocrinol Metab 2013;98:3785–92.
7. Moy V, Jindal S, Lieman H, Buyuk E. Obesity adversely affects serum anti-Müllerian hormone (AMH) levels in Caucasian women. J Assist Reprod Genet 2015;32:1305–11.
8. Gladman D, Ginzler E, Goldsmith C, Fortin P, Liang M, Urowitz M, et al. The development and initial validation of the Systemic Lupus International Collaborating Clinics/American College of Rheumatology Damage Index for systemic lupus erythematosus. Arthritis Rheum 1996;39:363–9.
9. Clowse ME, Harward L, Criscione-Schreiber L, Pisetsky D, Copland S. Anti–Müllerian hormone: a better marker of ovarian damage from cyclophosphamide. Arthritis Rheum 2012;64:1305–10.
10. El Hachmi M, Jadoul M, Lefèbvre C, Depresseux G, Houssiau FA. Relapses of lupus nephritis: incidence, risk factors, serology and impact on outcome. Lupus 2003;12:692–6.
11. Pankhurst MW, Clark CA, Zarek J, Laskin CA, McLennan IS. Changes in circulating ProAMH and total AMH during healthy pregnancy and post-partum: a longitudinal study. PloS One 2016;11:e0162509.
12. Lawrenz B, Henes J, Henes M, Neunhoeffer E, Schmalzing M, Fehm T, et al. Impact of systemic lupus erythematosus on ovarian reserve in premenopausal women: evaluation by using anti-Muellerian hormone. Lupus 2011;20:1193–7.

ARTHRITIS & RHEUMATOLOGY
Vol. 69, No. 6, June 2017, pp 1272–1279
DOI 10.1002/art.40057

Effect of Corticosteroids and Cyclophosphamide on Sex Hormone Profiles in Male Patients With Systemic Lupus Erythematosus or Systemic Sclerosis

Laurent Arnaud,[1] Annica Nordin,[2] Hannes Lundholm,[2] Elisabet Svenungsson,[2] Erik Hellbacher,[3] Johan Wikner,[4] Agneta Zickert,[2] and Iva Gunnarsson[2]

Objective. **Systemic lupus erythematosus (SLE) and systemic sclerosis (SSc) are autoimmune diseases that predominantly affect female patients, and therefore fewer investigations have been conducted in men. The aim of this study was to analyze sex hormone levels in male patients with SLE and those with SSc, compared to matched controls, in relation to the use of corticosteroids and cyclophosphamide (CYC).**

Methods. **Sex hormone levels were measured in fasting blood samples from male patients with SLE (n = 71) and those with SSc (n = 29) and compared to population-based, age-matched male controls. Relevant hormone profiles were identified using cluster analysis.**

Results. **Male SLE patients had higher levels of luteinizing hormone (LH) ($P < 0.0001$) and more frequent bioactive testosterone deficiency ($P = 0.02$) than their matched controls. The current dosage of prednisolone correlated inversely with the levels of bioactive testosterone ($r = -0.36$, $P = 0.03$). Cluster analysis identified a subset of SLE patients with increased levels of follicle-stimulating hormone, LH, and prolactin as well as lower levels of bioactive testosterone ($P < 0.0001$) in relation to higher daily doses of prednisolone. In male SSc patients, levels of testosterone ($P = 0.03$) and bioactive testosterone ($P = 0.02$) were significantly lower than those in matched controls. Use of CYC during the previous year was associated with lower bioactive testosterone levels in both SLE patients ($P = 0.02$) and SSc patients ($P = 0.01$), after adjustment for age.**

Conclusion. **The results of this study highlight the negative impact of corticosteroids on gonadal function in men with SLE. Furthermore, use of CYC during the year prior to study inclusion impaired bioactive testosterone levels in male patients with either SLE or SSc. Physicians should be more aware of the possibility of hypogonadism in male patients with autoimmune diseases. The need for hormonal supplementation remains to be formally evaluated in these patients.**

Systemic lupus erythematosus (SLE) is a chronic systemic autoimmune disease that affects women at a disproportionately high frequency (1). Female predominance has also been observed in patients with systemic sclerosis (SSc), but to a lesser extent (2). The causes of female predominance in autoimmune diseases are largely unknown, but a strong influence of hormones and genetic factors has been reported (3). The importance of these factors has been extensively shown in men with Klinefelter's syndrome (47,XXY karyotype), a condition in men usually accompanied by low testosterone levels and infertility, in whom the prevalence of SLE is 14 times higher compared to those with the 46,XY karyotype (4,5).

In addition to the role of genetics in contributing to disturbances in sex hormones, the extent of disease activity as well as treatments have been shown to influence circulating hormone levels. Negative effects of corticosteroids (CS) on free testosterone levels have been reported in chronic inflammatory disease (6) and respiratory disease (7,8), while cyclophosphamide (CYC), an alkylating agent

[1]Laurent Arnaud, MD, PhD: Centre National de Référence des Maladies Systémiques et Auto-immunes rares, Université de Strasbourg, INSERM UMR-S 1109, Strasbourg, France, and Karolinska University Hospital, Karolinska Institutet, Stockholm, Sweden; [2]Annica Nordin, MD, PhD, Hannes Lundholm, MD, Elisabet Svenungsson, MD, PhD, Agneta Zickert, MD, PhD, Iva Gunnarsson, MD, PhD: Karolinska University Hospital, Karolinska Institutet, Stockholm, Sweden; [3]Erik Hellbacher, MD: Uppsala University Hospital, Uppsala, Sweden; [4]Johan Wikner, MD, PhD: Karolinska Institutet and Södersjukhuset, Stockholm, Sweden.

Address correspondence to Iva Gunnarsson, MD, PhD, Department of Medicine, Unit of Rheumatology, Karolinska University Hospital, Karolinska Institute, S-171 76 Stockholm, Sweden. E-mail: iva.gunnarsson@karolinska.se.

Submitted for publication July 18, 2016; accepted in revised form January 24, 2017.

commonly used to treat severe manifestations of autoimmune disorders, is well known for its deleterious effects on the gonads and the reproductive system, especially in female patients with SLE and those with SSc (9).

The aim of the present study was to assess the levels of sex hormones in male patients with SLE and those with SSc as compared to age-matched male controls, and to analyze patterns of hormone levels in association with disease activity, damage, and use of CS or CYC treatments.

PATIENTS AND METHODS

Study design and inclusion criteria. This cross-sectional study included male patients with SLE who were being followed up at the Department of Rheumatology and/or the Department of Nephrology at Karolinska University Hospital. In addition, male patients with SSc from the population-based SSc cohort being followed up at the Department of Rheumatology at Karolinska University Hospital were also included. All of the patients with SLE fulfilled the 1982 revised classification criteria for SLE (10) or the Systemic Lupus International Collaborating Clinics (SLICC) 2012 criteria (11). For the diagnosis of SSc, the American College of Rheumatology/European League Against Rheumatism 2013 criteria were used (12). Patients receiving hormone replacement therapy at the time of study inclusion (n = 4 patients with SLE and n = 1 patient with SSc) were excluded from the study. Randomly selected age-matched men from the Swedish Population Registry were recruited as controls for the SLE and SSc patients. Ethics permission was obtained from the Regional Ethical Review Board in Stockholm, Sweden, and all patients and controls provided written informed consent.

Definitions and clinical data collection. In SLE patients, disease activity at the time of blood sampling was assessed using both the Systemic Lupus Activity Measure, Revised (SLAM-R) (13) and the SLE Disease Activity Index 2000 (SLEDAI-2K) (14). Organ damage was determined according to the SLICC Damage Index (SDI) (15).

In SSc patients, disease activity was evaluated using the European Scleroderma Study Group (ESSG) preliminary criteria for disease activity (16), and organ damage was assessed using the Medsger scale of disease damage (17). Severity of skin disease was assessed using the modified Rodnan skin thickness score (18), and SSc patients were classified as having either limited cutaneous SSc or diffuse cutaneous SSc according to the LeRoy and Medsger classification (19). Pulmonary fibrosis was defined as signs of fibrosis on high-resolution computed tomography.

For all patients, the body mass index (BMI), current use of prednisolone, and previous or current use of CYC (total dose in gm) were recorded at the time of study inclusion, after review of the medical charts. In addition, the presence of abnormal potency was determined based on patients' responses to a direct question at the inclusion interview. Depression was recorded as ever present, i.e., if the patients were ever treated with antidepressant medication. In patients with SLE, osteoporosis severity was defined according to the SDI (15). In patients with SSc, bone mineral density was investigated with dual x-ray absorptiometry scans of the lumbar spine (L1–L4) and the left and/or right hip. Osteoporosis was diagnosed if the patient had a T score of less than or equal to −2.5 SD in any investigated location.

Blood sample collection and laboratory methods. All blood samples were obtained from patients after overnight fasting, before 10:00 AM on the day of inclusion in the study. The samples were then frozen at −80°C and stored until analyzed. Serum creatinine levels were measured through standard laboratory methods, and renal function was estimated with the Modification of Diet in Renal Disease (MDRD) score, which was calculated with the standard MDRD formula (20). Total cholesterol levels were measured using an LX20 chemistry analyzer (Beckman Coulter) in accordance with routine clinical practice.

Hormone levels were measured in the laboratory at Karolinska University. Specifically, levels of testosterone (i.e., total testosterone), bioactive testosterone (i.e., not bound to sex hormone–binding globulin [SHBG]), SHBG, and prolactin were measured with chemiluminescent immunoassays using a UniCel DXL 800, in accordance with the manufacturer's instructions (Beckman Coulter). Levels of follicle-stimulating hormone (FSH) and luteinizing hormone (LH) were measured with fluorescence immunoassays (PerkinElmer). Hormonal abnormalities were defined according to the Karolinska University laboratory reference ranges for FSH (range 1.0–12.5 units/liter), LH (range 1.2–9.6 units/liter), SHBG (range 10–30 nmoles/liter), prolactin (range 56–278 mIU/liter), total testosterone (range 10–30 nmoles/liter), and bioactive testosterone (range 6.3–16 nmoles/liter for those ages 20–49 years, and 4.4–14 nmoles/liter for those ages ≥50 years).

Statistical analysis. Descriptive data are presented as the median (range) or count (percentage). Correlations between non–normally distributed data were analyzed using Spearman's correlation coefficients. Comparisons of dichotomous variables between independent samples were performed using the chi-square test, or the Fisher's exact test when appropriate. Comparisons of continuous variables between independent samples with non-normal distribution were performed using the nonparametric Mann-Whitney U test. Multivariate regression models were built to adjust the associations of interest for the levels of serum creatinine or the use of CYC. Sex hormone profiles were studied by hierarchical cluster analysis of the levels of FSH, LH, prolactin, SHBG, and bioactive testosterone, using Ward's method. Comparison of secondary outcomes known to be influenced by sex hormones (BMI, potency, cholesterol levels, depression, osteoporosis) was performed between the various groups of interest. All tests were bilateral, and *P* values less than 0.05 were considered statistically significant. Statistical analyses were performed using JMP8 (SAS Institute).

RESULTS

Comparison of hormone levels between SLE patients and their matched controls. A total of 71 male patients with SLE (median age 49 years, range 19–79 years) were included in the study. Characteristics of these SLE patients and their 25 population-based, age-matched male controls were similar (Table 1), except for a higher proportion of ever smokers among the SLE patients ($P = 0.048$). In SLE patients, the median SLAM-R score was 5 (range 0–19), the median SLEDAI-2K score was 2 (range 0–20), and the median SDI was 1 (range 0–6). Forty-three SLE patients (60.6%) had a history of lupus nephritis.

Table 1. Baseline characteristics of the patients with SLE and their matched controls*

	SLE patients (n = 71)	Matched controls (n = 25)	*P*
Male	71 (100)	25 (100)	1.00
Age, median (range) years	49 (19–79)	50 (23–70)	0.68
Ever smoker	39 (55)	8 (32)	0.048
Creatinine, median (range) μmoles/liter	82 (45–1,059)	81 (14–96)	0.21
Diabetes	3 (4)	0 (0)	0.30
Prednisolone dosage, median (range) mg/day	5.0 (0–40)	0 (0–7.5)	<0.0001
Cyclophosphamide			
Use within last 12 months	3 (4.2)	–	–
Ever use	26 (36.6)	–	–
Cumulative dose, median (range) gm	0 (0–27)	–	–

* Except where indicated otherwise, values are the number (%) of subjects. SLE = systemic lupus erythematosus.

Comparison of sex hormone levels revealed that the levels of LH were significantly higher in SLE patients than in matched controls ($P < 0.0001$). However, the levels of FSH, prolactin, SHBG, and testosterone were similar between the SLE patients and matched controls (Table 2).

The median age of the patients with SLE did not correlate with the levels of LH (Spearman's $r = 0.19$, $P = 0.11$). However, age was negatively correlated with the levels of bioactive testosterone (i.e., its fraction not bound to SHBG) in SLE patients ($r = -0.52$, $P < 0.0001$). Moreover, creatinine levels correlated with prolactin levels in SLE patients ($r = 0.28$, $P = 0.02$).

Compared to age-matched male controls, bioactive testosterone deficiency was significantly more frequent among SLE patients ($P = 0.02$) (Table 2), whereas the frequencies of increased levels of FSH, LH, and prolactin were similar in both groups. Furthermore, with regard to the combined finding of high levels of LH and low levels of bioactive testosterone, we observed no difference in frequency between SLE patients and their matched controls ($P = 0.33$). Notably, high levels of LH and high levels of prolactin were found only among SLE patients, at a frequency of 14.1% and 7%, respectively.

We also compared secondary outcomes known to be influenced by sex hormones (BMI, potency, total cholesterol levels, depression, osteoporosis) between SLE patients and their matched controls. The findings revealed no significant differences in any of these secondary outcomes (see Supplementary Document 1, available on the *Arthritis & Rheumatology* web site at http://onlinelibrary.wiley.com/doi/10.1002/art.40057/abstract).

Effect of hormone levels on disease activity and damage in SLE patients. In SLE patients, the SLAM-R score was correlated with the levels of LH (Spearman's $r = 0.35$, $P = 0.003$). Moreover, the SLAM-R score was inversely correlated with the levels of SHBG ($r = -0.29$, $P = 0.01$), levels of testosterone ($r = -0.34$, $P = 0.004$), and levels of bioactive testosterone ($r = -0.27$, $P = 0.02$). No correlation with the levels of FSH or prolactin was found (data not shown). We observed no associations between hormone levels and the SLEDAI-2K score. Conversely, the SDI was associated with the levels of prolactin ($P = 0.0003$) and inversely associated with the levels of

Table 2. Sex hormone profiles in patients with SLE and their matched controls*

	SLE patients (n = 71)	Matched controls (n = 25)	*P*
FSH			
Levels, median (range) units/liter	4.2 (1.2–30)	3.6 (1.9–16)	0.23
High FSH (>12.5 units/liter), no. (%)	11 (15.5)	1 (4)	0.18
LH			
Levels, median (range) units/liter	4.6 (1.3–20)	2.7 (1.6–7.1)	<0.0001
High LH (>9.6 units/liter), no. (%)	10 (14.1)	0 (0)	0.06
Prolactin			
Levels, median (range) mIU/liter	161 (23–1,022)	153 (47–339)	0.18
High prolactin (>278 mIU/liter), no. (%)	5 (7.0)	0 (0)	0.32
SHBG, median (range) nmoles/liter	32.0 (11–108)	29.0 (8.2–61)	0.33
Testosterone			
Levels, median (range) nmoles/liter	11.0 (4.0–32)	13.0 (3.4–27)	0.78
Low testosterone (<10 nmoles/liter), no. (%)	23 (32.4)	7 (28.0)	0.68
Bioactive testosterone			
Levels, median (range) nmoles/liter	6.3 (2.9–13)	7.2 (2.7–11)	0.20
Low bioactive testosterone, no. (%)†	24 (34)	2 (8)	0.02

* SLE = systemic lupus erythematosus; FSH = follicle-stimulating hormone; LH = luteinizing hormone; SHBG = sex hormone–binding globulin.
† Defined as <6.3 nmoles/liter for those ages 20–49 years and <4.4 nmoles/liter for those age ≥50 years.

Table 3. Characteristics and sex hormone profiles of the subjects (SLE patients and matched controls) in cluster A and cluster B*

	Cluster A (n = 80)	Cluster B (n = 16)	*P*
SLE patients, no. (%)	56 (70.0)	15 (93.8)	0.06
Age, median (range) years	46.5 (19–79)	59.5 (25–74)	0.03
Creatinine, median (range) μmoles/liter	80.5 (14–1,059)	97.0 (55–607)	0.002
MDRD score, median (range) ml/minute/1.73^2	90.5 (4–149)	75.5 (8–131)	0.002
FSH, median (range) units/liter	3.6 (1.2–11)	16.0 (1.9–30)	<0.0001
LH, median (range) units/liter	3.6 (1.3–14)	9.1 (1.5–20)	<0.0001
Prolactin, median (range) mIU/liter	151.3 (23.3–508.8)	224.5 (101.8–1,022)	0.008
SHBG, median (range) nmoles/liter	31.5 (8.2–108)	33 (11–38)	0.25
Testosterone, median (range) nmoles/liter	13 (3.4–32.0)	8.6 (4–18)	0.0001
Bioactive testosterone, median (range) nmoles/liter	6.9 (2.7–13.0)	4.25 (2.9–8.5)	<0.0001
Prednisolone dosage, median (range) mg/day	0 (0–40)	8.7 (0–40)	0.005
Cyclophosphamide			
Use within last 12 months, no. (%)	1 (1.79)	2 (13.3)	0.11
Ever use, no. (%)	19 (33.9)	7 (46.7)	0.36
Cumulative dose, median (range) gm	0 (0–27)	0 (0–26.4)	0.07

* SLE = systemic lupus erythematosus; MDRD = Modification of Diet in Renal Disease; FSH = follicle-stimulating hormone; LH = luteinizing hormone; SHBG = sex hormone–binding globulin.

testosterone ($P = 0.04$) and levels of bioactive testosterone ($P = 0.003$). However, the latter 2 associations did not remain significant after adjustment for age.

Cluster analysis of hormone profiles in SLE patients and their matched controls. Cluster analysis of the levels of FSH, LH, prolactin, SHBG, and bioactive testosterone in SLE patients and their matched controls allowed identification of 2 main clusters of subjects, namely, cluster A (n = 80) and cluster B (n = 16) (see Supplementary Document 2A, available on the *Arthritis & Rheumatology* web site at http://onlinelibrary.wiley.com/doi/10.1002/art.40057/abstract). Compared to cluster A, cluster B comprised a higher proportion of SLE patients (n = 15 [93.8%]), and those in cluster B had a higher median age ($P = 0.03$), higher levels of creatinine ($P = 0.002$), FSH ($P < 0.0001$), LH ($P < 0.0001$), and prolactin ($P = 0.008$), and lower levels of bioactive testosterone ($P < 0.0001$) (Table 3). Of note, the dosage of prednisolone was higher in cluster B ($P = 0.005$), whereas no difference between clusters was observed for previous use and total dose of CYC (Table 3). Comparison of secondary outcomes between cluster A and cluster B revealed no significant differences (Supplementary Document 1, http://onlinelibrary.wiley.com/doi/10.1002/art.40057/abstract).

Furthermore, cluster analysis of the same hormones limited to only SLE patients allowed identification of 2 main clusters of patients, namely, cluster C (n = 55) and cluster D (n = 16) (Supplementary Document 2B, http://onlinelibrary.wiley.com/doi/10.1002/art.40057/abstract). Cluster D comprised SLE patients whose median age was higher than that of patients in cluster C ($P = 0.02$). Moreover, compared to cluster C, those in cluster D had higher levels of creatinine ($P = 0.003$), FSH ($P < 0.0001$), LH ($P < 0.0001$), and prolactin ($P = 0.01$), and lower levels of bioactive testosterone ($P < 0.0001$) (Supplementary Document 3, available on the *Arthritis & Rheumatology* web site at http://onlinelibrary.wiley.com/doi/10.1002/art.40057/abstract). The proportion of patients with a history of lupus nephritis, as well as the SLAM, SLEDAI-2K, and SDI scores, were similar between cluster C and cluster D. Of note, the dosage of prednisolone was higher in cluster D ($P = 0.04$), whereas no difference between these 2 clusters was observed for previous use and total dose of CYC (Supplementary Document 3, http://onlinelibrary.wiley.com/doi/10.1002/art.40057/abstract). Comparison of secondary outcomes between cluster C and cluster D revealed no significant differences (Supplementary Document 1, http://onlinelibrary.wiley.com/doi/10.1002/art.40057/abstract).

Comparison of hormone levels between SSc patients and their matched controls. Baseline characteristics of the 29 male patients with SSc and their 17 matched male controls were similar (Table 4). Comparison of sex hormone levels between the SSc patients and matched controls revealed lower levels of testosterone ($P = 0.03$) and bioactive testosterone ($P = 0.02$) in the SSc patients, whereas the median levels of FSH, LH, prolactin, and SHBG were similar between SSc patients and controls (Table 5). The median age of the SSc patients did not correlate with the levels of testosterone (Spearman's r = 0.02, $P = 0.93$) or levels of bioactive testosterone (r = −0.29, $P = 0.12$). Moreover, in SSc patients, the levels of creatinine were associated with the levels of prolactin ($P < 0.0001$).

Table 4. Baseline characteristics of the patients with SSc and their matched controls*

	SSc patients (n = 29)	Matched controls (n = 17)
Age, median (range) years	60 (38–80)	61 (41–86)
Disease duration, median (range) years	4.9 (0.9–23.9)	–
dcSSc	8 (27.6)	–
History of digital ulcers	13 (44.8)	–
ESSG disease activity index, median (range)	0.5 (0–4)	–
Medsger SSc damage score, median (range)	5 (1–13)	–
Pulmonary fibrosis	12 (41.4)	–
Diabetes	1 (3.4)	2 (11.8)
Ever smoker	17 (59)	14 (82)
Creatinine, median (range) μmoles/liter	77 (66–575)	83 (62–269)
Cyclophosphamide		
Use within last 12 months	2 (7)	–
Ever use	9 (31)	–
Cumulative dose, median (range) gm	0 (0–25.1)	–

* Except where indicated otherwise, values are the number (%) of subjects. No significant differences were seen between the groups. SSc = systemic sclerosis; dcSSc = diffuse cutaneous SSc; ESSG = European Scleroderma Study Group.

Bioactive testosterone deficiency was significantly more frequent in SSc patients than in their controls ($P = 0.03$), whereas the frequencies of increased levels of FSH, LH, and prolactin were similar between the 2 groups (Table 5). Furthermore, we observed no significant difference in frequency of the combined finding of high LH levels and low bioactive testosterone levels between SSc patients and their matched controls ($P = 1.00$). Comparison of secondary outcomes known to be influenced by sex hormones between SSc patients and their controls revealed no significant differences (Supplementary Document 1, http://onlinelibrary.wiley.com/doi/10.1002/art.40057/abstract).

Effect of hormone levels on severity, disease activity, and damage in SSc patients. We observed no association between the levels of sex hormones and SSc subtypes, modified Rodnan skin thickness score, or history of digital ulcers (data not shown). Of note, SSc patients with pulmonary fibrosis had significantly higher levels of FSH ($P = 0.02$).

Interestingly, the ESSG disease activity score in patients with SSc was associated with the levels of FSH ($P = 0.002$), the levels of LH ($P = 0.008$), and low bioactive testosterone levels ($P = 0.02$), and this remained significant after adjustment for use of CYC ($P = 0.004$, $P = 0.02$, and $P = 0.01$, respectively). Conversely, the ESSG disease activity score was not associated with the levels of prolactin ($P = 0.95$) or SHBG ($P = 0.09$). Furthermore, the Medsger damage score was associated with the levels of prolactin ($P = 0.004$) and LH ($P = 0.02$), but after adjustment for the use of CYC, only the association with levels of prolactin remained significant ($P = 0.02$).

Cluster analysis of hormone profiles in SSc patients and their matched controls. Cluster analysis based on the levels of FSH, LH, prolactin, SHBG, and bioactive testosterone showed that SSc patients and their matched controls shared various hormone profiles,

Table 5. Sex hormone profiles in patients with SSc and their matched controls*

	SSc patients (n = 29)	Matched controls (n = 17)	*P*
FSH			
Levels, median (range) units/liter	3.8 (1.6–33)	5.5 (1.4–33)	0.84
High FSH (>12.5 units/liter), no. (%)	4 (13.8)	(23.5)	0.44
LH			
Levels, median (range) units/liter	3 (10.3)	1 (5.9)	1.00
High LH (>9.6 units/liter), no. (%)	4.4 (1.6–16)	3.3 (1.9–15)	0.43
Prolactin			
Levels, median (range) mIU/liter	143 (55–1,663)	107 (65–243)	0.35
High prolactin (>278 mIU/liter), no. (%)	1 (3.4)	0 (0)	1.00
SHBG, median (range) nmoles/liter	36 (14–64)	39 (9.8–63)	0.79
Testosterone			
Levels, median (range) nmoles/liter	10.0 (4.8–16.0)	13.0 (7.0–17.0)	0.03
Low testosterone (<10 nmoles/liter), no. (%)	12 (41.4)	4 (23.5)	0.34
Bioactive testosterone			
Levels, median (range) nmoles/liter	4.8 (2.2–7.2)	5.9 (2.4–8.2)	0.02
Low bioactive testosterone, no. (%)†	15 (52)	3 (18)	0.03

* SSc = systemic sclerosis; FSH = follicle-stimulating hormone; LH = luteinizing hormone; SHBG = sex hormone–binding globulin.
† Defined as <6.3 nmoles/liter for those ages 20–49 years and <4.4 nmoles/liter for those age ≥50 years.

but the analysis did not allow identification of any distinctive cluster. Similarly, cluster analysis in which only SSc patients were considered did not reveal any meaningful hormone profile (see results in Supplementary Documents 4A and B, available on the *Arthritis & Rheumatology* web site at http://onlinelibrary.wiley.com/doi/10.1002/art.40057/abstract).

Effects of CS use on hormone levels in patients with SLE and patients with SSc. In SLE patients, the daily dose of prednisolone correlated inversely with the levels of testosterone (Spearman's $r = -0.39$, $P = 0.0008$) and levels of bioactive testosterone ($r = -0.36$, $P = 0.03$), but not with any other hormones (data not shown). In SSc patients, no correlation between prednisolone dosage and sex hormone levels was observed.

Effects of CYC use on hormone levels in patients with SLE and patients with SSc. Twenty-six (37%) of the 71 male patients with SLE had been treated with CYC during the course of the disease (median cumulative dose of CYC 6.5 gm, range 0.5–27 gm), and 3 (4%) of the 71 patients had been given CYC during the last 12 months (Table 1). The use of CYC during the 12 months prior to study inclusion was associated with significantly lower levels of bioactive testosterone in the SLE patients, after adjustment for age ($P = 0.02$).

Nine (31%) of the 29 male patients with SSc had been treated with CYC during the course of the disease (median cumulative dose 8.7 gm, range 3.6–25.1 gm), of whom 2 (7%) were treated during the last 12 months. Similarly, the use of CYC during the 12 months prior to study inclusion was significantly associated with lower levels of bioactive testosterone in SSc patients, after adjustment for age ($P = 0.01$).

DISCUSSION

In the current study, we investigated sex hormone levels in male patients with 2 systemic autoimmune diseases characterized by a high female predominance. We found that the LH levels were significantly elevated among the male patients with SLE, and observed significant bioactive testosterone deficiencies in both the male patients with SLE and those with SSc, as compared to age-matched male controls. Using cluster analysis, we were able to characterize 2 main hormone patterns in SLE patients, and unveiled the association of one of these patterns with high frequency of CS use. Our analysis also revealed significant associations between sex hormone levels and disease activity and damage in both SLE and SSc. Furthermore, the dosage of prednisolone correlated inversely with the levels of testosterone and bioactive testosterone in SLE patients. Finally, treatment with CYC during the last 12 months before study entry was associated with testosterone deficiency in both SLE patients and SSc patients. These results further highlight the negative impact of CS in SLE, and also suggest that the gonadal toxicity of CYC, used at the doses recommended for autoimmune diseases, is not restricted to female patients.

Data regarding levels of sex hormones in male SLE patients are scarce, but the findings suggest a frequent dysfunction of the LH–FSH–testosterone axis (21). Previous studies (22,23) have demonstrated increased levels of FSH and LH in male SLE patients, but those findings were discrepant regarding testosterone levels. Importantly, only total testosterone was assessed in these studies, which may not reflect the effects of the bioactive (not bound to SHBG) testosterone fraction (22). Consistent with these findings, we observed that the levels of LH were significantly increased in male SLE patients as compared to controls, and also observed a significant deficit of bioactive testosterone in male SLE patients, at the group level. Based on our understanding of the physiology of the hypothalamic–pituitary–gonadal axis, a possible explanation for this finding is the presence of a partially compensated testosterone deficiency, in which testosterone levels are maintained by increased levels of LH (24). Conversely, we did not confirm the previously reported finding of generally increased prolactin levels in male SLE patients (21,25), but our results did corroborate the association of prolactin with creatinine levels (26). Therefore, differences in baseline renal function between our patients and those from previous studies (21,25) may account for the differences in prolactin levels observed.

In male SSc patients, we observed significantly lower levels of both total testosterone and bioactive testosterone, as compared to age-matched controls. Two previous studies (27,28) did not detect any alteration in sex hormone levels in male SSc patients, but those studies were limited by their sample size, while another study (29) showed that the levels of testosterone and SHBG were higher in male SSc patients compared to controls. This may be attributable to differences in sample size and inclusion criteria, since one of the studies (27) included patients with rheumatoid arthritis among the controls, and excluded SSc patients based on the presence of additional comorbidities, including 1 patient with Klinefelter's syndrome.

To further explore the clinical impact of sex hormones over the course of SLE and SSc, we studied the associations between hormone levels and validated indices of disease activity and damage. A previous study in SLE (22) indicated that the prolactin/testosterone fraction correlated with disease activity as estimated by the SLEDAI-2K score. In our study, we observed significant correlations between the levels of LH, SHBG, testosterone, and

bioactive testosterone and the disease activity as assessed by the SLAM-R index. Although the SLAM-R and SLEDAI-2K scores were correlated (data not shown), we did not observe any association between hormone levels and the SLEDAI-2K score. The fact that the SLAM-R score, but not the SLEDAI-2K score (30), better captures subjective findings such as fatigue, which have been linked to testosterone levels (31), may have contributed at least in part to our result.

In SSc, we observed an association between the levels of FSH, LH, prolactin, and bioactive testosterone and disease activity as assessed by the ESSG disease activity index. We also observed an association between prolactin levels and disease damage in patients with SSc. Taken together, these results further suggest a role of sex hormones over the course of SLE and SSc.

We were able to expand previous findings by studying not only the levels of individual hormones but also their combined patterns, using cluster analysis. We found 2 main hormone patterns in male SLE patients. One of these (cluster D) was characterized by significantly increased levels of the pituitary hormones FSH, LH, and prolactin, along with significantly decreased bioactive testosterone levels. Importantly, these SLE patients had been receiving higher daily doses of prednisolone than had SLE patients in the other cluster, which further highlights the deleterious impact of CS use in SLE. Furthermore, they had significantly increased creatinine levels, which further strengthens the relationship between renal function and prolactin levels in SLE (26).

Finally, one of the main findings of our study was the relationship between the use of immunosuppressive drugs and subsequent bioavailable testosterone deficiency in male patients with autoimmune diseases. Results of previous studies have suggested that treatment with CS may decrease testosterone levels in chronic inflammatory and respiratory diseases (7,8), and we herein confirmed this suppressive effect of CS on testosterone levels in SLE patients. Furthermore, we showed that treatment with CYC during the last 12 months before study entry was associated with significant testosterone deficiency in both SLE patients and SSc patients, even after adjustment for age. Although we are not seeking to make a case against the use of CS or CYC when indicated in SLE, we do believe that physicians should be more aware of the hormonal impact of these treatments, not only in female patients but also in male patients.

In the general population, primary hypogonadism tends to be more frequent among older male patients, even though no evidence was found for a further decrease in mean total testosterone levels with increasing age (32). Similarly, testosterone might have to be added to therapeutic regimens in male patients with SLE, in whom the levels of bioactive testosterone are critically low. Interestingly, in a pilot study of male patients receiving CYC (33), the small subgroup who were given depotestosterone supplementation were found to have both higher sperm counts and testosterone levels after therapy compared to nontreated individuals. Given the impact on testosterone levels and the potential risk of reduced fertility following CYC treatment (9), the effect of a limited period of testosterone supplementation remains to be formally evaluated during CYC therapy both in patients with SLE and in patients with SSc.

A major strength of the study is that blood sample collection was fully standardized to collection of fasting samples obtained before 10 AM, which is appropriate for most laboratory tests for hormones. However, prolactin levels peak around the time of waking up and do not normalize until about 3 hours later. Thus, we cannot exclude the possibility that for some participants, the blood sample may have been obtained <3 hours after waking up.

Limitations of the study include its sample size, particularly the limited number of patients receiving CYC during the 12 months before inclusion, which may impair the generalizability of our findings. Nevertheless, our study is one of the largest of its kind, and demonstrates that hormone abnormalities may be a common feature among men with systemic inflammatory diseases.

In summary, we observed more frequent bioactive testosterone deficiencies in male patients with SLE and those with SSc as compared to controls. The dosage of prednisolone correlated inversely with the levels of testosterone and bioactive testosterone in SLE patients, which further highlights the negative impact of CS treatment in SLE. Furthermore, CYC treatment during the 12 months prior to study inclusion was associated with testosterone deficiency in both SLE patients and SSc patients. With this knowledge, physicians should be more aware of the possibility of hypogonadism in male patients with autoimmune diseases treated with CS or CYC, and thus be more attentive to the various symptoms of testosterone deficiency. The need for hormonal supplementation remains to be formally evaluated in SLE patients with critically low levels of bioactive testosterone.

AUTHOR CONTRIBUTIONS

All authors were involved in drafting the article or revising it critically for important intellectual content, and all authors approved the final version to be published. Dr. Gunnarsson had full access to all of the data in the study and takes responsibility for the integrity of the data and the accuracy of the data analysis.

Study conception and design. Arnaud, Nordin, Gunnarsson.

Acquisition of data. Arnaud, Nordin, Gunnarsson.

Analysis and interpretation of data. Arnaud, Nordin, Lundholm, Svenungsson, Hellbacher, Wikner, Zickert, Gunnarsson.

REFERENCES

1. Cervera R, Khamashta MA, Font J, Sebastiani GD, Gil A, Lavilla P, et al. Systemic lupus erythematosus: clinical and immunologic patterns of disease expression in a cohort of 1,000 patients. The European Working Party on Systemic Lupus Erythematosus. Medicine (Baltimore) 1993;72:113–24.
2. Elhai M, Avouac J, Walker UA, Matucci-Cerinic M, Riemekasten G, Airo P, et al. A gender gap in primary and secondary heart dysfunctions in systemic sclerosis: a EUSTAR prospective study. Ann Rheum Dis 2016;75:163–9.
3. Quintero OL, Amador-Patarroyo MJ, Montoya-Ortiz G, Rojas-Villarraga A, Anaya JM. Autoimmune disease and gender: plausible mechanisms for the female predominance of autoimmunity. J Autoimmun 2012;38:J109–19.
4. Seminog OO, Seminog AB, Yeates D, Goldacre MJ. Associations between Klinefelter's syndrome and autoimmune diseases: English national record linkage studies. Autoimmunity 2015;48: 125–8.
5. Rovensky J, Imrich R, Lazurova I, Payer J. Rheumatic diseases and Klinefelter's syndrome. Ann N Y Acad Sci 2010;1193:1–9.
6. Fitzgerald RC, Skingle SJ, Crisp AJ. Testosterone concentrations in men on chronic glucocorticosteroid therapy. J R Coll Physicians Lond 1997;31:168–70.
7. Morrison D, Capewell S, Reynolds SP, Thomas J, Ali NJ, Read GF, et al. Testosterone levels during systemic and inhaled corticosteroid therapy. Respir Med 1994;88:659–63.
8. Reid IR, Ibbertson HK, France JT, Pybus J. Plasma testosterone concentrations in asthmatic men treated with glucocorticoids. Br Med J (Clin Res Ed) 1985;291:574.
9. Mersereau J, Dooley MA. Gonadal failure with cyclophosphamide therapy for lupus nephritis: advances in fertility preservation. Rheum Dis Clin North Am 2010;36:99–108, viii.
10. Tan EM, Cohen AS, Fries JF, Masi AT, McShane DJ, Rothfield NF, et al. The 1982 revised criteria for the classification of systemic lupus erythematosus. Arthritis Rheum 1982;25:1271–7.
11. Petri M, Orbai AM, Alarcon GS, Gordon C, Merrill JT, Fortin PR, et al. Derivation and validation of the Systemic Lupus International Collaborating Clinics classification criteria for systemic lupus erythematosus. Arthritis Rheum 2012;64:2677–86.
12. Van den Hoogen F, Khanna D, Fransen J, Johnson SR, Baron M, Tyndall A, et al. 2013 classification criteria for systemic sclerosis: an American College of Rheumatology/European League Against Rheumatism collaborative initiative. Arthritis Rheum 2013;65:2737–47.
13. Bae SC, Koh HK, Chang DK, Kim MH, Park JK, Kim SY. Reliability and validity of Systemic Lupus Activity Measure-Revised (SLAM-R) for measuring clinical disease activity in systemic lupus erythematosus. Lupus 2001;10:405–9.
14. Gladman DD, Ibanez D, Urowitz MB. Systemic Lupus Erythematosus Disease Activity Index 2000. J Rheumatol 2002;29:288–91.
15. Gladman D, Ginzler E, Goldsmith C, Fortin P, Liang M, Urowitz M, et al. Systemic Lupus International Collaborative Clinics: development of a damage index in systemic lupus erythematosus. J Rheumatol 1992;19:1820–1.
16. Valentini G, Silman AJ, Veale D. Assessment of disease activity. Clin Exp Rheumatol 2003;21 Suppl 29:S39–41.
17. Medsger TA Jr, Bombardieri S, Czirjak L, Scorza R, Della Rossa A, Bencivelli W. Assessment of disease severity and prognosis. Clin Exp Rheumatol 2003;21 Suppl 29:S42–6.
18. Clements P, Lachenbruch P, Siebold J, White B, Weiner S, Martin R, et al. Inter and intraobserver variability of total skin thickness score (modified Rodnan TSS) in systemic sclerosis. J Rheumatol 1995;22:1281–5.
19. LeRoy EC, Medsger TA Jr. Criteria for the classification of early systemic sclerosis. J Rheumatol 2001;28:1573–6.
20. Levey AS, Bosch JP, Lewis JB, Greene T, Rogers N, Roth D, for the Modification of Diet in Renal Disease Study Group. A more accurate method to estimate glomerular filtration rate from serum creatinine: a new prediction equation. Ann Intern Med 1999;130:461–70.
21. McMurray RW, May W. Sex hormones and systemic lupus erythematosus: review and meta-analysis [review]. Arthritis Rheum 2003;48:2100–10.
22. Mok CC, Lau CS. Profile of sex hormones in male patients with systemic lupus erythematosus. Lupus 2000;9:252–7.
23. Sequeira JF, Keser G, Greenstein B, Wheeler MJ, Duarte PC, Khamashta MA, et al. Systemic lupus erythematosus: sex hormones in male patients. Lupus 1993;2:315–7.
24. Basaria S. Male hypogonadism. Lancet 2014;383:1250–63.
25. Lavalle C, Loyo E, Paniagua R, Bermudez JA, Herrera J, Graef A, et al. Correlation study between prolactin and androgens in male patients with systemic lupus erythematosus. J Rheumatol 1987;14:268–72.
26. Hou SH, Grossman S, Molitch ME. Hyperprolactinemia in patients with renal insufficiency and chronic renal failure requiring hemodialysis or chronic ambulatory peritoneal dialysis. Am J Kidney Dis 1985;6:245–9.
27. Nowlin NS, Brick JE, Weaver DJ, Wilson DA, Judd HL, Lu JK, et al. Impotence in scleroderma. Ann Intern Med 1986;104: 794–8.
28. Klein LE, Posner MS. Progressive systemic sclerosis and impotence. Ann Intern Med 1981;95:658–9.
29. Jemec GB, Sindrup JH. Circulating androgens in male patients suffering from systemic scleroderma. Arch Dermatol Res 1991; 283:289–91.
30. Romero-Diaz J, Isenberg D, Ramsey-Goldman R. Measures of adult systemic lupus erythematosus: updated version of British Isles Lupus Assessment Group (BILAG 2004), European Consensus Lupus Activity Measurements (ECLAM), Systemic Lupus Activity Measure, Revised (SLAM-R), Systemic Lupus Activity Questionnaire for Population Studies (SLAQ), Systemic Lupus Erythematosus Disease Activity Index 2000 (SLEDAI-2K), and Systemic Lupus International Collaborating Clinics/American College of Rheumatology Damage Index (SDI). Arthritis Care Res (Hoboken) 2011;63 Suppl 11:S37–46.
31. Bercea RM, Mihaescu T, Cojocaru C, Bjorvatn B. Fatigue and serum testosterone in obstructive sleep apnea patients. Clin Respir J 2015;9:342–9.
32. Kelsey TW, Li LQ, Mitchell RT, Whelan A, Anderson RA, Wallace WH. A validated age-related normative model for male total testosterone shows increasing variance but no decline after age 40 years. PLoS One 2014;9:e109346.
33. Masala A, Faedda R, Alagna S, Satta A, Chiarelli G, Rovasio PP, et al. Use of testosterone to prevent cyclophosphamide-induced azoospermia. Ann Intern Med 1997;126:292–5.

ARTHRITIS & RHEUMATOLOGY
Vol. 69, No. 6, June 2017, pp 1280–1293
DOI 10.1002/art.40077

Pathogenesis of Diffuse Alveolar Hemorrhage in Murine Lupus

Haoyang Zhuang,[1] Shuhong Han,[1] Pui Y. Lee,[2] Ravil Khaybullin,[1] Stepan Shumyak,[1] Li Lu,[1] Amina Chatha,[1] Anan Afaneh,[1] Yuan Zhang,[1] Chao Xie,[1] Dina Nacionales,[1] Lyle Moldawer,[1] Xin Qi,[1] Li-Jun Yang,[1] and Westley H. Reeves[1]

Objective. **Diffuse alveolar hemorrhage (DAH) in lupus patients confers >50% mortality, and the cause is unknown. We undertook this study to examine the pathogenesis of DAH in C57BL/6 mice with pristane-induced lupus, a model of human lupus-associated DAH.**

Methods. **Clinical/pathologic and immunologic manifestations of DAH in pristane-induced lupus were compared with those of DAH in humans. Tissue distribution of pristane was examined by mass spectrometry. Cell types responsible for disease were determined by in vivo depletion using clodronate liposomes and anti-neutrophil monoclonal antibodies (anti–Ly-6G). The effect of complement depletion with cobra venom factor (CVF) was examined.**

Results. **After intraperitoneal injection, pristane migrated to the lung, causing cell death, small vessel vasculitis, and alveolar hemorrhage similar to that seen in DAH in humans. B cell–deficient mice were resistant to induction of DAH, but susceptibility was restored by infusing IgM. $C3^{-/-}$ and $CD18^{-/-}$ mice were also resistant, and DAH was prevented in wild-type mice by CVF. Induction of DAH was independent of Toll-like receptors, inflammasomes, and inducible nitric oxide. Mortality was increased in interleukin-10 (IL-10)–deficient mice, and pristane treatment decreased IL-10 receptor expression in monocytes and STAT-3 phosphorylation in lung macrophages. In vivo neutrophil depletion was not protective, while treatment with clodronate liposomes prevented DAH, which suggests that macrophage activation is central to DAH pathogenesis.**

Conclusion. **The pathogenesis of DAH involves opsonization of dead cells by natural IgM and complement followed by complement receptor–mediated lung inflammation. The disease is macrophage dependent, and IL-10 is protective. Complement inhibition and/or macrophage-targeted therapies may reduce mortality in lupus-associated DAH.**

Although frequently unrecognized, lung disease occurs in half of patients with systemic lupus erythematosus (SLE). Manifestations include pleuritis, pulmonary hypertension, and interstitial lung disease (1). Only ~3% of SLE patients develop diffuse alveolar hemorrhage (DAH), but it is a significant problem with >50% mortality (2,3). Clinical features include hemoptysis, falling hemoglobin levels, and a strong association with lupus nephritis (3,4). Pathologic examination reveals hemosiderin-laden macrophages, bland hemorrhage, and/or pulmonary capillaritis (3). The pathogenesis remains unclear.

C57BL/6 (B6) mice with pristane-induced lupus develop DAH manifested by alveolar and perivascular inflammation (capillaritis, small vessel vasculitis), hemorrhage, endothelial injury, and infiltration of macrophages, neutrophils, lymphocytes, and eosinophils (5,6). Anti-neutrophil cytoplasmic antibodies (ANCAs) are absent (6). Recruitment of macrophages and neutrophils precedes hemorrhage, starting 3 days after pristane injection and peaking at 2 weeks (7). DAH is independent of myeloid differentiation factor 88 (MyD88), Toll-like receptor 7 (TLR-7), Fcγ receptor, Fas, and T cells, but immunoglobulin-deficient (μMT) mice (7) are resistant. The present studies were carried out to further define the pathogenesis of DAH in this model.

Supported by the NIH (National Institute of Arthritis and Musculoskeletal and Skin Diseases grants R01-GM-40586-24 to Dr. Moldawer and R01-AR-44731 to Dr. Reeves) and the Lupus Research Institute (grant to Dr. Yang).

[1]Haoyang Zhuang, PhD, Shuhong Han, PhD, Ravil Khaybullin, PhD, Stepan Shumyak, BS, Li Lu, MD, Amina Chatha, MD, Anan Afaneh, MD, Yuan Zhang, MD, PhD, Chao Xie, MS, Dina Nacionales, MD, Lyle Moldawer, PhD, Xin Qi, PhD, Li-Jun Yang, MD, Westley H. Reeves, MD: University of Florida, Gainesville; [2]Pui Y. Lee, MD, PhD: Boston Children's Hospital, Boston, Massachusetts.

Address correspondence to Westley H. Reeves, MD, Division of Rheumatology and Clinical Immunology, University of Florida, PO Box 100221, Gainesville, FL 32610. E-mail: whreeves@ufl.edu.

Submitted for publication October 21, 2016; accepted in revised form February 14, 2017.

MATERIALS AND METHODS

Mice and pristane treatment. Mice were bred and maintained under specific pathogen–free conditions. Female 10–12-week-old B6, B6.129S2-*Ighm*^{tm1Cgn}/J (μMT), B6.129P2-*Il10*^{tm1Cgn}/J (interleukin-10–deficient [IL-10$^{-/-}$]), B6.129X1-*Elane*^{tm1Sds}/J (elastase-deficient), B6.129S4-*C3*^{tm1Crr}/J (C3$^{-/-}$), B6.129S7-*Itgb2*^{tm1Bay}/J (CD18$^{-/-}$), B6(Cg)-*Ifnar1*$^{tm1.2Ees}$/J (interferon-$\alpha/\beta/\omega$ receptor–deficient [IFNAR$^{-/-}$]), B6N.129S2-*Casp1*^{tm1Flv}/J (caspase 1–deficient), and B6.129P2-*Nos2*^{tm1Lau}/J (type 2 nitric oxide synthase–deficient [NOS2$^{-/-}$]) mice were from The Jackson Laboratory. C57BL/6J-*Ticam1*^{Lps2}/J (Trif^{Lps2}; TRIF$^{-/-}$) and B6.129P2(SJL)-*Myd88*$^{tm1.1Defr}$/J (MyD88$^{-/-}$) mice were bred at the University of Florida. To induce lupus, 0.5 ml of pristane (Sigma-Aldrich) was administered intraperitoneally (IP). Controls were left untreated. Peritoneal exudate cells were collected by lavage. In some experiments, bronchoalveolar lavage (BAL) was performed. After mice were euthanized, a small incision was cut in the trachea and the alveolar spaces were lavaged with 1 ml of phosphate buffered saline (PBS). Cells collected by BAL were resuspended in RPMI 1640 plus 10% fetal bovine serum (FBS) and incubated at 37°C for 1 hour before treating with IL-10 (1 ng/ml). After a 15-minute incubation, the cells were fixed, permeabilized, surface stained with anti-CD11b antibodies, and stained intracellularly with anti–phospho–STAT-3 antibodies as described below. These studies were approved by the Institutional Animal Care and Use Committee.

Immunoglobulin infusion in μMT mice. Similar to IFN production in pristane-treated mice (8), ischemia-reperfusion injury in mice is mediated by the early classical complement cascade and natural IgM (9). Human natural IgM is as effective as murine IgM at inducing ischemia-reperfusion injury (10). In light of these observations and in view of the relative ease of obtaining human IgM versus mouse IgM, the requirement for immunoglobulin in DAH was evaluated by administering purified human IgM (50 or 200 μg/mouse; Sigma-Aldrich), murine IgG (200 μg/mouse; Sigma-Aldrich), or PBS intravenously (IV) to μMT mice 1 day before and 7 days after pristane treatment. DAH was assessed at 14 days.

Cobra venom factor (CVF) treatment. Mice were treated with 10 μg CVF (CompTech) IP 1 day before and 7 days after pristane treatment. C3 depletion was monitored by enzyme-linked immunosorbent assay using anti-C3 antibodies (Bioss). DAH was assessed at 14 days.

Lung pathology. Formalin-fixed, paraffin-embedded archived lung biopsy tissue from a 19-year-old woman with lupus nephritis who had developed massive hemoptysis and DAH was sectioned (4 μm) and stained with hematoxylin and eosin (H&E). Pristane-treated mice were euthanized at 14 days, and lungs were fixed in formalin. DAH was evaluated by gross inspection of excised lungs and confirmed by microscopy. Tissue sections were subjected to antigen retrieval and analyzed by TUNEL assay (ApopTag Peroxidase In Situ Apoptosis Detection Kit; Chemicon/Millipore). Neutrophil elastase was detected by immunohistochemistry with polyclonal anti-rabbit anti-elastase antibodies at 1:50 dilution for 60 minutes (Abcam) and quantified morphometrically. The expression area and staining intensity were quantified using MetaMorph Premier Image Analysis Software (Molecular Devices). Staining intensity (thresholded area) was expressed as a percentage of total examined lung cell area after subtracting noncellular space from total area.

Staining with oil red O was performed on 10-μm frozen sections of lung tissue from pristane-treated mice or untreated controls (11). Tissue was counterstained with Mayer's hematoxylin and viewed under a microscope.

Pristane-induced in vitro cell death. Pristane or mineral oil (a hydrocarbon oil that does not cause lupus) was dissolved/emulsified in PBS containing 100 mg/ml bovine serum albumin (BSA). At saturation, the solution contained 37.2 mg/ml of pristane. Mineral oil was mixed with PBS/BSA at the same concentration. BW5147 cells (murine thymoma; ATCC) and RAW 264.7 cells (murine macrophage; ATCC) were incubated for 24 hours at 8×10^5/ml in RPMI 1640 containing 10% FBS and serial 2-fold dilutions of either pristane or mineral oil in PBS/BSA or in medium alone. Cell death (necrosis) was determined by flow cytometry with 7-aminoactinomycin D (7-AAD).

Mass spectrometry. Lung and bone marrow tissue was collected 1 week after pristane treatment and frozen in liquid nitrogen. Metabolites were extracted from 15–30 mg of tissue, which was homogenized with a mortar and pestle under liquid nitrogen. Precooled 80% methanol (0.7 ml) and chloroform (0.7 ml) were added, and the mixture was kept on ice and vortexed every 5 minutes for 30 minutes. Ice-cold double-distilled H_2O (0.5 ml) was added to ensure separation of the aqueous and organic layers. The tube was centrifuged at 3,200*g* for 10 minutes at 4°C. The organic layers extracted from pristane-treated and untreated mice were diluted in methanol for determining pristane level using a Thermo Scientific LTQ-Orbitrap-XL mass spectrometer. Mass spectra were analyzed using Sciex OS software.

Flow cytometry. Peritoneal exudate and bone marrow cells were surface stained with the following antibodies: Pacific Blue (PB)–conjugated anti-CD11b, allophycocyanin (APC)–Cy7–conjugated anti–Ly-6G or phycoerythrin (PE)–conjugated anti–Ly-6G (both clone RB6-8C5), and PE-conjugated IL-10 receptor (IL-10R) (all from BioLegend). In some cases, the cells were fixed, permeabilized with Perm/Fix buffer (eBioscience), and stained intracellularly with APC-conjugated anti–tumor necrosis factor (anti-TNF) (BioLegend). In some experiments, the cells were fixed with Cytofix/Perm buffer (BD Biosciences), permeabilized with PhosFlow Permeabilization buffer (BD Biosciences), and stained with PE-conjugated anti–phospho–STAT-3 antibodies (BD Biosciences). Flow cytometry was performed using an LSRII flow cytometer (Becton Dickinson). At least 5×10^5 events were collected per sample. Data were analyzed using FlowJo software (Tree Star).

In vivo depletion of neutrophils and macrophages. Neutrophils were depleted by treating with anti–Ly-6G monoclonal antibody IA8 (BioXcell) (250 μg IV per mouse 1 day before and 7 days after pristane treatment) (12). Mice were euthanized at 14 days for pathologic analysis of DAH. Depletion of neutrophils in the bone marrow, peripheral blood, and peritoneum was ascertained by flow cytometry (PE-conjugated anti–Ly-6G plus PB-conjugated anti-CD11b). Neutrophil depletion in the lung was evaluated by H&E staining and elastase immunohistochemistry.

Macrophages were depleted using clodronate liposomes (CloLip; www.ClodronateLiposomes.com) (13) at 50 μl IP per mouse 1 day before and 7 days after pristane treatment (14).

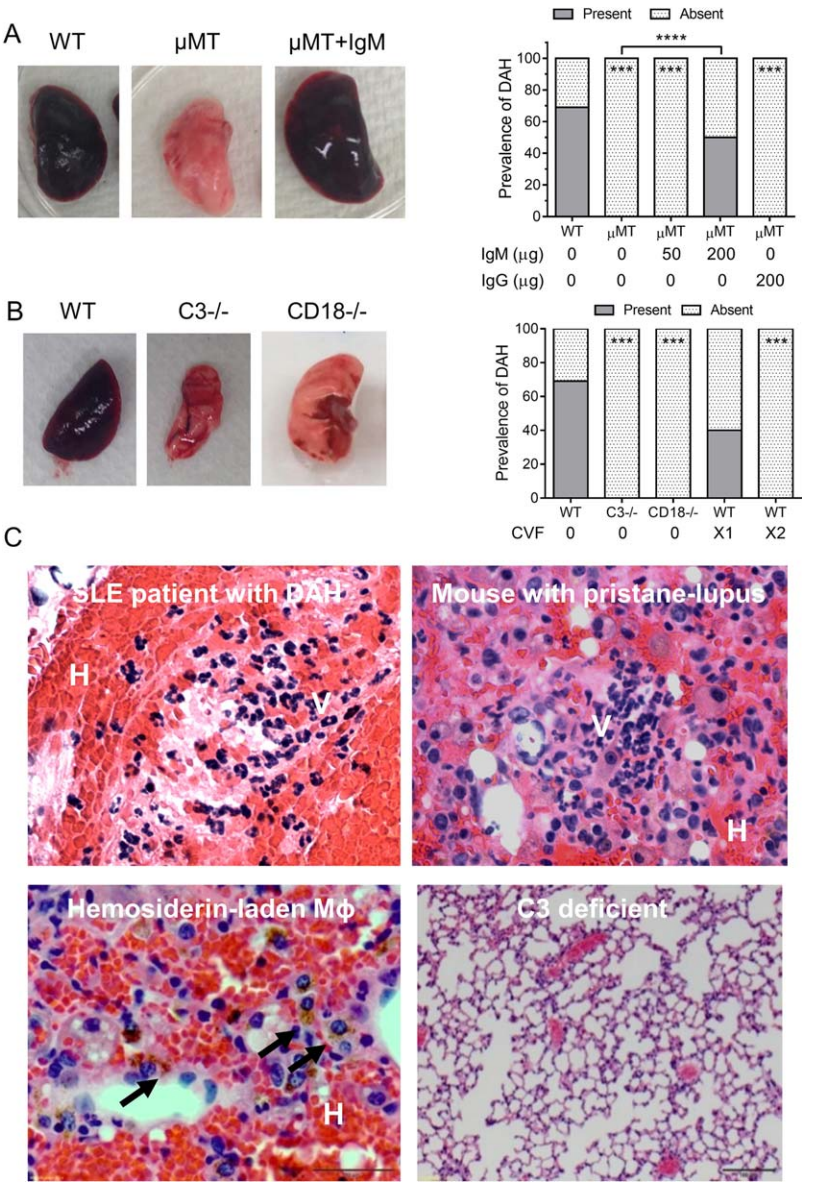

Figure 1. Diffuse alveolar hemorrhage (DAH) requires IgM, C3, and CD18. **A,** Wild-type (WT) and C57BL/6 (B6) immunoglobulin-deficient (μMT) mice were treated with pristane, and lungs were examined 14 days later. Some μMT mice received human IgM (50 or 200 μg intravenously [IV]) or murine IgG (200 μg IV) before pristane treatment (n = 4–6 per group). Left, Gross lung pathology. Right, Prevalence of DAH. *** = $P < 0.001$ versus WT mice; **** = $P < 0.001$, by Fisher's exact test. **B,** WT mice (n = 7), B6 $C3^{-/-}$ mice (n = 12), and B6 $CD18^{-/-}$ mice (n = 4) were treated with pristane, and lungs were examined for DAH 14 days later. Some WT mice were treated with cobra venom factor (CVF) to deplete complement 1 day before pristane treatment (X1; n = 6) or 1 day before and 7 days after pristane treatment (X2; n = 10). Left, Gross lung pathology. Right, Prevalence of DAH. *** = $P < 0.001$ versus WT mice not treated with CVF, by Fisher's exact test. **C,** Hematoxylin and eosin staining of lung tissue from a systemic lupus erythematosus (SLE) patient with DAH (top left) and a WT mouse with pristane-induced DAH (top right and bottom left) is shown. Lungs show bland hemorrhage (**H**), neutrophil-predominant small vessel vasculitis (**V**), and hemosiderin-laden macrophages (**MΦ**; **arrows**). These pathologic changes were absent in lungs from pristane-treated $C3^{-/-}$ mice (bottom right). Murine lung was examined 14 days after pristane treatment. Bars = 20 μm (bottom left); 100 μm (bottom right).

Mice were euthanized at 14 days for pathologic evaluation of DAH. Depletion of peritoneal monocytes and macrophages was ascertained by flow cytometry (fluorescein isothiocyanate–conjugated anti–Ly-6C [BioLegend] plus PB-conjugated anti-CD11b). Depletion in lung was evaluated by H&E staining and immunohistochemistry using horseradish peroxidase (HRP)–conjugated anti-F4/80 (clone BM8; Caltag Medsystems), HRP-conjugated anti-CD11b (clone 5C6; AbD Serotec), or HRP-conjugated anti-

CD11c (clone N418; Abcam) followed by staining with the immunoperoxidase substrate 3,3′-diaminobenzidine. Depletion of F4/80+ cells was quantified in a blinded manner by a pathologist (L-JY). Macrophage (F4/80) staining of the perivascular and alveolar regions of lungs from untreated mice (n = 7) and mice treated with pristane plus clodronate liposomes (n = 8) was graded as strongly positive (2+), weakly positive (1+), or absent (0+).

Statistical analysis. Data are representative of at least 2 independent experiments and are presented as the mean ± SD. For normally distributed data, comparisons were performed using Student's unpaired 2-tailed *t*-test (GraphPad Prism software, version 5). Non-normally distributed data were compared by Mann-Whitney U test. Frequency data were analyzed by Fisher's exact test. Correlations were analyzed using Spearman's rank correlation coefficient. *P* values less than 0.05 were considered significant.

RESULTS

Requirement of IgM, C3, and CD18 for DAH. B6 mice develop severe DAH 2–4 weeks after IP pristane injection (5), while B cell–deficient (μMT) mice are resistant (7). We investigated whether this was due to the absence of immunoglobulin or to another B cell function. Approximately 60–70% of pristane-treated wild-type (WT) B6 mice developed DAH, which was seen by gross examination of lung tissue (Figures 1A and B). In contrast, μMT mice did not develop DAH, while disease could be restored by IV injection of 200 μg per mouse (but not 50 μg per mouse) of normal human IgM ($P < 0.001$ by Fisher's exact test) (Figure 1A). Infusion of 200 μg per mouse of normal mouse IgG did not restore the ability of pristane to induce disease (Figure 1A). In contrast, μMT mice receiving 100 μl of normal mouse serum IV prior to pristane developed DAH (data not shown).

DAH was also absent in $C3^{-/-}$ and $CD18^{-/-}$ mice (Figure 1B). Pretreatment of WT mice with CVF 1 day before and 7 days after pristane treatment prevented DAH, while 69% of untreated mice developed DAH ($P < 0.001$ by Fisher's exact test) (Figure 1B). A single CVF treatment (1 day before pristane) was partially protective.

H&E-stained lung tissue from WT mice showed hemorrhage, pulmonary vasculitis with neutrophilic and mononuclear cell infiltrates surrounding the capillaries and small arteries, and hemosiderin-laden macrophages within the alveoli (Figure 1C). These changes were absent in $C3^{-/-}$ mice. Nearly identical changes were seen in H&E-stained tissue from a lupus patient with DAH (Figure 1C). Thus, DAH in pristane-induced lupus closely resembles human lupus-associated DAH pathologically and is mediated by IgM, C3, and CD18, a component of the C3b receptors CR3 and CR4.

Migration of pristane to lung after IP injection. We investigated the mechanism(s) responsible for DAH. Although pristane is injected IP, we hypothesized that it may gain access to the lungs. To examine that possibility, lung tissue was extracted 7 days after pristane treatment and analyzed by mass spectrometry (Figures 2A and B). A pristane standard yielded the characteristic fragmentation pattern of molecular ion peaks (M), with mass/charge ratios of 268 (M), 267 (M − 1), 269 (M + 1), and 270 (M + 2) (Figure 2A). The 4 characteristic peaks were seen in lung tissue of IP pristane–treated WT mice, but not untreated WT mice (Figure 2B). Pristane was also detected in the lung from treated $C3^{-/-}$ mice, but not untreated $C3^{-/-}$ mice (Figure 2B), indicating that C3 is not necessary for migration of pristane from peritoneum to lung. To confirm the presence of pristane in the lung, cryosections of lung tissue from pristane-treated mice were stained with oil red O, revealing numerous oil red O–positive droplets within the alveolar walls (Figure 2C). Oil red O–stained material was absent in lung from untreated mice, consistent with the mass spectrometry data. Peritoneal pristane injection also causes bone marrow inflammation (15), and pristane was detected by mass spectrometry in bone marrow of pristane-treated mice, but not in bone marrow of untreated mice (Figure 2D), which suggests that the oil was widely dispersed following IP injection.

Cell death induction by pristane. Examination of lung tissue by TUNEL assay revealed dead cells in pristane-treated mice but not in untreated controls (Figure 3A). Many TUNEL-positive cells were large, vacuolated cells located within the alveoli, reminiscent of alveolar macrophages, but smaller TUNEL-positive cells were also present. Dead cells also accumulate in the bone marrow of pristane-treated mice (15), which suggests that pristane might be cytotoxic. That possibility was examined by incubating mouse BW5147 T cells with pristane or mineral oil (the latter of which causes minimal alveolar hemorrhage [not shown]). BW5147 cells exposed in vitro to pristane, but not to mineral oil, exhibited dose-dependent induction of cell death (i.e., were 7-AAD+) (Figure 3B). In contrast, RAW 264.7 macrophages were resistant to the cytotoxic effects of pristane, with no significant 7-AAD staining (Figure 3C). Taken together, the data indicate that pristane migrates from the peritoneum to the lungs and other tissues, where it may cause death of certain cell types. Opsonization of these dead cells by IgM and C3 may promote pulmonary inflammation, as also seen in the peritoneum (8).

Role of macrophages in DAH. Normal lung contains several subsets of macrophages and dendritic cells, but bone marrow–derived monocytes and neutrophils are

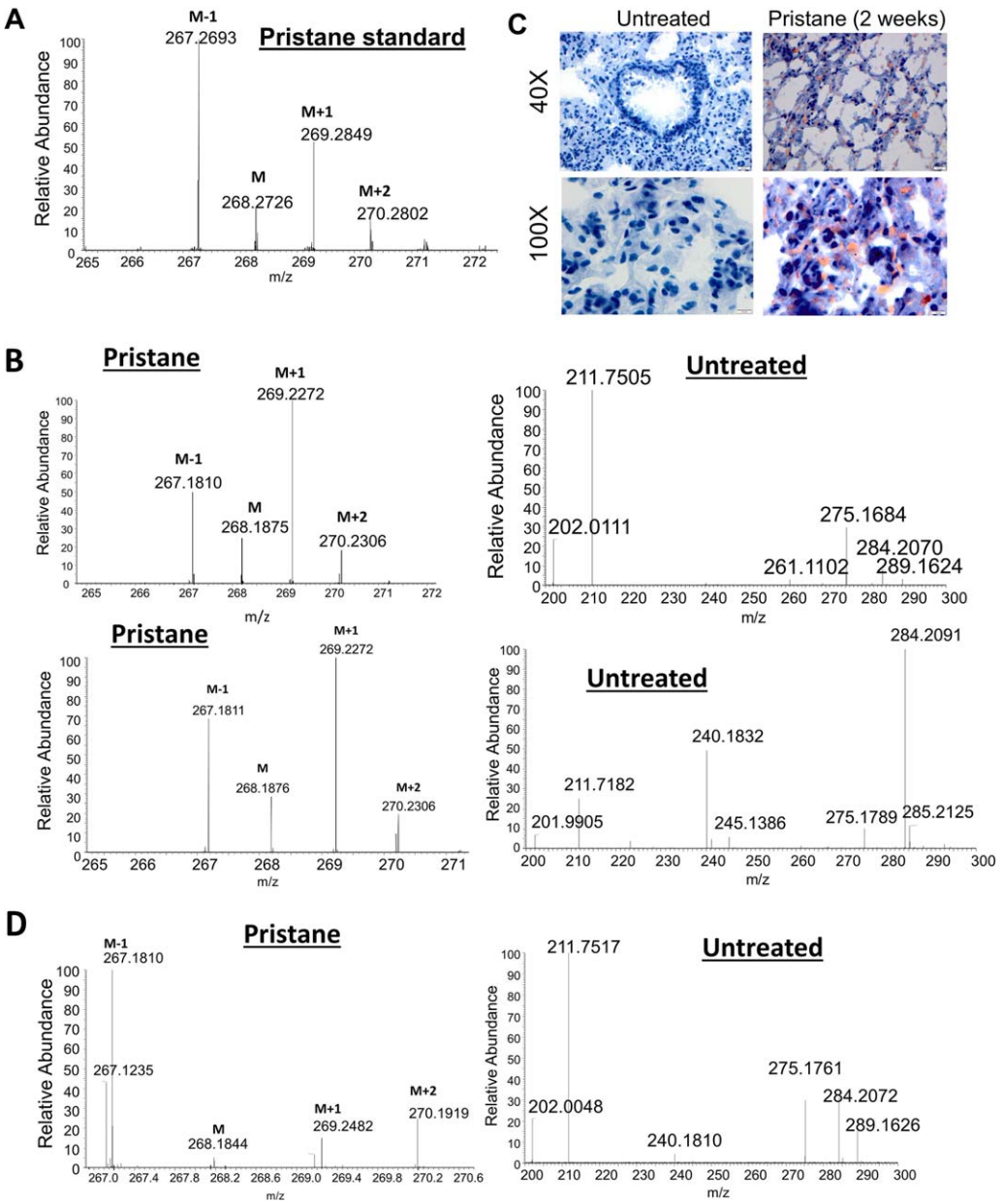

Figure 2. Migration of pristane from peritoneum to lung. **A,** Mass spectrum showing the 4 molecular ion peaks (M) characteristic of pristane: M (mass/charge [m/z] value 268), M − 1 (m/z value 267), M + 1 (m/z value 269), and M + 2 (m/z value 270). **B,** Representative mass spectra (m/z values between 265 and 271) from the organic phase of extracted lung tissue from wild-type (WT) mice (top) or $C3^{-/-}$ mice (bottom) treated 2 weeks earlier with pristane or left untreated. **C,** Oil red O staining of unfixed tissue (frozen sections) from untreated mice and mice treated 2 weeks earlier with pristane. **D,** Representative mass spectra (m/z values between 265 and 271) from the organic phase of extracted bone marrow from WT mice treated 2 weeks earlier with pristane or left untreated.

recruited during inflammation (16,17). We examined the role of monocyte/macrophages versus that of neutrophils in DAH by selectively depleting these subsets in WT mice. Neutrophil depletion with anti–Ly-6G antibodies greatly decreased total peritoneal neutrophils and peritoneal neutrophils containing intracellular TNF, but had little effect on bone marrow neutrophils (Figure 4A). In the lung, neutrophils were decreased in H&E- and neutrophil elastase–stained sections (Figure 4B). Perivascular neutrophilic infiltrates were markedly reduced (Figure 4B). However, numerous perivascular F4/80+ macrophages

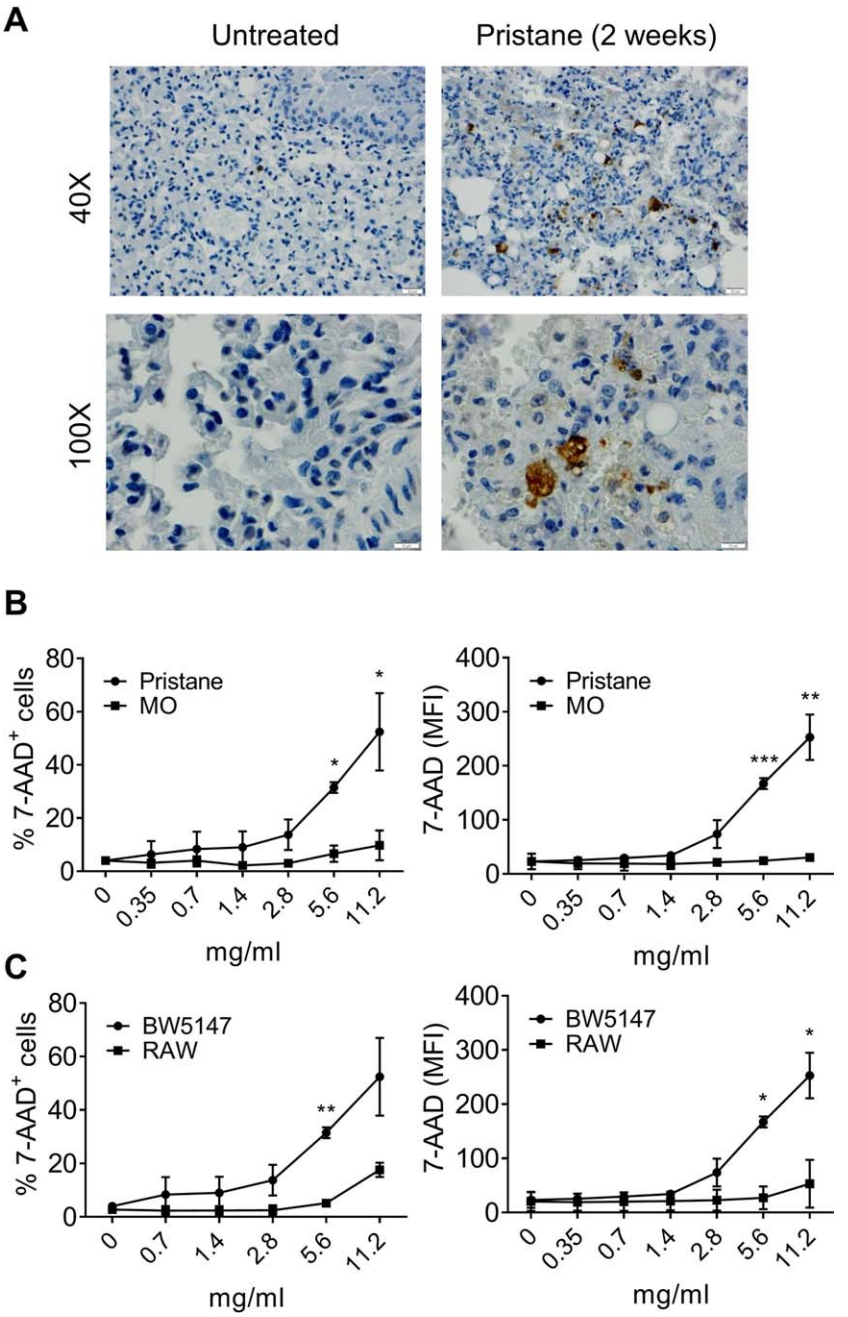

Figure 3. Pristane induces cell death. **A,** Fixed lung tissue from untreated mice and mice treated 2 weeks earlier with pristane was subjected to TUNEL staining. TUNEL-positive cells are brown. **B,** BW5147 cells were incubated for 24 hours at 37°C in medium containing the indicated concentrations of either pristane or mineral oil (MO). Afterward, cells were analyzed by flow cytometry after staining with 7-aminoactinomycin D (7-AAD). The percentage of 7-AAD–positive cells and mean fluorescence intensity (MFI) were determined. **C,** Comparison of 7-AAD staining of pristane-treated BW5147 and RAW 264.7 cells is shown. Cells were incubated in vitro with pristane as in **B,** followed by determination of the percentage of 7-AAD–positive cells and MFI. Values in **B** and **C** are the mean ± SD. $* = P < 0.05$; $** = P < 0.01$; $*** = P < 0.001$ versus mineral oil–treated cells in **B** and versus RAW 264.7 cells in **C**, by multiple *t*-test.

remained after anti–Ly-6G treatment (Figure 4C), despite depletion of elastase-positive cells (Figure 4D).

In contrast, treatment with clodronate liposomes, which depletes monocyte/macrophages (13), abolished the perivascular infiltrates in pristane-treated mice (Figure 4E).

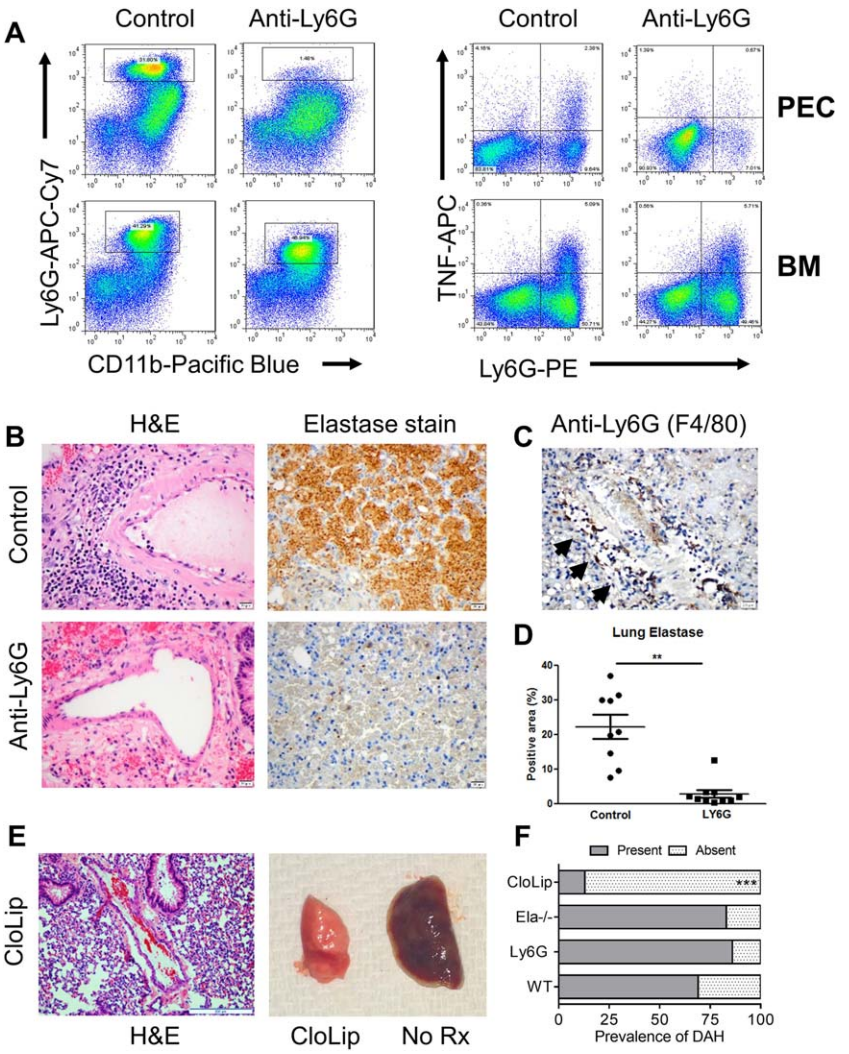

Figure 4. Role of neutrophils and monocyte/macrophages in diffuse alveolar hemorrhage (DAH). **A,** Flow cytometric analysis of peritoneal exudate cells (PEC) and bone marrow neutrophils (BM) from wild-type (WT) mice treated 14 days earlier with pristane, with depletion using anti–Ly-6G monoclonal antibody (mAb) IA8 or without depletion (Control). Left, Surface staining with allophycocyanin (APC)–Cy7–conjugated anti–Ly-6G (mAb RB6-8C5) and Pacific Blue–conjugated anti-CD11b showing depletion of neutrophils (boxed areas) from the peritoneum but not from the bone marrow. Right, Staining with phycoerythrin (PE)–conjugated anti–Ly-6G (mAb RB6-8C5) (surface stain) and APC-conjugated anti–tumor necrosis factor (anti-TNF) (intracellular stain) showing loss of intracellular TNF+ peritoneal, but not bone marrow, Ly-6G+ cells. **B,** Neutrophil depletion with anti–Ly-6G antibodies. WT mice were treated with anti–Ly-6G mAb 1 day before and 7 days after pristane treatment or left untreated (Control) (n = 6 per group). Hematoxylin and eosin (H&E) staining showed perivascular inflammatory cell infiltrates in control mice, but not in anti–Ly-6G–treated mice. Efficacy of neutrophil depletion in the lung was verified by staining with anti–neutrophil elastase antibodies. **C,** Anti-F4/80 staining of macrophages in WT mice after neutrophil depletion with anti–Ly-6G antibodies. **Arrows** indicate F4/80+ cells. **D,** Morphometric quantification of neutrophil elastase staining in lungs from control mice and anti–Ly-6G–treated mice. Symbols represent individual mice; bars show the mean ± SD. ** = $P < 0.01$ by *t*-test. **E,** H&E staining (left) and gross pathology (right) of lungs (14 days after pristane treatment) from WT mice either treated with clodronate liposomes (CloLip; n = 8) 1 day before and 7 days after pristane treatment or left untreated (No Rx; n = 6). Perivascular inflammatory cell infiltrates and DAH were absent after treatment with clodronate liposomes. **F,** Frequency of DAH in WT and elastase-deficient ($Ela^{-/-}$) mice 14 days after pristane treatment and in WT mice treated with anti–Ly-6G antibodies or with clodronate liposomes 1 day before and 7 days after pristane treatment. Pathology was assessed at 14 days. ** = $P < 0.01$ by *t*-test; *** = $P < 0.001$ versus WT mice, by Fisher's exact test. Bars = 20 μm in **B** and **C**; 200 μm in **E**.

The frequency of DAH was greatly reduced in mice treated with clodronate liposomes ($P < 0.001$ by Fisher's exact test), but was unaffected by neutrophil depletion (Figure 4F).

Like DAH, the localized Shwartzman reaction in skin is associated with thrombohemorrhagic vasculitis mediated by C3b–CR3 interactions (18). CR3-mediated

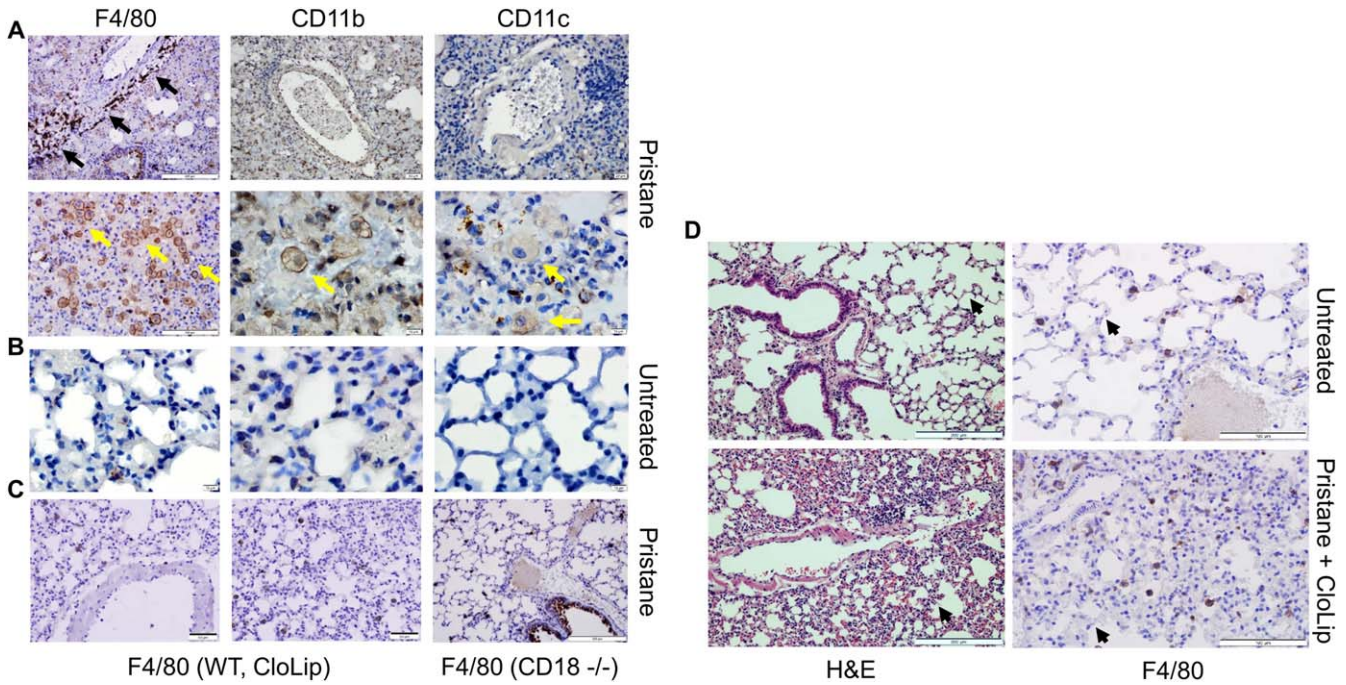

Figure 5. Macrophage subsets in diffuse alveolar hemorrhage (DAH). **A–C**, Immunohistochemistry of lungs from wild-type (WT) mice treated with pristane (**A** and **C**) or left untreated (**B**) and stained at 14 days with horseradish peroxidase–conjugated anti-F4/80, anti-CD11b, or anti-CD11c antibodies. Top, Perivascular F4/80^{high} cells (**arrows**). Bottom, Large F4/80+CD11b+CD11c^{low} alveolar macrophages (**arrows**). **B,** Staining of lung from untreated mice. **C,** Left and middle, F4/80 staining (at 14 days) of lung from WT mice receiving clodronate liposomes (CloLip) intraperitoneally 1 day before and 7 days after pristane treatment. The perivascular region (left) and alveolar spaces (middle) do not contain F4/80+ cells. Note the absence of perivascular and alveolar F4/80+ cells and the increased cellularity of the lung parenchyma. Right, F4/80 staining of lung from CD18$^{-/-}$ mice treated 14 days earlier with pristane, showing normal alveolar architecture and the absence of perivascular and alveolar F4/80+ cells. **D,** Hematoxylin and eosin (H&E) staining (left) and F4/80 immunohistochemistry (right) of normal lung from an untreated C57BL/6 (B6) mouse (top) compared with lung from a B6 mouse treated with pristane plus clodronate liposomes (bottom), showing mild thickening of the alveolar septa (**arrows**) despite the absence of alveolar hemorrhage. Bars = 10 μm in **A** and **B**; 50 μm (left and middle) and 200 μm (right) in **C**; 200 μm (left) and 100 μm (right) in **D**.

neutrophil activation results in vessel damage due to neutrophil elastase production. However, elastase-deficient mice were fully susceptible to pristane-induced DAH (Figure 4F). They also developed pulmonary vasculitis (not shown). Type I IFN and TNF production also remained intact in elastase-deficient mice (not shown). Thus, although it superficially resembles the localized Shwartzman reaction, DAH is not mediated by neutrophils and instead appears to be mediated by macrophages.

Depletion of alveolar and perivascular macrophages by clodronate liposomes. Perivascular inflammatory cell infiltrates in lungs from pristane-treated mice contained small F4/80^{high} cells (Figures 4C and 5A, top). Perivascular CD11b+ cells were also present (Figure 5A, top), but it could not be determined whether CD11b staining was associated with F4/80^{high} macrophages, F4/80− neutrophils, or both. The perivascular cells were uniformly CD11c− (Figure 5A, top right). The lung alveoli were consolidated by intraalveolar hemorrhage and inflammatory cells (Figure 5A). Numerous large F4/80^{low} alveolar macrophages were present in the alveolar spaces (Figure 5A, bottom). F4/80 staining of alveolar macrophages was less intense than on the smaller perivascular cells, and they were also CD11b+CD11c^{low} (Figure 5A, bottom). In addition, small F4/80− CD11b+CD11c− cells (monocytes and/or neutrophils) were present in the lung parenchyma (Figure 5A, top).

Although normal alveolar macrophages are F4/80+CD11b−CD11c^{low} (17), CD11b is induced by inflammation (19), which suggests that the large F4/80^{low} cells were activated alveolar macrophages. Lung from untreated mice did not contain perivascular F4/80^{high} cells and had lower numbers of F4/80^{low} alveolar macrophages (Figure 5B). F4/80−CD11b+CD11c− cells were absent in normal lung. Clodronate liposomes substantially depleted the F4/80+ macrophages (Figure 5C). Consistent with the marked reduction of alveolar hemorrhage (Figure 4F), treatment with clodronate liposomes decreased both vasculitis (perivascular F4/80^{high} cells)

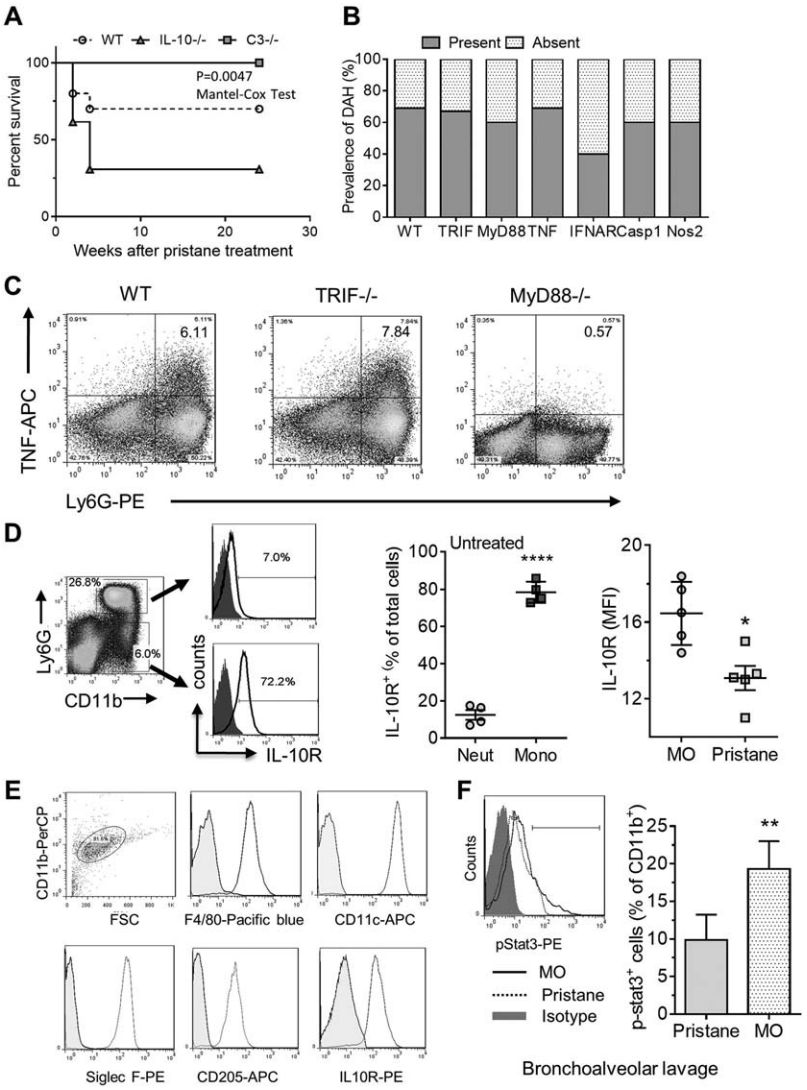

Figure 6. Pathogenesis of lung inflammation. **A,** Wild type (WT), interleukin-10–deficient (IL-$10^{-/-}$), and $C3^{-/-}$ mice were injected with pristane, and percent survival was compared among groups from baseline through 24 weeks after treatment. **B,** WT, $TRIF^{-/-}$, myeloid differentiation factor 88–deficient ($MyD88^{-/-}$), tumor necrosis factor–deficient ($TNF\alpha^{-/-}$), interferon-$\alpha/\beta/\omega$ receptor–deficient ($IFNAR^{-/-}$), caspase 1/caspase 11 (Casp1)–deficient, and type 2 nitric oxide synthase–deficient ($NOS2^{-/-}$) mice (n = 5–6 per group) were treated with pristane, and the prevalence of diffuse alveolar hemorrhage (DAH) was determined 14 days later. **C,** Flow cytometry of intracellular TNF in Ly-6G+ neutrophils from WT, $TRIF^{-/-}$, and $MyD88^{-/-}$ mice is shown. **D,** Left, Flow cytometry of IL-10 receptor (IL-10R) expression on bone marrow cells from untreated C57BL/6 (B6) mice is shown. Myeloid cells were identified by forward scatter/side scatter characteristics, and IL-10R expression was determined on CD11b+Ly-6G+ neutrophils (Neut) and CD11b+Ly-6G− monocytes (Mono). Middle, The percentage of IL-10R+ cells among total CD11b+Ly-6G+ and CD11b+Ly-6G− cells is shown. Right, IL-10R expression on CD11b+Ly-6G− bone marrow cells (mean fluorescence intensity [MFI], by flow cytometry) from mineral oil (MO)–treated mice and pristane-treated mice is shown. Symbols represent individual mice; bars show the mean ± SD. $* = P < 0.05$; $**** = P < 0.0001$, by *t*-test. **E,** Flow cytometry shows forward scatter and surface marker (F4/80, CD11c, Siglec F, CD205, and IL-10R) expression on CD11b+ alveolar macrophages collected by bronchoalveolar lavage (BAL) from untreated B6 mice. **F,** Activation (phosphorylation) of STAT-3 in IL-10–treated CD11b+ alveolar macrophages collected by BAL from mineral oil–treated mice (n = 8) and pristane-treated mice (n = 9) is shown. Left, Flow cytometry showing intracellular activated (phosphorylated) STAT-3 staining in CD11b+ alveolar macrophages. Right, Percentage of CD11b+ cells (from mineral oil–treated and pristane-treated mice) staining for phospho–STAT-3 after 15-minute exposure in vitro to IL-10. Values are the mean ± SD. $** = P < 0.02$ by *t*-test. APC = allophycocyanin; PE = phycoerythrin.

($P < 0.01$ by *t*-test) (not shown) and the large $F4/80^{low}$ alveolar macrophages ($P < 0.015$ by *t*-test) (not shown). However, occasional F4/80+ cells were still seen in the alveolar septa (Figure 5C). Interestingly, perivascular macrophages and neutrophils were both absent in mice treated with clodronate liposomes (Figure 5C, left).

The alveolar septa appeared thickened in clodronate liposome–treated mice, despite the absence of alveolar hemorrhage. There was no alveolar hemorrhage in 6 of 8 clodronate liposome–treated mice, while 2 mice exhibited mild alveolar hemorrhage ($P < 0.001$ by Fisher's exact test) (Figure 4F).

The severity of alveolar hemorrhage and vasculitis seemed to be related to the extent of F4/80+ macrophage depletion. Hemorrhage was absent in mice exhibiting complete depletion of the perivascular and alveolar F4/80+ cells, while the 2 mice with mild DAH had only partial depletion of F4/80+ cells, which suggests that clodronate liposome treatment was incomplete. Clodronate liposome treatment also depletes Ly-6C^{high}CD11b+ inflammatory macrophages from the peritoneum (14). Lung from pristane-treated CD18$^{-/-}$ mice showed no evidence of alveolar hemorrhage or F4/80+ macrophages, but in contrast to clodronate liposome–treated WT mice, alveolar architecture was normal (Figure 5C). Mild thickening of the alveolar septa in mice treated with pristane plus clodronate liposomes compared with untreated B6 controls was also apparent on H&E staining and F4/80 immunohistochemistry analysis (Figure 5D).

Mechanism of lung inflammation. Lung interstitial macrophages and epithelial cells are antiinflammatory and secrete IL-10 (20,21). Although alveolar macrophages are normally antiinflammatory, when activated via TLRs, IL-10R signal transduction is inhibited and they become proinflammatory (21,22). Thus, IL-10 is a crucial regulator of lung inflammation. Expression of CD11b suggested that alveolar macrophages from pristane-treated mice are activated (Figure 5A). Accordingly, we examined the effect of IL-10 on DAH. IL-10$^{-/-}$ mice had significantly increased mortality from DAH (Figure 6A). Pristane-treated B6 mice had mortality of ~40% at 1 month, but little additional mortality thereafter. There was no DAH (Figure 1B) or mortality up to 24 weeks after pristane treatment of C3$^{-/-}$ mice (Figure 6A). In contrast, mortality from DAH was nearly 75% in IL-10$^{-/-}$ mice ($P < 0.005$ by Mantel-Cox test) (Figure 6A).

TLR-activated genes are targeted by IL-10 (23), and pristane induces proinflammatory cytokine production via TLR-7 (24). Unexpectedly, MyD88$^{-/-}$ and TRIF$^{-/-}$ mice developed DAH at a frequency similar to that of WT mice (Figure 6B). Pristane also induced DAH in TNF$^{-/-}$ and IFNAR$^{-/-}$ mice. Consistent with our previous observations that proinflammatory cytokine production in pristane-treated mice is TLR-7/MyD88 dependent (15,24), neutrophils from pristane-treated MyD88$^{-/-}$ mice did not produce TNF, while neutrophils from TRIF$^{-/-}$ and WT mice exhibited similar TNF production (Figure 6C).

As IL-10 inhibits IL-1 production, we tested caspase 1–deficient mice, but we found no protection against DAH (Figure 6B). Although NO production can damage the alveolar wall (25), NOS2$^{-/-}$ mice were susceptible to pristane-induced DAH (Figure 6B).

To further examine the role of IL-10, we stained bone marrow myeloid cells from untreated and 1-month pristane–treated B6 mice with anti–IL-10R antibodies. As expected, CD11b+Ly-6G− monocytes expressed IL-10R, while neutrophils (CD11b+Ly-6G+) were mostly negative (Figure 6D). IL-10R staining of bone marrow monocytes was decreased in pristane-treated mice compared with mineral oil–treated mice (Figure 6D).

Alveolar macrophages (CD11b+F4/80+CD11c+ Siglec F positive CD205+) were present in BAL fluid from untreated mice (Figure 6E). As reported (22), they expressed IL-10R. IL-10R was also expressed by alveolar macrophages collected by BAL from mineral oil– and pristane-treated mice, with a trend toward lower expression in pristane-treated mice (data not shown). Alveolar macrophages collected by BAL from pristane-treated and mineral oil–treated mice were incubated for 15 minutes with IL-10, followed by staining with antibodies against CD11b (expressed by activated alveolar macrophages) and anti–phospho–STAT-3 antibodies. As shown in Figure 6F, STAT-3 activation was higher in alveolar macrophages from mineral oil–treated mice, which suggests that pristane treatment decreases the responsiveness of alveolar macrophages to IL-10.

DISCUSSION

Lupus-associated DAH has a mortality of >50% (2,3). Either bland hemorrhage or focal pulmonary capillaritis may be present in DAH due to lupus or vasculitis. Capillaritis occurs in 88% of patients, most commonly in granulomatosis with polyangiitis (Wegener's) (GPA), microscopic polyangiitis (MPA), and SLE (26), and it is often associated with fibrin thrombi occluding the intraalveolar capillaries and fibrinoid necrosis of the small blood vessels. It may be accompanied by inflammation of larger vessels and IgG/C3 deposition in the alveolar walls. In contrast to leukocytoclastic vasculitis, erythrocytes extravasate into the alveolar spaces (and not the interstitium) in DAH (26).

B6 mice with pristane-induced lupus develop hemorrhage and pulmonary capillaritis that is morphologically similar to human SLE–associated DAH (5–7) (Figure 1C). DAH required CD18 (a component of CR3 and CR4) and opsonization of dead cells by natural IgM and the early classical pathway of complement. Unexpectedly, macrophages, but not neutrophils, were

required for disease. Consistent with the importance of macrophage activation, disease was exacerbated in IL-$10^{-/-}$ mice. However, in contrast to the TLR-7 dependency of proinflammatory cytokine production (15,24), DAH was independent of MyD88, TRIF, TNF, and NOS2. Although both type I IFN (27) and inflammasomes (28) are involved in pristane-induced lupus, IFNAR$^{-/-}$ and caspase 1–deficient mice (which are also caspase 11–deficient [29]) were not protected. Thus, DAH was independent of IFN and the canonical and noncanonical inflammasome pathways.

Opsonization of dead cells may initiate lung injury. Defective clearance of dead cells by resident lung phagocytes contributes to inflammation in acute lung injury, asthma, cystic fibrosis, and chronic obstructive pulmonary disease (30). Human SLE and pristane-induced lupus both are associated with impaired apoptotic cell clearance, and mouse models suggest that this promotes lupus (31). Monocyte-derived macrophages from SLE patients are poorly phagocytic (32). Patients and lupus mice both exhibit increased numbers of uncleared apoptotic cells in tissues (15,33). Accumulation of dead cells in the lungs of pristane-treated mice may be partly due to the cytotoxicity of pristane. Consistent with an earlier report (34), pristane caused dose-dependent T cell death, but RAW 264.7 macrophages were resistant. Widespread dissemination of pristane after peritoneal injection may promote apoptosis and defective removal of dead cells in the lung (Han S: unpublished observations), as suggested by the TUNEL-positive cells in lungs of pristane-treated mice (Figure 3A) and consistent with the presence of dead cells in the lungs of SLE patients with DAH (data not shown).

Interestingly, TUNEL staining suggested that large cells whose appearance was consistent with that of alveolar macrophages were undergoing cell death. That possibility is supported by evidence that the recovery of alveolar macrophages by BAL was decreased in pristane-treated mice compared with mineral oil–treated mice (not shown). Thus, there may be differences in the susceptibility of various macrophage subsets to the induction of cell death by pristane. Although resident alveolar macrophages are generally more resistant to apoptosis than are macrophages recruited to the lung (35), engagement of the scavenger receptor macrophage receptor with collagenous structure (MARCO) sensitizes them to undergo apoptosis following uptake of silica (36). As MARCO is involved in the uptake of apoptotic cells in pristane-treated mice (Han S, et al: submitted for publication), the uptake of dead cells may sensitize alveolar macrophages to apoptosis. Further studies will be necessary to determine the cause of the differential susceptibility of alveolar macrophages and RAW 264.7 cells to pristane-induced apoptosis.

Our data suggest that DAH is mediated by opsonin-dependent uptake of dead cells, as natural IgM, C3, and CD18 are required. Induction of the IFN signature by pristane also requires IgM and C3 due to opsonization of dead cells and phagocytosis via CR3 and/or CR4 (8). Since CD11b$^{-/-}$ mice are protected against pristane-induced DAH (37), CR3 is likely to play an important role in the pathogenesis of lung inflammation. Our data suggest that the importance of CD11b and CD18 in lung inflammation lies in the role of CR3 as a phagocytic receptor rather than as a mediator of cell adhesion and migration. An additional role for CR4 (CD11c/CD18) cannot be excluded.

Alveolar hemorrhage is thought to emanate from neutrophilic inflammation of capillaries (capillaritis) (38), and neutrophils are also critical to the pathogenesis of acute lung injury induced by endotoxin, shock, and ischemia-reperfusion injury (39). The lungs of pristane-treated mice exhibited neutrophilic infiltration, but F4/80+ macrophages and other myeloid cells were also present. Although the pulmonary vasculitis superficially resembled a localized Shwartzman reaction (neutrophilic infiltration, erythrocyte extravasation, and dependence on C3 and neutrophil CR3) (18), neutrophil depletion had little effect on DAH. It was also unaffected by the absence of neutrophil elastase, a key mediator of the Schwartzman reaction (18). DAH was greatly attenuated by treatment with clodronate liposomes, suggesting that cells of the monocyte/macrophage lineage, rather than neutrophils, are central to the pathogenesis of lung hemorrhage. Although acute lung injury can be associated with alveolar hemorrhage, neutrophils, IL-1, and TNF are key mediators of inflammation (39), which suggests that pristane-induced DAH differs from acute lung injury.

At least 2 F4/80+ cell subsets were present in lungs of pristane-treated mice: small perivascular F4/80^{high}CD11^{low}CD11c− cells and large F4/80^{low}CD11b+ CD11c^{low} cells (Figure 5). Both were depleted by clodronate liposomes. Alveolar macrophages are long-lived, self-renewing resident macrophages (40). Although they are normally CD11b−, CD11b expression is induced on alveolar macrophages by inflammation (19). Thus, the large F4/80^{low}CD11b+CD11c^{low} cells are likely to be alveolar macrophages activated by the inflammatory response to pristane. The perivascular F4/80^{high}CD11^{low}CD11c− cells are probably bone marrow–derived inflammatory macrophages recruited to the inflamed lung. As both were depleted by clodronate liposomes and absent in CD18$^{-/-}$ mice, we cannot determine which subset causes lung injury.

IL-10 down-regulates proinflammatory cytokine production by macrophages at multiple (transcriptional and posttranscriptional) levels (41). Its constitutive

production by lung interstitial macrophages and epithelial cells helps maintain the antiinflammatory phenotype of alveolar macrophages, and BAL fluid from untreated mice contains IL-10 thought to be derived mainly from lung epithelial cells (20,42). DAH was more severe in IL-$10^{-/-}$ mice than in controls, which suggests that IL-10 protects against pristane-induced lung injury by interacting with IL-10R on alveolar macrophages or bone marrow–derived cells.

During inflammation, bone marrow–derived macrophages are recruited to the alveoli and differentiate into proinflammatory (M1-type) macrophages (25). IL-10R expression in untreated bone marrow was restricted to CD11b+Ly-6G− cells of the monocyte lineage. After pristane injection, these cells are recruited to the inflamed peritoneum via CCL2–CCR2 (43). In the absence of type I IFN, they develop into Ly-$6C^{low}$ macrophages, while maturation is inhibited by IFN. Decreased IL-10R expression on bone marrow monocytes from pristane-treated mice compared with controls (Figure 6) suggests that monocytes recruited to the inflamed lung in pristane-treated mice may be poorly responsive to the antiinflammatory effects of locally produced IL-10, consistent with the decreased STAT-3 phosphorylation in BAL cells from pristane-treated mice compared with those from mineral oil–treated mice. It will be of interest to see if the higher IL-10R expression by bone marrow monocytes from mineral oil–treated mice promotes differentiation into antiinflammatory (M2-type) macrophages, while low IL-10R expression in pristane-treated mice results in M1-type polarization.

The inflammatory pathway(s) activated when IgM/C3-opsonized dead cells engage CR3/CR4 on macrophages remain to be determined. IL-10 down-regulates TLR-stimulated transcription of proinflammatory cytokines by inducing ubiquitination and degradation of MyD88-dependent signaling molecules, such as TNF receptor–associated factor 6 and IL-1R–associated kinase 4 (44). In view of the importance of TLR-7 and MyD88 in pristane-induced proinflammatory cytokine production, it was surprising that DAH develops in TLR-$7^{-/-}$ (7) and MyD$88^{-/-}$ mice. DAH also developed in pristane-treated TRIF$^{-/-}$ mice. Thus, the pathogenesis of DAH may not involve TLR signaling, although it will be necessary to examine the susceptibility of MyD88/TRIF–double-deficient mice to exclude the possibility that TRIF and MyD88 can compensate for one another.

Pristane causes sterile inflammation, which is a result of innate immune recognition of damage-associated molecular patterns released from dead cells (45). Sterile inflammation is mediated by both neutrophils and monocytes. Neutrophil-mediated inflammation requires MyD88, IL-1α, and IL-1R, but not TRIF or TLRs, whereas the monocytic response is MyD88/IL-1R independent (46,47). The susceptibility of MyD$88^{-/-}$ mice and caspase 1/caspase 11–deficient mice (Figure 6B) further supports the idea that macrophages rather than neutrophils mediate DAH. Although NOS2 has been implicated in bleomycin-induced lung injury (48), it was not involved in pristane-induced DAH. Further studies are needed to define the inflammatory pathway(s) downstream of CR3/CR4 that lead to DAH.

DAH is an unusual manifestation of SLE with high mortality and unclear etiology (3,4). Although a variety of therapeutic interventions are used, their efficacy is unclear (3,4). The pathologic changes in pristane-induced DAH, especially the presence of capillaritis, closely resemble those in patients with DAH. Like DAH in SLE patients, murine DAH is not associated with ANCAs, and hemosiderin-laden macrophages are present (6) (Figure 1C). Moreover, dead cells accumulate in lung tissue from humans with DAH (Zhuang H: unpublished observations) as well as in lung tissue from animals with pristane-induced DAH. In contrast to chemical pneumonitis and ANCA-positive vasculitis syndromes, such as MPA and GPA, SLE-associated DAH is thought to be mediated by immune complexes with granular deposits of immunoglobulin, C3, and DNA in the alveolar capillary walls (49). The requirement for immunoglobulin and C3 in pristane-induced DAH is consistent with the role of immune complexes in this animal model, further underscoring the similarity between DAH in SLE patients and in mice.

Interestingly, hemoptysis and lung fibrosis have been seen in humans with inhalation, aspiration, or injection of mineral and other oils (50,51). Although humans are generally not exposed to pristane, the strong phenotypic and pathologic similarities (15,52) suggest that pristane exposure may activate inflammatory pathways similar to those in SLE patients. Respiratory infections, seen in 40–60% of patients with SLE-associated DAH (3,4,53), represent one mechanism that could drive the accumulation of apoptotic cells in the lungs, promoting DAH. It will be of interest to investigate the role of these infections in the pathogenesis of DAH in humans.

The response of pristane-induced DAH to CVF (Figure 1B) raises the possibility that complement depletion/inhibition may be a viable strategy for treating DAH in human SLE. Although CVF is too immunogenic for human use, “humanized” CVF is undergoing clinical testing (54), and compstatin, a 13-residue cyclic peptide that inhibits activation of the classical and

alternative complement pathways, is in clinical trials for macular degeneration (55). Complement inhibition also blocks pulmonary fibrosis (56), a long-term complication of DAH (57). As pulmonary fibrosis is also seen in lupus patients without prior overt episodes of DAH (1), it will be of interest to examine whether clinically silent DAH with alveolar microhemorrhage can cause pulmonary fibrosis. Finally, in view of the severity of disease in IL-10–deficient mice, it may be of interest to evaluate recombinant IL-10 as a potential therapy.

ACKNOWLEDGMENTS

We thank Ms Cathy Sun (University of Florida, Mouse Pathology Facility) for expert assistance with immunohistochemistry and Dr. Michael Carroll (Boston Children's Hospital, Boston, MA) for useful discussions.

AUTHOR CONTRIBUTIONS

All authors were involved in drafting the article or revising it critically for important intellectual content, and all authors approved the final version to be published. Dr. Reeves had full access to all of the data in the study and takes responsibility for the integrity of the data and the accuracy of the data analysis.

Study conception and design. Zhuang, Han, Lee, Khaybullin, Shumyak, Lu, Chatha, Afaneh, Zhang, Xie, Nacionales, Moldawer, Qi, Yang, Reeves.

Acquisition of data. Zhuang, Han, Lee, Khaybullin, Shumyak, Lu, Chatha, Afaneh, Zhang, Xie, Nacionales, Moldawer, Qi, Yang, Reeves.

Analysis and interpretation of data. Zhuang, Han, Lee, Khaybullin, Qi, Yang, Reeves.

REFERENCES

1. Mittoo S, Fell CD. Pulmonary manifestations of systemic lupus erythematosus. Semin Respir Crit Care Med 2014;35:249–54.
2. Kamen DL, Strange C. Pulmonary manifestations of systemic lupus erythematosus. Clin Chest Med 2010;31:479–88.
3. Zamora MR, Warner ML, Tuder R, Schwarz MI. Diffuse alveolar hemorrhage and systemic lupus erythematosus: clinical presentation, histology, survival, and outcome. Medicine (Baltimore) 1997; 76:192–202.
4. Martinez-Martinez MU, Abud-Mendoza C. Predictors of mortality in diffuse alveolar haemorrhage associated with systemic lupus erythematosus. Lupus 2011;20:568–74.
5. Satoh M, Weintraub JP, Yoshida H, Shaheen VM, Richards HB, Shaw M, et al. Fas and Fas ligand mutations inhibit autoantibody production in pristane-induced lupus. J Immunol 2000; 165:1036–43.
6. Chowdhary VR, Grande JP, Luthra HS, David CS. Characterization of haemorrhagic pulmonary capillaritis: another manifestation of pristane-induced lupus. Rheumatology (Oxford) 2007;46: 1405–10.
7. Barker TT, Lee PY, Kelly-Scumpia KM, Weinstein JS, Nacionales DC, Kumagai Y, et al. Pathogenic role of B cells in the development of diffuse alveolar hemorrhage induced by pristane. Lab Invest 2011;91:1540–50.
8. Zhuang H, Han S, Li Y, Kienhöfer D, Lee P, Shumyak S, et al. A novel mechanism for generating the interferon signature in lupus: opsonization of dead cells by complement and IgM. Arthritis Rheumatol 2016;68:2917–28.
9. Zhang M, Austen WG Jr, Chiu I, Alicot EM, Hung R, Ma M, et al. Identification of a specific self-reactive IgM antibody that initiates intestinal ischemia/reperfusion injury. Proc Natl Acad Sci U S A 2004;101:3886–91.
10. Zhang M, Alicot EM, Carroll MC. Human natural IgM can induce ischemia/reperfusion injury in a murine intestinal model. Mol Immunol 2008;45:4036–9.
11. Mehlem A, Hagberg CE, Muhl L, Eriksson U, Falkevall A. Imaging of neutral lipids by oil red O for analyzing the metabolic status in health and disease. Nat Protoc 2013;8:1149–54.
12. Daley JM, Thomay AA, Connolly MD, Reichner JS, Albina JE. Use of Ly6G-specific monoclonal antibody to deplete neutrophils in mice. J Leukoc Biol 2008;83:64–70.
13. Van Rooijen N, Sanders A. Liposome mediated depletion of macrophages: mechanism of action, preparation of liposomes and applications. J Immunol Methods 1994;174:83–93.
14. Lee PY, Weinstein JS, Nacionales DC, Scumpia PO, Li Y, Butfiloski E, et al. A novel type I IFN-producing cell subset in murine lupus. J Immunol 2008;180:5101–8.
15. Zhuang H, Han S, Xu Y, Li Y, Wang H, Yang LJ, et al. Toll-like receptor 7–stimulated tumor necrosis factor α causes bone marrow damage in systemic lupus erythematosus. Arthritis Rheumatol 2014;66:140–51.
16. Byrne AJ, Mathie SA, Gregory LG, Lloyd CM. Pulmonary macrophages: key players in the innate defence of the airways. Thorax 2015;70:1189–96.
17. Misharin AV, Morales-Nebreda L, Mutlu GM, Budinger GR, Perlman H. Flow cytometric analysis of macrophages and dendritic cell subsets in the mouse lung. Am J Respir Cell Mol Biol 2013;49:503–10.
18. Hirahashi J, Mekala D, van Ziffle J, Xiao L, Saffaripour S, Wagner DD, et al. Mac-1 signaling via Src-family and Syk kinases results in elastase-dependent thrombohemorrhagic vasculopathy. Immunity 2006;25:271–83.
19. Huaux F, Lo Re S, Giordano G, Uwambayinema F, Devosse R, Yakoub Y, et al. IL-1α induces CD11b^{low} alveolar macrophage proliferation and maturation during granuloma formation. J Pathol 2015;235:698–709.
20. Bedoret D, Wallemacq H, Marichal T, Desmet C, Quesada Calvo F, Henry E, et al. Lung interstitial macrophages alter dendritic cell functions to prevent airway allergy in mice. J Clin Invest 2009;119:3723–38.
21. Fernandez S, Jose P, Avdiushko MG, Kaplan AM, Cohen DA. Inhibition of IL-10 receptor function in alveolar macrophages by Toll-like receptor agonists. J Immunol 2004;172:2613–20.
22. Hussell T, Bell TJ. Alveolar macrophages: plasticity in a tissue-specific context. Nat Rev Immunol 2014;14:81–93.
23. Murray PJ, Smale ST. Restraint of inflammatory signaling by interdependent strata of negative regulatory pathways. Nat Immunol 2012;13:916–24.
24. Lee PY, Kumagai Y, Li Y, Takeuchi O, Yoshida H, Weinstein J, et al. TLR7-dependent and FcγR-independent production of type I interferon in experimental mouse lupus. J Exp Med 2008; 205:2995–3006.
25. Short KR, Kroeze EJ, Fouchier RA, Kuiken T. Pathogenesis of influenza-induced acute respiratory distress syndrome. Lancet Infect Dis 2014;14:57–69.
26. Franks TJ, Koss MN. Pulmonary capillaritis. Curr Opin Pulm Med 2000;6:430–5.
27. Nacionales DC, Kelly-Scumpia KM, Lee PY, Weinstein JS, Lyons R, Sobel E, et al. Deficiency of the type I interferon receptor protects mice from experimental lupus. Arthritis Rheum 2007;56:3770–83.
28. Kahlenberg JM, Yalavarthi S, Zhao W, Hodgin JB, Reed TJ, Tsuji NM, et al. An essential role of caspase 1 in the induction of murine lupus and its associated vascular damage. Arthritis Rheumatol 2014;66:152–62.
29. Kayagaki N, Warming S, Lamkanfi M, Vande Walle L, Louie S, Dong J, et al. Non-canonical inflammasome activation targets caspase-11. Nature 2011;479:117–21.

30. Robb CT, Regan KH, Dorward DA, Rossi AG. Key mechanisms governing resolution of lung inflammation. Semin Immunopathol 2016;38:425–48.
31. Nagata S, Hanayama R, Kawane K. Autoimmunity and the clearance of dead cells. Cell 2010;140:619–30.
32. Herrmann M, Voll RE, Zoller OM, Hagenhofer M, Ponner BB, Kalden JR. Impaired phagocytosis of apoptotic cell material by monocyte-derived macrophages from patients with systemic lupus erythematosus. Arthritis Rheum 1998;41:1241–50.
33. Gaipl US, Voll RE, Sheriff A, Franz S, Kalden JR, Herrmann M. Impaired clearance of dying cells in systemic lupus erythematosus. Autoimmun Rev 2005;4:189–94.
34. Calvani N, Caricchio R, Tucci M, Sobel ES, Silvestris F, Tartaglia P, et al. Induction of apoptosis by the hydrocarbon oil pristane: implications for pristane-induced lupus. J Immunol 2005;175:4777–82.
35. Janssen WJ, Barthel L, Muldrow A, Oberley-Deegan RE, Kearns MT, Jakubzick C, et al. Fas determines differential fates of resident and recruited macrophages during resolution of acute lung injury. Am J Respir Crit Care Med 2011;184:547–60.
36. Hamilton RF Jr, Thakur SA, Mayfair JK, Holian A. MARCO mediates silica uptake and toxicity in alveolar macrophages from C57BL/6 mice. J Biol Chem 2006;281:34218–26.
37. Shi Y, Tsuboi N, Furuhashi K, Du Q, Horinouchi A, Maeda K, et al. Pristane-induced granulocyte recruitment promotes phenotypic conversion of macrophages and protects against diffuse pulmonary hemorrhage in Mac-1 deficiency. J Immunol 2014; 193:5129–39.
38. Cordier JF, Cottin V. Alveolar hemorrhage in vasculitis: primary and secondary. Semin Respir Crit Care Med 2011;32:310–21.
39. Abraham E. Neutrophils and acute lung injury. Crit Care Med 2003;31 Suppl:S195–9.
40. Guilliams M, de Kleer I, Henri S, Post S, Vanhoutte L, de Prijck S, et al. Alveolar macrophages develop from fetal monocytes that differentiate into long-lived cells in the first week of life via GM-CSF. J Exp Med 2013;210:1977–92.
41. Moore KW, de Waal Malefyt R, Coffman RL, O'Garra A. Interleukin-10 and the interleukin-10 receptor. Annu Rev Immunol 2001;19:683–765.
42. Franke-Ullmann G, Pfortner C, Walter P, Steinmuller C, Lohmann-Matthes ML, Kobzik L. Characterization of murine lung interstitial macrophages in comparison with alveolar macrophages in vitro. J Immunol 1996;157:3097–104.
43. Lee PY, Li Y, Kumagai Y, Xu Y, Weinstein JS, Kellner ES, et al. Type-I interferon modulates monocyte recruitment and maturation in chronic inflammation. Am J Pathol 2009;175:2023–33.
44. Chang J, Kunkel SL, Chang CH. Negative regulation of MyD88-dependent signaling by IL-10 in dendritic cells. Proc Natl Acad Sci U S A 2009;106:18327–32.
45. Shen H, Kreisel D, Goldstein DR. Processes of sterile inflammation. J Immunol 2013;191:2857–63.
46. Chen CJ, Kono H, Golenbock D, Reed G, Akira S, Rock KL. Identification of a key pathway required for the sterile inflammatory response triggered by dying cells. Nat Med 2007;13:851–6.
47. Lee PY, Kumagai Y, Xu Y, Li Y, Barker T, Liu C, et al. IL-1α modulates neutrophil recruitment in chronic inflammation induced by hydrocarbon oil. J Immunol 2011;186:1747–54.
48. Guo C, Atochina-Vasserman E, Abramova H, George B, Manoj V, Scott P, et al. Role of NOS2 in pulmonary injury and repair in response to bleomycin. Free Radic Biol Med 2016;91:293–301.
49. Inoue T, Kanayama Y, Ohe A, Kato N, Horiguchi T, Ishii M, et al. Immunopathologic studies of pneumonitis in systemic lupus erythematosus. Ann Intern Med 1979;91:30–4.
50. Pielaszkiewicz-Wydra M, Homola-Piekarska B, Szczesniak E, Ciolek-Zdun M, Fall A. Exogenous lipoid pneumonia: a case report of a fire-eater. Pol J Radiol 2012;77:60–4.
51. Simmons A, Rouf E, Whittle J. Not your typical pneumonia: a case of exogenous lipoid pneumonia. J Gen Intern Med 2007;22:1613–6.
52. Reeves WH, Lee PY, Weinstein JS, Satoh M, Lu L. Induction of autoimmunity by pristane and other naturally occurring hydrocarbons. Trends Immunol 2009;30:455–64.
53. Shen M, Zeng X, Tian X, Zhang F, Zeng X, Zhang X, et al. Diffuse alveolar hemorrhage in systemic lupus erythematosus: a retrospective study in China. Lupus 2010;19:1326–30.
54. Vogel CW, Fritzinger DC, Gorsuch WB, Stahl GL. Complement depletion with humanised cobra venom factor: efficacy in preclinical models of vascular diseases. Thromb Haemost 2015;113: 548–52.
55. Ricklin D, Lambris JD. Compstatin: a complement inhibitor on its way to clinical application. Adv Exp Med Biol 2008;632:273–92.
56. Silasi-Mansat R, Zhu H, Georgescu C, Popescu N, Keshari RS, Peer G, et al. Complement inhibition decreases early fibrogenic events in the lung of septic baboons. J Cell Mol Med 2015;19:2549–63.
57. Lishnevsky M, Young LC, Woods SJ, Groshong SD, Basaraba RJ, Gilchrist JM, et al. Microhemorrhage is an early event in the pulmonary fibrotic disease of PECAM-1 deficient FVB/n mice. Exp Mol Pathol 2014;97:128–36.

ARTHRITIS & RHEUMATOLOGY
Vol. 69, No. 6, June 2017, pp 1294–1305
DOI 10.1002/art.40040

Genome-Wide Association Analysis Reveals Genetic Heterogeneity of Sjögren's Syndrome According to Ancestry

Kimberly E. Taylor,[1] Quenna Wong,[2] David M. Levine,[2] Caitlin McHugh,[2] Cathy Laurie,[2] Kimberly Doheny,[3] Mi Y. Lam,[1] Alan N. Baer,[3] Stephen Challacombe,[4] Hector Lanfranchi,[5] Morten Schiødt,[6] M. Srinivasan,[7] Hisanori Umehara,[8] Frederick B. Vivino,[9] Yan Zhao,[10] Stephen C. Shiboski,[1] Troy E. Daniels,[1] John S. Greenspan,[1] Caroline H. Shiboski,[1] and Lindsey A. Criswell[1]

Objective. **The Sjögren's International Collaborative Clinical Alliance (SICCA) is an international data registry and biorepository derived from a multisite observational study of participants in whom genotyping was performed on the Omni2.5M platform and who had undergone deep phenotyping using common protocol-directed methods. The aim of this study was to examine the genetic etiology of Sjögren's syndrome (SS) across ancestry and disease subsets.**

Methods. **We performed genome-wide association study analyses using SICCA subjects and external controls obtained from dbGaP data sets, one using all participants (1,405 cases, 1,622 SICCA controls, and 3,125 external controls), one using European participants (585, 966, and 580, respectively), and one using Asian participants (460, 224, and 901, respectively) with ancestry adjustments via principal components analyses. We also investigated whether subphenotype distributions differ by ethnicity, and whether this contributes to the heterogeneity of genetic associations.**

Results. **We observed significant associations in established regions of the major histocompatibility complex (MHC), *IRF5*, and *STAT4* ($P = 3 \times 10^{-42}$, $P = 3 \times 10^{-14}$, and $P = 9 \times 10^{-10}$, respectively), and several novel suggestive regions (those with 2 or more associations at $P < 1 \times 10^{-5}$). Two regions have been previously implicated in autoimmune disease: *KLRG1* ($P = 6 \times 10^{-7}$ [Asian cluster]) and *SH2D2A* ($P = 2 \times 10^{-6}$ [all participants]). We observed striking differences between the associations in Europeans and Asians, with high heterogeneity especially in the MHC; representative single-nucleotide polymorphisms from established and suggestive regions had highly significant differences in the allele frequencies in the study populations. We showed that SSA/SSB autoantibody production and the labial salivary gland focus score criteria were associated with the first worldwide principal component, indicative of higher non-European ancestry ($P = 4 \times 10^{-15}$ and $P = 4 \times 10^{-5}$, respectively), but that**

This article was not prepared in collaboration with the Susceptibility Loci for IgA Nephropathy Study (IGANGWAS) investigators and does not necessarily reflect the opinions or views of the IGANGWAS, dbGaP, or the National Institute of Diabetes and Digestive and Kidney Diseases.

The Sjögren's International Collaborative Clinical Alliance (SICCA) cohort was supported by the NIH (National Institute for Dental and Craniofacial Research [NIDCR], National Eye Institute, and Office of Research on Women's Health grant N01-DE-32626). The SICCA Biorepository and Data Registry is supported by NIH grant HHSN-26S201300057C from the NIDCR. Genotyping at the Johns Hopkins Center for Inherited Disease Research was supported by NIH grant HHSN-268201200008I. Dr. Baer's work was supported by NIH grant R01-DE-12354-15A1. Drs. Taylor and Criswell's work was supported by the Rosalind Russell/Ephraim P. Engleman Rheumatology Center of the University of California.

[1]Kimberly E. Taylor, PhD, MPH, Mi Y. Lam, MS, Stephen C. Shiboski, PhD, Troy E. Daniels, DDS, MS, John S. Greenspan, BDS, PhD, Caroline H. Shiboski, DDS, MPH, PhD, Lindsey A. Criswell, MD, MPH, DSc: University of California, San Francisco; [2]Quenna Wong, MS, David M. Levine, PhD, Caitlin McHugh, PhD, Cathy Laurie, BS, PhD: University of Washington, Seattle; [3]Kimberly Doheny, PhD, Alan N. Baer, MD: Johns Hopkins University, Baltimore, Maryland; [4]Stephen Challacombe, PhD, FDS: Guy's, King's, and St. Thomas' Dental Institute, King's College London, London, UK; [5]Hector Lanfranchi, DDS, PhD: University of Buenos Aires, Buenos Aires, Argentina; [6]Morten Schiødt, DDS, PhD: Rigshospitalet, Copenhagen, Denmark; [7]M. Srinivasan, MS, DO: Aravind Eye Hospital, Madurai, India; [8]Hisanori Umehara, MD, PhD: Kanazawa Medical University, Ishikawa, Japan; [9]Frederick B. Vivino, MD: University of Pennsylvania, Philadelphia; [10]Yan Zhao, MD: Peking Union Medical College Hospital, Beijing, China.

Address correspondence to Lindsey A. Criswell, MD, MPH, DSc, 513 Parnassus Avenue S-857, University of California, San Francisco, San Francisco, CA 94143. E-mail: Lindsey.Criswell@ucsf.edu.

Submitted for publication September 21, 2016; accepted in revised form January 5, 2017.

subphenotype differences did not explain most of the ancestry differences in genetic associations.

***Conclusion*. Genetic associations with SS differ markedly according to ancestry; however, this is not explained by differences in subphenotypes.**

Sjögren's syndrome (SS) is a systemic autoimmune disease affecting primarily the lacrimal and salivary glands and occurs in ~0.5–1% of the population (1). Patients typically present with dry eyes and/or dry mouth, but confirmation of the diagnosis using American College of Rheumatology (ACR) classification criteria requires a positive result for any 2 of the 3 following tests: presence of SS autoantibodies (primarily SSA and SSB), presence of focal lymphocytic sialadenitis in labial salivary gland (LSG) biopsy, and degree of eye damage due to keratoconjunctivitis sicca (KCS) (2).

While there have been relatively few family studies in SS compared to the number of family studies in other autoimmune diseases, there is an increased prevalence of autoimmune diseases in families with SS (3), and the sibling risk ratio in a Taiwanese population was recently estimated to be 19% (4). Genetic variants in multiple HLA class II genes in the major histocompatibility complex (MHC) region 6p21.3 have been well established as SS risk factors (5). More recently, a genome-wide association study (GWAS) of SS in subjects of European descent (6) established associations of SS with gene regions *IRF5–TNP03, STAT4, IL12A, FAM167A–BLK, DDX6–CXCR5,* and *TNIP1*. In addition, a GWAS of SS in Han Chinese participants identified *GTF2I* as a susceptibility locus in that population (7).

The Sjögren's International Collaborative Clinical Alliance (SICCA) is an international data registry and biorepository derived from a multisite observational study for which participants were enrolled between 2004 and 2012 from the University of Buenos Aires, Argentina; Peking Union Medical College, Beijing, China; Rigshopitalet, Copenhagen, Denmark; Kanazawa Medical University, Ishikawa, Japan; King's College, London, UK; University of California, San Francisco (UCSF), California; Aravind Eye Hospital, Madurai, India; Johns Hopkins University (JHU), Baltimore, Maryland; and University of Pennsylvania, Philadelphia, Pennsylvania. In addition to whole-genome genotyping, SICCA participants underwent extensive phenotyping using common comprehensive protocol-directed methods for collection of data and specimens across all sites (2,8). More information about the SICCA registry is available online at http://sicca-online.ucsf.edu. SICCA collaborators in addition to those who are authors are listed in Appendix A.

Although the small set of genes described above have been identified as contributing to SS susceptibility, relatively little is known compared with what is known about other autoimmune diseases, particularly how susceptibility and severity are affected by ancestry and how subphenotypes may be influenced by different genes and/or ethnicity. For example, in systemic lupus erythematosus (SLE), Northern Europeans have less severe disease including lower susceptibility for nephritis (9,10), and double-stranded DNA (dsDNA)–negative SLE has a genetic profile different from that of dsDNA-positive SLE (11). One population-based study of SS in a multiethnic cohort in the greater Paris area showed that non-European participants had a higher prevalence of SS, were younger, and were more likely to have SS autoantibodies and polyclonal hypergammaglobulinemia compared with non-European participants (12).

The SICCA registry offers a unique opportunity to expand our knowledge of the genetic etiology of SS in 2 principal ways: 1) it is the first international SS cohort including participants of non-European ancestry and participants of European ancestry genotyped together on a whole-genome platform, and 2) extensive phenotyping using consistent methods across all sites allows these genetic data to be analyzed in conjunction with clinical data on disease manifestations, enabling the combined effects of genetics, ancestry, and subphenotypes to be jointly examined.

PATIENTS AND METHODS

Study population and clinical data. *SICCA.* All SS patients are SICCA participants who fulfilled the ACR classification criteria for primary SS (2). This collection is described in detail in refs. 2 and 8. All research was approved by an institutional review board or appropriate ethics committee at each SICCA site. Table 1 shows the distribution of these participants according to self-reported ethnicity.

Evaluation of the classification criteria relies on the following measures from clinical data that we use in our analysis: 1) presence of SSA/Ro or SSB/La autoantibodies; 2) a focus score of >1, measuring the degree of focal sialadenitis in LSG biopsy specimens (13); and 3) an ocular staining score (OSS) of ≥3, measuring the degree of damage due to KCS (14). Fulfillment of 2 of the 3 criteria items described above is sufficient for classification as SS according to the ACR. SICCA participants who were unambiguously negative for SS (i.e., at least 2 of 3 criteria were known to be negative) were also included in the control group, along with healthy external (out-of-study) controls (see below).

External controls. Out-of-study controls were obtained from 3 dbGaP data sets: Age-Related Eye Disease Study (AREDS; phs000001.v3.p1) Genetic Variation of Refractive Error Substudy (phs000429.v1.p1), Collaborative Study of Nicotine Dependence (COGEND; phs000404.v1.p1), and IgA Nephropathy GWAS (IGANGWAS; phs000431.v2.p1). Table 1 shows the distribution of these participants according to self-reported ethnicity (see also Supplementary Methods, available on the *Arthritis & Rheumatology* web site at http://onlinelibrary.wiley.com/doi/10.1002/art.40040/abstract). Specimens obtained from

Table 1. Numbers of participants according to data source and self-reported ethnicity*

Registry	European	African	Asian	Hispanic/Native American	Mixed/other/ unspecified
SICCA					
All†	1,840	83	913	358	161
Participants with SS	669	51	570	164	59
Participants without SS	1,109	31	306	191	101
AREDS	1,659	0	0	0	0
COGEND	910	464	0	46	47
IGANGWAS	0	0	897	0	0
HapMap	18	11	8	16	0

* SICCA = Sjögren's International Collaborative Clinical Alliance; SS = Sjögren's syndrome; AREDS = Age-Related Eye Disease Study; COGEND = Collaborative Study of Nicotine Dependence; IGANGWAS = IgA Nephropathy genome-wide association study (GWAS).
† Includes participants with an ambiguous SS classification due to missing data and participants with secondary SS not included in the GWAS.

AREDS and COGEND participants were typed on the Illumina HumanOmni2.5M-4v1 platform, and IGANGWAS participants were typed on the Illumina Human610-Quad v1 platform.

Genotyping and quality assurance. DNA specimens obtained from SICCA participants were genotyped in 2 phases on the Illumina HumanOmni2.5-4v1 or Illumina HumanOmni2.5M-8v1-1 array (2.5 million single-nucleotide polymorphisms [SNPs] genome-wide) at the Center for Inherited Disease Research. Quality control and merging of genotypes from the 2 phases were performed at the University of Washington Genetics Coordinating Center, as previously described (15). SNPs were removed if they were monomorphic or positional duplicates; had a missing call rate of ≥2%; had 2 or more discordant calls in 170 SICCA duplicates; had 1 or more discordant calls in 38 cross-phase SICCA duplicates; had 5 or more Mendelian errors in 76 SICCA and HapMap trios; had a Hardy-Weinberg equilibrium test P value of $<10^{-4}$ in participants with self-identified European ancestry; or contained large chromosomal anomalies such as regions of aneuploidy. After quality control was performed (post–quality control), 1,444,884 SNPs were analyzed; these SICCA genotype data are available through dbGaP (accession no. phs000672.v1.p1). For this analysis, SNPs with a minor allele frequency (MAF) of <2% were removed.

Samples with unresolved identity issues (unexpected duplicates or genotypes inconsistent with expected family structure) or no case report form were removed. All remaining samples had call rates of ≥98%. For this analysis, family members were removed by selecting a maximum set of unrelated (through third-degree relationships via identical by descent analysis) participants. The numbers of post–quality control samples are shown in Table 1.

All external control data sets were filtered to have ≥2% MAFs and ≥98% genotyping of SNPs and individuals. Additional cross-study quality control performance is described in Supplementary Methods (available on the *Arthritis & Rheumatology* web site at http://onlinelibrary.wiley.com/doi/10.1002/art.40040/abstract). Overlap in post–quality control SNPs between the 1,444,884 SNPs from the Omni2.5M chip and the 483,279 SNPs from the Illumina 610K chip resulted in 302,689 SNPs for analyses in the Asian cluster, which included IGANGWAS controls; this is hereinafter referred to as the 300K overlap SNP set.

Statistical analysis. *Ancestry.* Principal components analysis (PCA) using EigenStrat (16) was used for ancestry estimation (see Supplementary Methods, available on the *Arthritis & Rheumatology* web site at http://onlinelibrary.wiley.com/doi/10.1002/art.40040/abstract). Three PCAs were performed: an intercontinental PCA of all participants (see Supplementary Figure 1, available on the *Arthritis & Rheumatology* web site at http://onlinelibrary.wiley.com/doi/10.1002/art.40040/abstract), yielding PC1 (principal component 1), PC2, and so on; an intracontinental PCA of a European-only cluster (Supplementary Figure 2), yielding EPC1 (European PC1), EPC2, and so on; and an intracontinental PCA of an Asian-only cluster (Supplementary Figure 3), yielding APC1 (Asian PC1), APC2, and so on. The Asian cluster was also split into Chinese and Japanese clusters (APC1 >0, APC1 <0) for some analyses.

Based on the leveling of the scree plots, we used EPC1 to adjust for ancestry within the European cluster, and we used APC1 and APC2 to adjust for ancestry within the Asian cluster. In the intercontinental PCA, the top 4 PCs were sufficient to cluster major populations: PC1 differentiated European versus Asian; similarly, PC2 differentiated African ancestry, PC3 differentiated American Indian ancestry, and PC4 differentiated Indian ancestry. PCs 5–9 were each highly correlated with one of the top 3 European or top 2 Asian PCs (see Supplementary Methods, available on the *Arthritis & Rheumatology* web site at http://onlinelibrary.wiley.com/doi/10.1002/art.40040/abstract); therefore, we adjusted for 9 PCs in our all-subjects regressions to account for both intercontinental substructure and the intracontinental substructure of these population groups.

GWAS. Due to the multiethnic and multiplatform nature of our study, we performed multiple phases of analysis using logistic regression for each SNP as a predictor of case–control status: 1) analysis of all SICCA participants and external controls (AREDS and COGEND) genotyped on the Omni2.5M platform (1,444,854 SNPs), adjusting for 9 PCs, sex, and smoking status (see Supplementary Methods, available on the *Arthritis & Rheumatology* web site at http://onlinelibrary.wiley.com/doi/10.1002/art.40040/abstract); 2) analysis of only the European cluster, adjusting for the top intra-European PC (EPC1), sex, and smoking status (see Supplementary Methods); 3) meta-analysis of the 2 Asian clusters, including Chinese external controls (IGANGWAS) typed on the Illumina 610 Quad, for SNPs in the 300K overlap set. Analysis of the China and Japan subgroups were performed via logistic regression, adjusting for the top 2

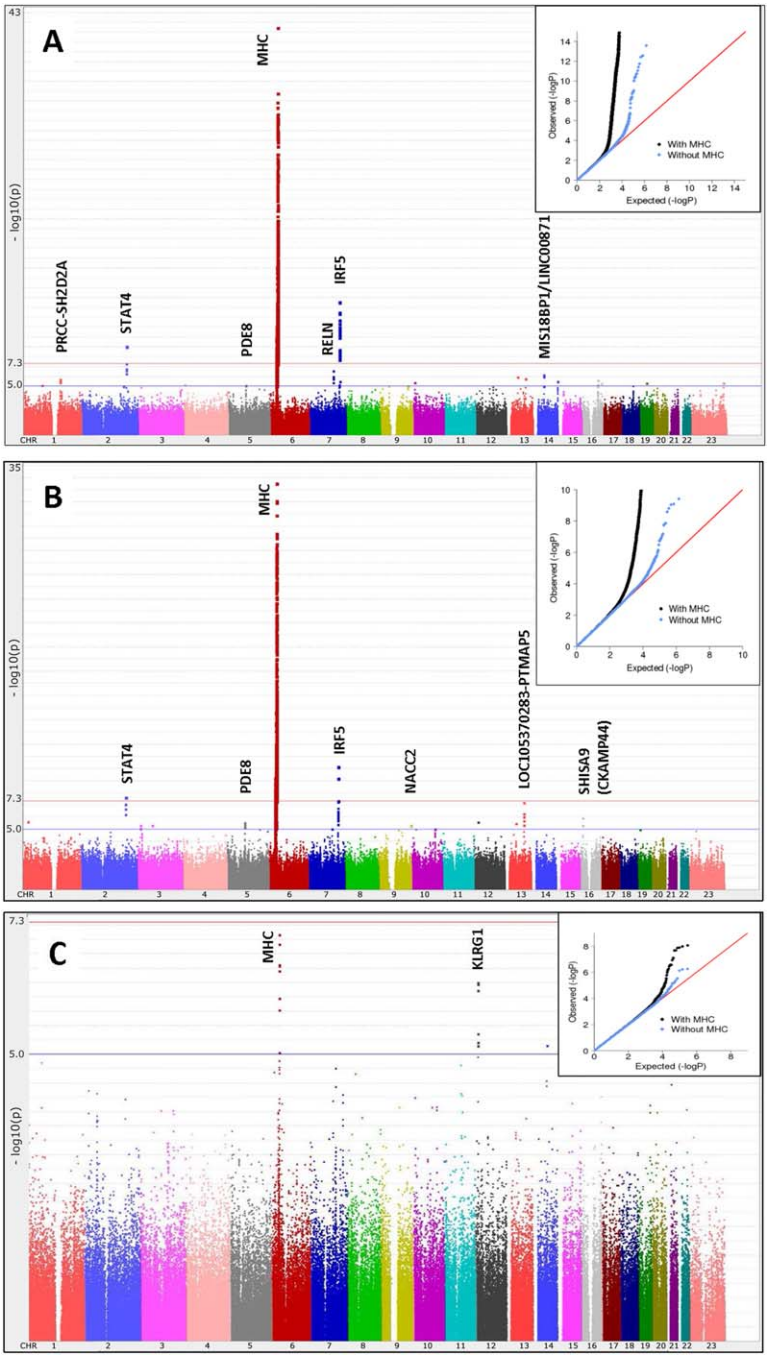

Figure 1. Manhattan plots of the results of the genome-wide association studies (GWAS) with logistic regression in patients with Sjögren's syndrome. **A,** Global GWAS (1,405 cases, 1,622 Sjögren's International Collaborative Clinical Alliance [SICCA] controls, and 3,125 external controls) using 1,444,854 single-nucleotide polymorphisms (SNPs), with adjustment for 9 intercontinental principal components (PCs) and smoking ($\lambda = 1.02$). **B,** European subgroup GWAS (585 cases, 966 SICCA controls, and 580 external controls) using the same set of SNPs described in **A,** with adjustment for 1 intra-European PC and smoking ($\lambda = 1.002$). **C,** Meta-analysis of the Chinese ($\lambda = 1.03$) and Japanese ($\lambda = 1.03$) subgroups of the Asian GWAS (460 cases, 224 SICCA controls, and 901 external controls) using 302,688 SNPs, with adjustment for 2 intra-Asian PCs. **Insets,** Q–Q plots. MHC = major histocompatibility complex; Chr. = chromosome.

Table 2. Top SNPs in regions having 2 or more suggestive or stronger associations in the case–control analyses*

GWAS	Chr. (kbp)	Gene region	SNP	OR	95% CI	*P*
All subjects	1 (156,774)	*PRCC/SH2D2A*	rs16837677	1.54	1.29–1.84	2×10^{-6}
All subjects	1 (156,774)	*PRCC/SH2D2A*	rs16837672	1.53	1.28–1.83	2×10^{-6}
All subjects	2 (191,944)	*STAT4*	rs11889341	1.40	1.26–1.56	9×10^{-10}
European	2 (191,965)	*STAT4*	rs7574865	1.51	1.31–1.75	2×10^{-8}
All subjects	2 (191,965)	*STAT4*	rs7574865	1.35	1.21–1.50	5×10^{-8}
Europeans	2 (191,969)	*STAT4*	rs8179673	1.48	1.28–1.71	8×10^{-8}
European	3 (14,715)	*GRIP2/CCDC174*	rs79407237	0.61	0.49–0.75	5×10^{-6}
European	3 (14,682)	*GRIP2/CCDC174*	rs17318848	0.63	0.51–0.77	9×10^{-6}
European	5 (76,591)	*PDE8B*	rs181851	0.67	0.56–0.79	3×10^{-6}
European	5 (76,600)	*PDE8B*	rs11949070	0.67	0.57–0.80	5×10^{-6}
All subjects	5 (76,620)	*PDE8B*	rs10474500	0.75	0.66–0.85	8×10^{-6}
All subjects	5 (76,553)	*PDE8B*	rs10464287	1.53	1.27–1.84	9×10^{-6}
All subjects	6 (32,591)	*MHC (HLA–DRB1, HLA–DQA1)*	rs9271573	2.02	1.82–2.23	3×10^{-42}
All subjects	6 (32,623)	*MHC (HLA–DQA1, HLA–DQB1)*	rs3021302	2.24	1.97–2.54	2×10^{-35}
European	6 (32,591)	*MHC (HLA–DRB1/HLA−DQA1)*	rs9271573	2.29	2.01–2.62	3×10^{-34}
European	6 (32,679)	*MHC (HLA–DQB1/HLA–DQA2)*	rs9275572	2.28	1.99–2.61	7×10^{-33}
Asian	6 (33,056)	*MHC (HLA–DPB1)*	rs9277554	1.65	1.37–2.00	3×10^{-7}
Asian	6 (33,053)	*MHC (HLA–DPB1)*	rs9277464	1.65	1.37–1.99	3×10^{-7}
All subjects	7 (128,580)	*IRF5/TNP03*	rs3823536	1.49	1.34–1.65	3×10^{-14}
All subjects	7 (128,716)	*IRF5/TNP03*	rs59110799	1.72	1.49–1.99	3×10^{-13}
European	7 (128,580)	*IRF5/TNP03*	rs3823536	1.54	1.36–1.76	7×10^{-11}
European	7 (128,581)	*IRF5/TNP03*	rs3807306	1.50	1.32–1.71	6×10^{-10}
All subjects	7 (103,405)	*RELN*	rs7341475	1.39	1.23–1.57	3×10^{-7}
All subjects	7 (103,404)	*RELN*	rs73180120	1.36	1.20–1.54	1×10^{-6}
European	7 (103,405)	*RELN*	rs7341475	1.43	1.22–1.68	9×10^{-6}
European	9 (138,947)	*NACC2*	rs4842091	1.39	1.21–1.61	5×10^{-6}
European	9 (138,948)	*NACC2*	rs11103291	1.39	1.21–1.61	5×10^{-6}
Asian	12 (9,163)	*KLRG1/M6PR*	rs1805673	0.62	0.51–0.74	6×10^{-7}
Asian	12 (9,154)	*KLRG1/M6PR*	rs11048434	0.63	0.53–0.75	6×10^{-7}
All subjects	13 (47,951)	*HTR2A/LINC00562*	rs7999279	1.42	1.23–1.63	1×10^{-6}
European	13 (47,951)	*HTR2A/LINC00562*	rs7999279	1.52	1.27–1.81	3×10^{-6}
European	13 (82,162)	*LOC105370283-PTMAP5*	rs17074492	1.53	1.31–1.79	6×10^{-8}
European	13 (82,177)	*LOC105370283-PTMAP5*	rs67218188	1.49	1.28–1.74	5×10^{-7}
All subjects	13 (82,162)	*LOC105370283-PTMAP5*	rs17074492	1.37	1.20–1.56	2×10^{-6}
All subjects	14 (46,407)	*MIS18BP1/LINC00871*	rs1957173	0.61	0.50–0.74	7×10^{-7}
All subjects	14 (46,375)	*MIS18BP1/LINC00871*	rs17116722	0.60	0.49–0.74	1×10^{-6}
All subjects	16 (69,704)	*NFAT5*	rs7192380	1.28	1.16–1.42	2×10^{-6}
All subjects	16 (69,633)	*NFAT5*	kgp11747098	1.26	1.14–1.40	7×10^{-6}
European	16 (13,002)	*SHISA9*	rs9938751	0.59	0.48–0.73	1×10^{-6}
European	16 (12,988)	*SHISA9*	rs8046800	0.61	0.50–0.76	5×10^{-6}

* Up to 2 single-nucleotide polymorphisms (SNPs) are included for each genome-wide association study (GWAS)/gene. Chr. = chromosome; OR = odds ratio; 95% CI = 95% confidence interval.

intra-Asian PCs (APC1 and APC2) and sex. The number of subjects included in each analysis is described in Figure 1 and Supplementary Table 1 (available on the *Arthritis & Rheumatology* web site at http://onlinelibrary.wiley.com/doi/10.1002/art.40040/abstract).

Regulatory evidence for sites of interest was collected from RegulomeDB (17) and ANNOVAR (18) data; evidence for association with related phenotypes was collected from National Center for Biotechnology Information Phenotype–Genotype Integrator (http://www.ncbi.nlm.nih.gov/gap/phegeni). For follow-up in the *KLRG1* region, we imputed genotypes for all European and Asian participants up to the 1000 Genomes reference panel starting from the 300K overlap SNP set, using IMPUTE2 software (19).

SNP selection for downstream analyses. We undertook several analyses in order to determine whether or not the apparent differences between Asian and European associations were true heterogeneity of association or were attributable to other factors such as differences in allele frequency between populations or disease heterogeneity between population groups and/or sites. For these analyses and for multivariate modeling, we chose representative SNPs from our case–control analyses: one SNP per region with at least 2 associations that were suggestive ($P \times 10^{-5}$) or stronger in any of our 3 GWAS (all participants, European cluster, and Asian cluster). We also selected representative SNPs from the top hits in published European (6) and Asian (7) GWAS. SNPs with the strongest association from the 300K overlap set were selected to allow comparisons and multivariate modeling with our full Asian control data; in some cases, a proxy SNP was chosen. A total of 24 SNPs were selected (see Supplementary Methods and Supplementary Table 2, available on the *Arthritis & Rheumatology* web site at http://onlinelibrary.wiley.com/doi/10.1002/art.40040/abstract).

Heterogeneity. We quantified heterogeneity between the European and Asian GWAS using Q and I^2 statistics from meta-analysis of the 2 studies, using Plink. For the MHC region, we also imputed HLA alleles using SNP2HLA (20) and the HapMap CEU (Utah residents with ancestry from northern and western Europe) reference panel for the Europeans and a Pan-Asian

reference panel (described in ref. 21) for the Asians. Associations with HLA allele doses in each population group were analyzed in Plink, and the results were meta-analyzed to assess heterogeneity. In order to investigate or exclude heterogeneity of disease subtypes, we repeated some analyses using only cases meeting all 3 of the classification criteria.

RESULTS

Global GWAS. Our global GWAS (Figure 1A) of the approximately 1.4 million post–quality control SNPs showed genome-wide significant peaks in established SS regions, namely the MHC, *STAT4*, and *IRF5*. We also observed several suggestive association peaks, as shown in Figure 1A and Table 2, with the most significant being in *RELN* (odds ratio [OR] 1.4, $P = 3 \times 10^{-7}$) on 7q22.1, and on 14q21.2 between *MIS18BP1* and *LINC00871* (OR 0.61, $P = 7 \times 10^{-7}$). A suggestive region on 1q23.1 (OR 1.5, $P = 2 \times 10^{-6}$) included *SH2D2A,* which has been shown to be associated with other autoimmune disorders. Our top SNPs in *SH2D2A* were located in peaks of DNase I hypersensitivity sites for numerous cell types, and this region has been shown via ChIP-Seq to bind to protein CCAAT/enhancer binding protein β (CEBPB), a known regulator of immune and inflammatory response genes. Additional suggestive regions were in *PDE8B* (OR 0.75, $P = 8 \times 10^{-6}$) on 5q13.3 and *NFAT5* (OR 1.28, $P = 2 \times 10^{-6}$) on 16q22.1.

European versus Asian GWAS. We performed subpopulation GWAS in our 2 largest ethnic groups. The European subgroup was analyzed using the same set of 1.4 million SNPs as described above; the Asian group was analyzed using the 300K set of SNPs overlapping with the Asian external controls that were added to increase power for this analysis. Figures 1B and C show Manhattan plots for the European and Asian GWAS, respectively, and details of the top SNPs are shown in Table 2. Two aspects are striking. First, the MHC region, while being the most significant region in the Asian participants, had a much weaker effect than that in the Europeans (in Europeans, peak OR 2.29, 95% confidence interval [95% CI] 2.01–2.62, $P = 3 \times 10^{-34}$; in Asians, peak OR 1.65, 95% CI 1.37–2.00, $P = 3 \times 10^{-7}$). Second, the *KLRG1* region (for the top SNP, OR 0.62, $P = 6 \times 10^{-7}$) had the next strongest associations in Asians but did not appear to be associated in Europeans. *KLRG1* has been shown to be associated with SLE (22). Top SNPs in this region show strong evidence of immune regulation; ChIP-Seq analysis has shown that they bind to multiple proteins including NF-κB subunit 1 in B lymphocytes and are within DNase I hypersensitivity sites of B lymphocytes, Th1 cells, and Th17 cells.

The European GWAS also showed multiple suggestive association peaks (Figure 1B and Table 2); the strongest association (OR 1.5, $P = 6 \times 10^{-8}$) was in *LOC105370283*, a noncoding RNA, on 13q31.1 and near pseudogene *PTMAP5*. Other suggestive gene regions were *CCDC174* (OR 0.61, $P = 5 \times 10^{-6}$) on 3p25.1, *NACC2* (OR 1.39, $P = 5 \times 10^{-6}$) on 9q34.3, and *SHISA9*/*CKAMP44* (OR 0.59, $P = 1 \times 10^{-6}$) on 16p13.12.

MHC region. Figures 2A and B show MHC region associations in the Asian and European clusters, respectively. In order to determine whether the observed differences were attributable to power differences, we randomly selected a subset of the European cases and controls, with sample sizes equal to those in the Asian analysis (460 cases and 1,125 controls) and repeated the analysis. Figure 2C shows the results of that analysis, which continued to demonstrate striking differences in significance and the location of peaks that are not explained by sample size differences. The top SNPs in Europeans were rs9271573 ($P = 3 \times 10^{-34}$) and rs9275572 ($P = 7 \times 10^{-33}$), which flank *HLA–DQA1* and *HLA–DQB1*, as shown in Figure 2B. The top SNP in a secondary peak, rs6937545 ($P = 6 \times 10^{-30}$), is downstream of *HLA–DRA*. The top SNPs in 2 association peaks in Asians (Figure 2A) were rs9277554 ($P = 3 \times 10^{-7}$) near *HLA–DPB1* and rs6903608 ($P = 1 \times 10^{-6}$) in *HLA–DRB9* (between *HLA–DRA* and *HLA–DRB1*).

We also analyzed associations in imputed HLA alleles in the European and Asian subsets (Supplementary Table 3, available on the *Arthritis & Rheumatology* web site at http://onlinelibrary.wiley.com/doi/10.1002/art.40040/abstract) and conducted a meta-analysis to assess heterogeneity. Of 41 alleles (of a total of 361) with significant ($P < 0.0001$) associations in Europeans, Asians, or in the meta-analysis, 17 had an I^2 value of >80%, indicating high heterogeneity, with an I^2 value of 96.4 for *HLA–DQA1*0103* (OR in Europeans [OR_{Euro}] 0.45, and OR in Asians [OR_{Asia}] 1.56) and an I^2 value of 94.9 for *HLA–DQB1*0201* (OR_{Euro} 2.38 and OR_{Asia} 1.03). In addition, 7 associations in Asians (all in *HLA–DPA1*/*DPB1*) could not be analyzed in Europeans due to low frequency.

KLRG1 region. In order to determine whether there might be associations in Europeans with untyped SNPs in the *KLRG1* region, we imputed up to the 1000 Genomes reference panel starting from the set of SNPs common to both the Omni2.5M and Illumina 610K platforms. Supplementary Figure 4 (available on the *Arthritis & Rheumatology* web site at http://onlinelibrary.wiley.com/doi/10.1002/art.40040/abstract) shows associations of genotyped and imputed SNPs in the *KLRG1* region for European and Asian participants separately. These data continued to show an Asian-only effect of multiple *KLRG1* SNPs on SS risk. Supplementary Table 4 (available on the *Arthritis & Rheumatology* web site at http://onlinelibrary.wiley.com/doi/10.1002/art.40040/abstract)

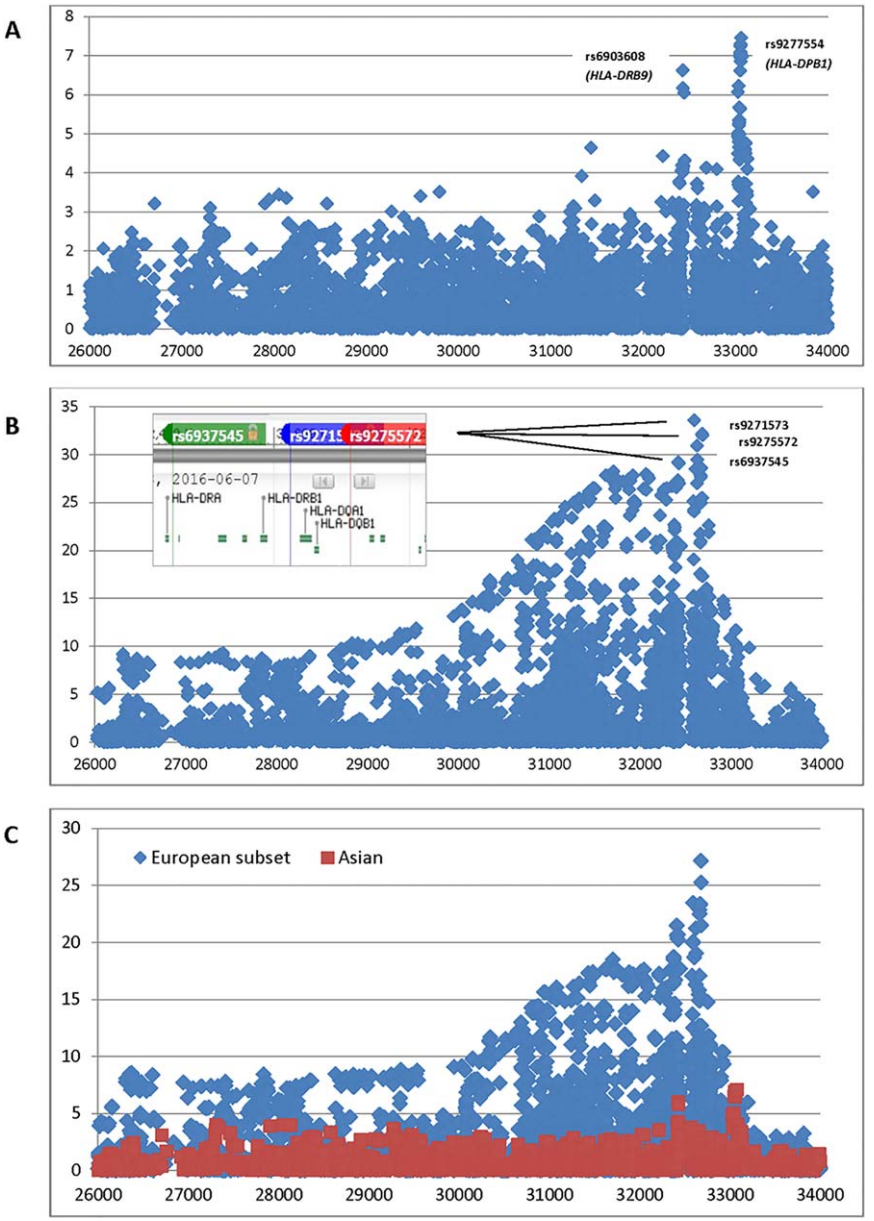

Figure 2. Major histocompatibility complex association plots. **A,** Asian subgroup. **B,** European subgroup. **Inset**. Relative positions of top single-nucleotide polymorphisms and HLA genes from dbSNP. **C,** European subgroup (blue) with sample sizes (460 cases and 1,125 controls) equal to those in the Asian subgroup (red).

shows the allele frequencies of the suggestive *KLRG1* SNPs in various participant subgroups in our data set, indicating that the external controls were similar to internal controls, and that effect sizes were higher in the Chinese cluster than in the Japanese cluster.

Representative SNPs and multivariate modeling. We selected 24 representative SNPs in 20 regions with at least 2 suggestive ($P < 1 \times 10^{-5}$) or stronger associations in any of our 3 GWAS (all subjects, Europeans, and Asians) and from the top hits (or proxies) in published European (6) and Asian (7) GWAS (see Patients and Methods). Supplementary Table 2 (available on the *Arthritis & Rheumatology* web site at http://onlinelibrary.wiley.com/doi/10.1002/art.40040/abstract) contains details of the SNP/proxy selection, and Supplementary Table 5 (available on the *Arthritis & Rheumatology* web site at http://onlinelibrary.wiley.com/doi/10.1002/art.40040/abstract) contains results from the 3 GWAS. Although *STAT4* and *IRF5* SNPs did not

Table 3. Subphenotype differences between the European and Asian clusters, and correlations with the top 3 worldwide PCs, in SICCA participants*

	SSA/SSB	Focus score	OSS
European cluster, no. meeting criteria/total no. (%)	553/1,663 (33)	526/1,568 (34)	1,126/1,600 (70)
Asian cluster, no. meeting criteria/total no. (%)	439/704 (62)	351/647 (54)	575/680 (85)
Top 3 worldwide PCs			
PC1, r (*P*)	-0.27 (5×10^{-47})	-0.18 (2×10^{-21})	-0.12 (2×10^{-14})
PC2, r (*P*)	-0.025 (0.16)	0.0053 (0.77)	-0.013 (0.49)
PC3, r (*P*)	-0.035 (0.055)	-0.054 (0.0034)	-0.050 (0.0059)

* PC1 = principal components cluster 1; SICCA = Sjögren's International Collaborative Clinical Alliance; OSS = ocular staining score.

meet the criteria for suggestive associations in our Asian GWAS, the ORs for these SNPs were similar across analyses. *TNFAIP3* also had similar ORs across analyses and has been implicated previously in both European (23) and Asian (7) studies. Interestingly, the results of this analysis suggested that one of the *GTF2I* SNPs may be associated in Europeans, although it previously was implicated only in Asians (7). According to our data, *BLK* and *CXCR5* SNPs had a stronger effect in Asians, whereas the effect of *IL2A* was much lower.

We also performed multivariate modeling of these SNPs in the European and Asian subgroups separately, adjusting for intra-European and intra-Asian PCs, respectively (see Patients and Methods). We executed logistic regression analysis with backward selection, with thresholds of $P < 0.01$ for the European subset and $P < 0.05$ for the Asian subset due to the smaller sample size. The results of this analysis are shown in Supplementary Table 6, available on the *Arthritis & Rheumatology* web site at http://onlinelibrary.wiley.com/doi/10.1002/art.40040/abstract. These data continue to support that *GTF2I* is a risk variant in Europeans and also indicate that the effect of the *PRCC–SH2D2A* region may be more prominent in Asians or non-Europeans.

Investigation of sources of heterogeneity. As shown in Supplementary Figure 5 (available on the *Arthritis & Rheumatology* web site at http://onlinelibrary.wiley.com/doi/10.1002/art.40040/abstract), we plotted the heterogeneity *P* value from the Q statistic for the 24 representative SNPs between the European and Asian analyses versus the difference in MAF between controls in the 2 population groups. Although most of these SNPs had highly significant allele frequency differences, there was also substantial heterogeneity of association; i.e., the frequency differences did not fully explain these differences in association.

One potential source of genetic heterogeneity is the heterogeneity of underlying subphenotypes in the population groups. Table 3 shows the percentage of cases positive for SSA/SSB autoantibodies, focus score criteria, and OSS criteria. The percentage of cases positive for these criteria was much higher in the Asian cluster compared with the European cluster, which may be attributable to ascertainment and/or associations between ethnicity and subphenotypes (see below). Next, we studied the degree to which global ancestry, represented by our top 3 worldwide PCs, correlates with the subphenotypes described above. As shown in Table 3, we observed strongly significant correlations between PC1 (European/Asian axis) and all 3 subphenotypes (for SSA/SSB, $r = -0.27$ [$P = 5 \times 10^{-47}$]; for focus score, $r = -0.18$ [$P = 2 \times 10^{-21}$]; for OSS, $r = -0.12$ [$P = 2 \times 10^{-14}$]). We also observed strongly significant correlations between PC3 (American Indian/non–American Indian axis) and the focus score and OSS, although the correlation coefficients were modest (absolute value <0.1).

Because it is possible that the relationship between ancestry and subphenotype was confounded by the geographic recruitment site, we adjusted for site via meta-analysis and provide site-specific statistics for PC1 (see Supplementary Table 7, available on the *Arthritis & Rheumatology* web site at http://onlinelibrary.wiley.com/doi/10.1002/art.40040/abstract). The mean value for PC1 was higher or equal throughout in the subphenotype-negative versus the subphenotype-positive cases, with the exception that values were slightly lower for the India site (SSA/SSB) or the Denmark and JHU sites (OSS). We observed a very strong association between SSA/SSB status and PC1, both adjusted for strata (meta-analysis $P = 4 \times 10^{-15}$, heterogeneity $Q = 0.38$) and within the sites having the most variance in PC1 (i.e., higher power to detect associations): for UCSF, $P = 8 \times 10^{-7}$; for Argentina, $P = 1 \times 10^{-5}$; for UK, $P = 0.00065$; and for JHU, $P = 0.0040$. For the focus score and OSS, the strata-adjusted *P* values were $P = 4 \times 10^{-5}$ and $P = 0.071$, respectively, and the most strongly

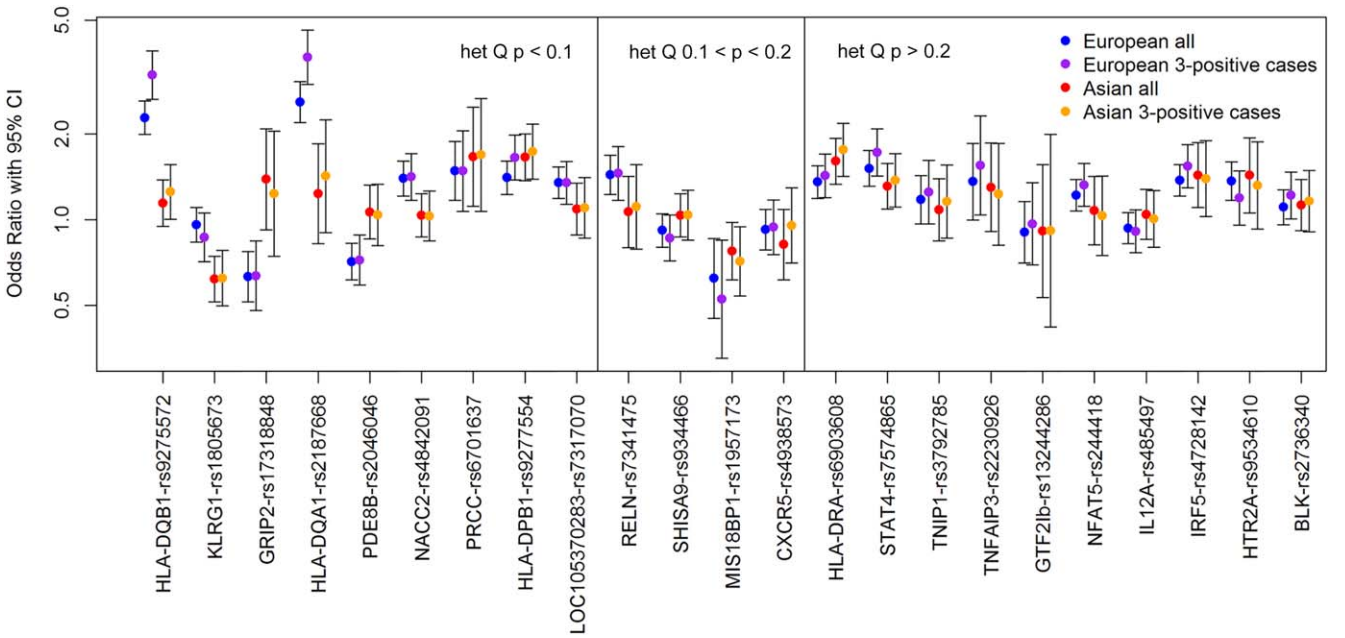

Figure 3. Associations in Europeans versus associations in Asians. Cases designated 3-positive are positive for the SSA/SSB, focus score, and ocular staining score criteria. The single-nucleotide polymorphisms are ordered according to decreasing heterogeneity (het) based on higher Q values. 95% CI = 95% confidence interval.

associated strata is Argentina for both ($P = 5 \times 10^{-6}$ and $P = 0.0061$, respectively). We concluded that the degree of European ancestry is likely to be protective for these subphenotypes (see Discussion).

Finally, to understand whether this difference was driving the apparent European and Asian heterogeneity, we re-analyzed our data using only cases positive for all 3 subphenotypes. As shown in Figure 3, we plotted the 95% CIs for associations in the European and Asian cases, for all SS cases, and for only those meeting all 3 subphenotype criteria. In most cases, the 95% CIs for associations in the 2 European groups and the 2 Asian groups were more similar to each other than to the 95% CIs for associations in the 2 groups meeting 3 criteria, indicating that subphenotypes are not driving differences in association. A notable exception was *HLA–DPB1*, for which the 95% CIs in Europeans became more similar to those in Asians when the analyses were restricted to cases positive for 3 criteria; *HLA–DPB1* was associated with positive SSA/SSB and focus score status in both Europeans (for SSA/SSB, OR 1.69 [$P = 1.3 \times 10^{-8}$]; for focus score, OR 1.36 [$P = 0.00071$]) and Asians (for SSA/SSB, OR 1.64 [$P = 0.00032$]; for focus score, OR 1.47 [$P = 0.0049$]). It was common in our study for effect sizes to become stronger when the analyses were restricted to cases positive for all 3 criteria; this was particularly true for *HLA–DQB1* and *HLA–DQA1* in Europeans. *HLA–DQA1* and *HLA–DQB1* alleles were very strongly associated with SSA/SSB and focus score status in the European participants (for SSA/SSB, OR 4.42 [$P = 1.2 \times 10^{-34}$] and OR 3.20 [$P = 1.0 \times 10^{-32}$], respectively; for focus score, OR 2.98 [$P = 1.6 \times 10^{-21}$] and OR 2.52 [$P = 3.7 \times 10^{-24}$], respectively) but not in the Asian participants.

DISCUSSION

The current study is the first international multiethnic GWAS of SS and to our knowledge is the only international cohort with standardized deep phenotyping. Thus, it is particularly well-suited to assess relationships between ancestry and genetic etiology and how these may differ depending on the clinical subtypes of SS, particularly for the 2 largest ethnic groups, Europeans and Asians.

The results of our GWAS implicate several novel suggestive regions of association (having at least 2 SNPs with a P value of less than 1×10^{-5}). Two of these, *SH2D2A* and *KLRG1*, have been associated with other autoimmune diseases. It has been suggested (24) that a P value more liberal than standard genome-wide significance ($P < 5 \times 10^{-8}$) is appropriate in this case, because genes are often associated with multiple autoimmune diseases and involve overlapping clinical subphenotypes. *SH2D2A* has been associated with juvenile rheumatoid arthritis (25), multiple sclerosis (26), and inflammatory neuropathies (27,28). *SH2D2A* encodes a T cell–specific adapter protein (TSAd) expressed in activated T cells, natural

killer cells, and endothelial cells and is thought to function in T cell signal transduction (29). We also found regulatory evidence for this region: it has been shown to bind to CEBPB, a regulator of immune and inflammatory responses, and our top SNPs in this region are within DNase I hypersensitivity peaks for numerous cell types. *KLRG1* has been shown to be associated with SLE in a previous study (22) that examined both adult and childhood-onset SLE in multiple ethnic groups. In that study, significant haplotypes varied by ethnicity, with the most significant haplotype being in Asian Americans, and with European Americans having no significantly associated haplotype. This corroborates our finding of *KLRG1* being associated with SS only in Asians.

The strongest novel region in our 3 GWAS was observed in the European GWAS (OR 1.5, $P = 6 \times 10^{-8}$) in *LOC105370283*, a noncoding RNA on 13q31.1 that is near pseudogene *PTMAP5*. This region was associated ($P = 5 \times 10^{-9}$) with C-reactive protein, a biomarker of inflammation, in the Framingham cohort (30) and contains a DNase I hypersensitivity site for human retinal epithelial cells. Another interesting suggestive region was *NFAT5*; members of the NF-AT family of proteins are transcription factors involved in the immune response.

Striking differences between our European and Asian GWAS pertain to the significance and locations of MHC associations. The locations of MHC peaks in Europeans are consistent with those observed in a previous study (6), which also identified genes *HLA–DQA1, HLA–DQB1*, and *HLA–DRA* as being most significant. The peaks observed in the Asians in our study are similar to the 2 previously reported independent association signals (7); both studies showed an association peak at *HLA–DPB1*. Although the top peak reported in ref. 7 was between *HLA–DRB1* and *HLA–DQA1*, *HLA–DRB9* is within the same region of long-range linkage disequilibrium in MHC class II. We observed high heterogeneity between European and Asian associations in our representative markers for the peak MHC regions. Similarly, high MHC heterogeneity between European and Chinese participants has recently been reported in SLE (31).

We have shown that the first worldwide ancestry PC is significantly associated with subphenotypes, especially SSA/SSB autoantibody production, even within sites and adjusting for site differences. Because this PC distinguishes between European and Asian clusters, this could be attributed to either the presence of Asian ancestry or the absence of European ancestry. However, association of PC1 with subphenotypes within Argentinians, and a much weaker association with the American Indian axis (PC3), leads us to believe that the degree of European ancestry is primarily driving the PC1 association. Further work is needed to confirm this finding, with more detailed ancestry admixture data. If European ancestry is indeed protective for all SS subphenotypes, this implies that European ancestry is protective for SS in general, as has been seen in SLE. This is consistent with a study by Maldini et al (12), which demonstrated a higher prevalence of SS and SS autoantibodies in non-Europeans versus Europeans in the greater Paris area. More population-based studies of SS prevalence are needed to confirm this hypothesis.

Finally, we demonstrate that the heterogeneity of association seen in many of the top regions is not explained, in most cases, by differing subphenotype distributions within different ethnic groups. Allele frequencies in these SNPs differed significantly between the European and Asian subgroups and likely reflect different underlying haplotype structures, as has been shown for *KLRG1* in SLE (22). Because associated variants are likely only tagging the actual causal variants, whether disease-causing mutations are present in some populations but not others or actually have different biologic effects in different populations, will be the subject of future research.

A limitation of the current study is the paucity of non-European control data sets. We included 2 European control data sets derived from dbGaP (AREDS and COGEND), which were genotyped on the same platform and in the same laboratory concurrently. We identified these in advance and thus were able to do duplicate genotyping in a small subset of cases, for quality control. We obtained a control data set for our Asian cluster, IGANGWAS; however, it was genotyped on the Illumina 610 Quad platform, with only ~300,000 SNPs common to both platforms. Thus, our Asian analysis was limited to this smaller set, and comparisons between the ancestry groups have this caveat. We performed an imputation of this data set up to the 1.4 million post–quality control SNPs of the Omni2.5M platform, and during the quality control process compared the frequencies of the imputed external versus internal controls (SICCA participants without SS) for each SNP. The resulting Q–Q plot indicated systematic bias of the imputed SNPs; therefore, we chose not to include these data in the final analysis. Related to this, the 24 SNPs that we used for heterogeneity comparisons and multivariate modeling were drawn from the 300K overlap SNP set, which sometimes resulted in weak proxies; this may have led to overestimation or underestimation of the heterogeneity of causal variants and their effects in multivariate models.

A related limitation of our study is that it may not have had sufficient power to identify novel variants; recently discovered variants in European (6) and Asian (7) cohorts have identified risk alleles with ORs as low as 1.28 and 1.44, respectively. Our all-subjects analysis had 80% power to

detect ORs of 1.31–1.50 (for MAFs of 0.1–0.45), while our European and Asian analyses had power to detect ORs of 1.49–1.75 and 1.65–2.01, respectively. We are very encouraged by the presence of suggestive genes already known to influence autoimmunity, which we consider the most promising for future follow-up. These data are also available for use in larger collaborations that may be more appropriately suited to establishing novel associations.

Our SS case–control comparison used the ACR 2012 criteria for SS and included SS-negative subjects who were positive for 1 criterion, with external Asian controls added to increase power. Our results for the top SNPs were very similar if the subjects positive for only 1 criterion are omitted or if the newer 2016 ACR/European League Against Rheumatism criteria (32) were used (see Supplementary Table 8, available on the *Arthritis & Rheumatology* web site at http://onlinelibrary.wiley.com/doi/10.1002/art.40040/abstract).

In summary, we have conducted the first multiethnic GWAS in SS and analyses of European versus Asian associations. Several suggestive association peaks warrant further follow-up in future studies, particularly in 2 regions previously implicated in autoimmune diseases. We observed strong associations between SS subphenotypes and genetic ancestry; however, this does not explain the heterogeneity of the associations seen in the European versus Asian subpopulations. Issues of genetic etiology, ancestry, and subphenotype heterogeneity have been studied very little in SS compared with autoimmune diseases such as SLE. Our study gives new insights into these relationships and provides a basis for future work on the genetic etiology of SS.

ACKNOWLEDGMENTS

We are very grateful to the SICCA participants for their time and dedication to this research. We would also like to thank the IGANGWAS, COGEND, and AREDS participants and researchers for their valuable contributions. We acknowledge the contribution of data from AREDS, which were accessed through dbGaP (accession no. phs000001.v3.p1). Funding support for AREDS was provided by the National Eye Institute (N01-EY-[NEI AREDS] April 21, 2010, version G Page 5 of 8 0-2127). We also acknowledge the contribution of data from Genetic Architecture of Smoking and Smoking Cessation, accessed through dbGaP (accession no. phs000404.v1.p1). Funding support for genotyping, which was performed at the Center for Inherited Disease Research (CIDR), was provided by 1 X01 HG005274-01. The CIDR is fully funded through a federal contract from the National Institutes of Health to Johns Hopkins University (contract no. HHSN268 200782096C). Assistance with the cleaning of genotype data, as well as with general study coordination, was provided by the Gene Environment Association Studies Coordinating Center (U01HG004 446). Funding support for the collection of data sets and samples was provided by the Collaborative Study of Nicotine Dependence (P01-CA089392) and the University of Wisconsin Transdisciplinary Tobacco Use Research Center (grants P50-DA019706 and P50-A084724). Finally, we acknowledge the contribution of data from IGANGWAS, conducted by the IGANGWAS investigators and supported by the NIDDK. The data from IGANGWAS reported herein were derived from dbGaP (accession no. phs000431.v2.p1).

AUTHOR CONTRIBUTIONS

All authors were involved in drafting the article or revising it critically for important intellectual content, and all authors approved the final version to be published. Dr. Criswell had full access to all of the data in the study and takes responsibility for the integrity of the data and the accuracy of the data analysis.

Study conception and design. Taylor, S. Shiboski, Daniels, Greenspan, C. Shiboski, Criswell.

Acquisition of data. Doheny, Lam, Baer, Challacombe, Lanfranchi, Schiødt, Srinivasan, Umehara, Vivino, Zhao, S. Shiboski, Daniels, Greenspan, C. Shiboski, Criswell.

Analysis and interpretation of data. Taylor, Wong, Levine, McHugh, Laurie, Lam, Criswell.

REFERENCES

1. Ice JA, Li H, Adrianto I, Lin PC, Kelly JA, Montgomery CG, et al. Genetics of Sjögren's syndrome in the genome-wide association era. J Autoimmun 2012;39:57–63.
2. Shiboski SC, Shiboski CH, Criswell L, Baer A, Challacombe S, Lanfranchi H, et al. American College of Rheumatology classification criteria for Sjögren's syndrome: a data-driven, expert consensus approach in the Sjögren's International Collaborative Clinical Alliance cohort. Arthritis Care Res (Hoboken) 2012;64:475–87.
3. Cobb BL, Lessard CJ, Harley JB, Moser KL. Genes and Sjögren's syndrome. Rheum Dis Clin North Am 2008;34:847–68, vii.
4. Kuo CF, Grainge MJ, Valdes AM, See LC, Luo SF, Yu KH, et al. Familial risk of Sjögren's syndrome and co-aggregation of autoimmune diseases in affected families: a nationwide population study. Arthritis Rheumatol 2015;67:1904–12.
5. Cruz-Tapias P, Rojas-Villarraga A, Maier-Moore S, Anaya JM. HLA and Sjögren's syndrome susceptibility: a meta-analysis of worldwide studies. Autoimmun Rev 2012;11:281–7.
6. Lessard CJ, Li H, Adrianto I, Ice JA, Rasmussen A, Grundahl KM, et al. Variants at multiple loci implicated in both innate and adaptive immune responses are associated with Sjögren's syndrome. Nat Genet 2013;45:1284–92.
7. Li Y, Zhang K, Chen H, Sun F, Xu J, Wu Z, et al. A genome-wide association study in Han Chinese identifies a susceptibility locus for primary Sjögren's syndrome at 7q11.23. Nat Genet 2013;45:1361–5.
8. Daniels TE, Criswell LA, Shiboski C, Shiboski S, Lanfranchi H, Dong Y, et al. An early view of the International Sjögren's Syndrome Registry. Arthritis Rheum 2009;61:711–4.
9. Chung SA, Tian C, Taylor KE, Lee AT, Ortmann WA, Hom G, et al. European population substructure is associated with mucocutaneous manifestations and autoantibody production in systemic lupus erythematosus. Arthritis Rheum 2009;60:2448–56.
10. Richman IB, Chung SA, Taylor KE, Kosoy R, Tian C, Ortmann WA, et al. European population substructure correlates with systemic lupus erythematosus endophenotypes in North Americans of European descent. Genes Immun 2010;11:515–21.
11. Chung SA, Taylor KE, Graham RR, Hom G, Ortmann WA, Lee AT, et al. Refining genome-wide association results for SLE according to anti-dsDNA autoantibody production [abstract]. Arthritis Rheum 2008;58 Suppl:S344.
12. Maldini C, Seror R, Fain O, Dhote R, Amoura Z, de Bandt M, et al. Epidemiology of primary Sjögren's syndrome in a French multiracial/multiethnic area. Arthritis Care Res (Hoboken) 2014;66:454–63.

13. Daniels TE, Cox D, Shiboski CH, Schiodt M, Wu A, Lanfranchi H, et al. Associations between salivary gland histopathologic diagnoses and phenotypic features of Sjögren's syndrome among 1,726 registry participants. Arthritis Rheum 2011;63:2021–30.
14. Whitcher JP, Shiboski CH, Shiboski SC, Heidenreich AM, Kitagawa K, Zhang S, et al. A simplified quantitative method for assessing keratoconjunctivitis sicca from the Sjögren's Syndrome International Registry. Am J Ophthalmol 2010;149:405–15.
15. Laurie CC, Doheny KF, Mirel DB, Pugh EW, Bierut LJ, Bhangale T, et al. Quality control and quality assurance in genotypic data for genome-wide association studies. Genet Epidemiol 2010;34:591–602.
16. Price AL, Patterson NJ, Plenge RM, Weinblatt ME, Shadick NA, Reich D. Principal components analysis corrects for stratification in genome-wide association studies. Nat Genet 2006;38: 904–9.
17. Boyle AP, Hong EL, Hariharan M, Cheng Y, Schaub MA, Kasowski M, et al. Annotation of functional variation in personal genomes using RegulomeDB. Genome Res 2012;22:1790–7.
18. Wang K, Li M, Hakonarson H. ANNOVAR: functional annotation of genetic variants from high-throughput sequencing data. Nucleic Acids Res 2010;38:e164.
19. Howie BN, Donnelly P, Marchini J. A flexible and accurate genotype imputation method for the next generation of genome-wide association studies. PLoS Genet 2009;5:e1000529.
20. Jia X, Han B, Onengut-Gumuscu S, Chen WM, Concannon PJ, Rich SS, et al. Imputing amino acid polymorphisms in human leukocyte antigens. PLoS One 2013;8:e64683.
21. Pillai NE, Okada Y, Saw WY, Ong RT, Wang X, Tantoso E, et al. Predicting HLA alleles from high-resolution SNP data in three Southeast Asian populations. Hum Mol Genet 2014;23: 4443–51.
22. Armstrong DL, Reiff A, Myones BL, Quismorio FP Jr, Kleiin-Gitelman M, McCurdy D, et al. Identification of new SLE-associated genes with a two-step Bayesian study design. Genes Immun 2009;10:446–56.
23. Nocturne G, Boudaoud S, Miceli-Richard C, Viengchareun S, Lazure T, Nititham J, et al. Germline and somatic genetic variations of TNFAIP3 in lymphoma complicating primary Sjögren's syndrome. Blood 2013;122:4068–76.
24. Zhernakova A, Stahl EA, Trynka G, Raychaudhuri S, Festen EA, Franke L, et al. Meta-analysis of genome-wide association studies in celiac disease and rheumatoid arthritis identifies fourteen non-HLA shared loci. PLoS Genet 2011;7:e1002004.
25. Smerdel A, Dai KZ, Lorentzen AR, Flato B, Maslinski S, Thorsby E, et al. Genetic association between juvenile rheumatoid arthritis and polymorphism in the SH2D2A gene. Genes Immun 2004;5:310–2.
26. Lorentzen AR, Smestad C, Lie BA, Oturai AB, Akesson E, Saarela J, et al. The SH2D2A gene and susceptibility to multiple sclerosis. J Neuroimmunol 2008;197:152–8.
27. Notturno F, Pace M, de Angelis MV, Caporale CM, Giovannini A, Uncini A. Susceptibility to chronic inflammatory demyelinating polyradiculoneuropathy is associated to polymorphic GA repeat in the SH2D2A gene. J Neuroimmunol 2008;197:124–7.
28. Uncini A, Notturno F, Pace M, Caporale CM. Polymorphism of CD1 and SH2D2A genes in inflammatory neuropathies. J Peripher Nerv Syst 2011;16 Suppl 1:48–51.
29. Pandya AD, Leergaard TB, Dissen E, Haraldsen G, Spurkland A. Expression of the T cell-specific adapter protein in human tissues. Scand J Immunol 2014;80:169–79.
30. Benjamin EJ, Dupuis J, Larson MG, Lunetta KL, Booth SL, Govindaraju DR, et al. Genome-wide association with select biomarker traits in the Framingham Heart study. BMC Med Genet 2007;8 Suppl 1:S11.
31. Morris DL, Sheng Y, Zhang Y, Wang YF, Zhu Z, Tombleson P, et al. Genome-wide association meta-analysis in Chinese and European individuals identifies ten new loci associated with systemic lupus erythematosus. Nat Genet 2016;48:940–6.
32. Shiboski CH, Shiboski SC, Seror R, Criswell LA, Labetoulle M, Lietman TM, et al. 2016 American College of Rheumatology/European League Against Rheumatism classification criteria for primary Sjögren's syndrome: a consensus and data-driven methodology involving three international patient cohorts. Arthritis Rheumatol 2017;69:35–45.

APPENDIX A: ADDITIONAL COLLABORATORS IN THE SJÖGREN'S INTERNATIONAL COLLABORATIVE CLINICAL ALLIANCE

Collaborators in the Sjögren's International Collaborative Clinical Alliance, in addition to the authors, are as follows: D. Cox, R. Jordan, D. Lee, Y. DeSouza, D. Drury, A. Do, L. Scott, J. Nespeco, J. Whiteford, M. Margaret, and K. Sack (University of California, San Francisco); I. Adler, A. C. Smith, A. M. Bisio, M. S. Gandolfo, A. M. Chirife, A. Keszler, S. Daverio, and V. Kambo (University of Buenos Aires and German Hospital, Buenos Aires, Argentina); Y. Dong, Y. Jiang, D. Xu, J. Su, D. Du, H. Wang, Z. Li, J. Xiao, Q. Wu, C. Zhang, W. Meng, and J. Zhang (Peking Union Medical College Hospital, Beijing, China); S. Johansen, S. Hamann, J. Schiødt, H. Holm, P. Ibsen, A. M. Manniche, S. P. Kreutzmann, and J. Villadsen (Rigshospitalet, Copenhagen, Denmark); S. Sugai, Y. Masaki, T. Sakai, N. Shibata, M. Honjo, N. Kurose, T. Nojima, T. Kawanami, T. Sawaki, and K. Fujimoto (Kanazawa Medical University, Ishikawa, Japan); E. Odell, P. Morgan, L. Fernandes-Naglik, B. Varghese-Jacob, S. Ali, and M. Adamson (King's College London, London, UK); S. Seghal, R. Mishra, V. Bunya, M. Massaro-Giordano, S. K. Abboud, A. Pinto, Y. W. Sia, and K. Dow (University of Pennsylvania, Philadelphia); E. Akpek, S. Ingrodi, W. Henderson, C. Gourin, and A. Keyes (Johns Hopkins University, Baltimore, Maryland); M. Srinivasan, J. Mascarenhas, M. Das, A. Kumar, P. Joshi, R. Banushree, U. Kim, B. Babu, A. Ram, R. Saravanan, K. N. Kannappan, and N. Kalyani (Aravind Eye Hospital, Madurai, India).

ARTHRITIS & RHEUMATOLOGY
Vol. 69, No. 6, June 2017, pp 1306–1312
DOI 10.1002/art.40065

BRIEF REPORT

Anti–RNPC-3 Antibodies As a Marker of Cancer-Associated Scleroderma

Ami A. Shah,[1] George Xu,[2] Antony Rosen,[1] Laura K. Hummers,[1] Fredrick M. Wigley,[1] Stephen J. Elledge,[3] and Livia Casciola-Rosen[1]

Objective. **Prior studies have demonstrated an increased risk of cancer-associated scleroderma in patients with anti–RNA polymerase III (anti–RNAP III) autoantibodies as well as in patients who are triple-negative for anticentromere (anti-CENP), anti–topoisomerase I (anti–topo I), and anti–RNAP III (also known as anti-POL) autoantibodies (referred to as CTP negative). In a recent study of 16 CTP-negative scleroderma patients with coincident cancer, 25% of the patients were found to have autoantibodies to RNPC-3, a member of the minor spliceosome complex. This investigation was undertaken to validate the relationship between anti–RNPC-3 antibodies and cancer and examine the associated clinical phenotype in a large sample of scleroderma patients.**

Methods. **Scleroderma patients with cancer were assayed for anti-CENP, anti–topo I, anti–RNAP III, and anti–RNPC-3 autoantibodies. Disease characteristics and the cancer–scleroderma interval were compared across autoantibody groups. The relationship between autoantibody status and cancer-associated scleroderma was assessed by logistic regression.**

Results. **Of 318 patients with scleroderma and cancer, 70 (22.0%) were positive for anti–RNAP III, 54 (17.0%) were positive for anti–topo I, and 96 (30.2%) were positive for anti-CENP. Twelve patients (3.8% of the overall group or 12.2% of CTP-negative patients) were positive for anti–RNPC-3. Patients with anti–RNPC-3 had a short cancer–scleroderma interval (median 0.9 years). Relative to patients with anti-CENP, patients with anti–RNPC-3 and those with anti–RNAP III had a >4-fold increased risk of cancer within 2 years of scleroderma onset (for anti–RNPC-3–positive patients, odds ratio [OR] 4.3, 95% confidence interval [95% CI] 1.10–16.9 [$P = 0.037$]; for anti–RNAP III–positive patients, OR 4.49, 95% CI 1.98–10.2 [$P < 0.001$]). Patients with anti–RNPC-3 had severe restrictive lung disease, gastrointestinal disease, Raynaud's phenomenon, and myopathy.**

Conclusion. **Anti–RNPC-3 autoantibodies, similar to anti–RNAP III autoantibodies, are associated with an increased risk of cancer at the onset of scleroderma. These data suggest the possibility of cancer-induced autoimmunity in this subset of patients with scleroderma.**

Patients with systemic sclerosis (SSc; scleroderma) have an elevated risk of cancer compared with individuals in the general population (1). Recent data have demonstrated that a close temporal relationship exists between the cancer diagnosis and the first clinical signs of scleroderma in a subset of patients (2,3). This clustering is most notable in patients with anti–RNA polymerase III (anti–RNAP III) autoantibodies (2–6), who have a >5-fold increased risk of cancer within 2 years of scleroderma onset (3). Findings from biologic studies have strongly suggested that paraneoplastic development of autoimmunity and scleroderma can occur in patients with anti–RNAP III autoantibodies. Genetic alterations (somatic mutations and/or loss of heterozygosity) of the *POLR3A* gene, which encodes for RNAP III, are also specifically identified in these patients' cancers, but not in the cancers in scleroderma patients with other autoantibodies (7). Furthermore, these patients develop mutation-specific T cell

Supported by the NIH (grant K23-AR-061439 from the National Institute of Arthritis and Musculoskeletal and Skin Diseases to Dr. Shah, and grant R01-DE-12354-15A1 to Drs. Rosen and Casciola-Rosen), the Ira T. Fine Discovery Fund, the Donald B. and Dorothy L. Stabler Foundation, and the Scleroderma Research Foundation. The Johns Hopkins Rheumatic Disease Research Core Center, where the antibody assays were performed, is supported by the NIH (grant P30-AR-053503).

[1]Ami A. Shah, MD, MHS, Antony Rosen, MD, Laura K. Hummers, MD, ScM, Fredrick M. Wigley, MD, Livia Casciola-Rosen, PhD: Johns Hopkins University School of Medicine, Baltimore, Maryland; [2]George Xu, PhD: Harvard University and Harvard–Massachusetts Institute of Technology Division of Health Sciences and Technology, Cambridge, Massachusetts, and Howard Hughes Medical Institute and Brigham and Women's Hospital, Boston, Massachusetts; [3]Stephen J. Elledge, PhD: Howard Hughes Medical Institute, Brigham and Women's Hospital, and Harvard University Medical School, Boston, Massachusetts.

Drs. Shah and Xu contributed equally to this work. Drs. Elledge and Casciola-Rosen contributed equally to this work.

Address correspondence to Ami A. Shah, MD, MHS, Johns Hopkins Scleroderma Center, 5501 Hopkins Bayview Circle, Room 1B32, Baltimore, MD 21224. E-mail: Ami.Shah@jhmi.edu.

Submitted for publication October 12, 2016; accepted in revised form February 2, 2017.

immune responses and anti–RNAP III autoantibodies that react with both mutant and wild-type RNAP III proteins (7). In aggregate, these studies suggest a model of cancer-induced autoimmunity in which autoantigen mutation in cancers may trigger the development of anti-tumor immune responses that then result in autoimmunity (8).

In addition to patients with anti–RNAP III autoantibodies, there are other subsets of scleroderma patients who demonstrate a similar clustering of cancer diagnosis with the first clinical signs of scleroderma. This clustering is most notable among older patients developing scleroderma who are positive for antinuclear antibodies (ANAs) but negative for the 3 most common scleroderma autoantibodies observed in US cohorts (anticentromere [anti-CENP], anti–topoisomerase I [anti–topo I], and anti–RNAP III [also known as anti-POL] autoantibodies [CTP negative]) (2,3). These individuals likely represent a heterogenous population of scleroderma patients in whom different autoantigens, both known and novel, are targeted.

We recently utilized phage-immunoprecipitation sequencing and PLATO (parallel analysis of in vitro translated open-reading frames) (9,10) to identify unique autoantibodies in CTP-negative scleroderma patients with a clustering of cancer diagnosis and scleroderma onset (11). Specifically, 16 CTP-negative patients with scleroderma and cancer and with a short cancer–scleroderma interval (≤5 years) were studied. Four (25%) of these 16 patients had autoantibodies to multiple adjacent peptides within RNA-binding protein–containing 3 (RNPC-3) (11), a 65-kd protein component of the minor spliceosome complex that participates in removal of U12-type introns from pre–messenger RNA (12,13). The minor spliceosome complex consists of several small nuclear RNAs (snRNAs) and multiple protein components, including the small nuclear ribonucleoproteins (snRNPs) 25, 35, and 48, programmed cell death protein 7, and the Sm proteins. RNPC-3 has 2 RNA recognition motifs, indicating that it likely contacts one of the snRNAs of the minor spliceosome. This anti–RNPC-3 specificity (also known as anti-U11/U12) has previously been described in patients with scleroderma, with a reported prevalence of 3.2% in the University of Pittsburgh scleroderma cohort (14).

In this investigation, we sought to verify whether anti–RNPC-3 antibodies are associated with a short cancer–scleroderma interval in a large sample of patients with scleroderma and cancer, as this would provide additional evidence to support a model of cancer-induced autoimmunity. We also compared the prevalence of anti–RNPC-3 antibodies in CTP-negative patients with and those without cancer to determine whether anti–RNPC-3 autoantibodies are a marker of cancer risk overall. Similarly, we examined the clinical phenotype in these patients to identify whether any unique clinical characteristics could be a sign of an underlying cancer. In addition, we assayed anti–RNPC-3 antibodies in cancer patients without scleroderma to define whether anti–RNPC-3 antibodies are cancer biomarkers more broadly.

PATIENTS AND METHODS

Study population. Patients with scleroderma and an available serum sample were identified through the institutional review board–approved Johns Hopkins Scleroderma Center database. All patients were diagnosed as having scleroderma according to the American College of Rheumatology (ACR) 2013 classification criteria or the ACR 1980 classification criteria (15,16), or according to whether they had at least 3 of 5 features of the CREST syndrome (calcinosis, Raynaud's phenomenon, esophageal dysmotility, sclerodactyly, telangiectasias). Demographic data, date of symptom onset, cutaneous SSc subtype (17), organ-specific disease severity scores (18,19), smoking status, and cancer diagnosis (date of onset, site, histologic findings, and therapy) were ascertained in all patients at the first visit and longitudinally at 6-month intervals for relevant parameters. All clinically obtained pulmonary function test results and echocardiogram findings were recorded. The date of scleroderma onset was defined as the date of the first scleroderma symptom, categorized as either Raynaud's or non-Raynaud's phenomenon. The date of cancer diagnosis was obtained from pathology reports or medical record review when available, and was otherwise defined by patient report. The cancer–scleroderma interval was calculated as the difference between these 2 dates.

Cancer cohort and autoantibody status. We first examined our entire cohort of scleroderma patients with cancer and an available serum sample (n = 325). The serum sample obtained closest to the date of cancer diagnosis was studied for each participant. Autoantibodies against topo I, RNAP III, and CENP-A/B were assayed by enzyme-linked immunosorbent assays (ELISAs) using commercially available kits (Inova Diagnostics), and autoantibody levels of ≥40 units were defined as a true positive finding for our primary analyses. A sensitivity analysis was also performed, with antibody positivity redefined as a threshold of ≥20 units. Autoantibodies to RNPC-3 were assayed by immunoprecipitation of ^{35}S-methionine–labeled protein, generated by in vitro transcription and translation from complementary DNA encoding full-length RNPC-3 (purchased from Origene Technologies) as described previously (20). Representative data from the immunoprecipitation assay to detect RNPC-3 antibodies are available upon request from the corresponding author. We restricted our primary analyses to patients who were positive for only 1 scleroderma autoantibody, as previously described (3). Of 325 patients with complete autoantibody data, only 7 patients were excluded from our analyses, because these patients were positive for multiple autoantibodies (largely overlapping with positivity for anti-CENP antibodies). Five of the 7 patients also had anti–RNPC-3 antibodies, of whom only 3 were moderately or strongly positive. Therefore, our study population consisted of 318 scleroderma patients with cancer.

Patients were subdivided into 5 autoantibody subgroups for analysis: patients positive for anti–RNAP III, anti–topo I, anti-CENP, or anti–RNPC-3 autoantibodies and patients negative for all 4 tested autoantibodies (anti-CENP, anti–topo I, anti–RNAP III, and anti–RNPC-3 [CTPR negative]). Demographic

Table 1. Characteristics of the study population*

Variable	Anti–RNAP III positive (n = 70)	Anti–topo I positive (n = 54)	Anti-CENP positive (n = 96)	Anti–RNPC-3 positive (n = 12)	CTPR negative (n = 86)	*P*
Age at SSc onset, mean ± SD years	52.7 ± 13.0	43.8 ± 16.3	43.8 ± 14.7	50.1 ± 11.7	47.9 ± 13.7	0.0007
Age at cancer diagnosis, mean ± SD years	56.3 ± 10.8	52.2 ± 14.8	56.3 ± 13.4	48.6 ± 13.2	56.3 ± 12.8	0.1059
SSc–cancer interval, median (IQR) years	1.0 (−1.3, 8.9)	7.7 (0.3, 14.1)	11.1 (1.3, 25.8)	0.9 (−5.0, 2.7)	7.5 (1.4, 16.7)	0.0001†
Non-RP–cancer interval, median (IQR) years	0.8 (−2.0, 5.5) (n = 69)	6.0 (−1.4, 13.0) (n = 52)	5.3 (−1.5, 13.8) (n = 95)	−0.1 (−8.5, 0.5)	3.7 (−1.2, 12.0) (n = 85)	0.0021†
RP–cancer interval, median (IQR) years	0.8 (−1.7, 8.5) (n = 68)	7.7 (0.3, 14.1)	9.2 (−0.1, 24.6)	0.9 (−5.0, 2.7)	8.7 (0.8, 16.4) (n = 78)	0.0008†
Disease duration at first visit, median (IQR) years	1.6 (1.0, 4.2)	3.6 (1.5, 12.2)	13.5 (5.1, 26.2)	2.2 (1.1, 6.6)	6.1 (1.0, 12.4)	0.0001†
Female sex, no. (%)	52 (74.3)	43 (79.6)	86 (89.6)	12 (100)	66 (76.7)	0.024
Race, no. (%)						
White	69 (98.6)	46 (85.2)	93 (97.9) (n = 95)	9 (75)	75 (88.2) (n = 85)	0.001
African American	1 (1.4)	5 (9.3)	2 (2.1) (n = 95)	3 (25)	8 (9.4) (n = 85)	
Other	0 (0)	3 (5.6)	0 (0) (n = 95)	0 (0)	2 (2.4) (n = 85)	
Smoking, no. (%)						
Never	33 (47.2)	27 (50)	48 (50.5) (n = 95)	7 (58.3)	35 (40.7)	0.912
Former	29 (41.4)	22 (40.7)	37 (39) (n = 95)	4 (33.3)	43 (50)	
Current	8 (11.4)	5 (9.3)	10 (10.5) (n = 95)	1 (8.3)	8 (9.3)	
ACR 2013 SSc classification criteria, no. (%)‡	92 (95.8)	70 (100)	54 (100)	12 (100)	82 (95.4)	0.201
Cutaneous SSc subtype, no. (%)						
Diffuse	54 (77.1)	23 (42.6)	6 (6.3)	3 (25)	29 (33.7)	<0.001
Limited	16 (22.9)	31 (57.4)	90 (93.8)	9 (75)	57 (66.3)	
Baseline MRSS, median (IQR)	18 (8, 30) (n = 69)	6 (3, 15) (n = 51)	2 (2, 4) (n = 91)	2 (2, 4)	4 (2, 13) (n = 77)	0.0001†
Baseline Medsger disease severity score, no. (%)§						
Severe RP (pits, ulcers, gangrene)	9 (12.9)	25 (46.3)	32 (33.3)	7 (58.3)	21 (25) (n = 84)	<0.001
Severe GI disease	5 (7.1)	12 (22.2)	21 (21.9)	3 (25)	26 (30.6) (n = 85)	0.005
Severe lung disease	17 (34) (n = 50)	23 (57.5) (n = 40)	29 (44.6) (n = 65)	8 (88.9) (n = 9)	31 (49.2) (n = 63)	0.019
Baseline FVC, mean ± SD % predicted	84.6 ± 14.3 (n = 62)	73.2 ± 16.9 (n = 49)	90.0 ± 16.1 (n = 91)	66.1 ± 17.8	77.7 ± 19.5 (n = 78)	<0.0001
Baseline DLco, mean ± SD % predicted	83.6 ± 20.2 (n = 55)	74.7 ± 22.4 (n = 46)	85.2 ± 25.1 (n = 79)	64.2 ± 23.4 (n = 8)	71.4 ± 22.1 (n = 70)	0.0005
Baseline RVSP, median (IQR) mm Hg	33.2 (26, 38) (n = 38)	31 (27.5, 35.5) (n = 32)	35 (28, 43) (n = 53)	43 (35, 51) (n = 6)	34 (30, 42) (n = 57)	0.0206†
FVC ever <70% of predicted, no. (%)	22 (31.4)	34 (63)	26 (27.1)	9 (75)	36 (41.9)	<0.001
RVSP ever >45 mm Hg, no. (%)	14 (20)	16 (29.6)	34 (35.4)	6 (50)	33 (38.4)	0.062
Myopathy ever, no. (%)¶	10 (14.3)	5 (9.3)	6 (6.3)	4 (33.3)	15 (17.4)	0.027
Tendon friction rubs ever, no. (%)	32 (45.7)	12 (22.2)	3 (3.1)	0 (0)	8 (9.3)	<0.001
Renal crisis, no. (%)	9 (12.9)	1 (1.9)	1 (1.0)	1 (8.3)	6 (7.0)	0.009
Death, no. (%)	25 (35.7)	21 (38.9)	26 (27.1)	7 (58.3)	35 (40.7)	0.134

Table 1. *(Cont'd)*

Variable	Anti–RNAP III positive (n = 70)	Anti–topo I positive (n = 54)	Anti-CENP positive (n = 96)	Anti–RNPC-3 positive (n = 12)	CTPR negative (n = 86)	*P*
Cancer site, no. (%)						
Female/gynecologic						
Breast	27 (38.6)	17 (31.5)	29 (30.2)	6 (50)	18 (20.9)	NT
Other gynecologic	5 (7.1)	3 (5.6)	9 (9.4)	2 (16.7)	7 (8.1)	NT
Lung	6 (8.6)	9 (16.7)	11 (11.5)	0 (0)	6 (7)	NT
Hematologic	3 (4.3)	0 (0)	8 (8.3)	2 (16.7)	11 (12.8)	NT
Skin	8 (11.4)	12 (22.2)	24 (25)	2 (16.7)	25 (29.1)	NT
Other	21 (30)	13 (24.1)	15 (15.6)	0 (0)	19 (22.1)	NT

* The study population comprised 318 patients with systemic sclerosis (SSc) and cancer in the autoantibody subgroups of patients who were positive for anti–RNA polymerase III (anti–RNAP III; also known as anti-POL), anti–topoisomerase I (anti–topo I), anticentromere (anti-CENP), or anti–RNPC-3 autoantibodies and patients who were quadruple-negative for anti-CENP/anti–topo I/anti–RNAP III/anti–RNPC-3 (CTPR negative). IQR = interquartile range; non-RP = non–Raynaud's phenomenon; MRSS = modified Rodnan skin thickness score; RVSP = right ventricular systolic pressure; NT = not tested.

† *P* values were determined using the Kruskal-Wallis test.

‡ The 4 remaining patients in the anti-CENP–positive group and 3 of the 4 in the CTPR-negative group met at least 3 of the 5 criteria for the CREST syndrome (calcinosis, Raynaud's phenomenon, esophageal dysmotility, sclerodactyly, telangiectasias); 1 patient in the CTPR-negative group met the American College of Rheumatology (ACR) 1980 classification criteria for SSc.

§ Severe RP (pits, ulcers, gangrene) was defined as a Medsger severity score of ≥2 at baseline. Severe gastrointestinal (GI) disease was defined as a requirement for high-dose medications to treat gastroesophageal reflux disease, antibiotics needed for bacterial overgrowth, presence of malabsorption syndrome, episodes of pseudoobstruction, or a requirement for total parenteral nutrition. Severe lung disease was defined as a forced vital capacity (FVC) or diffusing capacity for carbon monoxide (DLCO) of <70% of predicted.

¶ Myopathy was defined as a history of abnormal muscle enzyme levels or abnormal findings on electromyography, muscle biopsy, or magnetic resonance imaging.

features, the cancer–scleroderma interval, and scleroderma phenotypic features were compared across the autoantibody subgroups. For continuous variables, differences in mean values were assessed by analysis of variance, unless unequal variances were suggested by the Bartlett's test; in this instance, the Kruskal-Wallis test was applied as a nonparametric test. Dichotomous and categorical variables were compared using the Fisher's exact test. Characteristics were also compared between anti–RNPC-3–positive and anti–RNPC-3–negative patients using the Student's *t*-test or, where appropriate, the Fisher's exact test.

We also performed logistic regression analysis to examine whether anti–RNPC-3 and other autoantibodies were associated with an increased risk of cancer-associated scleroderma. Cancer-associated scleroderma was defined by a short cancer–scleroderma interval (±2 years), as previously described (3). The cancer–scleroderma interval was also examined graphically by generating scatterplots of age at scleroderma onset and age at cancer diagnosis for each autoantibody type.

Comparison cohort of CTP-negative scleroderma patients without cancer. Sixty CTP-negative scleroderma patients without cancer were also studied. The prevalence of anti–RNPC-3 positivity was compared between CTP-negative patients with cancer and those without cancer by chi-square test. We examined whether the clinical phenotype differed between anti–RNPC-3–positive patients with and those without cancer using the Wilcoxon–Mann-Whitney test or, where appropriate, the Fisher's exact test.

Comparison cohort of healthy controls and those with other disease states. Twenty-five healthy controls, 45 patients with pancreatic cancer, and 35 patients with lupus and cancer were also assayed for anti–RNPC-3 antibodies, in the same manner as described above.

Statistical analysis. All statistical analyses were performed using Stata version 13 (StataCorp). Two-sided *P* values less than 0.05 were considered statistically significant. Odds ratios (ORs) with 95% confidence intervals (95% CIs) were determined.

RESULTS

Patients. In total, 318 scleroderma patients with cancer were analyzed (Table 1). Seventy patients (22.0%) were positive for anti–RNAP III antibodies, 54 (17.0%) were positive for anti–topo I, 96 (30.2%) were positive for anti-CENP, and 12 (3.8%) were positive for anti–RNPC-3, leaving 86 patients (27.0%) in whom other autoantibody specificities are likely targeted (the CTPR-negative group). None of the controls (healthy subjects, patients with pancreatic cancer, or patients with lupus and cancer) had evidence of anti–RNPC-3 antibodies.

Association of anti–RNPC-3 autoantibodies with a short cancer–scleroderma interval and severe clinical phenotype. The cancer–scleroderma interval was significantly different across the 5 autoantibody subgroups. This finding persisted regardless of whether scleroderma onset was defined by the onset of Raynaud's phenomenon ($P = 0.0008$), onset of the first non–Raynaud's symptom ($P = 0.0021$), or onset of the first symptom (either Raynaud's or non–Raynaud's phenomenon; $P = 0.0001$). Patients with anti–RNPC-3 autoantibodies had a short cancer–scleroderma interval (median 0.9 years), similar to that observed in patients with anti–RNAP III antibodies (median 1.0 years). This temporal clustering between cancer and scleroderma in patients positive for

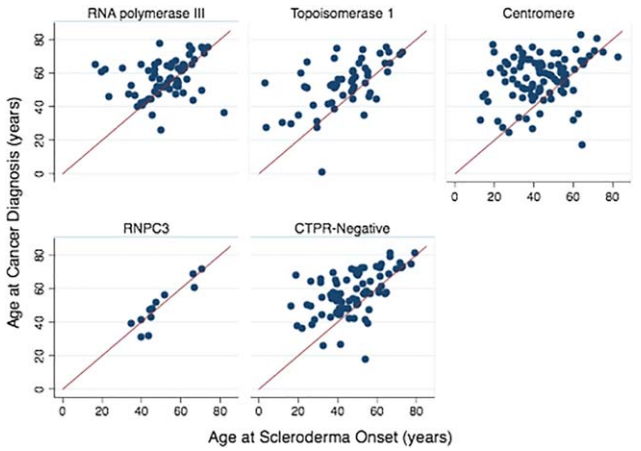

Figure 1. Relationship between age at cancer diagnosis and age at scleroderma onset. The red line in each graph denotes perfect agreement between age at cancer diagnosis and age at scleroderma onset (i.e., cancer–scleroderma interval of 0). CTPR-negative refers to the group of patients who were negative for all 4 autoantibodies tested (anticentromere [anti-CENP], anti–topoisomerase I, anti–RNA polymerase III [also known as anti-POL], and anti–RNPC-3).

anti–RNPC-3 and those positive for anti–RNAP III is shown in Figure 1. As illustrated, tight clustering on or around the line of perfect agreement (representing a cancer–scleroderma interval of 0) was seen for patients with anti–RNPC-3 autoantibodies (Figure 1), consistent with the possibility of an increased risk of cancer-associated scleroderma.

Relative to patients with anti-CENP autoantibodies, patients with anti–RNPC-3 antibodies and those with anti–RNAP III antibodies had a >4-fold increased risk of cancer within 2 years of scleroderma onset (for those with anti–RNPC-3, OR 4.3, 95% CI 1.10–16.9 [$P = 0.037$]; for those with anti–RNAP III, OR 4.49, 95% CI 1.98–10.2 [$P < 0.001$]) (Table 2). When we broadened our reference group to include patients with anti-CENP, patients with anti–topo I, and CTPR-negative patients, we found that patients with anti–RNPC-3 and those with anti–RNAP III had >3-fold increased odds of cancer within 2 years of scleroderma onset (for those with anti–RNPC-3, OR 3.57, 95% CI 1.01–12.6 [$P = 0.048$]; for those with anti–RNAP III, OR 3.72, 95% CI 1.99–6.98 [$P < 0.001$]). These findings persisted in our sensitivity analyses in which autoantibody positivity was redefined at a lower cutoff of ≥20 units (data not shown).

All of the patients with anti–RNPC-3 autoantibodies were female, and the patients in this autoantibody subset were more likely to be African American (25% of patients) (Table 1). There were statistically significant differences in age at scleroderma onset ($P = 0.0007$) and disease duration at first visit ($P = 0.0001$) across the autoantibody subgroups. Patients with anti–RNPC-3 antibodies and those with anti–RNAP III antibodies had a mean age at scleroderma onset of >50 years, and both subgroups had a shorter time to presentation for clinical evaluation than did the other autoantibody subgroups; this latter finding is likely attributable to the aggressive phenotype associated with these 2 autoantibodies (6,14). Patients with anti–RNPC-3 antibodies had less severe cutaneous and articular disease, as assessed by subtype distributions as well as by the modified Rodnan skin thickness score and the presence of tendon friction rubs. However, patients with anti–RNPC-3 antibodies had more severe restrictive lung disease at baseline, with a lower forced vital capacity and diffusing capacity for carbon monoxide and a higher Medsger severity score for lung disease compared with the other autoantibody subgroups. Anti–RNPC-3–positive patients also had associated pulmonary hypertension, which was defined as an elevated right ventricular systolic pressure (RVSP) on baseline echocardiography, although it is important to note the small size of the sample of patients with an estimated RVSP value available for this analysis. Anti–RNPC-3–positive patients had an associated myopathy (33.3% of patients) as well as severe gastrointestinal disease and severe Raynaud's phenomenon.

Given the small sample size, pairwise comparisons between the anti–RNPC-3 autoantibody subgroup and every other autoantibody subgroup were not performed because of the high likelihood that associations would be observed by chance alone. However, we compared anti–RNPC-3–positive and –negative patients and confirmed that anti–RNPC-3–positive patients had statistically significant associations, with a short cancer–scleroderma interval, severe restrictive lung disease consistent with interstitial lung disease, a higher baseline RVSP, severe Raynaud's phenomenon, and a history of myopathy (data not shown).

Although anti–RNPC-3 autoantibodies are not commercially available for clinical use, indirect immunofluorescence patterns on ANA testing may provide insights into autoantibody associations in CTP-negative

Table 2. Relative odds of cancer-associated scleroderma according to autoantibody subgroup*

Autoantibody	OR (95% CI)
Anti-CENP	Reference
Anti–RNA polymerase III	4.49 (1.98–10.2)
Anti–topoisomerase I	1.72 (0.65–4.54)
Anti–RNPC-3	4.3 (1.10–16.9)
Remaining (CTPR negative)	1.13 (0.45–2.87)

* Cancer-associated scleroderma was defined as cancer and scleroderma occurring within 2 years of each other. Values are the odds ratio (OR) (95% confidence interval [95% CI]) relative to the anticentromere (anti-CENP)–subgroup as reference. CTPR negative = quadruple-negative for anti-CENP/anti–topoisomerase I/anti–RNA polymerase III (also known as anti-POL)/anti–RNPC-3.

patients who might have this specificity. Of the 12 anti–RNPC-3–positive patients, 11 had available data on ANA patterns. Nine (81.8%) of the 11 patients had a speckled ANA pattern.

As some of the phenotypic features that are associated with anti–RNPC-3 autoantibodies are similar to that seen in patients with anti–U1 RNP autoantibodies, we also assessed whether anti–U1 RNP was present among these patients. No patient with anti–RNPC-3 autoantibodies was moderately to strongly positive for anti–U1 RNP on ELISA.

Patients with anti–RNPC-3 antibodies also had a worse prognosis, with a shorter time to death, as compared with patients in the other autoantibody subgroups (median survival 9.0 years in anti–RNPC-3–positive patients versus >20 years in all other antibody subgroups; $P < 0.0001$ by log-rank test) (details available upon request from the corresponding author). While statistical comparisons of all tumor types were not possible with our small sample size, it is noteworthy that most malignancies in the anti–RNPC-3–positive group (66.7% of patients) were gynecologic tumors in women, with 50% of these patients having breast cancer ($P = 0.075$ for comparison across antibody subgroups).

Prevalence of anti–RNPC-3 autoantibodies and clinical phenotype of anti–RNPC-3–positive patients does not differ by cancer status. Among the CTP-negative scleroderma patients, there were no significant differences in the prevalence of anti–RNPC-3 antibodies by cancer status (12 [12.2%] of 98 patients with cancer were anti–RNPC-3 positive, compared with 8 [13.3%] of 60 patients without cancer; $P = 0.842$). We examined whether unique phenotypic features could identify the subset of patients with an underlying cancer among anti–RNPC-3–positive patients, as clinical differences could aid in risk stratification for cancer screening. Our sample size was limited to 12 anti–RNPC-3–positive patients with cancer and 8 anti–RNPC-3–positive patients without cancer. There were no statistically significant differences in age at scleroderma onset, age at cancer diagnosis, disease duration at first visit, sex, race, cutaneous subtype, organ-specific severity scores, baseline pulmonary function, history of myopathy, or history of articular disease (data not shown).

DISCUSSION

This investigation found that scleroderma patients with anti–RNPC-3 autoantibodies have a short cancer–scleroderma interval (median 0.9 years), similar to that observed in patients with anti–RNAP III antibodies (median 1.0 years). Relative to patients with anti-CENP autoantibodies, patients with anti–RNPC-3 antibodies and those with anti–RNAP III antibodies had a >4-fold increased risk of cancer occuring within 2 years of scleroderma onset. The presence of anti–RNPC-3 autoantibodies did not signify an increased risk of cancer overall, but did identify a subset of patients who have an increased risk of cancer at the time of the first clinical manifestations of scleroderma. The temporal association between cancer and scleroderma in patients with anti–RNPC-3 antibodies is very similar to that observed in patients with anti–RNAP III antibodies, and strongly suggests that additional, serologically defined subsets of scleroderma patients may have cancer-induced autoimmunity (2,3,7,8). Although the mechanistic relationship between cancer and scleroderma among patients with anti–RNPC-3 antibodies is unknown, these data support the idea that cancer might initiate scleroderma-specific immune responses and also provide a rationale for targeted malignancy screening at the time of scleroderma onset.

In our study of scleroderma patients with cancer, patients with anti–RNPC-3 were more likely to be African American and to have severe interstitial lung disease, gastrointestinal disease, and Raynaud's phenomenon. Even among a cohort of patients with a history of cancer, patients with anti–RNPC-3 had a faster time to death from scleroderma onset than did patients without anti–RNPC-3, which may be consistent with the aggressive phenotype of these patients. Overall, our findings related to the clinical phenotype and prevalence estimates (3.8% in the Johns Hopkins cohort and 3.2% in the University of Pittsburgh cohort) are similar to those previously described for anti-U11/U12 antibodies in the University of Pittsburgh scleroderma cohort (14). Our data suggest that patients with anti–RNPC-3 may be more likely to have a myopathy, which has not been described before; further study is required to validate this finding in a larger cohort.

Recognizing that the prevalence of anti–RNPC-3 antibodies was low in our cohort, we were unable to identify any significant clinical phenotypic differences between anti–RNPC-3–positive patients with cancer compared with those without cancer. Anti–RNPC-3 autoantibodies were unique to scleroderma and were not found in cancer patients without scleroderma, demonstrating that anti–RNPC-3 antibodies are not cancer biomarkers in non-scleroderma populations.

As in patients with anti-RNAP III autoantibodies, these data support the practice of careful cancer screening at the onset of scleroderma in patients with anti–RNPC-3 autoantibodies. As we begin to identify more subsets of patients with possible cancer-associated scleroderma, it will be critical to consider evidence-based approaches to define the optimal cancer screening algorithm in these patients to maximize cancer dectection while minimizing the risks associated with false positive testing. The approach to cancer screening in scleroderma may vary by autoantibody subtype. In our small sample of

anti–RNPC-3–positive patients with cancer, 50% of the malignancies were breast cancers, suggesting that mammography is important. The remaining cancers seen in our anti–RNPC-3–positive patients were gynecologic, hematologic, and skin in origin.

Our study was conducted in the largest cohort of well-characterized patients with scleroderma and cancer to date, but it was limited by the small sample size of patients with anti–RNPC-3 autoantibodies. While we observed statistically significant differences, it is important to note that we could not perform pairwise comparisons between each pair of autoantibody subgroups, due to our sample size. In addition, our control group was restricted to scleroderma patients who were CTP negative and without cancer. Finally, although our data demonstrating a clustering of cancer diagnosis with scleroderma onset suggest a paraneoplastic mechanism of scleroderma onset, similar to that in patients with anti-RNAP III autoantibodies, this investigation did not examine whether genetic or posttranslational alterations of RNPC-3 are present in the cancer tissue of these patients.

In conclusion, anti–RNPC-3 autoantibodies are associated with an increased risk of cancer at scleroderma onset, similar to the findings in patients with anti–RNAP III autoantibodies. These data suggest the possibility of cancer-induced autoimmunity in this subset of patients with scleroderma, and biologic studies of autoantigen alterations in tissue samples from anti–RNPC-3–positive patients with cancer remain an important priority. Awareness of the association between anti–RNPC-3 antibodies and cancer in patients with scleroderma provides an opportunity for early cancer detection and intervention, which may improve overall outcomes.

ACKNOWLEDGMENTS

The authors would like to thank Adrianne Woods and Margaret Sampedro for excellent management of the database and biologic samples for this study.

AUTHOR CONTRIBUTIONS

All authors were involved in drafting the article or revising it critically for important intellectual content, and all authors approved the final version to be published. Dr. Shah had full access to all of the data in the study and takes responsibility for the integrity of the data and the accuracy of the data analysis.

Study conception and design. Shah, Rosen, Elledge, Casciola-Rosen.
Acquisition of data. Shah, Xu, Hummers, Wigley, Casciola-Rosen.
Analysis and interpretation of data. Shah, Xu, Rosen, Hummers, Elledge, Casciola-Rosen.

REFERENCES

1. Onishi A, Sugiyama D, Kumagai S, Morinobu A. Cancer incidence in systemic sclerosis: meta-analysis of population-based cohort studies. Arthritis Rheum 2013;65:1913–21.
2. Shah AA, Rosen A, Hummers L, Wigley F, Casciola-Rosen L. Close temporal relationship between onset of cancer and scleroderma in patients with RNA polymerase I/III antibodies. Arthritis Rheum 2010;62:2787–95.
3. Shah AA, Hummers LK, Casciola-Rosen L, Visvanathan K, Rosen A, Wigley FM. Examination of autoantibody status and clinical features associated with cancer risk and cancer-associated scleroderma. Arthritis Rheumatol 2015;67:1053–61.
4. Airo P, Ceribelli A, Cavazzana I, Taraborelli M, Zingarelli S, Franceschini F. Malignancies in Italian patients with systemic sclerosis positive for anti-RNA polymerase III antibodies. J Rheumatol 2011;38:1329–34.
5. Moinzadeh P, Fonseca C, Hellmich M, Shah AA, Chighizola C, Denton CP, et al. Association of anti-RNA polymerase III autoantibodies and cancer in scleroderma. Arthritis Res Ther 2014;16:R53.
6. Nikpour M, Hissaria P, Byron J, Sahhar J, Micallef M, Paspaliaris W, et al. Prevalence, correlates and clinical usefulness of antibodies to RNA polymerase III in systemic sclerosis: a cross-sectional analysis of data from an Australian cohort. Arthritis Res Ther 2011;13:R211.
7. Joseph CG, Darrah E, Shah AA, Skora AD, Casciola-Rosen LA, Wigley FM, et al. Association of the autoimmune disease scleroderma with an immunologic response to cancer. Science 2014;343:152–7.
8. Shah AA, Casciola-Rosen L, Rosen A. Cancer-induced autoimmunity in the rheumatic diseases [review]. Arthritis Rheumatol 2015;67:317–26.
9. Larman HB, Zhao Z, Laserson U, Li MZ, Ciccia A, Gakidis MA, et al. Autoantigen discovery with a synthetic human peptidome. Nat Biotechnol 2011;29:535–41.
10. Zhu J, Larman HB, Gao G, Somwar R, Zhang Z, Laserson U, et al. Protein interaction discovery using parallel analysis of translated ORFs (PLATO). Nat Biotechnol 2013;31:331–4.
11. Xu G, Shah AA, Li MZ, Xu Q, Rosen A, Casciola-Rosen L, et al. Systematic autoantigen analysis identifies a distinct subtype of scleroderma with coincident cancer. Proc Natl Acad Sci U S A 2016;113:E7526–34.
12. Benecke H, Luhrmann R, Will CL. The U11/U12 snRNP 65K protein acts as a molecular bridge, binding the U12 snRNA and U11-59K protein. EMBO J 2005;24:3057–69.
13. Netter C, Weber G, Benecke H, Wahl MC. Functional stabilization of an RNA recognition motif by a noncanonical N-terminal expansion. RNA 2009;15:1305–13.
14. Fertig N, Domsic RT, Rodriguez-Reyna T, Kuwana M, Lucas M, Medsger TA Jr, et al. Anti–U11/U12 RNP antibodies in systemic sclerosis: a new serologic marker associated with pulmonary fibrosis. Arthritis Rheum 2009;61:958–65.
15. Van den Hoogen F, Khanna D, Fransen J, Johnson SR, Baron M, Tyndall A, et al. 2013 classification criteria for systemic sclerosis: an American College of Rheumatology/European League Against Rheumatism collaborative initiative. Arthritis Rheum 2013;65:2737–47.
16. Subcommittee for Scleroderma Criteria of the American Rheumatism Association Diagnostic and Therapeutic Criteria Committee. Preliminary criteria for the classification of systemic sclerosis (scleroderma). Arthritis Rheum 1980;23:581–90.
17. LeRoy EC, Black C, Fleischmajer R, Jablonska S, Krieg T, Medsger TA Jr, et al. Scleroderma (systemic sclerosis): classification, subsets and pathogenesis. J Rheumatol 1988;15:202–5.
18. Clements PJ, Lachenbruch PA, Seibold JR, Zee B, Steen VD, Brennan P, et al. Skin thickness score in systemic sclerosis: an assessment of interobserver variability in 3 independent studies. J Rheumatol 1993;20:1892–6.
19. Medsger TA Jr, Silman AJ, Steen VD, Black CM, Akesson A, Bacon PA, et al. A disease severity scale for systemic sclerosis: development and testing. J Rheumatol 1999;26:2159–67.
20. Fiorentino DF, Chung LS, Christopher-Stine L, Zaba L, Li S, Mammen AL, et al. Most patients with cancer-associated dermatomyositis have antibodies to nuclear matrix protein NXP-2 or transcription intermediary factor 1γ. Arthritis Rheum 2013;65:2954–62.

ARTHRITIS & RHEUMATOLOGY
Vol. 69, No. 6, June 2017, pp 1313–1324
DOI 10.1002/art.40059

Enhanced Bruton's Tyrosine Kinase Activity in Peripheral Blood B Lymphocytes From Patients With Autoimmune Disease

Odilia B. J. Corneth,[1] Gwenny M. P. Verstappen,[2] Sandra M. J. Paulissen,[1] Marjolein J. W. de Bruijn,[1] Jasper Rip,[1] Melanie Lukkes,[1] Jan Piet van Hamburg,[1] Erik Lubberts,[1] Hendrika Bootsma,[2] Frans G. M. Kroese,[2] and Rudi W. Hendriks[1]

Objective. **Bruton's tyrosine kinase (BTK) transmits crucial survival signals from the B cell receptor (BCR) in B cells. Pharmacologic BTK inhibition effectively diminishes disease symptoms in mouse models of autoimmunity; conversely, transgenic BTK overexpression induces systemic autoimmunity in mice. We undertook this study to investigate BTK expression and activity in human B cells in the context of autoimmune disease.**

Methods. **Using intracellular flow cytometry, we quantified BTK expression and phosphorylation in subsets of peripheral blood B cells from 30 patients with rheumatoid arthritis (RA), 26 patients with primary Sjögren's syndrome (SS), and matched healthy controls.**

Results. **In circulating B cells, BTK protein expression levels correlated with BTK phosphorylation. BTK expression was up-regulated upon BCR stimulation in vitro and was significantly higher in CD27+ memory B cells than in CD27−IgD+ naive B cells. Importantly, BTK protein and phospho-BTK were significantly increased in B cells from anti–citrullinated protein antibody (ACPA)–positive RA patients but not in B cells from ACPA-negative RA patients. BTK was increased both in naive B cells and in memory B cells and correlated with frequencies of circulating CCR6+ Th17 cells. Likewise, BTK protein was increased in B cells from a major fraction of patients with primary SS and correlated with serum rheumatoid factor levels and parotid gland T cell infiltration. Interestingly, targeting T cell activation in patients with primary SS using the CTLA-4Ig fusion protein abatacept restored BTK protein expression in B cells to normal levels.**

Conclusion. **These data indicate that autoimmune disease in humans is characterized by enhanced BTK activity, which is linked not only to autoantibody formation but also to T cell activity.**

B lymphocytes play a crucial role in various systemic autoimmune diseases. This is evident from the characteristic autoantibody repertoire, the genetic associations identified, and the promising efficacy of B cell–targeted therapies in rheumatoid arthritis (RA), systemic lupus erythematosus (SLE), and Sjögren's syndrome (SS). Autoantibodies directed against nuclear self antigens in SLE and SS or anti–citrullinated protein antibodies (ACPAs) in RA often appear in patient serum before the onset of clinical symptoms (1–3). In primary SS (4), the presence of circulating nuclear autoantibodies and germinal centers (GCs) in salivary glands correlates with disease severity (5–7). Moreover, genetic studies have implicated several genes involved in activation and differentiation of B cells in the pathogenesis of primary SS and SLE, including *BLK*, *BANK1*, *LYN*, and *BAFF* (1,8,9). Next to being precursors of plasmablasts and plasma cells that secrete autoantibodies, B cells can engage T cells by supporting follicular Th cell differentiation, antigen presentation, production of inflammatory cytokines, and induction of tertiary lymphoid structures (10,11). Although effects of B

Supported by the Dutch Arthritis Foundation (Reumafonds, grants 09-1-302 and 13-2-301). The open-label Active Sjögren Abatacept Pilot study was supported by an unrestricted grant from Bristol-Myers Squibb, France, who also supplied study medication.

[1]Odilia B. J. Corneth, PhD, Sandra M. J. Paulissen, PhD, Marjolein J. W. de Bruijn, BSc, Jasper Rip, MSc, Melanie Lukkes, BSc, Jan Piet van Hamburg, PhD, Erik Lubberts, PhD, Rudi W. Hendriks, PhD: Erasmus Medical Center, Rotterdam, The Netherlands; [2]Gwenny M. P. Verstappen, MSc, Hendrika Bootsma, MD, PhD, Frans G. M. Kroese, PhD: University Medical Center Groningen, Groningen, The Netherlands.

Address correspondence to Rudi W. Hendriks, PhD, Department of Pulmonary Medicine, Room Ee2251a, Erasmus MC Rotterdam, PO Box 2040, NL 3000 CA Rotterdam, The Netherlands. E-mail: r.hendriks@erasmusmc.nl.

Submitted for publication June 17, 2016; accepted in revised form January 26, 2017.

cell–depleting regimens in primary SS are inconclusive (12–14), the efficacy of neutralizing BAFF in SLE and the efficacy of rituximab (an anti-CD20 antibody that eliminates B cells) in RA indicate that intelligent modulation of B cell function or survival may be key to successful treatment of systemic autoimmunity (1,15).

Promising drug candidates for autoimmune diseases include newly developed inhibitors of Bruton's tyrosine kinase (BTK), which is a pivotal signaling molecule that directly links B cell receptor (BCR) signals to B cell proliferation and survival through activation of the transcription factor NF-κB (16). The importance of BTK signaling to B cells is evident from the severe B cell deficiency in patients with X-linked agammaglobulinemia, who have mutations in the *BTK* gene (16,17). The BTK small-molecule inhibitors ibrutinib and acalabrutinib have shown robust antitumor activity and limited adverse effects in clinical studies in patients with various B cell malignancies (18,19). In murine models of SLE and RA, promising results have been obtained with BTK inhibition, which could prevent or ameliorate lupus nephritis or joint inflammation by correcting BCR-mediated B cell activation and autoantibody production (20–26) and also by dampening myeloid cell activation (18,24–26).

In the mouse, BTK protein expression levels in naive B cells are rapidly up-regulated upon BCR engagement or when B cells are activated by Toll-like receptor (TLR) or anti-CD40 stimulation (27,28). Several mechanisms are involved in this positive feedback regulation, including microRNA-185 and NF-κB signaling (29,30). Sufficient BTK expression is crucial for normal B cell development and function in mice (31,32). On the other hand, appropriate regulation of BTK protein expression in B cells is crucial for maintaining immune tolerance, because CD19-hBtk–transgenic mice (with modest B cell–restricted human BTK overexpression under control of the CD19 promoter) spontaneously develop SLE/primary SS–like disease pathology (28). In these mice, B cells are resistant to apoptosis, which aids their differentiation into autoantibody-producing plasma cells (28). CD19-hBtk–transgenic mice manifest spontaneous GC formation, antinuclear autoantibodies, and lymphocyte infiltration in various organs, including salivary glands (28). We recently found that BTK overexpression in B cells disrupts T cell homeostasis and promotes follicular Th cell differentiation, both in aging mice and in a collagen-induced arthritis model (33).

The finding that a modest increase in BTK expression in B cells is sufficient to induce systemic autoimmune disease in mice prompted us to examine BTK expression levels and regulation in B cell subsets in peripheral blood of healthy controls and patients with autoimmune disease. We show that human B cells also up-regulate BTK protein levels upon activation, and we provide data on aberrant expression levels and phosphorylation status of BTK in B cells from ACPA-positive RA patients. Likewise, we found that BTK protein was increased in B cells from a majority of patients with primary SS.

PATIENTS AND METHODS

Patients and healthy individuals. Data on characteristics of the patients and healthy controls are available upon request from the corresponding author.

RA patients. Cohorts of ACPA-positive and ACPA-negative treatment-naive patients with early RA who were matched for the Disease Activity Score (DAS) in 44 joints (34), the presence of rheumatoid factor (RF), and the duration of symptoms have been described previously (35). All patients met the American College of Rheumatology/European League Against Rheumatism (EULAR) 2010 classification criteria for RA (36). Fifteen ACPA-positive and 15 ACPA-negative patients were included and matched with 15 healthy controls.

Patients with primary SS. We included 26 patients with primary SS who were naive to treatment with biologic disease-modifying antirheumatic drugs (DMARDs) and who fulfilled the American–European Consensus Group criteria for SS (37); we matched these patients with 26 healthy controls. Fifteen of the patients with primary SS had participated in the previously reported Active Sjögren Abatacept Pilot (ASAP) study (METc2009.371) (38). They had been treated with intravenous abatacept on days 1, 15, and 29 and every 4 weeks thereafter until week 24, a regimen that improved disease activity as previously reported (38). Patients were not treated with DMARDs or prednisone for at least 1 month prior to or during this study.

Serum and peripheral blood mononuclear cells (PBMCs) were collected from all healthy controls and patients at baseline (untreated) and from the 15 abatacept-treated patients with primary SS at 4, 12, 24, 36, and 48 weeks after the first dose. Experimental procedures were approved by the Erasmus Medical Center and University Medical Center Groningen medical ethics committees. All patients provided written informed consent.

Isolation and culture of human peripheral blood B cells. PBMCs were isolated by standard Ficoll-Paque (GE Healthcare) density gradients. Subsequent purification of naive B cells was performed using a human Naive B Cell Isolation Kit II (Miltenyi Biotec), and B cell purity (>95%) was verified using flow cytometry. B cells were cultured in the presence of 10 μg/ml $F(ab')_2$ goat anti-mouse IgM (Jackson ImmunoResearch), 2 μg/ml recombinant CD40L (R&D Systems), or 2 ng/ml lipopolysaccharide (LPS) for 3 days.

Flow cytometry procedures. Fluorescence labeling of cells and measurement of intracellular BTK levels were performed as described previously (28) (a list of antibodies used is available upon request from the corresponding author). BTK gate settings were based on isotype controls, fluorescence minus one controls, and analysis of T cells, which lack BTK expression. For staining of phosphorylated BTK, PBMCs were left unstimulated or were stimulated for 30 seconds with $F(ab')_2$ anti-human IgM (20 μg/ml; SouthernBiotech) and subsequently fixed with Cytofix and permeabilized with Phosflow Perm Buffer III (BD Biosciences). Flow cytometric measurements were performed on an LSRII flow cytometer (BD Biosciences), and data were analyzed using FlowJo software (Tree Star).

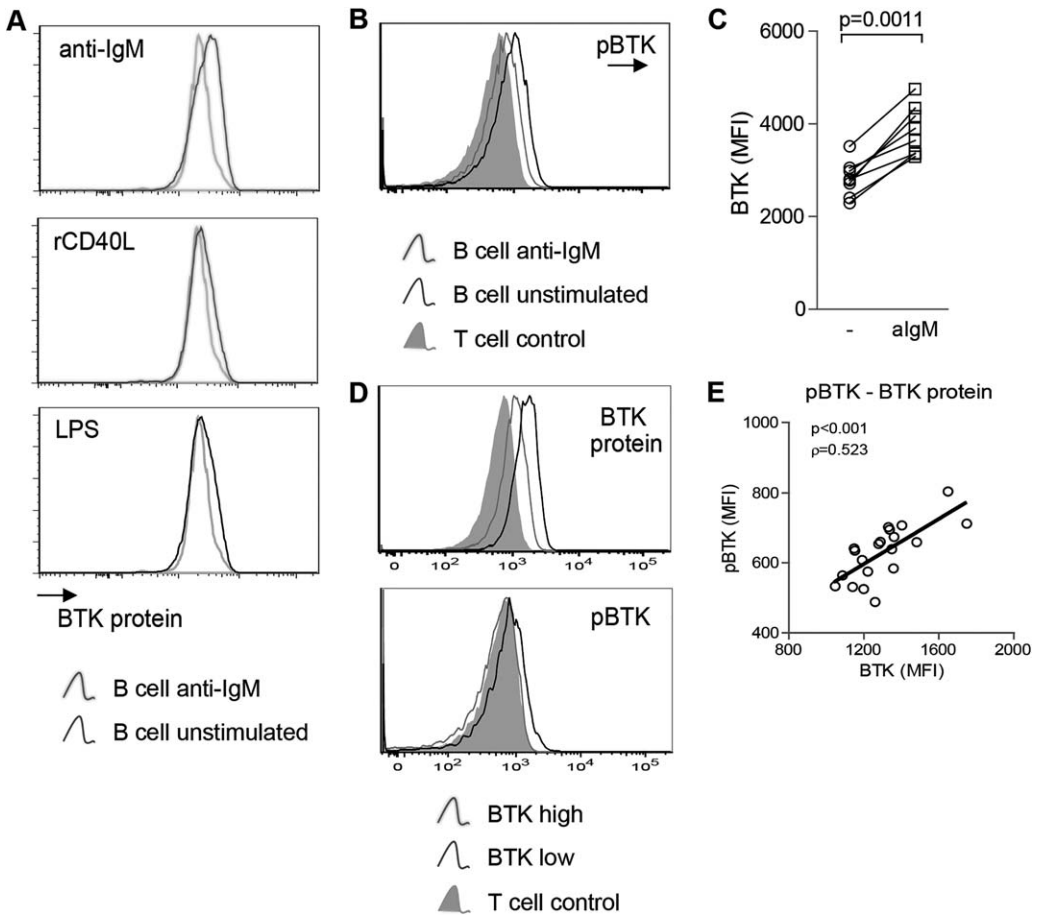

Figure 1. Bruton's tyrosine kinase (BTK) protein expression and phosphorylation in human B cells are correlated and up-regulated upon B cell receptor stimulation in vitro. **A,** Representative graph of intracellular BTK expression in magnetic-activated cell-sorted B cells from a healthy control after 3 days of stimulation with anti-IgM (10 μg/ml), recombinant CD40L (rCD40L; 2 μg/ml), or lipopolysaccharide (LPS; 2 ng/ml). **B,** Representative graph of BTK phosphorylation in healthy control B cells that were either left unstimulated or were stimulated for 30 seconds with anti-IgM (20 μg/ml). **C,** BTK expression in magnetic-activated cell-sorted B cells from healthy controls that were either left unstimulated or were stimulated for 3 days with anti-IgM (10 μg/ml). Symbols represent specimens from individual subjects. **D,** BTK protein and phospho-BTK expression in B cells from healthy controls expressing high or low levels of BTK at baseline. **E,** Correlation between BTK protein and phospho-BTK expression in B cells from 20 subjects. Data are representative of 2 individual experiments. MFI = mean fluorescence intensity.

Immunohistochemistry. Parotid gland biopsy specimens were obtained from 15 patients with primary SS at baseline, and paraffin-embedded sections were stained with rabbit anti-human CD3 antibody (Ventana Medical Systems) and counterstained with hematoxylin using standard procedures. Numbers of CD3+ cells/mm^2 were analyzed using HistoQuest software.

Laboratory assessments of serum. Baseline levels of serum immunoglobulin classes and RF were measured by nephelometry.

Statistical analysis. Significance of continuous data was calculated using the nonparametric Mann-Whitney U test or one-way analysis of variance (ANOVA) or repeated-measures ANOVA with Tukey's multiple comparison test. *P* values less than 0.05 were considered significant. Significance of correlations was determined with a nonparametric Spearman test. To determine the significance of the effect of abatacept on BTK levels in B cells within patients over time, a generalized estimating equation was performed using SPSS statistical software (IBM).

RESULTS

BTK protein expression is up-regulated in in vitro–activated human B cells and correlates with BTK phosphorylation. Upon BCR stimulation of human B cells, a signaling cascade is initiated whereby BTK is phosphorylated in its kinase domain at position Y^{551} (18). To verify this, we stimulated fractions of PBMCs from healthy controls with anti-IgM in vitro and found induction of phospho-BTK in B cells by phosphoflow analysis (Figure 1B).

Parallel to the findings in murine B cells (27,28), we observed that anti-IgM stimulation in vitro also induced an up-regulation of BTK protein expression in human B cells, as detected by intracellular flow cytometry; average mean fluorescence intensity values increased ~1.4-fold (Figures 1A and C). Other stimuli, including recombinant CD40L, LPS, and imiquimod

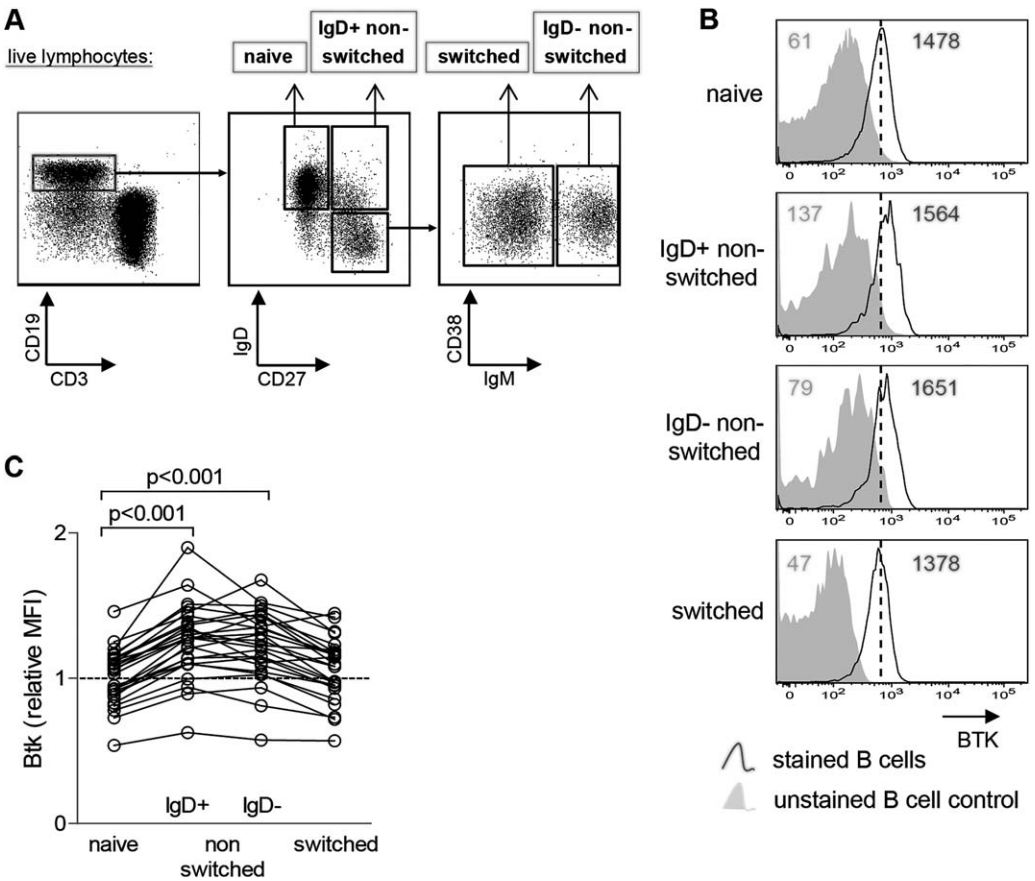

Figure 2. Differential expression of Bruton's tyrosine kinase (BTK) in subsets of peripheral B cells from healthy controls. **A,** Gating strategy for naive B cells, IgD+ and IgD− nonswitched memory B cells, and switched memory B cells used throughout the study. Live lymphocytes were gated based on the absence of a cell death marker and the forward scatter and side scatter. **B,** Representative histograms of BTK expression in several B cell subsets from a healthy control. Numbers indicate mean fluorescence intensity (MFI); dashed lines represent the peak in naive B cells. **C,** BTK expression in different B cell subsets in healthy controls. Symbols represent specimens from individual subjects. Dashed line indicates average MFI in total B cells. Data are representative of 6 individual experiments.

(a TLR-7 agonist), induced a limited but consistently detectable increase in BTK protein levels (Figure 1A and data not shown). To further study the relationship between BTK protein expression and phosphorylation of BTK at Y^{551} in human B cells, we measured BTK protein and phospho-BTK in gated CD19+ B cells from unstimulated fractions of PBMCs from 20 subjects. Signals for BTK protein and phospho-BTK varied considerably between individuals, but these were strongly correlated in individual subjects (Figures 1D and E). From these findings, we conclude that BTK protein expression levels are a sensitive and functional indicator of BTK activity in human B cells.

Differential expression of BTK protein in individual peripheral blood B cell subsets. In contrast to phosphoflow analysis, which is difficult to perform in conjunction with cell surface markers, the staining procedure for total BTK protein allows for quantification of BTK expression levels in individual B cell subsets. This enabled us to compare BTK expression between subsets of unstimulated peripheral blood B cells from healthy controls ex vivo (gating strategy is shown in Figure 2A). We observed that BTK expression levels were significantly higher in antigen-experienced CD27+IgD+ and CD27+IgD−IgM+ nonswitched memory B cells compared with CD27−IgD+ naive B cells and CD27+IgD−IgM− switched memory B cells (Figures 2B and C). These data indicate that BTK protein levels are tightly regulated during B cell differentiation and suggest that up-regulation of BTK expression in specific B cell subsets may have a physiologic function.

BTK protein and BTK phosphorylation are increased in peripheral blood B cells of ACPA-positive RA patients. To investigate BTK activity in the context of autoimmune disease, we studied peripheral blood B cells from 15 ACPA-positive and 15 ACPA-negative treatment-naive RA patients who were matched for the DAS, and we

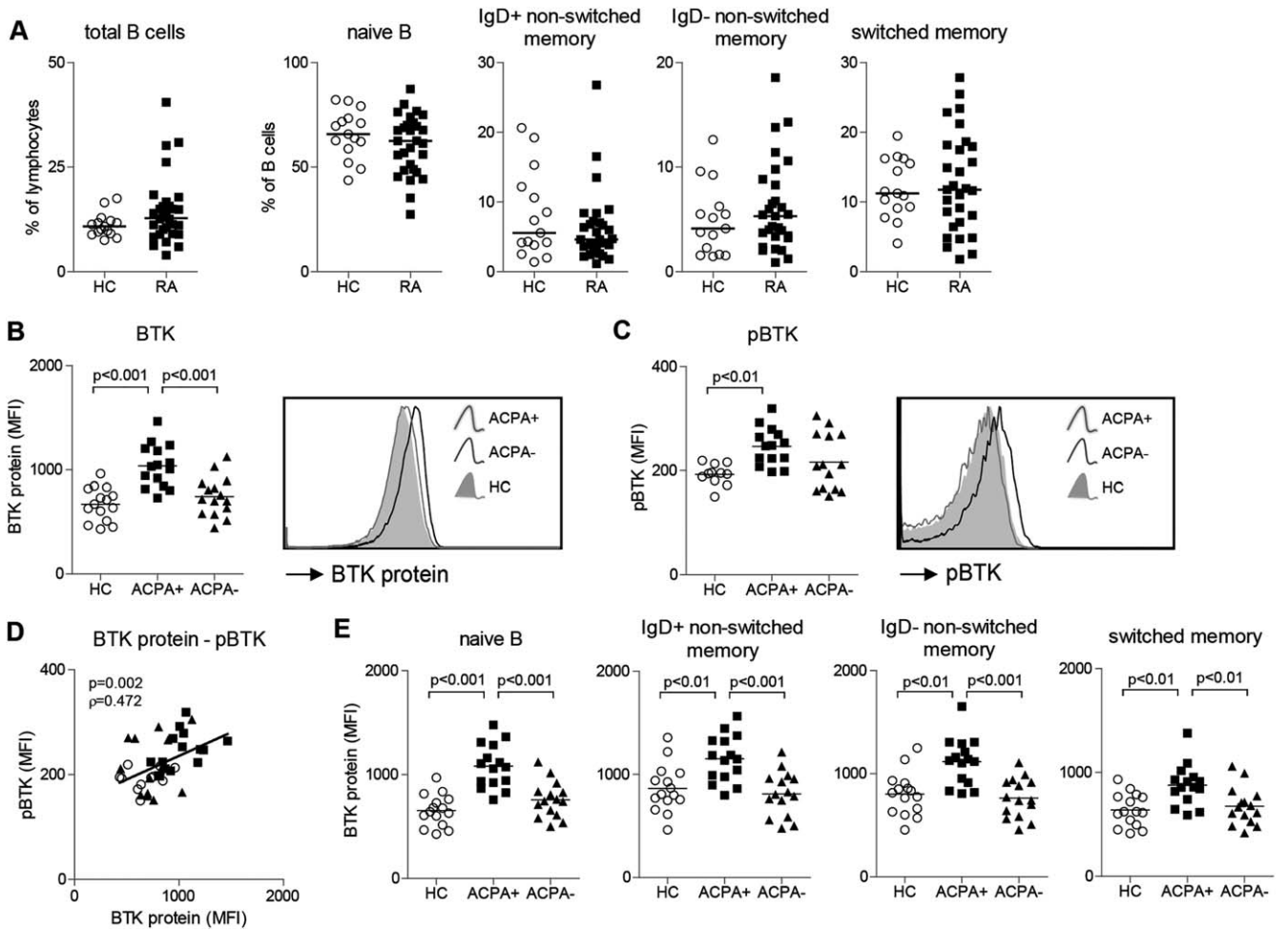

Figure 3. Increased expression of Bruton's tyrosine kinase (BTK) in B cells from anti–citrullinated protein antibody (ACPA)–positive patients with rheumatoid arthritis (RA). **A,** Proportions of total B cells among live cells and proportions of naive B cells, IgD+ and IgD− nonswitched memory B cells, and switched memory B cells among total B cells in RA patients and healthy controls (HC). **B,** BTK protein expression in total B cells. Representative flow plots show BTK protein expression in an ACPA-positive patient, an ACPA-negative patient, and a healthy control. **C,** Phospho-BTK expression in total B cells. Representative flow plots show phospho-BTK expression in an ACPA-positive patient, an ACPA-negative patient, and a healthy control. **D,** Correlation between BTK protein and phospho-BTK expression in ACPA-positive patients (squares), ACPA-negative patients (triangles), and healthy controls (circles). **E,** BTK protein expression in the indicated B cell subsets in RA patients and healthy controls. Symbols represent specimens from individual subjects; bars show the median. MFI = mean fluorescence intensity.

included 15 age/sex-matched healthy controls (further information is available upon request from the corresponding author). The proportions of total B cells and the distribution over naive and various memory B cell subsets were not significantly different between RA patients and healthy controls (Figure 3A). Interestingly, when we quantified BTK expression in total B cells, we found that BTK protein levels were significantly increased (~1.4-fold) in ACPA-positive RA patients compared with ACPA-negative RA patients and healthy controls (Figure 3B) (representative flow cytometry dot plots are available upon request from the corresponding author). Similar results were found for phospho-BTK levels in unstimulated B cells, consistent with the significant correlation observed between total BTK and phospho-BTK signals (Figures 3C and D). Compared with ACPA-negative RA patients and healthy controls, ACPA-positive RA patients showed increased BTK protein expression both in CD27−IgD+ naive B cells and in all the individual CD27+ memory B cell subsets (Figure 3E). In ACPA-positive RA patients, BTK was differentially expressed between different B cell subsets, as observed in healthy controls (further information is available upon request from the corresponding author). Taken together, our intracellular flow cytometry analyses demonstrate that in ACPA-positive RA patients, but not in ACPA-negative RA patients, relative BTK expression values were increased in all B cell subsets, including naive and memory B cells, compared with healthy controls.

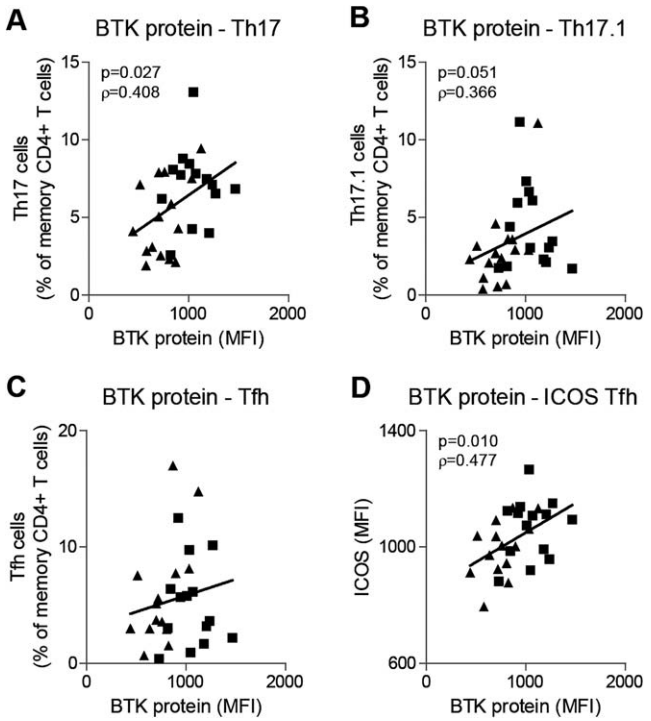

Figure 4. Correlation of Bruton's tyrosine kinase (BTK) expression with Th17-lineage cells and inducible costimulator (ICOS) expression on follicular helper T (Tfh) cells. Shown are correlations between BTK protein expression and Th17 cells (CCR6+CXCR3−) (**A**), Th17.1 cells (CCR6+CXCR3+) (**B**), Tfh cells (CXCR5+) (**C**), and ICOS expression by Tfh cells (**D**), measured by flow cytometry in specimens from ACPA-positive patients (squares) and ACPA-negative patients (triangles). MFI = mean fluorescence intensity.

BTK expression levels in B cells correlate with frequencies of circulating CCR6+ Th17 cells. Since we found that BTK-overexpressing B cells in transgenic mice have the capacity to disrupt T cell homeostasis (33), we wondered whether BTK expression levels in RA patients correlated with parameters of T cell activity. We found that BTK protein levels correlated significantly with frequencies in peripheral blood of Th17-lineage cells, which have recently been implicated in RA etiology (39) (Figures 4A and B) (gating strategy is available upon request from the corresponding author). Although BTK protein levels and frequencies of follicular helper T (Tfh) cells did not correlate significantly (Figure 4C), we did observe a positive correlation of BTK protein levels with inducible costimulator (ICOS) expression on Tfh cells (Figure 4D). The latter finding is interesting, because we previously found that in mice overexpressing BTK in B cells, the expression of ICOS on T cells, including Tfh cells, was increased (33). No correlation was found with other T cell subsets, including Th1 and Treg cells (data not shown). In summary, the finding that BTK protein levels correlate with the frequencies of Th17-lineage cells and with Tfh cell ICOS expression suggests that BTK activity is linked to T cell activation in RA.

Peripheral blood BTK protein expression is increased in a major fraction of patients with primary SS. To explore whether increased BTK activity is unique to RA or can also be found in other autoimmune disorders, we investigated BTK expression in 26 treatment-naive patients with primary SS and 26 age/sex-matched healthy controls. Because of the reported decrease in CD27+ memory B cells in patients (6,40–42), we first quantified peripheral B cell subsets. Proportions of B cells in PBMCs from patients with primary SS were higher than in those from healthy controls, possibly due to lymphopenia of CD4+ T cells, as absolute numbers were comparable. In patients with primary SS, more circulating B cells were naive, and proportions of nonswitched and switched memory B cells were decreased (Figure 5A and data not shown).

BTK protein levels were significantly increased in CD27−IgD+ naive B cells, CD27+IgD−IgM+ nonswitched memory B cells, and CD27+IgD−IgM− switched memory B cells in patients with primary SS compared with healthy controls (Figure 5B) (representative flow cytometry dot plots for total B cells are available upon request from the corresponding author). In 16 of 26 patients with primary SS (62%), relative BTK expression values in CD27−IgD+ naive B cells were >1.2-fold those in healthy controls. BTK levels were significantly increased in CD86+ cells within this population, although proportions of CD86+ naive B cells were similar to those in controls and still very low (0.25% of all naive B cells) (data not shown; further information is available upon request from the corresponding author). BTK expression correlated with CD86 expression on naive B cells in patients with primary SS and healthy controls (further information is available upon request from the corresponding author). Importantly, in patients with primary SS, BTK levels were increased even in naive CD86− B cells compared to levels in healthy controls. Patients with primary SS showed differential BTK expression between different B cell subsets, similar to ACPA-positive RA patients and healthy controls (further information is available upon request from the corresponding author). In summary, in a major proportion of patients with primary SS, we observed increased BTK protein expression in various B cell subsets, including naive B cells, paralleling our findings in ACPA-positive RA patients.

BTK expression levels in B cells correlate with serum autoantibodies and parotid gland T cell infiltration in patients with primary SS. Next, we wondered whether BTK levels correlated with clinical or immunologic parameters in patients with primary SS. Scores on the EULAR Sjögren's Syndrome Disease Activity Index (ESSDAI) (43) and serum IgG levels were not correlated with relative BTK levels (data not shown). However, total serum IgM

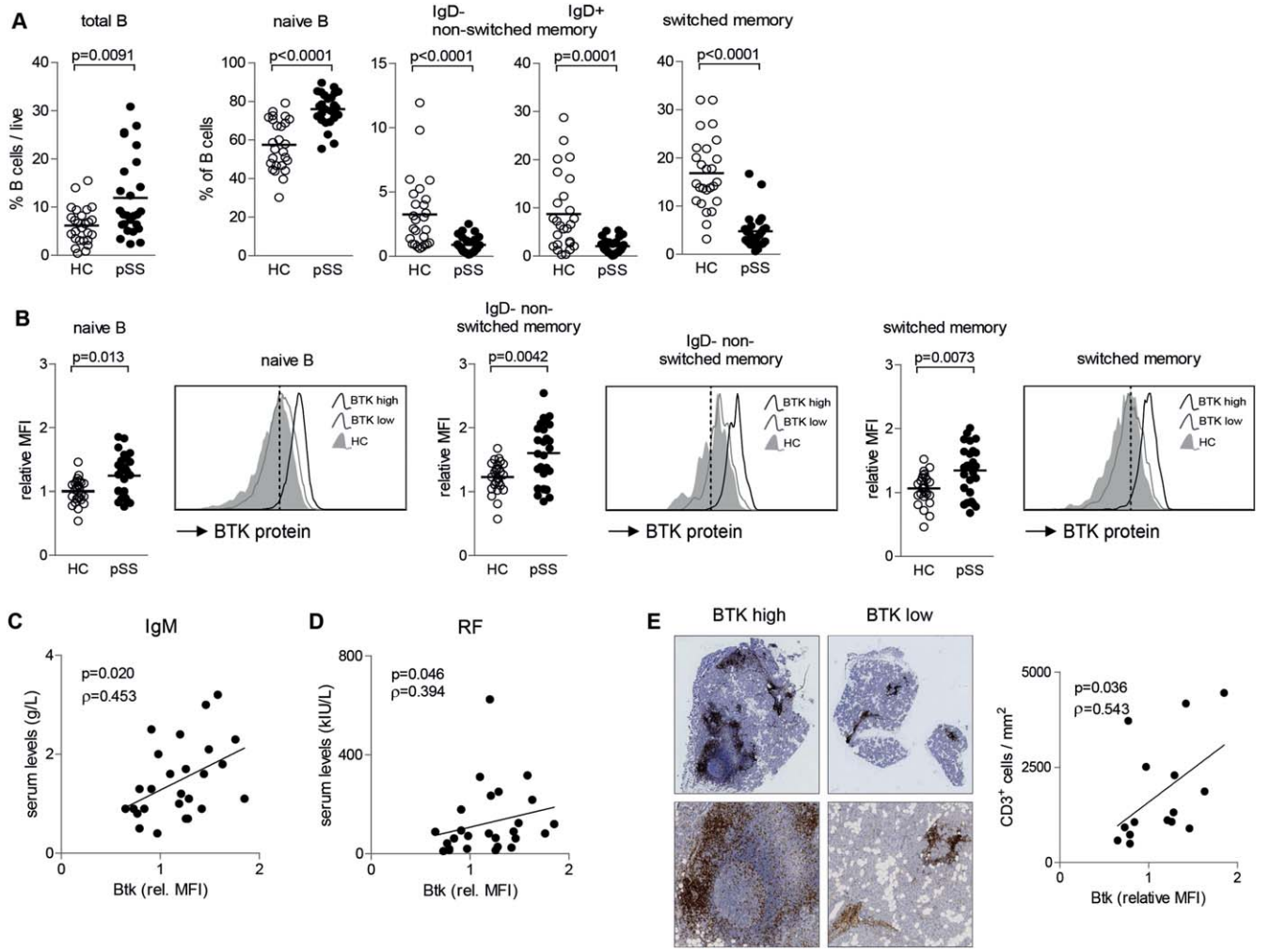

Figure 5. Increased expression of Bruton's tyrosine kinase (BTK) in B cells from patients with primary Sjögren's syndrome (pSS). **A,** Proportions of total B cells among live cells and proportions of naive B cells, IgD+ and IgD− nonswitched memory B cells, and switched memory B cells among total B cells in patients with primary SS and healthy controls (HC). **B,** BTK expression measured by intracellular flow cytometry in the indicated B cell subsets in patients with primary SS and healthy controls, normalized to BTK expression in total B cells of healthy controls, which was set to 1.0. Data shown are from 6 individual experiments. Representative flow plots show BTK protein expression in B cells from 1 patient with high levels of BTK at baseline, 1 patient with low levels of BTK at baseline, and 1 healthy control. Dashed lines represent the peak of BTK expression in naive B cells from the healthy control. **C** and **D,** Correlation of relative BTK levels in B cells with total serum IgM levels (**C**) and total serum rheumatoid factor (RF) levels (**D**) in patients with primary SS. **E,** Left, CD3+ T cells (brown) in parotid gland biopsy specimens from 2 patients with primary SS: 1 with high levels of BTK at baseline and 1 with low levels of BTK at baseline. Original magnification × 40 at top; higher-magnification views are shown at bottom. Right, Correlation of relative BTK expression in total B cells of patients with primary SS with CD3+ T cell infiltration of the parotid gland. Symbols represent specimens from individual subjects; bars in **A** and **B** show the median. MFI = mean fluorescence intensity. Color figure can be viewed in the online issue, which is available at http://onlinelibrary.wiley.com/doi/10.1002/art.40059/abstract.

and RF levels correlated significantly with relative BTK levels in total B cells in the 26 patients with primary SS (Figures 5C and D). Levels of Ro 52– and Ro 60–specific antibodies were higher in patients with high BTK expression, although this did not reach significance (data not shown). T cell infiltration in salivary glands is an important feature of primary SS. Strikingly, BTK expression levels in total peripheral B cells correlated significantly with numbers of infiltrating CD3+ T cells/mm^2 in parotid gland infiltrates (Figure 5E). These findings link BTK expression levels to autoantibody levels and salivary gland immune cell infiltration.

Abatacept treatment normalizes BTK expression in B cells from patients with primary SS. Next, we wanted to investigate whether the increase of BTK expression levels in autoimmunity was dependent on T cell activation. To this end, we examined our 15 patients with primary SS who had been treated for 24 weeks with the CTLA-4Ig fusion protein abatacept in the previously reported ASAP study (38), which was aimed at inhibiting

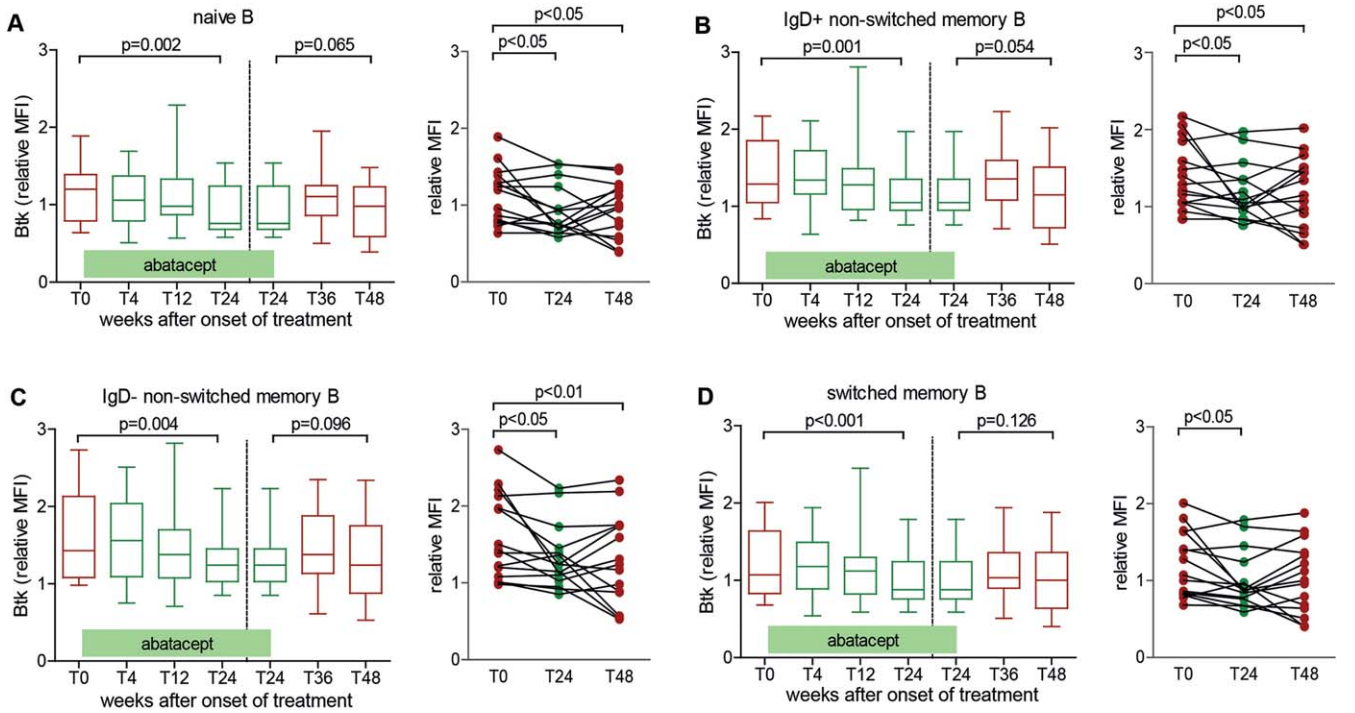

Figure 6. Normalization, upon treatment with abatacept, of Bruton's tyrosine kinase (BTK) expression levels in B cells from patients with primary Sjögren's syndrome (pSS). Shown is relative BTK expression in naive B cells (**A**), IgD+ nonswitched memory B cells (**B**), IgD− nonswitched memory B cells (**C**), and switched memory B cells (**D**) from 15 patients with primary SS at baseline (time 0 [T0]), upon abatacept treatment (T4, T12, and T24, indicating weeks after initiation of treatment), and after discontinuation of treatment (T36 and T48, indicating weeks after initiation of treatment), normalized to average BTK expression in total B cells from healthy controls (set to 1). Data at left are shown as box plots. Each box represents the 25th to 75th percentiles. Lines inside the boxes represent the median. Lines outside the boxes represent minimum and maximum values. Graphs at right show the same patients at T0, T24, and T48. MFI = mean fluorescence intensity.

T cell activity. Abatacept significantly reduced objective and subjective indicators of disease activity. Scores on the ESSDAI and EULAR Sjögren's Syndrome Patient Reported Index (44) as well as levels of RF and IgG decreased significantly, and health-related quality of life improved during abatacept treatment (38). Interestingly, abatacept treatment significantly restored BTK expression levels in CD27−IgD+ naive B cells, CD27+IgD+ and CD27+IgD−IgM+ nonswitched memory B cells, and CD27+IgD−IgM− switched memory B cells to levels comparable to those in healthy individuals (Figure 6). Taken together, these findings show that targeting T cell activation in patients with primary SS by abatacept restored BTK protein expression in B cells to normal levels after 24 weeks of treatment and suggest the involvement of a B cell– and T cell–driven proinflammatory loop in primary SS.

DISCUSSION

We previously found in CD19-hBtk–transgenic mice that increased BTK protein levels in B cells are sufficient to disrupt T cell homeostasis and to establish systemic autoimmunity. Therefore, we decided to investigate whether BTK-driven proinflammatory loops may also propagate the development of autoimmune disease in humans. Upon B cell activation, only a small fraction of the BTK molecules present in a cell become detectably phosphorylated in a transient manner. Therefore, in this study, we made use of the unique property of BTK that its protein expression levels are stably up-regulated upon B cell activation (28), allowing for very sensitive measurements of changes in BTK signaling by intracellular flow cytometry. Importantly, BTK protein expression levels correlated with phosphorylation of BTK at Y^{551}. In the present study, we show that BTK expression is up-regulated upon BCR stimulation in vitro and that BTK is differentially expressed in human B cell subsets ex vivo. Notably, in healthy controls, ex vivo BTK expression is significantly increased in CD27+IgD−IgM+ and CD27+IgD+ nonswitched memory B cells compared to CD27−IgD+ naive B cells and CD27+IgD−IgM− switched memory B cells. These findings suggest a role for BTK protein up-regulation in early activation of B cells prior to or during the GC reaction.

BTK protein and phospho-BTK were significantly increased in B cells from ACPA-positive RA patients but not in those from ACPA-negative RA patients. BTK was increased both in naive and in memory B cells and correlated with frequencies of circulating CCR6+ Th17 cells. As ACPA positivity is associated with a more severe disease course, our findings point toward a pathogenic role of BTK-mediated signaling in RA. Likewise, BTK protein was increased in naive and memory B cells from a major fraction (~62%) of patients with primary SS and correlated with serum RF levels and parotid gland T cell infiltration. Our data suggest that there were 2 subgroups of patients with primary SS, based on BTK expression levels. Although BTK levels correlated with autoantibody levels in serum, they did not show a clear distinction in disease severity (the ESSDAI score) in our cohort of 26 patients. In addition, BTK levels in patients expressing low levels of BTK at baseline decreased upon treatment with abatacept in a manner similar to that in patients expressing high levels of BTK at baseline. Therefore, from the present study, we cannot conclude that these 2 subgroups of patients with primary SS represent distinct subsets of patients, except for differences in BTK and autoantibody levels and T cell infiltrates in salivary glands. Analysis of a larger group of patients is needed to draw conclusions about the relationship between BTK expression and disease severity or frequencies of Th17 cells, and about the relationship between different clinical parameters.

We found increased BTK levels in subsets of patients with two distinct autoimmune diseases, indicating that disrupted BTK expression is not a unique feature of one disease but may be involved in more autoimmune diseases. Both RA and primary SS are systemic autoimmune diseases, but B cells and autoantibodies have also been implicated in nonsystemic autoimmune diseases. Our data show a clear link between high BTK expression and autoantibodies, suggesting that autoimmune diseases featuring autoantibody production may be interesting candidates for future studies.

Several of our findings point to an association of BTK activity in B cells with T cell activation. These include the observed correlations of BTK expression levels with the frequency of circulating Th17 cells and ICOS expression on Tfh cells in RA patients, and with salivary gland T cell infiltration in primary SS. In addition, the specific increase in BTK activity in ACPA-positive RA patients but not in ACPA-negative RA patients may require the involvement of T cells, since ACPA production is very likely T cell dependent (45–47). Interestingly, targeting T cell activation in patients with primary SS by treatment with abatacept restored BTK protein expression in B cells to normal levels, which suggests that increased BTK expression in circulating B cells of patients with primary SS depends on T cell activity. However, it is quite difficult to explain how abatacept treatment would reduce BTK expression in naive circulating B cells.

A direct effect of abatacept on naive B cells cannot be excluded, since it has been reported that expression of CD86 on B cells, even on naive B cells, is increased in patients with various autoimmune diseases (48,49), and we show in the present study that increased CD86 expression on naive B cells is correlated with higher BTK expression. Nevertheless, our data show that in patients with primary SS, BTK expression is even increased in naive resting CD86− B cells, indicating that elevated BTK levels do not simply reflect the massive B cell activation in these patients. In addition, B cell–T cell interaction through costimulatory molecules (50) and/or T cell–derived cytokines may also affect naive B cells. The observed correlation between BTK levels in peripheral blood B cells and parotid gland T cell infiltration suggests that at an early stage of disease, either T cell activity regulates the expression of BTK in the B cell lineage or elevated BTK levels contribute to local T cell activity. These two scenarios are not mutually exclusive and are supported by our findings in BTK-overexpressing mice, in which the spontaneous autoimmune phenotype is dependent on a B cell–T cell–mediated proinflammatory feedback loop through CD40–CD40L interaction (28,33). Further experiments are needed to reveal the molecular mechanisms that regulate BTK protein expression in naive B cells in patients with autoimmune disease.

Recent studies have pointed toward a pathogenic role for BTK signaling in autoimmune disease. In B cells from RA patients, BTK signaling was required for induction of interleukin-21 (IL-21) expression by B cells (51). Even though levels of phospho-BTK were not significantly different between RF-negative and RF-positive RA patients, there was a significant correlation between phospho-BTK and RF titer. In addition, disease activity in SLE was shown to correlate with expression in peripheral blood B cells of the transcription factor AT-rich–interactive domain–containing protein 3A (52), which interacts directly with BTK (53). It was recently reported that levels of phospho-Syk, an upstream activator of BTK that has the capacity to phosphorylate BTK at position Y^{551} (18), were higher in peripheral blood B cells from RA patients, particularly those who were ACPA positive (54). Those authors also found that treatment with abatacept significantly reduced the levels of phospho-Syk, but it is not known whether phospho-Syk levels are also modulated between different B cell subsets, similar to BTK. In this context, it is remarkable that increased phospho-Syk was found both in treatment-naive RA patients and in patients receiving methotrexate or methotrexate and biologic agents (54). A recent meta-analysis concluded that the Syk

inhibitor fostamatinib has moderate effects in the treatment of RA, with mostly mild-to-moderate adverse events and dose-dependent, transient neutropenia and hypertransaminasemia (55).

In summary, both naive and nonswitched memory B cells in peripheral blood from RA patients and a major fraction of patients with primary SS showed significantly increased BTK protein levels, which correlated with ACPA positivity and severity of salivary gland T cell infiltration, respectively. Conversely, in CD19-hBtk–transgenic mice, we have noticed that BTK overexpression alone is sufficient to disrupt T cell homeostasis and induce Tfh cell formation (28,33). Furthermore, CD19-hBtk–transgenic mouse B cells show higher production of the proinflammatory cytokines IL-6 and interferon-γ, which was dependent on T cells (33). Together, these findings point to a BTK-dependent proinflammatory feedback loop whereby B cell–T cell interactions through costimulatory molecules and proinflammatory cytokine production drive autoimmunity. Therefore, by interfering with the costimulatory pathways between T cells and CD80/CD86-expressing dendritic cells or activated B cells, abatacept treatment may disrupt this feedback loop. In this context, it is important that it has been shown that strong CD28 engagement to CD86 is crucial for generating the Tfh cells that support GC development (56). It is therefore attractive to speculate that in autoimmune disease, BTK-mediated signaling in B cells may establish or maintain T cell–propagated pathology and vice versa. Together with the observed beneficial effects of BTK inhibition in mouse models of autoimmune disease and its compelling safety and efficacy in patients with B cell malignancies (18,19), our findings would make BTK an attractive therapeutic target in autoimmune diseases, but we will have to await results of the ongoing clinical trials.

ACKNOWLEDGMENTS

We would like to thank Ilke Ilgaz, Peter Heukels, and Jennifer van Hulst for their technical assistance during experiments. We would also like to thank Erlin Haacke and Konstantina Delli for histopathologic analysis of the parotid gland biopsy specimens.

AUTHOR CONTRIBUTIONS

All authors were involved in drafting the article or revising it critically for important intellectual content, and all authors approved the final version to be published. Dr. Hendriks had full access to all of the data in the study and takes responsibility for the integrity of the data and the accuracy of the data analysis.

Study conception and design. Corneth, Verstappen, Kroese, Hendriks.

Acquisition of data. Corneth, Verstappen, Paulissen, de Bruijn, Rip, Lukkes, van Hamburg.

Analysis and interpretation of data. Corneth, Verstappen, Paulissen, de Bruijn, Rip, van Hamburg, Lubberts, Bootsma, Kroese, Hendriks.

REFERENCES

1. Kil LP, Hendriks RW. Aberrant B cell selection and activation in systemic lupus erythematosus. Int Rev Immunol 2013;32:445–70.
2. Nielen MM, van Schaardenburg D, Reesink HW, van de Stadt RJ, van der Horst-Bruinsma IE, de Koning MH, et al. Specific autoantibodies precede the symptoms of rheumatoid arthritis: a study of serial measurements in blood donors. Arthritis Rheum 2004;50:380–6.
3. Theander E, Jonsson R, Sjöström B, Brokstad K, Olsson P, Henriksson G. Prediction of Sjögren's syndrome years before diagnosis and identification of patients with early onset and severe disease course by autoantibody profiling. Arthritis Rheumatol 2015;67:2427–36.
4. Fox RI. Sjögren's syndrome. Lancet 2005;366:321–31.
5. Atkinson JC, Travis WD, Slocum L, Ebbs WL, Fox PC. Serum anti–SS-B/La and IgA rheumatoid factor are markers of salivary gland disease activity in primary Sjögren's syndrome. Arthritis Rheum 1992;35:1368–72.
6. Kroese FG, Abdulahad WH, Haacke E, Bos NA, Vissink A, Bootsma H. B-cell hyperactivity in primary Sjögren's syndrome. Expert Rev Clin Immunol 2014;10:483–99.
7. Ramos-Casals M, Brito-Zeron P, Solans R, Camps MT, Casanovas A, Sopena B, et al. Systemic involvement in primary Sjögren's syndrome evaluated by the EULAR-SS disease activity index: analysis of 921 Spanish patients (GEAS-SS registry). Rheumatology (Oxford) 2014;53:321–31.
8. Lessard CJ, Li H, Adrianto I, Ice JA, Rasmussen A, Grundahl KM, et al. Variants at multiple loci implicated in both innate and adaptive immune responses are associated with Sjögren's syndrome. Nat Genet 2013;45:1284–92.
9. Groom J, Kalled SL, Cutler AH, Olson C, Woodcock SA, Schneider P, et al. Association of BAFF/BLyS overexpression and altered B cell differentiation with Sjögren's syndrome. J Clin Invest 2002;109:59–68.
10. Baumjohann D, Preite S, Reboldi A, Ronchi F, Ansel KM, Lanzavecchia A, et al. Persistent antigen and germinal center B cells sustain T follicular helper cell responses and phenotype. Immunity 2013;38:596–605.
11. Shen P, Fillatreau S. Antibody-independent functions of B cells: a focus on cytokines. Nat Rev Immunol 2015;15:441–51.
12. Devauchelle-Pensec V, Mariette X, Jousse-Joulin S, Berthelot JM, Perdriger A, Puechal X, et al. Treatment of primary Sjögren syndrome with rituximab: a randomized trial. Ann Intern Med 2014;160:233–42.
13. Meijer JM, Pijpe J, Vissink A, Kallenberg CG, Bootsma H. Treatment of primary Sjögren syndrome with rituximab: extended follow-up, safety and efficacy of retreatment. Ann Rheum Dis 2009;68:284–5.
14. Carubbi F, Alunno A, Cipriani P, Bartoloni E, Ciccia F, Triolo G, et al. Rituximab in primary Sjögren's syndrome: a ten-year journey. Lupus 2014;23:1337–49.
15. Navarra SV, Guzman RM, Gallacher AE, Hall S, Levy RA, Jimenez RE, et al. Efficacy and safety of belimumab in patients with active systemic lupus erythematosus: a randomised, placebo-controlled, phase 3 trial. Lancet 2011;377:721–31.
16. Corneth OB, Klein Wolterink RG, Hendriks RW. BTK signaling in B cell differentiation and autoimmunity. Curr Top Microbiol Immunol 2016;393:67–105.
17. Conley ME, Broides A, Hernandez-Trujillo V, Howard V, Kanegane H, Miyawaki T, et al. Genetic analysis of patients with defects in early B-cell development. Immunol Rev 2005;203:216–34.
18. Hendriks RW, Yuvaraj S, Kil LP. Targeting Bruton's tyrosine kinase in B cell malignancies. Nat Rev Cancer 2014;14:219–32.
19. Byrd JC, Harrington B, O'Brien S, Jones JA, Schuh A, Devereux S, et al. Acalabrutinib (ACP-196) in relapsed chronic lymphocytic leukemia. N Engl J Med 2016;374:323–32.
20. Honigberg LA, Smith AM, Sirisawad M, Verner E, Loury D, Chang B, et al. The Bruton tyrosine kinase inhibitor PCI-32765

blocks B-cell activation and is efficacious in models of autoimmune disease and B-cell malignancy. Proc Natl Acad Sci U S A 2010;107:13075–80.
21. Hutcheson J, Vanarsa K, Bashmakov A, Grewal S, Sajitharan D, Chang BY, et al. Modulating proximal cell signaling by targeting Btk ameliorates humoral autoimmunity and end-organ disease in murine lupus. Arthritis Res Ther 2012;14:R243.
22. Mina-Osorio P, LaStant J, Keirstead N, Whittard T, Ayala J, Stefanova S, et al. Suppression of glomerulonephritis in lupus-prone NZB × NZW mice by RN486, a selective inhibitor of Bruton's tyrosine kinase. Arthritis Rheum 2013;65:2380–91.
23. Rankin AL, Seth N, Keegan S, Andreyeva T, Cook TA, Edmonds J, et al. Selective inhibition of BTK prevents murine lupus and antibody-mediated glomerulonephritis. J Immunol 2013;191:4540–50.
24. Xu D, Kim Y, Postelnek J, Vu MD, Hu DQ, Liao C, et al. RN486, a selective Bruton's tyrosine kinase inhibitor, abrogates immune hypersensitivity responses and arthritis in rodents. J Pharmacol Exp Ther 2012;341:90–103.
25. Chang BY, Huang MM, Francesco M, Chen J, Sokolove J, Magadala P, et al. The Bruton tyrosine kinase inhibitor PCI-32765 ameliorates autoimmune arthritis by inhibition of multiple effector cells. Arthritis Res Ther 2011;13:R115.
26. Di Paolo JA, Huang T, Balazs M, Barbosa J, Barck KH, Bravo BJ, et al. Specific Btk inhibition suppresses B cell- and myeloid cell-mediated arthritis. Nat Chem Biol 2011;7:41–50.
27. Nisitani S, Satterthwaite AB, Akashi K, Weissman IL, Witte ON, Wahl MI. Posttranscriptional regulation of Bruton's tyrosine kinase expression in antigen receptor-stimulated splenic B cells. Proc Natl Acad Sci U S A 2000;97:2737–42.
28. Kil LP, de Bruijn MJ, van Nimwegen M, Corneth OB, van Hamburg JP, Dingjan GM, et al. Btk levels set the threshold for B-cell activation and negative selection of autoreactive B cells in mice. Blood 2012;119:3744–56.
29. Belver L, de Yebenes VG, Ramiro AR. MicroRNAs prevent the generation of autoreactive antibodies. Immunity 2010;33:713–22.
30. Yu L, Mohamed AJ, Simonson OE, Vargas L, Blomberg KE, Bjorkstrand B, et al. Proteasome-dependent autoregulation of Bruton tyrosine kinase (Btk) promoter via NF-κB. Blood 2008; 111:4617–26.
31. Satterthwaite AB, Cheroutre H, Khan WN, Sideras P, Witte ON. Btk dosage determines sensitivity to B cell antigen receptor cross-linking. Proc Natl Acad Sci U S A 1997;94:13152–7.
32. Drabek D, Raguz S, de Wit TP, Dingjan GM, Savelkoul HF, Grosveld F, et al. Correction of the X-linked immunodeficiency phenotype by transgenic expression of human Bruton tyrosine kinase under the control of the class II major histocompatibility complex Ea locus control region. Proc Natl Acad Sci U S A 1997;94:610–5.
33. Corneth OB, de Bruijn MJ, Rip J, Asmawidjaja PS, Kil LP, Hendriks RW. Enhanced expression of Bruton's tyrosine kinase in B cells drives systemic autoimmunity by disrupting T cell homeostasis. J Immunol 2016;197:58–67.
34. Van der Heijde DM, van 't Hof MA, van Riel PL, Theunisse LM, Lubberts EW, van Leeuwen MA, et al. Judging disease activity in clinical practice in rheumatoid arthritis: first step in the development of a disease activity score. Ann Rheum Dis 1990;49:916–20.
35. Paulissen SM, van Hamburg JP, Davelaar N, Vroman H, Hazes JM, de Jong PH, et al. $CCR6^+$ Th cell populations distinguish ACPA positive from ACPA negative rheumatoid arthritis. Arthritis Res Ther 2015;17:344.
36. Aletaha D, Neogi T, Silman AJ, Funovits J, Felson DT, Bingham CO III, et al. 2010 rheumatoid arthritis classification criteria: an American College of Rheumatology/European League Against Rheumatism collaborative initiative. Arthritis Rheum 2010;62:2569–81.
37. Vitali C, Bombardieri S, Jonsson R, Moutsopoulos HM, Alexander EL, Carsons SE, et al. Classification criteria for Sjögren's syndrome: a revised version of the European criteria proposed by the American-European Consensus Group. Ann Rheum Dis 2002;61:554–8.
38. Meiners PM, Vissink A, Kroese FG, Spijkervet FK, Smitt-Kamminga NS, Abdulahad WH, et al. Abatacept treatment reduces disease activity in early primary Sjögren's syndrome (open-label proof of concept ASAP study). Ann Rheum Dis 2014;73:1393–6.
39. Paulissen SM, van Hamburg JP, Dankers W, Lubberts E. The role and modulation of CCR6+ Th17 cell populations in rheumatoid arthritis. Cytokine 2015;74:43–53.
40. Bohnhorst JO, Bjorgan MB, Thoen JE, Jonsson R, Natvig JB, Thompson KM. Abnormal B cell differentiation in primary Sjögren's syndrome results in a depressed percentage of circulating memory B cells and elevated levels of soluble CD27 that correlate with Serum IgG concentration. Clin Immunol 2002;103:79–88.
41. Hansen A, Odendahl M, Reiter K, Jacobi AM, Feist E, Scholze J, et al. Diminished peripheral blood memory B cells and accumulation of memory B cells in the salivary glands of patients with Sjögren's syndrome. Arthritis Rheum 2002;46:2160–71.
42. Rodriguez-Bayona B, Ramos-Amaya A, Perez-Venegas JJ, Rodriguez C, Brieva JA. Decreased frequency and activated phenotype of blood CD27 IgD IgM B lymphocytes is a permanent abnormality in systemic lupus erythematosus patients. Arthritis Res Ther 2010;12:R108.
43. Seror R, Ravaud P, Bowman SJ, Baron G, Tzioufas A, Theander E, et al, on behalf of the EULAR Sjögren's Task Force. EULAR Sjögren's Syndrome Disease Activity Index: development of a consensus systemic disease activity index for primary Sjögren's syndrome. Ann Rheum Dis 2010;69:1103–9.
44. Seror R, Ravaud P, Mariette X, Bootsma H, Theander E, Hansen A, et al. EULAR Sjögren's Syndrome Patient Reported Index (ESSPRI): development of a consensus patient index for primary Sjögren's syndrome. Ann Rheum Dis 2011;70:968–72.
45. Verpoort KN, Jol-van der Zijde CM, Papendrecht-van der Voort EA, Ioan-Facsinay A, Drijfhout JW, van Tol MJ, et al. Isotype distribution of anti–cyclic citrullinated peptide antibodies in undifferentiated arthritis and rheumatoid arthritis reflects an ongoing immune response. Arthritis Rheum 2006;54:3799–808.
46. Feitsma AL, van der Voort EI, Franken KL, el Bannoudi H, Elferink BG, Drijfhout JW, et al. Identification of citrullinated vimentin peptides as T cell epitopes in HLA–DR4–positive patients with rheumatoid arthritis. Arthritis Rheum 2010;62:117–25.
47. Von Delwig A, Locke J, Robinson JH, Ng WF. Response of Th17 cells to a citrullinated arthritogenic aggrecan peptide in patients with rheumatoid arthritis. Arthritis Rheum 2010;62: 143–9.
48. Folzenlogen D, Hofer MF, Leung DY, Freed JH, Newell MK. Analysis of CD80 and CD86 expression on peripheral blood B lymphocytes reveals increased expression of CD86 in lupus patients. Clin Immunol Immunopathol 1997;83:199–204.
49. Catalan D, Aravena O, Sabugo F, Wurmann P, Soto L, Kalergis AM, et al. B cells from rheumatoid arthritis patients show important alterations in the expression of CD86 and FcγRIIb, which are modulated by anti-tumor necrosis factor therapy. Arthritis Res Ther 2010;12:R68.
50. Schwartz MA, Kolhatkar NS, Thouvenel C, Khim S, Rawlings DJ. CD4+ T cells and CD40 participate in selection and homeostasis of peripheral B cells. J Immunol 2014; 193:3492–502.
51. Wang SP, Iwata S, Nakayamada S, Niiro H, Jabbarzadeh-Tabrizi S, Kondo M, et al. Amplification of IL-21 signalling pathway through Bruton's tyrosine kinase in human B cell activation. Rheumatology (Oxford) 2015;54:1488–97.
52. Ward JM, Rose K, Montgomery C, Adrianto I, James JA, Merrill JT, et al. Disease activity in systemic lupus erythematosus correlates with expression of the transcription factor AT-rich–interactive domain 3A. Arthritis Rheumatol 2014;66:3404–12.
53. Rajaiya J, Hatfield M, Nixon JC, Rawlings DJ, Webb CF. Bruton's tyrosine kinase regulates immunoglobulin promoter activation in association with the transcription factor Bright. Mol Cell Biol 2005;25:2073–84.

54. Iwata S, Nakayamada S, Fukuyo S, Kubo S, Yunoue N, Wang SP, et al. Activation of Syk in peripheral blood B cells in patients with rheumatoid arthritis: a potential target for abatacept therapy. Arthritis Rheumatol 2015;67:63–73.
55. Kunwar S, Devkota AR, Ghimire DK. Fostamatinib, an oral spleen tyrosine kinase inhibitor, in the treatment of rheumatoid arthritis: a meta-analysis of randomized controlled trials. Rheumatol Int 2016;36:1077–87.
56. Wang CJ, Heuts F, Ovcinnikovs V, Wardzinski L, Bowers C, Schmidt EM, et al. CTLA-4 controls follicular helper T-cell differentiation by regulating the strength of CD28 engagement. Proc Natl Acad Sci U S A 2015;112:524–9.

DOI: 10.1002/art.40081

Clinical Images: Progressive noninfectious anterior vertebral fusion (Copenhagen syndrome) in a 15-year-old boy

The patient, a 15-year-old boy, presented with major thoracolumbar kyphosis with spinal stiffness, but without pain, scoliosis, neurologic symptoms, or difficulty walking. Based on the findings of radiography and magnetic resonance imaging (MRI) of the spine and the absence of sacroiliac joint involvement, progressive noninfectious anterior vertebral fusion (PAVS) was diagnosed. Transpedicle osteotomy of T12–L1 was performed, which corrected this spinal deformity. Plain radiography revealed an anterior vertebral body fusion of T12, L1, and L2 (left). MRI sagittal scanning through the thoracolumbar levels (T2 fast spin-echo sequences) confirmed T12–L1 and L1–L2 fusion and multilevel lumbar anterior disc space obliteration and erosion (T12 through L5) (right). Narrowing and erosion of the end plates progresses over time from early childhood and tends to extend rapidly during adolescence, with eventual anterior bony ankylosis via a thick bony bridge. The narrowing can extend posteriorly, with complete vertebral fusion resulting. The process may affect one level or several contiguous or noncontiguous levels, and most frequently involves the thoracolumbar junction. Often referred to as "Copenhagen syndrome" (1–3), PAVS is a rare spine disorder mostly seen in childhood. The disease may be asymptomatic or may present with mild pain or stiffness. Thoracolumbar kyphosis is a characteristic finding. PAVS represents a distinct clinical and pathologic entity separate from anterior limbus vertebra, Scheuermann's disease, and thalidomide embryopathy in children, and from ankylosing spondylitis and diffuse idiopathic skeletal hyperostosis in adults, with which it shares some features. Its cause remains unknown, but a congenital etiology has been suggested. Treatment comprises bracing during childhood in order to slow progression, or surgical correction. The deformity is thought to stabilize in adulthood once fusion is complete.

1. Andersen J, Rostgaard-Christensen E. Progressive noninfectious anterior vertebral fusion. J Bone Joint Surg 1991;73:859–62.
2. Hughes RJ, Saifuddin A. Progressive non-infectious anterior vertebral fusion (Copenhagen syndrome) in three children: features on radiographs and MR imaging. Skeletal Radiol 2006;35:397–401.
3. Cebulski A, Nectoux E, Bigot J, Cagneaux M, Mézel A, Fron D, et al. Progressive anterior vertebral fusion: a report of three cases. Diagn Interv Imaging 2012;93:53–6.

Clément Prati, MD, PhD
Jean Langlais, MD
University Teaching Hospital
Sébastien Aubry, MD, PhD
Benoit Barbier Brion, MD
Clinique St. Vincent
Daniel Wendling, MD, PhD
University Teaching Hospital
Besançon, France

54. Iwata S, Nakayamada S, Fukuyo S, Kubo S, Yunoue N, Wang SP, et al. Activation of Syk in peripheral blood B cells in patients with rheumatoid arthritis: a potential target for abatacept therapy. Arthritis Rheumatol 2015;67:63–73.
55. Kunwar S, Devkota AR, Ghimire DK. Fostamatinib, an oral spleen tyrosine kinase inhibitor, in the treatment of rheumatoid arthritis: a meta-analysis of randomized controlled trials. Rheumatol Int 2016;36:1077–87.
56. Wang CJ, Heuts F, Ovcinnikovs V, Wardzinski L, Bowers C, Schmidt EM, et al. CTLA-4 controls follicular helper T-cell differentiation by regulating the strength of CD28 engagement. Proc Natl Acad Sci U S A 2015;112:524–9.

DOI: 10.1002/art.40081

Clinical Images: Progressive noninfectious anterior vertebral fusion (Copenhagen syndrome) in a 15-year-old boy

The patient, a 15-year-old boy, presented with major thoracolumbar kyphosis with spinal stiffness, but without pain, scoliosis, neurologic symptoms, or difficulty walking. Based on the findings of radiography and magnetic resonance imaging (MRI) of the spine and the absence of sacroiliac joint involvement, progressive noninfectious anterior vertebral fusion (PAVS) was diagnosed. Transpedicle osteotomy of T12–L1 was performed, which corrected this spinal deformity. Plain radiography revealed an anterior vertebral body fusion of T12, L1, and L2 (left). MRI sagittal scanning through the thoracolumbar levels (T2 fast spin-echo sequences) confirmed T12–L1 and L1–L2 fusion and multilevel lumbar anterior disc space obliteration and erosion (T12 through L5) (right). Narrowing and erosion of the end plates progresses over time from early childhood and tends to extend rapidly during adolescence, with eventual anterior bony ankylosis via a thick bony bridge. The narrowing can extend posteriorly, with complete vertebral fusion resulting. The process may affect one level or several contiguous or noncontiguous levels, and most frequently involves the thoracolumbar junction. Often referred to as "Copenhagen syndrome" (1–3), PAVS is a rare spine disorder mostly seen in childhood. The disease may be asymptomatic or may present with mild pain or stiffness. Thoracolumbar kyphosis is a characteristic finding. PAVS represents a distinct clinical and pathologic entity separate from anterior limbus vertebra, Scheuermann's disease, and thalidomide embryopathy in children, and from ankylosing spondylitis and diffuse idiopathic skeletal hyperostosis in adults, with which it shares some features. Its cause remains unknown, but a congenital etiology has been suggested. Treatment comprises bracing during childhood in order to slow progression, or surgical correction. The deformity is thought to stabilize in adulthood once fusion is complete.

1. Andersen J, Rostgaard-Christensen E. Progressive noninfectious anterior vertebral fusion. J Bone Joint Surg 1991;73:859–62.
2. Hughes RJ, Saifuddin A. Progressive non-infectious anterior vertebral fusion (Copenhagen syndrome) in three children: features on radiographs and MR imaging. Skeletal Radiol 2006;35:397–401.
3. Cebulski A, Nectoux E, Bigot J, Cagneaux M, Mézel A, Fron D, et al. Progressive anterior vertebral fusion: a report of three cases. Diagn Interv Imaging 2012;93:53–6.

Clément Prati, MD, PhD
Jean Langlais, MD
University Teaching Hospital
Sébastien Aubry, MD, PhD
Benoit Barbier Brion, MD
Clinique St. Vincent
Daniel Wendling, MD, PhD
University Teaching Hospital
Besançon, France

ARTHRITIS & RHEUMATOLOGY
Vol. 69, No. 6, June 2017, pp 1325–1336
DOI 10.1002/art.40055

Cerebrospinal Fluid Cytokines Correlate With Aseptic Meningitis and Blood–Brain Barrier Function in Neonatal-Onset Multisystem Inflammatory Disease

Central Nervous System Biomarkers in Neonatal-Onset Multisystem Inflammatory Disease Correlate With Central Nervous System Inflammation

Jackeline Rodriguez-Smith,[1] Yen-Chih Lin,[2] Wanxia Li Tsai,[3] Hanna Kim,[4] Gina Montealegre-Sanchez,[1] Dawn Chapelle,[1] Yan Huang,[1] Cailin H. Sibley,[5] Massimo Gadina,[3] Robert Wesley,[6] Bibiana Bielekova,[2] and Raphaela Goldbach-Mansky[1]

Objective. **To evaluate proinflammatory cytokines and leukocyte subpopulations in the cerebrospinal fluid (CSF) and blood of patients with neonatal-onset multisystem inflammatory disease (NOMID) after treatment, and to compare inflammatory cytokines in the CSF and blood in 6 patients treated with 2 interleukin-1 (IL-1) blockers—anakinra and canakinumab.**

Methods. **During routine follow-up visits between December 2011 and October 2013, we immunophenotyped the CSF of 17 pediatric NOMID patients who were treated with anakinra, and analyzed CSF cytokine levels in samples obtained at baseline and at 3–5-year follow-up visits and compared them to samples from healthy controls.***

Results. **CSF levels of IL-6, interferon-γ–inducible 10-kd protein (IP-10/CXCL10), and IL-18 and monocyte and granulocyte counts significantly decreased with anakinra treatment but did not normalize to levels in the controls, even in patients fulfilling criteria for clinical remission. CSF IL-6 and IL-18 levels significantly correlated with measures of blood–brain barrier function, specifically CSF protein ($r = 0.75$ and $r = 0.81$, respectively) and albumin quotient ($r = 0.79$ and $r = 0.68$, respectively). When patients were treated with canakinumab versus anakinra, median CSF white blood cell counts and IL-6 levels were significantly higher with canakinumab treatment (10.2 cells/mm^3 versus 3.7 cells/mm^3 and 150.7 pg/ml versus 28.5 pg/ml, respectively) despite similar serum cytokine levels.**

Conclusion. **CSF leukocyte subpopulations and cytokine levels significantly improve with optimized IL-1 blocking treatment, but do not normalize. The correlation of CSF IL-6, IP-10/CXCL10, and IL-18 levels with clinical laboratory measures of inflammation and**

ClinicalTrials.gov identifiers: NCT00059748; NCT00069329.

Supported by the NIH (Intramural Research Programs of the National Institute of Allergy and Infectious Diseases and of the National Institute of Arthritis and Musculoskeletal and Skin Diseases, the National Institute of Neurological Disorders and Stroke, and the NIH Clinical Center). Dr. Rodriguez-Smith's work was supported by the NIH (Medical Research Scholars Program, a public-private partnership supported jointly by the NIH and Pfizer, Inc.), the Doris Duke Charitable Foundation, Alexandria Real Estate Equities, Inc., Mr. and Mrs. Joel S. Marcus, the Howard Hughes Medical Institute, and private donors.

[1]Jackeline Rodriguez-Smith, MD, Gina Montealegre-Sanchez, MD, MPH, Dawn Chapelle, CRNP, Yan Huang, Raphaela Goldbach-Mansky, MD, MHS: Translational Autoinflammatory Disease Studies, Intramural Research Program, NIH, Bethesda, Maryland; [2]Yen-Chih Lin, PhD, Bibiana Bielekova, MD: Neuroimmunological Diseases Unit, National Institute of Neurological Disorders and Stroke, NIH, Bethesda, Maryland; [3]Wanxia Li Tsai, MS, Massimo Gadina, PhD: Translational Immunology Section, National Institute of Arthritis and Musculoskeletal and Skin Diseases, NIH, Bethesda, Maryland; [4]Hanna Kim, MD, MHS: Scholar's Program, National Institute of Arthritis and Musculoskeletal and Skin Diseases, NIH, Bethesda, Maryland; [5]Cailin H. Sibley, MD: Oregon Health & Science University, Portland, Oregon; [6]Robert Wesley, PhD: Clinical Center, NIH, Bethesda, Maryland.

Dr. Goldbach-Mansky has received grant support for clinical studies from Regeneron, Novartis, Sobi, Inc., and Eli Lilly.

Address correspondence to Raphaela Goldbach-Mansky, MD, MHS, Translational Autoinflammatory Disease Studies, NIH/NIAID/LCID, Building 10, Room 11C205, 10 Center Drive, Bethesda, MD 20892. E-mail: goldbacr@mail.nih.gov.

Submitted for publication February 24, 2016; accepted in revised form January 17, 2017.

* Correction added on May 19, 2017, after online publication: Text in this sentence has been updated to change "3–5 years" to "3–5-year follow-up visits."

blood–brain barrier function suggests that they may have a role as biomarkers in central nervous system (CNS) inflammation. The difference in inhibition of CSF biomarkers between 2 IL-1 blocking agents, anakinra and canakinumab, suggests differences in efficacy in the intrathecal compartment, with anakinra being more effective. Our data indicate that intrathecal immune responses shape CNS inflammation and should be assessed in addition to blood markers.

Neonatal-onset multisystem inflammatory disease (NOMID), also referred to as chronic infantile neurologic, cutaneous, articular syndrome, is the most severe clinical form of the disease spectrum of cryopyrin-associated periodic syndromes (CAPS). CAPS are caused by gain-of-function mutations in the *NLRP3* gene that encodes cryopyrin, a protein that is expressed in hematopoietic cells including granulocytes, monocytes, dendritic cells, and nonhematopoietic cells that include microglial and reactive astrocytes in the central nervous system (CNS) (1–3). Two-thirds of patients with NOMID have de novo germline mutations and ~30% have somatic mosaicism in *NLRP3* (4). Pathogenic *NLRP3* mutations lead to constitutive inflammasome activation with secretion of interleukin-1β (IL-1β) and to moderate elevations in levels of IL-18.

CAPS patients present with episodic (on the milder end of the disease spectrum) or continuous (on the more-severe end of the spectrum) systemic inflammation that includes recurrent fever flares with neutrophilic urticaria, arthralgia, and increased levels of acute-phase reactants. With increasing severity of CAPS, CNS and organ inflammation become more prevalent and chronic, which leads to organ damage. Cochlear inflammation leads to sensorineural hearing loss, chronic papilledema leads to optic nerve atrophy and peripheral visual field loss, and chronic increased intracranial pressure can lead to brain atrophy and mental retardation. These features are commonly observed in patients with NOMID, and are more variable or absent in the milder forms of CAPS (Muckle-Wells syndrome and familial cold autoinflammatory disease, respectively) (5,6).

Treatment with IL-1 blocking agents results in significant clinical and laboratory improvements in NOMID and has become the standard of care. NOMID patients with germline or somatic mosaicism do not differ in disease severity and respond equally to IL-1 blocking treatment (4,7). Anakinra can penetrate into the CNS and treatment improves CNS inflammation by decreasing cerebrospinal fluid (CSF) pleocytosis, opening pressure and protein levels, papilledema, and inner ear enhancement (6–8). It currently remains unclear whether adequate inflammatory control is achieved in NOMID patients with severe CNS inflammation receiving treatment with both short-acting (anakinra) and long-acting (canakinumab and rilonacept) IL-1 inhibitors. We have observed that normalization of acute-phase reactant levels in the blood does not preclude persistent, low-grade CNS pleocytosis (suggesting ongoing CNS inflammation) (4,9), and that dose escalations of the IL-1 blocking agent anakinra, beyond levels needed to control peripheral inflammation, are needed to optimally control CNS inflammation (7).

In a previous study we observed that IL-6 levels in the CSF of untreated NOMID patients were on average 6 times higher than IL-6 levels in the blood (6), suggesting that IL-6 may be produced in the CNS by resident cells, as suggested in CNS inflammation in patients with systemic lupus erythematosus (10) and in those with neuro-Behçet's syndrome (2). However, correlations of IL-6 levels with mononuclear cell subsets in the CSF (6), or their use as a potential biomarker for CNS disease in NOMID, have yet to be assessed.

In the present study we evaluated 9 cytokines (including IL-6) in the CSF compared to serum and determined the correlation between cytokine levels and blood–brain barrier function and CNS inflammation to assess their use as biomarkers for CNS inflammation. We further compared cytokine levels in 6 patients who sequentially received anakinra and canakinumab.

PATIENTS AND METHODS

Patients and controls. Between December 2011 and October 2013, we collected (for immunophenotyping) CSF samples from 17 consecutive anakinra-treated pediatric NOMID patients who were enrolled in a natural history and treatment study (NCT00069329) and had returned for routine follow-up. For the cytokine analyses, we used archived CSF and plasma/serum samples that were collected, spun, and frozen from baseline (before patients received IL-1 blocking treatments) and follow-up (after patients started IL-1 blocking treatments). We immunophenotyped CSF leukocyte subsets on freshly collected samples (11). One patient was excluded from the analyses of cell populations due to a technical problem with the staining procedure (see Supplementary Figures 1A and 1B, available on the *Arthritis & Rheumatology* web site at http://onlinelibrary.wiley.com/doi/10.1002/art.40055/abstract).

Archived baseline (prior to anakinra treatment) and posttreatment paired CSF and serum samples were available for 11 of the 17 patients. For the cytokine analyses we included samples from 4 additional patients with NOMID for whom matched baseline and posttreatment CSF and serum samples had been stored, but whose CSF had not been immunophenotyped for cell subsets (see Supplementary Figures 1A and B, http://onlinelibrary.wiley.com/doi/10.1002/art.40055/abstract).

Complete clinical remission was defined by the following criteria: erythrocyte sedimentation rate (ESR) $\leq$25 mm/hour, C-reactive protein (CRP) $\leq$0.5 mg/dl, CSF white blood cell

(WBC) count ≤5 cells/mm^3, and protein ≤40 mg/dl (7). Blood plasma/serum and CSF samples from patients with NOMID were compared to serum samples from 11 pediatric age-matched controls and to 7 CSF samples, respectively. Five of the CSF samples were from healthy adult controls recruited for another study (11), and 2 were from pediatric patients with undifferentiated autoinflammation who had undergone a diagnostic lumbar puncture but had no evidence of CNS inflammation according to medical history, imaging, and CSF markers (leukocytosis, opening pressure, and protein content).

Longitudinal cytokine analyses of all available CSF and serum samples were conducted for 21 patients (see Supplementary Figure 1B, available on the *Arthritis & Rheumatology* web site at http://onlinelibrary.wiley.com/doi/10.1002/art.40055/abstract). To assess the relevance of these biomarkers longitudinally, we included 6 patients who were initially treated with anakinra and subsequently switched to canakinumab (9).* Three of the 6 patients were ultimately switched back to anakinra.

Written informed consent was obtained from all patients and/or their legal guardians. The current study was conducted in accordance with the Declaration of Helsinki, and the local institutional review board approved the protocol.

Assessment of clinical laboratory CSF parameters. CSF WBC counts were assessed in the NIH clinical laboratory (from unspun CSF) and in the laboratory of one of the authors (BB) (from spun and 50-fold concentrated CSF), as described (11). Where applicable, CSF and serum samples were utilized to ascertain routine CSF protein and glucose levels, calculated CSF/serum albumin quotients, and IgG index to assess blood–brain barrier function (12).

Cytokine analyses. CSF and blood cytokines (IL-1β, IL-1 receptor antagonist [IL-1Ra], IL-6, IL-9, IL-10, IL-12p70, IL-12p40, IL-17, interferon-γ–inducible 10-kd protein [IP-10/CXCL10], interferon-γ [IFNγ], tumor necrosis factor [TNF], IL-1α, IL-18, and IFN-α2) were assessed via Bio-Plex multiplex assays (Bio-Rad), as previously reported (13). Samples were stored at −80°C and the majority (except for some baseline blood and CSF samples) had not been previously thawed. Of the cytokines assessed, 5 were not included in the tables or further analyzed (see Supplementary Table 1A, available on the *Arthritis & Rheumatology* web site at http://onlinelibrary.wiley.com/doi/10.1002/art.40055/abstract), including 2 that were undetectable in most of the CSF samples (IFN-α2, IL-1α), 2 whose levels were not significantly different from those in controls and did not change with treatment (IL-9, IL-12p40), and 1 with levels lower than in controls, with significant variability and no change with treatment (IL-17).

Immunophenotyping of leukocytes. We analyzed absolute values of 5 subpopulations of leukocytes, which included monocytes, granulocytes, natural killer cells, CD3+ cells, and B cells. Sample preparation and immunophenotyping of leukocytes by flow cytometry were performed as previously reported (11).

Correlation analyses. Correlations of CSF and blood cytokine levels with leukocyte subpopulations were mostly analyzed posttreatment; CSF and blood immunophenotyping were performed prior to initiation of IL-1 blocking therapy in only 2 patients. CSF cytokine levels were also correlated with the following parameters of inflammation in CSF: CSF opening pressures, WBC count, total protein, and albumin quotient. Two of the 21 patients had ventriculoperitoneal shunts and were excluded only from CSF inflammation parameter correlations; both had very high protein levels at baseline, consistent with decreased circulation of spinal cord CSF related to the mechanical shunt (14).

Statistical analysis. Statistical analyses and graphing were performed using GraphPad 6 and Stata (StataCorp) software. Differences between nonpaired data with parametric or nonparametric distributions were analyzed using Student's *t*-test and Wilcoxon's rank sum test, respectively. Paired CSF and blood samples were analyzed with Student's paired *t*-test using $\log_{10}$ transformation of raw values. Correlations were assessed with Spearman's correlation coefficient. Due to the pilot nature of the study, we provided raw *P* values, unadjusted for multiple comparisons.

Table 1. Demographic and baseline clinical characteristics of the 23 pediatric NOMID patients*

Age, mean ± SD years	6.3 ± 5.7
0–3	11 (46)
4–8	5 (25)
9–12	3 (13)
13–18	2 (8)
≥18	2 (8)
Sex, female/male	12 (50)/11 (50)
Race	
White	10 (46)
Latino	8 (33)
Asian	4 (17)
Black	1 (4)
American Indian	0
NLRP3 mutations†	23 (100)
Growth retardation (below third percentile)	17 (71)
CNS damage	
Stroke	2 (8)
Seizures	4 (17)
Papilledema‡	21 (100)
Below average cognitive function (IQ)	11 (46)
Extremely low (<70)	5 (21)
Borderline (70–79)	2 (8)
Low average (80–89)	4 (16)
Abnormalities on brain MRI	
Ventriculomegaly	12 (54)
Arachnoid adhesions	13 (54)
Leptomeningeal enhancement§	7 (43)
Dura enhancement§	7 (43)
Cochlear enhancement§	14 (94)
VP shunt	2 (8)
Inner ear damage (hearing loss)	19 (83)
Mild (>20 to ≤40 dB)	6 (32)
Moderate (>40 to ≤70 dB)	7 (37)
Severe (>70 to ≤95 dB)	5 (26)
Profound (>95 dB)	1 (5)
Bone damage	
Bone overgrowth	10 (46)
Joint contractures	13 (58)
Limb length discrepancies	4 (21)

* Except where indicated otherwise, values are the number (%) of patients. NOMID = neonatal-onset multisystem inflammatory disease; CNS = central nervous system; IQ = intelligence quotient; MRI = magnetic resonance imaging; VP = ventriculoperitoneal.
† Four patients had germline mosaicism.
‡ Recorded in 21 patients.
§ Assessed in 15 of 17 patients; 6 of 23 patients were being treated with anakinra prior to enrollment.

* Correction added on May 19, 2017, after online publication: The reference (9) has been added to this sentence.

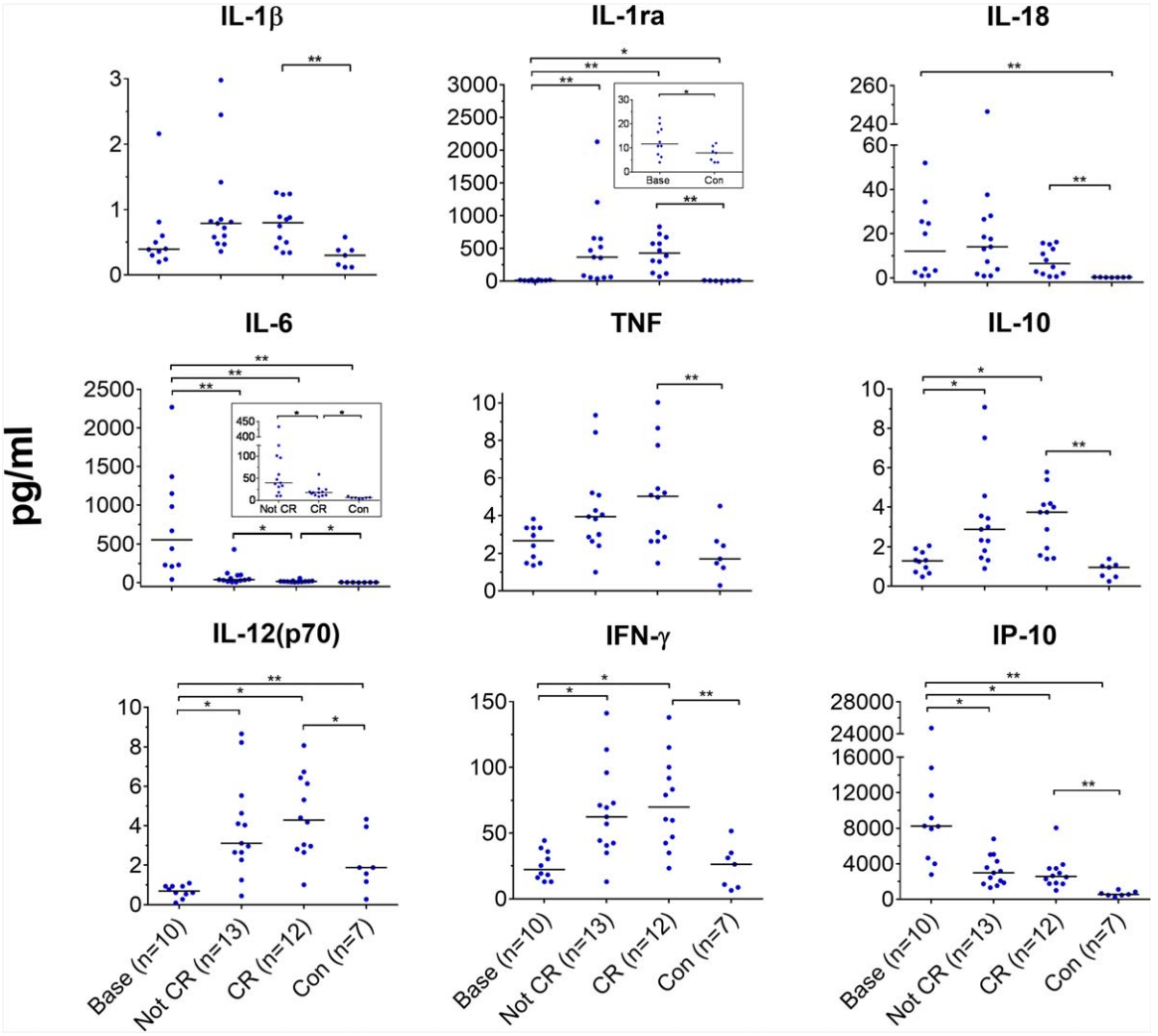

Figure 1. Cytokine levels in cerebrospinal fluid (CSF) from patients with neonatal-onset multisystem inflammatory disease at baseline (base), when disease was not in clinical remission (not CR), and when disease was in complete clinical remission. Paired CSF samples were analyzed by Student's paired *t*-test using $\log_{10}$ transformation of raw values. Unpaired comparisons were performed by Student's unpaired *t*-test or Wilcoxon's rank sum test, depending on data distribution. Symbols represent individual patients; bars show the median. $* = P < 0.05$; $** = P < 0.005$. IL-1Ra = interleukin-1 receptor antagonist; TNF = tumor necrosis factor; IFNγ = interferon-γ; IP-10 = interferon-γ–inducible 10-kd protein.

RESULTS

Demographic and clinical characteristics. The mean ± SD age of the NOMID patients at study enrollment was 6.3 ± 5.7 years. Nineteen of 23 patients had germline *NLRP3* mutations and 4 had somatic mosaicism (Table 1). At baseline, most patients had been receiving treatment with disease-modifying antirheumatic drugs (DMARDs) and/or steroids. Patients whose disease was in complete clinical remission who had been treated with anakinra had received a mean ± SD dosage of 4.6 ± 1.4 mg/kg/day and had been receiving treatment for 2.8 ± 2.8 years, compared to patients receiving anakinra whose disease was improved but not in complete remission, who had received an average dosage of 3.4 ± 1.4 mg/kg/day and were being treated with anakinra for 1.6 ± 1.3 years.* None of the patients were taking steroids or DMARDs posttreatment, except for 1 patient who was receiving methotrexate at the time of the sample collection.

Decrease in CSF and blood cytokine levels with IL-1 blocking treatment. Baseline CSF levels of IL-18, IL-6, and IP-10/CXCL10 were significantly higher in NOMID patients compared to healthy controls (median 12.07 pg/ml versus 0.29 pg/ml, 555.31 pg/ml versus 5.61 pg/ml, and 8,239.0 pg/ml versus 544.19 pg/ml, respectively), but there was no statistically significant difference in

* Correction added on May 19, 2017, after online publication: 1.7 years was changed to 2.8 years in this sentence.

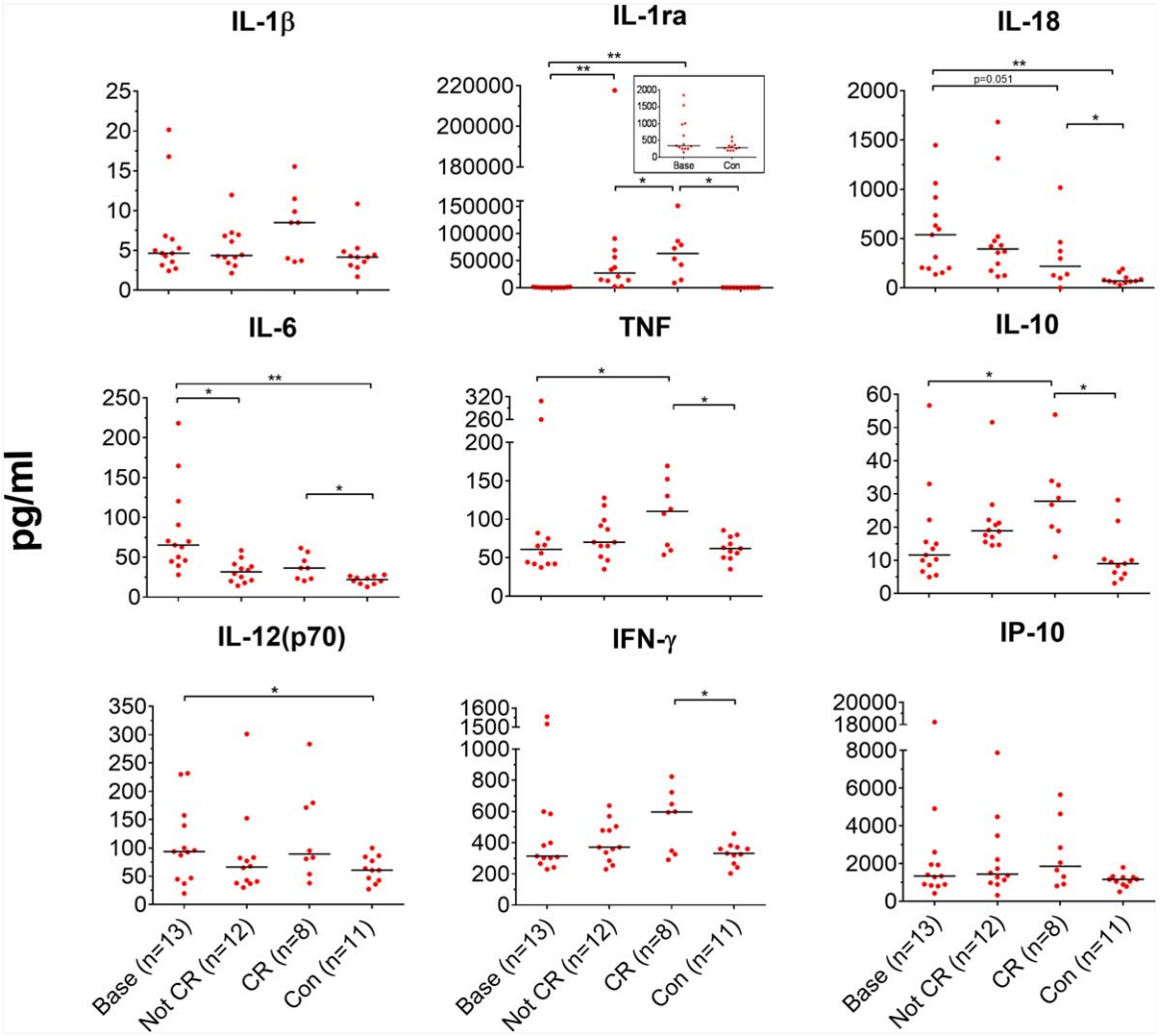

Figure 2. Cytokine levels in blood from patients with neonatal-onset multisystem inflammatory disease at baseline, when disease was not in clinical remission, and when disease was in complete clinical remission. Paired blood samples were analyzed by Student's paired *t*-test using $\log_{10}$ transformation of raw values. Unpaired comparisons were performed by Student's unpaired *t*-test or Wilcoxon's rank sum test, depending on data distribution. Symbols represent individual patients; bars show the median. $* = P < 0.05$; $** = P < 0.005$. For IL-6 levels, n = 10 controls. See Figure 1 for definitions.

blood levels of IP-10 in healthy controls versus patients (Figures 1 and 2). In contrast, CSF levels of IL-12p70 were significantly lower in patients versus healthy controls, and levels of TNF, IFNγ, and IL-10 in the CSF were not significantly different between the 2 groups (Figure 1). CSF IL-6 and IP-10/CXCL10 levels significantly decreased in patients receiving anakinra treatment (to a median of 17.5 pg/ml for IL-6 and 2,567.5 pg/ml for IP-10). CSF IL-6 levels were significantly lower in patients who were considered to have met criteria for clinical remission compared to those who had received treatment but had not met the criteria, but remained elevated compared to levels in healthy controls (Figure 1). CSF IL-18 levels decreased, particularly in patients with baseline IL-18 levels of >20 pg/ml, but this decrease was not statistically significant.

Levels of IL-1β, TNF, IL-12p70, IFNγ, and IL-10 in the CSF were elevated compared to baseline levels (significantly for IL-12p70, IFNγ, and IL-10). This elevation reached statistical significance in patients who met the criteria for clinical remission compared to healthy controls (IL-1β 0.8 pg/ml versus 0.3 pg/ml [$P = 0.001$], TNF 5.02 pg/ml versus 1.7 pg/ml [$P = 0.005$], IFNγ 69.8 pg/ml versus 26.3 pg/ml [$P = 0.001$], and IL-10 3.74 pg/ml versus 0.96 pg/ml [$P = 0.0001$]).

Similar to levels in the CSF, baseline blood levels of IL-18 and IL-6 were significantly higher in untreated

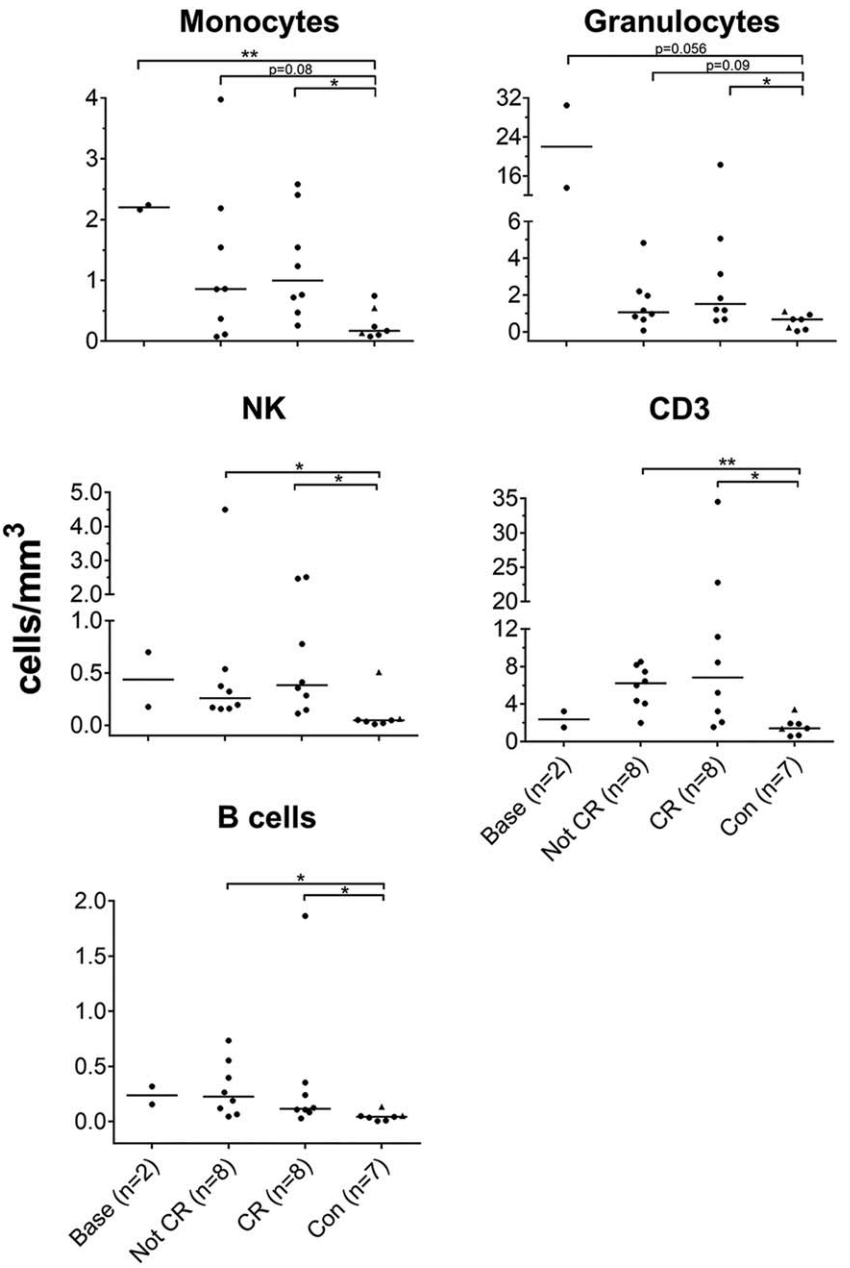

Figure 3. Leukocyte subpopulation absolute counts in CSF. Statistical analyses were performed by Student's unpaired *t*-test or Wilcoxon's rank sum test, depending on data distribution. Symbols represent individual patients; bars show the median. $* = P < 0.05$; $** = P < 0.005$. **Arrowheads** represent pediatric controls. NK = natural killer (see Figure 1 for other definitions).

NOMID patients than in controls (median 538.9 pg/ml versus 70.4 pg/ml [$P = 0.002$] and 65.3 pg/ml versus 22.0 pg/ml [$P = 0.002$], respectively) and decreased with treatment, but remained significantly higher relative to levels in healthy controls (Figure 2). Unlike levels in the CSF, baseline blood levels of IP-10/CXCL10 in patients were similar to levels in healthy controls. IL-12p70 levels, although lower in the CSF of patients with NOMID versus controls, were significantly higher in the blood of NOMID patients versus controls. Blood levels of IL-12p70 remained stable in patients receiving anakinra, while blood TNF, IL-10, and IFNγ levels increased (significantly for TNF and IL-10). Blood IP-10 levels remained unchanged with treatment. As we expected, after anakinra treatment, blood and CSF levels of IL-1Ra increased (as they reflect a sum of both endogenous

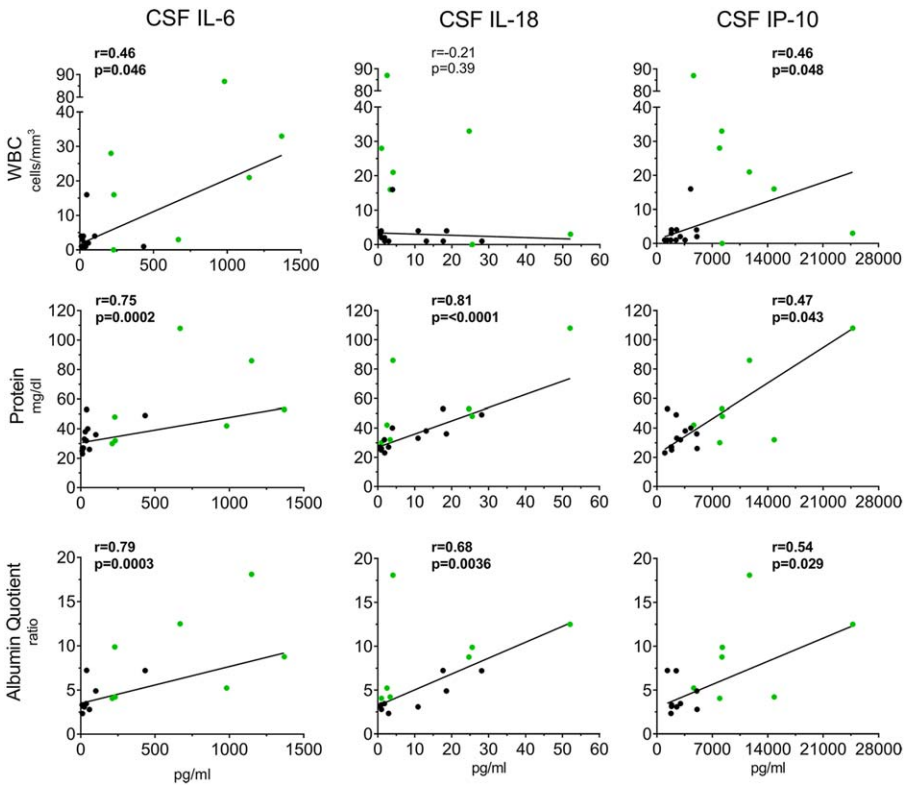

Figure 4. Correlations between levels of IL-6, IL-18, and IP-10/CXCL10 in the CSF with central nervous system parameters of inflammation. For each patient, baseline data (green; n = 7) were used if available and posttreatment data (black; n = 12) if baseline data were not available (total of 19 patients). Two patients were excluded because they had ventricular peritoneal shunts. Correlation coefficients and *P* values were assessed using Spearman's correlation coefficient. Non–linear regression robust straight lines are shown in each graph. WBC = white blood cells (see Figure 1 for other definitions).

and recombinant IL-1Ra or anakinra). IL-1β levels, which have been found only at very low levels in patients with NOMID (6), did not significantly increase.

To compare the amount of cytokine production in the CNS compared to the blood, matched CSF and blood samples were analyzed for cytokine CSF:blood ratios in the same assay, with appropriate serum and CSF controls. Consistent with results found in a previous study (6), baseline IL-6 levels were higher in the CSF than in blood samples; this was also observed for IP-10 levels in the CSF. Median CSF:blood ratios in patients were 31- and 11-fold higher than those in controls, with a median CSF:blood ratio of 5.2 for IL-6, and 8.7 for IP-10/CXCL10 (see Supplementary Figure 2, available on the *Arthritis & Rheumatology* web site at http://onlinelibrary.wiley.com/doi/10.1002/art.40055/abstract). The CSF:blood ratios for IL-6 and IP-10/CXCL10 progressively decreased with treatment and were lowest when disease was in clinical remission (0.5 and 1.2, respectively). The median CSF:blood ratios for the other cytokines (including IL-1β and IL-18) demonstrated lower levels in the CSF than in the blood (with ratios between 0.05 and 0.2) and did not significantly change with anakinra treatment, except that the IL-12p70 and IFNγ CSF:blood ratios increased (though not significantly) after treatment (due to a greater increase in the CSF than in blood levels).

Significant decrease in CSF monocyte and granulocyte counts, but no full normalization, during remission. Patients with NOMID have a predominant elevation of innate leukocytes in the CSF (11). Although adaptive immune cells (CD3+ cells and B cells) are mildly increased in the CSF of untreated and anakinra-treated patients, only numbers of innate immune cells (monocytes, granulocytes) were significantly higher in patients with NOMID compared to controls (Figure 3). Monocyte and granulocyte numbers decreased posttreatment, but monocyte numbers remained on average 3-fold higher in patients with NOMID who were treated with anakinra in comparison to controls, while neutrophils remained only ~1.5-fold higher in anakinra-treated NOMID patients versus controls

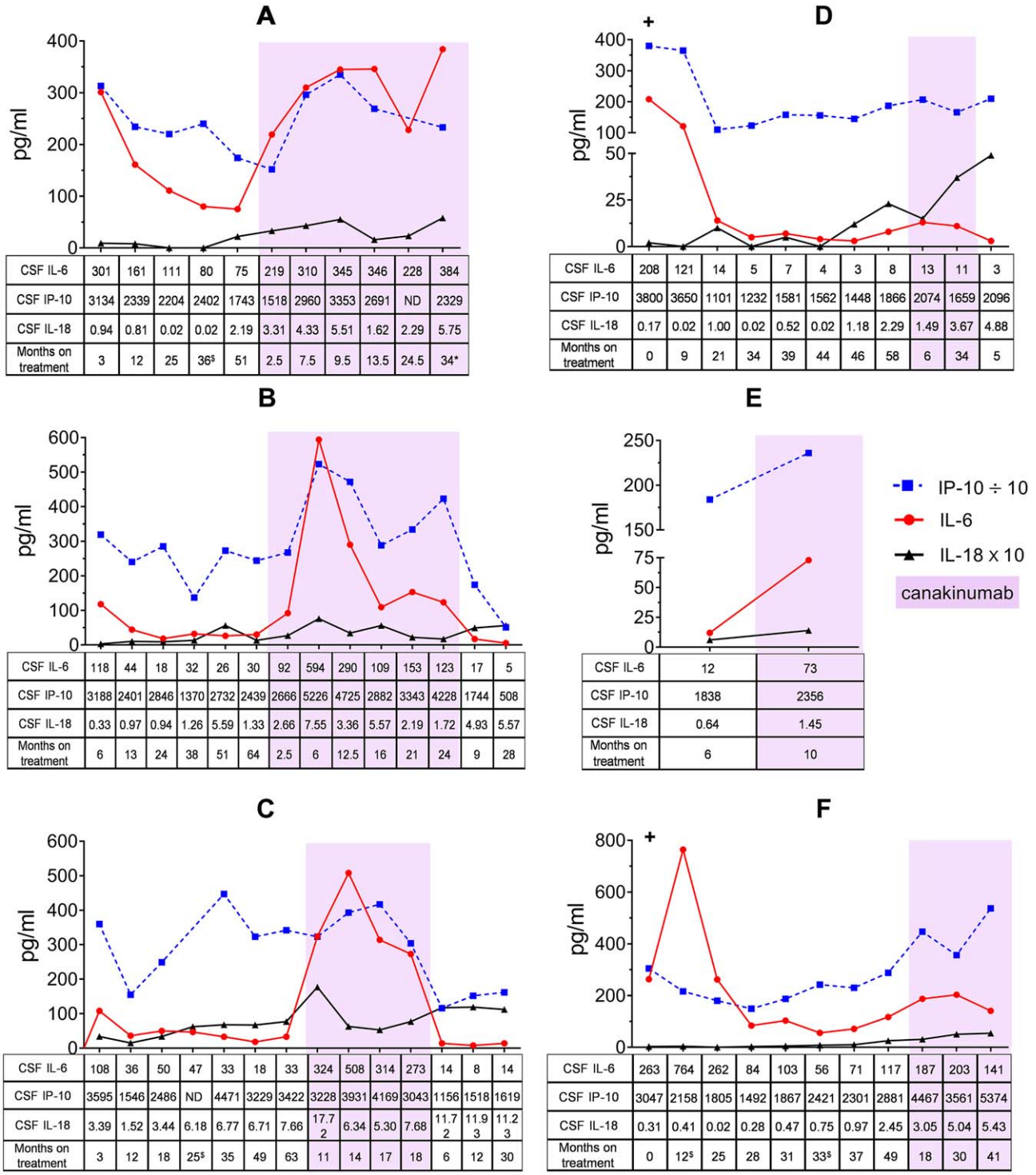

Figure 5. IL-6, IP-10/CXCL10, and IL-18 levels in the CSF of 6 pediatric neonatal-onset multisystem inflammatory disease patients who received anakinra and canakinumab in sequence. All 6 patients initially received anakinra and were then switched to canakinumab. After canakinumab, 3 patients' treatments were switched back to anakinra. Plus signs indicate baseline samples. $= patients with otitis media or sinusitis at time of procedure. * = patient was taking one-fourth of the prescribed dose. ND = not done due to no or insufficient CSF sample (see Figure 1 for other definitions).

Table 2. Comparison of CSF and blood cytokine measurements in pediatric NOMID patients receiving anakinra and subsequent canakinumab treatment*

Measure	Anakinra	Canakinumab	*P*
IL-6, pg/ml			
CSF	28.5 (14.4–62.7)	150.7 (84.3–275.5)	0.004
Blood†	3.0 (2.7–5.0)	2.8 (2.13–3.0)	0.17
IP-10/CXCL10, pg/ml			
CSF	2,148.1 (1,904.3–2,440.7)	3,119.0 (2,458.0–3,655.0)	0.037
Blood†	906.3 (878.7–1,071.4)	1,245.1 (732.8–1,385.7)	0.82
IL-18, pg/ml			
CSF	1.3 (0.83–2.3)	3.4 (3.2–4.3)	0.028
Blood†	179.7 (158.2–332.6)	145.5 (131.1–301.6)	0.10
CSF WBCs/mm^3‡	3.7 (1.6–6.0)	10.2 (3.6–23.9)	0.027
CSF protein, mg/dl§	39.0 (33.7–47.3)	44.3 (38.3–46.3)	0.69
CSF albumin quotient§	4.4 (3.1–7.0)	5.2 (4.0–5.5)	0.89

* For individual patients, mean anakinra and mean canakinumab values were obtained by taking the average of the last 3 values during anakinra treatment (prior to canakinumab treatment) and the average of the last 3 (for cerebrospinal fluid [CSF] measures) or last 2 (for blood measures) values during canakinumab treatment at steady state. For CSF measures, averages were not calculated for 1 patient who had only 1 value for both anakinra and canakinumab at steady state, and another patient who had only 1 value for canakinumab at steady state. For blood measures, averages were not calculated for 2 patients who had only 1 value for canakinumab at steady state. Due to small sample size, raw values were log transformed to be closely normally distributed, and analyzed by paired Student's *t*-test. Values are the back-transformed median (interquartile range). NOMID = neonatal-onset multisymptom inflammatory disease; IL-6 = interleukin-6; IP-10/CXCL10 = interferon-γ–inducible 10-kd protein; WBCs = white blood cells.
† Blood comparisons were performed among 5 patients due to missing data from canakinumab treatment in 1 patient.
‡ Due to a value of zero, raw values were transformed into arcsine.
§ Analyses were performed on 5 patients; CSF protein and albumin quotient were not recorded for 1 patient each for canakinumab treatment at steady state.

(*P* not significant). B cell counts remained stable, and CD3+ T cell counts increased significantly (~3–4-fold) with treatment.

Significant correlation of CSF IL-6 and IP-10/CXCL10 levels with monocyte counts during clinical remission. To investigate associations between inflammatory cells and cytokines, we analyzed correlations between CSF cytokine levels and CSF leukocyte subpopulations. Posttreatment, only CSF IL-6 levels correlated significantly with the number of CSF monocytes ($r = 0.51$, $P = 0.046$). When the illness was in remission, this correlation became stronger ($r = 0.88$, $P = 0.004$), and IP-10/CXCL10 levels also correlated significantly with CSF monocytes ($r = 0.81$, $P = 0.015$) (see Supplementary Tables 1B and C, available on the *Arthritis & Rheumatology* web site at http://onlinelibrary.wiley.com/doi/10.1002/art.40055/abstract). We found no relationship between levels of IL-18 or the other cytokines measured and subpopulations of CSF leukocytes.

Correlation of CSF IL-6 and IL-18 levels with CSF protein levels and albumin quotient. We assessed correlations of IL-18, IL-6, and IP-10 levels with measures of blood–brain barrier function, CSF total protein level and albumin quotient. Blood–brain barrier function measures, including total protein level and albumin quotient, correlated strongly with levels of IL-18 ($r = 0.81$, $P < 0.0001$ and $r = 0.68$, $P = 0.0036$, respectively) and IL-6 ($r = 0.75$, $P = 0.0002$ and $r = 0.79$, $P = 0.0003$, respectively), and moderately with IP-10/CXCL10 levels ($r = 0.47$, $P = 0.043$ and $r = 0.54$, $P = 0.029$, respectively) (Figure 4), but did not correlate with the other cytokines measured (see Supplementary Table 2, http://onlinelibrary.wiley.com/doi/10.1002/art.40055/abstract).

Increased within-patient CSF cytokine levels and CSF WBC counts when treated with "optimized" doses of canakinumab versus anakinra. To date, there are no published comparative studies comparing anakinra and the long-acting anti–IL-1β monoclonal antibody canakinumab for treatment of CNS inflammation. Since CSF IL-6, IP-10, and IL-18 levels correlated with clinical measures including monocyte counts and blood–brain barrier function in anakinra-treated patients with NOMID, we assessed serial CSF and blood IL-6, IP-10/CXCL10, and IL-18 levels as well as CNS inflammatory markers in 6 pediatric patients who were initially treated with anakinra and were then switched to canakinumab. Three of these patients were switched back to anakinra (Figure 5). We found that CSF IL-6, IP-10/CXCL10, and IL-18 levels and WBC counts were significantly higher when patients were receiving canakinumab than when they were receiving anakinra (Table 2), despite

only infrequent self-reports of headaches. The CSF cytokine levels and the WBC counts decreased in the 3 patients who switched back to anakinra after canakinumab treatment (see Figures 5B–D and Supplementary Tables 3B–D, available on the *Arthritis & Rheumatology* web site at http://onlinelibrary.wiley.com/doi/10.1002/art.40055/abstract); however, these results did not reach statistical significance due to the small number of patients. In patients receiving either anakinra or canakinumab treatment, ESRs and CRP levels were normal and blood IL-6, IP-10/CXCL10, and IL-18 levels did not significantly differ between treatments (see Table 2 and Supplementary Tables 3A–F, http://onlinelibrary.wiley.com/doi/10.1002/art.40055/abstract).

DISCUSSION

Increased *NLRP3* inflammasome assembly and IL-1β secretion cause the systemic disease manifestations of NOMID. However, the regulation of CNS inflammation, the contribution of CNS resident cells to the development of chronic aseptic meningitis and brain damage, and differences in the effects of various IL-1 blocking treatments on CNS inflammation remain unknown. Our data indicate that IL-6 and IP-10/CXCL10 levels are highly elevated in the CSF and decreased with treatment, but did not normalize in all patients. Furthermore, IL-18, IL-6, and IP-10/CXCL10 may be markers for blood–brain barrier function, and differences in treatment responses to the 2 IL-1 blocking agents anakinra and canakinumab suggest differences in CNS penetration. Collectively, our data suggest a role of serial CSF biomarker measurements in assessing and monitoring residual CNS inflammation in patients with NOMID receiving different IL-1 blocking treatments.

Elevated granulocyte counts, which represent >90% of abnormally elevated cell numbers in the CSF of untreated NOMID patients with aseptic meningitis, virtually normalized with IL-1 blocking treatment. In contrast, CSF monocyte levels decreased but remained significantly elevated even in patients with illness in clinical remission. Of the 9 inflammatory cytokines we examined to characterize potential low-grade inflammation, only IL-6 and IP-10/CXCL10 were expressed at higher levels in the CSF compared to corresponding serum samples; the levels of both cytokines were significantly lower (albeit not completely normalized) with anakinra treatment compared to canakinumab. Levels were lowest when patients' disease was in clinical remission compared to those in patients who were receiving treatment but did not fulfill clinical remission criteria. The presence of higher levels of IL-6 and IP-10 in the CSF compared to the blood suggests production of these cytokines in the CNS. Although monocytes in the CSF can produce IL-1, microglia and astrocytes can produce IL-6 and IP-10 in response to IL-1β during active disease and are a likely source for the cytokine production in the CNS in NOMID (15).

IP-10/CXCL10 is a known downstream marker of IFN signaling, and levels of IP-10/CXCL10 in the blood of patients with NOMID are not elevated above control levels. In contrast, levels of IP-10/CXCL10 in the blood are highly elevated in patients with IFN-mediated autoinflammatory diseases (16,17). While it is necessary to further evaluate the mechanisms that lead to elevation of IP-10/CXCL10 levels in the CSF but not the blood of untreated NOMID patients, IFN- and STAT-1–independent mechanisms of IP-10/CXCL10 up-regulation have been observed in astrocytes and microglia in the CNS in a murine HIV model (18). IP-10/CXCL10 production has also been observed in brain microvascular endothelial cells that form the blood–brain barrier in response to exposure to serum from patients with neuromyelitis optica (19). These observations raise the question of whether the elevation of IP-10/CXCL10 levels in the CSF may reflect astrocyte, microglial, and/or brain microvascular endothelial cell activation in response to blood–brain barrier damage in NOMID.

In contrast to IL-6, IP-10/CXCL10, and IL-18 levels, which all decreased with treatment, we observed small but significant increases in the levels of TNF, IL-12p70, IL-10, and IFNγ in the CSF with treatment (in the context of significant clinical improvement). The overall levels of these cytokines were much lower in the CSF than in the blood (10 pg/ml for TNF, IL-12p70, and IL-10, and 150 pg/ml for IFNγ); but the increase in these levels demonstrates the complexity of interpreting soluble biomarker levels in biologic fluids. The measured CSF cytokine levels represent the balance between their production/secretion and their binding/uptake by target cells and tissues. In that context the small increase in cytokine levels could reflect an altered balance of production and consumption, with fewer inflammatory or activated tissue cells being able to consume/bind these cytokines.

Upon treatment with anakinra, CSF protein and albumin levels declined (7), suggesting improvement of blood–brain barrier function. The CSF cytokines IL-6, IP-10/CXCL10, and IL-18 significantly correlated with measures of blood–brain barrier function. It has been implied that these cytokines, when elevated, cause the functional changes in the endothelial cells and astrocytes layer that constitutes the blood–brain barrier and cause or aggravate blood–brain barrier dysfunction/breakdown (19,20). While the elevated levels of IP-10 and IL-6 suggest

that they are produced intrathecally, the relatively stable IL-18 CSF:blood ratios before and after anakinra treatment and the lack of correlation between CSF IL-18 levels and WBC counts suggest that CSF IL-18 may mainly derive from passage across a "leaky" blood–brain barrier, although low levels of CNS production cannot be ruled out. Interestingly, elevations of IL-1 and IL-18 have been seen in patients with chronic tension headaches (21), and IL-18–mediated microglia/astrocyte interactions have been associated with the development of allodynia and may play a role in development of persistent headaches (22).

Our study is limited by the small sample size (due to the rarity of the disease) and the fact that we did not correct for the multiple exploratory analyses performed. However, serial, longitudinally collected, matched CSF and blood samples (including pretreatment CSF samples) were assayed simultaneously, which reduced interassay variability typically seen with cytokine analyses, and increases the reliability of our data interpretation. The markers we propose need to be validated in further follow-up studies and in other diseases. Multiplex cytokine assays allow for measurement of multiple cytokines simultaneously from a small sample volume, but their utility for the assessment of IL-1β and other low-expressing cytokines is limited. IL-1β is highly protein-bound; soluble serum, plasma, and CSF levels are often below 1 pg/ml, which is below the assay's detection range. Small variations in IL-1β levels can have large pathologic effects as seen in the cryopyrinopathies, but serum IL-1β measurements cannot reliably be interpreted, thus limiting their use as a biomarker. Although IL-6 is not a specific marker for inflammasome activation, it is a known downstream marker of systemic inflammation in patients with CAPS (23). In our study, IL-6 correlated best with clinical markers of CNS inflammation and may be a surrogate for assessing IL-1 activity in patients with CAPS.

This is the first published study to compare treatment with 2 IL-1 blocking agents, anakinra and canakinumab, and their effects on controlling CNS inflammation in NOMID/CAPS (6 patients). CSF levels of IL-6, IP-10/CXCL10, and IL-18 and WBC counts were significantly higher when patients were being treated with canakinumab at a time when steady-state kinetics had likely been established compared to when patients were receiving anakinra treatment at steady-state kinetics. CRP levels and ESRs, and blood levels of cytokines, including IL-6, IP-10/CXCL10, and IL-18, were similar during anakinra and canakinumab treatment. However, cytokine levels in the CSF were lower when patients were receiving anakinra compared to canakinumab treatment, and there was a trend for levels to go back down when anakinra was reinitiated, in the 3 patients who began treatment with anakinra, switched to canakinumab, and then back to anakinra. Differences in CSF penetration of the 2 drugs may contribute to the differences in low-grade CNS inflammation, which may be particularly relevant in "low inflammatory states" when the blood–brain barrier is less penetrant. All patients enrolled had chronic CNS inflammation prior to receiving IL-1 blocking treatment. Our data regarding CNS inflammation cannot be extrapolated to patients with milder forms of CAPS who have less-severe or only intermittent CNS disease.

The long-term clinical implications of chronic low elevation of CSF cytokine levels (including IL-1β, IL-6, IL-18, and IP-10) and persistently elevated monocyte counts in patients with NOMID are currently unknown, and complications from the illness can take many years to develop. Therefore, correlations with the longer-term development of symptoms and damage need to be studied in the future. Monocytes can confer proinflammatory and antiinflammatory properties (24); they play a role in wound repair and tissue surveillance and their persistence posttreatment may reflect a homeostatic adaptation (25). Similarly, IL-6 has pro- and antiinflammatory properties; however, chronically elevated IL-6 levels in the CSF are seen in acute and chronic neurologic conditions (26), and have been correlated with progression of brain atrophy in patients with neuro-Behçet's disease (27). Elevated IL-1β levels have also been associated with Alzheimer's disease (28) and with recurrent headaches (21). This study was not designed to investigate the long-term effects of chronic low-grade inflammation but rather was intended to identify biomarkers that may assist in the assessment and characterization of low-grade inflammation. Our data indicate the need for longitudinal assessment of patients' clinical function to determine whether the residual inflammation measured is benign or associated with long-term consequences such as headaches, cognition, and progression of brain atrophy.

In summary, our findings indicate that the regulation of inflammation in the CNS compartment cannot be predicted by blood markers of inflammation and that drugs that suppress systemic inflammation may not equally suppress CNS inflammation and suggest the value of a "personalized approach" guided by CSF biomarkers to assess residual inflammation and optimize treatment. Of the markers tested, IL-6, IL-18, and perhaps IP-10/CXCL10 may be used to monitor efficacy of IL-1 blocking therapy in controlling CNS inflammation in NOMID. Differences in blockade of CNS inflammation between anakinra and canakinumab suggest that assessment of CSF inflammation, drug penetration into

the CNS, and pharmacokinetics of IL-1β inhibitors should be included when designing studies of IL-1β inhibitors in NOMID and other neuroinflammatory diseases.

ACKNOWLEDGMENT

The authors would like to thank Usma Hussein for her help in organizing the data.

AUTHOR CONTRIBUTIONS

All authors were involved in drafting the article or revising it critically for important intellectual content, and all authors approved the final version to be published. Dr. Rodriguez-Smith had full access to all of the data in the study and takes responsibility for the integrity of the data and the accuracy of the data analysis.

Study conception and design. Rodriguez-Smith, Gadina, Goldbach-Mansky.

Acquisition of data. Rodriguez-Smith, Lin, Tsai, Kim, Montealegre-Sanchez, Chapelle, Huang, Sibley, Bielekova, Goldbach-Mansky.

Analysis and interpretation of data. Rodriguez-Smith, Wesley, Bielekova, Goldbach-Mansky.

REFERENCES

1. Guarda G, Zenger M, Yazdi AS, Schroder K, Ferrero I, Menu P, et al. Differential expression of NLRP3 among hematopoietic cells. J Immunol 2011;186:2529–34.
2. Hirohata S, Isshi K, Oguchi H, Ohse T, Haraoka H, Takeuchi A, et al. Cerebrospinal fluid interleukin-6 in progressive Neuro-Behcet's syndrome. Clin Immunol Immunopathol 1997;82:12–7.
3. Mankan AK, Dau T, Jenne D, Hornung V. The NLRP3/ASC/Caspase-1 axis regulates IL-1β processing in neutrophils. Eur J Immunol 2012;42:710–5.
4. Tanaka N, Izawa K, Saito MK, Sakuma M, Oshima K, Ohara O, et al. High incidence of NLRP3 somatic mosaicism in patients with chronic infantile neurologic, cutaneous, articular syndrome: results of an International Multicenter Collaborative study. Arthritis Rheum 2011;63:3625–32.
5. Goldbach-Mansky R. Current status of understanding the pathogenesis and management of patients with NOMID/CINCA. Curr Rheumatol Rep 2011;13:123–31.
6. Goldbach-Mansky R, Dailey NJ, Canna SW, Gelabert A, Jones J, Rubin BI, et al. Neonatal-onset multisystem inflammatory disease responsive to interleukin-1β inhibition. N Engl J Med 2006; 355:581–92.
7. Sibley CH, Plass N, Snow J, Wiggs EA, Brewer CC, King KA, et al. Sustained response and prevention of damage progression in patients with neonatal-onset multisystem inflammatory disease treated with anakinra: a cohort study to determine three- and five-year outcomes. Arthritis Rheum 2012;64:2375–86.
8. Fox E, Jayaprakash N, Pham TH, Rowley A, McCully CL, Pucino F, et al. The serum and cerebrospinal fluid pharmacokinetics of anakinra after intravenous administration to non-human primates. J Neuroimmunol 2010;223:138–40.
9. Sibley CH, Chioato A, Felix S, Colin L, Chakraborty A, Plass N, et al. A 24-month open-label study of canakinumab in neonatal-onset multisystem inflammatory disease. Ann Rheum Dis 2015; 74:1714–9.
10. Hirohata S, Miyamoto T. Elevated levels of interleukin-6 in cerebrospinal fluid from patients with systemic lupus erythematosus and central nervous system involvement. Arthritis Rheum 1990;33: 644–9.
11. Han S, Lin YC, Wu T, Salgado AD, Mexhitaj I, Wuest SC, et al. Comprehensive immunophenotyping of cerebrospinal fluid cells in patients with neuroimmunological diseases. J Immunol 2014;192:2551–63.
12. Reiber H, Peter JB. Cerebrospinal fluid analysis: disease-related data patterns and evaluation programs. J Neurol Sci 2001;184: 101–22.
13. Houser B. Bio-Rad's Bio-Plex® suspension array system, xMAP technology overview. Arch Physiol Biochem 2012;118:192–6.
14. Fox JL, McCullough DC, Green RC. Effect of cerebrospinal fluid shunts on intracranial pressure and on cerebrospinal fluid dynamics. 2. A new technique of pressure measurements: results and concepts. 3. A concept of hydrocephalus. J Neurol Neurosurg Psychiatry 1973;36:302–12.
15. Das S, Mishra MK, Ghosh J, Basu A. Japanese encephalitis virus infection induces IL-18 and IL-1β in microglia and astrocytes: correlation with in vitro cytokine responsiveness of glial cells and subsequent neuronal death. J Neuroimmunol 2008;195:60–72.
16. Liu Y, Ramot Y, Torrelo A, Paller AS, Si N, Babay S, et al. Mutations in proteasome subunit β type 8 cause chronic atypical neutrophilic dermatosis with lipodystrophy and elevated temperature with evidence of genetic and phenotypic heterogeneity. Arthritis Rheum 2012;64:895–907.
17. Liu Y, Jesus AA, Marrero B, Yang D, Ramsey SE, Montealegre Sanchez GA, et al. Activated STING in a vascular and pulmonary syndrome. N Engl J Med 2014;371:507–18.
18. Asensio VC, Maier J, Milner R, Boztug K, Kincaid C, Moulard M, et al. Interferon-independent, human immunodeficiency virus type 1 gp120-mediated induction of CXCL10/IP-10 gene expression by astrocytes in vivo and in vitro. J Virol 2001;75:7067–77.
19. Shimizu F, Nishihara H, Sano Y, Takeshita Y, Takahashi S, Maeda T, et al. Markedly increased IP-10 production by blood-brain barrier in neuromyelitis optica. PLoS One 2015;10:e0122000.
20. De Vries HE, Blom-Roosemalen MC, van Oosten M, de Boer AG, van Berkel TJ, Breimer DD, et al. The influence of cytokines on the integrity of the blood-brain barrier in vitro. J Neuroimmunol 1996;64:37–43.
21. Della Vedova C, Cathcart S, Dohnalek A, Lee V, Hutchinson MR, Immink MA, et al. Peripheral interleukin-1β levels are elevated in chronic tension-type headache patients. Pain Res Manag 2013;18:301–6.
22. Miyoshi K, Obata K, Kondo T, Okamura H, Noguchi K. Interleukin-18-mediated microglia/astrocyte interaction in the spinal cord enhances neuropathic pain processing after nerve injury. J Neurosci 2008;28:12775–87.
23. Hoffman HM, Rosengren S, Boyle DL, Cho JY, Nayar J, Mueller JL, et al. Prevention of cold-associated acute inflammation in familial cold autoinflammatory syndrome by interleukin-1 receptor antagonist. Lancet 2004;364:1779–85.
24. Grainger JR, Wohlfert EA, Fuss IJ, Bouladoux N, Askenase MH, Legrand F, et al. Inflammatory monocytes regulate pathologic responses to commensals during acute gastrointestinal infection. Nat Med 2013;19:713–21.
25. Aubert P, Suarez-Farinas M, Mitsui H, Johnson-Huang LM, Harden JL, Pierson KC, et al. Homeostatic tissue responses in skin biopsies from NOMID patients with constitutive overproduction of IL-1β. PLoS One 2012;7:e49408.
26. Erta M, Quintana A, Hidalgo J. Interleukin-6, a major cytokine in the central nervous system. Int J Biol Sci 2012;8:1254–66.
27. Kikuchi H, Takayama M, Hirohata S. Quantitative analysis of brainstem atrophy on magnetic resonance imaging in chronic progressive neuro-Behcet's disease. J Neurol Sci 2014;337:80–5.
28. Tan MS, Yu JT, Jiang T, Zhu XC, Tan L. The NLRP3 inflammasome in Alzheimer's disease. Mol Neurobiol 2013;48:875–82.

ARTHRITIS & RHEUMATOLOGY
Vol. 69, No. 6, June 2017, pp 1337–1338

CONCISE COMMUNICATION

DOI 10.1002/art.40058

Analysis of *ATP8B4* F436L missense variant in a large systemic sclerosis cohort

Over the last 7 years, knowledge of the systemic sclerosis (SSc) genetic component has increased considerably, due mainly to large genetic studies including genome-wide association studies (GWAS) and Immunochip analysis. However, there is still a large portion of SSc heritability that remains unexplained, as is the case with most complex traits (1). One hypothesis that has been proposed to explain the missing heritability for complex diseases involves rare and low-frequency variants. These types of genetic variations are not well covered by GWAS, which are mainly focused on common variants. However, the use of next-generation sequencing technologies, such as whole-exome sequencing, has rapidly overcome this problem. In this regard, Gao et al performed, for the first time, whole-exome sequencing in SSc and reported a novel gene, *ATP8B4*, as a risk factor for the disease (2). They suggested a missense rare variant (F436L [rs55687265]) as a potential causal variant for the association signal in *ATP8B4*. We therefore aimed to further evaluate the reported signal of association, taking advantage of our access to large cohorts of patients with SSc.

The *ATP8B4* rare variant rs55687265 was genotyped in 6 independent case–control cohorts of European ancestry (total 7,426 SSc patients and 13,087 healthy controls) (see Supplementary Table 1, on the *Arthritis & Rheumatology* web site at http://onlinelibrary.wiley.com/doi/10.1002/art.40058/abstract). All SSc patients fulfilled the American College of Rheumatology 1980 preliminary classification criteria for the disease (3) or exhibited at least 3 of 5 features of CREST syndrome (calcinosis, Raynaud's phenomenon, esophageal dysmotility, sclerodactyly, telangiectasias) (4). We first performed association analyses to test whether rs55687265 was associated with SSc susceptibility in each of the cohorts included in the present study (see Supplementary Methods, http://onlinelibrary.wiley.com/doi/10.1002/art.40058/abstract). A trend toward association ($P = 0.071$) was observed in the Spanish case–control set (odds ratio [OR] 1.58) (Table 1). However, we did not observe any suggestive or significant association signal in the remaining cohorts. We also observed opposite effects for the same allele in different populations. The meta-analysis combining all of the sample sets, which was performed using an inverse variance fixed-effects model, showed no significant association with the disease (OR 1.07, $P = 0.484$) (Table 1 and Supplementary Methods). In addition, stratified analysis based on different clinical sub-phenotypes of SSc (limited and diffuse cutaneous subtypes, and the presence of the SSc-specific autoantibodies anticentromere and anti–topoisomerase I) did not show significant associations (data not shown). Thus, we did not find statistically significant differences in the frequency of the *ATP8B4* rs55687265*C allele between the SSc patients and controls enrolled in the study. A meta-analysis combining the results of the present study with the results from the discovery phase of the study reported by Gao et al (2) was also performed, and again no significant *P* value was found (OR 1.36, $P_{random} = 0.212$, heterogeneity q value < 0.01, $I^2 = 82.68$).

The impact of rare variants on the development of autoimmune diseases remains an unanswered and controversial question (5). Moreover, it has long been recognized that the identification of rare variant associations with high-throughput DNA sequencing technologies, such as whole-exome sequencing, is substantially affected by technical artifacts, which may lead to Type I error. This issue becomes especially important when the sample size of the whole-exome sequencing study is not large enough, and when there is a large difference between the case cohort size and the control cohort size (6,7). The present study highlights the importance of validation of whole-exome sequencing results with other sequencing methods, as well as replication of the newly observed associations in independent studies, in order to detect actual disease-causing mutations.

In conclusion, in the present study we could not replicate the association of *ATP8B4* rs55687265 with susceptibility to SSc. However, because we did not attempt to evaluate associations of other rare or common variants with SSc

Table 1. Association analysis of the *ATP8B4* F436L variant in 6 independent systemic sclerosis cohorts, and meta-analysis*

	Minor/major allele	No. of cases/controls	MAF, cases	MAF, controls	OR (95% CI)
Cohort					
Spain	C/G	2,056/2,718	0.008	0.005	1.58 (0.96–2.61)
Germany	C/G	909/486	0.019	0.022	0.87 (0.50–1.50)
The Netherlands	C/G	435/783	0.013	0.007	1.78 (0.75–4.20)
Italy	C/G	1,114/980	0.006	0.011	0.56 (0.28–1.12)
UK	C/G	1,456/5,272	0.012	0.011	1.13 (0.77–1.67)
US	C/G	1,456/2,848	0.015	0.015	1.00 (0.69–1.45)
Meta-analysis†	C/G	7,426/13,087			1.07 (0.88–1.31)

* Self-reported ancestry and genome-wide association study or Immunochip data were used to remove outliers. None of the odds ratios (ORs) for minor allele frequency (MAF) in cases versus controls were statistically significant. In the Spanish cohort there was a trend toward significance ($P = 0.071$). 95% CI = 95% confidence interval.
† Heterogeneity q value = 0.17, $I^2 = 35.73$.

susceptibility, our findings do not eliminate the possibility that this gene plays a role.

Supported by the Spanish Ministry of Economy and Competitiveness (grant SAF2015-66761-P). The authors are grateful to the Spanish Scleroderma Group (whose members are listed in the Supplementary Appendix, on the Arthritis & Rheumatology web site at http://onlinelibrary.wiley.com/doi/10.1002/art.40058/abstract) for valuable contributions to the study.

Elena López-Isac, MSc
Lara Bossini-Castillo, PhD
Ana B. Palma, MSc
Institute of Parasitology and Biomedicine López-Neyra CSIC
Granada, Spain
Shervin Assassi, MD
Maureen D. Mayes, MD, MPH
The University of Texas Health Science Center
Houston, TX
Carmen P. Simeón, MD, PhD
Valle de Hebrón Hospital
Barcelona, Spain
Norberto Ortego-Centeno, MD
Clinic University Hospital
Granada, Spain
Esther Vicente, MD
Hospital La Princesa
Madrid, Spain
Carlos Tolosa, MD
Hospital Parc Tauli
Sabadell, Spain
Manuel Rubio-Rivas, MD*
Bellvitge University Hospital
Barcelona, Spain
José A. Román-Ivorra, MD
Hospital Universitari i Politecnic La Fe
Valencia, Spain
Lorenzo Beretta, MD
Fondazione IRCCS Ca' Granda Ospedale Maggiore Policlinico di Milano
Milan, Italy
Gianluca Moroncini, MD, PhD
Università Politecnica delle Marche and Ospedali Riuniti
Ancona, Italy
Nicolas Hunzelmann, MD
University of Cologne
Cologne, Germany
Jörg H. W. Distler, MD
University of Erlangen-Nuremberg
Erlangen, Germany
Gabriella Riemekasten, MD, PhD
University of Lübeck
Lübeck, Germany and German Lung Center
Borstel, Germany
Jeska de Vries-Bouwstra, MD, PhD
Leiden University Medical Center
Leiden, The Netherlands
Alexandre E. Voskuyl, MD
VU University Medical Center
Amsterdam, The Netherlands
Timothy R. D. J. Radstake, MD, PhD
University Medical Center Utrecht
Utrecht, The Netherlands
Ariane Herrick, MD, PhD
The University of Manchester Manchester Academic Health Science Centre
Manchester, UK
Christopher P. Denton, MD, PhD
Carmen Fonseca, MD, PhD
Royal Free and University College Medical School
London, UK
Javier Martín, MD, PhD
Institute of Parasitology and Biomedicine López-Neyra
Granada, Spain

AUTHOR CONTRIBUTIONS

All authors were involved in drafting the article or revising it critically for important intellectual content, and all authors approved the final version to be published. Ms López-Isac had full access to all of the data in the study and takes responsibility for the integrity of the data and the accuracy of the data analysis.

Study conception and design. López-Isac, Martín.

Acquisition of data. Bossini-Castillo, Assassi, Mayes, Simeón, Ortego-Centeno, Vicente, Tolosa, Rubio-Rivas, Román-Ivorra, Beretta, Moroncini, Hunzelmann, Distler, Riemekasten, de Vries-Bouwstra, Voskuyl, Radstake, Herrick, Denton, Fonseca, Martín.

Analysis and interpretation of data. López-Isac, Palma.

1. Bossini-Castillo L, Lopez-Isac E, Martin J. Immunogenetics of systemic sclerosis: defining heritability, functional variants and shared-autoimmunity pathways. J Autoimmun 2015;64:53–65.
2. Gao L, Emond MJ, Louie T, Cheadle C, Berger AE, Rafaels N, et al. Identification of rare variants in ATP8B4 as a risk factor for systemic sclerosis by whole-exome sequencing. Arthritis Rheumatol 2016;68:191–200.
3. Subcommittee for Scleroderma Criteria of the American Rheumatism Association Diagnostic and Therapeutic Criteria Committee. Preliminary criteria for the classification of systemic sclerosis (scleroderma). Arthritis Rheum 1980;23:581–90.
4. Mayes MD, Bossini-Castillo L, Gorlova O, Martin JE, Zhou X, Chen WV, et al. Immunochip analysis identifies multiple susceptibility loci for systemic sclerosis. Am J Hum Genet 2014;94:47–61.
5. Hunt KA, Mistry V, Bockett NA, Ahmad T, Ban M, Barker JN, et al. Negligible impact of rare autoimmune-locus coding-region variants on missing heritability. Nature 2013;498:232–5.
6. Goodwin S, McPherson JD, McCombie WR. Coming of age: ten years of next-generation sequencing technologies. Nat Rev Genet 2016;17:333–51.
7. Hu YJ, Liao P, Johnston HR, Allen AS, Satten GA. Testing rare-variant association without calling genotypes allows for systematic differences in sequencing between cases and controls. PLoS Genet 2016;12:e1006040.

* Correction added on May 19, 2017, after online publication: The spelling of the author name Manuel Rubio-Rivas has been corrected.

ARTHRITIS & RHEUMATOLOGY
Vol. 69, No. 6, June 2017, pp 1339–1342

LETTERS

DOI 10.1002/art.40048

Could γ/δ T cells explain adverse effects of zoledronic acid? Comment on the article by Reinhardt et al

To the Editor:

We read with interest the recent article by Reinhardt et al reporting on the abundance of activated γ/δ T cells in the enthesis, ciliary body, and aortic valve in *Tcrd-H2BeGFP* mice (1). The clinical implications of these findings might be relevant. We suggest, for example, that this particular localization of γ/δ T cells may explain the adverse effects of certain drugs.

Zoledronic acid is a drug used to treat osteoporosis, Paget's disease, and bone metastasis (2). The use of intravenous zoledronic acid is occasionally associated with the appearance of an acute-phase response within 24–36 hours, mainly characterized by fever, musculoskeletal symptoms (principally pain and stiffness of the joints, which suggest an inflammatory reaction, possibly enthesitis), and eye inflammation (3). In particular, in some cases, uveitis has been observed after infusion (4). Moreover, it is known that zoledronic acid might induce arrhythmias (atrial fibrillation, in particular) (5).

Nitrogen-containing bisphosphonates, such as zoledronic acid, inhibit osteoclastic bone resorption by blocking farnesyl pyrophosphate synthase, an enzyme in the mevalonate pathway, leading to accumulation of isopentenyl diphosphate and dimethyl-allyl diphosphate in monocytes. This results in the activation of adjacent γ/δ T cells and the release of interferon-γ and tumor necrosis factor (6). We have previously demonstrated that higher numbers of circulating γ/δ T cells before zoledronic acid infusion correlate with a higher risk of acute-phase reactions (7). In addition, γ/δ T cell numbers decrease after the infusion and were found to be lower than before zoledronic acid treatment, even at 12-month follow-up (8). This effect on circulating lymphocytes may be attributed to the activation, differentiation, and homing of these cells at tissue levels (9). Akitsu et al have found increased homing of γ/δ T cells in mice with inflammatory arthritis (10).

Given their localization in the enthesis and ciliary body of mice, we hypothesize that γ/δ T cells, activated by zoledronic acid, might induce articular inflammation and uveitis. Moreover, the localization of activated γ/δ T cells in the aortic valve may suggest that they have a role even in arrhythmias, in particular, atrial fibrillation, which has been reported as an adverse effect of zoledronic acid infusion.

Cristian Caimmi, MD
Maurizio Rossini, MD, PhD
Ombretta Viapiana, MD, PhD
Luca Idolazzi, MD, PhD
Giovanni Adami, MD
Davide Gatti, MD
University of Verona
Verona, Italy

1. Reinhardt A, Yevsa T, Worbs T, Lienenklaus S, Sandrock I, Oberdörfer L, et al. Interleukin-23–dependent γ/δ T cells produce interleukin-17 and accumulate in the enthesis, aortic valve, and ciliary body in mice. Arthritis Rheumatol 2016;68:2476–86.
2. Coleman R, Burkinshaw R, Winter M, Neville-Webbe H, Lester J, Woodward E, et al. Zoledronic acid. Expert Opin Drug Saf 2011;10:133–45.
3. Reid IR, Gamble GD, Mesenbrink P, Lakatos P, Black DM. Characterization of and risk factors for the acute-phase response after zoledronic acid. J Clin Endocrinol Metab 2010; 95:4380–7.
4. Patel DV, Horne A, House M, Reid IR, McGhee CN. The incidence of acute anterior uveitis after intravenous zoledronate. Ophthalmology 2013;120:773–6.
5. Black DM, Delmas PD, Eastell R, Reid IR, Boonen S, Cauley JA, et al. Once-yearly zoledronic acid for treatment of postmenopausal osteoporosis. N Engl J Med 2007;356:1809–22.
6. Roelofs AJ, Jauhiainen M, Monkkonen H, Rogers MJ, Monkkonen J, Thompson K. Peripheral blood monocytes are responsible for γδ T cell activation induced by zoledronic acid through accumulation of IPP/DMAPP. Br J Haematol 2009;144:245–50.
7. Rossini M, Adami S, Viapiana O, Ortolani R, Vella A, Fracassi E, et al. Circulating γδ T cells and the risk of acute-phase response after zoledronic acid administration. J Bone Miner Res 2012;27: 227–30.
8. Rossini M, Adami S, Viapiana O, Fracassi E, Ortolani R, Vella A, et al. Long-term effects of amino-bisphosphonates on circulating γδ T cells. Calcif Tissue Int 2012;91:395–9.
9. Dieli F, Gebbia N, Poccia F, Caccamo N, Montesano C, Fulfaro F, et al. Induction of γδ T-lymphocyte effector functions by bisphosphonate zoledronic acid in cancer patients in vivo. Blood 2003;102:2310–1.
10. Akitsu A, Ishigame H, Kakuta S, Chung SH, Ikeda S, Shimizu K, et al. IL-1 receptor antagonist-deficient mice develop autoimmune arthritis due to intrinsic activation of IL-17-producing $CCR2^{+}V\gamma6^{+}\gamma\delta$ T cells. Nat Commun 2015;25:7464.

DOI 10.1002/art.40050

Reply

To the Editor:

We thank Dr. Caimmi and colleagues for their thoughtful commentary on our recent publication. The authors speculate about a possible connection between tissue-resident interleukin-17 (IL-17)–producing γ/δ T cells and zoledronic acid–induced local inflammation in humans. Zoledronic acid indeed leads to an accumulation of intracellular isopentenyl pyrophosphate (IPP) in target cells, which in turn activates human Vγ9+Vδ2+ T cells. However, only a few reports to date have described the induction of IL-17 in human Vγ9+Vδ2+ T cells, either by zoledronate (1), or directly by phosphoantigens such as IPP (2–5) or the more potent microbial hydroxyl-3-methyl-but-2-enyl pyrophosphate (HMBPP) (6,7) (Table 1). Collectively, these studies showed that in healthy human blood only a minor γ/δ T cell population produces IL-17 upon stimulation with HMBPP or IPP, whereas IL-17–producing γ/δ T cell numbers can increase upon stimulation with specific cytokine mixtures, during infection or autoimmune and autoinflammatory diseases (Table 1). Although a very interesting hypothesis, it is thus presently far from established that intravenous injection of zoledronate could lead to a strong induction of IL-17 secretion by human tissue-resident γ/δ T cells.

Table 1. Evidence for phosphoantigen-induced IL-17 production by human Vγ9+Vδ2+ T cells*

Experimental system	Stimulus (% of IL-17–producing γ/δ T cells)	Ref.
Neonatal cord blood Vγ9+Vδ2+ T cells	Zoledronate (0.3%), zoledronate + IL-23 (2%)	1
Healthy PB Vγ9+Vδ2+ T cells	IPP (1–5%), IPP + IL-1β + IL-6 + IL-23 + TGFβ (35%)	2
BacMen PB or CSF Vγ9+Vδ2+ T cells	IPP (50–70%)	2
Healthy PB Vγ9+ T cells	IPP (<1%)	3
JIA PB or SF Vγ9+ T cells	IPP (4%)	3
Healthy PB Vγ9+Vδ2+ T cells	IPP (effector memory 91%, non–effector memory 25%)	4
Healthy PB Vγ9+Vδ2+ T cells	IPP (0.4%)	5
PsA PB or SF Vγ9+Vδ2+ T cells	IPP (1.5%)	5
Healthy PB Vγ9+Vδ2+ T cells	HMBPP + IL-1β + IL-23 + TGFβ (14%)	6
Neonatal cord blood Vγ9+Vδ2+ T cells	HMBPP + IL-1β + IL-6 + TGFβ (7%)	6
Psoriasis skin Vγ9+Vδ2+ T cells	HMBPP (0.5%)	7
Healthy PB Vγ9+Vδ2+ T cells	BrHPP (1%), BrHPP + activated PDCs (6%)	18

* IL-17 = interleukin-17; PB = peripheral blood; IPP = isopentenyl pyrophosphate; TGFβ = transforming growth factor β; BacMen = bacterial meningitis; CSF = cerebrospinal fluid; JIA = juvenile idiopathic arthritis; SF = synovial fluid; PsA = psoriatic arthritis; HMBPP = hydroxyl-3-methyl-but-2-enyl pyrophosphate; BrHPP = bromohydrin pyrophosphate; PDCs = plasmacytoid dendritic cells.

Data on the identification of entheseal T cells in humans are rare. Although IL-17–producing γ/δ T cells have been reported to be enriched in the peripheral blood of patients with ankylosing spondylitis (8), enthesitis-related arthritis (9), or psoriatic arthritis (5), presence of γ/δ T cells within entheseal tissue has not been systematically addressed to date. However, IL-17–producing α/β T cells (10), mast cells (11), or type 3 innate lymphoid cells (12) have been found in synovial fluid from spondyloarthritis patients, whereas IL-17–producing neutrophils were enriched within inflamed facet joints (13). The presence of CD8+ T cells (14) and macrophages within entheseal tissue has been described (15). Interestingly, γ/δ T cells were enriched in aqueous humor from patients with idiopathic uveitis (16), and IPP-responsive γ/δ T cells could be isolated from intraocular fluid from patients with Behçet's disease (17).

Nevertheless, cytokines other than IL-17 might be secreted by enthesis-, eye-, or heart-resident γ/δ T cells in humans, and contribute to the reported symptoms as well. Since zoledronic acid certainly potently induces secretion of interferon-γ (IFNγ), as well as tumor necrosis factor (TNF), by peripheral blood Vγ9+Vδ2+ T cells, it is conceivable that similar functions are also exerted by tissue-resident Vγ9+Vδ2+ T cells. In this context, production of IFNγ and TNF by peripheral blood Vγ9+Vδ2+ T cells could explain adverse effects such as fever and musculoskeletal symptoms that appear during the acute-phase reaction in response to zoledronic acid, as implied in the letter by Caimmi et al.

Assuming that zoledronic acid–inducible γ/δ T cells indeed reside within human entheseal, eye, or heart tissue, this would be of great interest for understanding zoledronic acid–induced local inflammation, irrespective of their IFNγ, TNF, or IL-17 production capacity. There is, therefore, an urgent need to determine whether γ/δ T cells are present in healthy and inflamed human entheseal, eye, and heart tissue, accounting for zoledronic acid–induced arrhythmias and atrial fibrillation, as well as articular and eye inflammation.

Annika Reinhardt, Dr. rer. nat.
Immo Prinz, Prof. Dr. rer. nat.
Hannover Medical School
Hannover, Germany

1. Moens E, Brouwer M, Dimova T, Goldman M, Willems F, Vermijlen D. IL-23R and TCR signaling drives the generation of neonatal Vγ9Vδ2 T cells expressing high levels of cytotoxic mediators and producing IFN-γ and IL-17. J Leukoc Biol 2011;89:743–52.
2. Caccamo N, La Mendola C, Orlando V, Meraviglia S, Todaro M, Stassi G, et al. Differentiation, phenotype, and function of interleukin-17-producing human Vγ9Vδ2 T cells. Blood 2011; 118:129–38.
3. Bendersky A, Marcu-Malina V, Berkun Y, Gerstein M, Nagar M, Goldstein I, et al. Cellular interactions of synovial fluid γδ T cells in juvenile idiopathic arthritis. J Immunol 2012;188:4349–59.
4. Hu C, Qian L, Miao Y, Huang Q, Miao P, Wang P, et al. Antigen-presenting effects of effector memory Vγ9Vδ2 T cells in rheumatoid arthritis. Cell Mol Immunol 2012;9:245–54.
5. Guggino G, Ciccia F, Di Liberto D, Lo Pizzo M, Ruscitti P, Cipriani P, et al. Interleukin (IL)-9/IL-9R axis drives γδ T cells activation in psoriatic arthritis patients. Clin Exp Immunol 2016; 186:277–83.

6. Ness-Schwickerath KJ, Jin C, Morita CT. Cytokine requirements for the differentiation and expansion of IL-17A- and IL-22-producing human Vγ2Vδ2 T cells. J Immunol 2010;184:7268–80.
7. Laggner U, Di Meglio P, Perera GK, Hundhausen C, Lacy KE, Ali N, et al. Identification of a novel proinflammatory human skin-homing Vγ9Vδ2 T cell subset with a potential role in psoriasis. J Immunol 2011;187:2783–93.
8. Kenna TJ, Davidson SI, Duan R, Bradbury LA, McFarlane J, Smith M, et al. Enrichment of circulating interleukin-17–secreting interleukin-23 receptor–positive γ/δ T cells in patients with active ankylosing spondylitis. Arthritis Rheum 2012;64:1420–9.
9. Gaur P, Misra R, Aggarwal A. Natural killer cells and γδ T cells alterations in enthesitis related arthritis category of juvenile idiopathic arthritis. Clin Immunol 2015;161:163–9.
10. Bowness P, Ridley A, Shaw J, Chan AT, Wong-Baeza I, Fleming M, et al. Th17 cells expressing KIR3DL2+ and responsive to HLA-B27 homodimers are increased in ankylosing spondylitis. J Immunol 2011;186:2672–80.
11. Noordenbos T, Yeremenko N, Gofita I, van de Sande M, Tak PP, Canete JD, et al. Interleukin-17–positive mast cells contribute to synovial inflammation in spondylarthritis. Arthritis Rheum 2012;64:99–109.
12. Ciccia F, Guggino G, Rizzo A, Saieva L, Peralta S, Giardina A, et al. Type 3 innate lymphoid cells producing IL-17 and IL-22 are expanded in the gut, in the peripheral blood, synovial fluid and bone marrow of patients with ankylosing spondylitis. Ann Rheum Dis 2015;74:1739–47.
13. Appel H, Maier R, Wu P, Scheer R, Hempfing A, Kayser R, et al. Analysis of IL-17^{+} cells in facet joints of patients with spondyloarthritis suggests that the innate immune pathway might be of greater relevance than the Th17-mediated adaptive immune response. Arthritis Res Ther 2011;13:R95.
14. Laloux L, Voisin MC, Allain J, Martin N, Kerboull L, Chevalier X, et al. Immunohistological study of entheses in spondyloarthropathies: comparison in rheumatoid arthritis and osteoarthritis. Ann Rheum Dis 2001;60:316–21.
15. McGonagle D, Marzo-Ortega H, O'Connor P, Gibbon W, Hawkey P, Henshaw K, et al. Histological assessment of the early enthesitis lesion in spondyloarthropathy. Ann Rheum Dis 2002;61:534–7.
16. Bertotto A, Spinozzi F, Vagliasindi C, Vaccaro R. γδ T cells in aqueous humour from untreated idiopathic uveitis patients. Br J Ophthalmol 1995;79:395.
17. Verjans GM, van Hagen PM, van der Kooi A, Osterhaus AD, Baarsma GS. Vγ9Vδ2 T cells recovered from eyes of patients with Behcet's disease recognize non-peptide prenyl pyrophosphate antigens. J Neuroimmunol 2002;130:46–54.
18. Lo Presti E, Caccamo N, Orlando V, Dieli F, Meraviglia S. Activation and selective IL-17 response of human Vγ9Vδ2 T lymphocytes by TLR-activated plasmacytoid dendritic cells. Oncotarget 2016;7:60896–905.

DOI 10.1002/art.40083

American College of Rheumatology/European League Against Rheumatism Sjögren's syndrome classification criteria may not be adequate for extraglandular disease and necessitate defining "seronegative Sjögren's syndrome": comment on the article by Shiboski et al

To the Editor:

The recently published American College of Rheumatology (ACR)/European League Against Rheumatism (EULAR) criteria for classifying primary Sjögren's syndrome (SS) (1) are based on a scoring system that can be applied to individuals who have a positive response on any of the screening questions or any positive item in the EULAR SS Disease Activity Index questionnaire (2). A patient is classified as having SS if she/he has a score of ≥4 from the classification criteria items. However, similar to previous SS classification criteria sets (3–6), there is an inherent problem: the criteria comprise only glandular manifestations. Most patients with primary SS who need aggressive treatment (immunosuppressive or biologic agents) are those with major organ involvement, and a significant proportion of these patients do not have glandular manifestations severe enough to fulfill the classification criteria. This might be due to symptoms and signs related to major organ involvement leading to earlier diagnosis compared to that in patients with only glandular symptoms. The new classification criteria do not seem to resolve this problem. We suggest that the criteria be modified to allow classification (maybe with fewer item scores) when there is major organ involvement. This would be similar to the ability to classify a patient with lupus renal involvement as having systemic lupus erythematosus (SLE) with fewer items when there is biopsy-proven disease, in the Systemic Lupus International Collaborating Clinics (SLICC) criteria (6,7).

Our second concern is that anti-SSA/Ro is the only immunologic marker in the new ACR/EULAR classification criteria. This is also similar to some of the previous criteria sets (3–6). The result is that a patient with no detectable autoantibodies may be classified as having primary SS. A few reports have used the term "seronegative primary SS," which usually denotes "anti-SSA/SSB negative." In clinical practice, our observation is that the majority of patients with primary SS who are negative for anti-SSA/SSB are positive for rheumatoid factor (RF) or antinuclear antibody (ANA). Therefore, there is an urgent need to define seronegative primary SS. The new, as well as most of the previous, classification criteria sets allow classification of individuals who are triple negative (for SSA/SSB, RF, and ANA) as having primary SS. However, this subgroup is not adequately defined or studied. We suggest that clinical and laboratory findings should be evaluated separately and fulfillment of at least 1 clinical and 1 laboratory criteria component should be required for classification, as in the 2012 SLICC classification criteria for SLE (7).

Mehmet E. Tezcan, MD
Kartal Dr. Lutfi Kirdar Training and Research Hospital
Istanbul, Turkey
Hamit Kucuk, MD
Berna Goker, MD
Gazi University School of Medicine
Ankara, Turkey

1. Shiboski CH, Shiboski SC, Seror R, Criswell LA, Labetoulle M, Lietman TM, et al. 2016 American College of Rheumatology/European League Against Rheumatism classification criteria for primary Sjögren's syndrome: a consensus and data-driven methodology involving three international patient cohorts. Arthritis Rheumatol 2017;69:35–45.
2. Seror R, Ravaud P, Bowman SJ, Baron G, Tzioufas A, Theander E, et al. EULAR Sjögren's Syndrome Disease Activity Index: development of a consensus systemic disease activity index for primary Sjögren's syndrome. Ann Rheum Dis 2010;69:1103–9.
3. Shiboski SC, Shiboski CH, Criswell LA, Baer AN, Challacombe S, Lanfranchi H, et al. American College of Rheumatology classifica-

tion criteria for Sjögren's syndrome: a data-driven, expert consensus approach in the Sjögren's International Collaborative Clinical Alliance cohort. Arthritis Care Res (Hoboken) 2012;64:475–87.
4. Vitali C, Bombardieri S, Jonsson R, Moutsopoulos HM, Alexander EL, Carsons SE, et al. Classification criteria for Sjögren's syndrome: a revised version of the European criteria proposed by the American-European Consensus Group. Ann Rheum Dis 2002;61:554–8.
5. Vitali C, Bombardieri S, Moutsopoulos HM, Coll J, Gerli R, Hatron PY, et al. Assessment of the European classification criteria for Sjögren's syndrome in a series of clinically defined cases: results of a prospective multicentre study. Ann Rheum Dis 1996;55:116–21.
6. Kabasakal Y, Kitapcioglu G, Karabulut G, Tezcan ME, Balkarli A, Aksoy A, et al. Criteria sets for primary Sjögren's syndrome are not adequate for those presenting with extraglandular organ involvements as their dominant clinical features. Rheumatol Int 2017;37:675–84. In press.
7. Petri M, Orbai AM, Alarcon GS, Gordon C, Merrill JT, Fortin PR, et al. Derivation and validation of the Systemic Lupus International Collaborating Clinics classification criteria for systemic lupus erythematosus. Arthritis Rheum 2012;64:2677–86.

DOI 10.1002/art.40085

Reply

To the Editor:

Drs. Tezcan and colleagues point out that some patients with clinically diagnosed SS, presenting with disease-related extraglandular features and anti-SSA/Ro antibodies (or a positive lip biopsy result) but without overt glandular manifestations (i.e., negative findings on salivary and lacrimal function tests), would not fulfill the new ACR/EULAR criteria for primary SS. Tezcan et al also indicate that, in their experience, these patients are often negative for anti-SSA/Ro antibodies and positive for RF and ANA, which are not included among the items in the new criteria set.

The fact that some patients with a given disorder cannot meet the classification criteria for it is not surprising. Classification criteria are not designed to assess the diagnosis in individual cases, but serve to define groups of patients with a given disease to be included in epidemiologic, clinical, and treatment studies. To be valid, classification criteria should have balanced and sufficiently high sensitivity and specificity to minimize the risk that patients without the disorder may be included in, and patients with clearcut disease may be excluded from, specifically designed studies (1). None of the classification criteria proposed for the different autoimmune rheumatic disorders, including those for SS, cover the entire spectrum of the disorder under consideration. To obtain this (in other words, to have a sensitivity of, or very close to, 100%) may be accompanied by an unacceptable loss of specificity.

The 2016 ACR/EULAR classification criteria for SS were developed using statistical methodology that has been approved by both the ACR and EULAR for this purpose and used to define classification criteria for other rheumatic diseases. Thus, the items selected and included in this criteria set were restricted to those that were most important from the perspective of both clinician expert opinion and statistical performance. From a methodologic point of view, classification criteria are quite distinct from diagnostic criteria. Clinicians should be cautious when adopting classification criteria in clinical practice, since a certain number of patients who do not meet the criteria for a given disorder will nonetheless have the disorder. In such cases, clinicians should adopt the therapeutic approach believed to be potentially beneficial for the patient, using their best clinical skill and independent of satisfaction of classification criteria. As pointed out in our report, the gold standard for the diagnosis of SS remains expert opinion.

Claudio Vitali, MD
Istituto Villa San Giuseppe
Como, Italy
and Casa di Cura di Lecco
Lecco, Italy
Hal Scofield, MD
Oklahoma Medical Research Foundation
University of Oklahoma Health Sciences Center
and Department of Veterans Affairs Medical Center
Oklahoma City, OK
Stephen C. Shiboski, PhD
Lindsey A. Criswell, MD, MPH, DSc
Thomas M. Lietman, MD
University of California San Francisco
Raphaèle Seror, MD, PhD
Marc Labetoulle, MD
Xavier Mariette, MD, PhD
Université Paris-Sud AP-HP
Hôpitaux Universitaires Paris-Sud
INSERM U1184
Paris, France
Astrid Rasmussen, MD, PhD
Oklahoma Medical Research Foundation
Oklahoma City, OK
Simon J. Bowman, PhD, FRCP
University Hospitals Birmingham
Birmingham, UK
Caroline H. Shiboski, DDS, MPH, PhD
University of California San Francisco

1. Johnson SR, Goek ON, Singh-Grewal D, Vlad SC, Feldman BM, Felson DT, et al. Classification criteria in rheumatic diseases: a review of methodologic properties. Arthritis Rheum 2007;57:1119–33.
2. Classification and Response Criteria Subcommittee of the American College of Rheumatology Committee on Quality Measures. Development of classification and response criteria for rheumatic diseases [editorial]. Arthritis Rheum 2006;55:348–52.
3. Dougados M, Gossec L. Classification criteria for rheumatic diseases: why and how? [editorial]. Arthritis Rheum 2007;57:1112–5.